PROCEEDINGS OF THE NUCLEAR PHYSICS AND SOLID STATE PHYSICS SYMPOSIUM 1970

MADURAI, DECEMBER 27-30, 1970

Volume II-Nuclear Physics

ORGANISED BY
THE PHYSICS COMMITTEE
OF THE DEPARTMENT OF ATOMIC ENERGY
GOVERNMENT OF INDIA

FOREWORD

The fifteenth Nuclear Physics and Solid State Physics Symposium sponsored by the Physics Committee of the Department of Atomic Energy was held at the American College Campus of the Madurai University during December 27-30, 1970. Prof. T. Meenakshisundaram, Vice-Chancellor, Madurai University, inaugurated the Symposium at the opening session which was presided over by Prof. B. D. Nag Chaudhuri, Chairman of the Physics Committee. About 400 physicists from all over the country participated in the Symposium.

Looking at the number of papers submitted to Nuclear Physics and Solid State Physics sections of the Symposium over the last few years, one finds that the number of contributed papers is tending to increase every year at the rate of roughly 20 papers per year. This year, 148 papers were submitted for the Nuclear Physics section and 167 papers for the Solid State Physics section. Although this trend may be taken to indicate a welcome feature of continuous growth of Nuclear Physics and Solid State Physics research in the country, the organizers of the Symposium are beginning to face the dilemma of how to programme such a large number of papers providing adequate time for an effective feed-back and discussion. We have followed this year, as in the previous ones, the practice of starring some papers in the Nuclear Physics Section and resorting to a few rapporteuring sessions in Solid State Physics Section. The number of invited talks in the combined sessions of the two sections was reduced to five this year and one joint session was devoted to a discussion of "Correlations" in both the Nuclear and Solid State Physics problems.

It has been increasingly felt that the usefulness of the proceedings of an annual symposium like this can be greatly enhanced by bringing out the proceedings as fast as possible. The Symposium Committee has taken some effective steps this year to avoid delay in the publication of the proceedings. The Vols. II and III containing contributed papers have, therefore, been prepared by the direct Xerographic reproduction of the submitted papers without any correction, revision or retyping. This was made possible only with the cooperation received from most of the authors in following the instructions for preparing the papers and in strictly observing the dead-lines. If any paper was not received within the prescribed dead-line, it was assumed that the author/s did not wish to publish the full paper in the proceedings, as they might have sent it for publication elsewhere. In such cases, only the abstracts of the papers presented have been included in the proceedings. Several

persons have contributed towards our efforts to bring out the proceedings as fast as possible; but it has been possible mainly due to the untiring efforts of Dr. B. A. Dasannacharya, Secretary, Solid State Physics Section, Dr. M. G. Betigeri, Secretary, Nuclear Physics Section, and the extreme cooperation of Dr. V. A. Kamath, Scientific Information Officer, BARC.

We would like to take this opportunity to record our thanks to the Vice-Chancellor, Madurai University, for his kind invitation to hold the symposium at Madurai. We are particularly grateful to Prof. K. S. Chandrasekaran and other members of the Physics Department of the Madurai University and the American College, Madurai, for their hospitality and the excellent arrangements made during the Symposium.

SSKapoor

(S. S. Kapoor)

Convener,
Nuclear Physics & Solid State
Physics Symposium Committee

CONTENTS

II. NUCLEAR THEORY

Page

Page

Page

NUCLEAR REACTIONS

THE LEVEL STRUCTURE OF ^{75}Se

Baldev Sahai and B. Lal
Tata Institute of Fundamental Research, Bombay-5.

I. INTRODUCTION

$^{75}_{34}Se_{41}$ is an odd A-odd N isotope expected to have a spin $9/2^+$ for the ground state according to the single particle shell model. It has, however, an anamalous[1] spin $5/2^+$; magnetic dipole moment $\mu = 0.9$ nm and the quadrupole moment $Q = 1.1 \pm 0.2$. These facts suggest that the study of low lying states in this nucleus should be interesting.

This nucleus has been studied in the past by two methods: As(p, n) reaction[2,3,4] and ^{75}Br decay[5,6]. However, no detailed work on the decay scheme has been done by studying gamma rays following the As(p, n) reaction wherein many more levels can be excited than in the beta decay of ^{75}Br. The present work was undertaken to make a detailed study of the level structure of ^{75}Se.

II. EXPERIMENTAL PROCEDURE

^{75}As(p, nγ)^{75}Se reaction has been studied with the 5.5 MeV Van de Graaff at the Bhabha Atomic Research Centre, Trombay. ^{75}As targets used were in two forms: firstly pellets made by pressing spec-pure arsenic powder obtained from Analytical Chemistry Division, B.A.R.C., Trombay; secondly thin targets deposited on thin carbon films. Former type is "infinitely" thick for the bombarding energies used whereas the latter had a thickness $\sim 100\ \mu g/cm^2$. Q value of the reaction leading to the ground state is - 1.647 MeV. We recorded the gamma spectra at progressively increasing bombarding energies starting at $E_p = 1.5$ to $E_p = 3.75$ MeV to find out the threshold for production of the various gamma rays. These spectra in the earlier

stages were recorded with a 30 c.c. Ge(Li) detector and a 400-channel T.M.C. analyser using pellet type targets. Fig.1 shows such a spectrum taken at E_p = 2.65 MeV and covering the energy range upto ~ 520 keV. The lines marked As are the lines arising from Coulomb excitation in As or from As(p, p') reaction. Fig.2 shows a gamma spectrum taken at E_p = 3.25 MeV and covering the higher energy range upto ~ 1500 keV. In the latter stages of the experiment a 4096 channel Nuclear Data analyser became available and some gamma-ray spectra were recorded at certain selected bombarding energies using thin targets. Thus the energies of the gamma ray could be more accurately determined. The resolution for 1332 keV gamma ray from ^{60}Co was 5.5 keV fwhm.

In addition, we have carried out gamma-gamma coincidence measurements at E_p = 3.0 and 3.5 MeV. Gating gamma rays were detected in NaI(Tl) crystals of 1/2" and 1" thickness, whereas the gated spectra were recorded with the 30 c.c. Ge(Li) detector. A conventional fast-slow set-up having a time resolution 2τ = 80 n.s. was used in the experiment. The gating gamma rays were the 112, 141.5, 286.5 and (491 + 511 + 516) keV gamma rays.

Recently, we have also carried out some conversion coefficient measurements by a six gap spectrometer[7] using the same (p, n) reaction.

III. RESULTS

Based on the coincidence measurements as well as the excitation functions of various gamma-rays, a decay scheme has been proposed in Fig.3. Many of the levels proposed agree with those in ref.3) and 4) observed by neutron time of flight technique. However, more accurate

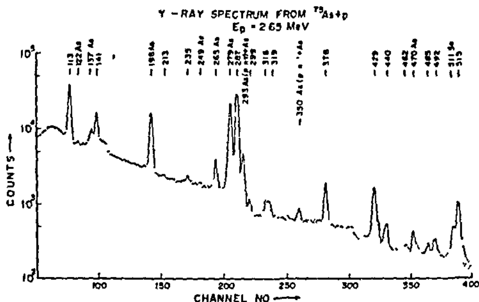


Fig.1. Gamma spectrum taken at E_p = 2.65 MeV covering the energy range upto 620 keV. As marked levels arise due to Coulomb excitation. Se implies gamma rays from ^{75}Se.

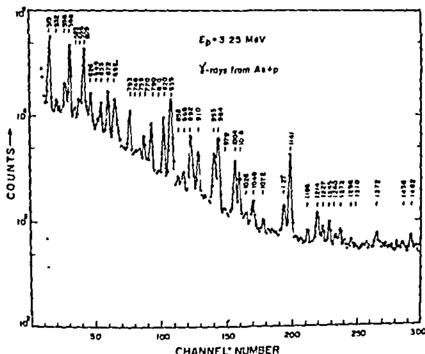


Fig.2. Gamma spectrum covering the range upto abo 1500 keV and taken at E_p = 3.25 MeV.

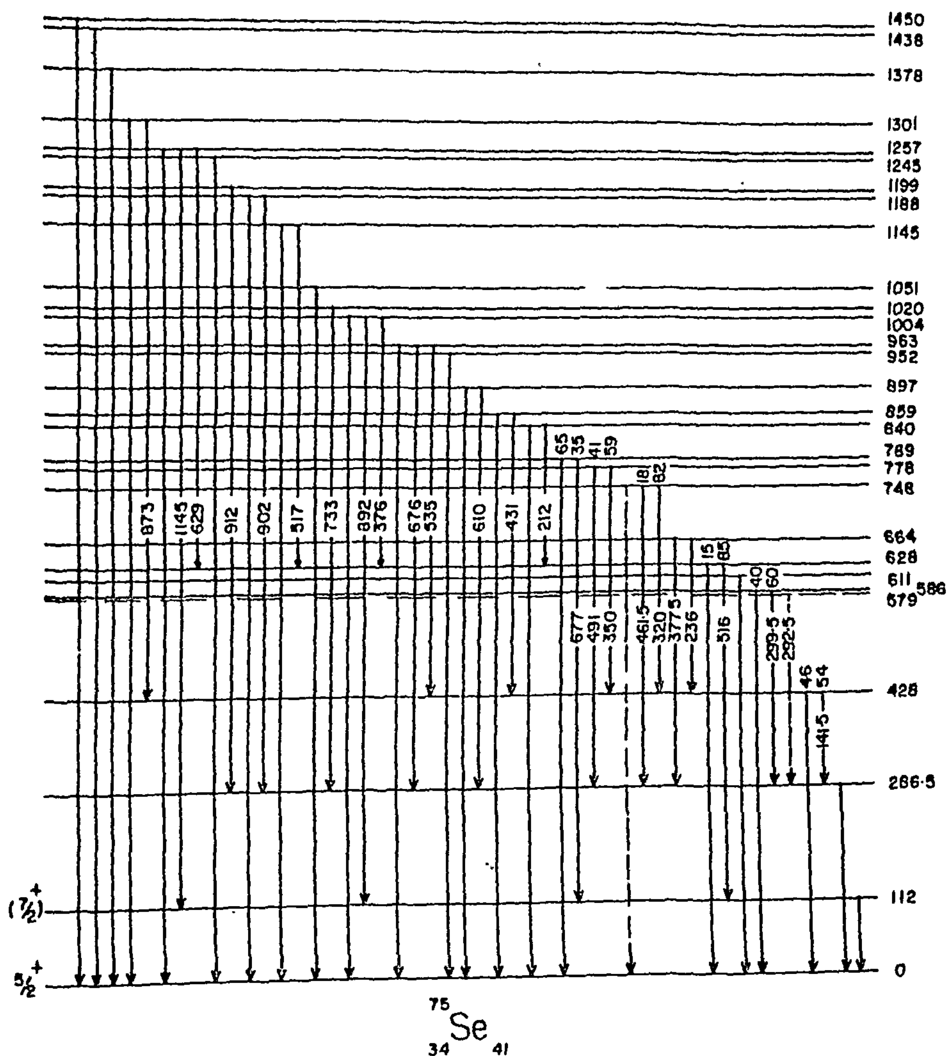


Fig.3. Proposed level scheme of ^{75}Se.

energy estimates are possible in the present experiment because of the use of Ge(Li) detector. The branching ratio have been worked out for those levels which decay through gamma rays of unique energies i.e. no comparable gamma ray exists which can be assigned to some other levels. These are summarized in Table 1.

TABLE I

BRANCHING RATIOS

Level	γ-rays arising from the level and % branching ratios in brackets.
112	112 (100)
286.5	286.5 (100)
428	141.5 (54), 428 (46)
579	292.5 (100)
586	299.5 (60), 586 (40)
611	611 (100)
628	516 (85), 628 (15)
664	377.5 (90), 236 (10)
748	461.5 (18), 320 (82)
778	491 (41), 550 (59)
952	952 (100)
1020	733 (100)
1051	1051 (100)
1199	912 (100)
1301	873 (76), 1301 (24)
1378	1378 (100)
1438	1438 (100)
1450	1450 (100)

In addition, levels at 789, 840, 859, 897, 983, 1004, 1145, 1188, 1245, 1257 decay through gamma rays which cannot be uniquely assigned.

Based on the preliminary conversion coefficient measurements, the spins of 112 and 286.5 keV levels appear to be $7/2^+$ and $3/2^-$ as the transitions are found to be M1 and E1 respectively and the fact that 286.5 keV level decays directly to the ground state supports this assignment.

References

1. Nuclear Data, Section B, B1-6-97.
2. B. Labkowicz and P. Marmier, Helv. Phys. Acta, 34, 85 (1961).
3. N.A. Tubbs, Thesis, Oxford University, 1966 (unpublished).
4. E. Finckh, U. Jahnke, B. Schreiber and A. Weidinger, Nucl. Phys. A144, 67 (1970).
5. S. Ray, J.N. Mo, S. Muszynski and S.K. Mark, Nucl. Phys. A138, 49 (1969).
6. I.M. Ladenbauer-Bellis and H. Bakhru, Phys. Rev. 178, 2019 (1969).
7. S.K. Ambardekar, S.M. Bharathi and C.V.K. Baba, Proc. Nucl. Physics & Solid State Physics Symposium, Roorkee, 1969.

DISCUSSION

V. Lakshminarayana: Since (p,α) is a positive value reaction, did you separate out $(p,\alpha\gamma)$ from your $(p,n\gamma)$.

B. Lal: Yes, it is very easy to separate them out as the γ-rays due to $(p,\alpha\gamma)$ and $(p,n\gamma)$ would be distinctly seen in the spectrum. However the cross-section for $(p,\alpha\gamma)$ is very low compared to that of $(p,n\gamma)$ reaction.

S. Ramamurty: Is the nucleus ^{75}Se expected to verify some model?

B. Lal: I would be interested to apply some model for this nucleus after the spins of some of the low lying levels in the ^{75}Se are confirmed.

LOW LYING LEVELS OF ^{51}Cr AND ^{59}Ni

B. Lal and Baldev Sahai
Tata Institute of Fundamental Research, Bombay-5.

I. INTRODUCTION

In continuation of our studies[1] of (p, nγ) reactions to measure the spins of the low lying levels in the residual nuclei, we have studied the angular distribution of gamma rays from $^{51}V(p, n\gamma)^{51}Cr$ and $^{59}Co(p, n\gamma)^{59}Ni$ reactions.

Though the spins in ^{51}Cr nucleus for the levels at 749, 778, 1350 are established[2] to be $3/2^-$, $1/2^-$ and $5/2^-$, the spin assignments of the levels at 1165, 1479 and 1557 have been rather doubtful. The levels at 1165 and 1479 have been clearly seen in stripping reaction $^{50}V(^3He, d)^{51}Cr$ by Dorenbusch[3] et al. Since the ground state spin of ^{50}V is 6^+ the spins of the levels excited in this reaction are expected to be high. Recently the $^{51}V(p, n\gamma)^{51}Cr$ studies performed by Tepel[4] et al. have shown the spins of 1165, 1479 and 1557 to be $9/2^-$, $11/2^-$ and $7/2^-$ respectively.

The ^{59}Ni nucleus has been investigated in the past by stripping and pick-up[5] reactions and also by (α, nγ) and (p, nγ) reactions by Birstein[6] et al.

We present here our results on angular distribution of ground state transitions from 749, 1165, 1350, 1479 and 1557 keV levels in ^{51}Cr and 339, 465 and 879 keV levels in ^{59}Ni. The results have been compared with the statistical model calculations.

II. EXPERIMENTAL PROCEDURE

Targets were prepared by evaporating spectroscopically pure vanadium and cobalt metals on gold backing. The thickness of the target obtained was roughly 800 $\mu gm/cm^2$ which is about 50 keV thick

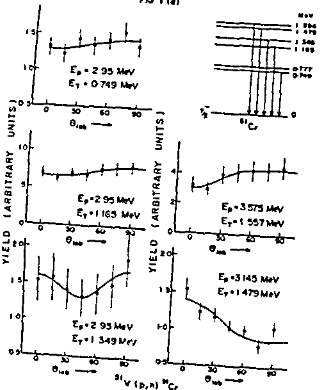
for 5.5 MeV proton. A 2 c.c. Ge(Li) detector used for detection of gamma-rays was mounted on a movable arm so that it could be moved on a circle around the target housed in an aluminium tube. A 3" x 3" NaI(Tl) detector kept at 90° on the other side of the beam was used as a monitor. The anisotropy resulting from the absorption of gamma-rays in the target backing and the target tube and also due to non-centering of the target was corrected by obtaining the angular distribution of gamma-rays of comparable energies from radioactive isotopes under experimental conditions.

III. RESULTS

Angular distributions obtained were fitted to even order Legendre Polynomial expansion

$$W(\theta) = 1 + a_2 P_2(\cos\theta) + a_4 P_4(\cos\theta)$$

The results obtained were compared with the theoretical calculations for the angular distribution of gamma-rays based on the expression given by Sheldon and van Patter[7]. The computer code HFMODEL[1] was used for this purpose. In the calculations the elastic, inelastic and (p, n) channels were considered for the decay of the compound nucleus and ℓ values upto 5 were taken into consideration for protons and neutrons. The transmission coefficients for protons and neutrons were obtained from the computer code "ABACUS"[8]. The results are shown in Fig.1 and 2. The shaded rectangle shows the experimental value along with its error and the curves are theoretical values calculated for different values of the multipole mixing ratio varying from $-\infty$ to $+\infty$. Each curve corresponds to a different value of spin assumed for the level whose decay is being considered.



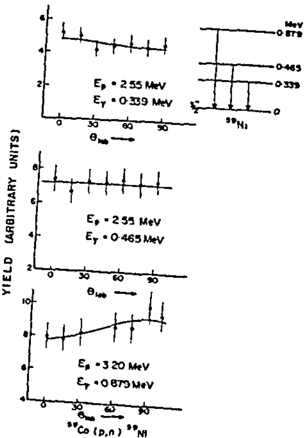
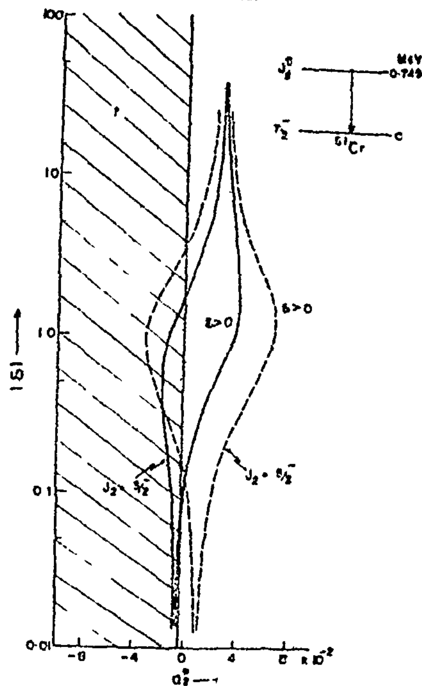
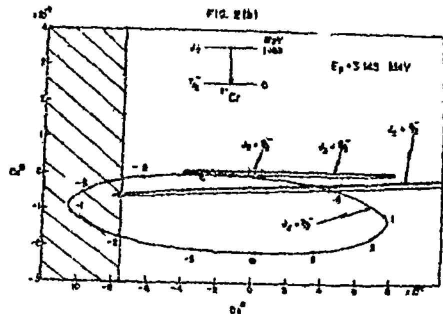
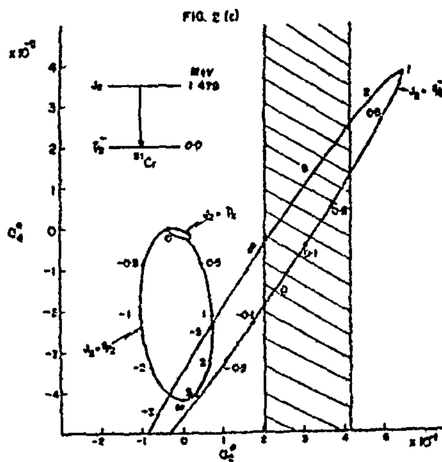


Fig.1(a) and (b) show the Legendre Polynomial fitting to the observed angular distribution of the gamma rays.







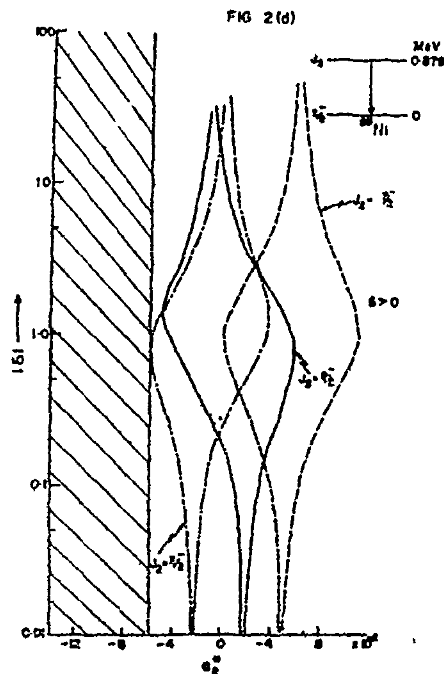


Fig.2(a), (b), (c) and (d) show the theoretically calculated curves a_2^* vs a_4^* or a_2^* vs δ -multipole mixing ratio, compared with the experimental data: ($a_n^* \equiv a_n/a_0$). Shaded area shows the experimental value along with its error.

References

1. K.V.K. Iyengar, B. Lal and S.K. Gupta, Nucl. Phys. A 108, 592 (1967).
2. J.R. Robertshaw, S. Mecca, A. Sperduto and W.W. Buechner, Phys. Rev. 170, 1013 (1968).
3. W.E. Dorenbusch, T.A. Belote and J. Rapaport, Nucl. Phys. A 133, 146 (1969).
4. J.W. Tepel, J.G. Malan and J.A.M. de Villiers, (Preprint).
5. E.R. Cosman, C.H. Paris, A. Sperduto and H.A. Enge, Phys. Rev. 142, 673 (1966).
6. L. Birstein, R. Chechik, Ch. Drory, E. Friedman, A.A. Jaffe and A. Wolf, Nucl. Phys. A 118, 193 (1968).
7. E. Sheldon and D.M. van Patter, Rev. Mod. Phys. 38, 143 (1966).
8. E.H. Auerbach, Report BNL-6562 (1962), unpublished.

DISCUSSION

P.P. Kane: How do you know that the lowest transition is M1 and not E2 + M1?

B. Lal: This is a tentative assignment.

K.G. Prasad: From the Multipolarity M1 of 112 keV transition, How do you fine the spin of 112 keV level to be $7/2^+$? It could be $3/2^+$ or $5/2^+$ also. Similarly it could be $5/2^-$ and $7/2^-$ in case of second excited state.

B. Lal: $5/2^-$ and $7/2^-$ assignments for second excited state viz 287 keV are ruled out from the log ft values fof this level from the decay of ^{75}Br, thus only $3/2^-$ is the likely assignment. The cascade transition from 287 keV to 112 keV does not exist hence the spin values for 112 keV, $3/2^+$ or $5/2^+$ could not be possible while on the other hand $7/2^+$ for 112 keV fulfils both the conditions of M1 transition as well as the 287 keV $(3/2^-) \rightarrow$ 112 keV $(7/2^+)$ being forbidden.

ON THE APPEARANCE OF PLATEAU IN THE NEUTRON TOTAL CROSS SECTION

A.N. Saharia and I. Ahmad
Dept. of Physics, Aligarh Muslim University, Aligarh (U.P.)

I. INTRODUCTION

It is quite well known that if the neutron total cross section is plotted as a function of $A^{1/3}$(depending on energy) there are certain regions over which the total cross section is essentially constant. Emmerich[1] by numerically integrating the Schrodinger equation, showed that the appearance of such plateau in the total cross section is well described by the nuclear optical model. However, a qualitative study of the plateau as regards to its nature and its dependence on the incident neutron energy and the target mass number is lacking. In the present note we show that the modified Glauber high energy scattering theory provides a qualitatively good description of the appearance of the plateau and use it to obtain an equation of the loci in the $A^{1/3}$-E plane.

II. THEORETICAL CONSIDERATIONS

In the Glauber high energy approximation the total cross-section is given by[2]

$$\sigma = 2\int(1 - \mathrm{Re}\, \exp(i\chi(\vec{b})))d\vec{b} \qquad (1)$$

where $\vec{b}$ is the impact parameter and $\chi(\vec{b})$ is the phase shift function.

$$\chi(\vec{b}) = -\frac{1}{\hbar v}\int_{-\infty}^{+\infty} V(\vec{b}+\vec{z})dz \qquad (2)$$

with V as the interaction potential. Eqs. (1) and (2) give a good account of total cross section provided $|E/V| \gg 1$, though the approximation is found to be valid at energies smaller than that given by this condition.

Franco[3] finds that if instead of using expression (2) for the phase shift function $\chi(\vec{b})$, one uses

$$\chi(\vec{b}) = \int_{-\infty}^{\infty}(K(\vec{b},z) - k)dz \, , \qquad (3)$$

where

$$K(\vec{b},z) = \sqrt{\left(\frac{2m}{\hbar^2}(E - V(\vec{b},z)\right)} \qquad (4)$$

the situation regarding the applicability of the Glauber theory to the relatively low energies improves. He uses this modified form of $\chi(\vec{b})$ to have a qualitative description of the appearance of of the giant resonances in the neutron total cross section with reasonable success.

Since our main aim in the present paper is to see how far the high energy approximation is able to describe the main features of the neutron total cross section σ as a function of $A^{1/3}$, we also use eqs.(3) and (1) according to which

$$\sigma = 2\pi R^2 + \frac{\pi}{\alpha^2}\left[1 - \cos 2\alpha R - 2\alpha R \sin 2\alpha R\right] \tag{5}$$

for a real square well potential, where $\alpha = K-k$ and R is the nuclear radius and

$$\sigma = \pi R^2\left[2 + \frac{(\lambda^2-\mu^2)}{(\lambda^2+\mu^2)^2} - \frac{e^{-2\mu}}{(\lambda^2+\mu^2)}\left\{\frac{(\lambda^2-\mu^2)\cos 2\lambda + 2\lambda\mu \sin 2\lambda}{(\lambda^2+\mu^2)} + 2\lambda \sin 2\lambda - 2\mu \cos 2\lambda\right\}\right] \tag{6}$$

for a complex square well potential with $(\lambda + i\mu) = (K-k)R$.

Differentiating eq. (5) with respect to R we obtain

$$\frac{\partial\sigma}{\partial R} = 4\pi R - 4\pi R \cos 2\alpha R \tag{7}$$

which gives $\frac{\partial\sigma}{\partial R} = 0$ at

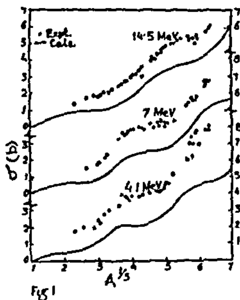
$$R = m\pi/\alpha \;, \quad m = 1, 2, 3 \ldots \tag{8}$$

Further differentiation shows that at $R = m\pi/\alpha$,

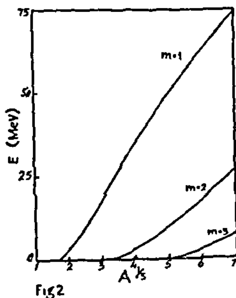
$\partial^2\sigma/\partial R^2 = 0$ and $\partial^3\sigma/\partial R^3 = 16 m\pi^2\alpha$ which shows that eq. (8) does not give an extremum point, rather a point of inflection. As discussed in next section, eq. (8) does actually describes the occurence of the plateau in σ when plotted as a function of $A^{1/3}$.

III. RESULTS AND DISCUSSION

In fig.1, the neutron total cross section given by eq. (6) is plotted as a function of $A^{1/3}$ with real and imaginary well depths (in MeV) as 46- .25 E and 0.125 E - .0004 E^2 respectively (as used by Fiedelday[4]) and R = 1.38 $A^{1/3}$ fm. It is seen that eq. (6) satisfactorily describes the qualitative features of the neutron total cross section even at an energy as low as 4.1 MeV. In particular the appearance of the plateau in the experimental data is well reproduced. The positions of the plateau predicted by eq. (8) being in good agreement with the ones observed experimentally. The loci of the plateau in $A^{1/3}$- E plane are given in fig.2, the plateau shifting to higher mass numbers with increasing energies. It is interesting to note that at very high energies (>75 MeV) no plateau should be observed. This seems to be



The neutron total cross section as a function of $A^{1/3}$.
Experimental data is taken from ref. 5).



Loci of the plateau in $A^{1/3}$–E plane.

confirmed by the high energy scattering data.

REFERENCES

1. K.S. Emmerich, Proc. International Conference on the Nuclear Optical Model, the Florida University, Tallahassee (1959) p.3
2. R.J. Glauber, Lectures in Theoretical Physics, (Interscience Publishers, Inc., New York, 1959), Vol. I, p. 315.
3. V.Franco, Phys. Rev. 140B, 1501 (1965).
4. C.A. Engelbrecht and H. Fiedeldey, Ann. Phys. 42, 262, (1967)
5. F.Perey and B.Buck, Nucl. Phys. 32, 353 (1962).

DISCUSSION

A.S. Divatia: Have you investigated the sensitivity of these results to the potential parameters?

A.N. Saharia: No. We have used only one value.

B.K. Jain: When one says that the Glauber theory is valid even at low energy, I don't think one means energ is like 10 - 20 MeV where you have applied it.

A.N. Saharia: We are interested only in the qualitativ behaviour of the total cross section when plotted as a function of $A^{1/3}$. As can be seen from the Fig.1. Glauber theory, with a modified form of the phase shift function does reproduce the qualitative aspects of the cross sections at these energies.

K. Srinivasa Rao: How is Glauber theory which is valid for high energies applicable to such low energies as $\sim$ 5 MeV? What is the validity?

A.N. Saharia: As has been discussed in ref.3, high energy approximation can be used at relatively low energies if one uses Eq.(3) for the phase shift func-

NEW ISOMERIC CROSS SECTION RATIOS IN NEUTRON CAPTURE REACTIONS

A. Lakshmana Rao, K. Parthasaradhi and J. Rama Rao
The Laboratories for Nuclear Research
Andhra University, Waltair, India.

I. Introduction

Studies on the isomer ratios in nuclear reactions have gained importance in recent years because of the valuable information they provide on the spin dependence of the nuclear level density. A survey of literature on neutron induced reaction shows that the work done at intermediate enenegies is comparitively less than at thermal or high energies. Hence a systematic study of the isomer ratios in neutron capture reactions at 24 keV has been taken up. The present paper reports some new experimental isomer ratios for (n,gamma) reactions at this energy leading to the isomeric pairs Ge-75m,g; Rb-86m,g; Pd-111m,g; Cd-117mg; Sb-122m,g; Eu-152m_1,m_2 and Pt-197m,g. The spin cut off factors are extracted for these cases using the Huizenga and Vandenbosch formalism(1-3) and are compared with the predictions(4,5) of the shifted Fermigas, Independent pairing and Super conductor models.

II. Experimental Details

An Sb-Be neutron source of strength 20C obtained from BARC Bombay was used to give neutrons of 25 ± 5 keV energy. Targets used were natural samples obtained in metalic powder or oxide form. These targets were put in thin perspex cylindrical tubes and were irradiated

at a height of 10 ft from the ground by remote control arrangement developed for the purpose. The activity produced was measured by absolute gamma counting technique using a calibrated 7F8 Harshaw crystal scintillation spectrometer and a 100 channel analyser. Symultaneously with the recording of gamma ray spectra, the half-live of the activity is also followed in a wide window single channel analyser-scaler-timer unit. This enables a unique identification of the reaction product. The neutron flux was determined by the secondary standard reaction $^{127}I(n,\gamma)^{128}I$ and the cross sections reported are relative to Iodine cross section which is taken to be 832 ± 26 mb. The spectroscopic data used in the calculations was taken largely from Nuclear Data Sheets and from other recent work in some cases. The cross sections for reactions leading to the isomer and ground states along with the isomer ratios (R) (R is defined in this paper as the ratio of the cross section for the high spin state to the total cross section) are given in Table 1.

III. Theoretical Analysis

In extracting the spin cut off factors using HV forlism the other parameters are fixed as follows. The level density parameter 'a' was calculated using the expression given by Abdelmalek and Stavinsky(6)

$$a = (0.095 \pm 0.007)\, A^{2/3}(\bar{J}_z + \bar{J}_n + 1)$$

where $\bar{J}_z$ and $\bar{J}_n$ are the average number of single particle levels for protons and neutrons respectively. The pairing energy values are taken from the smoothed out curves of

Table-I

S.No.	Reaction	$\sigma_{\text{High Spin}}$ in mb	$\sigma_{\text{Low Spin}}$ in mb	$R = \frac{\sigma_H}{\sigma_H + \sigma_L}$
1.	$^{74}Ge(n,\gamma)^{75m,g}Ge$	24.8±2	64.8±5	0.28±0.031
2.	$^{85}Rb(n,\gamma)^{86m,g}Rb$	35.1±2.8	334.5±28	0.1±0.011
3.	$^{110}Pd(n,\gamma)^{111m,g}Pd$	7.6±0.6	120±11	0.06±0.007
4.	$^{116}Cd(n,\gamma)^{117m,g}Cd$	18.2±1.5	61.2±4.8	0.23±0.025
5.	$^{121}Sb(n,\gamma)^{122m,g}Sb$	1.8±0.15	1062±82	0.002±0.0002
6.	$^{124}Sn(n,\gamma)^{125m,g}Sn$	69±5.6	42.1±3	0.62±0.07
7.	$^{151}Eu(n,\gamma)^{152m_1,m_2}Eu$	32.7±2.6	6586±510	0.005±0.0006
8.	$^{196}Pt(n,\gamma)^{197m,g}Pt$	12.6±1	42.2±3.3	0.23±0.025

Table-II

Target Isotope	σ_{exp}	$\sigma_{S.F.M.}$	$\sigma_{I.P.M}$	$\sigma_{S.C.M}$
$^{74}_{32}Ge_{42}$	2.2±0.2	4.0	2.9	3.3
$^{85}_{37}Rb_{48}$	2.4±0.1	4.7	3.3	3.9
$^{110}_{46}Pd_{64}$	5.2±1	4.9	3.4	3.7
$^{116}_{48}Cd_{68}$	4.9±1	4.8	3.3	3.5
$^{121}_{51}Sb_{70}$	1.9±0.02	5.7	3.9	5.0
$^{124}_{50}Sn_{74}$	> 8	5.1	3.6	3.8
$^{151}_{63}Eu_{88}$	2.0±0.03	6.1	4.1	4.9
$^{196}_{78}Pt_{118}$	6.5±1	7.2	4.9	5.2

Nemirovisky and Adamchuk[7]. In the treatement of the gamma cascade pure dipole emission was considered. The average number of gamma rays was calculated following Huizenga's treatment[3]. The computations are carried out using the CDC 3600 computer at TIFR. The experimental values of the spin cutt off factor, σ_{b}, are compared with the predictions of the shifted Fermi-gas model (S.F.M.), Independent pairing model (I.P.M.) and Super conductor model (S.C.M.) in Table II.

IV. Discussion

It may be noted from Table 2 that all the target nuclei investigated have an even neutron number. In targets where the proton number is also even, the capture of a neutron leads to an odd mass compound nucleus and for such cases there is good agreement between experimental and shifted Fermi-gas spin cut off factors. In the odd Z targets where the neutron capture leads to an odd compound nucleus it is observed that the experimental spin cut off factors agree better with the independent pairing model. The latter model is an improvement over the Fermi-gas model, by Ericson[8] and Lang and Lecouteur [9] taking into account the residual forces by simple form of pairing interaction. The spin cut off factors for these nuclei lead to reducedmoments of inertia compared to rigid body value, thereby indicating the relative importance of residual interactions in odd-odd nuclei.

- - -

V. References

1. J.R. Huizenga and R.Vandenbosch; Phys.Rev.120,1305 (1960).

2. R. Vandenbosch and J.R. Huizenga; Phys. Rev.120,1313 (1960).

3. H.K. Vonach, R. Vandenbosch and J.R. Huizenga;Nuc. Phys.60,70(1964)

4. R. Vandenbosch, L.Haskin and J.C. Norman; Phys. Rev.137,B1134(1965).

5. A. Lakshmana Rao, B.V. Thirumala Rao,P.Ramaprasad, and J. Rama Rao; Il Nuovo cimento 65B100(1970)

6. N.N. Abdelmalek and V.S. Stavinsky; Nuc.Phys.58,601 (1964)

7. P.E. Nemirovsky and Yu.V.Adamchuk; Nuc.Phys.39,551 (1962)

8. T. Ericson; Nuc.Phys.6,62(1958)

9 D.W. Lang and K.J. Lecouteur; Nuc.Phys.14,21(1959-60)

P-WAVE STRENGTH FUNCTIONS IN THE MASS REGION $140 < A < 160$.

B.V. Thirumala Rao, J. Rama Rao and E. Kondaiah*
Laboratories for Nuclear Research, Andhra University, Waltair.

I. INTRODUCTION

It is well known that the simple optical model of Feshbach, Porter and Weisskopf[1] could not explain the splittings of 2 p and 4 s giant resonances observed experimentally. Since 4 s resonance falls in the deformed region, Chase, Wilets and Edmonds[2,3] have explained the splitting in terms of strong, permanent deformations of the rare earth nuclei in this region. The splitting of the 3 p resonance near A ∽ 100 was attributed to spin-orbit interaction by Krueger and Margolis[4] who have shown that the resonance can be split by this mechanism for two to three times the normally accepted value. However, Buck and Pery[5] working on the idea of dynamical deformabilities for the nuclei in this region could reproduce the p-wave splitting on the pure quadrupole vibration model. Fiedeldey and Frahn[6] using a complex potential which is continuous and analytic with surface peaked absorption, have obtained closed expressions for s- and p- wave strength functions reproducing the same features of the strength functions. While a general agreement was noticed between the experimental and the various theoretical values of the strength functions on the crests of these resonances considerable discrepancies were observed in the valley

---

* Present Address: Tata Institute of Fundamental Research, Colaba, Bombay-5.

regions between the resonance peaks. For example in the mass region $140 < A < 160$, for p- wave strength function Fiedeldey and Frahn predict almost a constant strength function of value about 0.3×10^{-4} where as Buck and Pery calculations show structure in this region with the value of S_1 ranging between 1 and 2 ($\times 10^{-4}$). Previous experimental investigations in this region are rather scanty. In view of this the present work is under taken extracting the p-wave strength functions from average capture cross sections using 25 keV neutrons.

II. EXPERIMENTAL

The average neutron capture cross sections for the nuclei ^{146}Nd, ^{148}Nd, ^{150}Nd and ^{158}Gd in this region were determined at 25 keV using a 20 curie Sb-Be source and the activation technique. Gamma counting method was employed using a calibrated well type NaI(Tl) crystal and a 100 channel analyser. The p-wave strength functions for these isotopes are extracted from the average capture cross sections by the following method.

III. METHOD OF EXTRACTION OF P-WAVE STRENGTH FUNCTIONS

Since the present mass region $140 < A < 160$, corresponds to one of the crests of the 4 s resonance, there is good agreement between the experimental and theoretical s-wave strength functions. Taking advantage of this fact and making use of average resonance parameters for these isotopes in the keV region recently reported[7] at the Dubna conference the s-wave contributions were accurately

calculated and subtracted out from the average total cross sections to obtain the p-wave capture cross sections in these isotopes. It is found that these contributions are more than 50% in all cases, there by justifying the subtraction technique.

To extract the p-wave strength functions two assumptions are made. 1) The radiation width is assumed to be the same for s- and p- wave capture. 2) The average level spacing for p-waves is taken to be one-third of the s-wave level spacing. Using the formula developed by Bilpuch[8] for the partial cross sections

$$\sigma_c^{\,l} \simeq (2l+1)\,\frac{\pi}{2}\left(\frac{2.6\times10^{6}}{E_n}\right)\frac{\Gamma_{\gamma l}}{D_l}\left[1-\sqrt{b\pi}\;e^{b}\left\{1-\frac{2}{\sqrt{\pi}}\int_0^{\sqrt{b}}e^{-t^2}dt\right\}\right]$$

where $b = \dfrac{\Gamma_{\gamma l}}{2 v_l \Gamma^{\circ}_{nl}\sqrt{E_n}} \simeq \dfrac{\Gamma_{\gamma l}}{2 v_l \sqrt{E_n}\, S_l D_l}$

l is the angular momentum of the incident neutron, En is the energy of the incident neutron in ev, v_l is the penetration factor for the neutron of angular momentum l, and $\Gamma_{\gamma l}$, D_l and Γ°_{nl} are the experimentally measured radiation width, level spacing and reduced neutron width respectively; the p-wave strength function S_1 was obtained. These are compared with the theoretical predictions in Table I.

IV. RESULTS

It can be seen from the table that the experimentally derived p-wave strength functions fall in between the two theoretical predictions except for ^{158}Gd. It is

TABLE I

Isotope.	σ exp. (mb)	σ s-wave (mb)	σ p-wave (mb)	p-wave strength functions. $S_1 \times 10^4$		
				Exptl.	P.B.[5]	F.D.[6]
^{146}Nd	89±10	27	62	0.25±0.7	1.1	0.3
^{148}Nd	195±20	67	128	0.45±0.12	1.1	0.3
^{150}Nd	85±9	52	33	0.86±0.22	1.3	0.3
^{158}Gd	890±90	127	763	7.6±2	1.9	0.3

interesting to note that the present values show an increasing trend as predicted by Buck and Pery.

REFERENCES

1. H. Feshbech, L.E. Porter and V.F. Weisskopf; Phys. Rev, 96 (1954) 448.
2. B. Margolis and E.S. Troubetzky; Phys. Rev.106(1957) 105.
3. D.M. Chase, L. Wilets and A.R. Edmonds; Phys. Rev. 110 (1958) 1080.
4. T.K. Krueger and B. Margolis; Nuc. Phys.28 (1961)578.
5. B. Buck and Pery; Phys. Rev.Letters 8 (1962) 444.
6. H. Fiedeldey and W.E. Frahn; Ann.Phys.19 (1962) 428.
7. Proc. of the Dubna Conference USSR (1968) Article by L.B. Pikelner.
8. L.W. Weston, K.K. Seth, E.G. Bilpuch and H.W.Newson; Ann. Phys. 10 (1960) 455.

P-WAVE NEUTRON CAPTURE IN HEAVY NUCLEI AT 25 KEV

M. Sriramachandra Murty, K. Siddappa and J. Rama Rao
Laboratories For Nuclear Research
Andhra University, Waltair.

I. INTRODUCTION

While a number of experimental and theoretical papers have appeared in literature on the s-wave neutron capture and size resonances, relatively few investigations seem to have been carried out on the p-wave capture, particularly in heavy elements. The Optical model of Feshback, Požter and Weisskopf[1] predicted the 3p giant resonance of the neutron strength function around the mass number 216 which falls in the region of unstable nuclides. Even the more refined theories of Buck and Perey[2] and Fiedeldey and Frahn[3] have not appreciably changed the situation with regard to the 3p giant resonance. However, recent experimental measurements of Chaubey et al.[4] have indicated a peak around A=185 in the p-wave neutron capture cross-sections. It is felt that a systematic investigation on the p-wave neutron strength functions in the heavy nuclei would be interesting. As a part of this programme and to plug the gaps in the existing cross-section data at 25 keV, the average capture cross-sections for 13 isotopes have been measured using the activation method and absolute gamma counting technique. Using the low energy resonance parameters, wherever available, the s-wave contributions have been calculated and subtracted out from the experimental cross-sections to

obtain the p-wave contributions.

II. EXPERIMENTAL DETAILS

For the present work, a 20 curie Sb-Be neutron source was obtained from Bhabha Atomic Research Centre, Bombay, to give neutrons of energy 25 keV. The targets used were all either metal powders of oxides with purity greater than 99.9%. The samples were kept in thin cylindrical perspex tubes of diameter 13 mm and irradiated at a height of 10 feet from the ground in order to minimise scattering effects. A remote control arrangement was employed to operate the neutron source. A 7F8 Harshaw well-type crystal was used as a gamma detector. The effective photopeak and total efficiencies for the crystal for cylindrical sources placed in the well have been determined experimentally and used in the evaluation of the cross-sections. A 100 channel analyzer was used to record the gamma spectrum. The reaction $I^{127}(n,\gamma)I^{128}$ was used as a secondary standard for flux measurement, assuming its cross-section to be 836±26 mb.

III. METHOD

Using Breit and Wigner theory for nuclear resonances, E.G. Bilpuch[5] derived an expression for the capture cross-section as a sum of partial cross-sections for different l,

$$\sigma_c^{l} = (2l+1)\frac{\pi}{2}\frac{(2\cdot 6\times 10^{6})}{E_n}\frac{\Gamma_{\gamma l}}{D_l}\left[1-\sqrt{b\pi}\, e^{b}\left\{1-\frac{2}{\sqrt{\pi}}\int_0^{\sqrt{b}} e^{-t^2}dt\right\}\right]$$

where $b=\frac{\Gamma_{\gamma l}}{2\nu_l\Gamma_{nl}^{0}\sqrt{E_n}} = \frac{\Gamma_{\gamma l}}{2\nu_l\sqrt{E_n}\,S_l\,D_l}$

and l is the angular momentum of incident neutron, E_n is

the energy of the incident neutron expressed in ev and V_l is the penetration factor for the neutron of angular momentum l (taken equal to unity for l=0). The quantities D_l, Γ_n^l and $\Gamma_{\gamma l}$ are the experimentally measured average level spacing, reduced neutron width and radiation width respectively.

With the above expression, s-wave neutron contributions have been evaluated making ~~using~~ use of the low energy resonance parameters available in literature . The p-wave capture cross-sections have been obtained for these isotopes by subtracting the s-wave capture contributions from the experimentally measured total cross-sections. It is assumed that the contributions due to d-wave and higher partial waves are negligible at this energy.

IV. RESULTS AND DISCUSSION

The experimental cross-sections for the 13 reactions measured for the first time are reported in column 2 of table I. In cases where only the isomeric cross-section is measured or resonance parameters are not available, no attempt has been made to calculate the p-wave contribution. In rest of the cases, the s-wave and p-wave contributions are respectively shown in columns 3 and 4. It can be seen from the table that p-wave capture is quite predominant in heavy nuclei. The present results, although sketchy, seem to indicate a peak like structure in the p-wave cross-sections around A=168 similar to the one observed by Chaubey et al[4] around A=185. Systematic

investigations are in progress to extract the p-wave strength functions in this region to ascertain the nature of the observed peak.

TABLE I

Reaction	σ_{expt} (barns)	$\sigma_{s\text{-}wave}$ (barns)	$\sigma_{p\text{-}wave}$ (barns)
$^{74}Se(n,\gamma)Se^{75}$	2.383 ± 0.216	0.114	2.269
$^{84}Sr(n,\gamma)Sr^{85m}$	0.469 ± 0.047	.....	.....
$^{109}Ag(n,\gamma)Ag^{110m}$	0.015 ± 0.0015	.....	.....
$^{122}Te(n,\gamma)Te^{123m}$	0.177 ± 0.016	.....	.....
$^{159}Tb(n,\gamma)Tb^{160}$	6.243 ± 0.571	0.829	5.414
$^{168}Yb(n,\gamma)Yb^{169}$	48.97 ± 4.91	0.329	48.641
$^{174}Yb(n,\gamma)Yb^{175}$	2.403 ± 0.221	0.039	2.364
$^{176}Yb(n,\gamma)Yb^{177}$	0.107 ± 0.011	0.039	0.068
$^{169}Tm(n,\gamma)Tm^{170}$	2.202 ± 0.221	0.355	1.847
$^{178}Hf(n,\gamma)Hf^{179m}$	0.267 ± 0.025	.....	.....
$^{179}Hf(n,\gamma)Hf^{180m}$	0.013 ± 0.001	.....	.....
$^{191}Ir(n,\gamma)Ir^{192g}$	9.200 ± 0.911	1.082	8.118
$^{192}Os(n,\gamma)Os^{193}$	0.296 ± 0.027	.....	.....

REFERENCES

1. H. Feshbach, C.E. Porter and V.F. Weisskopf, Phys. Rev. 96, 448 (1954).

2. B. Buck and F. Perey, Phys. Rev. Letters 8, 444 (1962)

3. H. Fiedeldey and W.E. Frahn, Ann. Phys. (N.Y.) 19, 428 (1962).

4. A.K. Chaubey and M.L. Sehgal, Proceedings of the Nuclear Physics and Solid State Physics Symposium, 82, (1968).

5. E.G. Bilpuch, L.W. Weston and H.W. Newson, Ann. Phys., 10, 455 (1960).

STATISTICAL THEORY CALCULATIONS OF NEUTRON CAPTURE CROSS SECTIONS FROM 200 keV to 800 keV

H.V. Gupta, A.K. Chaubey and M.L. Sehgal
Department of Physics
Aligarh Muslim University, Aligarh, U.P.

ABSTRACT

Neutron capture cross sections have been calculated using statistical theory of nuclear reactions in the energy range from 200 keV to 800 keV for ^{75}As, ^{79}Br, ^{115}In and ^{197}Au. These calculated cross sections were compared with the experimental values of capture cross section to test the validity of statistical theory in the energy range 200 keV to 800 keV. Some excited states in these nuclei have more than one spin. It was tried from the calculations of neutron capture cross-section that which spin is more suitable.

STUDY OF P-WAVE NEUTRON STRENGTH FUNCTIONS

A.K. Chaubey and M.L. Sehgal
Department of Physics
Aligarh Muslim University, Aligarh, U.P.

ABSTRACT

P-wave neutron strength functions (Γ_n^1 /D) have been calculated using 24 keV neutron capture cross sections and low energy resonance parameters. These values of strength functions were compared with the previous reported values. Some interesting results have been obtained.

STATISTICAL THEORY CALCULATIONS OF NEUTRON CAPTURE CROSS SECTIONS AT 130 keV

J. Alam and A. Augusthy
Department of Physics
Aligarh Muslim University, Aligarh, U.P.

ABSTRACT

Neutron capture cross-sections have been calculated using statistical theory of nuclear reactions at 130 keV energy for a large number of cases. These calculated cross-sections are compared with the experimental values to obtain informations about the parameter ξ_{cal} ($= \frac{D}{2\pi \Gamma_\gamma}$). These values of ξ_{cal} are then compared with the known experimental values of ξ_{obs}, obtained from low energy resonance experiment to check the validity of the statistical theory.

14.8 MeV NEUTRON RADIATIVE CAPTURE CROSS SECTION

S.S. Hasan, R. Prasad and M.L. Sehgal
Department of Physics
Aligarh Muslim University, Aligarh, U.P.

ABSTRACT

Neutron radiative capture cross-sections have been measured for ^{103}Rh, ^{127}I and ^{175}Lu. Results of these measurements and those of earlier measurements have been used to check direct-semi-direct theory for radiative capture. A comparison of experimental and theoretical values reveals that for the nuclei near the closed neutron shell these agree well. However, for other nuclei only order of magnitudes agree. Shell effects in (n,γ) cross-sections at 14.8 MeV have also been observed.

LOWEST T = 3/2 STATE IN ^{33}Cl OBSERVED AS A RESONANCE IN ^{32}S(p,γ)^{33}Cl REACTION

M.A. Eswaran, M. Ismail and N.L. Ragoowansi
Nuclear Physics Division
Bhabha Atomic Research Centre, Trombay, Bombay-85

ABSTRACT

The yield of the reaction $^{32}S(p,\gamma)^{33}Cl$ near the lowest T = 3/2 state has been measured by counting the residual activity between bursts of a mechanically chopped beam. A natural target of Sb_2S_3 was employed and a Ge(Li) detector was used for counting the positron annihilation radiation from the decay of ^{33}Cl. The resonance was found to be at E_p = 3.371 ± 0.006 MeV in agreement with the elastic scattering experiments. By comparison of the thick target yield of this resonance with that of the resonance at E_p = 2.547 MeV the radiation width Γ_γ has been determined to be 0.56 ± 0.18 eV for this lowest T = 3/2 state. The branching of this state, is found to be ~ 90% to the $1/2^+$ first excited state in ^{33}Cl. This transition is likely to be from the analogue to the anti-analogue state and its radiation width corresponds to 0.22 Weisskopf unit.

A DOORWAY STATE OBSERVED AS A RESONANCE IN THE $^{35}Cl(p,p_0)^{35}Cl$ REACTION

S. K. Gupta, S. S. Kerekatte, S. Swami*, M. R. Dwarakanath, K. K. Sekharan** and A.S. Divatia
Bhabha Atomic Research Centre, Bombay-85.

I. INTRODUCTION

We have investigated the elastic proton scattering from the ^{35}Cl nucleus from $E_{p\ lab}$ = 2.380 MeV to 2.620 MeV. This reaction was studied to look for the isolated bound doorway states having a large coupling to the entrance channel. Doorway states were postulated to describe micoscopically, the mechanism of nuclear reactions. So far the isobaric analog states have been the only reported doorway states. The difficulties encountered in pinning down a doorway state of another type, experimentally and theoretically, are numerous. Once we concentrate our attention on the bound isolated doorway states with a large decay width to the entrance channel, the experimental identification becomes definite. Payne[1] has theoretically investigated the elastic scattering of neutrons from the single closed shell even-even nuclei. His calculations are approximate and are applicable to a very limited number of cases. The calculations for other cases are not actually available. The major difficulty in solving the doorway state problem theoretically is to deal with the complications of the nuclear

* Member of I.I.T., Powai, Bombay-76

** Now at the University of Kentucky, U.S.A.

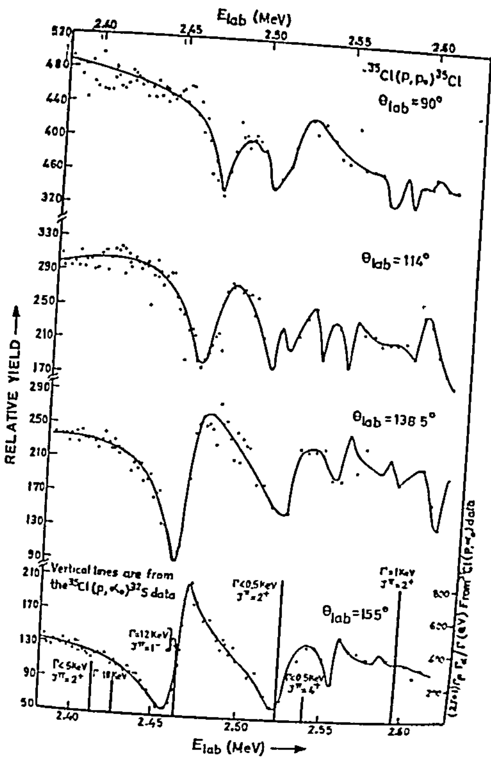
structure as well as the nuclear reaction calculations. Here we are describing briefly our results and an approximate comparison with the theoretical calculations.

II. EXPERIMENTAL METHOD AND RESULTS

The 5.5 MeV Van de Graaff accelerator was the source of protons. The targets were prepared using NaCl having ^{35}Cl enriched to 99.37% on carbon backings. The scattered particles were detected using four solid states detectors at lab. angles of 93°, 113.8°, 138.5° and 155°. The data was taken in 2 KeV steps. Bosnjakovic et al[2] have already investigated the $^{35}Cl(p,\alpha_0)^{32}S$ reaction in the same energy range. We show in Fig. 1 their results along with our data. A resonance at $E_{p\ lab}$ = 2.463 MeV with a width of 16 KeV appears only in the proton channel. As this resonance anomaly appears at all the four angles, it is consistent with an $l_p = 0$, $J^{\pi} = 2^+$ assignment. This assignment is not unique.

III. DISCUSSION

The calculations of Payne[1] reveal that the isolated bound doorway states should appear at an incident energy of 2-3 MeV with a typical width of 50 - 100 KeV in neutron elastic scattering. Taking into account the Coulomb effects, the width of the doorway state changes from 100 KeV to 15 KeV for $l_p = 0$ protons at E_p = 2.0 MeV. Glaudemans et al[3] have carried out bound state calculations within s-d shell using an empirically determined residual interaction. In the configuration space made up



E_lab (MeV)
$^{35}Cl(p,p_0)^{35}Cl$
θ_lab = 90°
θ_lab = 114°
θ_lab = 138.5°
θ_lab = 155°
RELATIVE YIELD
Vertical lines are from the $^{35}Cl(p,\alpha_0)^{32}S$ data
E_lab (MeV)

Fig. 1

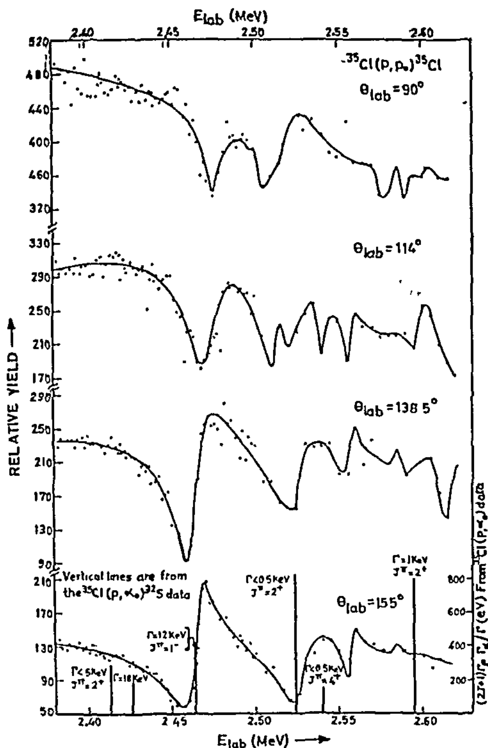
structure as well as the nuclear reaction calculations. Here we are describing briefly our results and an approximate comparison with the theoretical calculations.

II. EXPERIMENTAL METHOD AND RESULTS

The 5.5 MeV Van de Graaff accelerator was the source of protons. The targets were prepared using NaCl having ^{35}Cl enriched to 99.3[illegible]% on carbon backings. The scattered particles were detected using four solid states detectors at lab. angles of 93°, 113.8°, 138.5° and 155°. The data was taken in 2 KeV steps. Bosnjakovic et al[2] have already investigated the $^{35}Cl(p,\alpha_0)^{32}S$ reaction in the same energy range. We show in Fig.1 their results along with our data. A resonance at $E_{p\ lab} = 2.463$ MeV with a width of 16 KeV appears only in the proton channel. As this resonance anomaly appears at all the four angles, it is consistent with an $l_p = 0$, $J^{\pi} = 2^{+}$ assignment. This assignment is not unique.

III. DISCUSSION

The calculations of Payne[1] reveal that the isolated bound doorway states should appear at an incident energy of 2-3 MeV with a typical width of 50 - 100 KeV in neutron elastic scattering. Taking into account the Coulomb effects, the width of the doorway state changes from 100 KeV to 15 KeV for $l_p = 0$ protons at $E_p = 2.0$ MeV. Glaudemans et al[3] have carried out bound state calculations within s-d shell using an empirically determined residual interaction. In the configuration space made up



Elab (MeV)
RELATIVE YIELD
^{35}Cl(p,p$_o$)^{35}Cl
θlab=90°
θlab=114°
θlab=138 5°
θlab=155°
Vertical lines are from the ^{35}Cl(p,α$_o$)^{32}S data
Elab (MeV)

Fig. 1

of $s_{1/2}$ and $d_{3/2}$ subshells, the doorway states can have only $(s_{1/2})^3 (d_{3/2})^5$ or $(s_{1/2})^4 (d_{3/2})^4$ configurations. Glaudemans et al find a level at an excitation of 10.5 MeV with $J^{\pi} = 2^+$, $T = 0$ in ^{36}Ar with a 67% $(s_{1/2})^3(d_{3/2})^5$ and a 11% $(s_{1/2})^4 (d_{3/2})^4$ configuration. The resonance observed by us corresponds to a state in ^{36}Ar at 10.901 ± .005 MeV with a c.m. width of 15 KeV. Thus our observations are consistent with the expected behaviour of the doorway states as calculated by Payne as well as the shell model calculations for bound states which will not differ substantially for the unbound states. Further work is in progress on this problem.

REFERENCES

1. G.L. Payne, Phys. Rev. 174, 1227(1968)

2. B. Bosnjakovic, J. Bouwmeester, J. A. Van Best and H. S. Pruys, Nucl. Phys. A114,7 (1968).

3. P.W. Glaudemans, G. Wiechers and P.J. Brussard,Nucl. Phys. 56, 529(1964); 56, 548(1964).

DISCUSSION

B.K. Jain: The 10.5 MeV state in Glaudemans' work is a bound state while the state you observe is not a bound state. Therefore, just because these two energy positions agree, how much are you justified in identifying them with each other. In Glaudemans' picture the configuration of a unbound state at 10.5 MeV may be quite different from that of bound state at that energy.

S.K. Gupta: There will be a level shift in the observed resonance corresponding to the doorway state and this shift will be not very large. Anyway, the present comparison is only a tentative one.

M. Balakrishnan: What is the average value of compound nucleus resonance width and their level spacing known from other experiments, if any?

S.K. Gupta: The (p, α_0) data shows six states, each with a width $\sim$ 1 keV in 200 keV range of the excitation function. This is the experimental data available and should be taken as it is. The reason for the smaller value of $\langle\Gamma\rangle/\langle D\rangle$ may be due to the even-even compound nucleus.

M. Balakrishnan: A $\langle\Gamma\rangle/\langle D\rangle$ value of 1/50 seems small in the region of 10 MeV excitation, when we compare with similar quantity for the nearby elements.

A STUDY OF THE $^{64}Ni(p,n)^{64}Cu$ REACTION

S. S. Kerekatte, S. K. Gupta and A. S. Divatia
Nuclear Physics Division
Bhabha Atomic Research Centre, Bombay-85

I. INTRODUCTION

The (p,n) reaction on a ^{64}Ni target, was investigated to identify the isobaric analog resonances in the nucleus ^{65}Cu, corresponding to the parent nucleus ^{65}Ni. Recently, this reaction has also been studied by the Duke Group[1] from $E_p = 2.5 - 3.3$ MeV. In the energy range $E_p = 2.5 - 5.5$ MeV scanned by us, strong resonances have been observed which are superimposed upon the Ericson type statistical fluctuations.

II. EXPERIMENTAL METHOD AND MEASUREMENTS

A metallic ^{64}Ni target (enriched to 97.92%) was prepared by evaporating ^{64}Ni metal from a heated tungsten ribbon on to a tantalum backing foil. A 4π - geometry neutron counter was used to measure the yield of the reaction. The absolute cross-section has not been extracted. The relative cross-section is accurate to within $\pm$ 5%. The measured excitation function is shown in Fig.1.

III. DISCUSSION

The threshold of the reaction has been observed at $E_p = 2.500 \pm .005$ MeV. The average cross-section gradually increases with the incident proton energy due to the increase in the penetrability factor. The cross-section shows fluctuations. The average width of the compound

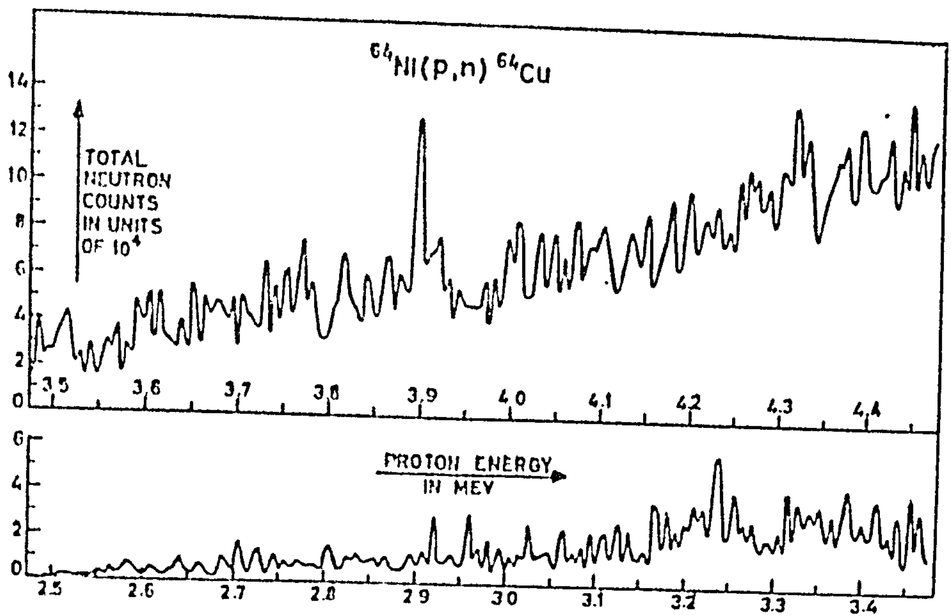


Figure 1(a):Total neutron yield in the $^{64}Ni(p,n)^{64}Cu$ reaction for incident proton energies between 2.5 and 4.475 MeV.

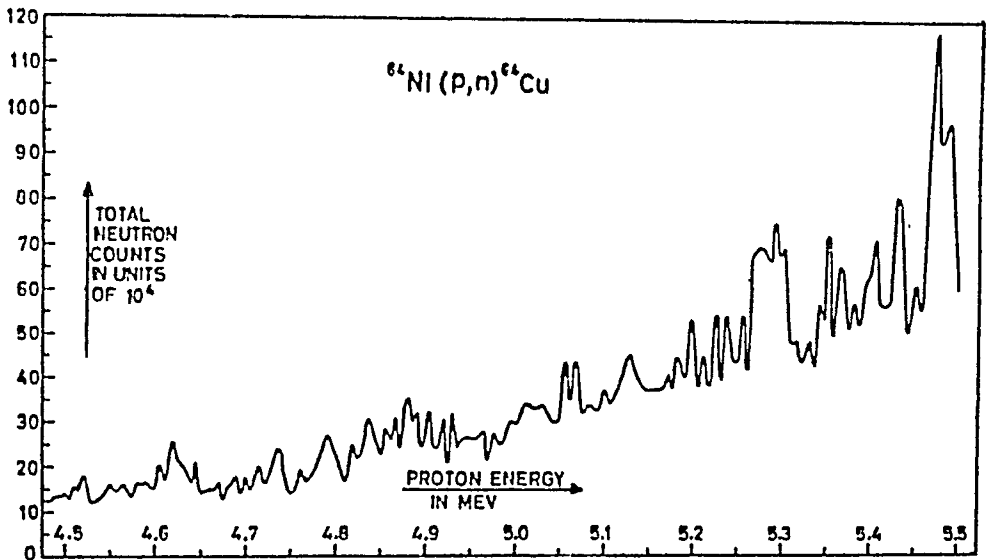


Figure 1(b):Total neutron yield in the $^{64}Ni(p,n)^{64}Cu$ reaction for incident proton energies between 4.475 and 5.5 MeV.

nuclear levels is calculated to be $\sim 7 \pm 1.5$ KeV, using the peak counting method(2) and has been approximately corrected for the experimental resolution.

The g.s. analog of ^{65}Ni cannot be observed because it is due to $l_p = 3$. The Duke group observed the analog of the first excited state at $E_p = 3.217$ MeV. Accordingly, the other analog resonances are expected at $E_{p,lab} = 3.471$, 3.861, 4.188, 4.502, 4.591, 4.779, 4.958, 5.100 and 5.338 MeV. Out of these, on the basis of the spectroscopic factor for the parent states observed through the $^{64}Ni(d,p)^{65}Ni$ reaction(3) and the penetration factor criterion, the resonances at 3.861, 4.591, 4.779 and 5.338 MeV are strong. Experimentally, we observe strong resonances at $E_{p,lab} = 3.895$, 4.620 and 4.790 MeV, corresponding to the expected resonances. Strong resonances are observed at $E_{p,lab} = 3.235$, 4.310 and 5.470 MeV which do not correspond to the known levels in ^{65}Ni. The resonance at $E_p = 3.895$ MeV is having the asymmetry predicted by Robson et al(4) in the (p,n) reactions.

A more detailed analysis of the data is in progress.

REFERENCES

1. J.C. Browne, H.W. Newson, E.G. Bilpuch and G.E. Mitchell, Nucl.Phys. A153,481 (1970).

2. A.Van der Woude, Nucl.Phys. 80,14(1966).

3. R.H. Fulmer and A.L. McCarthy, Phys.Rev.131,2133(1963).

4. D. Robson, J.D. Fox, P. Richard and C.P. Moore, Phys. Letters, 18,86(1965).

DISCUSSION

D.K. Sood: What was the criterian for assignment of isobar analogue states to some selected resonances?.

S.S. Kerekatte: The criteria were the spectroscopic factor obtained from (d,p) data and the penetrability factor and also the ℓ values. The assignments will be confirmed by detailed analysis later and also by doing the ^{64}Ni(p,p) scattering experiments.

S. Ramamurty: How is it that isobaric analogue states of only the 3rd and the 6th excited states of ^{65}Ni are observed in ^{65}Cu (and not for other states of ^{65}Ni)?

S.S. Kerekatte: The others may not be expected on the basis of the spectroscopic factor and penetration factor criteria.

EVIDENCE FOR DOORWAY STATES IN $^{29}Si(\alpha,n)^{32}S$ REACTION

M. Balakrishnan, M. K. Mehta and A. S. Divatia
Nuclear Physics Division
Bhabha Atomic Research Centre, Bombay-85

I. INTRODUCTION

According to Feshbach et.al(1) doorway states will be most readily observable if the number of open channels which are detected experimentally is small, so that total cross-section in a neutron induced reaction is least sensitive to the presence of doorway states. Hence the most suitable case for detection of a doorway state is in the crosse-section measurements for light nuclei at low energies, wherein the spreading width $\Gamma_d \downarrow$ can be relatively small. From this point of view the reaction $^{28}Si(\alpha,n)^{32}S$ seems appropriate.

II. EXPERIMENTAL

Fig.1 shows the experimental data, the details for which are given elsewhere(2). There is good agreement between the two separate sets of data.

III. RESULTS

An examination of data shows following details.
a) Resonances are about 10 KeV wide, and $\langle\Gamma\rangle/\langle D\rangle 0.3$ for the region of excitation around 10 MeV in ^{33}S. This is in agreement with the widths and $\langle\Gamma\rangle/\langle D\rangle$ ratio known for ^{33}S in this region(3,4). (b) There is an indication for the presence of gross structures, superposing the finer variations in cross-sections with energy. (c) The

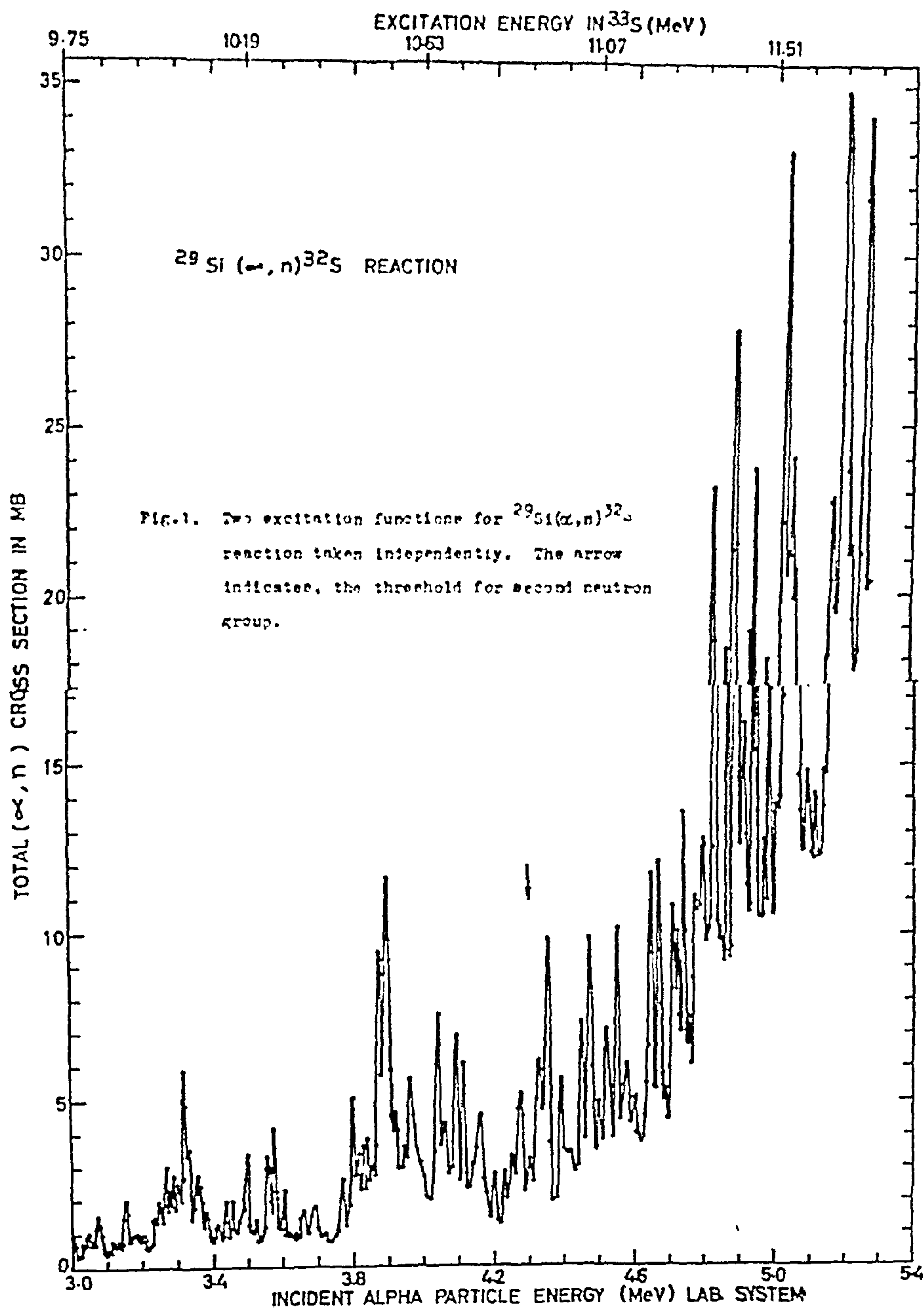


Fig.1. Two excitation functions for ^{29}Si(α,n)^{32}S reaction taken independently. The arrow indicates the threshold for second neutron group.

gross structures are not distributed at random, but there is a regularity in the distribution of widths and energy spacings of these structures. (d) The cross sections shows more intense peaks within each of these broad structures than in between them.

The excitation function averaged over 100 KeV are shown in Fig.2, where structures of width around 270 KeV with spacing of 500 KeV are present. From observation (a), it can be seen that we are not in the region of excitation where Ericson fluctuations[5] are valid. This is also supported by the fact that (n,α) and (n,p) correlation exists[6] in ^{32}S-and that compound nucleus cross - sections are not damped. Hence accidental lumping of resonance states as discussed by Singh et al.[7], wherein spurious "intermediate" like structures are built up, can be ruled out. For the region of excitation where $\langle\Gamma\rangle/\langle D\rangle$ is not too large and correlation exists between various entrance or exit channels, the structures have been qualitatively explained as due to statistical fluctuations in the average level densities of the compound nuclei involved[8]. From the observations (b) and (c) above, it is improbable that such an explanation can account for these structures.

A more realistic possibility is to explain these structures as due to simple modes of excitation of the compound nucleus. The reduced alpha width, for the single particle Wigner limit $\theta^2 = 3\hbar^2/2MR^2$ is 430 KeV which is twice as great as the observed width 270 KeV. Doorway

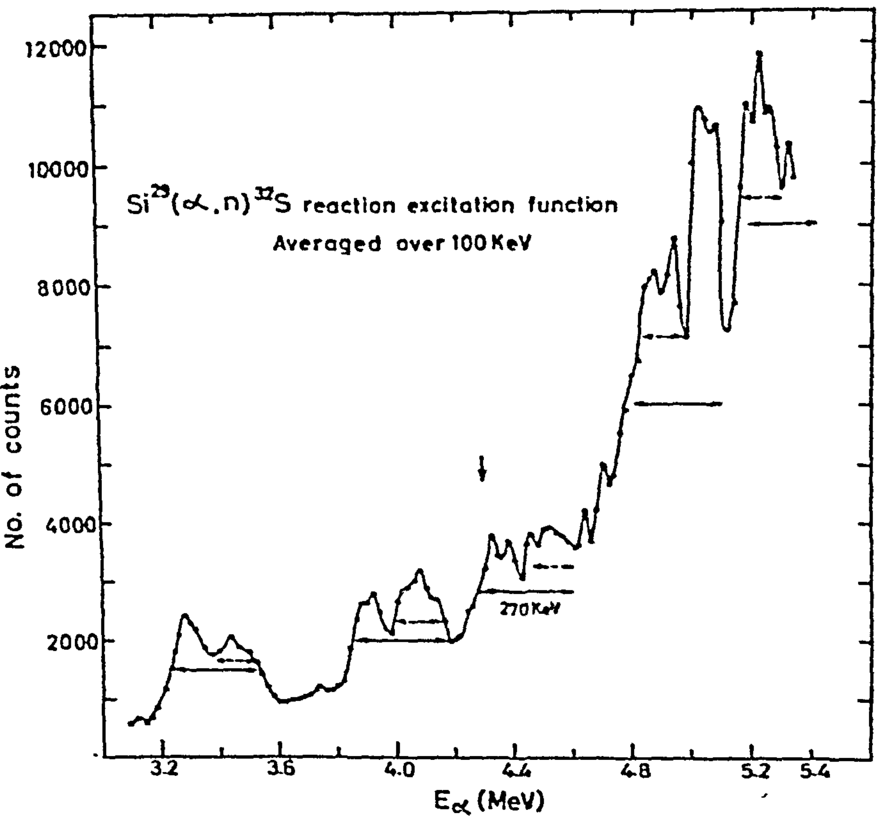


FIG.2

rne excitation function averaged over 100 KeV, showing the presence of broader structures.

states described as three quasi-particle states can account for a width of about 200 to 250 KeV for nuclei in this mass region[1]. Shakin[9], Lande and Block[10] estimated that the number of three quasi-particle states that can occur per MeV energy spread is around three, in this region of excitation for medium heavy nuclei. This is consistent with the separation of 500 KeV observed for light nuclei as in the present experiment. Since each three quasi-particle states should be characterised by a unique angular momentum, it will be quite interesting to see the differential cross-sections for these structures, to check whether a unique angular momentum can be attributed to each of them. The expected spreading of the doorway states over many compound nuclear states (observation (d)) may make it more difficult to observe this.

<u>REFERENCES</u>

1. H. Feshbach, A.K. Kerman and R.H. Lemmer; Ann. Phys. (N.Y.) <u>41</u>, 230 (1967)

2. M. Balkrishnan, K. K. Sekharan, M. K. Mehta and A. S. Divatia; Proceedings of Nucl. Phys. & Solid State Phys. Symp., December 1968, p.57.

3. P.M. Endt and C. Van der Leun; Nucl.Phys.<u>A105</u>,216(1967)

4. A.D. Carlson and H.H. Barschall; Phys. Rev.<u>158</u>,1142(1967)

5.i)T. Ericson; Phys. Rev.Lett. <u>5</u>,430 (1960)

ii)T.Ericson; Ann. Phys. (N.Y.) <u>23</u>,390 (1963)

6. A. Agodi, G. Pappalardo, R. Ricamo and D. Vinciguerra; Nuovo Cimento <u>23</u>, 1136 (1962)

7. P.P. Singh, P. Hoffman-Pinther and D.W. Lang; Phys.Lett. <u>23</u>, 255 (1966)

8.i)G. Calvi, R. Ricamo, A. Rubbino and D. Zubke; Nucl.Phys. Nucl.Phys. <u>48</u>,408 (1963)

ii)A. Agodi and G. Pappalardo; Nucl.Phys.<u>47</u>,129(1963)

9) C. Shakin; Ann.Phys. (N.Y.) 22,373 (1963).

10) A. Lande and B. Block; Phys. Rev.Lett.12,334(1964).

ISOBARIC ANALOGUE STATES IN ^{67}Ga

M.G. Betigeri, C.M. Lamba, D.K. Sood, N. Sarma and N.S. Thampi
Bhabha Atomic Research Centre, Bombay - 85

In this work the observation and study of the isobaric analogue states of ^{67}Zn in the compound nucleus ^{67}Ga which is formed by the proton bombardment on ^{66}Zn is reported.

Excitation functions at three angles θ_{cm} = 90°, 125° and 165° were measured in the incident protons energy range of 2.9 to 3.9 MeV. A thin target of ^{66}Zn (enriched to ~ 90%) evaporated on thin carbon backing (~ 10 μg/cm) was bombarded with protons from 5.5 MeV Van de Graaff accelerator at the Bhabha Atomic Research Centre. The error on the measurement is 2% including the statistical error.

At high excitation energies in medium weight nuclei the level width is much larger than spacing. On this background of compound nucleus states of isospin $T_<$ the analogue state with isospin $T_>$ stands out as an anomaly in the cross section. Interference also occures between potential and resonant scattering. These anomalies have been observed in ^{67}Ga which are analogues of 93, 184, 390, 978 and 1142 keV levels in ^{67}Zn. The states analogues to the ground and 602 keV states could not be observed because of high ℓ values involved. The resonances have been fitted with the program BRIGIT as modified for the CDC-3600 computer[1]. Values for the resonances energy

9) O. Shakin; Ann.Phys. (N.Y.) 22,373 (1963).
10) A. Lando and B. Block; Phys. Rev.Lett.12,334(1964).

ISOBARIC ANALOGUE STATES IN ^{67}Ga

M.G. Betigeri, C.M.Lamba, D.K. Sood, N.Sarma and N.S.Thampi
Bhabha Atomic Research Centre, Bombay - 85

In this work the observation and study of the isobaric analogue states of ^{67}Zn in the compound nucleus ^{67}Ga which is formed by the proton bombardment on ^{66}Zn is reported.

Excitation functions at three angles θ_{cm}= 90°,125° and 165° were measured in the incident protons energy range of 2.9 to 3.9 MeV. A thin target of ^{66}Zn (enriched to ~ 90%) evaporated on thin carbon backing (~ 10 μg/cm) was bombarded with protons from 5.5 MeV Van de Graaff accelerator at the Bhabha Atomic Research Centre. The error on the measurement is 2% including the statistical error.

At high excitation energies in medium weight nuclei the level width is much larger than spacing. On this background of compound nucleus states of isospin $T_<$ the analogue state with isospin $T_>$ stands out as an anomaly in the cross section. Interference also occures between potential and resonant scattering. These anomalies have been observed in ^{67}Ga which are analogues of 93, 184, 390, 978 and 1142 keV levels in ^{67}Zn. The states analogues to the ground and 602 keV states could not be observed because of high ℓ values involved. The resonances have been fitted with the program BRIGIT as modified for the CDC-3600 computer[1]. Values for the resonances energy

total width and partial widths are obtained. The results are shown in Table 1.

Table 1

Energies of levels in ^{67}Zn keV	Previous assignments J^{π}	Γ keV	Γ_p	Present assignments l	J
184	$3/2^-$	3.62	0.04	1	$3/2^-$
978	$5/2^+$	10.54	0.34	1	$1/2^-$
		No unique fit		2	$5/2^+$
1142	$1/2^-$	14.10	0.75	1	$1/2^-$

The ℓ and j values for the various resonances agree with the results obtained from (d,p) reaction data except for the 978 keV level. The present experiment suggests a value of l = 1 for this resonance. No unique fitting can be obtained for this level for ℓ = 2 assignment.

REFERENCE

1. M.G. Betigeri, C.M. Lamba, N. Sarma, D.K. Sood and N.S. Thampi, Nucl. Phys A133(1969)465.

FRAGMENT ANGULAR DISTRIBUTIONS IN THE 14 MeV NEUTRON INDUCED FISSION OF Th^{232}, U^{233}, U^{235}, U^{238}, Np^{237}, Pu^{239} AND Am^{241} USING SOLID-STATE TRACK DETECTORS

by

R.H. Iyer and M.L. Sagu,
Radiochemistry Division,
Bhabha Atomic Research Centre,
Trombay, Bombay-85.

I. INTRODUCTION

The first ever attempt to observe angular distribution of fission fragments was made by Halpern and Winhold[1], who studied the photofission of Th^{232} induced by 16 MeV x-rays. Since then, several studies in fission fragments angular distribution have been made by several authors using a variety of targets, and projectiles and over a wide range of energies[2]. Most of the measurements involve experimental set ups employing fission chambers or solid-state counters coupled with elaborate electronic circuitry, and occasionally radiochemical techniques[3]. Very recently solid-state track detectors have been used[4] for these measurements.

Brolley and Dickinson[5-7] studied the angular distribution of Th^{232}, U^{233}, U^{235}, U^{238} and Np^{237} induced by thermal and 14 MeV neutrons. They have also found that the anistropy $W(0°)/W(90°)$, varies with neutron energy[8].

Since angular distributions of fission fragments are very much tied up with many properties such as spin, orbital angular momentum, fissionability, etc. of the compound nucleus, these studies particularly those involving near threshold excitation energy, can give valuable information about the nucleus at a crucial stage (transition state) of the fission process.

One of the aims of the present paper is to report the results of a study of the angular distribution of fission fragments of Th^{232}, U^{233}, U^{235}, U^{238}, Np^{237}, Pu^{239} and Am^{241} induced by 14 MeV neutrons and to compare them with other published data. The merit of the present work is its simplicity using Lexan solid-state

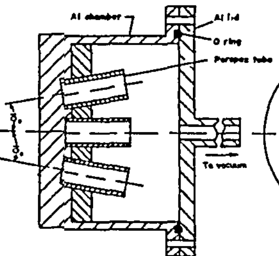
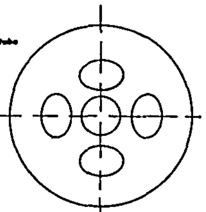
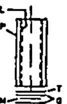


Fig-1(a) RECOIL CHAMBER



The locations of perspex tubes in Al chamber



L - Lucon detector
P Perspex tube (10mm I.D)
T - Target
G - Al. Gaurd
M - Al neutron monitor

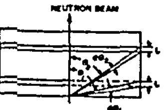


Fig-1(b)

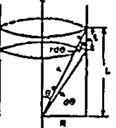
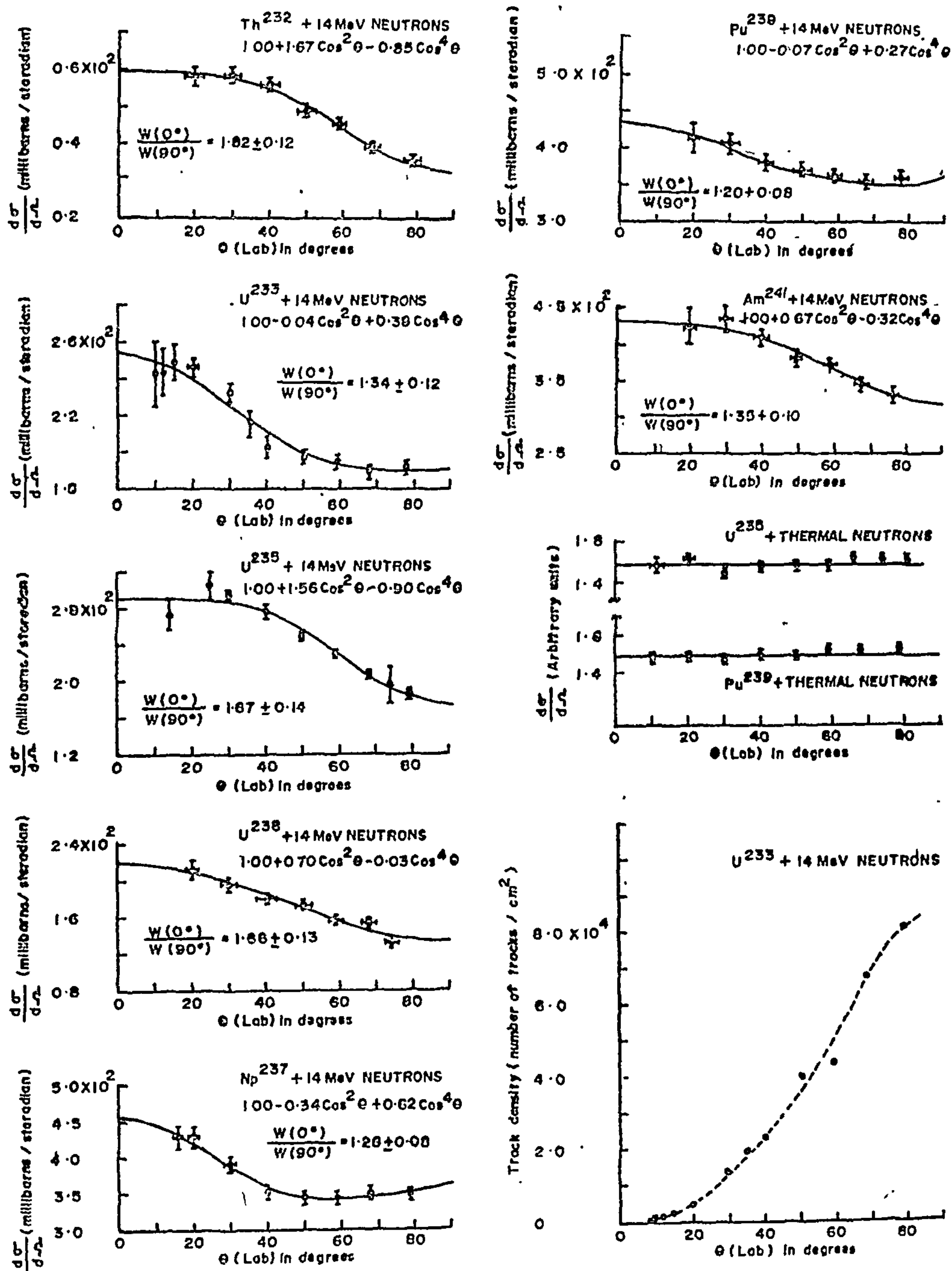


Fig-1(c)


FIGURE - 2
FISSION FRAGMENT ANGULAR DISTRIBUTION USING SOLID-STATE TRACK DETECTORS
Least squares fit A + B Cos²θ + C Cos⁴θ
(A is normalised to unity)
Experimental data
Th232 + 14 MeV NEUTRONS
1·00+1·67 Cos²θ - 0·85 Cos⁴θ
W(0°)/W(90°) = 1·82±0·12
Pu239 + 14 MeV NEUTRONS
1·00-0·07 Cos²θ + 0·27 Cos⁴θ
W(0°)/W(90°) = 1·20+0·08
U233 + 14 MeV NEUTRONS
1·00-0·04 Cos²θ + 0·39 Cos⁴θ
W(0°)/W(90°) = 1·34 ± 0·12
Am241 + 14 MeV NEUTRONS
1·00+0·67 Cos²θ - 0·32 Cos⁴θ
W(0°)/W(90°) = 1·35+0·10
U235 + 14 MeV NEUTRONS
1·00+1·56 Cos²θ - 0·90 Cos⁴θ
W(0°)/W(90°) = 1·67 ± 0·14
U235 + THERMAL NEUTRONS
Pu239 + THERMAL NEUTRONS
(Arbitrary units)
U238 + 14 MeV NEUTRONS
1·00+0·70 Cos²θ - 0·03 Cos⁴θ
W(0°)/W(90°) = 1·66±0·13
Np237 + 14 MeV NEUTRONS
1·00-0·34 Cos²θ + 0·62 Cos⁴θ
W(0°)/W(90°) = 1·26±0·08
U233 + 14 MeV NEUTRONS
Track density (number of tracks / cm²)
dσ/dΩ (millibarns / steradian)
θ (Lab) in degrees

The measured angular distributions were normalised to the total fission cross section by the relation

$$W(\theta_i) = \frac{\left(\frac{d\sigma}{d\Omega}\right)_{\theta_i} \cdot \sigma_{f_{total}}}{\sum_{1}^{n}\left(\frac{d\sigma}{d\Omega}\right)_{\theta_n}} \qquad \ldots\ldots\ldots \quad (2)$$

where $\left(\frac{d\sigma}{d\Omega}\right)_{\theta}$ the differential cross section at the lab angle θ, in terms of the number of tracks per unit solid angle. $\sigma_{f_{total}}$ were taken from our previous work(9). The experimental angular distributions, $W(\theta)$ were thus converted into millibarns per steradian and are plotted in Figure 2. The working of experimental set up and the method was tested for thermal fission of U^{235} and Pu^{239} both of which gave isotropic distributions (see Figure 2).

From a least squares fit of the experimental points with the expression of the form $W(\theta) = A + B \cos^2\theta + C \cos^4\theta$, the anisotropies, $W(0°)/W(90°)$ were calculated. The fitted curves are also shown in Figure 2. The calculated anisotropies are listed in Table I, other reported values are also included in the table. It is seen that the results of these experiments agree well with other reported data. The effect of target thickness on the shape of the angular distribution and on the anisotropy was looked into by measuring the angular distribution of fragments from a thin U^{235} source ($\sim$100 $\mu g/cm^2$) and comparing that with the 1.7 mg/cm^2 source (120 μg). It was found that both the shape and anisotropy depended on the target thickness. Using the thin source $W(0°)/W(90°)$ was found to be 1.37 (Table I) in close agreement with other reported values. A similar observation has been made by Brolley et al(5). In the present geometry, the intensity of fragments emitted in a direction normal to the beam will be reduced by absorption and scattering effects due to the increased target thickness as compared to those emitted along the beam. This apparent reduction in intensity along 90° gives rise to an increase in anisotropy.

As expected, systematic decrease in anisotropy with increase in $(Z^2/A)_{C.N}$ (increase in fissionability) is observed(10). This is illustrated in Figure 3.

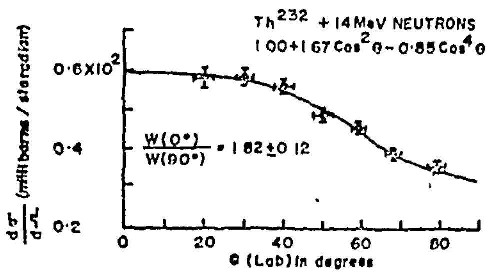
Interpretation of the results at higher excitation energies is complicated because more than one nucleus can undergo fission

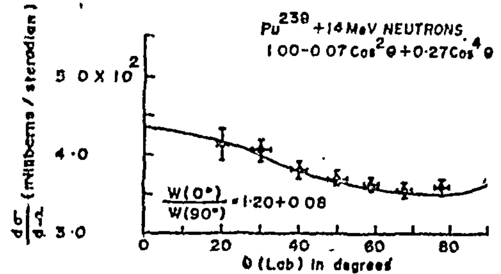
FIGURE - 2

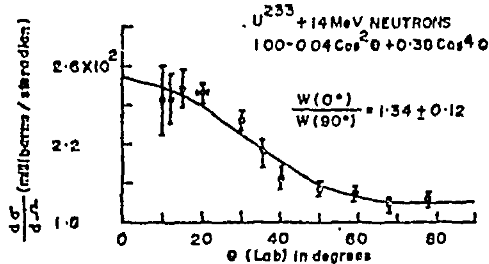
FISSION FRAGMENT ANGULAR DISTRIBUTION USING SOLID-STATE TRACK DETECTORS

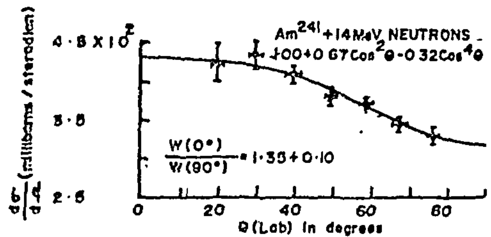
—— Least squares fit $A + B\cos^2\theta + C\cos^4\theta$ (A is normalised to unity)

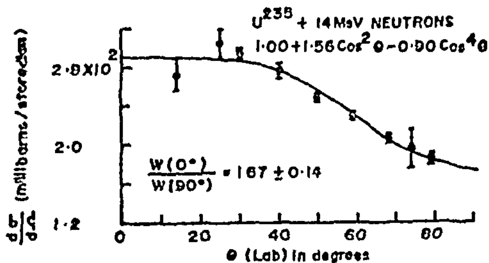
Experimental data

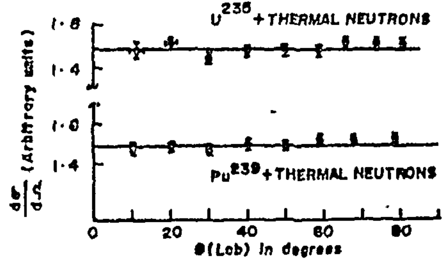


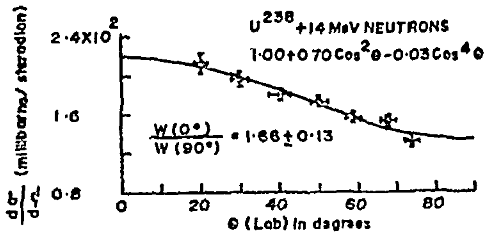


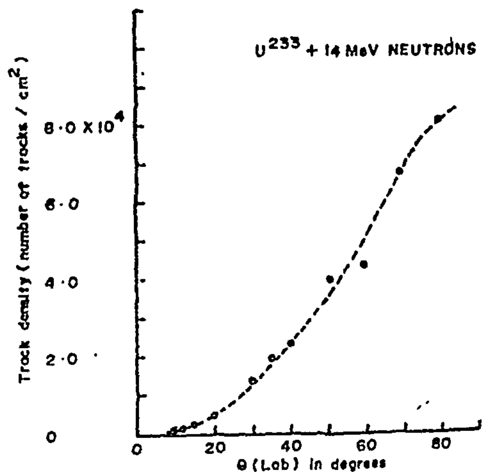


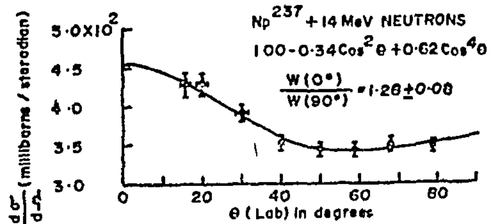












The measured angular distributions were normalised to the total fission cross section by the relation

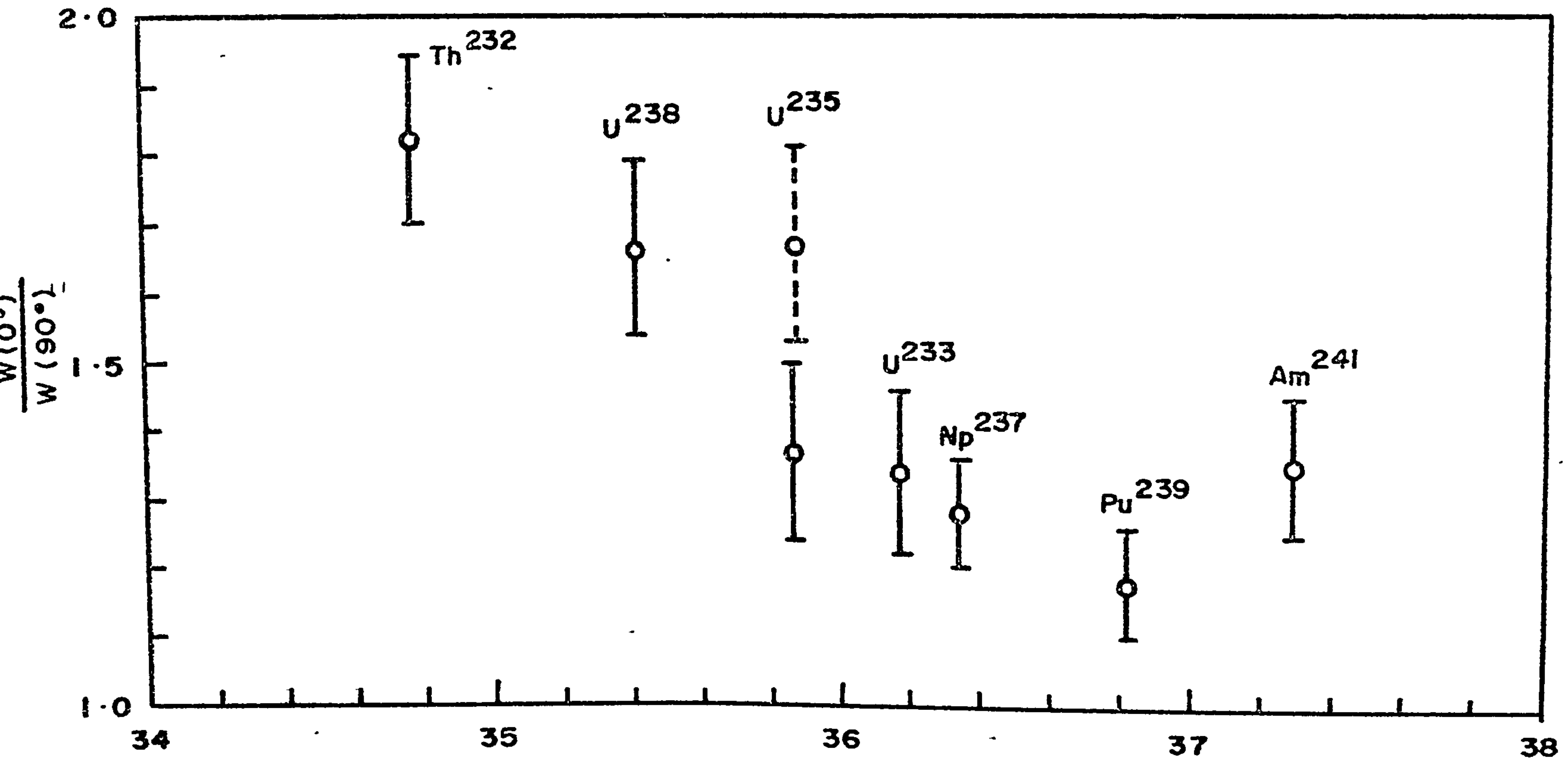
$$W(\theta_i) = \frac{\left(\frac{d\sigma}{d\Omega}\right)_{\theta_i} \cdot \sigma_{f\,total}}{\sum_i^n \left(\frac{d\sigma}{d\Omega}\right)_{\theta_n}} \qquad \ldots\ldots\ (2)$$

where $\left(\frac{d\sigma}{d\Omega}\right)_{\theta}$, the differential cross section at the lab angle θ, in terms of the number of tracks per unit solid angle. $\sigma_{f\,total}$ were taken from our previous work[9]. The experimental angular distributions, $W(\theta)$ were thus converted into millibarns per steradian and are plotted in Figure 2. The working of experimental set up and the method was tested for thermal fission of U^{235} and Pu^{239} both of which gave isotropic distributions (see Figure 2).

From a least squares fit of the experimental points with the expression of the form $W(\theta) = A + B\cos^2\theta + C\cos^4\theta$, the anisotropies, $W(0°)/W(90°)$ were calculated. The fitted curves are also shown in Figure 2. The calculated anisotropies are listed in Table I, other reported values are also included in the table. It is seen that the results of these experiments agree well with other reported data. The effect of target thickness on the shape of the angular distribution and on the anisotropy was looked into by measuring the angular distribution of fragments from a thin U^{235} source ($\sim 100\ \mu g/cm^2$) and comparing that with the 1.7 mg/cm^2 source (120 μg). It was found that both the shape and anisotropy depended on the target thickness. Using the thin source $W(0°)/W(90°)$ was found to be 1.37 (Table I) in close agreement with other reported values. A similar observation has been made by Brolley et al[5]. In the present geometry, the intensity of fragments emitted in a direction normal to the beam will be reduced by absorption and scattering effects due to the increased target thickness as compared to those emitted along the beam. This apparent reduction in intensity along 90° gives rise to an increase in anisotropy.

As expected, systematic decrease in anisotropy with increase in $(Z^2/A)_{C.N}$ (increase in fissionability) is observed[10]. This is illustrated in Figure 3.

Interpretation of the results at higher excitation energies is complicated because more than one nucleus can undergo fission making



2·0
1·5
1·0
W(0°)/W(90°)
34
35
36
37
38
Th232
U238
U235
U233
Np237
Pu239
Am241
(Z2/A) compound nucleus

FIGURE - 3

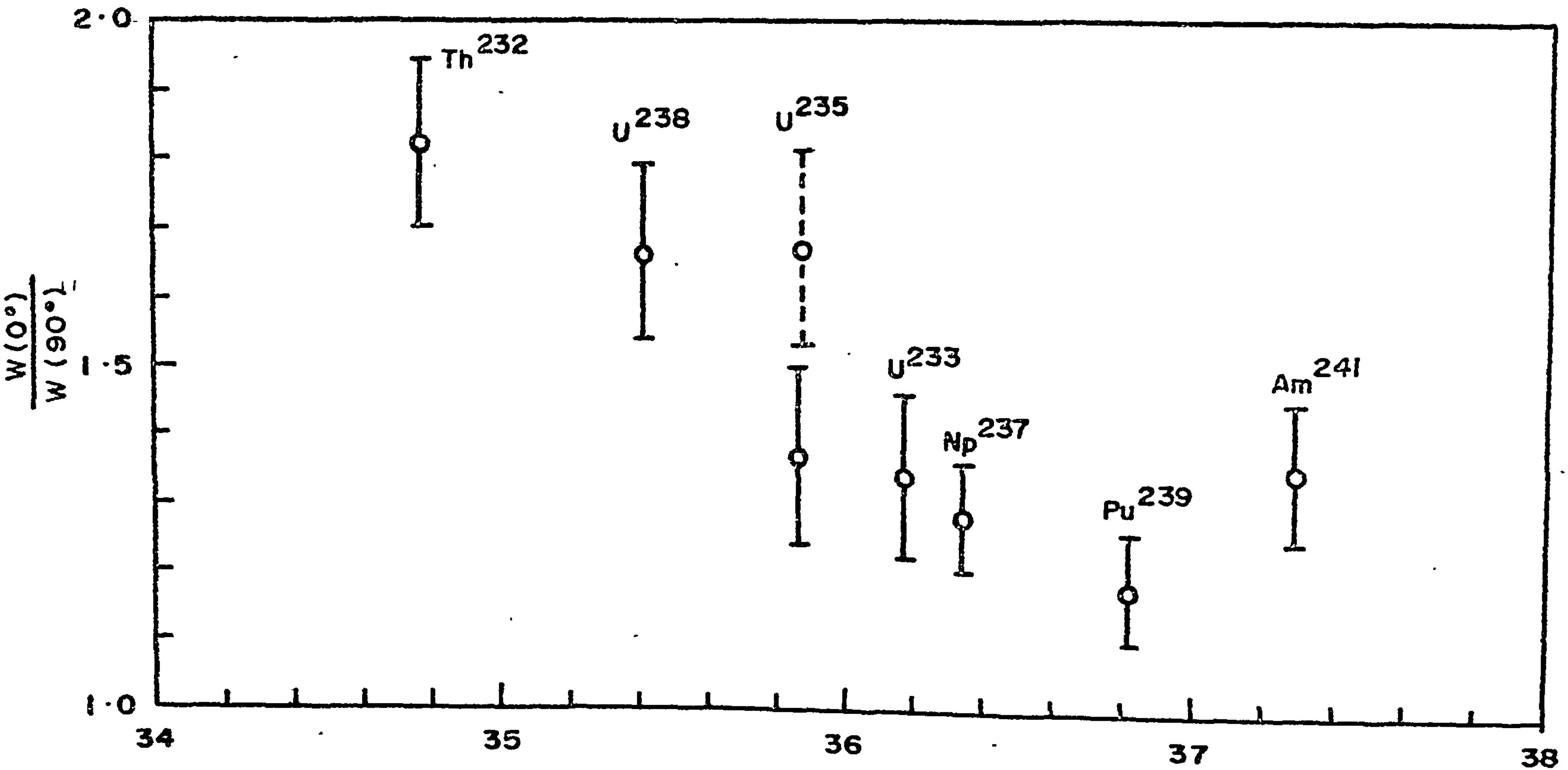
Table 1

Fission fragment anisotropy (15.8 ± 0.5 MeV)

	Neutron energy (MeV)	Anisotropy	Reference
Th^{232}	15.8 ± 0.5	1.82 ± 0.12	present work
	14.0	1.53 ± 0.17	6,7
	14.0	1.88 ± 0.30	10
	14.1 ± 0.1	1.40 ± 0.04	14
	14.5 ± 0.3	1.96 ± 0.38	8
		1.85 ± 0.80	8
U^{233}	15.8 ± 0.5	1.34 ± 0.12	present work
	14.0	1.32 ± 0.11	5
	14.0	1.32 ± 0.05	6,7
	14.0	1.30 ± 0.05	10
U^{235}	15.8 ± 0.5	1.67 ± 0.14[a]	present work
		1.37 ± 0.13[b]	present work
	14.0	1.27 ± 0.17	5
	14.0	1.27 ± 0.08	6,7
	14.0	1.23 ± 0.08	10
	14.8	1.28 ± 0.07	13
	14.1 ± 0.1	1.27 ± 0.01	14
U^{238}	15.8 ± 0.5	1.66 ± 0.13	present work
	14.0	1.31 ± 0.05	6,7
	14.0	1.37 ± 0.13	10
	14.9	1.25 ± 0.02	12
	14.1 ± 0.1	1.31 ± 0.02	14
	14.5 ± 0.5	1.40 ± 0.14	8
Np^{237}	15.8 ± 0.5	1.28 ± 0.08	present work
	14.0	1.15 ± 0.04	6,7
	14.0	1.14 ± 0.04	10
	14.7	1.16 ± 0.02	11
	14.1 ± 0.1	1.12 ± 0.05	14
Pu^{239}	15.8 ± 0.5	1.20 ± 0.08	present work
	14.8	1.15 ± 0.05	13
Am^{241}	15.8 ± 0.5	1.35 ± 0.10	present work
	14.7	1.08 ± 0.06	11

[a] target thickness 1.7 mg/cm^2

[b] target thickness 100 $\mu g/cm^2$



2·0
1·5
1·0
W(0°) / W(90°)
Th232
U238
U235
U233
Np237
Pu239
Am241
34
35
36
37
38
(Z2/A)compound nucleus

FIGURE - 3

Table 1

Fission fragment anisotropy (15.8 ± 0.5 MeV)

	Neutron energy (MeV)	Anisotropy	Reference
Th^{232}	15.8 ± 0.5	1.82 ± 0.12	present work
	14.0	1.53 ± 0.17	6,7
	14.0	1.88 ± 0.30	10
	14.1 ± 0.1	1.40 ± 0.04	14
	14.5 ± 0.3	1.96 ± 0.38 1.85 ± 0.80	8
U^{233}	15.8 ± 0.5	1.34 ± 0.12	present work
	14.0	1.32 ± 0.11	5
	14.0	1.32 ± 0.05	6,7
	14.0	1.30 ± 0.05	10
U^{235}	15.8 ± 0.5	1.67 ± 0.14[a] 1.37 ± 0.13[b]	present work
	14.0	1.27 ± 0.17	5
	14.0	1.27 ± 0.08	6,7
	14.0	1.23 ± 0.08	10
	14.8	1.28 ± 0.07	13
	14.1 ± 0.1	1.27 ± 0.01	14
U^{238}	15.8 ± 0.5	1.66 ± 0.13	present work
	14.0	1.31 ± 0.05	6,7
	14.0	1.37 ± 0.13	10
	14.9	1.25 ± 0.02	12
	14.1 ± 0.1	1.31 ± 0.02	14
	14.5 ± 0.5	1.40 ± 0.14	8
Np^{237}	15.8 ± 0.5	1.28 ± 0.08	present work
	14.0	1.15 ± 0.04	6,7
	14.0	1.14 ± 0.04	10
	14.7	1.16 ± 0.02	11
	14.1 ± 0.1	1.12 ± 0.05	14
Pu^{239}	15.8 ± 0.5	1.20 ± 0.08	present work
	14.8	1.15 ± 0.05	13
Am^{241}	15.8 ± 0.5	1.35 ± 0.10	present work
	14.7	1.08 ± 0.06	11

[a] target thickness 1.7 mg/cm^2

[b] target thickness 100 $\mu g/cm^2$

the observed angular distribution superposition of distributions from several nuclei. At present efforts are under way to disentangle the superpositions from a knowledge of the fissionabilities of the species involved and also to extend these measurements to near threshold excitation energies.

ACKNOWLEDGEMENT

It is a pleasure to express our thanks to Dr. M.V. Ramaniah, Head, Radiochemistry Division, for his continued interest, encouragement and support of the work. Thanks are also due to Mr. U.T.Raheja of T.I.F.R for his help in the neutron irradiations. We acknowledge the assistance of Mr. R. Sampathkumar in the initial phases of these experiments.

APPENDIX

SOLID ANGLE $\Omega = 2\pi(1-\cos\theta)$ ....(1)

OR $d\Omega = 2\pi \sin\theta \, d\theta$ ....(2)

FROM FIGURE 1(C) $\frac{r\,d\theta}{\ell} = \sin\theta = \frac{R}{r}$ ...(3)

$d\theta = \frac{\ell \sin\theta}{r} = \frac{\ell \sin^2\theta}{R}$ ...(4)

PUTTING THE VALUE OF $d\theta$ IN EQUATION (2)

$d\Omega = \frac{2\pi \ell \sin^3\theta}{R}$ .....(5)

$d\sigma = (\text{CONSTANT}) \times 2\pi R \ell \times (\text{TRACK DENSITY})$

$\frac{d\sigma}{d\Omega} = \frac{(\text{CONSTANT}) \times R^2 \times (\text{TRACK DENSITY})}{\sin^3\theta}$

WHERE,

Ω, SOLID ANGLE

θ, ANGLE BETWEEN NEUTRON BEAM AND DIRECTION OF FLIGHT OF F. FRAGMENT

ℓ, WIDTH OF STRIP

r, DISTANCE OF STRIP FROM CENTRE OF BASE OF THE CYLINDER

R, RADIUS OF CYLINDER

REFERENCES

1. I.Halpern and Winhold, Phy.Rev.87, 1139 (1952); 85, 728 (1952).
2. G.E.Gindler and J.R.Huizenga, Nuclear Chemistry, Vol.II, p.1, edited by L.Yaffee, (1968).
3. B.L.Cohen et al, Phys.Rev., 94, 625 (1954).
4. A.N.Behkami, J.R.Huizenga et al, Phys.Rev. 171, 1267 (1968).
5. J.E.Brolley and W.C.Dickinson, Phys.Rev., 90, 388 (1953).
6. J.E.Brolley and W.C.Dickinson, Phys.Rev., 94, 640 (1954).
7. J.E.Brolley and W.C.Dickinson, Phys.Rev., 99, 159 (1955).
8. R.L.Henkel and J.E.Brolley, Phys.Rev., 103, 1292 (1956).
9. R.H.Iyer and R.Sampath Kumar, Nuclear Physics and Solid State Physics Symposium (University of Roorkee, N79, Dec.28-31 (1969).
10. I.Halpern and V.M.Strutinski, 2nd Geneva Confc.Vol.15, 408 (1958)
11. A.N.Protopopov and V.P.Eismont, Soviet Physics JETP,9, 650 (1959).
12. A.N.Protopopov, V.P.Eismont et al, Soviet Physics JETP,9,1143 (1959)
13. A.N.Protopopov and V.P.Eismont,Soviet Physics JETP,7,173 (1958).
14. R.B.Leachman and L.Blumberg, Phys.Rev., 137, B814 (1965).

DISCUSSION

D.S. Srivastava: The plastic detector's efficiency is limited by a critical angle that exists for every dielectric-detector. How did you account for it? Also what led you prefer Lexan detector over mica which has 100% detection efficiency?

R.H. Iyer: Our measurements were restriected between 10° and 80° with respect to the neutron beam and in this range, the fragments make well-defined tracks with 100% efficiency.

Lexan being a synthetic plastic consisting mainly of carbon and Hydrogen is expected to be free of any heavy element contamination and this makes it very attractive for determining even low fission cross sections. More over, Lexan is more flexible than mica and this was a great advantage in our particular experimental set-up.

/

EXCITATION FUNCTIONS FOR THE NEUTRON INDUCED FISSION OF HEAVY NUCLEI

K.N. Iyengar*, R.H. Iyer, S.S. Kapoor, D.M. Nadkarni and M.L. Sagu,
Bhabha Atomic Research Centre, Trombay, Bombay-85.

INTRODUCTION

The presence of a second minimum in the fission barrier predicted by recent theoretical developments(1,2) is supported by several experimental findings. The gradual disappearance of structure in the near threshold fission anisotropy data as one goes from ^{231}Th to heavier actinide odd A compound nuclei has been attributed to the presence of a double-humped barrier with the height of the second barrier decreasing with A. It is therefore of interest to see if the lack of structure in the angular distribution of fission fragments in reactions of the type 241 Am(n,f) is also accompanied by the absence of any structure in the fission excitation functions.(2) The latter may still show a structure associated with the channels (saddle point states) over the first barrier(2) which is presumed to be higher. In the present work we have carried out experiments to measure the fission cross sections of several nuclei namely ^{232}Th, ^{233}U, ^{237}Np, ^{239}Pu and ^{241}Am relative to that of ^{235}U in the neutron energy region of 0.32 Mev to 2.1 Mev at energy intervals of about 100 Kev. In the present paper we present the fission cross section data on ^{241}Am(n,f) as it is more relevant to the points mentioned above. Only limited data were available at the time of starting these investigations.

---

* Tata Institute of Fundamental Research, Colaba, Bombay-5.

Experimental method and results

Fission events were recorded using solid state track detector (Lexan poly carbonate). This technique[3] is particularly suited to the present purpose because of the very low fission cross sections near and below the fission barrier. Further, ^{241}Am having a very high specific activity can cause complications of pile up pulses etc in the conventional methods. Lexan detectors prove to be invaluable as detectors of fission fragments in high backgrounds of relatively low ionizing radiations such as X-rays, γ-rays, α-particles etc as these detectors are nearly insensitive to these radiations. Also these being integral threshold detectors experimental data can be collected over long periods of time without any complications.

Targets were prepared[4] by electrodeposition of the radioactive substance on to gold plated aluminium foils. Natural thorium, depleted Uranium (^{238}U), pure ^{233}U($>$ 99.0%), 93% enriched ^{235}U, pure ^{237}Np($>$ 99.0%), ^{239}Pu($>$95.0%) and pure ^{241}Am($>$99.0%) were used for electro deposition. In the case of ^{232}Th and ^{238}U known amounts of solutions were spiked with known amounts ($\sim$ 1000 cpm) of ^{234}Th and ^{233}U tracers respectively before plating and the amounts deposited were assayed by counting the tracer activity. In the case of ^{233}U, ^{239}Pu and ^{241}Am the amounts plated were estimated by assaying the plating solution before and after plating. In all other cases the amount deposited was estimated by direct alpha counting. Targets of 1 cm diameter were prepared with the amounts of coating, for different isotopes, varying from 1 μg to 25 μg. Lexan strips of 3 mil thick were used and the targets and the lexan pieces were stacked one above the other such that the lexan strip was in contact with the coated side of the target thus providing a 2π geometry for fragment detection.

These stacks were covered by cadmium sheets to shield against any thermal neutrons. Monoenergetic neutrons in the energy range 0.32 to 2.1 MeV were generated with $^3H(p,n)^3He$ reaction using the protons from the 5.5 MeV Van de Graaff accelerator. The spread in the neutron energy was estimated to be in the range of ± 30 Kev to ± 50 Kev. These stacks were irradiated with the fast neutron beams for periods ranging from 20 to 50 hours. After irradiation the lexan foils were etched in 6N NaOH solution at 60°c for 60 minutes and the tracks were counted with an optical microscope with a magnification of 400 X. The cross sections were calculated relative to that of ^{235}U using the following relation

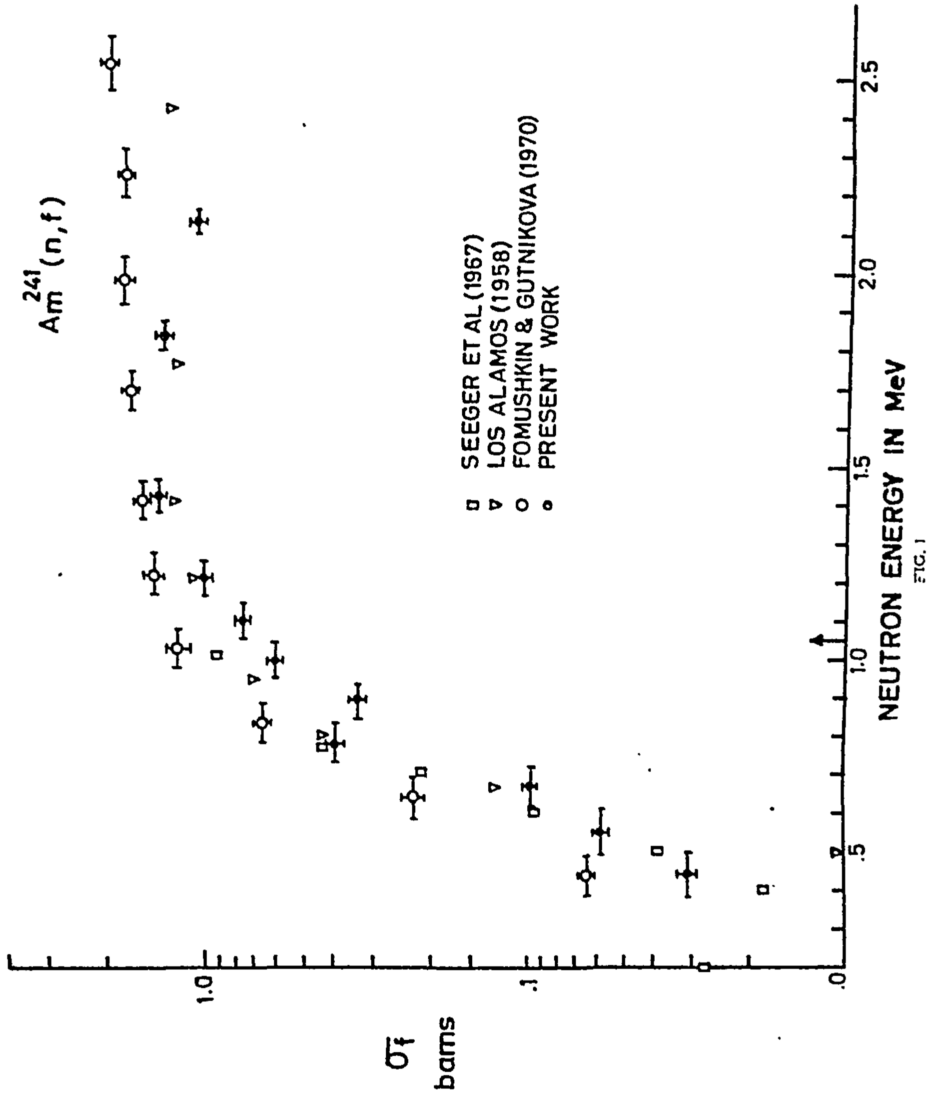
$$\sigma_2 = \frac{N_2 M_1 A_2 \phi_1}{N_1 M_2 A_1 \phi_2} \sigma_1$$

where N is the total number of tracks, M the amount of target material, A the mass number, ϕ the flux of fast neutrons and σ the fission cross section. The subscripts 1 and 2 refer to the standard (^{235}U) and the target whose cross section is to be determined respectively.

The fission cross section for ^{241}Am thus calculated is plotted as a function of incident neutron energy in Fig. 1. For the sake of comparision, we have also shown in the same figure the unpublished Los Alamos data[5], the results of Seeger et al[6] and the recent results of Fomushkin et al[7]. The errors shown in the figure include those due to uncertainties in the estimation of the amounts of the target.

Discussion

The fission cross sections measured in the present work (Fig 1)


$Am^{241}(n,f)$
SEEGER ET AL (1967)
LOS ALAMOS (1958)
FOMUSHKIN & GUTNIKOVA (1970)
PRESENT WORK
σ_f
bams
.01
.1
1.0
.5
1.0
1.5
2.0
2.5
NEUTRON ENERGY IN MeV
FIG. 1

are in fair agreement with results of measurements from other laboratories reported recently except at the low energy point of E_n = 0.5 Mev where our value is larger than the Los Alamos value. However at this energy the recently published data of Fomushkin et al[7] gives a much higher cross section than obtained in the present work. The fission cross section obtained in the present work shows a plateau at neutron energies En 1.4 MeV. In the present work a little structure in the fission cross section is noticeable at the incident neutron energy of 0.78 ± 0.05 Mev. However, no similar structure is observed in the data of other workers (Fig 1). In order to obtain more definite information about this point more data is required in this energy region at still smaller energy intervals.

REFERENCES

1. V.M. Strutinsky Nucl. Phys. A 95, 420 (1967), A 122, 1, (1968)

2. S. Bjornholm and V.M. Strutinsky Nucl. Phys. A 136, 1, (1969)

3. R.L. Fleischer, P.B. Price and R.M. Walker, Ann.Rev. Nucl. Sci. 15, 1, (1965)

4. R.H. Iyer and R. Sampathkumar Paper N 79, Nuclear Physics and Solid State Physics Symposium, Roorkee (1969)

5. BNL - 325 (Second Edition) 1958

6. P.A. Seeger, A. Hemmendinger and B.C. Diven. Nucl. Phys. A 96, 605 (1967)

7. E.F. Fomushkin and E.K. Gutnikova Soviet Jour. Nucl. Phys. 10, no 5, 529 (1970)

EMISSION OF LONG RANGE CHARGED PARTICLES IN THE FISSION OF ^{235}U BY THERMAL TO 4 MeV NEUTRONS

D.M. Nadkarni and S.S. Kapoor
Nuclear Physics Division
Bhabha Atomic Research Centre, Bombay- 85

INTRODUCTION

Several studies of the emission of Long Range Charged Particles (LRCP), in fission have shown that these particles originate towards the last stages of the fission process and therefore the probability of LRCP emission may depend on the configuration of the scission point nucleus. The dependence of the emission probability on the excitation energy of the fissioning nucleus may provide useful understanding on the complex mechanism of emission of these particles. Early measurements (1-3) on the yield of LRCP in the spontaneous fission of ^{240}Pu, thermal neutron fission of ^{239}Pu and in the 14 MeV neutron fission of ^{235}U indicated that the probability of LRCP emission goes down rapidly with increasing excitation energy. Later measurements with incident 2.5 MeV neutrons on ^{235}U by two groups were reported. In one(4) of these these(4) a higher probability of LRCP emission than in thermal neutron fission was found and in the second(5) same probability as in thermal fission was found. Also in high energy proton and α-particle induced fission measurements(6,7) a steep increase in the probability of LRCP was observed whereas Loveland et al(8) reported that the emission probability remains constant (within $\pm$ 15%) in the high energy fission reactions. It

that in these high energy measurements a substantial fraction (> 50%) of fission events taking place are second- and higher chance fissions and consequently the observed probability of LRCP yield is a result ~~out~~ of yields from a number of nuclear species fissioning at different excitation energies. Therefore there is a considerable uncertainty about the excitation energy dependence of LRCP emission probability. In the present work we have measured the probability of LRCP emission in 2,3 and 4 MeV neutron induced fission of ^{235}U relative to that in thermal neutron fission.

EXPERIMENTAL METHOD

In the present experiment the yield of LRCP in coincidence with fission fragment were determined by recording the energy spectrum of these particles and simultaneously monitoring the fission events taking place. The LRCP were detected with a surface barrier detector which had a sensitive area of 2 cm^2 and was operated with a depletion depth sufficient to stop alpha particles of up to 30 MeV. Fission fragments were detected in a 2π geometry using an ionization chamber filled with pure Argon gas and operated with an electric field of 100 V/m. This method has the advantage that no corrections need be made for the possible excitation energy dependence of LRCP-fragment angular correlation. The ^{235}U target was about 1 mg/cm^2 thick coated over an area of 1.5 cm^2 on to a 8 mg/cm^2 aluminium backing and was prepared by the electroplating technique. This thickness of the backing

is sufficient to stop all natural alpha particles and fission fragments so that only LRCP can pass through and get detected in the LRCP detector. The ^{235}U target formed the cathode of the ionization chamber. Neutrons of maximum energy 2.1 and 4.2 MeV were produced with the $^{3}H(p,n)^{3}He$ reaction using the proton beam from the Trombay 5.5 MeV Van de Graaff accelerator. The neutron energy spread, caused mainly due to the slowing down of the protons in the target, was estimated to be about 50-60 keV. The neutron flux at the fissile target was estimated to be about 5×10^{5} $/cm^{2}/sec$. The pulse from the LRCP detector and the ionization chamber were amplified and fed, through a pair of discriminators, to a coincidence circuit of 1 μsec resolving time. The out put of the coincidence circuit opened a linear gate through which the LRCP pulse was passed and its output pulse height distribution was recorded with a 400-channel analyser. Before and after each fast neutron irradiation, thermal neutron irradiations were carried out by surrounding the fission chamber with paraffin blocks. Typical count rates of LRCP-fragments coincidences in fast neutron irradiations were about 16 per hour.

RESULTS AND DISCUSSION

The observed yields of LRCP in 2 and 4 MeV neutron fission of ^{235}U relative to that in thermal fission are shown in Fig.1. where the yield of LRCP per fission in thermal neutron fission, $(2.02 \pm .17) \times 10^{-3}$ represents the weighted average of the results of several

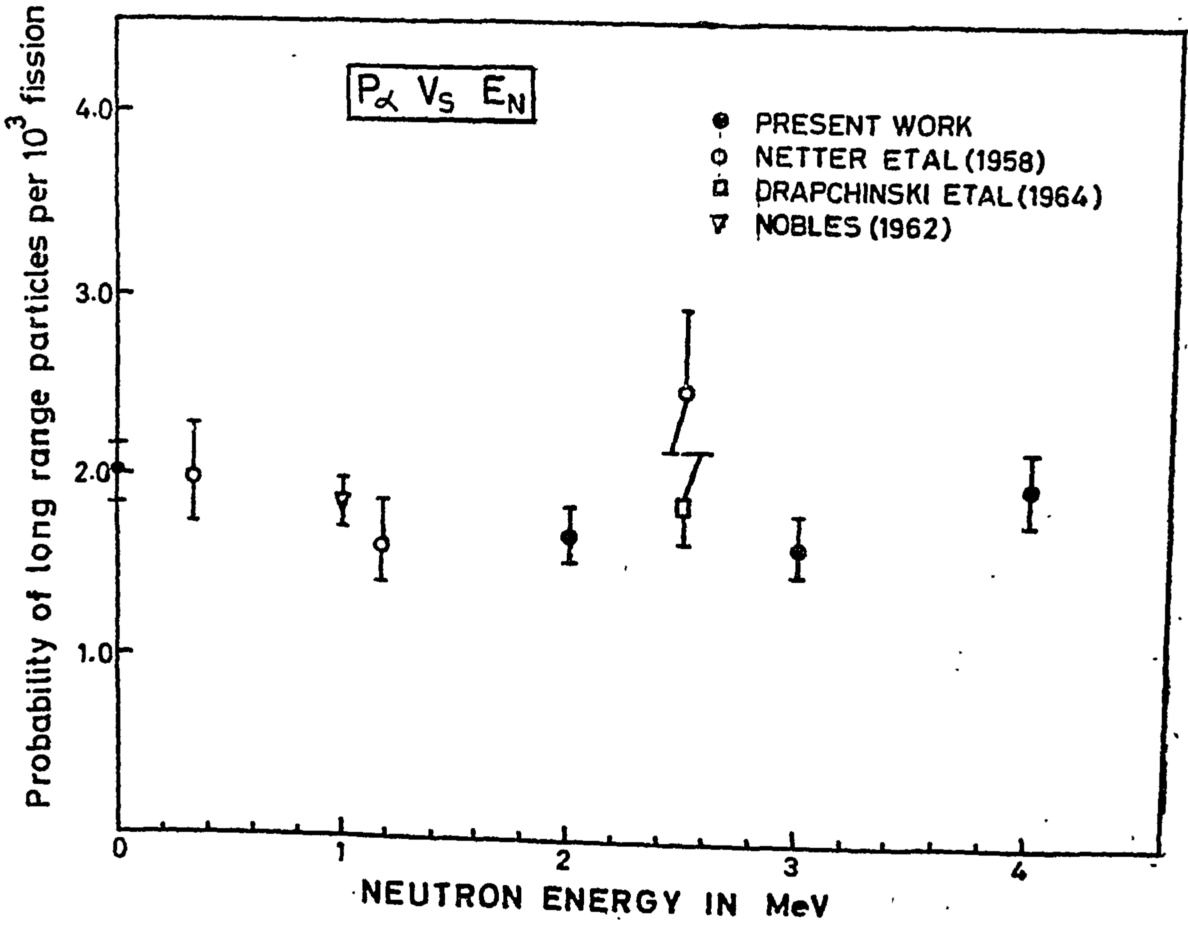

Pα Vs EN
PRESENT WORK
NETTER ETAL (1958)
DRAPCHINSKI ETAL (1964)
NOBLES (1962)
Probability of long range particles per 10³ fission
4.0
3.0
2.0
1.0
0
1
2
3
4
NEUTRON ENERGY IN MeV

FIG. 1

measurements[7]. Also shown in the figure is the result of our earlier measurement[9] of the yield of LRCP in 3 MeV neutron fission of ^{235}U using a similar method and the result of other workers[2,4,5]. The measured yields of LRCP per fission in 2 and 3 MeV neutron fission are found to be $(1.71 \pm 0.15) \times 10^{-3}$ and $(1.68 \pm 0.17) \times 10^{-3}$ respectively, which are in conformity with the yield in 2.5 MeV neutron fission reported by Drapchinski et al[5] but not in agreement with the rather large yield reported by Netter et al[4] at the same energy. In the present work the yield of LRCP per fission in 4 MeV neutron fission was found to be equal to that in the thermal neutron fission. From these results it is concluded that the LRCP emission probability is not sensitively dependent on the bombarding energy of the neutrons.

The reason for the near constancy of the emission probability of LRCP with the increase in the excitation energy of the fissioning compound nucleus-nucleus ^{236}U is intimately connected with the details of the emission mechanism of these particles. Although there are a few qualitative models[10,11] about LRCP emission, the exact mechanism is not yet known. If, however, the probability of emission of LRCP depends sensitively on the energy available for particle emission at scission and on the configuration of the fissioning nucleus at the last stage, as is assumed in these models, then it is concluded on the basis of the present results, that both the energy available for LRCP emission at

the shape of the scission point nucleus are insensitive to the initial excitation energy of the compound nucleus ^{236}U. The excess energy put in is locked up as deformation energy and is not available for particle emission. These interpretations are consistent with the observed[12] near constancy of the kinetic energy of fission fragments with the increase in neutron bombarding energy.

REFERENCES

1. T.A. Mostovaya, Reported by V.I. Mostovoi, Proc. Int. Conf. Peaceful Uses Atom. Energy, 2, 226 (1956)

2. R.A. Nobles, Phys. Rev. 126, 1508 (1962).

3. N.A. Perfilov, Z.I. Soloneva and R.A. Filov, Sov. Jr. Atom. Energy 14, 601 (1963).

4. M.F. Netter, H. Faraggi, A. Garin-Bonnet, M.J. Julien, C. Corge and J. Turkiewicz, Proc. Second Int. Conf. Peaceful Uses Atom. Energy 15, 418 (1958).

5. L.V. Drapchinski, S.S. Kovalenko, K.A. Petrzhak and I.I. Iyutyugin, Sov. Jr. Atom. Energy 16, 164 (1964).

6. J.A. Coleman, A.W. Fairhall and I. Halpern, Phys. Rev. 133, B731 (1964).

7. T.D. Thomas and S.L. Whetstone, Phys. Rev. 144, 1060 (1966).

8. W.D. Loveland, A.W. Fairhall and I. Halpern, Phys. Rev. 163, 1315 (1967).

9. V.A. Hattangadi, T. Methasiri, D.M. Nadkarni, R. Ramanna and P.N. Rama Rao, Phys. & Chemistry of Fission, 2, 397 (1965).

10. R. Ramanna, K.G. Nair and S.S. Kapoor, Phys. Rev. 129, 1350 (1963).

11. I. Halpern, Phys. & Chemistry of Fission, 2, 369 (1965).

12. See, for example, E.K. Hyde, Nuclear Properties of Heavy Elements, 3, (1964).

KINETIC ENERGY DISTRIBUTION IN THE REACTOR NEUTRON INDUCED FISSION OF ^{241}Am

Satya Prakash, S.B. Manohar, S.P. Dange,
A. Ramaswami and M.V. Ramaniah
Radiochemistry Division,
Bhabha Atomic Research Centre,
Trombay, Bombay-85.

I. INTRODUCTION

With an aim to understand the distribution of the kinetic energy released and the kinetic energy deficit, as a function of charge and the mass of the fissioning nucleus, we have determined the recoil ranges in the fission of ^{232}Th (1), ^{233}U and ^{239}Pu (2). This paper, which is a part of these studies, describes the measurements of recoil-ranges and hence the kinetic energies of the fission fragments in the reactor neutron induced fission of ^{241}Am, for which there is no data on kinetic energy released.

II. EXPERIMENTAL

Thin-target, thin-catcher technique was used in the determination of recoil ranges of fission products, in which the mean range 'R' is related to the activities in different catchers by equation (1)

$$R = \left[1 + \frac{A_2 + A_3 \ldots}{A_1} \ldots \right] \left[t + \tfrac{1}{2} CW \right] \quad \ldots\ldots (1)$$

R, t and W are the mean range of the fission product, the thickness of the first catcher and the thickness of the target respectively. A_1, A_2, A_3 etc. are the activities of the fission fragment in different catcher foils. 'C' is the correction factor for the difference in stopping power of the target and the catcher materials.

The uniform targets of about 100 ugm of ^{241}Am

gold plated aluminium foils by electrodeposition.

covered with 0.3 mil super pure aluminium catcher foils, and the whole assembly was wrapped in 1 mil aluminium foil. The irradiations were done at the CIRUS reactor with a neutron flux of 10^{13} n./cm^2/sec. for the duration of 10 to 24 hours. After the irradiations catcher foils were separated and the activities corresponding to different fission products were determined, either by γ-spectroscopy using a 2 cc Ge(Li) detector, or by standard radiochemical methods. The γ-spectroscopy was useful only in the region of high fission yields, and therefore the recoil-ranges in the symmetric region were determined by radiochemical methods.

The recoil ranges were converted into the kinetic energies of the secondary fragments using three different range energy relations. The first one is the emperical formula given by Alexander and Gazdik[3]

$$R = K\,E^{2/3} \qquad \ldots\ldots \qquad (2)$$

In this the constant 'K' which varies with the mass of the fission product was calculated using recoil range data of Aras[4] et al and the kinetic energy data of Schmitt et al[5]. The modified form of L.S.S. treatment by Noshkin and Sugihara[6] was also used, but it was found that it gives too high values of kinetic energies in the light mass region and too low values in the heavy mass region.

The third range energy relationship which was derived by us (to be published) was also used. In this the mean range 'R' is related to the kinetic energy of the fission product by equation (3)

$$R = \frac{V_o}{2.d} \cdot \frac{E^{\frac{1}{2}} \cdot M_1^{\frac{1}{2}}}{Z_p^{2/3}\,\xi} \qquad \ldots\ldots \qquad (3)$$

where $\xi = 1.486 \times 10^{18} \left[\frac{\rho_2}{\ldots} \cdot \frac{Z_p^{0.894}\ \ Z_o}{\ldots} \right] (A_1 + A_2)^{\frac{1}{2}} \quad \ldots (4)$

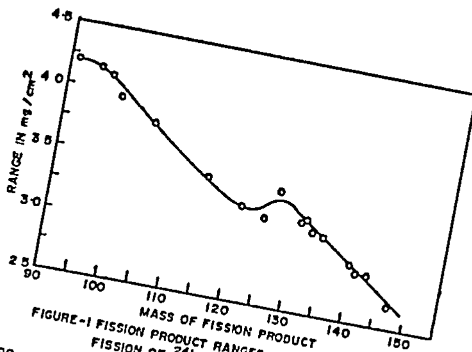


FIGURE-1 FISSION PRODUCT RANGES IN ALUMINIUM IN THE FISSION OF ^{241}Am

Ek (TOTAL KINETIC ENERGY RELEASE IN MeV)

190
180
170
160
150

—o— USING ALEXANDER-GAZDIK FORMULA

—△— USING NEW FORMULA

1·0 1·1 1·2 1·3 1·4 1·5 1·6

MASS RATIO

FIGURE-2 KINETIC ENERGY RELEASE AS A FUNCTION OF MASS RATIO IN ^{241}Am FISSION

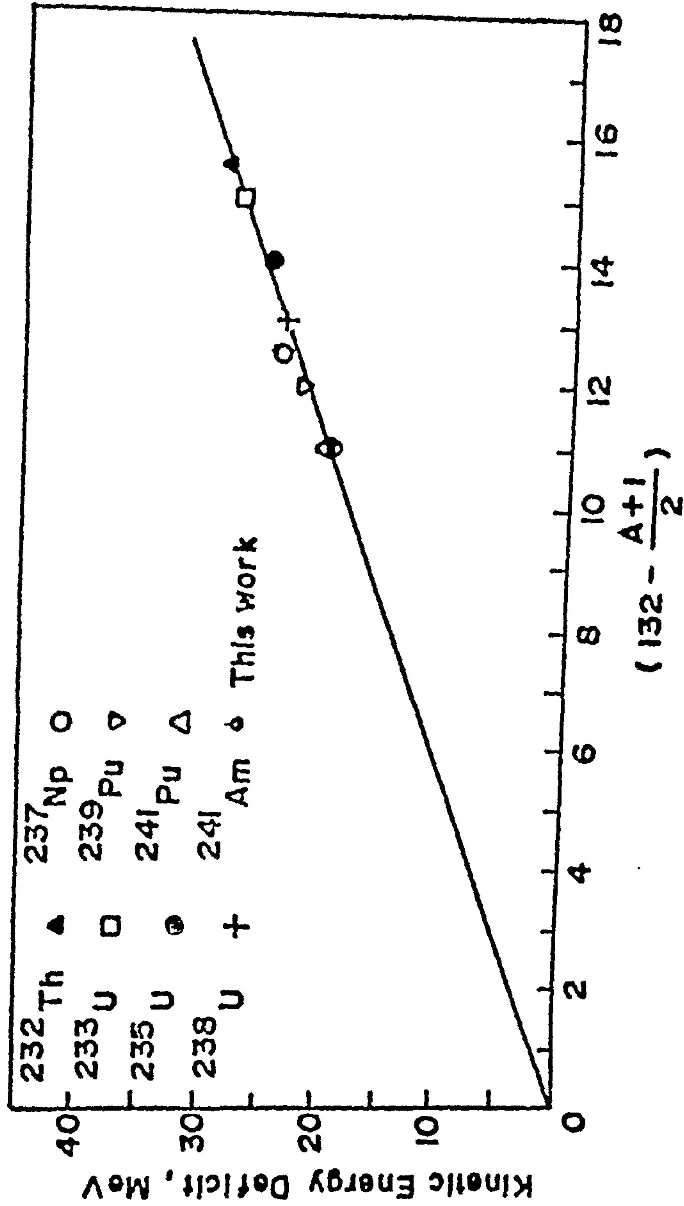


FIGURE-3. Correlation of K.E.D. with shell structure

V_0 is the velocity of an electron in the first orbit of hydrogen atom, e is the charge of the electron, Z_p and Z_o are the nuclear charges of the fission product and the stopping atom,
$Z_0 = [Z_p^{2/3} + Z_o^{2/3}]$ and M_1 is the mass of the fission product.

The kinetic energies of the primary fragments were calculated by making corrections for neutron evaporation. The primary kinetic energies were converted to the corresponding total kinetic energies for the different splits.

III. RESULTS

Fig. (1) shows the plot of recoil ranges as a function of mass of the fission product. Fig. (2) shows the plot of total kinetic energy released as a function of mass split. It can be seen that the kinetic energy deficit is about 19.0 MeV and this value fits well in our earlier correlation[1] with shell structure as seen in the Fig.(3)

ACKNOWLEDGEMENT

Authors are thankful to Shri A.G.C. Nair and Shri R.J. Singh for their help in this work.

REFERENCES

1. Satya Prakash, S.B. Manohar, C.L. Rao and M.V. Ramaniah; J.Inorg. Nucl. Chem. 31, 1217 (1969).
2. S.P. Dange, S.B. Manohar, Satya Prakash, A. Ramaswamy and M.V. Ramaniah; D.A.E. Chemistry Symposium, 1969, Chandigarh.
3. J.M. Alexander, M.F. Gazdik, A.R. Trips and S. Wasif; Phys. Rev. 129, 2659 (1963).
4. N.K. Aras; M.P. Menon and G.E. Gordon; Nucl. Phys. 69, 337 (1965).
5. H.W. Schmitt. J.H. Nieler and F.J. Walter; Phys.Rev.141, 1189(1966)
6. V.E. Noshkin and T.T. Sugihara; J.Inorg. Nucl.Chem. 27, 943 (1965)

HIGH ENERGY REACTIONS AND SHELL MODEL WAVEFUNCTIONS OF ^7Li

G. Ramachandran
Indian Statistical Institute, Calcutta- 35

The important role which high energy reactions could play in elucidating nuclear structure has well been demonstrated by the successful use of high energy electron scattering on nuclei. Apart from this particular process, we have at hand a number of other high energy processes like pion scattering, photoproduction etc., which could be expected to yield important insights into nuclear structure. We wish to suggest that experiments involving such high energy processes could be used to study experimentally the nuclear shell model radial wave functions. One advantage in using the processes like pion scattering or photoproduction rather than electron scattering being that these reactions possess strong spin-dependent parts which are comparable to the spin-independent amplitude on a nucleon. As a concrete example, we consider the case of ^7Li for the discussion.

We refer to an earlier paper[1] for details of the theoretical model used to discuss such processes leading to the ground as well as to excited states of the nucleus using the nuclear shell model. The first excited state of ^7Li which we take to be $[3]^{22}P_{1/2}$ state is a low lying state with excitation energy of only 0.48 MeV and it is usually difficult experimentally to resolve this inelastic contribution from the elastic cross section. Adding therefore the two, the cross section is given on the basis of our model by

$$\frac{d\sigma}{d\Omega} = \left| F_{os} (2L_p + 2L_n) + F_{op} (2L_n + L_p) \right|^2$$

$$+ \frac{13}{25} F_{2p}^2 \left| 2L_n + L_p \right|^2 + (F_{op}^2 + \frac{18}{25} F_{2p}^2) \left| K_p \right|^2 \quad (1)$$

where L and K denote respectively the nucleon spin-independent and spin-dependent parts of the amplitude for the process on a nucleon, whose charge state is denoted by the suffix p or n. F_{os}, F_{op} and F_{2p} refer respectively to the radial integrals

$$F_{os} = \int u_s^*(r)\, j_o(kr)\, u_s(r)\, dr \qquad (2)$$

$$F_{op} = \int u_p^*(r)\, j_o(kr)\, u_p(r)\, dr \qquad (3)$$

$$F_{2p} = \int u_p^*(r)\, j_2(kr)\, u_p(r)\, dr \qquad (4)$$

where u_s, u_p denote the radial wavefunctions in the s- and p- shells respectively and $j_\ell(kr)$ denote spherical Bessel functions, k being the momentum transferred to the nucleus.

The next excited state of the nucleus is taken as $[3]^{22}F$ with $J \leq 7/2$(2). Since the ground state is $[3]^{22}P$ it is obvious that an orbital angular momentum $\ell = 2$ at least, should be transferred to the nucleus to lead to this excited state and if this is to be brought about through the transition of a p- shell nucleon, $\ell = 2$ is the only allowed value for the orbital angular momentum transfer. Therefore, only the radial integral F_{2p} is involved here and we have

$$\frac{d\sigma}{d\Omega} = \left(\frac{37}{45} F_{2p}\right)^2 \left[\frac{46}{21} |\underset{\sim}{K}_p|^2 + \frac{16}{21} |\underset{\sim}{K}_p \cdot \underset{\sim}{k}|^2\right] \quad (5)$$

$$\frac{d\sigma}{d\Omega} = \left(\frac{37}{45} F_{2p}\right)^2 \left[\frac{52}{21} |\underset{\sim}{K}_p|^2 - \frac{16}{21} |\underset{\sim}{K}_p \cdot \underset{\sim}{k}|^2\right] \quad (6)$$

for this reaction, the alternative expressions (5) and (6) referring respectively to either of the possibilities $J = 5/2$ or $J = 7/2$ for the excited state.

The interesting point is that knowing the J- value one can readily estimate the form factor F_{2p} empirically from experimental studies of inelastic high energy reactions leading to this excited state.

Just as in the case of electron scattering, where the Coulomb scattering tends to zero at 180°, we have in the case of photoproduction of neutral pions that the spin independent contributions go to zero in the forward as well as in the backward production angles. This circumstance *could be taken advantage of to eliminate the form factor* F_{os} in (1) and determine empirically the combination $(F_{op}^2 + \frac{18}{25} F_{2p}^2)$ directly from experimental measurements of

$$\frac{d\sigma}{d\Omega} = \left(F_{op}^2 + \frac{18}{25} F_{2p}^2 \right) |\underset{\sim}{K}_p|^2 \quad (7)$$

at production angles $\theta = 0^{\circ}$ and 180°.

The knowledge of the two form factors F_{op} and F_{2p} thus gained could then be used in (1) and hence estimate empirically the form factor F_{os}.

It is also interesting to observe that in the oscillator model, the ratios F_{op}/F_{os} and F_{2p}/F_{os} are linear functions of k^2. It should be possible to test this feature easily using the empirical knowledge gained of the form factors and thus serve as an elegant check on the model.

REFERENCES

1) G. Ramachandran, N. D. Prabhakar and A. K. Rej, Nucl. Phys. B 22 (1970) 369

2) T. Lauritsen and F. Ajzenberg-Selove, Nucl. Phys. 78(1966)

DISCUSSION

B.K. Jain: First question is what specific reactions you have in mind to which you would like to apply your formalism to study the radial distribution of single nucleon in nuclei. Secondly how the information obtained from this procedure compares with that extracted by the single nucleon transfer reactions.

G. Ramachandran: As I have mentioned at the begining of my talk, pion scattering photo-production of pions, kaons etc. (as well as electro-production) and neutrino reactions etc. are the types of reactions to which the formalism could be applied. It would be adviseable, however, to check for regions of energy and momentum transfer in each of these reactions where the impulse approximation would be expected to be good. I understand that experimentalists have ways of checking this from certain kinematical requirements. As regards the second question, I do not think that the types of information that you get from the model I have been discussioning and that for single nucleon transfer reactions are the same for the simple reason that in the first problem it is a single nucleon that is supposed to feature in the reaction where as in the reaction which you refer to, it is a pair of nucleons that are supposed to be responsible for the reaction to go through.

IS THERE A PHASE DIFFERENCE BETWEEN THE S- AND D- STATES OF THE DEUTERON?

G. Ramachandran
Indian Statistical Institute, Calcutta - 35

ABSTRACT

Experimental data on the magnetic scattering of electrons on deuterons suggest a possibility of there being a phase difference between the S- and D- states of the deuteron. Other scattering data are also examined to check this possibility. The calculations are based on the Glendenning-Kramer and the Hamada-Johnston models of the deuteron. The implications of a possible phase difference to theories of violation of time reversal invariance are also discussed.

IS THERE A PHASE DIFFERENCE BETWEEN THE S- AND D- STATES OF THE DEUTERON?

G. Ramachandran
Indian Statistical Institute, Calcutta - 35

ABSTRACT

Experimental data on the magnetic scattering of electrons on deuterons suggest a possibility of there being a phase difference between the S- and D- states of the deuteron. Other scattering data are also examined to check this possibility. The calculations are based on the Glendenning-Kramer and the Hamada-Johnston models of the deuteron. The implications of a possible phase difference to theories of violation of time reversal invariance are also discussed.

SPECTRAL AVERAGES FOR SINGLE-NUCLEON TRANSFER REACTIONS FOR NEUTRON-RICH-MULTI-SHELL TARGET STATES

R.K. Bansal
Department of Physics, Panjab University, Chandigarh-14.

During the last many years sum rules have been developed and used within the framework of Shell Model in nuclear spectroscopy in, both for predicting strengths[1,2] and the nature of the residual interaction, using data on single nucleon transfer reactions. In continuation of our basic work[3,4], we recently extended[5] the sum-rules methods to predict spectroscopic averages of the spectra of the nuclei (Residual nuclei) obtained after doing single nucleon transfer reactions on target-states which have only neutrons in their active shell and the nuclear reaction (like $Ca^{43}(He^{3}, d)\ Sc^{44}$) transfers particle to the same shell i.e. the transfer is that of an Equivalent Particle (Inequivalent transfers have been dealth with earlier[4]).

It is quite interesting and useful to theoretically predict spectroscopic average of the spectra of the residual nucleus where the target has more then one neutron-rich active shells and the incoming nucleon (or hole) is added to any one of these active shells.

For single nucleon transfer reactions, the basic sum rules equations, incorporating the spectroscopic factors and the energies of the states of the residual nucleus are:

$$\sum_{\Gamma} (-1)^{\Gamma_0 + \rho_i - \Gamma} (2\Gamma+1)^{1/2} U(\Gamma_0 \rho_i \Gamma_0 \rho_i ; \Gamma \Lambda) \mathcal{S}_{\Gamma}^{(+)}(\Gamma_0 x_0 + \rho_i \to \Gamma) E_{\Gamma}^{(+)}$$
$$= (-1)^{\Lambda} \langle n \Gamma_0 x_0 \| (B^{\rho_i} \times H \times A^{\rho_i})^{\Lambda} \| n \Gamma_0 x_0 \rangle \qquad \text{---(1)}$$

and

$$\sum_{\Gamma} (-1)^{\Gamma_0 + \rho_i - \Gamma} (2\Gamma_0+1)(2\Gamma+1)^{-1/2} U(\Gamma_0 \rho_i \Gamma_0 \rho_i ; \Gamma \Lambda) \mathcal{S}_{\Gamma}^{(-)}(\Gamma_0 x_0 \to \Gamma\,[illegible]) E_{\Gamma}^{(-)}$$
$$= (-1)^{\Lambda} \langle n \Gamma_0 x_0 \| (A^{\rho_i} \times H \times B^{\rho_i}) \| n \Gamma_0 x_0 \rangle \qquad \text{--- (2)}$$

In equations (1) and (2) $\mathcal{S}_{\Gamma}^{(\pm)}$ and $E_{\Gamma}^{(\pm)}$ are the spectroscopic factors and energies of the states of the residual nucleus (+ sign indicates stripping reactions and (-) sign refers to the pick up cases). The symbol $\Gamma_0 \equiv J_0 T_0$, $\rho_i \equiv j\tfrac{1}{2}$ and $\Gamma \equiv JT$ refer to the angular momentum and iso spin of the target state, the transferred nucleon and the residual state (State of the residual nucleus) respectively; A^{ρ_i} and B^{ρ_i} are the properly symmetrized creation and destruction operators (for the first time used by Professor J.B. French) for the nucleon and $\Lambda(\equiv k\tau)$ is the appropriate rank of the relevant tensor in the product space. The quantum number x_0 and x are designed to make the target state and the final state unique.

If the target state $|n\Gamma_0 x_0\rangle$ has many active shells (occupied by neutrons only) labelled by ρ_j and ρ_i

labels the transferred nucleon, then equations (1) and (2) lead to the following result for the stripping and the pick up cases.

$$\overline{E_T^{(+)}} = \frac{\sum_J \mathcal{S}_{JT}^{(+)} E_{JT}^{(+)}}{\sum_J \mathcal{S}_{JT}^{(+)}}$$

$$= \Big\{ \Big[\sum_j \Big(p_T^{(+)}(i-j) + (1+\delta_{ij}(N_i-2))\, q_T^{(+)}(i-j) W^{T=1}(i-j) + (1+\delta_{ij} N_i)\, r_T^{(+)} W^{T=0}(i-j) \Big) \Big] \div \Big[\sum_J \mathcal{S}_{JT} \Big] \Big\} + E(N+Z) \quad \text{--- (3)}$$

where

$$p_T^{(+)}(i-j) = -\frac{(1+\delta_{ij})}{2} E_t(\ell_i-\ell_j)\left(1+\frac{f(T)}{T_0}\right) \quad \text{--- (4)}$$

$$q_T^{(+)}(i-j) = \left(3/4\, n_j + \frac{f(T)}{2T_0} T_{0j}\right) \quad \text{--- (5)}$$

$$r_T^{(+)}(i-j) = \left(\frac{1}{4} n_j - \frac{f(T)}{2T_0} T_{0j}\right) \quad \text{--- (6)}$$

where

$$n_j \equiv \langle n_j(op) \rangle_j$$

i.e. the number of active nucleons in the jth shell and $E_t(\ell_i-\ell_j)$ is the two body energy due to interactions of the nucleons in the ith shell with those in the jth shell i.e. it is $\langle n\Gamma_0 x_0 | H_{ij} | n\Gamma\xi \rangle$ and $f(T)$ and N_i are given by

$$f(T) = (T(T+1) - 3/4 - T_0(T_0+1))$$

$$N_i = (2j_i+1)$$

and T_{oj} is the iso spin due to neutrons in the jth shell E(RIZ) (is the residual interaction zero which) is defined to be the energy of the final nucleus when the interaction between the transferred nucleon and the active nucleons is switched off. Equations (3),(4),(5) and (6) reduce to the results for the single active shell case as known by our previous works[5].

For pick up case we can pick up only a neutron (the active nucleons in the target being neutrons only) and therefore only $E^{(-)}_{T_>}$ is attainable; this is given by

$$\overline{E^{(-)}_{T_>}} = \frac{\sum_J S^{(-)}_{J T_>} E^{(-)}_{J T_>}}{\sum_J S^{(-)}_{J T_>}}$$

$$= \frac{-\frac{1}{2}(1+\delta_{ij}) \sum_j E_t (e_i - e_j')}{\sum_J S^{(-)}_{J T_>}} + E^{(-)}(RIZ) \quad \text{---(8)}$$

The denominator in equations (3) and (8) is given by the well known Non-Energy weighted[1,2] sum Rules.

Interesting applications of Equations (3) and (8) are in the process of being worked out.

REFERENCES

1. J.B. French and M.Macfarlane, Nuclear Physics, 26, 168 (1961).

2. J.B. French, Physics letters 13, 249 (1964).

3. R.K. Bansal and J.B. French, Physics letters 19, 223 (1965).

4. R.K. Bansal, Proceedings of Nuclear Physics and Solid State Physics Symposium, Bombay (1968).

5. R.K. Bansal, Physics letters 27B, 184 (1968).

CALCULATION OF THE REAL PART OF THE NUCLEON-NUCLEUS OPTICAL POTENTIAL

H.R. Kidwai* and J.R. Rook
Nuclear Physics Laboratory, Oxford

The real part of the optical model potential for nucleon-nucleus scattering can be written as

$$\tilde{V}_1(\underline{r}_1) = \int \rho_m(\underline{r})\, v_1(\underline{r}_1,\underline{r})\, d\underline{r} \qquad (1)$$

where $\rho_m(\underline{r})$ is the nucleon density distribution and $v_1(\underline{r}_1,\underline{r})$ is the internucleon potential. This expression has been used very successfully by Greenlees, Pyle and Tang[1] to analyse proton elastic scattering data for several nuclei upto 40 MeV. Eqn. (1) however, is obtained without taking internucleon correlations into account. Also, in this form we cannot use realistic hard core potentials in eqn. (1).

In order to remove this deficiency we consider only two-body correlations between the incident nucleon and one of the target nucleons and obtain the expression

$$\tilde{V}_1(\underline{r}_1) = \int \rho_m(\underline{r})\, t(\underline{r}_1,\underline{r})\, d\underline{r} \qquad (2)$$

for the optical model potential. Now in this form we can use realistic hard core potentials. In our calculations we have used the Hamada-Johnston potential[2]. For matter distribution inside the nucleus we have used the independent fermion model. And to calculate the reaction matrix we have used the reference spectrum method of Bethe, Brandow and Petschek[3]. The parameters m^* and γ of the reference wave equation

$$\left[\frac{d^2}{dr^2} - \frac{l'(l'+1)}{r^2} - \gamma^2\right]\chi^{JS}_{ll'}(r) = -m^* \sum_{l''} v^{JS}_{l'l''}(r)\, f^{JS}_{ll''}(r) \qquad (3)$$

---

*Present address: Physics Department, Indian Institute of Technology, Kanpur-16 (U.P.)

can be obtained by comparison with experiment. In this way we find the values $m^* = 1$ and $\gamma = 0.7$ fm for these parameters. This value of γ corresponds to a healing distance of 1.4 fm which is less than the internucleon separation distance at the centre of a nucleus. Therefore we seem to be justified in considering only two-body correlations in our calculations.

Now as we can see from curve 1 in fig. 1 our calculation of the optical model potential is quite in disagreement with experimental result at high energies. The reason for this seems to be that although at high energies the effect of Pauli exclusion principle is quite small, eqn. (3) does not reduce to that of scattering of free nucleons. Now the important contribution to the reaction matrix comes from small distances. If we consider the following modification of the reference wave equation

$$\left[\frac{d^2}{dr^2} - \frac{l'(l'+1)}{r^2} - \{\gamma^2(1-e^{-\eta\gamma^2r^2}) - k^2e^{-\eta\gamma^2r^2}\} - \sum_{l'} v_{ll'}^{JS}(r)\right] f_{ll'}^{JS}(r)$$

$$= -[k^2 + \{\gamma^2(1-e^{-\eta\gamma^2r^2}) - k^2e^{-\eta\gamma^2r^2}\}]\delta_{ll'}j_l(r) \qquad (4)$$

we notice that this equation does reduce to that of free scattering for small values of r. This incidently is in agreement with Moszkowski and Scott[(4)]. At large distances this equation reduces to the usual reference wave equation. Eqn. (4), however, has the advantage that it can be used in any spin-isospin state.

We have obtained the energy dependence of the optical model potential by using the modified reference wave equation to calculate the reaction matrix, and as we can see in fig. 1 the result is in better agreement with experiment. The shape of the potential at a range of energies, fig. 2, and the isospin part, fig. 3, have also been obtained in this way.

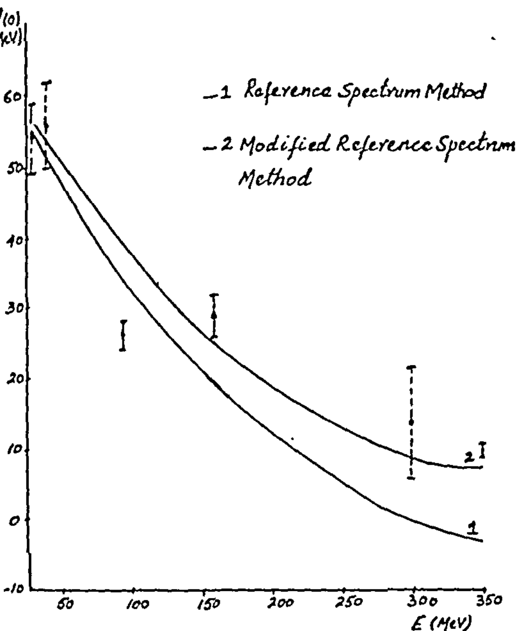


FIG. 1

Proton Optical potential at the centre of $^{208}_{82}$Pb as a function of the incident energy.

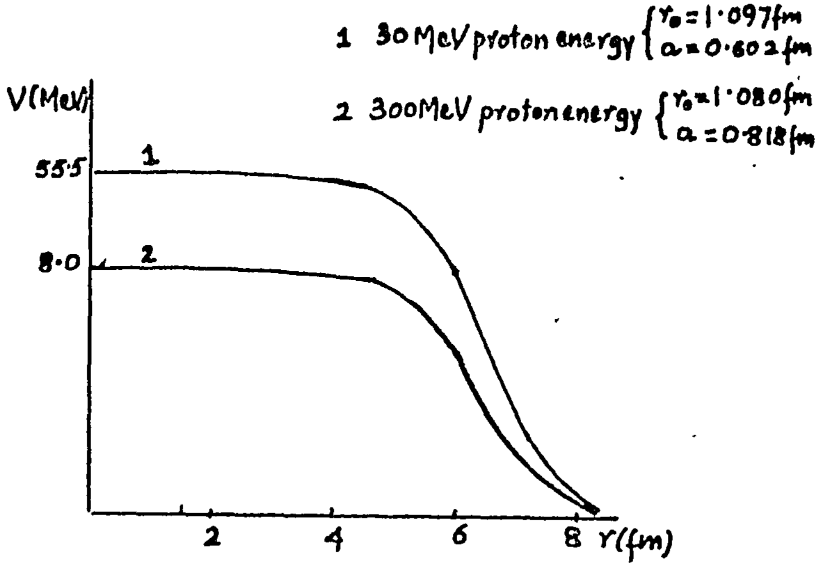


FIG. 2

Protons optical potential for $^{208}_{82}Pb$ at 30 MeV and 300 MeV calculated with modified reference spectrum method.

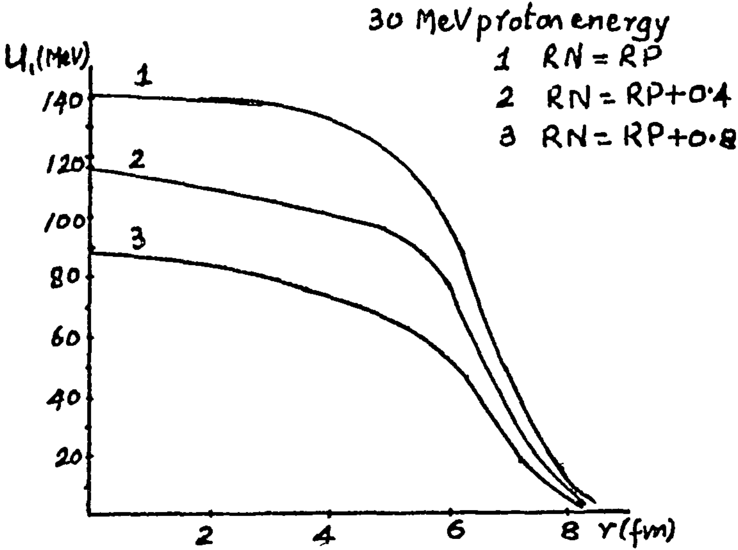


FIG. 3

Isospin part of the optical potential for $^{208}_{82}Pb$ calculated for different neutron radii, RN, corresponding to a given proton radius RP.

Thus we can say that realistic internucleon potentials can be used to evaluate the real part of the optical model potential provide one takes at least two-body correlations into account.

References

1. G.W. Greenlees, G.J. Pyle and Y.C. Tang, Phys. Rev. 171(1968) 111
2. T. Hamada and I.D. Johnston, Nucl. Phys. 34(1962) 382.
3. H.A. Bethe, B.H. Brandow and A.G. Petschek, Phys. Rev. 129(1963)
4. S.A. Moszkowski and B.L. Scott, Ann. Phys. 11(1960) 65.

DISCUSSION

N.K. Ganguly: In view of the fact that you have taken into account correlation, have you considered the effect of antisymmetrization?

H.R. Lidwai: Yes, we have considered the antisymmetrization of the incident nucleon with the target nucleons. This gives rise to the non-local potential. We find that the non-local potential is very small compared to the local potential.

- -

(t,α) REACTION ON ^{130}Te AT 12 MeV+

M.L. Chatterjee
Saha Institute of Nuclear Physics, Calcutta
and
N. Cindro**, M. Conjeaud*, S. Harar*,
B. Fernandez* and M. Turk**

ABSTRACT

The (t,α) reaction on ^{130}Te has been studied with 12 MeV triton beam from Aldermaston Van-de-Graaff. The data were registered in a multigap magnetic spectrograph. The work is still in process. Preliminary data and their DWBA analyses indicate that the strongly excited states of ^{129}Sb show good evidence of 2p-1h configurations.

+ This work was done at Institute Rudjer Boskovich Zagreb in collaboration with C.E.N., Saclay.

** I.R.B., Zagreb.

* S.P.N.B.E., C.E.N., Saclay.

OPTICAL POTENTIAL FOR DEUTERON

S. K. SAMADDAR and SUPROKASH MUKHERJEE
Saha Institute of Nuclear Physics, Calcutta - 9.

I. INTRODUCTION:

In a recent paper[1] it has been proposed that a linear energy dependence in the nucleon optical potential (OP) immaginary depth may not be a good approximation as far as the deuteron OP for elastic scattering is concerned in the formalism given in (2). Moreover, it is felt that the nucleon OP parameters should have larger radius for the imaginary part compared to nuclear radius. The OP parameters of Engelbrecht and Piedeldey[3] for neutron satisfy both the requirements and in this paper we study the deuteron OP generated according to the formalism of (2) using nucleon OP of (3).

II. FORMALISM:

The OP parameters for nucleon used here are those given by eqns.(29) and (30) of (3) which involves exponential energy dependence. So we need matrix element M

$$M = \langle \chi_0 | f(r_n)\, e^{a T_r} | \chi_0 \rangle, \qquad (1)$$

where $f(r_n)$ is the nucleon OP form factor, 'a' is a constant, T_r is the K.E. operator for the relative motion of neutron and proton in the deuteron and χ_0 is its ground state wavefunction which is generally taken as Hulthen form i.e.,

$$\chi_0(r) = N\,(e^{-\alpha r} - e^{-\beta r})/r$$

The form of $\chi_0(r)$ as given by eqn.(2) is unsuitable for our purpose as operation of T_r^n for $n > 1$ gives rise to $\delta(\vec{r})$ and its derivatives and M given by eqn.(1) becomes divergent. So we choose

$$\chi_0(r) = (2\alpha/\pi)^{3/4} e^{-\alpha r^2}, \tag{3}$$

with $\alpha = 0.06\ fm^{-2}$ and this form of $\chi_0(r)$ is free from the above mentioned unwanted feature. It is interesting to note that $e^{aT_r} e^{-\alpha r^2}$ is a Gaussian function in r as we can write

$$e^{-\alpha r^2} = \frac{2}{\pi}\int_0^\infty g(k)\ \frac{\sin kr}{r}\ dk, \tag{4}$$

where
$$g(k) = \frac{\sqrt{\pi}}{4\alpha^{3/2}}\ k\ \exp(-k^2/4\alpha). \tag{5}$$

Also

$$e^{aT_r}\ \frac{\sin kr}{r} = \exp(a\hbar^2 k^2/m)\ \frac{\sin kr}{r}, \tag{6}$$

m being the nucleon mass.

Operating both sides of eqn.(4) by e^{aT_r} and using eqns.(5) and (6) it is easy to see that $e^{aT_r} e^{-\alpha r^2}$ is a Gaussian function.

It is now straightforward to write down the expression for the deuteron OP for elastic scattering[1,2].

The real part of the calculated potential is fitted by

$$V(R) = -V_0/[1+\exp(\frac{R-R_0}{a_0})], \tag{7a}$$

and the imaginary part by

$$W(R) = -W_v / [1 + \exp(\frac{R - R_v}{a_v})] - 4W_s S(R) / [1 + S(R)]^2, \quad (7b)$$

where

$$S(R) = \exp(\frac{R - R_s}{a_s}).$$

III. RESULTS AND DISCUSSIONS:

In Fig.1 the angular distributions for elastic scattering of deuteron from Ni at energies 11.8, 13.5 and 21.6 MeV are shown along with the experimental results; the corresponding potential parameters are shown in Table I. We have calculated for several other targets as well, and the quality of fit is same as shown in Fig.1. If, one compares the quality of fit of our calculations and those of Perey and Perey[4] then it is observed that the goodness of our fit lies in between their "average geometrical parameters calculations" and "six parameters variation calculations". So we conclude that the formalism used here can reproduce the deuteron OP for elastic scattering satisfactorily with proper choice of nucleon OP.

REFERENCES:

1. S. K. Samaddar, R. K. Satpathy and Suprokash Mukherjee; Nucl.Phys. A160, 655 (1970).

2. S. Mukherjee, ibid A118, 423 (1968).

3. C. A. Engelbrecht and H. Fiedeldey; Ann.of Phys. 42, 262(1967).

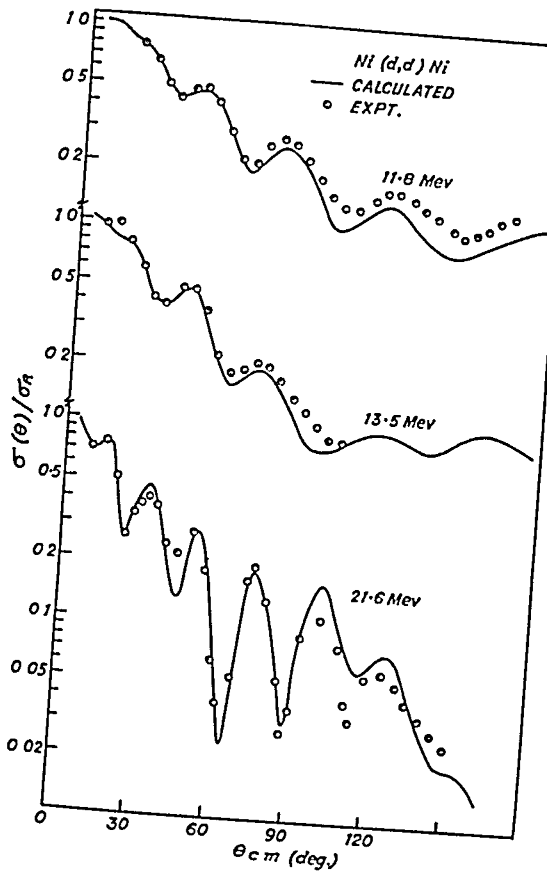
4. C. M. Perey and F. G. Perey; Phys.Rev. 132, 755(1963).

Table I

E(MeV)	V_o(MeV)	W_v(MeV)	r_v (fm)	a_v(fm)	W_s (MeV)
11.8	50.0	2.8	1.240	0.88	14.1
13.5	48.0	3.5	1.245	0.87	13.7
21.6	40.0	6.8	1.260	0.84	12.0

For all cases: r_o = 1.28 fm, a_o = 0.82 fm,

r_s = 1.41 fm and a_s = 0.61 fm.



Ni (d,d) Ni
CALCULATED
EXPT.
11·8 Mev
13·5 Mev
21·6 Mev
σ(θ)/σR
1·0
0·5
0·2
0·1
0·05
0·02
0
30
60
90
120
θ c m (deg.)

PHOTOPRODUCTION OF CHARGED PIONS FROM ^{12}C

K. Srinivasa Rao
MATSCIENCE, The Institute of Mathematical Science, Madras-20
and
V. Devanathan and G N S Prasad
Department of Nuclear Physics, University of Madras, Madras-25

ABSTRACT

The photoproduction of π^+ from $^{12}C(o^+, g.s.)$ leading to the five bound states $J^{\pi} = 1^+, 2^+, 2^-, 1^-, 3^-$ of ^{12}B and the photoproduction of from $^{12}C(o^+, g.s.)$ leading to the ground state of $^{12}N(J^{\pi} = 1^+)$ are studied by means of a transition operator obtained in the impulse approximation, assuming the ground state (g.s.) of ^{12}C to be spherical and using the particle-hole wavefunction calculated in the Tamm-Dancoff Approximation by Gillet and Vinh Mau[1] for the final nuclear states of ^{12}B and ^{12}N. The volume and surface production mechanisms have been used in the study.

The total cross-sections for $^{12}C(\gamma, \pi^+)^{12}B$ (obtained as a sum of 'partial' cross sections) and $^{12}C(\gamma, \pi^-)^{12}N$ exhibit a smooth variation with incident photon energy in the case of the surface production mechanism. We point out and emphasize that the reaction $^{12}C(\gamma, \pi^-)^{12}N$ is most favourable for drawing definite conclusions about the mechanism for photoproduction, since the only final nuclear state which is stable against nucleon emission is the ground state of $^{12}N(J^{\pi} = 1^+)$ in this case.

1. V. Gillet and N. Vinh Mau, Nucl. Phys 54, 321 (1964)

PHOTOPRODUCTION OF PIONS AND THE GROUND STATE WAVEFUNCTION OF ^{16}O

K. Srinivasa Rao
MATSCIENCE, The Institute of Mathematical Sciences, Madras-20

and

V. Devanathan
Department of Nuclear Physics, University of Madras, Madras-25

ABSTRACT

The existenceof 'deformed' components in the ground state wavefunction of ^{16}O, predicted by Brown and Green[1], has been recently confirmed by Purser et al[2]. We study the effect of these two-particle-two-hole correlations on the reaction,



$$\gamma + {}^{16}O(0^+, g.s.) \rightarrow \pi^+ + {}^{16}N(0^-, 1^-, 2^-, 3^-, \text{bound}) \quad \ldots\ldots\ldots (1)$$

From our analysis using various particle-hole wave functions for the bound states of ^{16}N, we draw the following conclusion: Without invoking the phenomenological surface production mechanism, a better agreement between theory and experiment for (1) can be obtained using the Kuo wave-functions with screening for ^{16}N states together with the deformed ground state wavefunction of ^{16}O obtained by Purser et al from an analysis of the $^{16}O(d, {}^{3}He)^{15}N$ experiment.

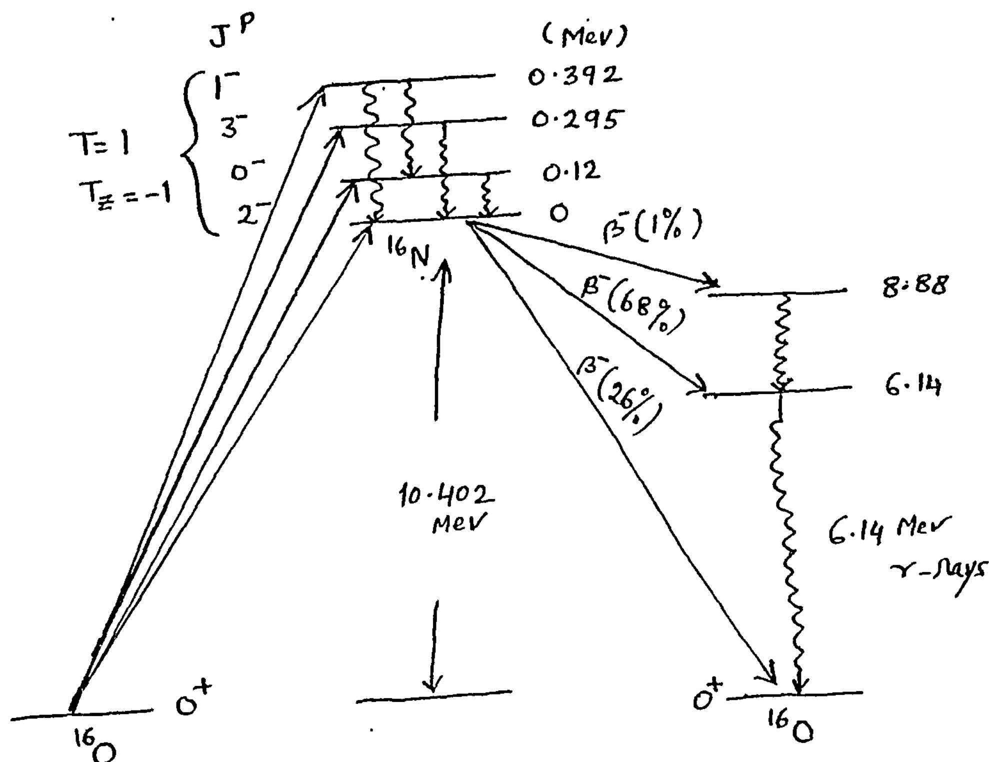
1. G. E. Brown and A. M. Green, Nucl. Phys. 75, 401 (1966).

2. K. H. Purser, W. P. Alford, D. Clines, H. W. Fulbright, H. E. Gove and M. S. Krick, Nucl. Phys. A132, 75 (1969).

DISCUSSION

N. Sarma: How are you sure it is a (γ, π^+) reaction?

K. Srinivasa Rao: The incident photon energies are above the threshold for pion production. In the experiment for $^{16}O(\gamma,\pi^+)^{16}N$, Meyer et al. (Phys. Rev. 138, B1421 (1965)) measure the 6.14 MeV γ-rays in ^{16}O shown in figure below. Though they do not look for the outgoing pion, the reaction kinematics ensure pion photoproduction, and the experimentalists, I believe, are sure about this.



Level scheme for the reaction $^{16}O(\gamma,\pi^+)^{16}N$ and subsequent decays. Solid upward arrows on the left show the photon induced transitions, while the solid downward arrows on the right indicate the β-decays with branching ratios and the wiggly arrows show the γ-de-excitations. The experimentalists measure only the 6.14 MeV γ-rays in ^{16}O.

PHOTOPRODUCTION OF CHARGED PIONS FROM ^{27}Al, ^{51}V AND ^{60}Ni

V. Devanathan and G. N. S. Prasad
Department of Nuclear Physics, University of Madras, Madras-25

and

K. Srinivasa Rao
MATSCIENCE, The Institute of Mathematical Sciences, Madras-20

ABSTRACT

A good agreement between theory and experiment was obtained for the reactions $^{16}O(\gamma,\pi^+)^{16}N$ and $^{11}B(\gamma,\pi^+)^{11}Be$, for which the final nuclear bound states that are stable against nucleon emission are well-known. Here, we extend our calculations to a few more reactions of this type: $^{27}Al(\gamma,\pi^+)^{27}Mg$, $^{51}V(\gamma,\pi^+)^{51}Ti$ and $^{60}Ni(\gamma,\pi^-)^{60}Cu$, for which experimental data are also available. The final bound states of the nuclei ^{27}Mg, ^{51}Ti and ^{60}Cu that are obtained in these reactions, are the low-lying states which are stable against nucleon emission and for which the complete information regarding the level scheme and spin-parity assignments are not available from spectroscopic data. It is suggested that the reactions of the type $A(\gamma,\pi^{\mp})B$ can be employed to extract information regarding the low-lying states of the nucleus B which are stable against nucleon emission.

EFFECT OF MULTIPLE SCATTERING ON POSITRON-ELECTRON RANGES

R.K. Batra, R.C.Grover+ and M.L. Sehgal
Physics Department, Aligarh Muslim University, Aligarh.

I. INTRODUCTION

The measurements on the ranges of positrons and electrons performed recently by Takhar[1] using coincidence technique and those reported earlier[2,3] indicate that the ranges $R^{\pm}(T)$ is a decreasing function of the atomic number of the absorber. As yet, there is no concrete theoretical interpretation to the measured data on ranges. In this paper, we propose to tackle the problem semi-theoretically.

II. PROCEDURE

According to the continuous-slowing-down-approximation[4], the c.s.d.a. range is given by

$$R^{\pm}(T) = \int_0^T \left[-\frac{1}{\rho}\left(\frac{dE}{dx}\right)^{\pm}_{Tot} \right]^{-1} dT \quad \cdots\cdots \quad (1)$$

Where
$$-\frac{1}{\rho}\left(\frac{dE}{dx}\right)^{\pm}_{Tot} = -\frac{1}{\rho}\left(\frac{dE}{dx}\right)^{\pm}_{col.} - \frac{1}{\rho}\left(\frac{dE}{dx}\right)^{\pm}_{rad.} \quad \cdots \quad (2)$$

The upper and the lower signs correspond to positrons and electrons respectively. The standard expressions of the energy loss of electrons and positrons due to collision and bremsstrahlung loss are available in the literature.[5,6] Since the expression for the total stopping power is very rigorous, the integral in eq.(1) can

---

+ University Polytechnic, A.M.U. Aligarh.

be evaluated either numerically or empirically. Berger and Seltzer[4] have calculated $R^{\pm}(T)$ by solving eq.(1) numerically. However, we have used our empirical relations[7] to find out $R^{\pm}(T)$. The c.s.d.a. range thus obtained for a given energy T, increases with the higher value of Z, the atomic number. Thus, it is concluded that the c.s.d.a. ranges do not explain the experimental ranges.

While passing through matter, electrons and positrons undergo both elastic and inelastic interactions. We know that in the treatment of the c.s.d.a. ranges, the inelastic interactions have been considered alone. Large angle Rutherford scattering in the course of penetration is a rare event but small angle multiple scattering, especially near the end of the electrons' range, introduces large deviations from the electrons' straight path.

The method of applying multiple scattering consists in expressing the mean square angle of multiple scattering as a function of kinetic energy $T = (\gamma-1) m_0 c^2$ and then making use of the Wilson's[8] assumption that the electrons move in the initial direction till their energy drops to a value for which the calculated value of $\langle \theta^2 \rangle$ has attained such a large value that the electrons thereafter start diffusing in a random way which contributes to straggling only. Let $\langle \theta_r^2 \rangle$ represent such an angle.

When electrons traverse through a foil of thickness 'dx' and N the number of target atoms per c.c.; the mean square angle of multiple scattering[9] is given by

$$\langle \theta^2 \rangle = 2\pi N \int_0^x dx \int_{\theta_s}^{\pi} \theta^2 \sigma(\theta) \sin\theta \, d\theta \quad ----(3)$$

where $\sigma(\theta)$ is the elastic scattering cross-section and θ_s the screening angle[9]. Substituting the value of 'dx' from our empirical relations[7] and integrating eq.(3), we obtain $\langle \theta^2 \rangle$ in terms of the total incident energy γ_0 and γ the energy of the electrons at an instant of penetration. The circumstance of the experiment of transmission of electrons is that the projection ϕ of the total scattering angle θ on the plane containing the initial trajectory should be considered. It is easy to prove[9] that $2\langle \phi^2 \rangle = \langle \theta^2 \rangle$. From the definition of the transport mean free path together with the Wilson's assumption[8], it follows that $\langle \theta_r^2 \rangle = 2$ and hence $\langle \phi_r^2 \rangle = 1$. This simplification permits to compute T_r . So, for an incident kinetic energy T of electrons, Tr can always be computed. Subracting the c.s.d.a. R(Tr) from R(T), we find a quantity which is very close to the experimental range.

III. CONCLUSIONS

Multiple scattering correction reduces the c.s.d.a. ranges of electrons. The similar correction for positrons need further inclusion of the differentiating term between positrons and electrons in the general expression of $\langle \theta^2 \rangle$. The calculations on this basis has yet to done.

REFERENCES

1. P.S. Takhar, Phys. Rev. 157, 257 (1967).

2. H.H. Seliger, Phys. Rev. 100, 1029 (1955).

3. K. Gubernator, Z. Physik 152, 183 (1958).

4. M. J. Berger and S.M. Seltzer, National Research Council Publication No.1133, 205-208 (1964).

5. F. Rohrlich and B.C. Carlson, Phys. Rev. 93, 39 (1954).

6. H.W. Koch and J.W. Motz, Rev.Mod.Phys. 31, 920(1959).

7. R.K. Batra and M.L. Sehgal, Nucl. Phys. A156, 314 (1970

8. R.R. Wilson, Phys. Rev. 84, 100 (1951).

9. B. Rossi and K. Greisen, Rev. Mod. Phys. 13, 262 (1941

K^- ABSORPTION IN $^{157}_{64}Gd$

D. Chattarji
Department of Physics, Visva-Bharati University,
Santiniketan, West Bengal.

From a recent survey of kaonic X-ray intensities for different atoms, Wiegand and Kunselman [1] have concluded that nuclear matter - very probably neutrons - extends further than the charge distribution. By using the intensity of the last X-ray transition observed in a given element as a built-in calibration for the probability of nuclear K^- capture in its upper orbit, they made quantitative estimates for the corresponding capture rate. For example, in kaonic gadolinium ^{157}Gd the experimentally calibrated capture rate from the 7i orbit ($n=7$, $l=6$) turns out to be 1.2×10^{16} sec^{-1}. Using a Woods-Saxon distribution for nuclear matter

$$\rho(r) = \frac{\rho(0)}{1+\exp(r-R_o/a)}, \tag{1}$$

a theoretical estimate of the capture rate was approximated by the overlap integral

$$P_{cap} = \frac{W}{\hbar}\int \rho(r)\, R^2_{n,n-1}\, r^2 dr. \tag{2}$$

W, the imaginary part of the K^--nucleus optical potential, was chosen to be the "conveniently round figure" of 100 MeV on the assumption that its precise value would not be material to the question of nuclear matter distribution. $R_{n,n-1}$ is the normalized hydrogenic radial wave-function for K^-. With identical parameters for protons and neutrons, i.e. $\rho(0) = 0.14$ nucleons per F^3,

R_o = 1.07 $A^{1/3}$F, a = 0.55 F, Wiegand and Kunselman obtained a theoretical capture rate of 2.5 x 10^{14} sec^{-1}, which is a factor of 50 less than the calibrated rate. In trying to bring the theoretical estimate into agreement with the experiment, the following points were made.

(i) W is a multiplying factor and cannot account for this discrepancy.

(ii) Kaons react about equally on neutrons and protons through the reactions $K^- + N \rightarrow$ hyperon + pion. Since the proton distribution is well-determined through electron-scattering experiments, the above discrepancy is deemed to imply a neutron tail extending beyond the conventional nuclear surface.

We wish to point out here that the magnitude of W is quite relevant to this calculation. The possible range of values from 30 to 300 MeV cited by the authors in itself introduces an uncertainty amounting to a factor of 10. Moreover, the points (i) and (ii) above are quite closely related, because W depends on the imaginary parts of a_o and a_1, the scattering lengths for the I=0 and I=1 isospin channels. It so happens that Im $a_o \approx$ Im a_1, so that Im $a_o \approx$ Im $\frac{a_o+a_1}{2}$ and the cross-sections for the K^-n and K^-p channels are nearly equal [2]. This makes W approximately proportional to the imaginary part of $\bar{a}$, the average of a_o and a_1, which is far from arbitrary. In fact, the scattering lengths are strongly momentum - dependent and even an approximate calculation must tie them to the nuclear Fermi momenta. Following previous studies [3], we have used an average relative momentum of 160 MeV/c for the K^--nucleon system, for which the effective K^--p cross-section σ_p=338 mb and the effective K^--n

cross-section σ_n=155 mb. Correspondingly, $\bar{\sigma}$, the average weighted $\bar{K}$-nucleon cross-section, is given by

$$\bar{\sigma} = \frac{2W}{\hbar} \tag{3}$$

where

$$W = (77 - 29\frac{N-Z}{A})\ \mathrm{MeV}. \tag{4}$$

Another important point is that ^{157}Gd is a strongly deformed nucleus with a quadrupole moment of 2.05 barns. Writing

$$R(\theta) = R_o\left[1+\beta Y_2^0(\theta,\varphi)\right] , \tag{5}$$

and using the approximate expansion

$$\frac{1}{1+\exp(r-R(\theta)/a)} = \frac{1}{1+\exp(r-R_o/a)} + \beta Y_2^0(\theta,\varphi)\frac{\exp(r-R_o/a)}{[1+\exp(r-R_o/a)]^2} \tag{6}$$

it can be shown that the quadrupole term makes a quite large contribution to the capture rate. Using identical parameters for the neutron and proton distributions, namely, $\rho(0)$ = 0.14 nucleons per F^3, R_o=1.07$A^{1/3}$F and a = 0.55 F, i.e. the values used by Wiegand and Kunselman for the proton distribution, we get P_{cap}=4.08 x 10^{16} sec^{-1}. Since the calibrated rate of 1.2 x 10^{16} sec^{-1} provides, after all, a lower limit for the actual value, we can see that even such a rough calculation agrees fairly well with experiment. Using the more realistic value of R_o = 1.1 $A^{1/3}$F characteristic of heavier nuclei, and surface thickness a = 0.523 F for deformed nuclei [4], the slightly lower capture rate of 3.8 x 10^{16} sec^{-1} is obtained. It seems, therefore, that there is no need to postulate a neutron distribution with parameters different from the proton parameters in order to explain the experimental results. In particular, since

these parameters are the quantities under investigation, it is desirable that the other variants in the model be chosen as realistically as possible before definite assertions can be made about the distribution of nuclear matter in the surface region.

A more detailed calculation along the above lines is now in progress and will be reported shortly.

The author would like to acknowledge some helpful discussions with B.K. Talukdar.

REFERENCES

1 C.E. Wiegand and R. Kunselman, International Conference on Hypernuclear Physics, Argonne National Laboratory, Argonne, Illinois (1969) 669; also C.E. Wiegand, Phys. Rev. Letters 22, 1235 (1969).

2 J.K. Kim, Phys. Rev. Letters 19 (1967) 1079; also J.K. Kim and F. von Hippel, Phys. Rev. Letters 20 (1968) 1303.

3 J.R. Rook, Nucl. Phys. 39 (1962) 479; ibid B9 (1968) 441; E.H.S. Burhop, Nucl. Phys. B1 (1967) 438.

4 L.R.B. Elton, Nuclear charge distributions; in Landolt - Bornstein, Numerical Data and Functional Relationships in Science and Technology, New Series, ed. by K.H. Hellwege, Group I, Vol. 2 (Springer Verlag, Berlin-Heidelberg New York, 1967), p. 1.

Min - Yi Chen, Nuclear Polarization in muonic atoms, Columbia Univ. Preprint 1969.

PHOTODISINTEGRATION OF THE ALPHA PARTICLE

H.L.Yadav, D.Mahanti and B.K.Srivastava
Department of Physics, Indian Institute of Technology, Kharagpur.

In the present paper we calculate the integrated and the bremsstrahlung-weighted cross sections for the photodisintegration of the alpha particle using the sum rules of Levinger and Bethe[1] as extended by Rustagi and Levinger [2]. We have used the velocity-dependent potential of Nestor et.al.[3] which contains a tensor component also.

The form of the Nestor [3] two-body potential is

$$U_j = \left[V_j^c(r) + \left\{ \left(\frac{p^2}{\hbar^2}\right) \omega_j(r) + \omega_j(r) \left(\frac{p^2}{\hbar^2}\right) \right\} + V_j^T(r) S_{12} + V_j^{LS}(r) \vec{L}\cdot\vec{S} \right], \qquad (1)$$

where index j stands for the four parts of the interaction singlet even, singlet odd, triplet even and triplet odd.

The ground state of the alpha particle is described by the Irving wave function[4] which contains a mixture of the $^1S_0$ and the principal $^5D_0$ states. The values of the wave function parameters are obtained from a variational calculation of the binding energy of the alpha particle.

Foldy [5] has shown that for a nucleus whose ground state wave function is completely symmetric in the space coordinates of all the nucleons, bremsstrahlung weighted cross section σ_b is given by

$$\sigma_b = \int_0^\infty \left(\frac{\sigma}{W}\right) dW = \left(\frac{4\pi^2}{3}\right)\left(\frac{e^2}{\hbar c}\right)\left\{\frac{NZ}{A-1}\right\}\langle r^2 \rangle_{00}, \qquad (2)$$

Where $\langle r^2 \rangle_{00}$ is the mean square charge radius of the alpha particle. Using the parameters obtained, the value of the root mean square charge radius for the alpha particle comes out to be 1.41 fm. which is quite close to the experimental value of 1.44 fm. obtained from electron-helium experiments (6). Eq. (2) then gives

$$\sigma_b = 2{\cdot}56 \text{ mb.} \tag{3}$$

The integrated cross section $\sigma_{int.}$ in the electric dipole approximation is proportional to the summed oscillator strength $\sum_n f_{0n}$

$$\sigma_{int.} = \frac{2\pi^2 e^2 \hbar}{mc} \sum_n f_{0n} \tag{4}$$

We evaluate different matrix elements in eq. (4) using the integral transform (7)

$$\exp(-ar) = \frac{1}{2} a \pi^{-\frac{1}{2}} \int_0^\infty s^{-\frac{3}{2}} \exp\left[-(a^2/4s) - s r^2\right] ds \tag{5}$$

The integration over the transformation variable s is carried out numerically. Finally we obtain

$$\sigma_{int.} = \frac{2\pi^2 e^2 \hbar}{mc} \left\{1 + 0{\cdot}1612 + 0{\cdot}6354\left(x + \tfrac{1}{2} y\right) + 0{\cdot}1480 x'\right\} \tag{6}$$

Where x and y are respectively the fractions of Majorana and Heisenberg exchange forces in the central part of the static potential while x' is the fraction of the Majorana exchange force in the tensor part of the potential.

Assuming $x = x'$, we get

$\sigma_{int.}$ = 93.2 MeV mb (for Serber mixture)

= 108.1 MeV mb (for Rosenfeld mixture)

Table I shows our results along with those of other workers.

Table I

Values of the integrated and the bremsstrahlung weighted cross sections for ^4He.

Reference	σ_{int} (MeV mb) Serber mixture	Rosenfeld mixture	σ_b (mb)
Present calculation	93.2	108.1	2.56
Rustgi and Levinger[(a)]	86.3	102.0	1.23
Goldhammer and Valk[(b)]	107.0	-	2.73
Srivastava and Jain[(c)]	101.0	123.0	3.08
Experimental [(d)]	95± 7		2.40 ± 0.15

a) Ref;(2) Using tensor potential without hard core.

b) Ref: (9) Using tensor potential with hard core.

c) Ref:(10) Using central velocity-dependent potential.

d) Ref: (8)

A comparison of our results with those of previous calculations shows that our results are in better agreement with the experimental values of Gorbunov and Spiridonov[(8)]. Also comparison of our results with those of Goldhammer and Valk[(9)] establishes reasonably well the equivalance of hard core and the velocity-dependent potentials. in photoeffect calculations.

REFERENCES :

1. J.S.Levinger and H.A.Bethe; Phys. Rev. 78,115 (1950)

2. M.L.Rustgi and J.S.Levinger; Phys. Rev. 106,530 (1957)

3. C.W.Nestor,Jr.,K.T.R.Davies,S.J.Krieger and M.Baranger; Nucl. Phys. A113, 14 (1968)

4. J.Irving ; Proc. Phys. Soc; London, 66A,17 (1953)

5. L.L.Foldy; Phys. Rev. 107, 1303 (1957)

6. R.Hofstadter; Rev. Mod. Phys. 28,214 (1956)

7. P.A.Roberts; Nucl. Phys. 81,387,(1966)

8. A.N.Gorbunov and V.M.Spiridonov ; Zh.Eksperim. i Teor. Fiz. 33, 21 (1957)

9. P.Goldhammer and H.S.Valk; Phys. Rev. 127, 945 (1962)

10. B.K.Srivastava and S.C.Jain; Phys. Rev. 164,1223(1967)

STUDY OF THE TWO HOLE STATES IN ^{12}C NUCLEUS WITH THE (π^-, nn) REACTION

B.K Jain
Nuclear Physics Division, Bhabha Atomic Research Centre, Bombay.

It is known now that due to kinematical considerations the absorption of negative pions on nuclei takes place preferentially on higly correlated pairs of nucleons. It is therefore expected that the process can be used to study dynamic correlations in nuclei. Reactions like (π^-, NN) may also be used to study the two hole states in nuclei. For the latter type of study it is more useful to employ a semi-phenomenological procedure for the absorption process. With this idea, using the two nucleon absorption model of Eckstein[1], we developed a formalism[2] to study these two hole states. The present note presents a simplified version of this formalism and uses it to analyse the recent available data on the $^{12}C(\pi^-,nn)$ reaction.

The reaction cross-section for the absorption of a pion from a 1s orbit is written

$$dw \;\propto\; \rho \, |M_{fi}|^2 \qquad (1)$$

where ρ is the phase space factor. The matrix element M_{fi} consists of two terms and is given by

$$M_{fi} = \left[g_0 G_0 + (T_f\, 1\, \nu_f\, 0 \,/\, T_i\, \nu_i)\, g_1 G_1 \right] \qquad (2)$$

Here $(T_f\ 1\ \nu_f 0 \,/\, T_i\ \nu_i\ )$ is the iso-spin Clebsch-Gordon coefficient. G_0 and G_1 correspond respectively to the

contributions from the T = 0 and T = 1 states of two nucleons in the nucleus. g_0 and g_1 are the interaction parameters which are obtained from the analysis of pion production reactions at threshold; their values recently obtained by Figureau and Ericson[3] from the analysis of experimental data are

$$|g_0|^2 = 0.64 \pm 0.05 \text{ fm}^8, \text{and}, \ |g_1|^2 = 0.155 \pm 0.08 \text{ fm}^8$$

As we see from eqn.(2) T = 0 and T = 1 terms contribute coherently. Therefore, the computation of M_{fi} demands the knowledge of the relative phase of g_0 and g_1. It is not possible to get this information from pion production reactions. However it is not necessary to know the relative phase of g_0 and g_1 if either the initial or the final nuclear states have zero iso-spin. In that case the contribution to M_{fi} will come only from one of the two values of T. For these nuclei we can therefore write

$$|M_{fi}|^2 = |g_0|^2 \, |G_0|^2, \text{ for } T = 0 \qquad \ldots \quad (3)$$

and,

$$|M_{fi}|^2 = (T_f 1 \nu_f 0 | T_i \nu_i)^2 \, |g_1|^2 \, |G_1|^2, \text{for } T = 1$$

These equations are applicable to the absorption reaction on most of the even mass number nuclei (viz. ^6Li, ^{12}C, ^{16}O etc) Again, if we consider the back to back emission of neutrons the expressions for G_0 and G_1 are very much simplified. They are as follows:

$$G_0^{\ 2} = k^2 \sum_{J, M=\pm 1} (2J+1)^{-1} \Big| \sum_L \mathcal{G}_{fi}(L\ S = 1J\ T=0)(L10M|JM)E_{L0}\Big|^2 \qquad \ldots \quad (4)$$

$$|a_1|^2 = k^2 \sum_{J=L} (2J+1)^{-1} \left| \mathcal{G}_{fi}(LS=0J\ T=1) \right|^2 \left| F_{L,0} \right|^2 ,$$

where

$$F_{L,0} = \int d\vec{R}\ \chi^{(-)*}(\vec{k}_1,\vec{R})\ \chi^{(-)*}(\vec{k}_2,\vec{R})\ \phi_{L,0}(\vec{k},\vec{R})\ \phi_{\pi}(\vec{R}). \quad (5)$$

$\mathcal{G}_{fi}$ is the spectroscopic amplitude and measures the probability of taking out two nucleons with quantum numbers (LSJT) from the initial nuclear state i and leaving the residual nucleus in state f. χ's are the distorted waves for the two neutrons. $\vec{k}$ ($= (\vec{k}_1 - \vec{k}_2)/2$) is the momentum vector conjugate to the position vector of two neutrons.

^{12}C nucleus in its ground state has iso-spin, $T_i=0$ and spin, $J_i = 0^+$. The simplified expressions (3) and (4) are therefore directly applicable to it. Recently Cheshire and Sobottka[4] reported the (π^-,nn) reaction on ^{12}C. In this experiment they observe the peaks in the excitation energy spectrum of ^{10}B corresponding to the emission of nucleons from $(1p)^2$,(1s1p) and $(1s)^2$ configurations. We have analysed the emission from $(1p)^2$ configuration. Using the wave functions of Boyarkina[5] for ^{12}C and ^{10}B the relative strengths of the peak cross-section to various excited states of ^{10}B are as follows:

Exc.Energy (MeV)	0	0.717	1.74	2.15	3.59	4.72	5.16	5.5}
J_f,T_f	3^+0	1^+0	0^+1	1^+0	2^+0	3^+0	2^+1	2^+0
Relative Strength	1	25	45	108	~0	~0	~0	2

From this we note that a good resolution experiment should show the structure of three peaks in the $(1p)^2$

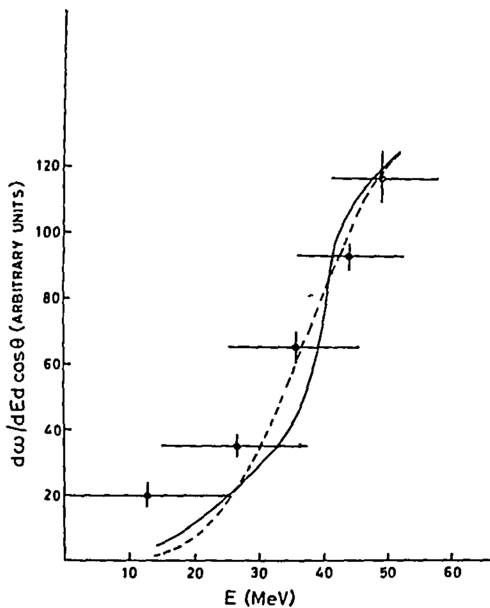
peak corresponding to the fi... three excited states of ^{10}B. Their strengths would roughly be in the ratio of 1:2:4. For the present analysis we have compared the experimental cross-section with the summed cross-section for these three states. This is shown in fig.1. The agreement is satisfactory. In order to estimate the effect of distortion of outgoing neutrons by the residual nucleus we have also plotted in fig.1 the result from a plane wave analysis. The introduction of distortions reduces the peak cross-section by a factor of 2.6.

It is important to note the agreement between experiment and our results which consider absorption from only the 1S orbit is in contradiction to the inference from pi-mesic X-ray data[6].

The X-ray data suggest that the absorption from 1S and 2p pionic orbit is comparable in ^{12}C. While analysing their (π^-,nn) data Cheshire and Sabottka also reached the same conclusion as ours. They were, however, not confident of their findings as the scattering of outgoing neutrons by the residual nucleus could not be computed in their formulation. In order to estimate the quantitatively the fractional contribution of 2P orbit to (π^-,nn) reaction, calculations are in progress.

REFERENCES

1. S.G. Eckstein, Phys.Rev. 129(1963)413.
2. B.K. Jain and B.Banerjee, Nuovo Cimento (in press)
   B.K. Jain, B.A.R.C. report (in press)
3. A. Figureau and M. Ericson, Nucl.Phys.B10(1969)349
4. D.L. Cheshire and S.E.Sobottka, Phys.Lett.30B(1969)244
5. A. Boyarkina, Eng.Trans. Bull.Acad. Sci.U.S.S.R.(Phys. Ser.)28(1964)255


dω/dEd cosθ (ARBITRARY UNITS)
120
100
80
60
40
20
10
20
30
40
50
60
E (MeV)

DISCUSSION

G. Ramachandran: I wish to make a couple of comments i) that the (π^-, nn) reaction is akin to the single nucleon transfer reactions that you referred to which needs a couple of nucleons in the nucleus to participate and therefore there could be a greater amount of similarities between types of information that you get from the reactions that you discuss and the single nucleon transfer reactions ii) Although the cross section for the (π^-, nn) reaction involves the Fourier transform of the relative wavefunction of the pair of nucleons, it may not be possible to empirically extract information about the nucleon-nucleon correlations from the experimental studies. I think the situation here is akin to what I have come across in a discussion of double charge exchange reactions (Nucl. Phys. 87, 107 (1966)) where integrals of this type over the two nucleon wave function occur but the Fourier transform gets once again integrated with respect to the momentum transferred.

V. Devanathan: Your results seem to indicate that the final state interactions are not very important. If that be so, it is in contradiction with the findings of Eisenberg and LeTourneax that the final state interactions are much more important than the two-nuclear correlations within the nucleus.

B.K. Jain: No, this is not true. Our results indicate that the shape of the angular correlation of the outgoing neutrons is not much changed by the final state interaction. The magnitude of the cross-section, however, is reduced appreciably. Therefore I don't think that our results are in apparent contradiction with that of Eisenberg and LeToureax.

P.P. Kane: The pi-mesonic $\times$-ray data establish very well the rate of absorption of the pion from the 2p-state. So the precise significance of your remark that this state does not agree with the absorption rate required by your model is not clear.

TRITON KNOCK-OUT FROM ^{7}Li NUCLEUS

A.K. Jain and N. Sarma
Nuclear Physics Division
Bhabha Atomic Research Centre, Bombay-85

Knock-out reactions provide information about the momentum distribution of the particles within the target nucleus. Direct observation of the clustering effects in nuclei should therefore be possible through knock-out reactions such as (p,pd),(p,pt),(p,pα) and (α,2α) reactions. The analysis of the reaction ^{6}Li(p,pd)^{4}He in terms of the cluster model of ^{6}Li has been very successful[1] and encourages us to analyse the ^{7}Li(p,pt)^{4}He reaction using a (α+ t) cluster model of ^{7}Li. Data on the ^{7}Li(p,pt)^{4}He reaction is available at 55 MeV incident energy from Hendrie et.al.[2]. These results have been analysed using a plane wave impulse approximation but a detailed analysis has tobe carried out before a definite statement can be made about clustering in ^{7}Li. Such a detailed analysis requires firstly, the antisymmetrization of the target wave function Secondly, as has been pointed out in many discussions, the intercluster wave function should have the correct asymptotic behaviour. A wave function with the correct asymptotic behaviour has been used in this work and we find it is of great importance in the determination of the angular distributions of the emitted particles. However the use of such correct wave functions creates computational difficulties. Finally the interaction of the incident and emergent particles with the initial and final nuclei has to be included through the use of distorted waves (i.e.,

DWIA matrix element for the transition is then given by

$$t_{if}(\underline{q},\underline{k}_3) = t_{pt}(q)\langle \Psi_f^{(-)} | \delta(\underline{r}_0 - \underline{r}_t) | \Psi_i^{(+)} \rangle ,$$
$$= t_{pt}(q)\, g_{if}(\underline{q},\underline{k}_3) ,$$

$t_{pt}(q)$ is the free p-t scattering amplitude and is a function of the momentum transfer q while $g_{if}(\underline{q},\underline{k}_3)$ is the momentum transform of the overlap integral of the final state with the initial state and is a function of $\underline{q}$ and the recoil momentum $\underline{k}_3$. The initial and final state wave functions $\Psi_i^{(+)}$ and $\Psi_f^{(-)}$ are given as follows,

$$\Psi_i^{(+)} = N_i\, \Phi_A(1234;567)\, \chi_i^{(+)}(\underline{k}_{0A}, \underline{r}_{0A}) ,$$
$$\Psi_f^{(-)} = N_f\, \Phi_\alpha(1234)\, \Phi_t(567) \chi_1^{(-)}(\underline{k}_{0\alpha}, \underline{r}_{0\alpha}) \chi_2^{(-)}(\underline{k}_{t\alpha}, \underline{R}).$$

The χ's here are the distorted waves and Φ's are the wave functions of the bound systems. The wave functions of the target nucleus is given by

$$\Phi_A(1234;567) = \mathcal{A}\{\psi_A(1234;567)\, \xi_A(1234;567)\} ,$$

ξ and ψ are respectively the spin and space parts of Φ and $\mathcal{A}$ is the antisymmetrizer. The space part ψ_A is expressed in the cluster model as a product of the internal wave functions of the clusters and the intercluster wave function. The form of ψ_A as given by Tang et.al[3] is

$$\psi_A(1234;567) = \exp\left\{-\frac{\alpha}{2}\sum_{i=1}^{4}\rho_i^2 - \frac{\beta}{2}\sum_{j=5}^{7}\rho_j^2\right\} \phi(\underline{R}) ;$$

ρ's are the coordinates of the particles with respect to the centres of mass of the clusters, and $\phi(R)$ has the form $R^3 \exp(-\frac{6}{7}\gamma R^2)\, Y_1^M(\hat{\underline{R}})$. The parameters α, β and γ were obtained by variational calculations. Using a partial wave expansion for χ's and summing over all the spin functions

and integrating over internal coordinates we get

$$g_{if}(\underline{q},\underline{k}_3) = \int X_{\underline{q},\underline{k}_3}(R)\{B_{NE}(R) - 3B_{SE}(R) + 3B_{DE}(R) - B_{TE}(R)\}\,dR$$

Here $X_{q,k_3}(R)$ comes from the three distorted waves and $\hat{\underline{R}}$ part of bound wave functions on summing over the partial waves. The subscripts NE,SE,DE and TE correspond to no, single, double and triple exchange of particle coordinates in the alpha and triton cluster wave function of the target nucleus.

To obtain the correct asymptotic behaviour,we have used an intercluster wave function

$$\varphi(R) = R^3 \exp\left(-\frac{6}{7}\gamma R^2\right) \quad , \quad R \leq 3.53\ fm,$$

$$= \left(\frac{1}{fR} + \frac{1}{f^2R^2}\right) \exp(-fR) \quad , \quad R \geq 3.53\ fm$$

The parameter $f\ \{= (2\mu_{t\alpha} E_{t\alpha}/\hbar^2)^{1/2}\}$ corresponds to the α-t separation energy $E_{t\alpha}$ = 2.47 MeV, $\mu_{t\alpha}$ is the reduced mass. In order to evaluate the exchange terms, it is found necessary to expand this correct intercluster wave function in terms of a series of Gaussians.

The numerical evaluation of the results is in progress for the 55 MeV data.

REFERENCES

1. A.K. Jain, N. Sarma and B. Banerjee;Nucl.Phys.A142 (1970)330.
2. D.L. Hendrie, M. Chabre and H.G. Pugh;UCRL report 16580, page 146.
3. Y.C. Tang, K. Wildermuth and L.D. Pearlstein, Phys. Rev. 123 (1961)548.

POSITRON-ELECTRON SCATTERING CROSS-SECTION

M.G. Shukla and M.R. Bhiday
Department of Physics
University of Poona, Poona-7

ABSTRACT

In order to verify Bhabha exchange term and to find the cross-section at half energy transfer, movable scintillation counters are used to increase the accuracy of measurements of coincidence counts. The gamma background from the source was reduced considerably by using a 60° double focussing sector magnet which also helped in selecting the beam energy.

The positron-electron scattering cross-section is not symmetrical about half energy transfer. In addition to the spin interaction found in Moller formula, Bhabha anticipated an exchange interaction due to virtual annihilation. This is a contribution to the scattering cross-section arising from virtual annihilation and recreation of a positron and an electron which go off in new directions. The net result will be scattering.

The results were corrected for multiple-scattering, annihilation of positron, decay of source, losses due to absorption in the foils etc.

The Bhabha-formula is verified with an accuracy of $\sim 8\%$. The ratio of electron-electron to positron-electron scattering cross-section was also verified both with and without the exchange effect. The results are in good agreement with the Bhabha theory.

ANALYSIS OF (p,2p) AND (e,e'p) REACTIONS ON ^{12}C NUCLEUS

R. Shanta and B.K. Jain, Nuclear
Physics Division, Bhabha Atomic Research Centre, Trombay

Recently there has been some confusion due to the reports published by Boffi et al., and Epp et al., about the analysis of the (e,e'p) and (e,e) reactions on ^{12}C. They observe that the bound state wave functions which fit the (e,e'p) data do not fit the (e,e) data on the same nucleus. This is in contradiction with the observation of Jain and Jackson who concluded that if the distortion of the incoming and outgoing protons is taken into account properly the wave function which fits the (e,e) data also fits the (p,2p) on the same nucleus. Their analysis however was restricted to (p,2p) data in the incident proton energy range of 155-185 MeV. Recently Simpson et al., have reported (p,2p) data on ^{12}C at 1GeV. Data at 460 MeV incident energy are already available in literature. We, therefore, have analysed in this report these high energy (p,2p) data on ^{12}C along with the (e,e'p) data at 600 MeV of Amaldi et al., using the single particle bound state wave function of Elton and Swift. These wave functions were derived to fit the $^{12}C(e,e)$ data.

The cross-section for the (p,2p) reaction in DWIA is written as

$$\frac{d^3\sigma}{d\Omega_1 d\Omega_2\, dE_p} = F_{pp}(\theta)\frac{d\sigma}{d\Omega_{pp}}\, P_{pp}(Q) \qquad (1)$$

Here F_{pp} is the kinematic factor, $\frac{d\sigma}{d\Omega_{pp}}$ is the free proton-proton cross-section and $P_{pp}(Q)$ is the distorted

momentum distribution. In the di-proton model,

$$P_{pp}(Q) = \sum_{jm} \left| (2\pi)^{-3/2} \int d\vec{r}\, \chi_p^{(-)*} \chi_k^{(+)} \psi_{jm}^{fi} \right|^2$$

where χ_p and χ_k are the distorted waves for the ce
of-mass of the outgoing protons and incoming proton re
ctively. $\psi_{jm}^{fi} \left(= \langle J_f M_f \mid J_i M_i \rangle\right)$ is the over
integral, and is related to the bound state wave func
of the struck proton. θ is the angle of each of the
outgoing protons with respect to the incident beam di
tion and E_p their energy. $\vec{Q}$ is the momentum of the r
sidual nucleus in the laboratory system.

For the (e,e'p) reaction the cross-section in
DWIA is written as

$$\frac{d^4\sigma}{dE_e\, d\Omega_e\, dE_p\, d\Omega_p} = F_{ep} \frac{d\sigma}{d\Omega_{ep}} P_{ep}(Q) \qquad ($$

where

$$P_{ep}(Q) = \sum_{jm} \left| (2\pi)^{-3/2} \int d\vec{r}\, e^{i\vec{q}\cdot\vec{r}} \chi_p^{(-)*} \psi_{jm}^{fi} \right|^2 \qquad ($$

$\vec{q}$ is the electron momentum transfer. Other factors
carry the same meaning as in eqn.(1) except that now t
refer to (e,e'p) reaction.

In the present paper we have analysed the angu
correlation distribution of the two reactions correspo
ing to the knock-out of 1p protons. In figs.1 and 2

sponding experimental points for the (p,2p) reaction at 460 MeV and 1GeV energies respectively. At 460 MeV we see that the shape of the cross-section is correctly reproduced. At 1GeV the experimental momentum distribution peaks around 150 MeV/c while the theoretical distribution at 100 MeV/c. In fig.3 we have plotted the (e,e'p) cross-section in arbitrary units. The positions of the experimental and theoretical peaks are at 70 MeV/c and 110 MeV/c respectively. The experimental full width at half maximum (FWHM) in the (e,e'p) reaction is however in agreement with that of the theoretical curve. The spectroscopic factor from the (p,2p) reaction by normalizing the theoretical peaks to the experimental ones are 4.76 and 9.74 at 460 MeV and 1GeV respectively. The corresponding value from sum rule is 8.

In the (e,e'p) reaction since the FWHM is the same for the experimental and theoretical curves the theoretical curve will fall mostly on experimental points if all the experimental points are displaced towards the right hand side by about 40 MeV/c. Hence before any definite conclusion is drawn from the shift of the theoretical peak from the experimental one new experimental information on this reaction is highly desirable. In the (p,2p) reaction at 1GeV the shift of the experimental peak towards higher momenta may be due to the rather short wave length (0.15 fm) of the projectile. This calls for the inclusion of the effect of the short range correlations in the treatment of the scattered protons. Further investigation of these observations is in progress.

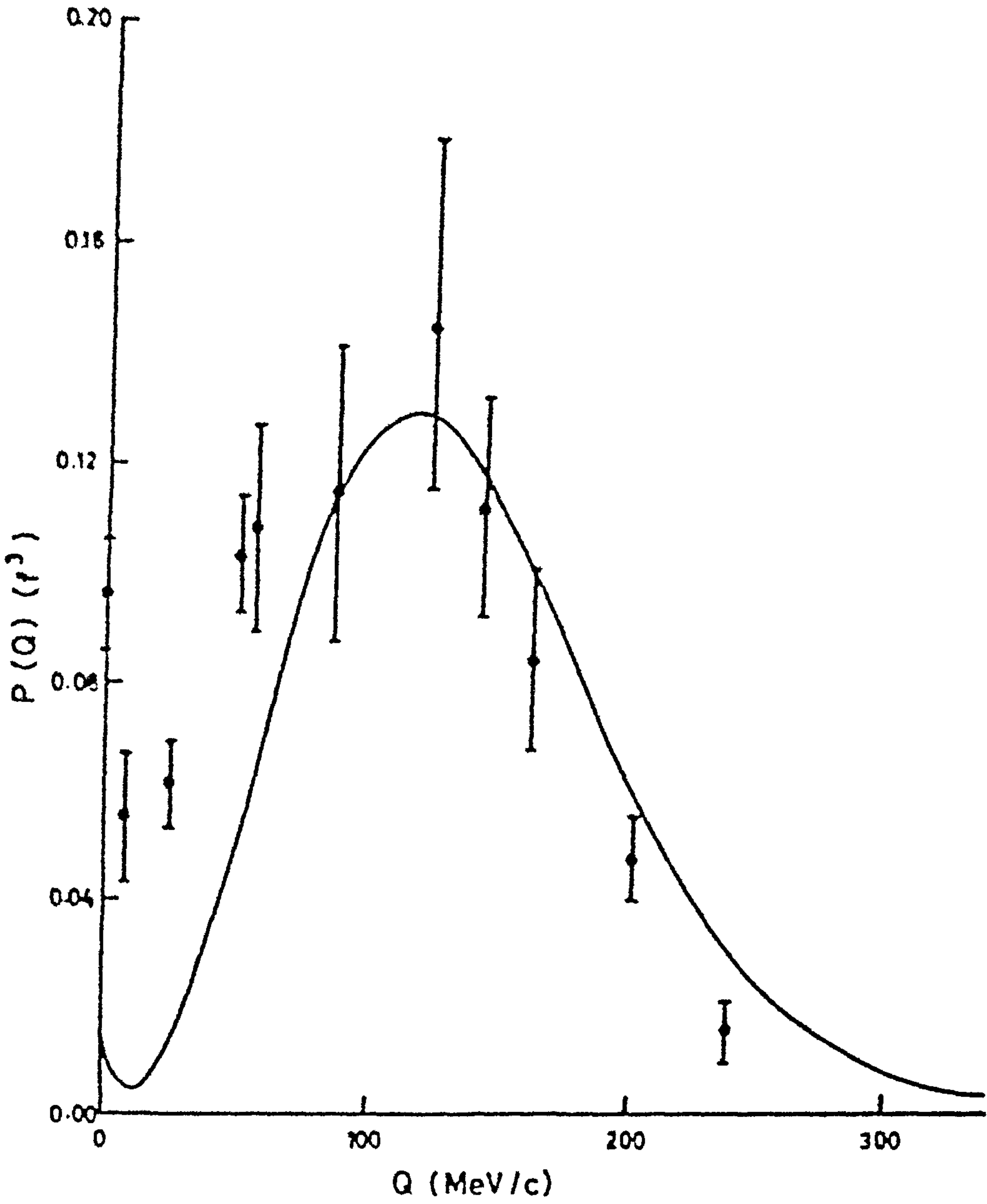


FIG.1

: Angular correlation distribution for (p,2p) reaction at 460 MeV.

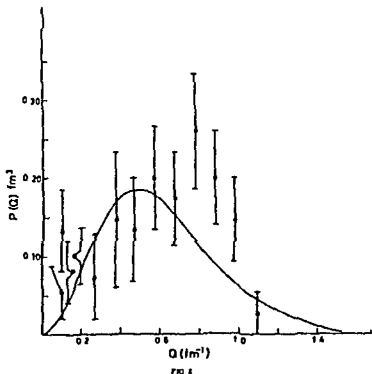


FIG 2

Angular correlation distribution for (p,2p) reaction at 1 GeV.

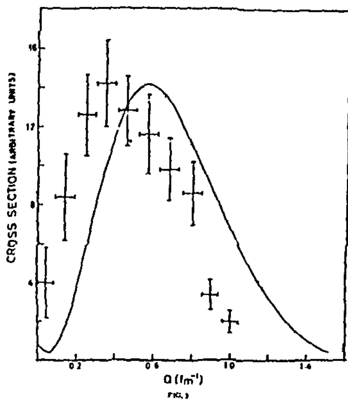


FIG. 3

Angular correlation distribution for (e e p) reaction

DISCUSSION

N. K. Ganguly: You have distorted the proton wave. What effect would the distortion in the electron wave would have.

R. Shanta: It is hardly effective since it is a pure electromagnetic interaction.

V. Devanathan: I would like to comment on as to why the distortion effects on the electron was not considered. It may be pointed out that the perturbation theory works admirably well for the electromagnetic interaction. In the case of electron scattering, the first term i.e. Born term should be quite sufficient since the second term would be smaller by the square of the coupling constant, viz. $\frac{1}{137}$ and as a consequence its contribution is less than 1%.

I wish to make another comment. The author has used essentially an impulse approximation and obtained the nuclear cross section in terms of the electron-proton cross section. In this treatment, off-the-energy shell effects are not properly taken into account. I have studied this process earlier (Ann. Phys. 1967) and therein I have pointed out that the momentum dependent effects of the bound nucleon may be correctly included by using McVoy - Van Hove effective Hamiltonian for the electron-proton interaction. Although, I have used a plane-wave approximation for the outgoing proton for simplicity, the distortion effects of the emitted proton was taken into account recently by Epp and Griffy (Phys. Rev. 19'0).

CONFIGURATION MIXING vs. EFFECTIVE SHELL MODEL

Raj K. Gupta and Ram K. Bansal
Department of Physics, Panjab University, Chandigarh-14.

In recent years, one of the outstanding problems in nuclear spectroscopy has been the demand for 'good' nuclear wave-functions— a demand which may or may not be met with the upto-date theoretical tools. In the shell model calculations a choice of configuration space, which determines the amount of configuration mixing, is intimately related to the quality of shell model wave-functions. This choice, however, is always dictated by certain practical considerations; i.e. either by the availability of only a fewer single-particle excitation energies or the desire to limit the size of the Hamiltonian matrix. Specifically, the mixed shell model calculations have been done with the configuration space, mixing single particle orbitals upto 2.5 - 3 MeV excitations such that one has remained contented with the consideration of non-mixed parity configurations (only positive or negative parity states) and the perdictions of the structure of low lying nuclear states only. In general, the choice of configuration space and residual interaction which shall give a good wave function for a particular nucleus, has always been a problem in shell model and efforts have been made to simplify this situation.

In view of these general considerations, Cohn, Lawson and Soper[1,2] reported a calculation based on the socalled pseudo-nuclei, and thus put shell model to a critical test. They considered models of two isolated, degenerate single particle levels (in one case[1] neutrons in $1d_{3/2}$, $1f_{7/2}$ orbitals and in the other[2] both neutrons and protons in $1p_{\frac{1}{2}}$, $1d_{3/2}$ orbitals), solved them exactly and treated the results as 'pseudo - experimental' data. This way one had a set of (imaginary)

nuclei whose configuration is exactly known and its comparison with a second calculation using the effective shell model approximation (in terms of an inert core--$1d_{3/2}$ in one case and $1p_{\frac{1}{2}}$ in another) was sought. It was reported that not only the low lying levels of appropriate parity have their spins in agreement with the effective shell model configurations but also many other nuclear properties such as binding energies, magnetic moments, M1 transitions, log ft values for β-decay, the single nucleon spectroscopic factors and many B(E2) values and quadrupole moments are extremely insensitive to this large configuration mixing. Following this study Gupta and Trainor [3,4] have shown that such a situation is by no means general. They considered a case[3] of non-mixed parity configurations (neutrons in $2s_{\frac{1}{2}}$ and $1d_{5/2}$) and found that the 'pseudo-experimental' level ordering is not appropriate to the shell model approximation. Also, the degenerate aspect of the models has been shown to be rather misleading. The consideration of the two levels to be non-degenerate has also been found[4] to be essential even for the mixed parity configurations (taking neutrons in $1p_{\frac{1}{2}}$ and $1d_{5/2}$ orbitals). The results of all these four cases have been interpreted[4] to mean that it is much easier to conceal configuration mixing and core excitation in shell model studies where such effects involve mixed parity configurations (only two-particle-two-hole excitations) than it is for studies of non-mixed parity configurations (n particle-n hole excitations). This conclusion has been further supported by their[3,4] preliminary investigation using inelastic electron scattering for Coulomb excitation alone. It is found that the dependence of the electromagnetic form factors on momentum transfer is a sensitive test for configuration mixing.

In the cases studied, so far, we notice that though both odd-

and even-parity orbitals have been considered for exact calculations but, for the effective shell model, only a single orbital has been taken. In other words, the comparison of the 'pseudo-experimental' data consisting of either only positive or both positive and negative parity states has been made with the shell model theory based on only single (positive or negative) parity states. It is thus important to extend these large configuration mixing effects to a case of three, isolated, orbitals such that under the assumption of effective shell model (filling the lower most subshell) one has two active orbitals (rather than one) giving mixed (both positive and negative) parity states. Secondly, it seems useful to perform a more systematic study of the inelastic electron scattering form factors for both the transverse and Coulomb (longitudinal) excitation contributions in order to see whether the proposition of Gupta and Trainor (based on a preliminary calculation) is more real than apparent.

We have selected a model of three isolated levels $2s_{\frac{1}{2}}$, $1d_{3/2}$ and $1f_{7/2}$ (giving mixed parity states) such that in shell model approximation (taking $2s_{\frac{1}{2}}$ as inert core) also we get both positive and negative parity states. We refer to these (imaginary) nuclei as pseudo-sulphur (Psp) nuclei. Unfortunately, if we try to consider both neutrons and protons, filling these three levels, it is an enormous problem; thus we consider only the neutrons. The method of analysis is similar to that discussed in the references 3 and 4. We are now in the process of making computation and unfortunately do not have any numbers to report.

REFERENCES

1. S. Cohen, R.D.Lawson and J.M. Soper, Phys. Lett. 21, 306 (1966).

2. R.D. Lawson and J.M. Soper, Proc. Int. Conf. on nuclear physics, Gatlinburg, Tenn. (1966) p. 511.

3. L.E. H. Trainor and R.K. Gupta, Nucl. Phys. A108, 257 (1968).

4. R.K. Gupta and L.E.H. Trainor, Nucl. Phys. A120, 273 (1968).

DISCUSSION

N.G. Puttaswamy: For the case of pseudonium, is it established that the electromagnetic properties are insensitive to configuration mixing?

R.K. Bansal: This is the claim made by Argonne National Lab. Group around 1963 or so.

STUDY OF THE $^{37}Cl(p,\gamma)^{38}Ar$ REACTION FOR E_p=1.5 to 4 MeV

N.G. Puttaswamy
Department of Physics, Bangalore University, Bangalore, and
Argonne National Laboratory, Argonne, Illinois, U.S.A.
and
R.E. Segel
Argonne National Laboratory, Argonne, Illinois, U.S.A.

I. INTRODUCTION

Photonuclear reactions and particle capture reactions are powerful means of studying the giant-dipole resonance in nuclei. The capture reactions in particular can be performed under high resolution. Giant resonances in ^{36}Ar and ^{38}Ar are of interest because they can provide information about the isospin splitting of the giant resonance[1]. As ^{38}Ar is not a self-conjugate nucleus, both T=1 and T=2 components are expected. The $^{37}Cl(p,\gamma)^{38}Ar$ reaction has been studied earlier for E_p=4 to 14 MeV[2] and by many groups of workers for E_p below 2 MeV[3]. The present experiment is performed to fill the gap; the yield curves for gamma rays leading to the ground (γ_0) and the first excited (γ_1) states in ^{38}Ar are obtained for E_p=1.5 to 4 MeV.

II. EXPERIMENTAL PROCEDURE

The experiment was performed using the 4-MV Van-de-Graaff accelerator of Argonne National Laboratory, U.S.A. A 250 $\mu g/cm^2$ thick barium target, containing ^{37}Cl isotope and evaporated on a thick tantalum backing, was used. A 10"-diam. by 12"-thick NaI(Tl) crystal with an electronics setup capable of pileup suppression was used to detect the gamma rays and the spectrum was recorded on a

400-channel analyzer. A typical spectrum is shown in Fig. 1. for E_p=3.3 MeV. The peaks due to γ_0 and γ_1 are easily identified and the areas A and B are used to obtain the yield of the gamma rays. Cosmic ray background is estimated from the higher part of the spectrum and is subtracted in each case. The insert in Fig. 1 shows the γ_0 yield for the resonance at 2.125 MeV. The 21-keV width observed in this case is all due to target thickness and the actual width of the resonance is much smaller; this has been checked at the 1.54-MeV γ_1 resonance which is known to be very narrow.

III. RESULTS

The yield curves for γ_0 and γ_1 are shown in Fig. 2. Above 3 MeV pileup effects start becoming important (because the threshold for the ^{37}Cl(p,n) reaction is at 1.64 MeV) and the expected background due to pileup for γ_1 is indicated in the figure. The differential cross section at the peak of the 2.13-MeV γ_0 resonance is found to be approximately 1.74 μb/sr.

The yield curves are dominated by narrow resonances and most of the width observed experimentally is essentially the target thickness, the resonance width being much smaller. Strong γ_0 resonances are observed at E_p=1.85, 2.13 and 3.27 MeV; the one at 3.27 MeV could be conveniently used for target thickness measurement when only higher energy proton beams are available, as in the tandem Van-de-Graaff energy region. The yield curve for γ_1 shows strong peaks at E_p=1.54 and 1.60 MeV, but none very strong

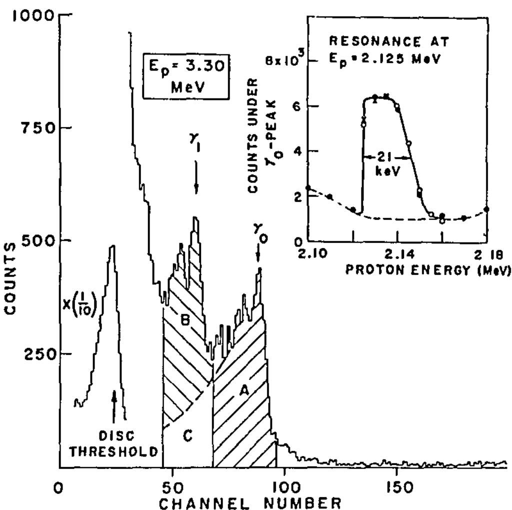


FIG. 1

Gamma-ray spectrum for the $^{37}Cl(p,\gamma)^{38}Ar$ reaction at E_p = 3.30 MeV. The insert shows the $\gamma 0$ yield taken over the 2.125-MeV resonance

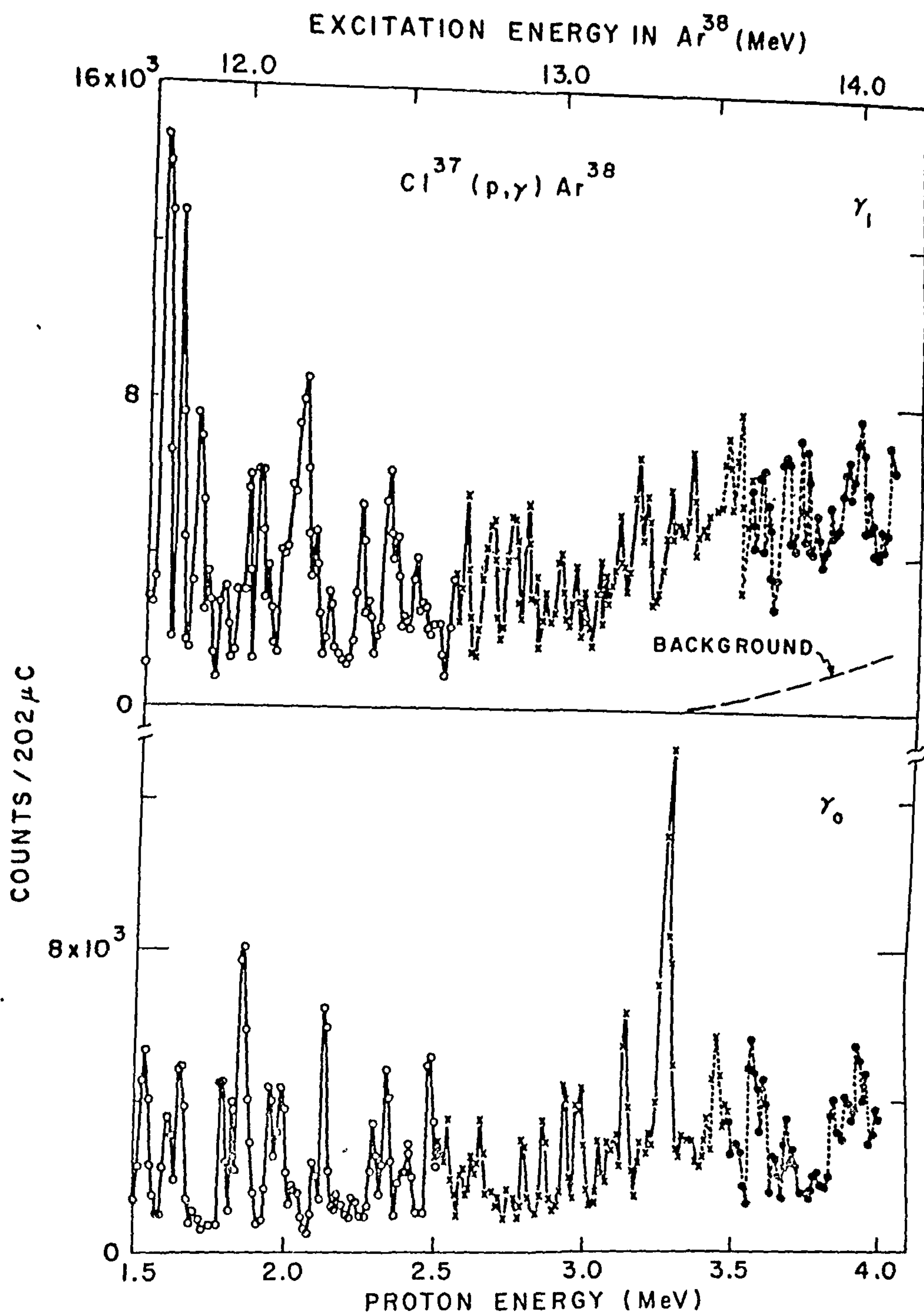


FIG. 2

Yield curves for γ_0 and γ_1 from the $^{37}Cl(p, \gamma)^{38}Ar$ reaction. The experimental points from three different runs are indicated by different symbols. The excitation energy in ^{38}Ar is also shown at the top of the plots.

between 2 and 4 MeV. For E_p above 3 MeV, the γ_0 yield begins to show a broader structure on which the narrow resonances are superposed. The integrated $^{38}Ar(\gamma,p_0)$ cross section in the region between E_p=1.5 to 4 MeV is less than 1% of the classical electric-dipole sum of 0.55 MeV-b. A further study upto E_p=14 MeV[2] reveals that the γ_0 yield appears as two broad peaks at 6 MeV and 11 MeV with widths of about 6 MeV and 3 MeV, respectively and these may be attributed to a splitting of the ^{38}Ar giant-dipole resonance into the T=1 and T=2 components.

REFERENCES

1. M.H. Macfarlane, Proceedings of the Conference on Isobaric Spin in Nuclear Physics, U.S.A., 1966, page 383.

2. R.E. Segel, L. Meyer-Schutzmeister, D.S. Gemmell, R.C. Bearse, N.G. Puttaswamy, H.T. Fortune, J.V. Maher, and E.L. Sprenkel-Segel, Bull. Am. Phys. Soc. 15, 47 (1970).

3. P.M. Endt and C. Van der Leun, Nucl. Phys. A105, 1 (1967).

DISCUSSION.

M.K. Mehta: You said you were not interested in the fine structure at all so probably you were not curious about the very striking sharp resonance at the low energy or in establishing the general nature of the "fine" structure over the higher energy range.

N.G. Puttaswamy: By the 'fine structure' I mean the narrow resonances which are there in plenty in the low energy region. These are interesting from the nuclear spectroscopy point of view. What is of more importance in the giant resonance region is the intermediate structure which can be attributed to the particle-hole states. Secondly, one wants to know the total integrated cross section.

N. Lingappa: How does the integrated cross-section exhaust the sum-rule in your case?

N.G. Puttaswamy: The integrated (γ, p_0) cross section for E_p between 4 and 14 MeV has been found to be about 14% of the sum rule and below 4 MeV it is less than 1%. Hence a substantial part of the sum rule is in the other channels.

S.K. Gupta: 1) The integrated cross section should include (γ, n) cross section which may dominate.
2) We observe a structure of intermediate width in $^{37}Cl(p,n)$ reaction at 2.13 MeV. This has also been found in the (p, α_0) data.

N.G. Puttaswamy: (γ,n) and (n,p) cross-sections are usually of the same order of magnitude.

A.S. Divatia: Is elastic scattering data on $^{37}Cl(p,p_0)^{37}Cl$ reaction available?

N.G. Puttaswamy: I don't think that there is any data above $E_p = 2$ MeV.

COULOMB EXCITATION OF SELENIUM ISOTOPES

A.P. Agnihotry, K.P. Gopinathan, M.C. Joshi and M.G. Prasad
Tata Institute of Fundamental Research, Bombay

As part of a program for measurement of g factors of levels excited in nuclear reactions by the technique of perturbed angular distribution of γ-rays using high resolution Ge(Li) detector, we report the preliminary results of the Coulomb excitation of Se^{77} levels and of the even even nuclei of Se.

EXPERIMENTAL

A thick target of natural selenium metal was exposed to singly charged helium ions from the 5.5 MeV Van-de-Graaff accelerator at Trombay. To reduce the loss of selenium by volatalization the beam current was kept low and the target cooled by a cold finger kept at liquid nitrogen temperature. The γ-ray spectra following Coulomb excitation of the selenium isotopes were observed at 55 degrees with respect to the beam by a 20 cc Ge(Li) detector. A typical spectrum with beam energy 5.001 MeV is shown in Fig. 1 where the γ-ray peaks of various Se isotopes are identified. The relative intensities of the γ-rays were determined after correcting for the efficiencies. The photopeak efficiencies for Ge(Li) detector as a function of energies of γ-rays were determined by taking spectra of [illegible], Ir^{192} and [illegible] having γ-rays of known relative intensities. The absolute photopeak efficiencies were obtained by using I.A.E.A. standard sources of [illegible], [illegible], [illegible] and [illegible]. The relative yields of γ-rays were calculated after correcting for relative abundance of the isotopes. [illegible] of Se^{78} was taken from the measurement of [illegible] (38.5 ± 0.[illegible]) e^2 [illegible]. [illegible]

10 APR (1970)
Se (α, α' γ)
E_α = 5·001 MeV
20 cc. Ge (Li) DETECTOR
1·46 keV / CHANNEL

65·6 (Ta) 88 136·3 (Ta) 165·4 (Ta) 200·5 (Se^{77}) 239·3 (Se^{77}) 250·2 (Se^{77}) 302·2 (Ta) 351·4

417·2 439·8 (Se^{77}) 511 559·4 (Se^{76}) 613·7 (Se^{78}) 634·9 (Se^{74}) 654·7 (Se^{82}) 666·2 (Se^{80})

COUNT RATE

CHANNEL NUMBER

FIG. 1

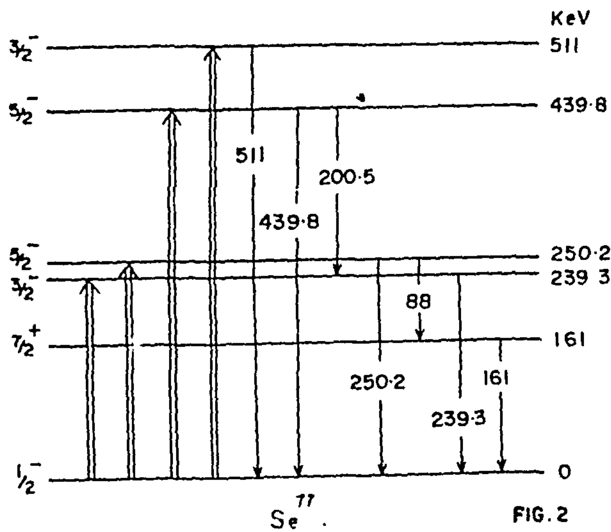


FIG. 2

the other even-even nuclei are calculated and compared with other measurements[1,2] in Table - 1.

Table - 1. Coulomb excitation of Se isotopes

A	E keV	Relative yield	B (E2)↑ (e^2 cm^4 10^{-50}) Present work	Earlier values	B(E2) / B(E2)	$T_{\frac{1}{2}}$	β
74	634.9	0.064	48 ± 15	44[a]	53	5.7 ps	0.3
76	553.4	1.17	45 ± 4	48.0 ± 0.9[b]	48	11.4 ps	0.3
78	613.7	1.00	38.5[b]	38.5 ± 0.9[b]	39.6	8.4 ps	0.2
80	666.2	0.74	27.6 ± 2.5	28.5 ± 0.9[b]	27.4	7.8 ps	0.2
82	654.7	0.524	20.1 ± 4	21.3 ± 0.9[b]	19.3	11.6 ps	0.2
77	239.3	0.76	18.6 ± 2.0	17.7 ± 1.6[c]	48.7	25 ps	
77	250.2	0.097	1.06 ± .2	0.94 ± .26[c]	1.6	10.0 ns	
77	439.8	0.814	22.8 ± 2.0	25.9 ± 1.7[d]	39.8	27 ps	
77	510.9	0.57	-	1.0 ± 0.2[d]	-	-	

a) Ref. 2 b) value from ref. 1

c) Ref. 4 d) Ref. 3

Coulomb excited levels of Se^{77} are 239.3, 250.2 and 439.8 keV (Fig. 2). The 510.9 keV peak is mainly due to annihilation radiation from nuclear reaction products in low Z impurities in the target. The branching ratios of the γ rays from the 250.2 and 439.8 keV levels were obtained from the γ spectrum. The B(E2)↑ values for the Se^{77} levels are also shown in Table 1 and compared with earlier measurements[3,4].

From the B(E2) values the half-lives and the ratios of B(E2)↓ to single particle B(E2)↓ values were deduced.

DISCUSSION

In the case of Se^{77} the present measurement ...

values of the 239.3 and 250.2 keV levels more accurately as the two γ rays were well resolved in our spectra. The half life of the 250.2 keV level as deduced from the B(E2) value is 10.0×10^{-9} sec in reasonable agreement with the value 9.3 ± 0.4 as measured by delayed coincidence[5,6]. The small B(E2) value of this level suggests it is of single particle character while the enhanced B(E2) values of the 239.3 ($3/2^-$) and 439.8 ($5/2^-$) keV levels are suggestive of their collective character. These are explained as arising from the coupling of the $\frac{1}{2}^-$ ground state with the phonon level.

The B(E2) values of even-even Se nuclei are all enhanced. The root mean square deformation, β_{rms} values deduced from B(E2) values, are listed in Table 1. They seem to decrease from Se^{74} to Se^{82} as the closed neutron shell at 50 is approached as can be expected.

This work demonstrates the usefulness of high resolution Ge(Li) detector in one single measurement without having to use enriched isotopes.

REFERENCES

1. P.H. Stelson and F.K. Mc Gowan, Nucl. Phys. 32, 652 (1962).
2. D.S. Andreev et al., Izv. Akad. Nauk SSSR, Ser. Fiz., 25, 832 (1961).

   R.L. Robinson, F.K. Mc Gowan and P.H. Stelson, Phys. Rev. 125, 1373 (1962).

4. R.L. Robinson et al., Nucl. Phys. 74, 281 (1965).
5. W. Engles et al. Phys. Letters 11, 57 (1964).
6. S. Monaro, Nuovo Cimento 30, 1379 (1963).

DISCUSSION:

Jyothi Parikh: Are you aware of any spectroscopic analysis which indicates the mixing of $g_{9/2}$ with p-f shell in ^{74}Se.

K.P. Gopinathan: No. You may use the experimental B(E2) and try to get the mixing.

values of the 239.3 and 250.2 keV levels more accurately as the two γ rays were well resolved in our spectra. The half life of the 250.2 keV level as deduced from the B(E2) value is 10.0×10^{-9} sec in reasonable agreement with the value 9.3 ± 0.4 as measured by delayed coincidence[5,6]. The small B(E2) value of this level suggests it is of single particle character while the enhanced B(E2) values of the 239.3 ($3/2^-$) and 439.8 ($5/2^-$) keV levels are suggestive of their collective character. These are explained as arising from the coupling of the $\frac{1}{2}^-$ ground state with the phonon level.

The B(E2) values of even-even Se nuclei are all enhanced. The root mean square deformation, β_{rms} values deduced from B(E2) values, are listed in Table 1. They seem to decrease from Se^{74} to Se^{82} as the closed neutron shell at 50 is approached as can be expected.

This work demonstrates the usefulness of high resolution Ge(Li) detector in one single measurement without having to use enriched isotopes.

REFERENCES

1. P.H. Stelson and F.K. Mc Gowan, Nucl. Phys. 32, 652 (1962).
2. D.S. Andreev et al., Izv. Akad. Nauk SSSR, Ser. Fiz., 25, 832 (1961).
3. R.L. Robinson, F.K. Mc Gowan and P.H. Stelson, Phys. Rev. 125, 1373 (1962).
4. R.L. Robinson et al., Nucl. Phys. 74, 281 (1965).
5. W. Engles et al. Phys. Letters 11, 57 (1964).
6. S. Monaro, Nuovo Cimento 30, 1379 (1963).

DISCUSSION.

Jyothi Parikh: Are you aware of any spectroscopic analysis which indicates the mixing of $g_{9/2}$ with p-f shell in ^{74}Se.

K.P. Gopinathan: No. You may use the experimental B(E2) and try to get the mixing.

IS LUNAR MATTER DIFFERENT FROM TERRESTRIAL MATTER?

K. Kondaiah
Tata Institute of Fundamental Research, Bombay.

Until the successful return of Apollo 11 mission in July 1969, the only extra terrestrial objects that could be handled in the laboratory were meteorites. Unlike the meteorites, the lunar samples come from a planetary object whose location is well known. Apart from the question whether the Moon was a part of our earth long ago, the most interesting question one would like to raise is whether the moon was made from the same primordial material as earth.

Reports[1,2] of investigations on lunar samples carried out so far showed that even though the elemental constituents of lunar samples are in general the same as those found on earth, there are several significant differences in composition, for example, unusually high concentrations of refractory materials like Ti, Zr etc. and low abundances of Na, K and Rb; such differences in elemental abundances are attributed to geochemical and physical processes that the moon might have gone through after its formation some four billion or more years ago. Unlike the elemental composition, the isotopic composition of elements should be unaffected by physical and chemical processes. So, a study of the isotopic composition of elements in lunar matter can, in principle, give a definite answer to the question whether lunar matter is the same as terrestrial matter.

However, it is well known that the isotopic abundances of elements can be disturbed by natural fission and nuclear reactions (spallation) arising from exposure to solar wind and cosmic rays. After taking into account these extraneous effects, if one finds significant differences in the isotopic composition of elements in lunar matter from that in terrestrial matter, one can conclude th-

lunar matter is made primordially under different physical conditions from the terrestrial matter. The likelihood of such a possibility may be remote as it is difficult to understand how a planet made from a galactic composition different from that in which the solar system originated, could wander into our proximity. Nevertheless, such a possibility cannot be ruled out as it has been found that the abundance of heavy elements relative to Hydrogen is a function of both time and location of formation of a star in the galaxy[3]. Prof. Alfven has a theory[9] that Moon and Mars are condensed from a "cloud" different from the one from which the other terrestrial planets were produced.

After the discovery of Technicium in some stars[4) it is generally accepted that Nature manufactures elements in stars through processes of nucleo-synthesis; light elements upto Iron are deemed to be manufactured by the capture of charged particles whereas elements heavier than Iron are manufactured by neutron captures and photo-nuclear reactions. The slow (s-) process capture of neutrons involves time scales of the order of thousands of years and thorough mixing of matter may be possible during the s-process occurance; on the other hand, the rapid (r-) process capture of neutrons is supposed to occur in super-novae explosions which may last at most a few seconds. Thus, matter manufactured in different supernovae explosions may show different isotopic compositions depending on the physical conditions such as composition of the star at the time of explosion, and its temperature, pressure etc. at the location of the r-process occurance.

Some of the heavy elements are reliably known to possess one or more isotopes made entirely by s-process and others predominantly by r-process[5,6]. Whereas the isotopic abundances of light elements are affected by solar wind, cosmic ray and spallation reactions, those

of the heavy elements beyond Iron are least affected by such extraneous causes after they are formed. Radiogenic influences on isotopic abundances etc. are sufficiently known by now so that one can concentrate on isotopes of elements that are not affected by such processes of enrichment or depletion. An examination of the isotope chart shows that there are some sixteen elements which are known to have pure s- and predominantly r-process stable isotopes. If one can show conclusively even for a few of these cases that either the (s-/r-) ratios or pure r-process abundances of these elements in lunar matter are different from those in terrestrial matter, one may be justified in concluding that lunar matter is in fact different from terrestrial matter. Till now, it is generally assumed that the composition of other galaxies are roughly comparable to our own; this is because, it is the simplest hypothesis. If lunar matter happens to have a different isotopic composition from that of terrestrial matter, this assumption may be questioned.

Isotopic analysis of Xenon was reported by Marti et al.[7] among others; the second column of Table I below is computed from their values. Only those isotopes of Xenon which are either predominantly s- or r-process nuclei are considered. The third column of Table I is computed from the Table of Isotopes[8].

Table I shows that in all the cases, the lunar (s-/r-) ratio is high compared to terrestrial matter. Xenon is the only heavy element for which isotopic abundances in lunar matter are reported so far. It is not possible to conclude from this single case of Xenon, that lunar matter is different from terrestrial matter, mainly because the low mass Xenon isotopes (Xe^{128} and Xe^{130}) can be produced by spallation[7] and the heavy Xenon isotopes (Xe^{134} and Xe^{136}) may have

some contributions from fission products. It is worthwhile to carry out isotopic analysis of the following elements in lunar matter: Ge, Se, Pd, Cd, Te, Nd, Yb, Pt and Hg. All these elements have at least one pure s- and one pure r-process isotopes.

Table I. (s-/r-) ratios for Xenon isotopes.

Isotopes	L = Lunar ratios (a)	T = Terrestrial ratios (b)	$(\frac{L-T}{T})\%$
Xe^{128}(s-)/Xe^{134}(r-)	0.237	0.185	28
Xe^{128}(s-)/Xe^{136}(r-)	0.293	0.216	36
Xe^{130}(s-)/Xe^{134}(r-)	0.451	0.392	15
Xe^{130}(s-)/Xe^{136}(r-)	0.557	0.460	21

(a) Compiled from data given in ref.(7).

(b) Compiled from data given in ref.(8).

References:

1. Science 165, 1211 (19th Sept. 1969).
2. Science 167, 3918 (30th Jan. 1970).
3. "Nucleo-Synthesis" edited by A.G.W. Cameron (p.29), Proc. by NASA (25-26 Jan. 1965).
4. P.W. Merrill, Science 115, 484 (1952).
5. D.D. Clayton et al., Ann. Phy. 12, 331 (1961).
6. A.G.W. Cameron, Astro. Phy. Jour. 129, 676 (1959).

7. K. Marti et al., Science 167, 548 (30th Jan. 1970).

8. "Table of Isotopes" - Sixth edition, C.M. Ledrer et al., John Wiley and Sons, N.Y. (1967).

9. H. Alfven, Icarus 1, 357 (1963).

DISCUSSION

J.C. Palathingal: Is there any sample variation in the ratios of the isotopes and how does they check with expectations?

E. Kondaiah: The isotopic abudances of any element should normally be the same wherever from the sample is taken from the Moon, except for the fact that some consideration as follows do change the isotopic ratios specially in the case of Xenon. (i) Natural fission gives rise to higher mass isotopes of Xenon (ii) Spallation reactions due to solar wind and Cosmic rays give rise to lower mass isotopes of Xe and this effect will depend on the depth from which the sample is taken from the Moon. (iii) Finally Mass-fractionation effect more the lower Mass isotopes of Xe. Due to the above, I submit the Xenon isotopic analysis of lunar samples does not answer the question raised in this paper full. One has to study many other cases.

071

COMPTON SCATTERING BY K-SHELL ELECTRONS AT LARGE SCATTERING ANGLE.

D.V. Krishna Reddy, V. Govinda Reddy and D.S.R. Murty,
Department of Physics, Osmania University, Hyderabad-7

I. *INTRODUCTION*

The incoherent scattering of gamma rays by atomic electrons is well known as 'Compton Effect', in which the scattering electron is considered to be free and stationary. It is well established quantitatively by Klein-Nishina formula. This relation is not valid in the practical cases where the scattering electron is tightly bound. For tightly bound electron a correction factor has to be incorporated with the Klein-Nishina formula, termed as the incoherent scattering function to get the theoretical cross-section for the bound electron.

Studies on compton scattering of gamma rays by K-shell electrons have been taken up by some workers during the past few years. Some of them[1-4] noticed the influence of binding on the scattered gamma rays spectra by K-shell electrons, showing up the broadening of the compton photo peak and tail of it extending upto 500 keV even at large scattering angles and some[1,4] of them found small shift of the photo peak towards the lower energy side at smaller scattering angles.

In the present paper the authors present the differential cross-section ratio $d\sigma_K / d\sigma_F$ for 662 keV gamma rays scattered at 125^0 by K-shell electrons of platinum and thorium using a conventional fast-slow

coincidence technique. The energy distributions and cross-section ratios for different thicknesses of the targets were studied.

II. EXPERIMENTAL

The experimental procedure followed in the present work is almost similar to the previous workers and it was already explained in detail earlier[5,6].

The measurement of the spectral distributions is basically the same as that employed in the case of angular distributions and it consists of selecting the coincidences between the scattered photons and fluorescent K X-rays using the usual fast-slow coincidence method. The resolving time of the fast coincidence circuit is about 100 nanoseconds. The gamma rays scattered by the K-shell electrons are displayed on a twenty channel analyser.

III. RESULTS

Studies were made with different thicknesses of platinum and thorium in order to observe the variation of the shape of the energy distribution spectra and also the differential cross-section ratios with respect to the thickness of the target and atomic number of the target.

The differential cross-section ratio for thorium is found to be equal for the two thicknesses (4.888 and 11.590 mg/cm^2) within the experimental errors. It shows that the thickness effects are negligible for the thicknesses less than 15 mg/cm^2 in the case of thorium. The shape of the energy distribution spectra for these two

targets are found to be almost similar. That shows the secondary effects reduced to the minimum in these two spectra. As the thickness of the target increases the secondary effects will dominate and the shape of the spectra changes.

The differential cross-section ratios for the thinnest targets of platinum and thorium determined experimentally are given in the Table-I. The ratios are compared with the available theoretical results. The experimental values are not in agreement with the existing theoretical values.

TABLE-I

Target	Thickness mg/cm^2	Experimental	Incoherent scattering function (S_K)
Platinum	11.650	1.660 ± 0.115	1.246
Thorium	4.888	1.845 ± 0.161	0.889

Shimizu et al[7] used the theory of compton scattering by a free electron with nonzero velocity developed by Jauch and Rohrlich[8] and showed that the experimental values for higher scattering angles are in good agreement with the theoretically calculated values using the above theory. But with the same theory the authors got very low value even less than unity for the differential cross-section ratio for platinum, calculated on computer. Recently Pingot[9] showed that the first relation given for the smaller angles by Shimizu et al[7] can be used for all the scattering angles and his experimental values are in

good agreement with theoretical values. Using their[7] second relation he got very smaller values less than unity, which are in good agreement with our calculated value with the same relation. But the experimental values of Pingot[9] are comparatively less than the values got by many workers.

The energy distribution of the incoherently scattered gamma rays at 125° by K-shell electrons of platinum and thorium targets are displayed on a twenty channel analyser. A clear shift in the compton coincidence peak is not seen in the present investigation.

The authors are much grateful to the Department of Atomic Energy for the financial assistance.

REFERENCES

1. Z. Sujkowski, and B. Nagel; Arkiv Fysik 20 , 323 (1961)
2. J. Varma and M.A. Eswaran; Phys. Rev. 127 , 1197 (1962)
3. A. Ramalinga Reddy, V. Lakshminarayana and Swami Jnanananda; Ind. J. P. and App. Phys. 4, 371 (1966).
4. M.A. Di Lazzaro and G. Missoni; Reports of Instituto Superiore Di Sanita Nos. 66/6, 66/7 and 66/8.
5. D.V. Krishna Reddy, E. Narasimhacharyulu and D.S.R. Murty; Proc. Ind. Acad. Sci. Vol LXXII 185 (1970).
6. D.V.Krishna Reddy, E. Narasimhacharyulu and D.S.R. Murty; Proc. Nucl. Phys. and Solid State Physics Symposium, Roorkee (1969).
7. S. Shimizu, Y. Nakayama and T. Mukoyama; Phys. Rev. 140 , No. 3A , A806 (1965).
8. J. M. Jauch and F. Rohrlich; The Theory of photons and electrons (Addison-Wesley Publ. Co., Cambridge, Massachusetts, 1955) p. 230.
9. O. Pingot; Nucl. Phys. A119 , 667 (1968).

INELASTIC SCATTERING OF GAMMA RAYS BY K-SHELL ELECTRONS

D.V.Krishna Reddy, E.Narasimhacharyulu and D.S.R.Murty,
Department of Physics, Osmania University, Hyderabad-7.

I. INTRODUCTION

The inelastic scattering of gamma rays by electrons in an atom was studied for the first time by Compton. His theory considers the scattering electrons as stationary and their binding energy negligible compared to the incident energy. In the case of the K-shell electrons of high 'Z' elements the above conditions donot hold good and the Klein-Nishina equation, which estimates the free electron cross-section fails to give the correct picture in the case of the bound electrons of high 'Z' elements.

The incoherent scattering of gamma rays by bound electrons was studied for the first time by Dumond[1]. But he used low 'Z' elements like carbon as scatterers. Bloch has calculated by non-relativistictreatment the shift and shape of the compton line for the scattering of X-rays by free electrons in atomic shells. But for the tightly bound electrons in atomic shells of heavy elements relativistic calculations are needed but are not available at present. Work on the experimental side was taken up in recent times and is quite limited.

The compton scattering by bound electrons has been studied in recent times[2-4] with a view to understand the influence of binding on the differential cross-sections of the scattered gamma rays. As information available from the experiments conducted so far is quite

authors have undertaken a study of this phenomenon.

II. EXPERIMENTAL

To detect the gammas scattered by K-shell electrons a fast-slow coincidence system has been used between the scattered gammas and the fluorescent X-rays due to the ejection of the K-electron from its orbit. For this purpose a 6.0 curie Caesium-137 source has been used. Blocking oscillators giving 50 ns pulses have been used on the fast coincidence side which includes a 6BN6 valve as a mixer. The slow coincidence has two inputs one from the X-spectrometer and the other from the fast coincidence circuit. The slow coincidence output is given to the gate of a twenty channel analyser. The input to the amplifier section of the twenty channel analyser comes from the γ-detector direct. The spectra are recorded on the twenty channel analyser. Platinum, and thorium have been used as scatterers at two scattering angles namely 70° and 105°.

The experimental differential cross-section ratio between the bound electron scattering and free electron scattering is determined from the following equation:

$$\frac{d\sigma_K}{d\sigma_F}(\theta) = \frac{N_K}{N_F} \cdot \frac{1}{\omega_x \epsilon_x \epsilon_c \nu_K} \cdot \frac{\epsilon_\gamma}{\epsilon_{\gamma(K)}} \cdot \frac{\nu_\gamma}{\nu_{\gamma(K)}} \cdot \frac{1}{\nu_x} \cdot \frac{d'}{d} \cdot \frac{A}{A'} \cdot \frac{13}{2}$$

In this equation the symbols have the same significance as in our previous report[5].

III. RESULTS

The cross-section ratios obtained making use of

the above equation at scattering angles of 70° and 105° have been reported in the table for the above two targets. *The spectra of the inelastically scattered* gamma rays by K-electrons have been studied on a twenty channel analyser.

The experimental differential cross-section ratios have been compared with theoretically computed values. In all these theories a correction factor has been introduced in the bound electron cross-section defined as the in-*coherent scattering function.*

$$\frac{d\sigma_K}{d\Omega}(\theta) = S_K(q, z)\, \frac{d\sigma_{KN}}{d\Omega}(\theta)$$

This is computed making use of a non-relativistic theory. From a formula based on the Thomas-Fermi model given by Shimizu et al[6] the value of the function $S_k(q, z)$ has been evaluated at these two angles for these scatterers. They are also presented in the table along with the experimental values for comparison.

TABLE

Incident Energy ($h\nu$) = 662 keV

		Platinum ($11.64\ mg/cm^2$)	Thorium ($11.59\ mg/cm^2$)
70°	Exptl.	1.160 ± 0.098	1.120 ± 0.074
	Theoretical S_k	0.876	0.631
105°	Exptl.	1.380 ± 0.169	1.487 ± 0.180
	Theoretical S_k	1.157	0.827

The energy spectrum of the incoherently scattered gamma rays by the K-shell electrons of a 11.64 mg/cm^2 thick platinum target recorded on the twenty channel analyser has been presented.

It is compared with the spectrum computed on the basis of a non-relativistic theory given by Schnaidt[7].

The authors thank the Department of Atomic Energy for financing this research project.

REFERENCES

1. J.W.M. Dumond; Rev. Mod. Phys. 5 , 1 (1933).

2. Z. Sujkowski and B. Nagel; Arkiv Fysik 20, 323 (1961).

3. J.W. Motz and G. Missoni; Phys. Rev. 124, 1458 (1961).

4. J. Varma and M.A. Eswaran; ibid. 127, 1197 (1962).

5. D.V. Krishna Reddy, E. Narasimhacharyulu and D.S.R. Murty; Proc. Ind. Acad. Sci. 72 , 185 (1970).

6. S. Shimizu, Y. Nakayama and T. Mukeyama; Phys. Rev. 140 , 3A , A806 (1965).

7. F. Schnaidt; Ann. d. Physik 21 , 89 (1934).

...

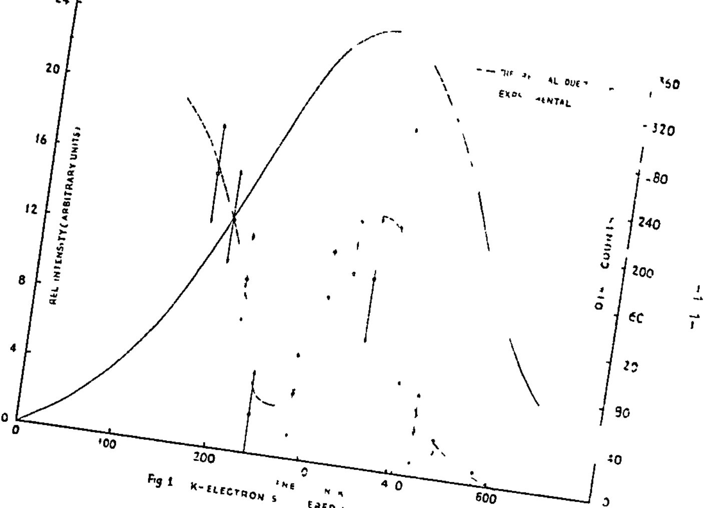


Fig 1 K-ELECTRON S EREDS

ANALYTICAL FORMULATION OF K-SHELL PHOTOEFFECT

M.Biswas*, S.C.Roy and A.M.Ghose,

Nuclear Physics Laboratory, Bose Institute, Calcutta-9.

I. INTRODUCTION.

The photoelectric effect being one of the major way of interaction of gamma rays with matter is a subject of interest to evaluate exact theoretical values, using high speed computers. Unfortunately, no simple analytical formula of photoeffect exists in the literature and the extraction of photoelectric cross-section for a specific element and gamma energy requires formidable amount of computation time. An attempt was made by Hla et al[1] to develop an analytical formula for K-shell photoeffect which is valid for intermediate and high Z atoms only. Further the formula appears to be a little complicated. The object of the present investigation is to develop a simple analytical formula for K-shell photoeffect which is valid for any element of the periodic table and over wide energy range. Of all the existing theoretical calculations, the calculation due to Schmickley and Pratt[2] will be considered as the most accurate calculations. The accurate calculation of K-shell photoeffect exists in the literature due to Pratt[3].

---

* Guest worker from New Alipore College, Calcutta-53.

Therefore our proposed equation will reproduce the cross-section values due to Schmickley and Pratt[2] at intermediate energies and to Pratt[3] at high energies.

II. DEVELOPMENT OF THE FORMULA.

The calculation of K-shell photoeffect by Sauter[4] using relativistic Born approximation when approximated to low energy reduces to the form

$$\sigma_K = \sigma_0\left(1+\frac{x}{2}\right)^{3/2}\left[\frac{8\sqrt{2}}{3x^{5/2}} - \frac{2\sqrt{2}}{3x^{3/2}}\right] \qquad (1)$$

where,

$$\sigma_0 = \frac{3}{2}\,\varphi_0\,\frac{a^5}{\alpha}\cdot\frac{1}{x}.$$

$$\varphi_0 = \frac{8\pi}{3}\left(\frac{e^2}{mc^2}\right)^2$$

$$x = h\nu/mc^2 \quad ; \quad a = \alpha Z = \frac{Z}{137}$$

Calculation of Nagasaka indicated that the structure of Sauter's equation should be retained even at higher energies. At high energy Sauter's equation reduces to

$$\sigma_K = \sigma_0$$

Pratt[3] has shown that more accurately the limiting K-shell photoeffect is given by

$$\sigma_K = \sigma_0 F(a)$$

The above formula can be justified on theoretical grounds for photon energy greater than 2 MeV. It has been found that F(a) can be expressed accurately by

$$F(a) = \exp\left(-3.440a + 1.655a^2 - 0.0415\right)$$

By plotting the theoretical values of σ_K/σ_0 against $1/x$ in a semi-log paper we obtain a straight line with

slope 0.4040 for intermediate and higher energies. The value of the intercept on the Y-axis almost corresponds to the values of F(a). Thus from the above discussion it is clear that the expression takes the form as

$$\sigma_K = \sigma_0 \left(1+\frac{x}{2}\right)^{3/2} \frac{2\sqrt{2}\,F(a)}{x^{3/2}} \exp\left(\frac{0.4040}{x}\right) \qquad (2)$$

It has been observed that the slope of the line varies a little from element to element. The above formula *is an exact fit for intermediate Z elements.* This effect has been compensated by introducing a Z-dependent term in the exponent of equation (2). Thus the final form of the formula for K-shell photoelectric cross-section stands as

$$\sigma_K = \sigma_0 \left(1+\frac{x}{2}\right)^{3/2} \frac{2\sqrt{2}\,F(a)}{x^{3/2}} \exp\left[\frac{0.4040}{x} + 0.0018(Z-42)\right] \qquad (3)$$

III. RESULTS:

The cross-section σ_K was calculated from this formula for Z starting from 13 to 92 over an energy range 200 KeV to 5,000 KeV. The agreement of the equation with Schmickley and Pratt's result for intermediate energies and with Pratt for high energies as well as with experimental results is satisfactory. We conclude, therefore, that this formula can be used for any elements of the periodic table above 200 Kev photon energy for the rapid estimation of K-shell photoelectric cross-sections. Fur

the formula reproduces Pratt's exact calculation at high energy the formula can be safely used to above 5 MeV, where exact computations of photoelectric cross-sections have not yet been made.

Acknowledgement

Thanks are due to Dr. S.M.Sircar, Director, Bose Institute, for his kind interest in this work. One of the author (S.C.R.) is thankful to DAE for awarding him a Senior Research Fellowship. Financial support for this work came from PL-480 project sponsored by the National Bureau of Standards, U.S.A.

References

1. Hla Yin Yin, et al : Proc. Nucl. Phys. Symposium (Roorkee), 1969, Vol.II. (in press).

2. Schmickley R.D. and Pratt R.H. : Phys. Rev. 164 (1967), 105.

3. Pratt, R.H. : Phys. Rev. 117 (1960), 1017.

4. Sauter, F. : Ann. d. Phys. 11, (1931) 454.

COMPTON SCATTERING BY K-SHELL ELECTRONS AT 1.12 MEV

P.N. Baba Prasad and P.P. Kane[x]
Department of Physics,
Indian Institute of Technology, Bombay-76.

In recent years, the old problem of photon scattering from bound atomic electrons has again received considerable theoretical and experimental attention. In the case of electrons bound in hydrogen, accurate field theoretic expressions for the scattering amplitudes are now available in the dipole approximation[1,2]. In the paper presented last year, references have been given to the previous experimental work performed with gamma rays. Experiments with monoergic gamma sources had been done only upto an energy of 0.662 MeV. A preliminary study of Compton scattering of 1.12 MeV photons from a zinc-65 source by a gold scatterer at 120° scattering angle was reported last year. Since then, we have made similar measurements with tantalum at 120°; tin, gold and thorium at 90°; tin, gold, lead and thorium at 60° and thorium at 25°. We have also studied the dependence of the results on the bias level in the gamma channel.

The principal results of the earlier experiments at lower energies, relevant to this work, are summarised here. At angles of scattering larger than about 70°, the Compton scattering cross section of a K-shell electron of a heavy

x Work supported by a grant from the National Bureau of Standards, Washington, D.C. under the PL-480 programme.

atom such as that of gold or lead for 0.662 MeV gamma rays is between 1.0 to 1.8 times the value predicted by the Klein-Nishina formula on the assumption of free electrons at rest. At smaller scattering angles, and also generally for somewhat lower energies, the ratio $d\sigma_K / d\sigma_{KN}$ of the K-shell electron cross section $d\sigma_K / d\Omega$ to the Klein - Nishina value $d\sigma_{KN} / d\Omega$ tends to be significantly less than unity. Since the photons scattered from the K-shell electrons can have any energy between zero and $E_o - I_k$, the spectral distribution of these photons is obviously different from that expected under the Klein-Nishina theory. Here, E_o is the incident photon energy and I_k is the binding energy of the K-shell electron. It is very difficult to determine accurately the spectral distribution on account of secondary effects associated with bremsstrahlung and K-X-rays arising through ionisation of the scatterer atoms by photoelectrons and Compton electrons. The importance of the secondary effects increases at least as the second power of the target thickness. Thus, it is really necessary to use target thicknesses not much greater than about 10-15 mg/cm^2. Unfortunately, the counting times then become prohibitively long. Varma and Eswaran[4] studied the spectral distribution in the case of 0.662 MeV photon scattering through 60° and 124° with 28.6 mg/cm^2, 58.8 mg/cm^2 and 93.3 mg/cm^2 lead scatterers and tried to ascertain, through a detailed analysis, the nature of the true spectrum characteristic of a thin target. The deduced spectrum was much broader than the 'free Compton'

spectrum and was shifted towards higher energies. The shift can be understood as an effect of binding[5]. However, with a 7.27 mg/cm^2 gold scatterer and for the same primary energy, Missoni and Lazzaro[6] found, after about 1800 hours of counting, a negligible shift at 75^0 scattering angle, a shift towards lower energies at 25^0 and also a large subsidiary peak in the neighbourhood of 160 KeV energy. Thus, the nature of the true spectral distribution is uncertain and puzzling.

In view of this background and in view of the fact that measurements at an energy as high as 1.12 MeV were being attempted for the first time, we decided to use relatively thin targets and pursue a slightly limited objective. With a gold target and at 60^0 scattering angle, the ratio $d\sigma_K/d\sigma_{KN}$ was determined as a function of the lower bias in the gamma counter channel. For scattered gamma energies in excess of 130 KeV, 150 KeV and 165 KeV, the ratio $d\sigma_K/d\sigma_{KN}$ turned out to be 1.16 ± 0.10, 1.20 ± 0.11 and 0.94 ± 0.11 respectively. It is interesting to compare these results with the above mentioned results of Lazzaro and Missoni for 0.662 MeV with a gold scatterer at 75^0. An analysis of their results leads to the ratio values of 1.45, 1.28 and 1.19 respectively for approximately the same bias levels. With thorium at 60^0, the cross-section ratios measured by us turn out to be 1.34 ± 0.16 and 1.27 ± 0.13 for bias levels of 165 KeV and 185 KeV respectively. The higher bias levels were chosen in this case since the

thorium K-X-ray energy is around 97 KeV. By way of comparison, Lazzaro and Missoni obtained, with a uranium target at 75°, the ratio values of 1.50 and 1.44 respectively. Further at 60° and a bias of 165 KeV, the cross-section ratios measured by us with 19.7 mg/cm^2 and 12.9 mg/cm^2 gold scatterers turned out to be 0.94 ± 0.11 and 0.82 ± 0.12 respectively, indicating agreement within statistics.

The data obtained after a counting time of about 1500 hours are summarised in Table I. The cross-sections measured even for this relatively high energy conform to the general trends described earlier.

The experimental details relevant to this work are somewhat different from those reported earlier[3]. The gamma counter was a 44 mm diameter x 38 mm height sodium iodide crystal mounted on RCA 6342 A photomultiplier. A 1.38 mm copper absorber was used in front of the gamma counter. The distance between the center of the target and the gamma counter was increased to 13.0 cm for the 60° and 90° measurements, and to 21.0 cm for the 25° measurements.

REFERENCES

1. M. Gavrila; Phys. Rev. 163, 147 (1967).

2. C. Fronsdal; Phys. Rev. 179, 1513 (1969).

3. P.P. Kane and P.N. Baba Prasad; Proc. of the Nuclear and Solid State Physics Symposium, Roorkee (1969).

4. J. Varma and M.A. Eswaran; Phys. Rev. 127, 1197 (1962).

5. H.A, Kirkpatrick and J.W.M. Dumond; Phys. Rev. 54, 802 (1938).

6. M.A. Di Lazzaro and G. Missoni; Instituto Superiore Di Sanita Report ISS 66/6 (1966) unpublished.

7. D.V. Krishna Reddy, E. Narasimhacharyulu and D.S.R. Murthy; Proc. of the Nuclear and Solid State Physics Symposium, Roorkee (1969).

TABLE I

Preliminary values of the ratio $d\sigma_K/d\sigma_{KN}$ for 1.12 MeV. α is the angle between the direction of the incident beam and the normal to the target plane.

Angle of scattering	Scatterer	Thickness in mg/cm^2	Gamma channel bias in KeV	$d\sigma_K/d\sigma_{KN}$
25^0 $\alpha=0$	Thorium	14.9	300	0.74 ± 0.18
60^0	Thorium	14.9	165	1.34 ± 0.16
$\alpha=0$	Lead	14.0	165	0.87 ± 0.10
	Gold	19.7	165	0.94 ± 0.11
	Gold	12.9	165	0.82 ± 0.12
	Tin	18.8	165	0.97 ± 0.08
90^0	Thorium	14.9	165	1.88 ± 0.11
$\alpha=30^0$	Gold	12.9	165	1.39 ± 0.12
	Tin	18.8	165	1.09 ± 0.09
120^0				
$\alpha=40^0$	Gold	19.7	100	1.18 ± 0.12
$\alpha=0$	Tantalum	22.1	100	0.96 ± 0.26

NUCLEAR THEORY

NUCLEAR ENERGY LEVEL CALCULATIONS OF THE BARIUM ISOTOPES IN THE UNIFIED MODEL.

C.R. CHANDRAN, M.N. SITARAMANATH, M.V. RAMANAMURTY and S. RAMAMURTY.
Laboratories for Nuclear Research, Andhra university,Waltair.

The intermediate coupling approach has beenused to investigate the nuclear properties of various nuclei by several authors. The present calculations are attempted to account for the energy level structure of Ba^{131} and Ba^{135}. For this purpose it is assumed that the above nuclei consist of an even-even core with an extra neutron outside the core. The last odd neutron has available to it, the $3s_{1/2}$ and $2d_{3/2}$ orbits. This odd neutron is coupled to the quadrupole vibrations of the even-even core and the resulting matrices for the $1/2^+$, $3/2^+$, $5/2^+$ and $7/2^+$ states are diagonalised. The eigen values and the eigen vectors are obtained in this way.

The main parameters that enter in to our calculations are: 1) hw, the phonon energy which is taken to be the energy of the first excited state of the corresponding even-even core, 2) ϵ , the energy spacing of the $3s_{1/2}$ and $2d_{3/2}$ states and 3) Z, the coupling strength. As there is not much experimental results ~~are~~ available for ϵ , the values of ϵ and Z are taken as parameters and the best fit for the experimental energy level structure is taken.

BASIC FORMULAE : We shall give a brief description of the formalism of the Unified model and of the wavefunctions

in question and explicitely give the necessary matrix elements.

The hamiltonian is $H = H_{coll} + H_{sp} + H_{int}$

The basis vectors are taken to be of the form :

$$|j;NR;IM\rangle = \sum_{m,m'} (jRmm'|jRIM)|jm\rangle |NRm'\rangle,$$

The basis eigen vectors satisfy the eigen value equation

$$(H_c + H_{SP})|j;NR;IM\rangle = (N\hbar\omega + E_j)|j;NR;IM\rangle,$$

The off diagonal matrix elements are calculated from

$$\langle j';N'R';IM|H_{int}|j;NR;IM\rangle = (-1)^{R'+j'+1}\sqrt{\tfrac{1}{5}\pi}\,z\hbar\omega \times \sqrt{(2j'+1)(2R+1)}$$
$$\times\langle N'R'\|b\|NR\rangle\langle l'sj\|Y_2\|lsj\rangle \times W(R'Rj'j;2I), \quad \text{for } N'<N$$

The eigen functions are then a linear combination of the basis vectors; $|E;IM\rangle = \sum_{j,N,R} A(jNRI|E)|j;NR;IM\rangle,$

In the above formalism H_{int} and Z are defined by

$$H_{int} = -\sqrt{\tfrac{1}{5}\pi}\,z\hbar\omega \sum_{\mu} (b_\mu + (-)^\mu b^+_{-\mu})\, Y_{2\mu}(\theta\phi),$$
$$z = K\sqrt{5/2\pi\hbar\omega C},$$

The values of the reduced matrix elements are tabulated by Choudhury[1].

RESULTS: The matrices which are diagonalised range in size from 4 x 4 for I = 1/2 to 6x6 for I = 3/2. The various parameters which are used in our calculations are given in Table 1. The experimental and the theoretical levels are compared in the Table 2. The energy values are plotted as a function of the dimensionless parameter Z but due to shortage of space they are not included here. As can be seen from the Table 2, very good agreement is obtained between the levels found experimentally and the levels determined theoretically . Some states which are not observed experimentally are also predicted in this model.

In the above calculations we have restricted ourselves to only the $3s_{1/2}$ d and $2d_{3/2}$ particle states and the coupling is done to the first two phonon states. The level $11/2^-$ is not predicted in our model because the positive parity states are only predicted as mixing of parities is not included.

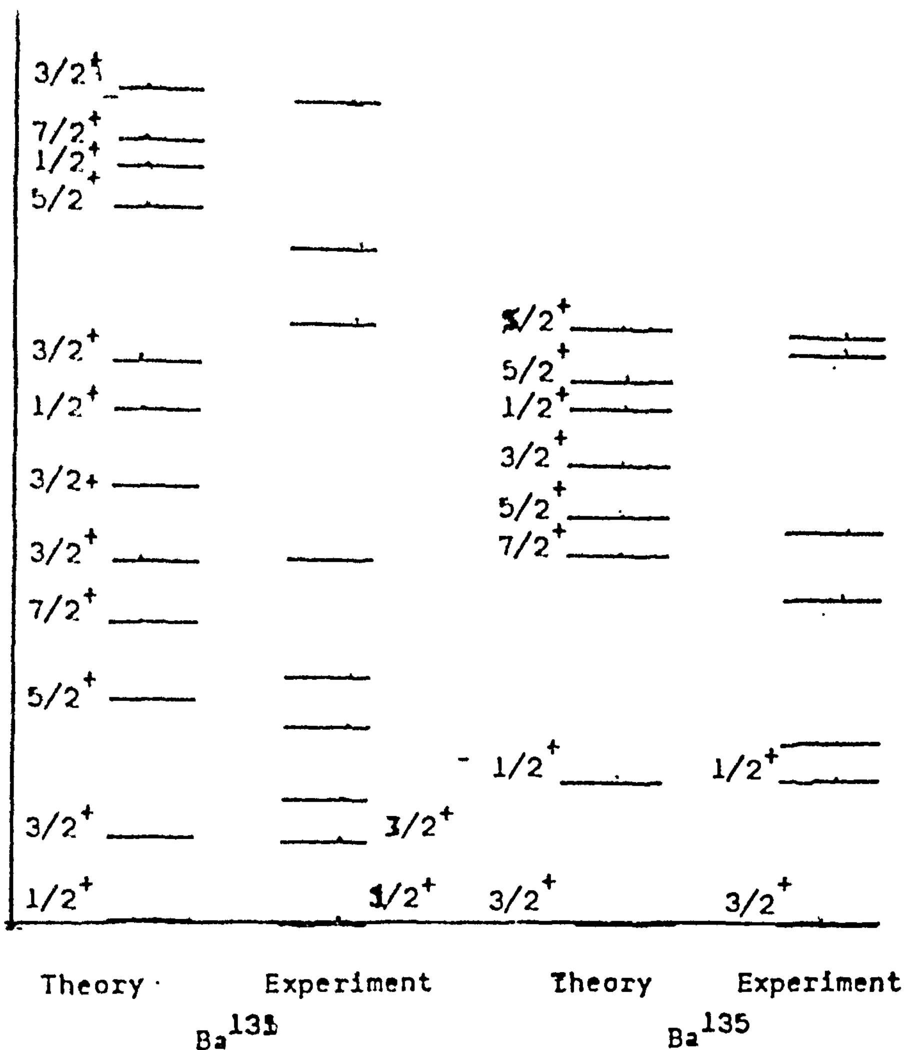
The wave functions obtained are being used for the calculation of the electromagnetic moments and transition rates and this part of the work is in progress. The validity of the model is not complete without these values.

TABLE 1

Values of the various parameters used in the calculations.

Parameter	Ba^{131}	Ba^{135}
$\hbar w$ (Kev)	356	604.6
$\epsilon = (E_{3/2} - E_{1/2})$ (Kev)	210	280
Z (the dimensionless parameter)	1.4	0.5

$\hbar w$ is taken from the spectra of the corresponding doubly even Barium nuclei, which was considered to form the core of the odd mass Barium nuclei.



Two of the authors(C.R.C and M.V.R) are thankful to the C.S.I.R for awarding them junior research fellowships.

REFERENCES:

1) D.C. Choudhury, Mat.Fys,Medd.Dan.Vid.Selsk.27(1953)

2) D.C. Choudhury, Nuclear Physics A93(1967)300
and T.F.O'Dwyer

3) Hyde and Brussaard, Nuclear Physics A104 (1967)81

EFFECT OF PAIRING ON PARTICLE-CORE COUPLING CALCULATIONS

K. V. Chalapati Rao
Saha Institute of Nuclear Physics, Calcutta-9

The single-particle transfer reactions involve direct transfer of a neutron or proton to the target nucleus. Thus, if the reaction is done on a doubly closed shell nucleus, only one level will be excited for each spin-parity state, since the whole single-particle strength will be concentrated in a single nuclear level. Away from the closed shells, the single-particle strength will be distributed over several nuclear levels. Thus, in a (d,p) reaction on a nucleus away from closed shells, several levels will be excited with the same spin-parity, each with a spectroscopic factor determined by the single particle content of the state. We have attempted to understand this fragmentation of single-particle strength through a core-particle coupling model[1], which pictures an odd-nucleus as a coupled system of the odd-particle and the even-even core. The excited states of the core are treated as phonons, the value of the phonon energy, being given by the energy of the first 2^+ - state of the neighbouring even-even nucleus.

If we assume that a single-particle state available to the odd-particle is fully empty, the spectroscopic factor is, in our model, the square of the zero-phonon amplitude, a_{jooj}. However it is well known that pairing effects cause the single-particle state to be partially occupied in the core. We take this effect

into account by taking the emptiness of the single-particle state as U_j^2 instead of unity. The spectroscopic factor is then $a_{jooj}^2 \times U_j^2$. The value of U_j^2 for each single-particle state is taken as the ratio of experimental spectroscopic factor and a_{jooj}^2 for the member of the group of j states containing the maximum single-particle strength.

The nuclei $^{111,113,115,117}Cd$, $^{113,115,117,119,121}Sn$ in the 3s-2d-1g shell and $^{59,61,63}Ni$ in the 2p-1f shell have been studied. In the former set the neutron occupies the single-particle states $s_{1/2}$, $d_{3/2}$, $d_{5/2}$ and $g_{7/2}$ and in the latter $p_{1/2}$, $p_{3/2}$ and $f_{5/2}$. The values of U_j^2 calculated as described above, together with those obtained from stripping reactions[2] are given in table(1) The values from the calculations of Kisslinger and Sorensen[3] are also given for comparison. It can be seen that our values agree very well with experiment in almost all the cases. The modified spectroscopic factors have been found to agree better with experiment. As an example, the case of ^{113}Cd is shown in fig (1).

REFERENCES

1. D. C. Choudhury, Mat. Fys. Medd. Dan. Vid. Selsk. 28, No. 4 (1954).

2. B. Rosner, Phys. Rev. 136 (1964) B 664.

R. J. Silva and G. E. Gordan, Phys. Rev. 136 (1964) B 618.

B. L. Cohen et al., Phys. Rev. 165 (1968) 1287.

E. Schneid et al., Phys. Rev. 156 (1967) 1316.

E. R. Cosman et al., Phys. Rev. 142 (1966) 673; ibid. 163 (1967) 1134.

3. L. S. Kisslinger and R. A. Sorensen, Mat. Fys. Medd. Dan. Vid. Selsk. 32 No. 9 (1958).

Table(1) U_j^2 - values

S.P. states →	$3s_{1/2}$			$2d_{3/2}$			$2d_{5/2}$			$1g_{7/2}$		
↓Nucleus	P	E	K	P	E	K	P	E	K	P	E	K
^{111}Cd	.43	.83	.51	.54	.64	.89	.25	.25	.86	.36	.25	.85
^{113}Cd	.45	.66	.60	.77	.76	.85	.28	.25	.89	.56	.55	.79
^{115}Cd	.44	.55	.69	.94	1.00	.80	.22	.28	.91	.37	.62	.73
^{117}Cd	.48	.62	—	.66	.70	—	.37	.16	—	.32	—	—
^{113}Sn	1.0	.89	.55	1.0	.86	.90	.20	.30	.85	.33	.31	.87
^{115}Sn	1.0	.73	.57	.85	.72	.87	.27	.31	.89	.22	.19	.82
^{117}Sn	.71	.60	.68	.75	.64	.83	.19	.18	.91	.19	.13	.76
^{119}Sn	.48	.45	.75	.67	.60	.76	.24	.21	.93	.29	.21	.67
^{121}Sn	.49	.30	.83	.52	.50	.67	.28	.19	.95	.51	.19	.57
	$2p_{1/2}$			$2p_{3/2}$			$1f_{5/2}$					
^{59}Ni	1.0	1.1	.89	.78	.78	.89	.80	.79	.73			
^{61}Ni	.96	.98	.80	.42	.48	.80	.58	.65	.53			
^{63}Ni	.46	.71	.65	.31	.34	.67	.46	.40	.66			

P - present, E - Experiment, K- Kisslinger and Sorensen

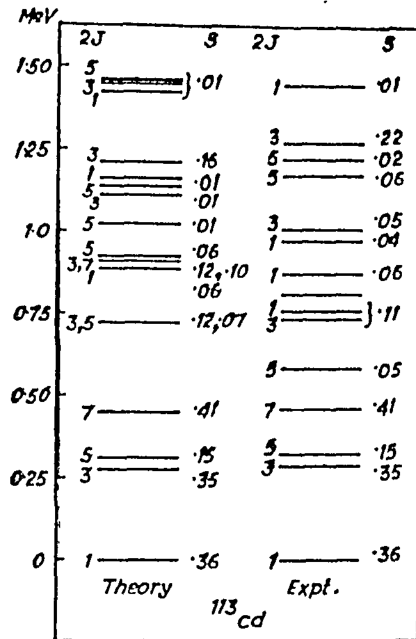


Fig.(1) : Experimental levels and spectroscopic factors together with the theoretical levels and modified spectroscopic factors for ^{113}Cd .

DISCUSSION

J. Dey: Could you please explain a bit about these emptiness parameter U^2.

K.V. Chalapati Rao: U^2 and V^2 are the pairing theory parameters. U^2 gives the extent to which the single particle state is empty. If a single-particle state is fully empty, $U^2 = 1$; other wise it is less than one.

CHARACTERISTICS OF α-α INTERACTION

P.C. Joshi and P.C. Sood
Physics Department, Banaras Hindu University, Varanasi-5

The alpha particle model for nuclei has its basis in the observation that inter alpha binding in these nuclei is much smaller than the intra-alpha binding energy. It has been believed that about 90% of the binding energy in light nuclei results from the internal binding within the constituent α particles whereas the interactions between the α particles constitute only 10% of the binding energy. As early as 1937 it was empirically concluded that this residual binding energy is closely proportional to the number of classical "bonds" between the α particles, with about 2.4 MeV per bond[2]. Recently, there have been several attempts[3] at calculating this inter-alpha binding energy starting with phenomenalogical α-α interactions[4]. However these attempts have not been very successful.

We have tried to look at this problem in analogy with the nuclear many body problem. In the nuclear case the significant basis is the saturation of the nuclear forces as revealed through the semi-empirical mass formula. Accordingly we seek the fundamental characteristics of the α-α force through examination of the masses (or simply the residual binding energies) of the α- nuclei. These energies, as calculated from the mass tables, are

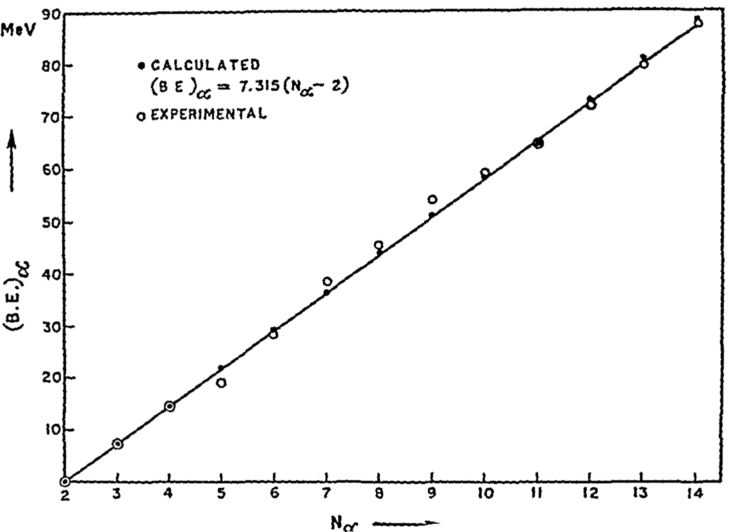
shown by open circles in fig.1. The points are seen to approximately fall on a straight line with an intercept at N_{α} very close to two. For simplicity of expression we assume the α- binding energy of ^{8}Be ($N_{\alpha} = 2$) to be zero (rather than the experimental value of -0.105 MeV). Then a least squares fit of the data yields the relation

$$(B.E.)_{\alpha} = (7.315 \pm 0.122)\ (N_{\alpha} - 2)\ MeV \ \ldots\ldots \quad (1)$$

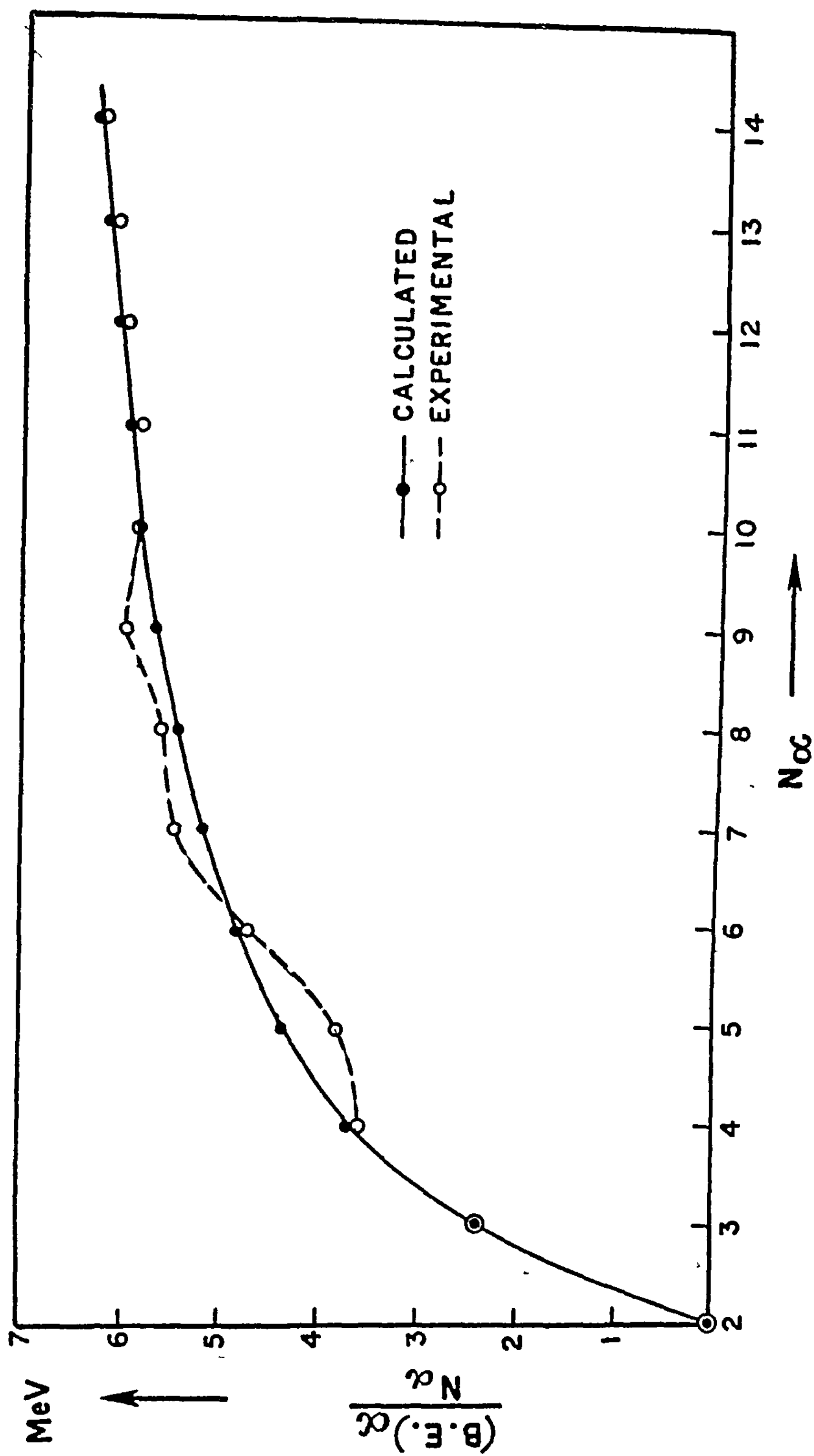
the deviation as shown being only about 1.7%. The comparison with the experimental values for individual nuclei is better brought out in fig.2 where we have plotted $(B.E.)_{\alpha} / N_{\alpha}$ versus N_{α}. It is seen that ^{20}Ne, the 5α structure, is quite loosely bound relative to any other nucleus. For all other nuclei there is a fair agreement with the experiment.

Thus it appears more reasonable to assume 7.3 MeV additional binding per α as the basic characteristic of the α- force rather than the ordinarily accepted concept of "bond" energy of about 2.4 MeV[(2)]. To put it in another way, the ratio of inter alpha binding to intraalpha binding is only 4 : 1 (and not 9 : 1 as mentioned in the beginning) !

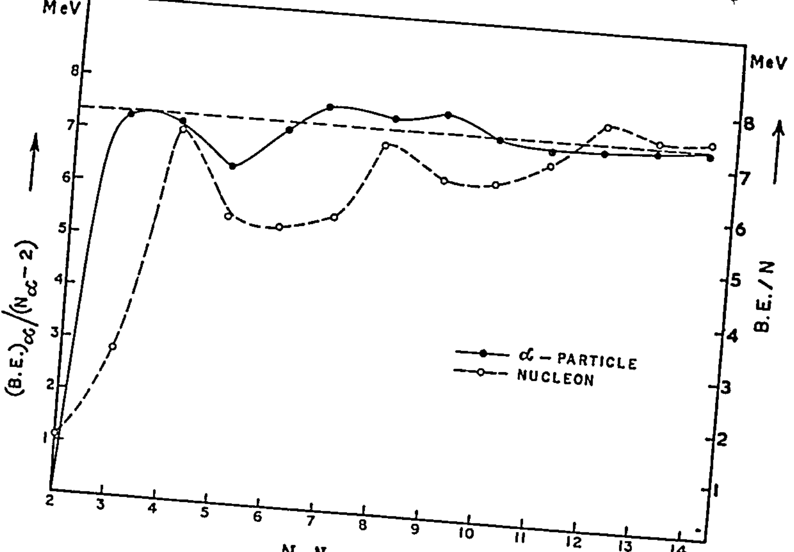
In order to study the fluctuations about, and the approach to, this "saturation" value for $\alpha - \alpha$ force we have plotted $(B.E.)_{\alpha} / (N_{\alpha} - 2)$ versus N_{α} in fig.3. It is seen that the "saturation" value is reached almost abruptly in going from the unbound system for $N_{\alpha} = 2$ to the three - α nucleus ^{12}C.



MeV
90
80
70
60
50
40
30
20
10
• CALCULATED
(B E)$_\alpha$ = 7.315 (N$_\alpha$ − 2)
o EXPERIMENTAL
(B.E.)$_\alpha$
2
3
4
5
6
7
8
9
10
11
12
13
14
N$_\alpha$



MeV
$\frac{(B.E.)_\alpha}{N_\alpha}$
CALCULATED
EXPERIMENTAL
N_α
1
2
3
4
5
6
7
2
3
4
5
6
7
8
9
10
11
12
13
14


MeV
MeV
$(B.E.)_\alpha/(N_\alpha - 2)$
B.E./N
α – PARTICLE
NUCLEON
1
2
3
4
5
6
7
8
2
3
4
5
6
7
8
9
10
11
12
13
14

Except for the distinct minimum for ^{20}Ne already pointed out above, the curve shows very little fluctuations about the "saturation" value. These fluctuations may result from the geometrical spacing of the various α particles inside the nucleus which may bring about these variations due to Coulomb contributions etc.

It is interesting to look at this curve in conjunction with the binding energy per nucleon versus nucleon number curve which is shown as dashed in fig.3. It is seen that whereas the latter shows distinct sub-shell structures, the α binding curve does not exhibit any such regular features. This corresponds to the statement that in α- particle nuclei there is no such distinction as the core or the valence particles; all the α- particles are a priori on rather equal footing.

REFERENCES

1. S.A. Moszkowski, in Handbuch der Phys. 39, 461(1957)

2. W. Wefelmeier, Naturewiss. 25, 525 (1937);
Z. Phys. 107, 332 (1937).

3. Abdul-Magd, Nucl. Phys. A 122, 610 (1969);
G.B.L. Das, Ph.D. Thesis, Dibrugarh Univ.(India), 1969, Unpublished.

4. S.A. Afzal, A.A.Z. Ahmed and S. Ali, Revs. Mod. Phys. 41, 247 (1969).

SHELL MODEL DESCRIPTION OF $(5/2)^n$ CONFIGURATIONS OF IDENTICAL PARTICLES

A.K. Nigam and P.C. Sood
Physics Department, Banaras Hindu University, Varanasi-5.

In the effective interaction approach for description of nuclear spectra one defines this interaction as a two body interaction whose matrix elements in n particle configurations are linear combinations of its matrix elements in two particle configurations. Thus, knowing the two particle spectra, one can calculate the energy levels for $n > 2$ cases for comparison with observed spectra and/or prediction of yet unobserved levels. Further the two body interaction may, in general, contain terms explicitly related to different coupling schemes such that the respective coefficients, when evaluated from observed spectra, provide an estimate of the relative contributions from the competing coupling schemes. In this paper we examine these features for $(5/2)^n$ configurations of n identical particles (protons or neutrons). It may be noted that this analysis does not distinguish between d5/2 and f5/2 orbitals in as much as the allowed J values for $(j)^n$ configurations are the same in both cases.

For $(5/2)^2$ case the allowed J values a 0^+, 2^+ and 4^+, and the corresponding experimental data can be used to define a three parameter interaction. Following Talmi (Rev. Mod. Phys. 34, 704, (1962)) we take the two body interaction as

$$H_{int}(ik) = a + 2b\,\vec{j}_i\cdot\vec{j}_k + c\,q.$$

whose matrix elements in the n particle case are

$$\left\langle j^n J v \right| \sum_i H_{int}(ik) \left| j^n J v \right\rangle = a\,\frac{n(n-1)}{2} + b\left[J(J+1) - n j(j+1)\right] + c\left(\frac{n-v}{2}\right)(2j+3-n-v) \qquad (2)$$

where q_{ik} is the pairing operator and v is the seniority quantum number. Evidently the relative excitation energies are functions of only two parameters b and c. For n = 2 we get from eq. (2) the relations

$$b = \frac{E(4^+) - E(2^+)}{14}\ ; \quad c = \frac{3\,E(4^+) - 10\,E(2^+)}{42}. \qquad (3)$$

Out of $(5/2)^n$ configurations only case of interest left now is with n = 3 since n = 1(5) are single particle (hole) states and n = 4 (two holes) is same as n = 2. For n = 3, the allowed j-j coupled states have J = 3/2, 5/2 and 9/2 only. Their relative separations in terms of b and c, as obtained by using eq. (2), are as follows:

$$E(5/2) - E(3/2) = 5b + 4c\ ;\ E(9/2) - E(5/2) = 16b - 4c \qquad (4)$$

Thus, provided two particle spectra are known, the three particle spectra can be calculated.

We have carried out calculations for sixteen n = 2, 3 sets of nuclei listed below:

Orbital	Nucleon No.	Neutron nuclei	Proton nuclei
1 d5/2	10 - 11	$^{18,19}O$; $^{20,21}Ne$	^{20}Ne-^{21}Na, ^{22}Ne-^{23}Na
1 f5/2	34 - 35	$^{62,63}Ni$; $^{64,65}Zn$	Se-Br with A values 76-77, 78-79, 80-81, 82-83
2 d5/2	52 - 53	$^{90,91}Sr$; $^{92,93}Zr$; $^{94,95}Mo$	Te-I with A values 124-125, 126-127, 128-129

The results are available in a tabular form but Talmi

had suggested a graphic representation, which also brings out the competing roles of the pairing (b = 0 limit) and the long range (c = 0 limit) coupling schemes. These graphs are shown in figs. 1 and 2 separately for the proton and the neutron cases.

The following are some of the important observations based on this study :

(a) We obtain a very simple criterion for $(5/2)^3$ cases for which the 3/2 state will lie lower than the 5/2 state. From eqs. (3) and (4) this is found to occur for nuclei in which the energy ratio $E(4^+)/E(2^+)$ for the neighbouring even-even nucleus is greater than 2.037, i.e. the so-called 'vibrational' criterion in even-even nuclei also corresponds to lowering of (j-1) state in odd mass nucleus. This is found to be approximately so except for ^{65}Zn wherein a second 5/2 state also appears at 206 keV excitation.

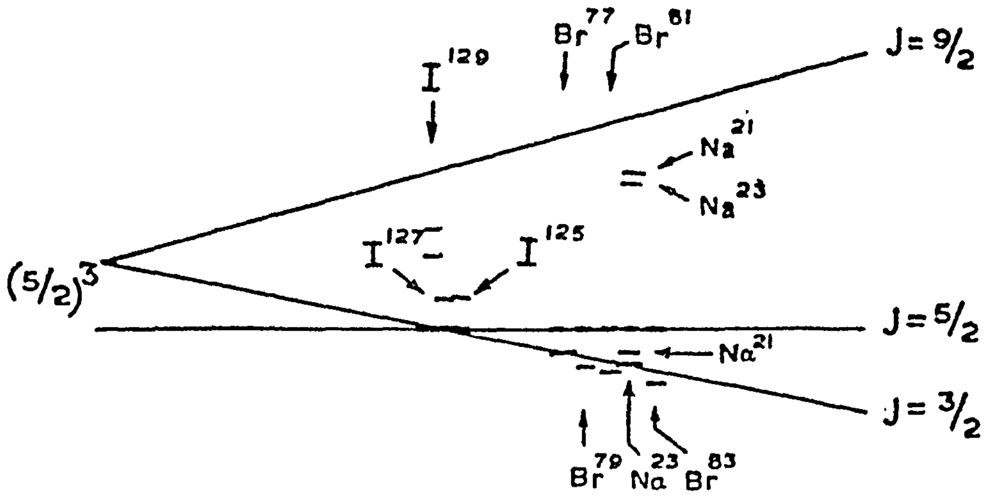
(b) Although for ^{23}Na the agreement is quite good, for ^{21}Na and ^{21}Ne the predictions are quite low.

(c) In Iodine isotopes the theory predicts 3/2 to be nearly degenerate with 5/2 whereas experimentally we find it at about 200 keV in A = 125 and 127, and at 559 keV in A = 129.

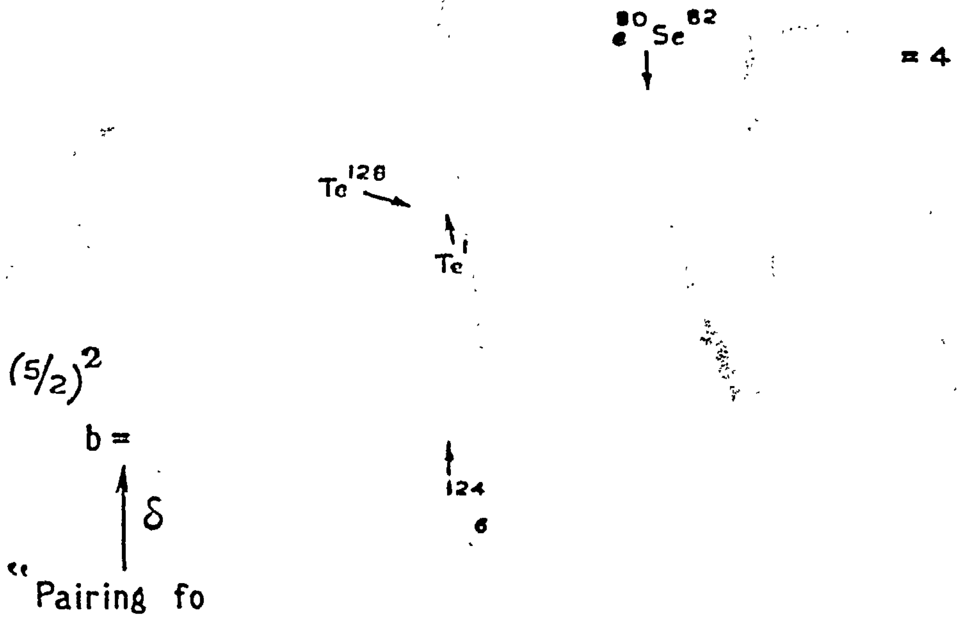
(d) In other cases the agreement is fair to moderate; best agreement is obtained for ^{93}Zr and ^{77}Br wherein 9/2 levels are predicted at 1.10 and 1.17 MeV respectively.

On the whole it may be concluded that this formulation has not been found satisfactory for quantitative

PROTON CASE



I^{129}
Br^{77}
Br^{81}
J= 9/2
Na^{21}
Na^{23}
I^{127}
I^{125}
$(5/2)^3$
J= 5/2
Na^{21}
J= 3/2
Br^{79}
Na^{23}
Br^{83}



Se
= 4
Te
$(5/2)^2$
b =
δ
"Pairing fo

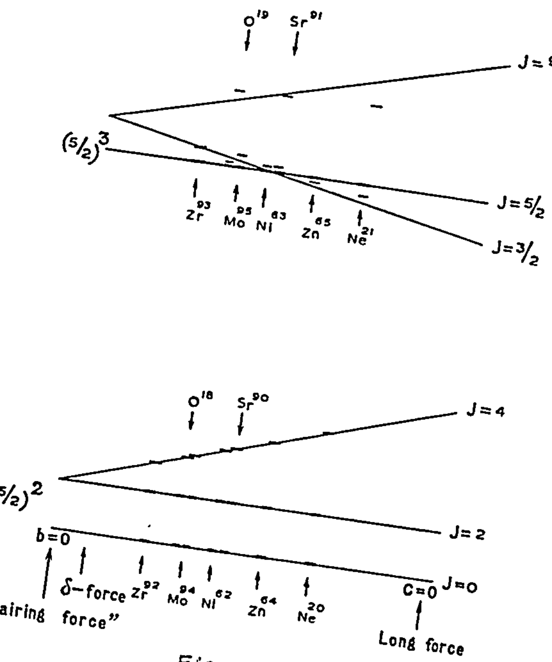

NEUTRON CASE
O^{19}
Sr^{91}
$(5/2)^3$
J = 5/2
J = 3/2
Zr^{93}
Mo^{95}
Ni^{63}
Zn^{65}
Ne^{21}
O^{18}
Sr^{90}
J = 4
$(5/2)^2$
J = 2
b = 0
J = 0
δ-force
Zr^{92}
Mo^{94}
Ni^{62}
Zn^{64}
Ne^{20}
C = 0
airing force"
Long force

Fig-2

description of nuclear spectra. This may result from different admixtures of various configurations in even-even and odd mass nuclei (so that the matrix elements of the effective interaction do not remain the same) or alternatively this may point to the relatively different contributions from the competing coupling schemes. Anyway the simple shell model scheme is actually found to be not so simple here!

SHELL MODEL DESCRIPTION OF $(d_{3/2})^n$ NUCLEI

A.N. Mantri and P.C. Sood
Physics Department, Banaras Hindu University, Varanasi-5.

The detailed description of nuclear energy levels in the shell model scheme involves the use of an effective interaction. The nuclear spectra are then calculated under the assumption that the parameters (or the matrix elements) of this interaction do not vary appreciably from nucleus to nucleus within any given configuration. In the Talmi approach one determines these matrix elements from the experimental data itself for, say, $(j)^2$ configuration and these are then used to calculate the energy levels for n particles in the same configuration.

In this paper we discuss the energy levels of $(d_{3/2})^n$ nuclei in the mass region $34 \leq A \leq 38$. The j-j coupled states in the seniority scheme may be labelled by four quantum numbers, i.e. total angular momentum J, total isospin T, seniority V, and reduced isospin t. For $(3/2)^2$ case four such (JTvt) states are possible which, if experimentally known, can be used to determine a four parameter effective interaction. Such an interaction may be taken as [1]

$$H_{int}(12) = a + 2b\vec{t}_1.\vec{t}_2 + cq_{12} + 2d\vec{j}_1.\vec{j}_2 \ \ldots\ldots \quad (1)$$

With this interaction, the energy in the n particle case can be written down in the form of a closed expression as given below :

$$\langle j^nJTvt/\sum_i H_{int}(ij)/j^nJTvt\rangle = \left[\frac{n(n-1)}{2}\right]a + \left[T(T+1) - \tfrac{3}{4}n\right]b + \left\{\left(\frac{n-v}{4}\right)(4j+8-n-v) - T(T+1)+t(t+1)\right\}c + \left\{J(J+1) - nj(j+1)\right\}d. \quad \ldots\ldots (2)$$

It is clear from eqn.(2) that the excitation energies of various levels in a given nucleus depend only on the three parameters b, c and d.

Nuclei with n = 2

For two identical nucleous we have $|T_z| = 1$ and hence T = 0 states of $(3/2)^2$ configuration do not appear for these even-even nuclei. For two non-identical nucleons we have four (JTvt) states which, as mentioned above, can be used to determine the three parameters. Such nuclei are ^{34}Cl and ^{38}K. The experimental[3,4] level schemes for these nuclei are shown in fig.1. It is seen that the spectra for these two nuclei is not identical; aside from the differences in the excitation energies, even the ordering of the 0^+ and 3^+ states is found to be reversed between them. Thus a single set of parameters cannot exactly describe both these spectra. We have chosen an average set of parameters with values

b = 0.953 MeV, c = - 0.626 MeV, d = - 0.049 MeV...(3)

These values put both the 0^+ and the 3^+ levels at zero energy. The relative separation of the 0^+ and the 2^+ levels comes out to be 2.21 MeV which is also in good agreement with the experimental data for even nuclei as shown in fig. 1.

Nuclei with n = 3

The calculated energy levels for $(d_{3/2})^3$ configuration using the parameters given in eq.(3) above are shown in fig.2 in comparison with the available experimental data for corresponding nuclei. The comparison reveals the interesting fact that not only there is disagreement on the excitation energies but rather a complete reversal of the level ordering seems to have appeared. We shall comment on this serious discrepancy later on.

Nuclei with n = 4

For n = 4 the experimental information is available only for one nucleus in each of the two classes -- the odd-odd nucleus ^{36}Cl and the even-even nucleus ^{36}Ar. The observed spectra for these two nuclei are compared with the calculated values in fig.3(a) and (b) respectively. In ^{36}Cl there is ambiguity about the 1^+ level and although several unassigned levels are known around 4 MeV, the $0^+(T = 2)$ level has not been identified. In view of these factors the agreement can be termed only qualitative. For ^{36}Ar again the nature of the agreement is not much different.

Concluding Remarks

Our analysis shows that the effective interaction parameters as determined from n = 2 spectra are not satisfactory for the description of t.

$(d_{\frac{3}{2}})^2$ CONFIG.

odd – odd

even – even

MeV $J^{\pi}(T, v, t)$

2.16 2^+

2.40 2^+

2.21 $2^+(1,2,1)$

2.13 2^+

2.1 2^+

2.17 2^+

2.20 2^+

0.67 1^+

0.46 1^+

0.50 $1^+(0,2,0)$

0.15 3^+ 0^+

0.13 0^+ 3^+

$0^+(1,0,0)$ $3^+(0,2,0)$

0^+ 0^+ 0^+ 0^+

$_{17}Cl_{17}$ $_{19}K_{19}$ $_{16}S_{18}$ $_{18}Ar_{16}$ $_{18}Ar_{20}$ $_{20}Ca_{18}$

EXPT

CALC

EXPT

FIG. 1.

MeV $J^{\pi}(T, v, t)$

$(d_{\frac{3}{2}})^3$ CONFIG.

$_{17}Cl_{18}$: 2.64 $(\frac{7}{2})$; 1.76 $\frac{3}{2}^+$; 1.22 $\frac{1}{2}^+$; 0 $\frac{3}{2}^+$

$_{18}Ar_{17}$: 2.7; 1.60; 1.20; 0 $\frac{3}{2}^+$

$_{18}Ar_{19}$: 2.8 $\frac{5}{2}^+$; 2.22; 1.41 $\frac{1}{2}^+$; 0 $\frac{3}{2}^+$

$_{19}K_{18}$: 3.08 $\frac{5}{2}$; 2.75 $(\frac{3}{2},\frac{5}{2})^+$; 2.28; 1.37 $(\frac{1}{2}+)$; 0 $\frac{3}{2}^+$

CALC: 4.74 $\frac{3}{2}^+(\frac{3}{2}, 1, \frac{1}{2})$; 3.26 $\frac{1}{2}^+(\frac{1}{2}, 3, \frac{1}{2})$; 2.68 $\frac{5}{2}^+(\frac{1}{2}, 3, \frac{1}{2})$; 2.54 $\frac{7}{2}^+(\frac{1}{2}, 3, \frac{1}{2})$; 0 $\frac{3}{2}^+(\frac{1}{2}, 1, \frac{1}{2})$

EXPT

CALC

FIG 2

$(d_{\frac{3}{2}})^4$ CONFIG.

odd – odd | even – even

J^{π} (T.v.t)

9.47 — 0^+ (2,0,0)

7.18 — 3^+

6.82 — 1^+ (1,2,0)

6.61 — 2^+ T=1 Level

6.33 — 3^+ (1,2,0)

5.97 — 2^+ (0,4,0)

MeV J^{π} (T.v.t)

5.67 — 2^+ (1,2,1)

5.28 — 4^+ (0,4,0)

4.98 — (2^+)

4.44 — (2^+)

4.41 — 4^+

4.11 — 0^+ (2,0,0)

2.21 — 2^+ (0,2,1)

1.97 — 2^+

1.60 — $(1.2)^+$

1.45 — 1^+ (1,2,0)

0.96 — 3^+ (1,2,0)

0.78 — 3^+

— 2^+ — 2^+ (1,2,1) — 0^+ — 0^+ (0,0,0)

$_{17}Cl_{19}$ | $_{18}Ar_{18}$

EXPT CALC | EXPT CALC

FIG. 3 (a) | FIG. 3 (b)

spectra and fail rather miserably for n = 3 nuclei. The latter situation cannot be remedied simply by minor adjustment of the parameters of the effective interaction but possibly corresponds to an abrupt change in the relative contributions of the pairing and the long range terms in the interaction with its related implications about the nuclear shapes in these nuclei. These features are presently being investigated.

REFERENCES

1. Talmi and Unna, Ann. Rev. Nucl. Sci., 10. 353(1960).
2. Racah, Phys. Rev. 63, 367 (1943).
3. Endt, Van derLeun, Nucl. Phys. A 105, 1, (1967).
4. Fortune, Puttaswamy, and Yntema., Phys. Rev. 185, 1550 (1969).

DISCUSSION

B.K. Jain: What is V_{12} in the interaction term?

A.M. Mantri: V_{12} is pairing interaction term with its matrix element given as follows

$$\langle j^2 J | V_{12} | j^2 J \rangle = (2j+1)\, \delta_{J0}$$

THE DEPENDENCE OF NUCLEAR MATTER BINDING ENERGY ON THE HIGH ENERGY PHASE SHIFTS

M.K. Srivastava
Department of Physics, University of Roorkee, Roorkee

I. INTRODUCTION

Recently Fiedeldey[1] has investigated the effect of the high energy phase shifts on the triton binding energy E_T. The low energy phase shifts were kept fixed while in the high energy region arbitrary changes were made. The potentials were obtained by using the solution of the inverse scattering problem for rank two separable potentials. He finds that these modifications in the standard phase shifts at high energies produce large variations in the triton binding energy (as much as 70% in some cases). This result is surprising since previous calculations by Tabakin[2] have indicated only 5-10% change in the binding energy by replacing a soft potential with a hard core one.

In this note we study the effect of arbitrary changes in the high energy S-wave phase shifts (E_{lab}>350MeV) on the binding energy per particle E_{NM} in nuclear matter. The object is two fold: (i) To see whether we get much larger variations in E_{NM}. This is, a priori, expected since nuclear matter is denser than triton. (ii) To examine whether the trend of variation of E_{NM} is the same as that of E_T. In the study of the off-shell effects with phase shift equivalent rank two separable potentials we found that they have opposite trend of variation.[3,4]

II. CONSTRUCTION OF THE POTENTIALS

Our standard phase shifts δ_0 are those given by

Tabakin.[2] These are the average between the singlet-S and the triplet-S NN phase shifts and have been generated by a second rank separable potential of the form

$$V(k,k') = \frac{\hbar^2}{2m\pi^2}\left[-g(k)g(k') + h(k)h(k')\right], \qquad (1)$$

with

$$g(k) = \frac{\alpha}{k^2+a^2}, \quad \alpha = 2.074\ \text{fm}^{-3/2}, \quad a = 1.1881\ \text{fm}^{-1}, \qquad (2)$$

and

$$h(k) = \frac{\beta k^2}{\{(k-d)^2+b^2\}\{(k+d)^2+b^2\}}$$

$$\beta = 2.664\ \text{fm}^{-3/2}, \quad b = 1.248\ \text{fm}^{-1}, \quad d = 1.444\ \text{fm}^{-1}. \qquad (3)$$

Arbitrary variations in the phase shifts in the high energy region (E>350 Mev lab) have been produced in the following way:

$$\delta_m(k) = \begin{cases} \delta_0(k) & k \leq k_c \\ \delta_0(k_c) + C(k-k_c)\exp\{(k_c-k)/100\}/\{1+m(k-k_c)^n\} & k > k_c \end{cases} \qquad (4)$$

We have taken $C = (d\delta_0/dk)_{k_c} = -15.03$ degrees fm and $k_c = (350m/2\hbar^2)^{1/2} = 2.054\ \text{fm}^{-1}$. This avoids any kink in δ_m at $k = k_c$. The factor $\exp[-(k-k_c)/100]$ ensures that δ_m goes to zero fast enough as $k \to \infty$. This improves the convergence of the integrals over δ_m without effecting the phase shifts in the interesting region. The parameters m and n produce the required arbitrary changes in the phase shifts.

The attractive form factor g(k) of the potential and the two body binding energy $E_D = \frac{\hbar^2}{m}k_D^2 = 0.43$ Mev were kept fixed at the values given by Tabakin.[2] The repulsive form factor h(k) in the potential was obtained in each case by solving the inverse scattering problem

for rank two separable potentials as suggested by Fiedeldey.[5]

III. CALCULATION

Nuclear matter calculations were done in the reference spectrum approximation. First and second order terms in the reference G-matrix were evaluated, taking the unoccupied state spectrum for the single particle potential to be zero. The higher order terms were estimated by the geometric series approximation of Dahll et.al.[6] Self-consistency with respect to the reference spectrum gap parameter Δ and the effective mass m^* for the occupied spectrum was achieved by iteration.

IV. RESULTS AND DISCUSSION

E_{NM} does not seem to depend very much on the phase shifts for $k > k_c$. At saturation $k_F \simeq 2.1\ fm^{-1}$, E_{NM} varies from 29.1 Mev to 29.3 Mev. Slightly larger variation is observed at $k_F = 2.4\ fm^{-1}$. More repulsive phase shifts always lead to decrease in the binding energy. Similar nuclear matter calculations were reported by Law.[7] By assuming positive phase shifts and using rank one separable potentials he got much larger changes in E_{NM} by varying the phase shifts in the region $k \sim 1 fm^{-1}$. This is expected since this region is rather important. We have limited our study to E>350 Mev lab because it is in this region where the phase shifts are not known accurately and unambigously.

It appears that 'physically reasonable' forces would not produce large variations in the binding energy either in nuclear matter or in triton. Large changes in

E_T, reported by Fiedeldey,[1] were obtained only when the attractive form factor was made unrealistically short ranged (0.2 - 0.6 fm).

Our results confirm the findings of Elliott et.al.[8] that nuclear structure calculations do not depend significantly on the high energy phase shifts.

REFERENCES

1. H. Fiedeldey; preprint.

2. F. Tabakin; Phys. Rev. 137, B75 (1965).

3. H. Fiedeldey; Phys. Lett. 30B, 603(1969).

4. M.K. Srivastava, Yogeshwar Singh and R.K. Bhaduri; Phys. Lett., 32B, 333(1970).

5. H. Fiedeldey; Nuc. Phys. A135, 353 (1969).

6. G. Dahll, E. Ostgaard and B.H. Brandow; Nuc. Phys. A124, 481(1969).

7. J. Law; Nuovo Cimento 58, 258 (1968).

8. J.P. Elliott, H.A. Mavromatis and E.A. Sanderson; Phys. Lett. 24B, 358(1967); J.P. Elliott, A.D. Jackson, H.A. Mavromatis, E.A. Sanderson and B. Singh; Nuc. Phys. 121A, 241(1968).

*****

DISCUSSION

H.R. Kidwai: Can you tell us the values of the parameters in your calculations.

M.K. Srivastava: $\Delta \simeq 0.9$
$m^* \simeq 0.4$

C.S. Warke: In view of the fact that the π-threshold is at 290 MeV. How much is it meaningful to consider a potential between the nucleons at very high energy?

M.K. Srivastava: Assuming a phenomenological potential, the purpose is to study how its characteristics are reflected in the many-body calculations.

THE DUAL CORE MODEL FOR B^{10} NUCLEUS

K.L.Narayana and Shamrao B.Desai *
Department of Physics, Shivaji University,
Kolhapur.

-o-

INTRODUCTION

The estimates of binding energy made by De Shalit and Talmi[1,2] indicate a quantitative extra-core nucleons contributions especially for the nucleii which fall in the middle of the shells. De Shalit and Talmi have attempted to explain the exact contributions to the binding energy both by taking into account the inter-configurational mixing and deformation effects.

However in view of the fact that the extra-core nucleon contributions are significant an attempt has been made earlier by Narayana[3] to estimate the binding energy of the boron nucleus with the assumption that B^{10} may be considered as resonating structure of a single and possible multiple core structures. His calculations indicate a 40% dual core component (with Gaussian wave function and 50 Mev strength) in the total nuclear wave function. This result is contradictory to the conclusion arrived at by Wergeland[4]. The later has made a variational calculations in which the α -model wave function is modified by an admixture of an elliptical model wave function. He takes $\Psi = \Psi_H + \lambda \Psi_\alpha$ where Ψ_α is an antisymmetric sum of product of eight Heitler-London form of nucleon orbitals and Ψ_H a similar wave function for

* U.G.C. Research Scholar, Shivaji University, Kolhapur.

elliptical model . The variational calculation gave rise to a value of λ = 1.3 suggesting that nucleus remains somewhat closer to the elliptical model that the α-model. However, elliptical model itself resembles α-model much more than the shell (a central) model. Thus this result suggests a pronounced role of the dual core component.

The object of the present investigation is to improve the wave function which describes the dual core structure by inclusion of higher order radial and angular orbitals in constructing the extra core nucleon wave function.

METHOD AND CALCULATION

Based on the considerations of (a) Flexibility of the wave function to incorporate deformation effects and description in terms of the probable clusters, (b) Accurate account of the correlation effects, (c) Optimum convergency property of the wave function with relatively few terms of higher order orbitals mixing, the wave function has chosen to be of the form,

$$\Psi = \Sigma_i C_i \Phi_i[1,2] \{1+P_{12}\} \chi \, \xi$$

$$\Phi_i[1,2] = e^{-\alpha_1 \xi_1^2 - \alpha_2 \xi_2^2 - \beta_1 \xi_1 \eta_1 - \beta_2 \xi_2 \eta_2} \cdot \xi_1^{m_i} \xi_2^{n_i} \eta_1^{j_i} \eta_2^{k_i} \rho^{p_i}$$

where ξ and the corresponding η are the distance and angular parameters of a nucleon relative to the centre of the nucleus and ρ is the dimensionless parameter associated with the separation of the two nucleons. The χ and ξ functions are respectively the ordinary and isotopic functions (for T = 0 and J = 3^+ state). The exponents (α_i, β_i) and C_i are the variational parameters.

A preferential[5] coordinate system viz. the body system of the coordinates which moves much slower than the motion of the nucleons itself has been used.

RESULTS;

Three different wave functions $\phi_1(1,2)$, $\phi_2(1,2)$, $\phi_3(1,2)$ are chosen at first to compute the ground state energy with the values for (m_1, n_1, j_1, k_1, p_1) respectively as (00000), (10000), (00002). The energies[θ] that would give rise to directly with the Hamiltonian H previously mentioned[D)] for B^{10} nucleus are E_{11} = -46 Mev, E_{22} = -39 Mev, and E_{33} = -222 Mev where E_{ij} stands for $\langle \phi_i(1,2) | H | \phi_j(1,2) \rangle$. The first two correspond to the energies one obtains with the assumption of pure shell model s and p orbitals for the outer most nucleons.

The lowest ground state energy for the B^{10} nucleus with 10 Mev -force turned out to be - 62 Mev when all the three basis wave functions given above are admixed. The amounts of the admixture are 10%, 19%, 71% respectively for the three basis wave functions. The low 10% Is character is in conformity with the studies[6] of the (p, 2p) scattering experiments.

The author (K.L.N.) is deeply indebted to Professor K.Rangadhama Rao and Professor O.M.P.Bilaniuk, Swarthmore college, Swarthmore, U.S.A. for their interest and encouragement.

REFERENCES

1. De-Shalit A. and Talmi I., Nuclear Shell theory, Academic Press, New York (1963).

2. I.Talmi and R.Thiorberger; Phys. Rev. 103 , 719(1956

3. K.L.Narayana; Curr. Sci. 38, 261 (1969).
Ibid, 38, 487 (1969).

K.L.Narayana; Proc. Nucl. and Solid State Physics Symposium, BARC, Bombay, held at Roorkee, 1969.

K.L.Narayana and S.B.Desai ; Shivaji University Journal (1970).

4. H.Wergeland ; Norske Videnskabers Selskabs Skrifter, 1, 1941.

5. D.R.Inglis; Rev. Mod. Phys. 25, 390 (1953).

D.R.Inglis; Phy. Rev. 126, 1789 (1962).

6. T.Berggren and G.Jacob; Nucl. Phys. 47, 481 (1963).
T.Berggren and G.Jacob; Phys. Lett. 1, 258 (1962).

J.M.Hansteen and M.I.Kanestro ; Nucl. Phys. 46, 303 (1963).

-oooo0ooo-

MODEL INDEPENDENT NO PARAMETER ANALYSIS OF SINGLE PARTICLE LEVELS OF LIGHT NUCLEI USING THE PHASE SHIFT METHODS OF ELLIOTT.

Jishnu Dey
Department of Physics, Chandernagore College, Hoogly

I. INTRODUCTION

Much attention has been drawn recently to methods due to Elliott, of getting nuclear matrix elements directly from phase shifts. The value of these matrix elements was shown to be remarkably independent of the parameters of the auxiliary potential which fits the phases roughly at a given energy, this value being the integral of this potential with the eigenfunction at this energy plus the born term for the difference of phase shifts. The relevant energy, as the eigenvalue, is dependent, through matching conditions, on the laboratory energy as well as the depth of the potential so that the shift in the eigenvalue coupled with the energy variation property of the phase shifts make the matrix independent of the auxiliary potential.[1] The matching also ensures healing of the wavefunction.[2]

The set of matrix elements given by Elliott and his co-workers were applied to nuclear matter by him and the present author, - and in first order reasonable binding was obtained at reasonable densities.[3] The The second born type corrections gave small contribution.[4]

Other corrections from the core are neccessary for saturation at high density[3], their nature was indicated[5], and their magnitude estimated[4]. It was found that they have the correct sign and magnitude at high density - so that they may yield the required satruation.

Deuteron properties[6] and properties of other nuclei were calculated with these matrix elements by Elliott and his collaborators, including the present author[3].

Earlier, using born approximation without any auxiliary potential, a set of matrix elements were deduced by Elliott, Mavromatis and Sanderson[7] for P and D relative channels, and these were found to yield good spin orbit splittings in light nuclei. The method was applied to S-states as well, and extensive sets of matrix elements were deduced by Sprung, Srivastava and Jopko. It is possible to interpret these as matrix elements of a free reaction matrix, t_{free}, following suggestions by Brink, Peierls and others. Some of our finite nucleus calculations were repeated for this t_{free} and comparison of these with other calculations reveal interesting results. It is found for example, that the b = 2.0 fm, matrix elements upto N = 6 published by Sprung et. al.[8] are enough to get a binding of 2.2 Mev for deuteron. For this b value even for the Elliott matrix elements[1] it is not necessary to extrapolate, and for N = 6 quanta a binding of 2.4 Mev and for N = 8, 3.2 Mev are obtained.

More details of the calculation will be given elsewhere but the conclusions of Elliott and Jackson [(6)] based on calculations using much smaller b, seem to need some modification. A general result seems to be that the data upto 300 Mev is sufficient, and both the methods tend to overbind : through the underestimated core in the Elliott method and through overestimated long range part by neglect of the Pauli operator in the t_{free}.

II. SECOND ORDER CALCULATION OF SINGLE PARTICLE SPECTRUM.

In a consistent calculation of the energy difference between a closed shell plus one and closed shell, one should include, in addition to the first order, five types of second order diagrams. This involves ladder type and Hartree type diagrams involving particle and hole lines in each type, and the two involving holes are repulsive while the two involving particles are attractive. For light nuclei the hole diagrams contribute little or nothing and the Hartree type diagrams are small. The fifth diagram is a cross between the two types and was first pointed out by Elliott. This shifts a level j by :

$$dE_j = (4j+2)^{-1}\sum_p (2p+1)^{-1}\sum_{h_1} (2J_1+1)(2T_1+1)\langle jh_1J_1T_1|\bar{V}|jpJ_1T_1\rangle$$

$$\sum_{h_2}(2J_2+1(2T_2+1)\langle h_2h_1J_2T_2|\bar{V}|h_2pJ_2T_2\rangle/2\hbar w \qquad (1)$$

in the standard notation. $\bar{V}$ here stands for the nuclear potential minus the relative oscillator, the

proportional to hw/A. With this the last sum in (1) may be seen to be the binding energy of the closed shell differentiated with respect to b.[1] Thus for the Elliott method, due to the lack of saturation, this diagram is always repulsive making the total second order contribution small or even repulsive. This does not help the absolute position of the levels or the l-splitting problems of Dey et al.[3] For example, in Oxygen 17, the $0d_{5/2}$ is 4 Mev unbound while the $1s_{\frac{1}{2}}$ gets 1 Mev below the $0d_{5/2}$. This way the lack of saturation through the neglect of the core gets in here as well.

III. CALCULATIONS WITH t_{free} AND CONCLUSIONS.

An easy first order calculation with t_{free} yields better results. The $0d_{5/2}$ level of the Oxygen nucleus for example is now 1 Mev overbound and the $1s_{\frac{1}{2}}$ is 0.1 Mev above it. It is reasonable to suppose that if the Pauli operator effects are taken care of properly the levels will be shifted up, the s-level more than the other. Hence, to get good single particle spectra the core has to be treated as an important factor.

REFERENCES

1. J.P.Elliott, A.D.Jackson, H.A.Mavromatis, E.A.Sanderson, and B.Singh; Nucl. Phys. 121,241(1968).

2. E. Ley Koo and M.De Llano; Phys. Lett. 31B,261(1969).

3. J.Dey, J.P.Elliott, A.D.Jackson, H.A.Mavromatis, E. A. Sanderson and B.Singh; Nucl.Phys. A134,385 (1969).

4. J.Dey; D. Phil. Thesis under J.P.Elliott, University of Sussex.

5. A.D. Jackson, H.A.Mavromatis and E.A. Sanderson; Nucl. Phys.A124,1(1969).

6. J.P.Elliott and A.D.Jackson; Nucl.Phys.121,242(1968)

7. J.P.Elliott, H.A.Mavromatis and E.A.Sanderson ; Phys. Lett.24B,358(1967).

8. A.M.Jopko, M.K.Srivastava and D.W.L.Sprung; Can.J. Phy. 47, 2459(1969).

REACTION MATRIX CALCULATION WITH A NON-LOCAL SEPERABLE POTENTIAL

Q.N. Usmani
Department of Physics
Aligarh Muslim University, Aligarh, U.P.

ABSTRACT

Kallio and Day version of the reference spectrum method has been applied to calculate the reaction matrix elements of a non-local separable potential. The basic equation has been reduced to non-homogeneous second order integro-differential equation, which is then solved by the Green's function method. The Pauli operator Q has been treated very accuratly in singlet as well as in triplet states.

General Comments by C.S. Warke

In view of the fact that now-a-days one does (Oak ridge group) nuclear spectroscopic calculations with 500 to 550 component wave functions, one should ask one self, how far can he stretch the single minded calculations of the same properties using j^n one component wave-functions and a phonon particle model. I must add that such calculations are always welcomed to explain new physical results but spectroscopic calculations certainly should be avoided.

In low energy nuclear physics we use N-N potentials which fit the scattering data upto 350 to 400 MeV and deutron properties. One gets many potentials which give the same experimental results. The question then arise is how to choose or discard some potential from these. Of course one could test these potentials against the data on p- p bremstrahlung and photo disintegration of deuteron. However, due to the fact that these do not go very far off the shell and with the large experimental errors and these potentials reproduce these results. Therefore one would like to test various potentials against the nuclear binding and energy levels, and see whether these are the sensitive functions of the potential. This was the aim of the papers of M.K. Srivastava and J. Dey.

AN UNIFIED THEORY ON THE STRUCTURE OF ATOMS AND NUCLEI

R Ramanna and S Jyothi
Bhabha Atomic Research Centre, Bombay

A manifold can be defined as a set of overlapping patches of coordinate systems which are individually euclidean but globally non-euclidean E Cartan's geometric theory of partial differential equations consists in defining a partial differential equation on each coordinate patch of the manifold In the overlapping region of the manifold the two differential equations must be invariant Depending on the nature of this manifold, this invariance gives rise to special results.

If the differential equations represent quantum-physical equations i. e., the Schrodinger equations and the coordinate systems are of space and time, it can be shown that the energy of the system is minimised if the coordinates of the first system (x_1, t_1) are related to those of the second system (x_2, t_2) by the Cauchy-Riemann relations

$$\frac{\partial x_1}{\partial x_2} = \frac{\partial t_1}{\partial t_2} = p \quad \text{and} \quad \frac{\partial x_1}{c\,\partial t_2} = -c\,\frac{\partial t_1}{\partial x_2} = q \qquad (1)$$

We multiply all quantities involving time by c, the velocity of light, to make p and q dimensionless quantities.

The minimisation of energy is shown with the help of the Dirichlet principle, which states that the integral

$$I = \iint_{D_t D_s} |a|^2 + |b|^2 \, dx\, dt \qquad (2)$$

is a minimum if $|a| + i|b|$, $|a| - i|b|$ are harmonic functions. Here $|a|$ and $|b|$ are functions of x and t and D_t, D_s are the domains of the integral over x and t.

Consider two Schrodinger equations defined in two overlapping domains with different coordinate systems (x_1, t_1) and (x_2, t_2)

$$\frac{\hbar^2}{2m_1}\frac{\partial^2 \psi_1(x_1,t_1)}{\partial x_1^2} + V_1(x_1,t_1)\psi_1(x_1,t_1) = i\hbar\frac{\partial \psi_1(x_1,t_1)}{\partial t_1} \quad (3)$$

$$\frac{\hbar^2}{2m_2}\frac{\partial^2 \psi_2(x_2,t_2)}{\partial x_2^2} + V_2(x_2,t_2)\psi_2(x_2,t_2) = i\hbar\frac{\partial \psi_2(x_2,t_2)}{\partial t_2} \quad (4)$$

By a coordinate transformation of (x_2, t_2) into (x_1, t_1) according to (1), it can be shown that in the overlap region due to invariance, the following equation holds:

$$p\,\frac{\partial^2 p}{\partial x_1^2} - \frac{1}{2}\left(\frac{\partial p}{\partial x_1}\right)^2 - \frac{2m_2c^2}{\hbar^2}\frac{(m_2-m_1p)(3m_2-m_1p)}{(2m_2-m_1p)} = \frac{4}{\hbar^2}(m_2V_2-m_1p^2) \quad (5)$$

The systems considered are stationary (time independendent) and the potentials V_1, V_2 are real.

Equation (5) is a standard non-linear differential equation which is invariant to automorphic transformations i.e., the solutions could be elliptic functions.

The function used to explain atomic structure is

$$p = A\exp\left[-\mu\, \mathrm{Sn}\frac{4Kx_1}{n\alpha_H}\,\mathrm{dn}\frac{4Kx_1}{n\alpha_H}\right] + B \quad (6)$$

where A, B are constants, n is an integer, $\mu = \frac{\text{mass of electron}}{\text{mass of proton}}$, α_H is the radius of the first Bohr orbit, the modulus of the elliptic functions $\mathrm{Sn}\frac{4Kx_1}{n\alpha_H}$, $\mathrm{dn}\frac{4Kx_1}{n\alpha_H}$ is $k = \sin 45^\circ = 1/\sqrt{2}$ and K = complete elliptic integral of the first type with modulus $= k = 1/\sqrt{2}$.

Putting (6) in (5) it can be shown that for certain fixed values of A, B and for small values of x_1, v_1 approximates to a $1/x$ law. From Eq (1) and (6) it can be shown that

$$x_2 = \frac{x_1}{\sqrt{S}} - \frac{n\alpha_H}{4K} \frac{A\mu}{S} \ln \frac{4Kx_1}{n\alpha_H} + Q \qquad (7)$$

where Q is a constant of integration and S is a scaling factor relating the potentials V_1, V_2 at a point in the overlap region by the equation

$S = m_2 V_2 / m_1 V_1$

We define the radius of the Bohr orbit as the distance between the origins of the two overlapping coordinate systems measured in one of the systems. If $(x_1)_{x_2=0}$ is the distance measured in the x_1 system for the point corresponding to $x_2 = 0$ in the x_2 system and $(x_2)_{x_1=0}$ is the distance measured in the x_2 system for the point corresponding to $x_1 = 0$ in the x_1 system, then from (7) it is easily deduced that

$$(x_1)_{x_2=0} = n^2 \alpha_H \qquad (8)$$

where $n = 1, 2, \ldots\ldots\ldots$ This is the usual expression for the Bohr orbits.

The energy of the many body system can be obtained from Eq (2) in the following manner. We assume

$$|a| + i|b| = Sn\left(\frac{4Kx}{n\alpha_H} + \frac{i4Kt}{nT_0}\right) dn\left(\frac{4Kx}{n\alpha_H} + \frac{i4Kt}{nT_0}\right)$$
$$|a| - i|b| = Sn\left(\frac{4Kx}{n\alpha_H} - \frac{i4Kt}{nT_0}\right) dn\left(\frac{4Kx}{n\alpha_H} - \frac{i4Kt}{nT_0}\right) \qquad (9)$$

For a characteristic time $t = T_0$, due to the double-periodicity of the integrand of (2) we can write

$$E^2 = Q \int_{\Omega_t} \partial\left(\frac{4Kt}{nT_0}\right) \int_{\Omega_S} Sn^2\left(\frac{4Kx}{n\alpha_H}\right) dn^2\left(\frac{4Kx}{n\alpha}\right) d\left(\frac{4Kx}{n\alpha}\right)$$

The energy given by the integral is the energy associated with a given domain. It is assumed that it is distributed over the corresponding domain in the complex plane. An atom in its stable state is characterised by its average position and the domain width Δ . The average position of the atom has a real part and an imaginary part. It is assumed that no two atoms can have domains of the same width unless they differ in their average positions either in their real parts or in imaginary parts. The shell structure arises because of the restriction that no two atoms can have the same three parameters viz. the real and imaginary parts of the average position and the domain-width. The above restriction is considered as the geometrical equivalent of the Pauli principle which gives rise to a shell-behaviour in the usual quantum theory of atomic structure.

To compare the measured energies of atoms in stable state with those predicted by the present theory, the domain-measures of these atoms are mapped into an order on the real line by a Schwarz-Christoffel transformation. Consider the lattice of points in the complex plane implied in (9). The points of this lattice form the vertices of isosceles right angled triangles. It can be shown that all lattice points along the sides of right-angled isosceles triangles with base lengths equal to 2, 7 or 14 in some arbitrary units can be considered for mapping. Along the real and imaginary axes oddmultiples of K for domain-widths lead to stable states, while along the hypotenuses all multiples of (-K + iK') for domain-widths are allowed.

Figure 1 gives the selected points on the complex plane.
When each point is fill-d with the appropriate atom with even atomic
number, it is seen that the entire periodic table is reproduced. We
note the following:

(I) All the rare gases fall along the vertices of the triangles
and the chemical similarities among the elements can be traced in an
exactly similar manner as in the usual periodic table of elements.

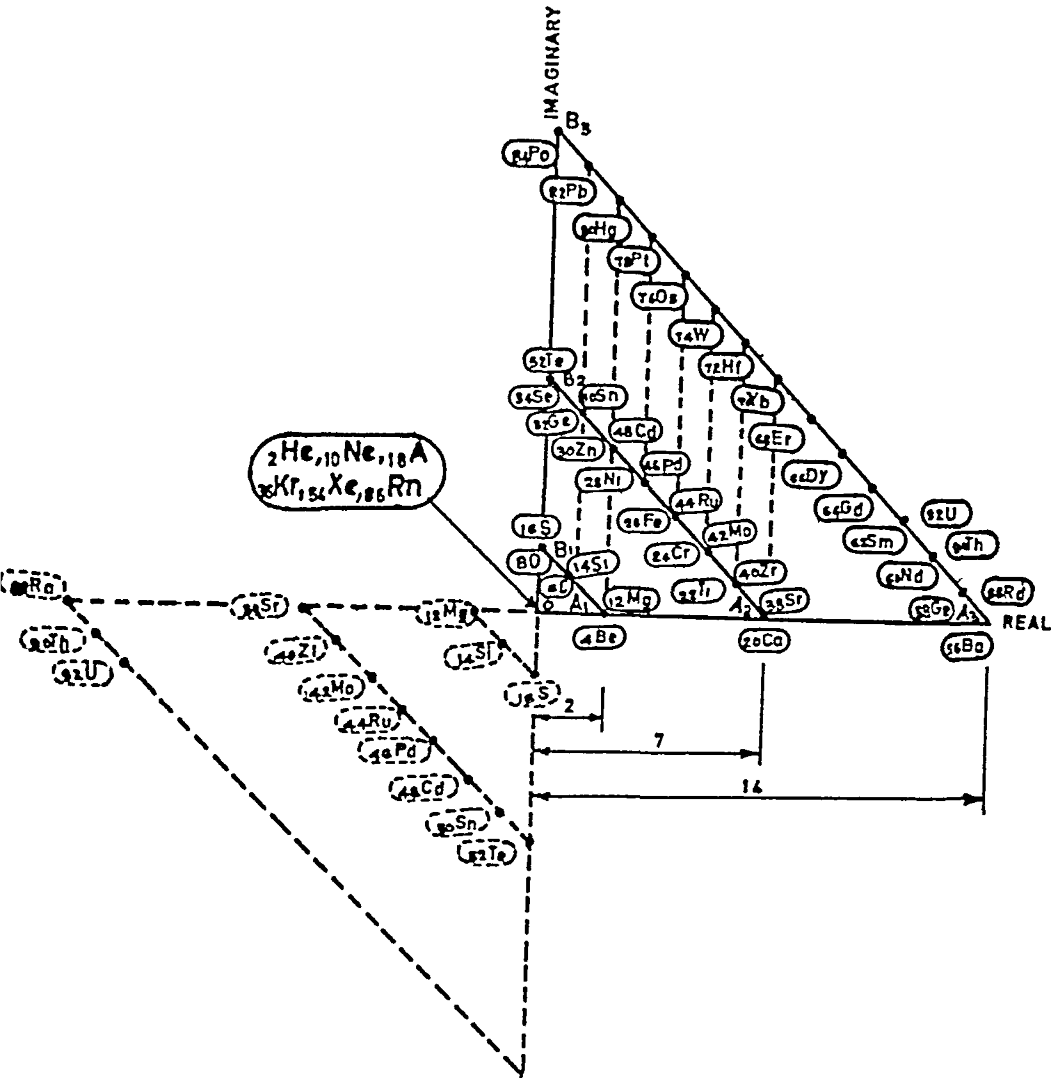
(II) It is necessary to have two entries at each permitted point
along the hypotenuse of each triangle, or, each triangular shell can
have a mirror reflection through the vertex.

The atomic binding energy E, after the Schwarz mapping of the
domain-widths onto the real lines, is given by

$$E = \left[Z m_o c^2 \alpha^2\right] \cdot \Delta \cdot F(\theta, 45^\circ) \qquad (10)$$

where α is the fine-structure constant, $F(\theta, 45^\circ)$ is the first type
elliptic integral with modulus = $1/\sqrt{2}$ and Δ, θ depend on Z, the
tomic number.

Table I, gives the calculated values of the binding energies
stable, spinless atoms. The agreement with the few experimental
ues is pretty good being within 3% and the agreement with the
turbation theories is quite impressive especially considering the
that no arbitrary parameter has been used in the present theory



The periodic table of elements obtained by arranging the even number atoms on the sides of right angled isosceles triangles on the complex plane. The Pauli principle appears as the exclusion of more than one atom with real or imaginary position having the same domain width. The dotted-lines drawn vertically link up atoms with similar chemical properties.

TABLE I

Electron-binding energy values in electron-volts of present theory compared with experimental values and the existing calculated values based on the Fermi-Thomas model and that due to Foldy

Z	Exptl E_B	E_B Foldy	E_B Fermi	E_B Cal
2	78 884	78 63	79 27	78 884
4	399 033	400 30	399 50	408 300
6	1029 805	1041 00	1029 00	1067 100
8	2043 189	2068 00	2013 00	2055 400
10	-	3535 00	3389 00	3373 100
18	-	-	1 336x10^4	1 523x10^4
20	-	1 833x10^4	1 708x10^4	2 100x10^4
30	-	4 811x10^4	4 399x10^4	3 573x10^4
36	-	-	6 731x10^4	5 674x10^4
40	-	9 590x10^4	8 607x10^4	1 173x10^5
50	-	1 637x10^5	1 449x10^5	1 528x10^5
54	-	-	1 734x10^5	1 813x10^5
60	-	2 532x10^5	2 217x10^5	2 245x10^5
70	-	3 663x10^5	3 177x10^5	2 620x10^5
80	-	5 049x10^5	4 388x10^5	3 041x10^5
86	-	-	5 135x10^5	3 796x10^5

DISCUSSION

H. S. Hans: Your theory seems to be not physical, but somewhat symbolic. How can we get the Hamiltonian between two nucleons, or two electrons.

R. Ramanna: The theory is no more non-physical than any other conventional theory of nucleus or the atom. If one believes that the Schrodinger equation describes a physical system and that we are not dealing with two-body problems, but many-body problems, the theory is as physical as in any other quantum mechanical approach to many-body problems. It may look somewhat symbolic in the sense that the appropriate space which has been determined, in which each point represents the state of the many-body system in its ground state and in this space there is straight-forward geometric symmetry in an abstract complex space.

B. K. Jain: In conventional nuclear physics calculations Hamiltonian used has the two body interaction only. More than two body interactions are neglected. Now in your model you don't have Hamiltonian as such. But could you say if the interaction which somehow or other has gone in your theory corresponds to the Hamiltonian of conventional theories, which have two, three, four body interactions in it. If it is so your theory would be much better in some respect at least.

R Ramanna The present theory is one in which the whole assembly of particles is treated as a single system, i e globablly and the theory is developed in such a way that the individual two-body interactions loose their meaning In this form the theory has many great advantages It is however shown that under certain approximations the two-body forces which one usually assumes in conventional theory comes out as a limiting situation (Coulomb law etc.)

S Ramamurthi 1) What is there in the physical notion of the atom - nucleus surrounded by electrons - to suggest the manifold you have used? 2) Similarly, what in the nucleus suggests the terms? 3) Can us say that you have shown that solving Schodinger's wave equations in certain manifolds you are getting mathmatical expressions which are what are encountered in the physics of certain systems?

R Ramanna 1) The physical notion of an atom, i e a nucleus surrounded by electrons, is suggested by the fact that the Bohr orbits can be obtained directly from the theory under the assumption when the proton is in the origin of one coordinate system, the electrons are respectively in the centre of the overlapping coordinate systems, which together form the manifold

2) Whether it be the atom or a nucleus the space time

manifold is defined on the surface of a torus which is another way of saying that the solutions to the nonlinear differential equation are invariant to automorphic transformation, i.e. solutions which are doubly periodic. It will be recalled that when the surface is that of a sphere one obtains spherical harmonics and when the surface is that of a singly punctured topological object, the solutions are elliptic functions. For higher punctured surfaces, one gets abelian integrals. All these solutions correspond to cases where the energy is minimised. 3) Yes.

T. V. Ramakrishnan: Can solutions describing molecules, solids etc. be obtained?

R. Ramanna: I have in the present paper extended the theory from the nucleus to the atom and shown that both can be satisfactorily described. In principle it should be possible to extend it to molecules and solids, but it may perhaps turn out to be trivial since the symmetry in molecules and solids is the symmetry in Euclidean space. It will be noted that the two solutions used in the cases of atom and nucleus respectively are the only ones which lead to single-valued solutions. There it is possible that a description of molecules and solids may come under this category. In any case, I would not use this theory for determining the struct ure of molecules and solids.

C S Warke 1) Could you suggest an experiment to test your theory 2) If it has a triangular geometric structure, could such a structure be found from the X-ray scattering experiment

R Ramanna 1) The theory gives consistently different values for the total binding energies of heavy atoms compared to the usual Hartree-Fock calculations If one can measure the binding energies of atoms of heavy elements one can clearly say which of the theories is correct But it is very difficult to perform such experiments as it involves stripping of several electrons simultaneously for a medium or heavy element atom. 2) There is no question of a triangular geometric structure which can be obtained by means of X-ray scattering experiments as the geometric structure is in an abstract space i e complex space, and is only a representation. Any determination of structure by means of an X-ray experiment can only be done in Euclidean space, whereas this theory is based on the theory of manifold which involves the over lapping of Euclidean patches which are globally non-Euclidean

C Biswas With a given mapping property for parameters of non-linear equation how much can you say about the uniqueness of the solution?

Ramanna. The two solutions used in the case of atoms of nuclei respectively are the only ones which lead to single valued solutions mapped to the inside of a circle for a unique value of the D (See Kober's Dictionary of Conformal T t on

CORE-EXCITATION EFFECTS IN HARTREE-FOCK CALCULATIONS

D.R. Kulkarni, S.B. Khadkikar and S.P. Pandya,
Physical Research Laboratory, Ahmedabad-9.

Recent trend in nuclear structure calculations is to use realistic nucleon-nucleon interactions; however one has to use a renormalised effective interaction which includes the effect of core-polarization and configuration truncation, for a few valence nucleons outside the core[1]. A comparison of Hartree-Fock (HF) calculations for d-s shell nuclei for bare and renormalised interaction is an interesting way to look into the nature of the core-excitation effects and degree to which quadrupole and pairing components of the interaction get enhanced. An alternative way to take core-excitation into account is to carry out the HF calculations with projection in a sufficiently large configuration space by explicitely treating all the nucleons[2]. Therefore it will be instructive to compare the angular momentum projected spectra from both HF calculations.

We have performed axial HF calculations in the space of d-s shell for ^{20}Ne, ^{24}Mg and ^{28}Si employing a) bare and b) renormalised interactions with the experimental single particle energies. The interaction matrix elements are those given by Kuo[3], extracted from Hamada-Johnstone potential. The results for the lowest HF states are displayed in table 1. It is seen that the HF energies (EHF) give more binding with the renormalised interaction indicating an overall increase in the interaction str

The intrinsic mass quadrupole moments (QHF) are very near to those of the appropriate maximum weight SU_3 states, however those with case b) are slightly smaller. This shows that the SU_3 symmetry is broken to a slightly larger extent with renormalisation, probably due to an increase in 'pairing' type of matrix elements. The overlaps with the asymptotic Nilsson orbits displayed in table 2 confirm the near SU_3 symmetry of the HF states in the a) and b) cases. An increase in HF gap between the last occupied and the first unoccupied orbits found in case b) relative to case a) may also be the result of the breaking of the SU_3 symmetry to some extent and should result in a more spread out spectrum.

The spectra obtained by projecting good angular momentum states from the various HF states (PHF) are shown in the Fig.1. The comparison of the PHF spectrum (b) for ^{20}Ne with that of shell model calculation of Halbert et.al[4] (d) shows a good agreement. The spectra (b) with renormalised interaction are consistentely more spread out as compared to those (a) with bare interaction.

We note that Kuo[3] has considered configuration space of first four major shells to calculate the effect of virtual one particle-one hole, two particle and two hole excitations in renormalising the bare interaction. We employ the same configuration space for a multi-shell PHF calculation for ^{20}Ne and show the resulting spectrum in Fig.1, in column (c). The d-s shell HF calculation for ^{20}Ne with "bare" interaction of Elliot et.al[5] yields

results in close agreement with those in case a). The matrix elements in two cases are also close within a few percent. Hence we employ the interaction of Elliot et.al. in this multi-shell PHF calculation (c) and compare the spectrum with that in case b). The agreement is quite good. Also the multi-shell HF results in a larger gap at the Fermi surface as compared with that in d-s shell calculation. This establishes a nice parallelism between the two methods of taking the core-excitations into account.

REFERENCES.

1) T.T.S. Kuo and Brown G.E. Nucl. Phys. 85(1966),40.

2) M.R. Gunye and S.B. Khadkikar, Phys. Rev. Lett.24(1970)910.

3) T.T.S. Kuo, Nucl. Phys. A 103 (1967), 71.

4) E.C. Halbert et.al. Preprint (to be published in Advances in Nuclear Physics)

5) J.P. Elliot, A.D. Jackson, H.A., Mavromatis, E.A. Sanderson and B. Singh, Nucl. Phys. A 121(1968), 241.

TABLE-I

Hartree-Fock energies (EHF) and intrinsic quadrupole moments (QHF) for a) bare b) renormalised interaction. The SU_3 limit values for intrinsic quadrupole moments are in the last column, with appropriate symmetry (λ, μ).

Nucleus	EHF		QHF (in units of b^2)		$Q(\lambda,\mu)$
	a	b	a	b	
^{20}Ne	-17.66	-21.22	15.59	15.46	16 (8.0)
^{24}Mg	-45.61	-50.34	19.35	19.23	20 (8.4)
^{28}Si	-94.32	-97.88	-23.03	-22.96	-24 (8.12)

TABLE - II

Overlaps of asymptotic Nilsson orbits with occupied HF orbits calculated with bare interaction.

Nucleus	K=1/2	K=3/2	K=5/2
^{20}Ne(prolate)	0.984	-	-
^{24}Mg(prolate)	0.986	0.987	-
^{28}Si(oblate)	0.992	0.967	1.00

A SCHEMATIC DESCRIPTION OF 'COLLECTIVE' STATES OF NUCLEI

S.K. Sharma, K.H. Bhatt and S.B. Khadkikar
Physical Research Laboratory
Ahmedabad-9.

An approximate but microscopic and unified description of both the configuration-mixing calculations for near-closed shell nuclei as well as the low-lying states of 'rotating' deformed nuclei is obtained by projecting out states with good angular momentum from an intrinsic state obtained by variational procedures such as Hartree-Fock or Hartree-Fock-Bogoliubov[1] formalisms. This implies that the low-lying states of nuclei can be obtained by the various couplings of the set of states with different angular momenta $|J_p\rangle$ and $|J_n\rangle$ of the Proton and Neutron groups in the intrinsic state and our attempt in this direction as described in this paper has been further motivated by the observation that in a well-deformed nucleus the states $|J_p\rangle$ and $|J_n\rangle$ separately exhibit rotation-like features. Thus the expectation value of the proton(neutron) parts of the Hamiltonian in the states $|J_p\rangle$ ($|J_n\rangle$) have rotation-like spectra and the E2 transitions between these states would be large.

The total Hamiltonian of the system is $H = H_n + H_p + H_{np}$ where $H_n (H_p)$ is the neutron (proton) part of the Hamiltonian. Since one of the dominant terms of a reasonably long-range two-body interaction has quadrupole-quadrupole form, the p-n interaction here can be assumed to be quadrupole-quadrupole type. Thus we have $H_{pn} = \Sigma_{(pn} \chi_{pn} q_p q_n = \chi_{pn} Q_p \cdot Q_n$, where $Q_p = \Sigma_{prot.} q_p$ and $Q_n = \Sigma_{Neut.} q_n$.

In our schematic model we consider two types of collective states-rotational collective states and vibrational collective states for representing the states belonging to proton(neutron) groups. Thus when the states belonging to proton(neutron) groups are rotational the reduced matrix element of the quadrupole operator and the spectrum for proton(neutron) part of the total Hamiltonian are given as

$$\langle J_p' \| Q_p \| J_p \rangle = (J_p 2 0 0 | J_p' 0)\, Q_0^p \quad ; \quad \langle J_p | H_p | J_p \rangle = A_p J_p (J_p + 1) \qquad \text{-------(1)}$$

Here the factor $(J_p 200 | J_p' \, o)$ is a Clebsch-Gorden Coefficient and $Q_o^p(Q_o^n)$ is the intrinsic quadrupole moment for the proton(neutron) group. In the case of vibrational collective states on the other hand we have (denoting the vibrational collective state as $|nJ\rangle$ where n is the phonon no.),

$$\langle n'J' \| Q \| n J \rangle = C (-1)^{J'-J} \sqrt{2J+1} \left\{ \langle n-1\, J' | n J \rangle \sqrt{n}\, \delta_{n', n-1} + \langle n+1\, J' | n J \rangle \sqrt{n+1}\, \delta_{n', n+1} \right\} \qquad \text{---(2)}$$

Here $\langle nJ | n'J \rangle$ is a coefficient of fractional parantage. We discuss below the results of calculations for cases when a> the states of proton- as well as neutron-groups are assumed to be rotational, b> the states belonging to the proton groups are assumed to be vibrational and c> the states belonging to proton-as well as neutron groups are taken as vibrational in nature. Hamiltonian matrices are set up and diagonalized in each case after putting some angular momentum cut-off in the spectra of protons and neutrons.

In case (a) where the states $|J_p\rangle$ and $|J_n\rangle$ are rotational, the matrix elements of the total Hamiltonian with the states $|[J_p \times J_n]\ J\rangle$ as basis state can be written as

$$\langle [J_p J_n] J | H | [J_p' J_n'] J \rangle = [A_p J_p(J_p+1) + A_n J_n(J_n+1)]\delta_{J_p J_p'}\delta_{J_n J_n'} +$$
$$\chi' (-1)^{J_p' + J_n - J} \sqrt{(2J_p+1)(2J_n+1)}\, W(J_p J_n J_p' J_n'; J2)(J_p 2 0 0 | J_p' 0)(J_n 2 0 0 | J_n' 0) \quad (3)$$

In addition to A_p and A_n we also take the product $\chi' = \chi_{pn}\, Q_o^p\, Q_o^n$ as a parameter. With $A_p = A_n = 0.3$ MeV and for sufficiently large values of the parameter χ' such as -15 MeV, we observe that i) approximately rotational spectrum results for the total H and ii) the low-lying states exhibit 'collectivity' in the sense that each of them can be projected from an assumed 'intrinsic' state to a good extent. These results have been shown in the figure R-R(a). Similar results are obtained for odd nuclei where we take $J_p = 0, 2, 4, 6$ and $J_n = 3/2, 5/2, 7/2, 9/2$ and the energy spectra is shown in figure R-R(b). Apart from the emergence of rotational spectra for the low-lying states the moment of inertia parameter($A = \hbar^2/2\mathcal{J}$) for the spectra in both the cases is nearly half of the parameter $A_p (= A_n)$. Further if the states $|J_n\rangle$ are assumed to have $K = 1/2$ band parantage and accordingly when we employ the spectrum $\langle J_n | H_n | J_n \rangle = A_n J_n(J_n+1) + a_n(-1)^{J_n+1/2}(J_n+1/2)$, the decoupling parameter for the final spectrum also turns out as nearly half of a_n. The energy spectrum in this case is shown in fig. R-R(c).

In case (b) where the states $|J_p\rangle$ are rotational but the states $|J_n\rangle$ are vibrational, the matrix-elements of H_{np} become $\langle (J_p, n J_n) J | H_{np} | (J_p', n' J_n') J \rangle =$

$$\chi_{pn} (-1)^{J_p' + J_n - J} \sqrt{(2J_p+1)}\, W(J_p J_n J_p' J_n'; J2)\, Q_o^p (J_p 2 0 0 | J_p' 0)\langle n J_n \| Q_n \| n' J_n' \rangle \quad (4)$$

The matrix-element $\langle n J_n \| Q^2 \| n' J_n' \rangle$ is evaluated by making use of equation (2). The product of χ_{pn}, Q_o^p and the constant c is considered as a parameter here r

ON THE ORIGIN OF HARD-CORE

Kamalesh Bhaumik
Saha Institute of Nuclear Physics, Calcutta-9

ABSTRACT

We have tried to give a theoretical explanation of the origin of repulsive-core in N-N interaction. We have been able to form a successful OBEP model which can generate a soft repulsive core. This soft core is, of course, hard enough to account for the observed change in the sign of the $^1S_0$ phase-shifts. The consistency of this model is being checked in explanining the experimentally observed quantities e.g. scattering lengths effective ranges, phase-shift parameters etc.

DISCUSSION

S. Ramamurty: Please inform whether, on this approache the K-meson has any relations to the hard core.

K. Bhaumik: This is N-N interaction. Since nucleons are particles of 1/2 isospin, there is no provision for exchanging any isospinor object.

G. Ramachandran: Can you tell me what numerical value of $g^2_{\omega NN}/4\pi$ is in your calculations and how it compares with the value of $g^2_{A_1 NN}/4\pi = 10$, which you have mentioned?

K. Bhaumki: The value of $g^2_{\omega NN}$ comes out to be 1.8. But some more contribution comes from the Pauli part of the coupling, which makes $V_\omega = 5.4 \frac{e^{-m_\omega r}}{r}$. The value of $g_{A_1 NN}$ should not be relied much, as most of the short -range effects are made responsible of A_1 in our model.

FISSION PROPERTIES OF SUPERHEAVY NUCLEI

S. Ramamurty, M.V. Ramanamurty, K.Parthasaradhi and C. R. Chandran,
Laboratories for Nuclear Research, Andhra University, Waltair.(A.P.) India.

I. INTRODUCTION

Many studies have been made on the liquid drop theory of nuclear fission. J.R. Nix, in a recent paper discussed the fission properties of some superheavy nuclei. An extensive table is now prepared for the mapping of the fission properties of superheavy nuclei in the Z-range 110-134 and mass region 288-324. Actually studies are being made concerning the existence of these superheavy nuclei. It is definite that if such nuclei exist, their fission properties can be extensively exploited. For instance, the neutron out turn of the nucleus ($\frac{134}{324}$) is calculated here to be as big as 9/ fission and the energy release per binary fission alone is 469 MeV. The large value of the number of neutrons emitted per binary fission of the superheavy nuclei is due to the fact that neutron separation energy is low. These predicted fission properties can be verified when experimental information is available. A new process is here investigated for the first time to our knowledge viz quarternary fission. It may be of in appreciable importance for the nuclei. Our calculations extend upto the heaviest of nucleus which can exist according to UCRL-11980, viz ($\frac{134}{324}$). The masses used for these calculations are taken from UCRL-11980.

The quantities calculated are the coulomb and surface energies and the fissility parameter of the superheavy nuclei, the energy release in binary, ternary and quarternary fission of these nuclei, the kinetic energy, the excitation energy and the temperature Θ of the fission fragments in binary fission and the quantity $n = \frac{4}{3}\,\Theta$. It is hoped that the present tabulation is sufficiently extensive to indicate the trend as regards these quantities

II. RESULTS:

1.	2.	3.	4.	5.	6.	7.	8.	9.	10.	11
$\binom{110}{288}$	0.9015	707	1292	291	352	364	81	203	1.5	8.8
$\binom{110}{300}$	0.8927	710	1258	276	349	368	68	1.794	1.34	9.2
$\binom{111}{300}$	0.9025	715	1281	293	348	394	79	1.933	1.35	14.2
$\binom{111}{312}$	0.8963	701	1281	287	342	-	77	1.87	1.42	16
$\binom{112}{300}$	0.9125	712	1321	300	-	391	76	2.4	1.42	9.6
$\binom{112}{312}$	0.9055	733	1304	296	335	400	76	1.862	1.3	11.1
$\binom{113}{300}$	0.9226	717	1346	306	363	390	80	1.94	1.46	13
$\binom{114}{300}$	0.9329	722	1370	310	384	410	72	1.85	1.38	11
$\binom{115}{300}$	0.9434	726	1393	319	382	427	74	1.87	1.39	11
$\binom{116}{300}$	0.9495	738	1418	327	402	426	72	1.84	1.38	6.8
$\binom{117}{300}$	0.9650	743	1442	317	406	430	61	1.7	1.27	6.6
$\binom{117}{306}$	0.9591	734	1433	334	404	429	81	1.93	1.45	12
$\binom{118}{300}$	0.9760	747	1468	341	412	448	72	1.84	1.38	6.4

$\binom{119}{312}$	0.9749	751	1472	348	439	479	93	2.06	1.54	13.5
$\binom{120}{300}$	0.9987	758	1518	361	446	468	95	2.12	1.59	6
$\binom{120}{300}$	0.9854	756	1497	356	439	479	95	2.08	1.56	11
$\binom{121}{300}$	1.0113	759	1543	369	454	479	96	2.13	1.60	10.2
$\binom{121}{312}$	0.9962	760	1523	362	442	481	96	2.09	1.57	13
$\binom{122}{300}$	1.0221	762	1569	375	469	494	93	2.09	1.57	8.5
$\binom{122}{312}$	1.0071	764	1548	367	460	491	96	2.09	1.57	10.5
$\binom{123}{300}$	1.0341	766	1594	387	477	513	104	2.21	1.66	10.4
$\binom{123}{312}$	1.0182	769	1573	377	465	506	97	2.10	1.57	12.1
$\binom{124}{300}$	1.0463	789	1620	398	485	520	98	2.15	1.12	8.5
$\binom{124}{312}$	1.0295	772	1603	385	467	508	95	2.08	1.56	9.7
$\binom{125}{300}$	1.0587	773	1646	405	512	531	93	2.10	1.57	8
$\binom{125}{312}$	1.0409	776	1625	391	498	514	97	2.10	1.57	10.85
$\binom{126}{300}$	1.0713	776	1673	412	521	545	98	2.15	1.61	7
$\binom{126}{312}$	1.0526	780	1651	396	502	535	93	2.06	1.54	9
$\binom{127}{312}$	1.0492	785	1657	407	504	560	101	2.10	1.58	7.4
$\binom{127}{324}$	1.0464	784	1677	408	510	558	95	2.08	1.56	10.4
$\binom{128}{324}$	1.0604	789	1683	417	523	564	102	2.11	1.58	10.4
$\binom{128}{312}$	1.0764	787	1704	418	524	565	95	2.08	1.56	7.3
$\binom{129}{324}$	1.0717	793	1709	418	523	564	97	2.06	1.55	11.3
$\binom{130}{312}$	1.1010	790	1757	436	546	589	100	2.13	1.60	7.4
$\binom{130}{324}$	1.0832	798	1736	432	535	588	108	2.15	[illegible]	

$\binom{131}{324}$	1.0948	800	1763	448	566	610	107	2.17	1.62	11.7
$\binom{132}{324}$	1.1067	804	1789	453	572	615	107	2.17	1.62	9.8
$\binom{134}{324}$	1.1309	811	1844	469	595	640	103	2.13	1.60	9

3. (1) Element $\binom{A}{Z}$ (2) Fissility parameter (3) Surface energy (4) Coulomb energy (5), (6), (7) energy release during binary, ternary and quarternary fission, (8) Excitation energy, (9) Nuclear temperature and (10) n , (11) Number of neutrons released during binary fission.

The authors acknowledge their indebtedness to Dr. J.R. Nix for discussion and communication of his research papers to them.

REFERENCES:

1. J.R. Nix,
   Physics Letters, 30, B11 (1969).

2. J.R. Nix,
   Nuclear Physics, A130, 241 (1969).

DISCUSSION

S.S. Kapoor: Will you explain what was the exact formulation for calculating the kinetic energy released?

S. Ramamurty: It is done on the basis of Nix's work.

LEVEL DENSITY PARAMETERS AND NUCLEAR STRUCTURE

S. Ramamurty, K. Parthasaradhi, M.V. Ramanamurty and C.R. Chandran,
The Laboratories for Nuclear Research, Andhra University, Waltair.(A.P.)India.

I. INTRODUCTION

An extensive data on level density parameters using Lang's [1] expression with the effective momentum values taken from Lym's[2] book are presented here. These calculations cover the mass region 32-209, especially near magic numbers in rare earths and for isotopes of any abundance and for which experimental data happen to be available. The region Z 83 is avoided. The available experimental data on separated isotopes given by Dastar Pooo9[3] along with the present calculations are given in Table I.

It can be seen from Table I, that the level density parameter increases as the mass number increases except in the vicinity of magic numbers. It can also be seen that the agreement between the experiment and theory is within 40%, except in ^{206}Pb and ^{209}Bi. Taking value of Lang[1] in the formula $a =$ $(j_N + j_p + 1)\ A^{2/3}$ as correct on a overall survey, this points to the need to sharply reduce the values of effective angular momenta j_N and j_p near Z = 82 and N = 126. It is hoped that data on separated isotopes will become available to test this point as also the formula $a =$ $(j_N + j_Z + 1)\ A^{2/3}$.

II. RESULTS

TABLE I

LEVEL DENSITY PARAMETERS

(Values in the brackets are experimental values taken from DASTAR P009[3])

Proforma :
Mass No. - Element - Proton No. Value

32-S-16	2.013	66-Zn-30	8.024	92-Zr-40	8.744
35-Cl-17	2.934	69-Ga-31	5.454	94-Zr-40	8.249
37-Cl-17	3.596	71-Ga-31	5.560	93-Nd-41	10.85 (13.3)
40-A-18	5.249	70-Gl-32	5.932	92-Mo-42	14.03
40-A-19	4.015	72-Ge-32	6.045	95-Mo-42	12.46
40-Ca-20	4.667	74-Ge-32	9.672	96-Mo-42	12.55 (14.8)
45-Sc-21	6.942	78-Se-34	10.92	98-Mo-42	13.99
		79-Se-34	11.02 (12.7)		
48-Ti-22	7.903 (6.00)	80-Se-34	11.11	105-Pd-46	16.64
51-V-23	7.536 (6.5)	79-Br-35	11.02	106-Pd-46	16.75
52-Cr-24	7.648 (5.8)	81-Br-35	11.2	108-Pd-46	16.96
55-Mn-25	6.491 (5.9)	82-Kr-36	11.29	110-Pd-46	17.18
56-Fe-26	6.569 (8.5)	83-Kr-36	11.39	107-Ag-47	16.86
59-Co-27	7.181 (8.1)	84-Kr-36	11.48	109-Ag-47	17.06
58-Ni-28	5.978	86-Kr-36	10.49	110-Cd-48	17.18
59-Ni-28	7.181 (9.5)	85-Rb-37	11.57	111-Cd-48	17.28
60-Ni-28	6.498	87-Rb-37	10.54	112-Cd-48	17.38 (14.8)
63-Cu-29	6.71	88-Rb-38	9.672	113-Cd-48	17.49
64-Cu-29	(12.4)	88-Sr-38	9.672	114-Cd-48	17.58
65-Cu-29	6.85	89-Y-39	8.746	116-Cd-48	17.79
64-Zn-30	5.985	90-Zr-40	9.815	115-Zn-49	17.34
65-Zn-30	6.108 (9.8)	91-Zr-40	9.285 (11.4)	116-Sn-50	17.08
118-Sn-50	17.28	139-La-57	13.04	156-Gd-64	20.16
119-Sn-50	17.38 (11.6)	138-Ce-58	11.58	157-Gd-64	20.68
120-Sn-50	17.48	140-Ce-58	13.31	158-Gd-64	20.77
121-Sb-51	17.2	142-Ce-58	13.47	160-Gd-64	20.99
123-Sb-51	17.39	141-Pr-59	13.58	159-Cd-65	20.85
126-Ce-52	15.2 (10.7)	143-Nd-60	14.72	162-Dy-66	21.12

130-Te-52	13.05	144-Nd-60	16.03	163-Dy-66	21.2
127-I-53	17.01	146-Nd-60	17.43	164-Dy-66	21.29
129-Xe-54	16.04	147-Sn-62	17.70	165-Mo-67	21.38
131-Xe-54	13.90	148-Sn-62	17.78	166-Er-68	21.46
132-Xe-54	12.8	149-Sn-62	17.86	167-Er-68	21.55
134-Xe-54	10.96	152-Sn-62	18.96	168-Er-68	21.64
133-Cs-55	12.86	151-Eu-63	18.03	170-Er-68	21.81
137-Ba-56	11.92	153-Eu-63	19.04	169-Tm-69	21.74
138-Ba-56	12.78	155-Gd-64	19.63	171-Yb-70	21.89

172-Yb-70	21.98	198-Hg-80	16.77		
173-Yb-70	22.06	174-Yb-70	22.14	176-Yb-70	22.31
175-Lu-71	22.23	177-Hf-72	22.4	178-Hf-72	22.48
179-Hf-72	22.57	180-Hf-72	22.66	184-W-74	22.96 (17.5)
184-Pt-78	18.80	185-Pt-78	18.87	196-Pt-78	18.93
197-Au-79	17.22	198-Hg-80	16.77	199-Hg-80	15.3
200-Hg-80	13.81	201-Hg-80	12.46	202-Hg-80	10.81
203-Te-81	12.4	205-Tl-81	9.883	206-Pb-82	11.48 (6.1)
207-Pb-82	13.09 (5.3)	208-Pb-82	14.71	209-Bi-83	16.33 (5.6)

REFERENCES.

1. D.W. Lang,
   Nuclear Physics, 26, 434 (1961).

2. J.E. Lym,
   The theory of Neutron.

3. DASTAR-P009.

SHELL EFFECTS ON NUCLEAR LEVEL DENSITIES

V.S. Ramamurthy, S.S. Kapoor and S.K. Kataria
Nuclear Physics Division
Bhabha Atomic Research Centre, Bombay- 85

In a previous publication(1) we reported microscopic calculations of nuclear level densities on the basis of a realistic shell model. It was shown that the nuclear shell effects on the level density disappear even at medium excitation energies of the order of 30-40 MeV. Recently Kahn and Rosenzweig(2) and Gilbert(3) have calculated nuclear level densities versus excitation energies for a degenerate system of Fermions moving in arbitrary periodic single-particle energy level schemes. They have concluded that the influence of the structure and the ground state occupancy of the level sequences on level densities persists at all excitation energies. This conclusion is in complete disagreement with the results of our work(1). In order to resolve the discrepancy, we have extended our calculations to a system of Fermions moving in a periodic level scheme identical to the one used by Kahn and Rosenzweig(2). It is shown that the numerical results of our calculations of level densities are in complete agreement with those of Kahn and Rosenzweig and the apparent discrepancy between our conclusions and those of these authors(2,3) arises due to a misinterpretation of the shell effects on the ground state energies by these authors(2,3).

The mathematical formulation of the present calculations is based on the well known formulae of statis-

tical thermodynamics. For a system containing N non-interacting Fermions with total energy E, the following relations hold:

$$N = \sum n_k \qquad \text{......... (1)}$$

$$E = \sum \epsilon_k n_k \qquad \text{......... (2)}$$

where ϵ_k is the energy of the k-th single particle state. The Fermi-Dirac distribution function n_k and the entropy S of the system are given by

$$n_k = \frac{1}{1+\exp[(\epsilon_k - \mu)/T]} \qquad \text{........ (3)}$$

$$S = -\left[\sum n_k \ln n_k + \overline{1-n_k} \ln \overline{1-n_k}\right] \qquad \text{........ (4)}$$

μ and T being the chemical potential and the thermodynamic temperature of the system respectively. The ground-state energy E_0 is the energy of the system when T = 0 and is given by

$$E_0 = \sum_{k=1}^{N} \epsilon_k \qquad \text{.........(5)}$$

Kahn and Rosenzweig have used in their studies, for , a simple periodic single particle-level scheme defined by the relation

$$\epsilon(k,\ell) = k + \eta(\ell)\ , \quad \begin{matrix} k = 0,1,2,\cdots \\ \ell = 1,2,3,\cdots g \end{matrix} \qquad \text{.... (6)}$$

with $$\sum_{\ell=1}^{g} \eta(\ell) = 0 \qquad \text{......... (7)}$$

The integer k specifies the position of the "center of gravity" of the k-th shell, and the numbers $\eta(\ell)$ represent the positional deviations of the g levels from the center of gravity. In the present work we consider only the two simple structures: (i) each shell consists of one g-fold degenerate level with $\eta(\ell) \equiv 0$ and (ii) the single particle levels are uniformly spaced with $\eta(\ell) \equiv u(\ell) = \frac{1}{g}[\ell - \frac{1}{2}(g+1)]$

The two level sequences are illustrated in Fig.2(a) and 2(b). The unit of energy has been set equal to the spacing between the centers of gravity of successive shells.

Making use of the periodicity of the level scheme Kahn and Rosenzweig have derived closed expressions for the density of states and the entropy of the system. The resulting expression for the entropy is

$$S(E,N) = \pi \left(\tfrac{2}{3} g Q^{*} \right)^{1/2} \quad \ldots\ldots\ldots\ldots (8)$$

where the effective excitation energy Q^{*} is related to the actual excitation energy $Q (= E - E_0)$ by the relation

$$Q^{*} = Q - (24g)^{-1} + \sum_{l=1}^{n} [\eta(l) - u(l)] + \frac{1}{2} \sum_{g=1}^{g} [\eta^{2}(l) - u^{2}(l)] \quad (9)$$

we have carried out a numerical evaluation of S for the same system by solving Eqs.(1) - (4) in a self-consistent manner for various excitation energies. The results of our calculations for a system with 96 particles and a degeneracy g = 8 and the corresponding predictions of Eq.(9) are shown in Fig.(1), where we have plotted S^2 against the excitation energy. It is seen that in the asymptotic region, the results of our numerical calculations are identical with the prediction of the Eq.(9) of Kahn and Rosenzweig, bringing out the consistency of the two calculations. One can also notice the asymptotic relation of the form

$$S^2 = C\,(Q + \Delta) \quad \ldots\ldots\ldots\ldots (10)$$

In our earlier work, we have identified the correction term Δ as the shell correction to the ground state energy of the nucleus and interpreted thi   lt

as an indication of the washing out of the shell effects at high excitation energies. This conclusion has also been verified in the present calculations by generating a continuous uniform level scheme using Strutinsky's smearing procedure[4] and comparing the ground state of the smeared scheme with that of the bunched scheme.

On the other hand the interpretation of Δ by Kahn and Rosenzweig differs from ours in the following respects: They have identified the difference $\Delta_S = \sum_{\ell=1}^{n} [\eta(\ell) - u(\ell)]$ between the ground state energies of N particles calculated in the two schemes as the ground state shell correction. To bring out the drawbacks of this association, we have shown in Fig.2(d), the variation of Δ_S and Δ with particle number n outside a closed shell. It is seen that Δ_S is always positive and is zero for a closed shell system. On the other hand Δ , which is shifted relative to Δ_S by a constant amount of $-g/24$, exhibits the familiar positive and negative variation, with maximum negative correction for closed shell systems. One can also see intutively that a discrete uniform distribution of levels is equivalent to another closed shell system with g = 1. On the other hand the evaluation of the ground state shell corrections based on a Strutinsky's smeared continuous level distribution as shown in Fig.2(c) predicts a negative shell correction for all closed shell systems including those with g = 1. The magnitude of the shell correction as defined above for a discrete uniform sequence of levels

can also be analytically obtained making use of the familiar Euler-Maclaurin summation formula. For the total energy E, one can write Eq.(2) as

$$E = \sum \epsilon_K n_K = \int \epsilon g(\epsilon) n(\epsilon) d\epsilon - \frac{1}{24}$$

As $T \to 0$, $E_g = \bar{E}_g - \frac{1}{24}$

In other words, the ground state of a system of particles moving in a discrete uniform level sequence is depressed with respect to a system with a continuous distribution of levels having the same density of states by an amount $-\frac{1}{24}$ energy units. If each level is degenerate with adegeneracy g, the ground state depression is proportionally increased to $-\gamma/24$. As can be seen from Fig.2(d), this depression exactly equals the difference between Δ, the additive correction to the excitation energy in the level density expression and Δ_S, the shell correction to the ground state energy as defined by Kahn and Rosenzweig. One can therefore conclude that if one uses a system with a continuous uniform distribution of levels as the reference for determining the ground state shell correction, the results of Kahn and Rosenzweig also imply that the effective excitation energy in the calculation of level density has to be measured from a ground state stripped off its shell effects. In general one can conclude that for an actual nucleus, the liquid drop mass corresponds to a "continuous uniform" distribution of levels and the Strutinsky method of evaluating the ground state shell correction is consistent with this definition.

N = 96
g = 8

$(\text{ENTROPY})^2$

50.0

0.0

530.0 530.5 531.0 531.5

TOTAL ENERGY

FIG. 1

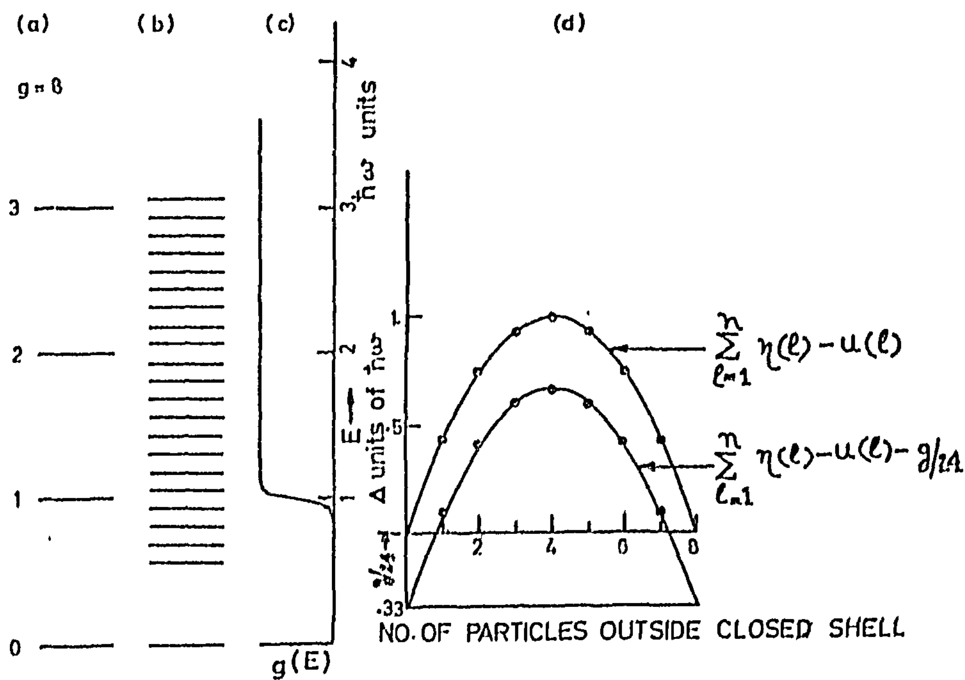


FIG. 2

REFERENCES

1. V.S. Ramamurthy, S.S. Kapoor and S.K. Kataria, Phys. Rev. Letters 25, 386 (1970).

2. P.B. Kahn and N. Rosenzweig, Phys. Rev. 187, 1193 (1970)

3. A. Gilbert, UCRL - 18095 (1968).

4. V.M. Strutinsky, Nucl. Phys. A95, 420 (1967).

DISCUSSION

R.K. Bansal: I would like to know whether your single particle energies include spin-orbit effects. If not, your calculation can be in trouble.

V.S. Ramamurthy: The calculations of level density for a Nilsson level scheme with spin-orbit coupling terms have been reported earlier (Phys. Rev. Letters 25, 1970 page 386). The present calculations were mainly aimed at comparing our results with those of Kahn and Rosenveig for the same level scheme as used by them.

ON THE PRODUCTION POSSIBILITY OF SUPERHEAVY NUCLEI

V.S. Ramamurthy and S.S. Kapoor
Nuclear Physics Division
Bhabha Atomic Research Centre, Bombay - 85

Recent work of Swiatecki[1] and Strutinsky[2] on the concept of "generalised shells" in deformed nuclei has led to the prediction that nuclei in the region $Z \simeq 114$ and $N \simeq 182$ might be relatively stable against α, β and fission modes of decay and have a measurably long half-life. This prediction has initiated on one hand an extensive search for the possible presence of these nuclei in nature and on the other hand attempts to synthesize these nuclei in the laboratory mainly by fusing heavy ions into heavy target nuclei. In all the attempts that are currently being made to produce superheavy nuclei by heavy ion bombardment, the compound nucleus is formed with an excitation energy of the order of a few tens of MeV and it is expected that the nucleus will undergo a cascade of neutron emission before it reaches the relatively stable ground state, where it is predicted to have an appreciably long half life for further decay. The probability that such a neutron cascade ultimately leads to the formation of the cold superheavy nucleus sensitively depends on the relative magnitudes of the neutron and the fission widths of the excited compound nucleus.

Theoretical estimates of the fission and neutron widths of excited heavy nucleus are usually made on the basis of the Bohr-Wheeler transition state theory[3]. On the basis of this theory, one can write for Γ_{fi} Γ_n

width Γ_f the expression

$$\Gamma_f = \frac{1}{2\pi\ \rho(E)} \cdot N_f \qquad \text{.......... (1)}$$

where $\rho(E)$ is the level density of the compound nucleus at the given excitation energy E and N_f is the effective number of open channels at the saddle point configuration. Representing the level spectrum of the saddle point nucleus at excitation energy X by a level density $\rho^*(X)$ and taking into account barrier penetrability one can write for N_f as

$$N_f = \int_0^E \frac{\rho^*(x)\, dx}{1 + \exp\left[-2\pi(E - B_f - x)/\hbar\omega\right]} \qquad \text{.....(2)}$$

where B_f is the fission barrier height and $\hbar\omega$ is a measure of its thickness. One can similarly write for the neutron width

$$\Gamma_n = \frac{1}{\pi\ \rho(E)} \int_0^{E-B_n} \rho^{**}(x) \left(\frac{t}{t_0}\right) dx \qquad \text{.....(3)}$$

where $\rho^{**}(X)$ is the level density of the residual nucleus after neutron emission at excitation energy X, t is the kinetic energy of the emitted neutron and $t_0 = \hbar/2mR^2$ where R is the radius of the residual nucleus.

Though Eqs (1)-(3) have been extensively used in the past for the prediction of fission and neutron widths and for the estimation of fission barriers from measured fission excitation functions, one usually encounters serious difficulties in fitting these equations over a wide range of excitation energies(4). It is also now very well known that many of the existing difficulties mainly arise as a result of our lack of understanding of nuclear level densities, in particular their dependence on excitation energy and nuclear shell effects.

5. D.S. Burnett, R.C. Gatti, F. Plasil, P.B. Price, W.J. Swiatecki and S.G. Thompson, Phys. Rev. B134, 952 (1964).

6. V.S. Ramamurthy, S.S. Kapoor and S.K. Kataria, Phys. Rev. Letter, 25, 386 (1970).

7. L.G. Moretto (Private Communication) 1970.

shown in Fig.(2). It is seen that in general there is a washing out of nuclear shell effects on entropy as the excitation energy increases. There is also a shift of the point of minimum entropy towards the spherical liquid drop ground state deformation with increasing excitation energy. Having located the saddle point, one can use Eqs (1)-(3) for the calculations of the fission and neutron widths for various excitation energies of the nucleus. The results of our calculations for the nucleus $_{114}X^{296}$ are shown in Fig.(3) where we have plotted the calculated Γ_f/Γ_n as a function of the excitation energy. It is seen that at about 30-40 MeV excitation, the probability of neutron emission is of the order of a few percent only. Similar calculations by Moretto[7] lead to 0.25 for Γ_n/Γ_T

The actual production cross section of the cold superheavy nucleus depends not only on the probability of a favourable neutron cascade, but also on the formation cross section of the compound nucleus. The latter quantity depends on the target-projectile combination used and the bombarding energy. Systematic studies of these quantities for various combinations of projectile and target are in progress.

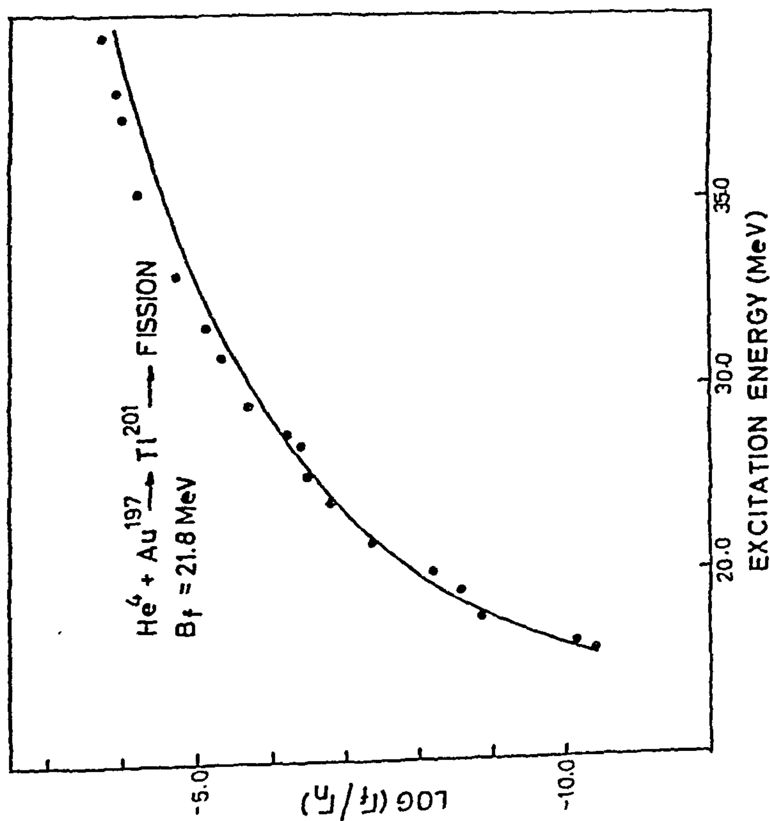
REFERENCES

1. W.D. Myers and W.J. Swiatecki, Nucl. Phys. 81, 1(1966).
2. V.M. Strutinsky, Nucl. Phys. A95, 420 (1967); Nucl. Phys. A122, 1 (1968).
3. N. Bohr and J.A. Wheeler, Phys. Rev. 56, 426 (1939).
4. Arastoo Khodai-Jaoopari, UCRL - 16489 (1966).

5. D.S. Burnett, R.C. Gatti, F. Plasil, P.B. Price, W.J. Swiatecki and S.G. Thompson, Phys. Rev. B134, 952 (1964).

6. V.S. Ramamurthy, S.S. Kapoor and S.K. Kataria, Phys. Rev. Letter, 25, 386 (1970).

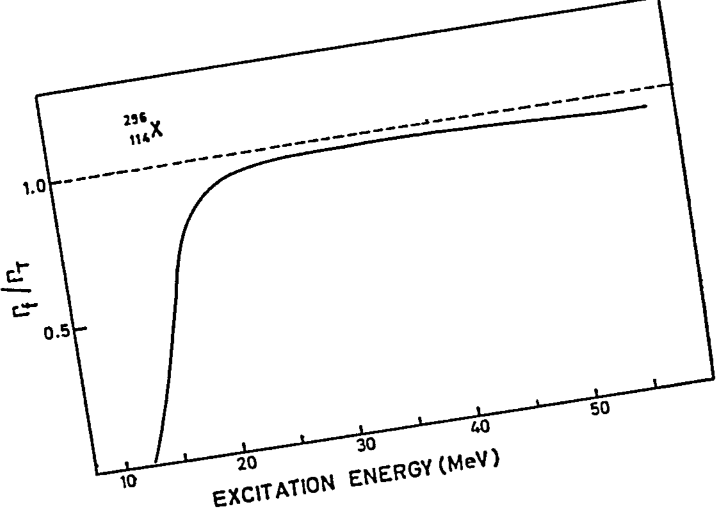
7. L.G. Moretto (Private Communication) 1970.



$He^4 + Au^{197} \longrightarrow Tl^{201} \longrightarrow$ FISSION
B_f = 21.8 MeV
LOG (Γ_f/Γ_n)
-5.0
-10.0
20.0
30.0
35.0
EXCITATION ENERGY (MeV)

FIG. 1

FIG. 2



$^{296}_{114}X$
1.0
0.5
Γ_f / Γ_T
10
20
30
40
50
EXCITATION ENERGY (MeV)

FIG. 3

EFFECT OF HEXADECAPOLE DEFORMATION ON NILSSON ORBITAL CROSSING

G. Ramakrishna
Saha Institute of Nuclear Physics, Calcutta.

The recent experimental evidences[1,2], through stripping and pick-up reactions, of strong $\Delta N=2$ mixing between the $3/_2^+$ [651] and $3/_2^+$ [402] pair on one hand and $1/_2^+$ [660] and $1/_2^+$ [400] pair on the other, has drawn the attention [redacted] of quite a few theoreticians. These two pairs of levels are the ones which actually *cross in the original Nilsson diagrams*[3] *for a quadrupole* deformation of $\delta_2 \sim 0.3$. The main features of the problem are the large spacings between the two levels of such a pair and the observability of $\Delta N = 2$ mixing over a wide range of nuclei. Andersen[4] has observed on the basis of a simple model of two interacting states that any theoretical calculation should be able to reproduce a matrix element $\langle N j_z | H_{\delta_2 f} | N \pm 2 j_z \rangle$ $\sim$ 80 KeV to be consistent with the large spacing (193 KeV in ^{159}Gd) of the two $1/_2^+$ levels and their (d,t) cross sections. The Nilsson Hamiltonian of [3] which is known to mix two such levels yields a matrix element $\sim$ 7 KeV for both the $1/_2^+$ and $3/_2^+$ cases. Andersen has shown that by invoking a deformed Saxon-Woods potential it is possible to get the matrix element of the right order of magnitude, mentioned above.

In this paper it will be shown that in the typical case of the two $3/_2^+$ levels the spacing ΔE ($\sim$150 KeV in ^{155}Gd) can be reproduced with the inclusion of

EFFECT OF HEXADECAPOLE DEFORMATION ON NILSSON ORBITAL CROSSING

G. Ramakrishna
Saha Institute of Nuclear Physics, Calcutta.

The recent experimental evidences[1,2], through stripping and pick-up reactions, of strong $\Delta N=2$ mixing between the $3/2^+$ [651] and $3/2^+$ [402] pair on one hand and $1/2^+$ [660] and $1/2^+$ [400] pair on the other, has drawn the attention [redacted] [redacted] of quite a few theoreticians. These two pairs of levels are the ones which actually cross in the original Nilsson diagrams[3] for a quadrupole deformation of $\delta_2 \sim 0.3$. The main features of the problem are the large spacings between the two levels of such a pair and the observability of $\Delta N = 2$ mixing over a wide range of nuclei. Andersen[4] has observed on the basis of a simple model of two interacting states that any theoretical calculation should be able to reproduce a matrix element $\langle N\, j_z | H_{def} | N \pm 2\, j_z \rangle \sim 80$ KeV to be consistent with the large spacing (193 KeV in ^{159}Gd) of the two $1/2^+$ levels and their (d,t) cross sections. The Nilsson Hamiltonian of [3] which is known to mix two such levels yields a matrix element ~ 7 KeV for both the $1/2^+$ and $3/2^+$ cases. Andersen has shown that by invoking a deformed Saxon-Woods potential it is possible to get the matrix element of the right order of magnitude, mentioned above.

In this paper it will be shown that in the typical case of the two $3/2^+$ levels the spacing ΔE (~ 160 KeV in ^{155}Gd) can be reproduced with the inclusion of

hexadecapole deformation in the Nilsson Hamiltonian retaining his original representation(3). The potential with the hexadecapole deformation is

$$V = \tfrac{1}{2}\hbar\omega_0(\delta_2,\delta_4)\, r^2\left(1 - \tfrac{4}{3}\delta_2\sqrt{\tfrac{4\pi}{5}}\, Y_0^2 + 2\delta_4 Y_{40}\right) - \chi\hbar\omega_0^0\left[2\vec{l}\cdot\vec{s} + \mu\left(\vec{l}^2 - \langle l^2\rangle_{av}\right)\right]$$

δ_4 is the deformation parameter characterising the hexadecapole deformation. The inclusion of δ_4 term in this form is in the same spirit ~~as~~ the recent calculations of Nilsson and his associates(5). The essential difference is that we retain Nilssons original δ- scheme where as Nilsson's group choose his alternative ϵ -scheme. The resulting wave function is

$$|\Omega|j_z\rangle = \sum_{N\ell j} C_{N\ell j}(j_z)\ |N\ell j\rangle$$

we have included basic states of N from 0→ 8. This choice of including N= 8 states for rare earth orbitals is from evidences of reference(6) and the support that it is a fair approximation from reference(7).

The matrices have been generated and diaognalised on an IBM 7044 machine at the IIT, Kanpur employing the values of χ and μ reported by Nilsson's group at the lysekil symposium(5). The minimum separation ΔE of the two $3/2^+$ levels has been estimated for a range of values of δ_4 changing δ_2 in closer steps for each δ_4. The resulting ΔE are shown in Table 1 for A= 157.

TABLE 1

DELTA 4	0	-0.05	-0.075	-0.10	-0.125	-0.15
ΔE(kev)	16.4	61.6	60.0	24.1	48.1	164.8

The separation of ~ 16 KeV at δ_4 = 0 increases to

~160 KeV (around the experimental value) at δ_4=-0.15. The sign of δ_4 is in accordance with the experimental finding of positive β in the samarium region[8] where ΔN =2 mixing is observed. Apparent from these resuts is the marked dependence of ΔE on δ_4. This is due to the fact that certain matrix elements of $\langle L L_3 | Y_2 | L' L_3' \rangle$ and $\langle L L_3 | Y_4 | L' L_3' \rangle$ are of opposite signs and as a consequence the total matrix element actually undergoes a sign change in a few cases at δ_4 = -0.125.

A noteworthy feature of the results of the present investigation is the broadening of the range in δ_2 ($\Delta \delta_2$) over which the ΔN= 2 mixing is observable. This observability in the case of the two $3/2^+$ levels is essentially determined by the amplitudes $C_{423/2}$ in both the $3/2^+$ levels. At δ_4= 0 these amplitudes are present in both the $3/2^+$ levels in appreciable amounts only over a narrow range of deformation namely $\Delta \delta_2$ = 0.002. As δ_4 is increased this range broadens and at δ_4 ≈-0.15 it is as much as 0.025. This effect is shown in Fig. 1 for the two representative cases δ_4= 0.0 and δ_4 = -0.15 . This remarkable behaviour of $C_{423/2}$ may account for the observation of Δ N = 2 mixing effects over a wide range of nuclei which essentially means a wide range of deformation.

REFERENCES :

1. R. K. Sheline et al. Phys. Lett. 26B, 14(1967)

2. B. Elbek and P.O. Tjøm Mat.Fys. Medd. Dan. Vid. Selsk. 36 nr.8 (1967)

3. S. G. Nilsson Mat.Fys. Medd. Dan.Vid

4. B. L. Andersen Nucl. Pyys. A112 , 443 (1968)

5. C. Gustafson, I.L.Lamm, B. Nilsson and S. G. Nilsson Ark.Fys. 36 nr. 69 (1967).

6. (a) P. E. Nemirovsky and V.A.Chepurnov Sov.J.Nucl. Phys. 3 , 730(1966)

(b) P. Mukherjee and G. Ramakrishna, unpublished

7. P. Quentin and R. Babinet Nucl.Phys. A156, 365 (1970)

8. D. L. Hendrie et al. Proc.of Int.Conf.on Nucl. Structure, Tokyo 306 (1967).

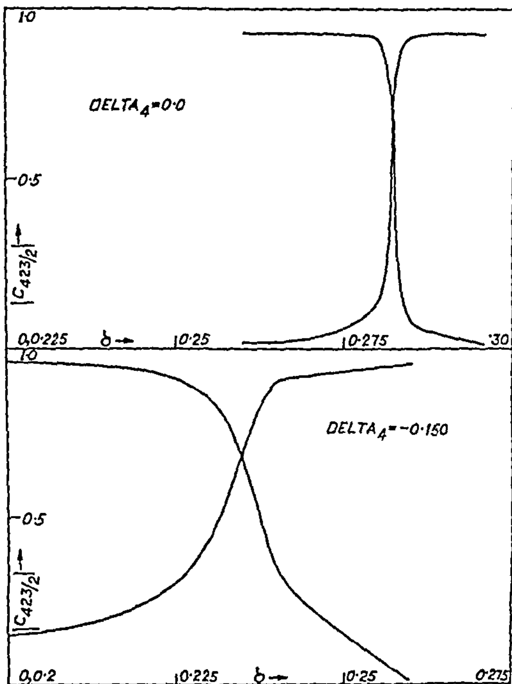


Fig. 1 Plot of $C_{4 2 3/2}$ Vs. δ_2

DISCUSSION

P.G. Hansen: I wonder what the significance of your result is. The S-W potential is believed to be a better approximation to the nuclear potential than is the Nilsson potential. The S-W potential gives the right result, is it then of any use to "doctor" the Nilsson potential by a hexadecapole term to predict the mixing? Does your hexadecapole deformation represent anything but one more free parameter.

G. Ramakrishnan: The significance of our result is the retaining of the harmonic oscillator representation and to point out that the general belief that Nilsson model cannot account such finer details as N = 2 mixing is not correct. Of course Saxon woods potential is a more realistic potential but difficult to work with.

As for the doctoring the Nilsson potential, there are ample experimental evidence that nuclei have hexadecapole deformation over and above the usual quadrupole deformations. To incorporate them and to study their effect on the observed phenomena is a natural consequence of the urge to understand. Though it is difficult at this stage to say correctly regarding the physics of the hexadecapole term, one can say, that this parameterisation is a representation of the deformed shell model potential.

SYSTEMATICS OF ROTATIONAL NUCLEI ON THE BASIS OF TWO-CENTRE MODEL

V.R.Prakash, B.H.Bahal and V.K.Deshpande
Department of Physics
Indian Institute of Technology, Kanpur, India.

I. INTRODUCTION :-

A Two-Centre(TC) model in which a deformed even-even nucleus is represented by two mass points with a phenomenological potential as a function of the distance between them was previously investigated[1]. The model successfully predicted energies of the low lying rotational levels of these nuclei to within a few percent. In the present investigation we wish to point out that in the region $158 \leq A \leq 182$ the model predicts moments of inertia which are in better agreement with those predicted on the basis of the quadrupole moment data than the rigid-body or the hydrodynamic model[2]. Calculations are done using the harmonic oscillator and the Morse potentials of which the latter gave improved results. Variation of stiffness as a function of the neutron and the proton number is studied.

The low lying rotational levels of even-even nuclei in the rare-earth and actinide regions are given by

$$E_I = (\hbar^2/2\mathcal{J})I(I+1) \qquad (1)$$

where I=0,2,4 etc., and $\mathcal{J}$ is the nuclear moment of inertia. For spheroidal shape, the rigid-body moment of inertia is

$$\mathcal{J}_R = (2/5)MR_o^2(1+0.31\beta+0.42\beta^2+.....) \qquad (2)$$

where M is the nuclear mass, R_o is the radius of the equal-volume sphere and β the quadrupole deformation parameter, which can be estimated from the intrinsic quadrupole moment given by

$$(Q/e)=(3/\sqrt{5\pi})ZR_o^2(\beta+0.16\beta^2+....) \qquad (3)$$

The hydrodynamic[2] value of the moment inertia is

$$\mathcal{J}_H=(9/8\pi)MR_o^2\beta^2 = 3B\beta^2 \qquad (4)$$

It is found that $\mathcal{J}_R$ is often twice and $\mathcal{J}_H$ about one-fifth of $\mathcal{J}$.

In the governor model[3] the moment of inertia of a spheroid of semi-major axis 'a' and semi-minor axis 'b', in which the contribution to $\mathcal{J}$ by the central sphere of radius 'b' is removed, is

$$\mathcal{J}_G = 0.53\, MR_o^2(\beta-0.47\beta^2+....) \qquad (5)$$

The TC-moment of inertia $\mathcal{J}_T$ is $(M\rho^2/4)$ where ρ is the distance between the two centres. For a spheroid, ρ is given by

$$\rho = (3R_o/4)(1+\sqrt{5/4\pi}\,\beta) \qquad (6)$$

From equation (3) we therefore have

$$(\mathcal{J}_T/Q) = 0.19 \frac{M(1+0.63\beta)}{Ze(\beta+0.16\beta^2)} \qquad (7)$$

which is independent of R_o. Similar ratio for the rigid-spheroid, the hydrodynamic and the governor models can be got using $\mathcal{J}_R$, $\mathcal{J}_H$, $\mathcal{J}_G$ in place of $\mathcal{J}_T$.

II. CALCULATIONS:- Using the experimental values[4] of the quadrupole moment and the values of moment of inertia from equation(1) (got by assuming the energy of the lowest 2^+ state), the value of β is got from equation (7) and is used to get R_o from equation (3). For governor model β thus obtained is negative in most cases. Plots of R_o as a function of the neutron number N are shown in fig.1. The values of R_o for the TC-model are close to those given by the equation R_o=1.2 $A^{\frac{1}{3}}$fm. In this region, $R_o \simeq$ 6.5 fm for the TC-model, $R_o \simeq$ 4.5fm for the rigid-spheroid model and $R_o \simeq$ 2fm for the hydrodynamic model. Thus the nuclear flow which is neither irrotational nor rigid corresponds to TC-motion.

The procedure for calculating energies of K=0 band levels is given in the previous report[1]. With the harmonic potential, the maximum departure for the highest known level is less than 1% for 28 nuclei, less than 2% for 6 nuclei and more than 2% for 16 nuclei. The values of k, C, $\mathcal{J}_o$ and (ΔE)max are given in table 1. The values of C obtained are about 50% larger than those obtained by Mariscotti et al[5], and are smaller than those of Mosel and Greiner[6]. The variation of C with the neutron and proton numbers are shown in figs.2 and 3 respectively. On the whole the stiffness increases with the addition of neutron and decreases with the addition of protons.

With the anharmonic Morse potential the value of $(\Delta E)_{max}$ was less than 1% for 41 nuclei, less than 2% for 6 nuclei and more than 2% for 3 nuclei. Marked improvement was possible for osmium isotopes and neutron deficient nuclei.

The experimental energies[7] of the $0^{+'}$ (β-vibrational)level was on an average found to be higher by about 55% compared to those calculated with the parameters needed to fit the lowest rotational levels. However, when a least squares fit to the rotational levels and the $0^{+'}$ level was made, it was possible to obtain fits to within a maximum departure of 6% as shown in table 2.

REFERENCES:

* 1. V.K.Deshpande, V.R.Prakash and B.M.Bahal Proc.Nuc.and Solid State Physics Sym. N90,(1969)

(Contd., under table 1)

Table 1.

Parameters with harmonic Potential.

NUCLEUS	C (MeV)	$\mathcal{J}_0$ (10^{-19} kev sec^2)	ΔE_{max} %	NUCLEUS	C (MeV)	$\mathcal{J}_0$ (10^{-19} kev sec^2)	ΔE_{max} %
^{150}Nd	1.639	94.6	1.4	^{174}Yb	9.040	158.2	1.8
^{152}Sm	1.551	102.6	5.0	^{176}Yb	8.405	147.9	0.3
^{154}Sm	3.891	149.3	3.0	^{166}Hf	2.337	78.6	5.0
^{154}Gd	1.561	101.5	7.2	^{168}Hf	2.828	100.5	4.8
^{156}Gd	4.205	137.8	0.4	^{170}Hf	3.760	123.5	0.5
^{158}Gd	6.125	152.7	0.4	^{172}Hf	5.987	129.6	1.6
^{160}Gd	6.745	161.0	0.4	^{174}Hf	7.032	134.1	0.9
^{156}Dy	1.434	90.3	2.5	^{176}Hf	9.110	137.5	0.1
^{158}Dy	3.392	125.1	0.4	^{178}Hf	11.420	130.2	0.3
^{160}Dy	6.176	140.6	0.6	^{180}Hf	20.560	129.0	0.1
^{162}Dy	8.622	150.0	0.3	^{172}W	2.393	101.5	1.7
^{164}Dy	7.727	164.7	0.2	^{174}W	3.767	110.8	1.4
^{158}Er	1.461	63.2	10.0	^{176}W	2.430	113.7	0.3
^{160}Er	2.471	98.7	6.8	^{178}W	8.262	116.6	3.0
^{162}Er	4.982	121.6	0.8	^{180}W	8.224	118.2	0.3
^{164}Er	7.729	133.4	1.0	^{182}W	14.500	121.2	0.1
^{166}Er	6.525	150.7	0.1	^{184}W	12.170	109.7	0.4
^{168}Er	13.740	150.9	0.1	^{186}W	13.660	99.9	0.2
^{170}Er	11.880	152.7	0.1	^{178}Os	1.816	94.9	4.0
^{162}Yb	2.108	74.8	6.2	^{180}Os	3.392	94.3	0.9
^{164}Yb	3.168	101.1	4.0	^{182}Os	4.557	97.9	1.8
^{166}Yb	5.454	120.7	0.2	^{184}Os	5.944	103.2	5.0
^{168}Yb	5.793	139.0	0.9	^{186}Os	5.855	90.5	3.6
^{170}Yb	10.400	143.7	0.4	^{188}Os	4.708	80.5	6.2
^{172}Yb	10.5100	153.3	0.6	^{190}Os	3.623	66.8	6.5

References (Contd):

2. A.Bohr and B.R.Mottelson, Kgl.Danske.Videnskab.Selskab.Mat.Fys.Medd. 27 (1953) 16
3. R.K.Gupta, Can. J. Phys. 47(1969)299
4. P.H.Stelson and L.Grodzins, Nuc. Data A1(1965)21
5. M.A.J.Mariscotti, G.S.Goldhaber and B.Buck, Phys. Rev. 178(1969)1864
6. U.Mosel and W.Greiner, Z.Phyk. 217(1968)256
7. C.M.Lederer, J.M.Hollander and I.Perlman, Table (6th edition, John Wiley, New York, 1967)

Table 2.

NUCLEUS	k (10^{29} kev/cm^2)	ρ_0 (fm)	$(\Delta E)_{max}$ %	D (MeV)	α (10^{12} cm^{-1})	ρ_1 (fm)	$(\Delta E)_{max}$ %
^{150}Nd	0.39	5.275	4.6	10.5	1.4	5.170	5.0
^{152}Sm	0.38	5.475	5.9	9.0	1.5	5.320	6.1
^{154}Sm	1.08	6.455	1.7	45.5	1.1	6.380	1.8
^{154}Gd	0.39	5.410	4.7	8.0	1.6	5.280	6.2
^{156}Gd	0.96	6.197	2.6	40.5	1.1	6.130	2.7
^{158}Dy	0.84	5.880	5.0	36.5	1.1	5.800	4.0
^{160}Dy	1.47	6.175	2.5	52.5	1.2	6.110	2.5
^{164}Er	1.46	5.945	2.4	51.5	1.2	5.880	2.4
^{166}Er	2.02	6.270	2.4	72.0	1.2	6.200	2.0
^{168}Yb	1.27	6.015	3.1	33.5	1.4	5.950	2.7
^{170}Yb	1.15	6.075	0.4	48.0	1.1	5.960	0.7
^{172}Yb	1.11	6.135	0.6	40.0	1.2	6.110	0.5
^{174}Yb	1.91	5.610	0.5	47.0	1.4	6.160	0.6
^{174}Hf	0.71	5.750	0.6	36.0	1.0	5.680	0.6
^{176}Hf	1.50	5.610	0.8	45.5	1.3	5.540	0.9
^{182}W	1.60	5.346	0.5	63.0	1.1	5.285	0.3
^{188}Os	1.21	4.350	4.7	51.0	1.1	4.320	5.0

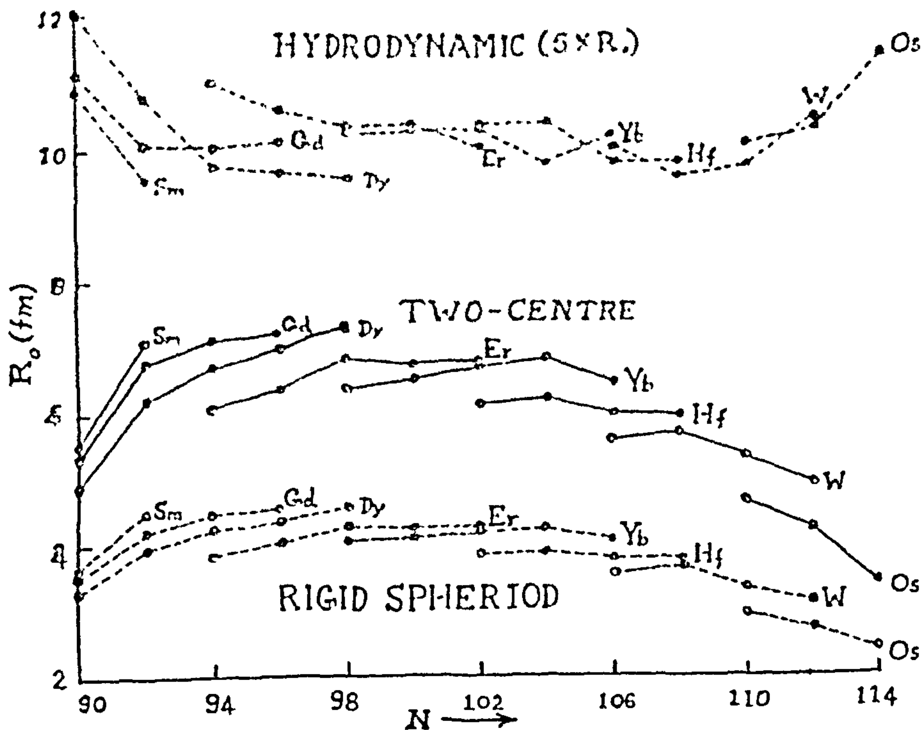
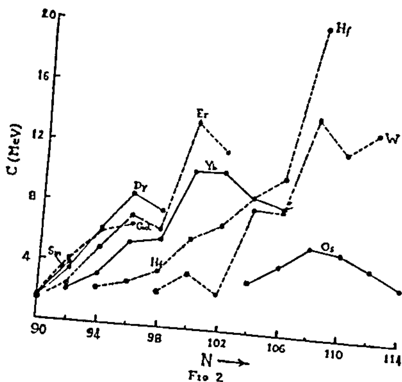
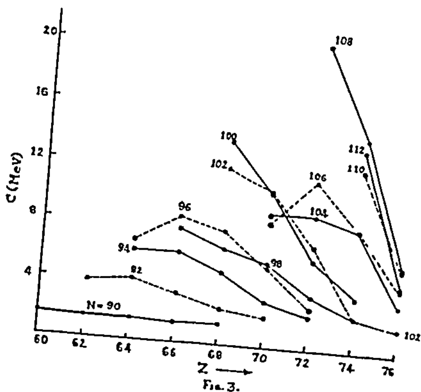


Fig. 1.



C (MeV)
20
16
12
8
4
90
94
98
102
106
110
114
N
Hf
Er
W
Yb
Dy
Gd
Sm
Hf
Os

Fig 2



C (MeV)
20
16
12
8
4
60
62
64
66
68
70
72
74
76
Z
108
100
112
102
110
106
96
104
94
98
92
N = 90
102

Fig. 3.

GROUND STATE ENERGIES OF DOUBLY EVEN NUCLEI ($12 \leq A \leq 40$)

K.M.Khanna and M.L.Sharma *
Dibrugarh University Dibrugarh (Assam)
*K. G. K. College, Moradabad (U.P.)

I INTRODUCTION

Recently [1], the cluster structure of alpha-particles nuclei has been studied by calculating the lower bounds to the ground state energy of N alpha particles interacting via a potential determined by alpha-alpha scattering experiments. The values so calculated were compared with ground state energies of nuclei with 2N protons and 2N neutrons, measured relative to the threshold of N alpha break up. In view of the excellent agreement with the measured values it seems to us that in principle doubly even nuclei can be represented as systems of rigid and structureless alpha particles. In this paper we have shown that by a suitable choice of the potentials excellent agreements can be obtained.

II ENERGY CALCULATIONS

Let us consider a system of N alpha particles enclosed in a volume V. The assembly of alpha particles is assumed to be interacting through a potential composed of a hard core followed by a square well of the form[2]

$$V_{\alpha\alpha}(r) = \begin{cases} +\infty & r < a \\ -V_0 & \text{for} \quad a < r < b \\ 0 & r > b \end{cases} \qquad \text{-----(1)}$$

The ground state energy has been calculated by using the theory developed by Brueckner and Sawada [3]. It is given by

$$E_0/N = \frac{1}{2} \, k \, t_{\ldots} = -(\hbar^2/\ldots)\left[\frac{1}{[\text{illegible}]} - 4\pi \int_a^{\infty} dr\, r^2 V_0(r) \left\{1 - \frac{[\text{illegible}]}{[\text{illegible}]}\right\}^2\right] \qquad \text{---(2)}$$

E_0 is ground state energy, ρ alpha particles number density

Go (a,r) and Go (a,a,)are the Green's functions to be dertermined from

$$G_0(a,a) = -\left(\frac{1}{2\pi}\right)^3 \int_0^\infty dq \left\{J_0(qa)\right\}^2 \Big[\frac{q^2}{m_\alpha} + 2\rho_\alpha \Big\{-2 \sum_{l \leq l_{\max}} (2l+1)\Big[\left[J_l\left(\tfrac{qa}{2}\right)\right]^2 / G_0(a,a)$$
$$+ 4\pi \int_a^\infty dr\, r^2 \Big\{J_l\left(\tfrac{qa}{2}\right)\frac{G_l(a,r)}{G_l(a,a)} - J_l\left(\tfrac{qr}{2}\right)\Big\} V_{\alpha\alpha}(r)\, \psi^l_{k/2}(r)\Big] + \frac{1}{G_0(a,a)}$$
$$- 4\pi \int_0^\infty dr\, r^2 \Big[1 - \frac{G_0(a,r)}{G_0(a,a)}\Big] V_{\alpha\alpha}(r)\, \psi_0^0(r)\Big\}\Big]^{-1} \quad \text{------} (3)$$

similar expression follows for Go(a,r).

Here J stands for spherical Bessel functions. The energy ~~educations~~ calculations are done by taking into account the wave distortion due to the potential given by eqn(1) so long as too,oo and the energy denominators are positive. Calculations of Go (a,a) and Go (a,r) are done with the following simplifying assumptions.

$$\psi_l^l(r) \cong J_l(lr) - J_l(la)\, G_l(a,r)/G_l(a,a) \quad \text{------} (4)$$
$$G_l(a,r)/G_l(a,a) \cong G_0(a,r)/G_0(a,a) = \frac{-m_\alpha / 4\pi\hbar^2 r}{-m_\alpha / 4\pi\hbar^2 a} = \frac{a}{r} \quad \text{------} (5)$$

The appropriate substitutions in eqn.(3) for the S state and its furtherr simplifications gives

$$G_0(a,a) = -\frac{1}{2\pi^2}\int_0^\infty dq\, \frac{\sin^2 qa}{q^2 a^2}\left[\frac{q^2\hbar^2}{m_\alpha} - \frac{2\rho_\alpha a^2}{G_0(a,a)} - 34.7\times 10^{-26}\times 2\pi V \rho_\alpha a^3\right]^{-1} \quad \text{-----} (6)$$

The integral on the R.H.S. of (6) is solved by iteration method upto third order. This gives us

$$-\left[G_0(a,a)\right]^{-1} = \frac{4\pi a}{m_\alpha}\left[1 + (8\pi)^{1/2}(\rho_\alpha a^3)^{1/2} + \frac{16\pi}{3}\rho_\alpha a^3\right] \quad \text{-----} (7)$$

Substituting from eqn.(1),(5),(7) in eqn.(2) and soluing it further we get

$$\frac{E_0}{N} = \frac{\rho_\alpha}{2}\left[\frac{4\pi a\hbar^2}{m_\alpha}\left\{1 + (8\pi\rho_\alpha a^3)^{1/2} + \frac{16\pi}{3}\rho_\alpha a^3\right\} - \frac{4\pi V_0}{3}(b-a)^3\right]. \quad \text{----} (8)$$

(ii) <u>Gaussain Potential Calculations.</u>

If, however, the interacting potential is composed of a hard core followed by a ~~Gaussian potent~~ Gaussian potential of the form

$$V_{\alpha\alpha}(r) = \begin{cases} +\infty & r < a \\ V_R e^{-\mu_R r^2} + V_A e^{-\mu_A r^2} & r > a \end{cases} \quad \text{----} (9)$$

We get the following expression for Eo/N

$$E_0/N = \frac{2\pi\hbar^2 a \rho_\alpha}{m_\alpha} + 2\pi\rho_\alpha\Big\{V_R\Big[\frac{1}{4}\sqrt{\frac{\pi}{\mu_R^3}} - \frac{a}{\mu_R} + \frac{a^2}{2}\sqrt{\frac{\pi}{\mu_R}}\Big] + V_A\Big[\frac{1}{4}\sqrt{\frac{\pi}{\mu_A^3}} - \frac{a}{\mu_A} + \frac{a^2}{2}\sqrt{\frac{\pi}{\mu_A}}\Big]\Big\} \quad \text{----} (10)$$

TABLE- I

$\frac{E_o}{N}$ for hard core = 6.76 MEV.

$\frac{E_o}{N}$ for Potential well = 12.37 MEV.

V_c = 15 Mev
a = 1.5 f
b = 1.2 f

Nucleus	N	$-E_{g.s}$ (Mev)	$k = 2.00 \times 10^{37}$ particles cm^{-3} Eo/N= (6.76-12.37) Mev. Hard core contribution (Mev)	Potential well contribution	Total $-E_o$(Mev.)
C^{12}	3	7.3	20.29	30.11	16.82
O^{16}	4	14.4	27.06	49.48	22.42
Ne^{20}	5	19.2	33.82	61.85	28.03
Mg^{24}	6	28.5	40.58	78.22	33.64
Si^{28}	7	38.5	47.35	86.59	39.24
S^{32}	8	45.4	54.11	98.96	44.85
Ar^{36}	9	52.1	60.88	111.33	50.45
Ca^{40}	10	59.1	67.64	123.70	56.06

TABLE -II

Nucleus	N	$-E_{g.S}$ (Mev)	$k = 0.36 \times 10^{38}$ particles $cm.^{-3}$ Eo/N= (4.21-9.47) Mev. Hard core contribution.	Gaussian potential contribution.	Total $-E_o$(Mev.)
C^{12}	3	7.3	12.63	28.41	15.78
O^{16}	4	14.4	16.84	37.88	20.04
Ne^{20}	5	19.2	21.05	47.35	26.30
Mg^{24}	6	28.5	25.26	56.82	31.56
Si^{28}	7	38.5	29.47	66.29	36.82
S^{32}	8	45.4	83.68	75.76	42.08
Ar^{36}	9	52.1	37.89	85.23	47.34
Ca^{40}	10	59.1	42.10	94.70	52.60

V_R = 320 Mev , V_A = -325 Mev , a = 180 f

Go (a,r) and Go (a,a,) are the Green's functions to be dortermined from

$$G_0(a,a) = -\left(\frac{1}{2\pi}\right)^3 \int_0^\infty dq \left[J_0(qa)\right]^2 \left[\frac{q^2}{m_\alpha} + 2\rho_\alpha \left[-2\sum_{l\neq 0}(2l+1)\left[\left\{J_l\left(\tfrac{qa}{2}\right)\right\}\right]^2 / G_l(a,a) \right.\right.$$
$$+ 4\pi \int_a^\infty dr\, r^2 \left[J_l\left(\tfrac{qa}{2}\right)\frac{G_l(a,r)}{G_l(a,a)} - J_l\left(\tfrac{qr}{2}\right)\right] V_{\alpha\alpha}(r)\, \Psi^l_{k}(r)\Big] + \frac{1}{G_0(a,a)}$$
$$\left. - 4\pi \int_a^\infty dr\, r^2 \left[1 - \frac{G_0(a,r)}{G_0(a,a)}\right] V_{\alpha\alpha}(r)\, \Psi^0(r) \right\}^{-1} \quad \text{- - - - - (3)}$$

similar expression follows for Go(a,r).

Here J stands for spherical Bessel functions. The energy ~~educationals~~ calculations are done by taking into account the wave distortion due to the potential given by eqn(1) so long as too,oo and the energy denominators are positive. Calculations of Go (a,a) and Go (a,r) are done with the following simplifying assumptions.

$$\Psi^l_k(r) \cong J_l(kr) - J_l(ka)\, G_l(a,r)/G_l(a,a) \quad \text{- - - - - - (4)}$$

$$G_l(a,r)/G_l(a,a) \cong G_0(a,r)/G_0(a,a) = \frac{-m_\alpha/4\pi\hbar^2 r}{-m_\alpha/4\pi\hbar^2 a} = \frac{a}{r} \quad \text{- - - - - (5)}$$

The appropriate substitutions in eqn.(3) for the S state and its furtherr simplifications gives

$$G_0(a,a) = -\frac{1}{2\pi^2}\int_0^\infty dq\, \frac{\sin^2 qa}{q^2 a^2}\left[\frac{q^2\hbar^2}{m_\alpha} - \frac{2\rho_\alpha a^2}{G_0(a,a)} - 56.7\,\pi\hbar^{-2}\, 2\pi\, V\rho_\alpha a^3\right]^{-1} \quad \text{- - - - - (6)}$$

The integral on the R.H.S. of (6) is solved by iteration method upto third order. This gives us

$$-\left[G_0(a,a)\right]^{-1} = \frac{4\pi a}{m_\alpha}\left[1 + (8\pi)^{1/2}(\rho_\alpha a^3)^{1/2} + \frac{16\pi}{5}\rho_\alpha a^3\right] \quad \text{- - - - - (7)}$$

Substituting from eqn.(1),(5),(7) in eqn.(2) and soluing it further we get

$$\frac{E_0}{N} = \frac{\rho_\alpha}{2}\left[\frac{4\pi a\hbar^2}{m_\alpha}\left\{1 + (8\pi\rho_\alpha a^3)^{1/2} + \frac{16\pi}{5}\rho_\alpha a^3\right\} - \frac{4\pi V_0}{3}(b-a)^3\right]. \quad \text{- - - - (8)}$$

(iii) <u>Gaussain Potential Calculations.</u>

If, however, the interacting potential is composed of a hard core followed by a ~~[illegible]~~ Gaussian potential of the form

$$V_{\alpha\alpha}(r) = \begin{cases} +\infty & r < a \\ V_R\, e^{-\mu_R r^2} + V_A\, e^{-\mu_A r^2} & r > a \end{cases} \quad \text{- - - - (9)}$$

We get the following expression for Eo/N

$$E_0/N = \frac{2\pi\hbar^2 a\rho_\alpha}{m_\alpha} + 2\pi\rho_\alpha\left\{V_R\left[\frac{1}{4}\sqrt{\frac{\pi}{\mu_R^3}} - \frac{a}{\mu_R} + \frac{a^2}{2}\sqrt{\frac{\pi}{\mu_R}}\right] + V_A\left[\frac{1}{4}\sqrt{\frac{\pi}{\mu_A^3}} - \frac{a}{\mu_A} + \frac{a^2}{2}\sqrt{\frac{\pi}{\mu_A}}\right]\right\} \quad \text{- - - - (10)}$$

b

TABLE- I

$\frac{Eo}{N}$ for hard core = 6.76 MEV.

$\frac{Eo}{N}$ for Potential well = 12.37 MEV.

V_0 = 15 Mev
a = 1.5 f
b = [illegible] f

Nucleus	N	$-E_{g.s}$ (Mev)	$k = 2.00 \times 10^{37}$ particles cm^{-3} Eo/N= (6.76-12.37) Mev. Hard core contribution ([illegible]ev)	Potential well contribution	Total -Eo(Mev.)
C^{12}	3	7.3	20.29	30.11	16.82
O^{16}	4	14.4	27.06	49.48	22.42
Ne^{20}	5	19.2	33.82	61.85	28.03
Mg^{24}	6	28.5	40.5?	78.22	33.64
Si^{28}	7	38.5	47.35	86.59	39.24
S^{32}	8	45.4	54.11	98.96	44.85
Ar^{36}	9	52.1	60.88	111.33	50.45
Ca^{40}	10	59.1	67.64	123.70	56.06

TABLE -II

V_R = 320 Mev , V_A = -335 Mev, a = 1.80 f

Nucleus	N	$-E_{g.S}$ (Mev)	$k = 0.36 \times 10^{38}$ particles cm^{-3} Eo/N= (4.21-9.47) Mev. Hard core contribution.	Gaussian potential contribution.	Total -Eo(Mev.)
C^{12}	3	7.3	12.63	28.41	[illegible]
O^{16}	4	14.4	16.84	37.83	[illegible]
Ne^{20}	5	19.2	21.05	47.35	[illegible]
Mg^{24}	6	28.5	25.26	56.82	[illegible]
Si^{28}	7	38.5	29.47	66.29	[illegible]
S^{32}	8	45.4	83.68	75.75	[illegible]
Ar^{36}	9	52.1	37.89	[illegible]	[illegible]
Ca^{40}	10	59.1	42.10	[illegible]	[illegible]

III ALPHA-PARTICLE DENSITY IN THE SURFACE REGION OF NUCLEAR MATTER.

We have estimated the density of alpha particles in the surface region of nuclear matter. From eqn.(8) we find that Eo/N varies with ρ . Eo/N will be minimum for some value of ρ provided $\frac{\partial(E_0/N)}{\partial\rho} = 0$ and $\frac{\partial^2(E_0/N)}{\partial\rho^2}$ is positive for that value of ρ . The value of ρ at which Eo/N is minimum comes out to be $\rho = 2{\cdot}57 \times 10^{37}$ particles cm^{-3}. If we plot a graph between Eo/N and ρ , minima Eo/N actually lies at $\rho = 2.6 \times 10^{37}$ particles cm^{-3}

IV DISCUSSION

Looking at the results given in the table (I), we find that for high value of ρ the agreement for these nuclei becomes better when $\alpha\alpha$ potential has a hard core followed by a square well. Excellent agreement is obtained for $\rho = 2 \times 10^{37}$ particles cm^{-3}. Thus the existence of alpha clusters in doubly even nuclei seems to be a reasonable possibility.

Our calculations, therefore, assert that the local potential should be of the form of a hard core followed by a Gaussian potential. This potential should be more suitable since the repulsive part of the Gaussian potential well indirectly contain in itself the coulomb effects between the ~~potential~~ charged alpha particles.

REFERENCES

1. A.Y.Abul. Magd. Nucl. Phy. A 129 (1969)610.
2. E Vander spuy and H.J. Pienaar. Nucl.Phys. 7 (1956) 397
3. K.A. Brueckner and K. Sawada. Phy.Rev.106 (1957) 1157.

DISCUSSION

R. Shanta: The attractive Gaussian potential you have considered has a range of 4 fm. Haven't considered the long range Coulomb repulsion in your calculations?

M.L. Sharma: In the potential composed of Hard core followed by Gaussian well, we have used the combination of both the attractive as well as repulsive part. The form is following:

$$V_{\alpha\alpha}(r) = \begin{cases} \infty & r < a \\ V_R e^{-\mu_R r^2} + V_A e^{-\mu_A r^2} & r > a \end{cases}$$

where V_R and V_A are the strengths of repulsive as well as attractive parts and $\sqrt{\mu_A}$, $\sqrt{\mu_R}$ are the corresponding inverse ranges.

M.L. Chatterjee: Your calculation should presumably work in the low mass region where there is good evidence for α-clustering width even in the ground state. But what about the heavy mass region where the neutron and proton orbitals are far different from each other?

K.M. Khanna: In fact, we have not examined this expect in our calculations. Hope to report it at some later date.

TWO-PARTICLE TWO-HOLE EXCITATIONS AND INTRINSIC SHAPES OF DEFORMED NUCLEI

M.R. Gunye and C.S. Warke
Tata Institute of Fundamental Research, Bombay 5, India

and

S.B. Khadkikar
Physical Research Laboratory, Ahmedabad 9, India

The Hartree-Fock (HF) method has been extensively used to describe the equilibrium shapes of the ground states of light and medium mass nuclei(1). It is found that almost all the deformed even-Z even-N nuclei in p- and sd-shell have axially symmetric shape with a few notable exceptions like ^{24}Mg which have non-axial shapes. These results are in agreement with the prediction of SU3-classification scheme(2). Both the SU3 and HF methods leave out nuclear pairing correlations which are known to affect the equilibrium deformations(3,4). The pairing correlations are induced by the 'residual interactions' ignored in HF theory. The residual interactions, however, give rise to many types of correlations in HF state as a result of two-particle two-hole (2p-2h) excitations. We propose to study the effect of residual interaction in a perturbation formalism by incorporating 2p-2h excitations in the HF state.

After the completion of calculations reported here, the work done by Padjen and Ripka(5) came to our notice. These authors have given a self-consistent approach for including 2p-2h admixtures in the ground state. The method is applied to sd-shell nuclei in a configuration space of single sd-shell. Their numerical applications are, however, restricted to axially symmetric states. These authors have tressed the need of including 2p-2h admixtures in non-axial state in rder to determine whether ^{24}Mg has an axial or non-axial shape in resence of 2p-2h excitations.

The second-order perturbation theory gives the following expressions for energy E and mass quadrupole moment Q:

$$E = E_{HF} - \sum_{i<j} \sum_{i'<j'} A_{i'j'ij} \; V_{i'j'ij}$$
$$Q = Q_{HF} - \frac{1}{C} \sum_{i<j} \sum_{i'<j'} (A_{i'j'ij})^2 (q_{i'i'} + q_{j'j'} - q_{ii} - q_{jj})$$
$$C = 1 + \sum_{i<j} \sum_{i'<j'} (A_{i'j'ij})^2$$

The sums over primed (unprimed) indices run over the unoccupied (occupied) single-particle HF orbitals. The energy and mass quadrupole moment in the HF state is denoted by E_{HF} and Q_{HF} respectively. The amplitude $A_{i'j'ij}$ is given by

$$A_{i'j'ij} = V_{i'j'ij} / (\varepsilon_{i'} + \varepsilon_{j'} - \varepsilon_i - \varepsilon_j)$$

where ε_m is the single-particle energy in HF orbital m and $v_{i'j'ij}$ is an antisymmetrized matrix element of the nucleon-nucleon (NN) interaction. The matrix element of the quadrupole operator[1] between the single-particle HF orbitals m and n is denoted by q_{mn}.

The calculations reported here are performed in a large configuration space of first four major shells by employing the effective NN interaction of Elliott et al[6]. Three typical nuclei ^{20}Ne, ^{24}Mg and ^{28}Si in sd-shell are considered in view of their characteristically different equilibrium shapes as found from bare HF calculations. The results of the calculations with oscillator size parameter b=1.7 fm are presented in Table I. It is found that the 2p-2h contribution is only $\lesssim$3% of the potential energy, justifying the perturbation treatment. It should be stressed here that the second-order perturbation treatment is valid even in case of HF solutions with small gaps at the Fermi surface. The second-order change in the mass quadrupole moment is also found to be small.

The bare HF calculations favour a prolate and oblate shape for intrinsic states of ^{20}Ne and ^{28}Si respectively. The second-order energy contribution, though quite small in comparison with the

potential energy, decreases the relative energy separation between prolate and oblate solutions of both ^{20}Ne and ^{28}Si but does not alter the conclusions of bare HF calculations as seen from Table I. In ^{24}Mg, however, the non-axial HF solution is lower than the prolate solution by 1.65 MeV. It is in this case that the 2p-2h excitations play a vital role in lowering the prolate solution by 3.35 MeV more than the non-axial solution, thus favouring the prolate shape for the ground state of ^{24}Mg.

It is found that both T=0 and T=1 states contribute comparably to the second-order energy gain, from 2p-2h excitations. The T=0 and T=1 perturbation contributions to the three HF solutions of ^{24}Mg are shown in Table II. That the T=1 pairing between identical nucleons alone is not enough to lower the prolate solution below the non-axial solution is clear from the HFB calculations[7] which yield a relative lowering of ≈ 1 MeV comparable to 1.50 MeV obtained from T=1 states of identical nucleons in the present calculations. However, the relative lowering of 4.3 MeV obtained[4] from the T=0 pairing correlations does not agree with the present calculations which give only 1.10 MeV relative lowering from T=0 2p-2h contributions. We feel that the estimation obtained[4] from T=0 pairing correlations is rather uncertain possibly due to simplified model calculations and particularly due to non-conservation of the number of neutron-proton pairs.

The prolate HF states of ^{24}Mg and ^{28}Si as well as oblate HF state of ^{20}Ne display pairing correlations[5] as a result of small HF gaps characterizing these states. The energy contribution from 2p-2h excitations is relatively more in these states than in the other HF states with large gaps. The relative 'second-order' lowering of one HF state with respect to other can thus be interpreted as a consequence of pairing correlations. In ^{24}Mg, the · on

HF calculation does not remain valid since the pairing correlations in prolate HF state actually lower that state below the non-axial state. We thus conclude that the ground state of ^{24}Mg has a prolate shape with both T=1 and T=0 pair correlations of comparable strengths.

In support of our conclusion, we mention that the spectroscopic factors for ^{24}Mg (d,p) ^{25}Mg can be explained[8] by assuming a prolate and not a non-axial intrinsic state for ^{24}Mg. The calculations carried out by using both the prolate[9] and the non-axial[10] HF states give a compressed spectrum for ^{24}Mg. This is not surprising in view of the present results. It is found[11] that the T=1 pairing correlations have a significant effect in spreading the compressed HF spectra of many even-Z even-N nuclei. It is therefore essential to include pairing correlations in the prolate intrinsic state to explain the excited state spectrum of ^{24}Mg.

References

1. J. Bar-Touv and I. Kelson, Phys. Rev. 138B, 1035; (1965); S.B. Khadkikar and M.R. Gunye, Nucl. Phys. A110, 472 (1968).
2. M.K. Banerjee, C.A. Levinson and S. Meshkov, Phys. Rev. 130, 1064 (1963).
3. S.B. Khadkikar and M.R. Gunye, Nucl. Phys. A144, 289 (1970).
4. A.L.Goodman, G.L.Struble and A.Goswami, Phys.Letters 26B, 260(1968)
5. R. Padjen and G. Ripka, Nucl. Phys. A149, 273 (1970).
6. J.P. Elliott, A.D. Jackson, H.A. Mavromatis, E.A. Sanderson and B. Singh, Nucl. Phys. A121, 241 (1968).
7. S.B. Khadkikar and M.R. Gunye, Proc. of Low Energy Nuclear Physics Symposium, Roorkee (India), 1969.
8. J.C. Parikh, Phys. Letters 26B, 607 (1968)
9. M.R. Gunye and C.S. Warke, Phys. Rev. 156, 1087 (1967).
10. B. Giraud and P.U. Sauer, Phys. Letters 30B, 218 (1969).
11. M.R. Gunye and S.B. Khadkikar, Phys.Rev.Letters 24, 910 (1970).

Table I

The energies (in MeV) of the low-lying HF states for ^{20}Ne, ^{24}Mg and ^{28}Si. E_{HF} is the HF energy and E includes second-order correction.

Shape of HF state	^{20}Ne E_{HF}	^{20}Ne E	^{24}Mg E_{HF}	^{24}Mg E	^{28}Si E_{HF}	^{28}Si E
Oblate	− 95.52	− 110.77	− 132.76	− 149.20	− 189.03	− 197.15
Prolate	− 103.50	− 114.52	− 138.15	− 152.52	− 184.43	− 195.15
Non-Axial			− 139.70	− 150.72		

Table II

The energy contributions from the T=1 and T=0 states of 2p-2h excitations in the prolate, oblate and non-axial HF states of ^{24}Mg.

	Oblate	Prolate	Non-Axial
T = 1	6.90	6.21	5.96
T = 0	9.55	8.15	7.03

EFFECTIVE INTERACTION AND ENERGY LEVELS OF NUCLEI WITH REALISTIC INTERACTIONS

M.C. Jain
Department of Physics
Indian Institute of Technology, Kanpur-16

ABSTRACT

Effective interactions of nuclei with two particles in the p-, sd- and fp- shells are calculated using the interaction of Shakin et al, obtained from the Yale potential following the Unitary-Model-Operator approach. Core-excitation corrections are evaluated following the method of Kuo and Brown. Detailed comparison is made with the works of Kuo-Brown and their collaborators, and of Becker and MacKollar. It is found that the differences in the effective interaction matrix elements calculated by different groups of workers can lead to large differences in the spectra, indicating that one can not get any conclusive information from the renormalization *calculations unless* the reaction matrix elements are evaluated with greater precision.

A VARIATIONAL APPROACH TO THE ^{18}O NUCLEUS

Jadunath De
Saha Institute of Nuclear Physics, Calcutta-9

ABSTRACT

Hartree-Fock calculations have been performed for the ^{18}O nucleus with two realistic potentials i) the hard-core Hamada-Johnston potential and ii) the nonsingular potential of Tabakin in harmonic-oscillator basis, the basis extending upto p-f shell. The binding energy for nucleus and the r.m.s. value were found to be reasonable though the gap was found to be quite small. Projection of states of good angular momentum was carried out from the Hartree-Fock intrinsic state. The resulting spectrum was found to be very compressed compared to the experimental one. BE_2 transition probabily ($2^+ \longrightarrow 0^+$) was also calculated and was found to be 3-times greater than the experimental value. 2p-2h type excitations are included in the calculation recently to include pairing correlations. It is hoped that this pairing-correlation would in effect dilute the spectrum and diminish the BE_2 value.

H F B CALCULATIONS IN p.f. SHELL NUCLEI (I) EVEN-EVEN NUCLEI

Jyoti K. Parikh
Bhabha Atomic Research Centre, Bombay-85

ABSTRACT

p.f. shell nuclei are studied using projected H F B formalism.

(1) Oblate shaped Zn isotopes are studied.

(2) Lifetimes of prolate shaped Ti isotopes and oblate shaped Zn isotopes are calculated and are found to be in very good agreement with the experimental values.

(3) The nuclei have prolate shape near ^{40}Ca region (Ti, Cr, Fe isotopes), in the middle (Ni isotopes) they are energetically degenerate in shape, and at the end of p.f. shell (Zn isotopes) they acquire oblate shape. It is also interesting to note that near ^{40}Ca region, protons show far more pairing than neutrons whereas near the other end of p.f. shell neutrons show more pairing.

H F B CALCULATIONS FOR p.f. SHELL NUCLEI (II) ODD-EVEN NUCLEI

Jyoti K. Parikh
Bhabha Atomic Research Centre, Bombay-85.

ABSTRACT

Variational H F B calculations are carried out for odd-even nuclei. The odd particle occupies a state with probability 1. This leads to blocking effect which has been taken into account in the self consistent calculations. The questions of time reversal invariance and axial symmetry are discussed. Odd-even mass differences are calculated and compared with the experiment.

GROUND STATE AND BETA-VIBRATIONAL BANDS OF NUCLEI IN THE RARE-EARTH REGION

A. Ansari and S.C.K. Nair
Saha Institute of Nuclear Physics, Calcutta-9

ABSTRACT

Hartree-Fock-Bogoliubov (HFB) calculations have been carried out for the ground intrinsic shape of ^{152}Sm with pairing + Q.Q two-body interaction followed by angular momentum projection s to study the various properties of the ground state rotational band. The projection results are compared with that of the semiclassical approaches and experimental data. The projected energy spectrum is found to be closer to the cranking model predictions. Further, the possibility of calculating the properties of the beta-vibrational band by solving the Hill-Wheeler integral equation in the Gaussian-Overlap-Approximation (GOA), with the deformation parameter as the generator co-ordinate, will be discussed.

A SIMPLE THOMAS-FERMI METHOD FOR NUCLEAR MATTER AND NUCLEI

S. Bhattacharyya
Sibpur Dinabandhu College, Howrah
and
M.K. Roy
Department of Physics, Calcutta University

ABSTRACT

The Thomas-Fermi method of Kumar, Le Couteur and Roy has been extended here to include higher powers in particle density and higher powers and orders in density gradient in the energy expression for nuclear matter and nuclei. We have worked with a realistic potential (viz. Reid's hard-core potential) and have used the Moszkowski-Scott separation method to take care of the short-range repulsive force. As a test case we have considered the ^1S and ^3S state potentials, and have calculated the energies and compressibilities of nuclear matter. The energies agree quite well with those of Dahlblom's calculations and the values of compressibilities are also reasonable. It is also found that of the three relations

(i) $R = {}^3S/{}^1S = 2.55 - 0.96\ k_F$ (Sprung and Bhargava's calculations)

(ii) $= 1.46 - 0.28\ k_F^2$, (Dahlblom's calculations)

(iii) $= 1.85 - 0.67\ k_F$ (Dahlblom's calculations)

which fit well with the ratio R of ^3S to ^1S contribution, (i) and (ii) give correct energies and compressibilities for nuclear matter.

SU_3 SYMMETRY IN f-p SHELL

D.R. Kulkarni and K.H. Bhatt
Physical Research Laboratory
Ahmedabad-9.

Unlike in d-s shell, nuclei in the beginning of f-p shell do not exhibit well-developed rotational spec This is generally attributed to the enhanced pairing effect in f-p shell as indicated(1) by greater stability of the HFB intrinsic state compared to HF intrinsic state We consider that the increase in pairing correlations in f-p shell is more due to its sequence of single particle states than to the presence of large pairing component in the two-body interaction. In fact we presume that two-body interaction is still predominantly quadrupole-quadrupole type but the unfavourable ordering of single particle states hinders the formation of rotational band. To see this point explicitely consider the hamiltonian-

$$H = H_o - A\,(Q.Q) \qquad (1)$$

Where $Q = q_1 + q_2$ is the total quadrupole operator, H_o, the harmonic oscillator potential and A, the strength of the interaction. This hamiltonian gives rotational spectra belonging to unique SU_3 representations(2).

Substituting for Q in (1) we get

$$H = H_o - A\sum_i C_i + 3A\sum_i l_i^2 - 2A\sum_{i<j} q_i \cdot q_j \qquad (2)$$

Where C_i denotes the single particle SU_3 casimir operator. The expression (2) shows that by adjusting the strength of single particle interaction l^2, it is possible to restore the SU_3 symmetry and thereby the rotatio[illegible] ded two-body interaction is q.q typ[illegible] pro-

same criteria to test the two-body interaction in our calculations.

The two-body wave functions are obtained using the Kuo-Brown interaction(3) and the following three choices of single particle energies a) experimental b) p and f degenerate c) p orbit below f (no spin-orbit interaction). An SU_3 decomposition of these wave functions shows that in case a) all SU_3 components are considerably mixed. The admixture of components with different space symmetry is due to the single particle spin-orbit interaction. In case b) the admixture of SU_3 components belonging to different space symmetry is absent but that of same space symmetry is still retained . This latter admixture is greatly reduced in case c). In this case separation of p and f is varied till the maximum SU_3 symmetry is restored. The average separation of p and f states required to resotre the SU_3 symmetry to about 95% for all J states is 1.5 MeV in T=1 interaction while corresponding number for T=0 interaction is 2 MeV. This difference in separation of p and f states reflects the fact that T=0 interaction is about 1.5 times stronger than T=1 interaction. Table I shows the result for the case J=0. T=1 for all three cases considered above. Fig. I shows the spectrum which tends to become more rotational as we use more favourable single particle states.

According to our criteria stated above these results suggest that the two-body interaction is mainly quadrupole-quadrupole type and that the absence of rotational spectra in f-p shell is mostly due to the unfavourable

sequence of physical single particle states.

The restoration of SU_3 symmetry by adjusting single particle states can be looked from a different point of view. We may say that if the two-body interaction contains any SU_3 breaking components, the suitable single particle states nullifies the effect of those components and SU_3 symmetry is recovered. The identification of SU_3 breaking component is easy if it is decomposed into various radial integrals. The study of each radial integral separately from the point of SU_3 symmetry reveals that the radial integrals I_{0s}, I_{3s}, I_{3d}, I_{1g} and I_{0i} act only in symmetric (60) representation while the radial integrals I_{2p}, I_{1f} and I_{0h} act uniquely in antisymmetric (41) representation. All other radial integrals mix the SU_3 representations.

REFERENCES:-

1) K.R. Sandhya Devi, S.B. Khadkikar, J.K. Parikh and B. Banarjee, Phys. Lett., 32B (1970), 179.

2) M. Harvey, Advances in Nuclear Physics, Vol. I, edited by M. Baranger and E. Vogt(Plenum Press, New York, 1968).

3) Kuo T.T.S. and Brown G.E., Nucl. Phys. A 114(1968) 241.

TABLE I

SU_3 decomposition for J=0, T=1 wave functions.

SU_3 component	a	b	c
$(60)_0$	0.5346	0.7787	0.9837
$(22)_0$	0.6948	0.6272	0.1794
$(41)_1$	-0.3680	-0.0053	0
$(03)_1$	-0.3098	-0.0128	-0.0139

NUCLEAR SPECTROSCOPY

PENETRATION EFFECTS IN THE INTERNAL CONVERSION OF L -FORBIDDEN M_1 - TRANSITIONS

M.S. Rajput
Department of Physics
Aligarh Muslim University, Aligarh, U.P.

ABSTRACT

Penetration factors λ have been calculated for some l- forbidden M_1 transitions according to General formulae of Church and Wenlsor from the experimental K-conversion coefficients. It has been observed that there is a trend for λ to increase with neutron number. Effect of mixing ratio parameter "δ" is also observed.

INTERNAL CONVERSION COEFFICIENT MEASUREMENTS IN ^{133}Ba DECAY

C. Narasimha Rao, B. Mallikarjuna Rao, K. Venkata RamanaiaH and K. Venkata Reddy,
The Laboratories for Nuclear Research, Andhra University, Waltair.

I. INTRODUCTION

The internal conversion coefficients studies for transitions 223, 276, 303 and 384 keV in ^{133}Ba decay have been made by several authors [(1-5)]. The α k (223) has been measured by Donnelly et al and Bosch et al. But these are not in agreement with the theoretical value. This discrepancy between the experimental and theoretical results has prompted us to carry out an accurate measurement of the α k(223). The K-conversion coefficients of the other transitions, 276, 303 and 384 keV have also been measured. In the present work we normalised our conversion line, intensities with the gamma intensities of Donnelly et al[1] (Table I) through the intense 356 keV transition which is known to be a pure E2 with α k =0.021 as calculated by Sliv and Band[6].

II. EXPERIMENTAL

Siegbahn-Slatis intermediate image beta ray spectrometer is used in the energy and intensity measurements. The source dependent background at every measurement point (current setting) is taken. Typical collection times are 3.6×10^3 sec.

III. RESULTS

Using our relative K-electron intensity (table I) and

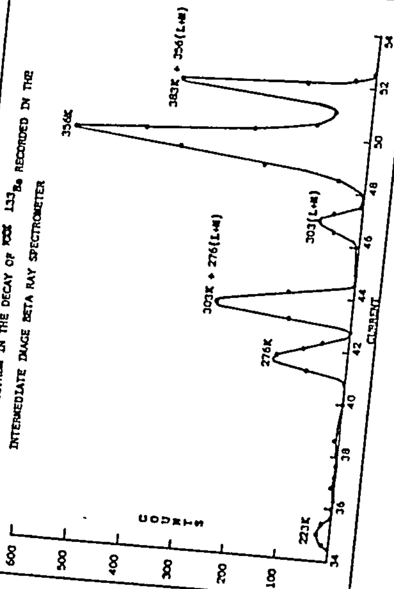
the gamma ray relative intensity of Donnelly et al(table I) the α k(223) is determined relative to αk(356). Our result is α k(223) = 0.0925±0.017. The αk of 276 keV transition has been obtained assuming the conversion coefficient of 356 keV as 0.021 and applying the same technique.

In the case of 303 k line there is a contribution from the 276(L+M) line as observed in our spectrometer. This contribution is subtracted using the K/L+M ... ratio for a 356 keV E2 transition. Similarly in the case of the 384 k line there is a contribution of about 65% of the 356 (L+M) line and this is subtracted and the α k is determined.

The results are shown in the Table II together with the conversion coefficients of Donnelly et al, Mann et al Thun et al, Bosch et al and Gupta et al.

TABLE I

Transition Energy keV	Electron relative intensity	Gamma relative intensity
223	3.22	0.72
278	26.49	11.62
303	51.26	29.40
356	100.00	100.00
384	11.40	14.30


ELECTRON SPECTRUM IN THE DECAY OF 133Ba RECORDED IN THE
INTERMEDIATE IMAGE BETA RAY SPECTROMETER
COUNTS
CURRENT
600
500
400
300
200
100
34
36
38
40
42
44
46
48
50
52
54
223K
276K
303K + 276(L+M)
303(L+M)
356K
383K + 356(L+M)

the gamma ray relative intensity of Donnelly et al(table I) the α k(223) is determined relative to αk(356). Our result is α k(223) = 0.0925±0.017. The αk of 276 keV transition has been obtained assuming the conversion coefficient of 356 keV as 0.021 and applying the same technique.

In the case of 303 k line there is a contribution fbom the 276(L+M) line as observed in our spectrometer. This contribution is subtracted using the K/L+M ... ratio for a 356 keV E2 transition. Similarly in the case of the 384 k line there is a contribution of about 65% of the 356 (L+M) line and this is subtracted and the α k is determined.

The results are shown in the Table II together with the conversion coefficients of Donnelly et al, Mann et al Thun et al, Bosch et al and Gupta et al.

TABLE I

Transition Energy keV	Electron relative intensity	Gamma relative intensity
223	3.22	0.72
278	26.49	11.62
303	51.26	29.40
356	100.00	100.00
384	11.40	14.30

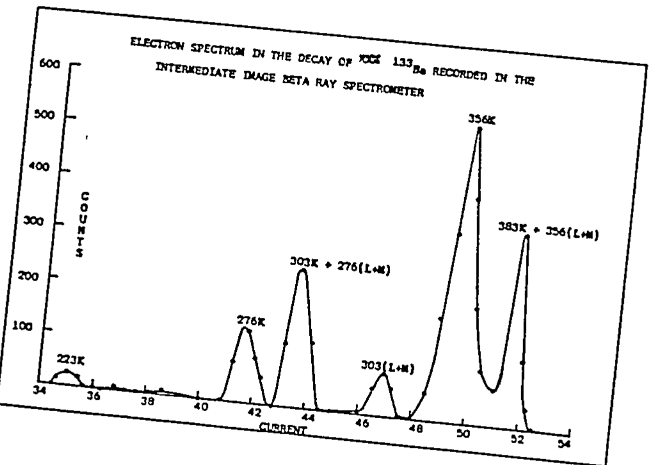

ELECTRON SPECTRUM IN THE DECAY OF 133Ba RECORDED IN THE
INTERMEDIATE IMAGE BETA RAY SPECTROMETER
356K
383K + 356(L+M)
303K + 276(L+M)
276K
303(L+M)
223K
COUNTS
CURRENT
600
500
400
300
200
100
34
36
38
40
42
44
46
48
50
52
54

TABLE II

Conversion coefficients.

Transition energy. keV	Donnelly.	Thun.	Mann.	Bosch.	Gupta.	Present work	Theoretical M1	Theoretical E2
223	0.76 ± 0.012	-	-	0.068	-	0.092 ± 0.017	0.083	0.092
276	0.046 ± 0.006	0.059 ± 0.008	0.047	-	0.0.106	0.048 ± 0.0045	0.047	0.045
303	0.037 ± 0.005	0.037 ± 0.006	0.036 ± 0.004	-	0.0235	0.037 ± 0.003	0.037	0.034
356	-	-	-	-	-	0.021	0.024	0.021
384	0.017 ± 0.002	0.017 ± 0.004	0.020 ± 0.013	-	-	0.017 ± 0.0019	00.020	0.017

REFERENCES

1. D.P. Donnelly et al, Phy.Rev.Vol.173,4,(1968)1198.
2. J.E. Thun et al, Nucl.Phy.88(1966) 289.
3. K.C. Mann et al, Can.J.Phy.41 (1963) 932.
4. H.E. Bosch et al, Nucl.Instr.Meth.52 (1967) 289.
5. R.K. Gupta et al, Nuovo Cimento, 8 (1958) 48.
6. L.A. Sliv and I.M. Band, Alpha, beta, gamma ray spectroscopy, edited by Kai Siegbahn, North Holland Publication, Amsterdam 1965, Vol.2.

HIGH RESOLUTION SPECTROSCOPY OF ^{164}Ho

B. P. Pathak and S. K. Mukherjee
Saha Institute of Nuclear Physics, Calcutta-9

and

S. C. Gujrathi
Department of Chemistry, Simon Fraser University, Burnaby-2, Vancouver, B. C., Canada.

1. INTRODUCTION

The radiations from the two isomers of ^{164}Ho (^{164m} & ^{g}Ho) have been studied by a number of investigators[1-6]. Although high resolution magnetic spectrometers were used by the earlier authors[1,2] to study the electron spectra, the γ-ray spectrometers used by these workers, were of poorer resolution and therefore, the disintegration properties obtained from the γ-ray spectroscopic data were subject to appreciable errors. In a recent work[4] a 2 cm^3 Ge(Li) detector was used to study the decay of ^{164m} & ^{g}Ho but the closely spaced X- and γ-rays could not be distinctly resolved.

The present investigation was carried out with the aim of obtaining further knowledge regarding the decay scheme of ^{164m} & ^{g}Ho using a high resolution Ge(Li) X-ray spectrometer. Precise energies and relative intensities of γ- and X-rays, and the half-life of the metastable state have been obtained. The X-ray intensities were utilised to calculate the intensity of electron capture branches of ^{164g}Ho and the K-conversion coefficients of 91.26 and 56.64 keV γ-rays. The results are compared with earlier works.

II. EXPERIMENTAL

The radioactive sources of $^{164m\,\&\,g}Ho$ were obtained through the (n,2n) reaction on the spectroscopically pure Holmium oxide with 14 MeV neutrons. The photon spectra were studied using a 5.5 mm diam x 6.0 mm deep Ge(Li) X-ray detector in conjunction with a 4096-channel analyzer. The resolution of the system was 585 eV for the 80.997 keV γ-ray of ^{133}Ba. The results of the measurements are summarised in table I. Apart from the photon peaks quoted in the spectrum a weak peak was observed at 94.0 keV.

By following the decay of 37.33 and 56.64 keV gamma rays, and the Ho X-rays, the half-life of ^{164m}Ho was found to be 36 ± 1 min. This value is in excellent agreement with those reported by earlier authors(2,8).

The isomeric cross-section ratio for the reaction $^{164}Ho\ (n,2n)\ ^{164m\,\&\,g}Ho$ was estimated to be 1.0 ± 0.25 by following the decay of the intensities of photopeaks of 73.40 and 91.26 keV gamma rays and the beta rays of ^{164g}Ho. The value obtained is in fair agreement with the one reported by Sethi et al(3). but differs from that of Steiner et al(7).

In view of the recent work by da Silva et al(6). a search for high energy gamma rays was made using a 3 gm sample of Ho_2O_3 and a 23.8 cc. coaxial Ge(Li) detector. The existence of 689 and 762 keV gamma rays could not be confirmed.

III. RESULTS

With the help of the results obtained in this work a revised decay scheme of $^{164m \& g}Ho$ is proposed(Fig.1). For the intensity of the negaton branches to the ground and first excited states of ^{164}Er, the results of Jorgensen et al.[2] were utilised. The electron capture branches to the first excited and ground states of Dy were calculated from the analysis of the Dy K X-ray intensities. From the intensities of the Ho and Er K X-rays the K-conversion coefficients (α_K) for the 56.64 and 91.26 keV gamma rays were found to be 19.0 ± 2 and 1.16 + 0.12, respectively. The value of α_K for the 56.64 keV transition is found to be 12 by analyzing the results of Jorgensen et al.[2] The K-conversion coefficient for the 91.26 keV transition, obtained in this work is in good agreement with that reported by Boneau et al.[5] In fig.1, the 94.0 keV transition is shown by dotted lines as the nature of the photopeak could not be ascertained.

REFERENCES

1. H. N. Brown and R. A. Becker, Phys. Rev. 96, 1372 (1954).
2. M. H. Jorgensen, O.B.Nielsen and O.Skilbreid, Nucl.Phys. 84, 569 (1966).
3. B. Sethi and S. K. Mukherjee, Nucl.Phys. 85, 227 (1966).
4. B. P. Pathak and S. K. Mukherjee, to be published in Nucl.Phys.
5. D. . Boneau and E. N. Hatch, Phys. 115A (1959)235.
6. A. G. da Silva, R. H. Topke, S. de Barros and Calzavara, Notas Fis. Centro Brasil Pesquisas Fis. 14, 226 (1968).
7. E. Steiner, P. Huber, W. Salathe and R. Wagner. Helv. Phys. Acta 43, 17(1970).

8. C.Ekstrom, T. Noreland, M.Olsmats and B.Wannberg, Nucl.Phys. A135, 289 (1969).

9. R. S. Hager and E. C. Seltzer, Nuclear Data A4(1968) No.1 & 2.

Table - I

Energies and relative intensities of X- and γ-rays from ^{164m} & ^{g}Ho.

Photon Energy (keV)	Relative intensity	Origin	α total [a)]	Transition intensity per 100 decays of ^{164m}Ho.
37.33	100	^{164m}Ho	8.1	100
45.21	310	Dy K_{α_2}		
46.00	570	Dy K_{α_1}		
46.70	230	Ho K_{α_2}		
47.55	420	Ho K_{α_1}		
49.13	34.7	Er K_{α_1}		
52.06	176	Dy K_{β_1}		
53.75	171	Dy K_{β_2} + Ho K_{β_1}		
55.37	38.7	Ho K_{β_2} + Er K_{β_1}		
56.64	48.1	^{164m}Ho	21.2 [b)]	117
73.40	35.1	^{164g}Ho	9.1	39
91.26	61.3	^{164g}Ho	4.2	35

a) Obtained from the approximate relation $\alpha_{total} \approx \alpha_K + 1.33\,\alpha_L$. The values of α_K and α_L are taken from ref[9].

b) Experimental value of α_K and the theoretical value of α_L have been used in finding the value of α_{total}.

DISCUSSION

P.N. Trehan: 1) How much accuracy you could attain in your intensity measurements of γ-rays. 2) What was the percentage error on your α_K values.

B.P. Pathak: 1) The gamma ray intensities reported in this work are subject to an error of about 5%. 2) The percentage error on the values of α_K obtained by us is approximately 10%.

MAGNETIC MOMENT OF THE 280 keV $5/2^-$ STATE OF ^{75}As

B.K. Sinha and R. Bhattacharyya
Saha Institute of Nuclear Physics, Calcutta-9

ABSTRACT

The magnetic moment of the 280 keV $5/2^-$ level of ^{75}As has been measured using a modified IRP method. This has resulted in a better accuracy of the measured value 10% compared to an accuracy of 20-30% as found in the published literatures.

DELAYED GAMMA-RAY EMISSION IN THE SPONTANEOUS FISSION OF ^{252}Cf

N.N. Ajitanand
Nuclear Physics Division
Bhabha Atomic Research Centre, Trombay, Bombay-85

I. INTRODUCTION

The bulk of the excitation energy of fragments formed in fission is given up in the form of neutrons and gamma rays emitted promptly i.e. within 10^{-11} seconds after the formation of the fragments. This leaves the fragments in various isomeric states from which they decay to their ground states by emission of the so-called delayed gamma-rays. The half-lives of these delayed gamma-rays ranges from a few nanoseconds to several microseconds[1-3].

Recently Guy[4] carried out a study of the delayed gamma-rays arising from various fragment masses in ^{252}Cf spontaneous fission. The present work also deals with a similar investigation but uses a very different experimental method and serves mainly as a check on the energies, half-lives and intensities of the long-lived gamma-rays reported by Guy.

II. EXPERIMENTAL PROCEDURE

A 10.7 C.C. ORTEC lithium drifted germanium detector was used to detect the gamma rays in coincidence with the fission fragments which were detected in a shallow argon-methane gas flow ionisation chamber, mounted on the face of the gamma ray detector to give a maximum possible detection efficiency as shown in fig. 1(a). The ^{252}Cf source had a spontaneous fission rate of 2.05 x 10^5 min^{-1}.

The electronics employed schematically is shown in fig. 1(b). The prompt gamma-rays were prevented from being recorded in the following way. The ionisation chamber had an efficiency of 95% so that almost every fission event caused the inhibit unit to be blocked for 300 nanosec. The width of the prompt gamma ray peak was only 55 nanosec. so that hardly any of these gamma rays were allowed through the inhibit unit. The pulses from the fission discriminator were given to the START input of the time-to-amplitude Converter (TAC) while the output of the inhibit unit went to the STOP input of the TAC. The output of the TAC and the linearly amplified gamma ray pulses were given to the two-parameter analyser of the PDP-7 on-line computer. The time parameter was divided into six equal intervals of 0.79 microsec each by means of digital windows and the delayed gamma-ray spectrum coming in coincidence with the TAC pulses were recorded in six corresponding regions of 1024 channels each. The typical coincidence count rate was 50 Sec^{-1} of which about 5% was due to chance coincidence. The lines arising from fission neutron bombardment of the gamma-ray detector were determined by using a 0.8 cm. thick lead absorber between the source and the detector.

III. RESULTS AND DISCUSSION

The data was analysed on an IBM 360 Computer. A least squares smoothing programme was utilised to remove the background continuum from each of the six spectra. The peak intensities were determined simply by adding up the counts in each peak. A simple exponential fitting programme was then used to determine the half-lives of the various decaying gamma-ray lines. The yields for the various gamma

rays were calculated from the gamma detection efficiency, total number of fission events and the half-lives.

Shown in Table I. are the energies, half-lives and intensities averaged over the results obtained for the four experimental runs and compared with the results of Guy[4]. The intensities have been normalised so as to obtain agreement for the 131.1 keV line. The energies agree with one percent and the half-lives within ten percent in most cases. The intensities are of the same order of magnitude.

In his work Guy has reported a number of delayed gamma rays of very low intensities. Of these only the 169.8 and 225.7 keV lines could be resolved in the present experiment, presumably due to lack of fragment mass identification. In addition, Guy has also obtained 86.3, 153.6 and 197.3 keV lines with half-lives 149, 110 and 2800 nanoseconds respectively and fairly high intensities (60 x 10^{-4} photons per fission). These lines have also been identified in the present experiment although the data did not permit a proper analysis of intensities and half-lives. The present data indicated the presence of some very long lived components (· 10 microseconds half-life) with energies of 276, 281 and 294 keV respectively.

The author is very grateful to Dr.J.W. Boldeman and Mr.R.L. Walsh for helpful discussions and to the Physics Division of the A.A.E.C. for providing experimental facilities.

REFERENCES

1. S.A.E. Johansson, Nucl. Phys. 64, 147 (1965)
2. L.A. Popeko et.al., Nucl. Energy 20, 611 (1968)
3. R.B.Walton and R.E. Sund, Phys. Rev. 178, 1894 (1969)
4. F.W.Guy, Delayed Gamma-Rays from ^{252}Cf, UCLA (

TABLE I

Energy (keV) (resolution 3 keV)		Half-life (nanoseconds)		Intensity (Number per 10^{-4} fission)	
Present Expt.	Ref. 6	Present Expt.	Ref. 6	Present Expt.	Ref. 6
66.2	66.2	200	140 ± 14		60 ± 6
96.7	96.2	600 ± 20	550 ± 40	74 ± 4	80 ± 7
115.2	115.0	250	162 ± 12		61 ± 4
122.4	121.4	2240 ± 700	360 ± 36	12 ± 5	48 ± 5
131.1	129.8	370 ± 30	340 ± 50	29 ± 2	29 ± 4
142.2	141.7	690 ± 130	2400 ± 140	3 ± 1	9 ± 1
172.1	170.5	1570 ± 250	1100 ± 220	8 ± 1	20 ± 4
192.9	191.6	1800 ± 210	850 ± 140	13 ± 2	14 ± 3
205.5	204.0	4000	3000		
326.7	324.5	630 ± 50	570 ± 50	25 ± 2	31 ± 3
383.5	380.7	3380 ± 350	3400 ± 270	39 ± 9	73 ± 6

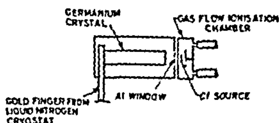


FIG 1(a)

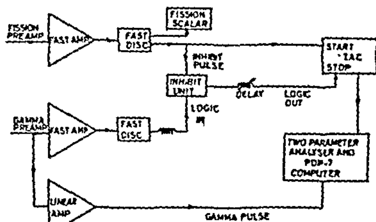


FIG 1(b)

DISCUSSION

C.V.K. Baba: Do you know the nucleus which gives rise to any of these transitions?

N.N. Ajitanand: The present experiment does not determine the masses associated with the various gamma-ray lines. However, Guy[6] has been able to identify the emitting fragment masses and has listed them in a table.

$L/_K$ CAPTURE RATIO FROM Ge(Li) SPECTRUM

B. K. Dasmahapatra
Saha Institute of Nuclear Physics, Calcutta-9

I. *INTRODUCTION*

Until now the methods developed for the determination of $L/_K$ electron capture ratio, adopt either the comparison of the relative intensities of the K- and L-x-rays or the coincidence of the K-X-rays with cascade gamma quantum in the decay scheme. While the first method has limited sphere of application, the second method with many modified techniques has been used extensively for the measurement of the capture ratios. The method however cannot be regarded as the most reliable one. Thus considering the decay of ^{133}Ba, the L/K ratio determined by this method varies in a wide range(1-7).

The purpose of the present investigation was to avoid the coincidence technique completely, as it appears that the inconsistency among the different work might be due to the inherent difficulties in the technique itself. The present method uses the decay scheme of the nucleus under investigation; measurement of the intensity of the K-X-rays relative to the cascade γ-ray yields the capture ratio in a very straight forward way as will be seen in section II.

As a test, the method has been applied to the decay of ^{133}Ba. The observed value 1.42 ± ^ differs from the works done recently(5-7)

II. PRINCIPLE OF THE METHOD

Considering the decay scheme of ^{133}Ba, if I_K and I_L be the intensities of the total K and L electrons capture respectively, then

$$I_K + I_L = I_{81}(1+\alpha_T^{81}) + I_{384}(1+\alpha_T^{384}) + I_{160}(1+\alpha_T^{160} ...$$

where I_{81} etc. are the gamma intensities and α_T are the total internal conversion coefficients. Use of the α_T values from (3,8) and relative intensities of gamma rays from (8) gives

$$I_K + I_L = I_{81}(2.90 \pm 0.06) \quad ..(1)$$

Let $I_{K\alpha}$ and $I_{K\beta}$ be the relative intensities of the K_α- and K_β- X-rays, then

$$I_{K\alpha} + I_{K\beta} = \omega_K [I_K + \alpha_K^{53} I_{53} + \alpha_K^{80} I_{80} + \alpha_K^{81} I_{81} + ...$$

where ω_K is the K flourescence yield in Cs. Neglecting the contribution from high energy transitions,

$$I_{K\alpha} + I_{K\beta} = \omega_K [I_K + I_{81}(1.78 \pm 0.06)] \quad .(2)$$

From the equations (1) and (2),

$$I_L/I_K = \frac{2.90 \pm 0.06}{\frac{I_{K\alpha}+I_{K\beta}}{\omega_K I_{81}} - (1.78 \pm 0.06)} - 1$$

$$= \frac{2.90 \pm 0.06}{(f_{K\beta}\, I_{K\beta}/\omega_K I_{81}) - (1.78 \pm 0.06)} - 1 \quad --(3)$$

where $f_{K\beta} = (I_{K\alpha}+I_{K\beta})/I_{K\beta}$, relative X-ray transition probabilities to the K shell, known accurately[9]. ω_K values are also known and can be used from (10).

For the present nucleus ^{133}Ba, however, the knowledge of ω_k is not necessary. If one uses a ^{137}Cs source for calibrating the efficiency in the K-X-ray region then the equation (3) becomes

$$I_L/I_K = \frac{2.90 \pm 0.06}{\dfrac{A_{K\beta}\, A_{661}\, \epsilon_{81}\, \alpha_K^{661}}{A_{81}\, A'_{K\beta}\, \epsilon_{661}} - (1.78 \pm 0.06)} - 1 \quad ..(4)$$

Where $A_{K\beta}$, A_{81} refer to the areas under the peaks K_β -X-ray and 81 KeV gamma-ray in the decay of ^{133}Ba, and $A'_{K\beta}$, A_{661} refer to the areas under the peaks K_β -X-ray and 661 KeV γ -ray in the decay of ^{137}Cs. ϵ_{81}, ϵ_{661} refer to the detector efficiencies for the respective transitions.

III. EXPERIMENT AND RESULTS

A 2 c.c. ORTEC Ge(Li) detector with a Laben 4096 channel Analyser have been used for the analysis of the spectra. The efficiency curve for the detector has been plotted by taking the standard intensity values of 152 (11) and ^{133}Ba (8). The curve has been extended to the low energy region by the determination of the efficiency of the detector for the K_β (34.7 KeV) X-ray. Taking the α_K value for the 661 KeV γ -ray as 0.093 (10), equation(4) reads I_L/I_K = 1.42 ± 0.13

Recent determinations of the L/K capture ratio for the decay of ^{133}Ba yield 0.37 - 0.38 (5-7). The value 1.42 ± 0.13 determined by us differs appreciably from the above wark .

The large difference in the L/K capture ratios between the three recent work and the present experiment is very difficult to explain. In view of the rather accurate determination of the K_β intensity in the present investigation, the major source of error is probably the decay scheme we have used. More work along this line will be worthwhile.

REFERENCES

1. R. K. Gupta et al — Nuovocemento 8,48(1958)
2. M. K. Ramaswamy et al — Nucl.Phys.19, 299(1960)
3. J. E. Thun et al — Nucl.Phys.88 ,289(1966)
4. M.McDonnel and M. K. Ramaswamy — Phys.Rev.168 1393(1968)
5. G. Schulz — Zeit.Phys 203,289(1967)
6. V.Narang and H.Houtermans. — Proc.Conf.EC and higher order processes in Nuclear Decays.Debreeen Hungary,p. 97 (1968).
7. S.Tornkvist and S. Strom — Arkiv For Fysik 38,261 (1968)
8. H. E. Bosch et al — Nucl.Phys.A108,209(1968)
9. J. S. Hansen et al — Nucl.Phys A142,604(1970)
10. C. M. Lederer et al — Table of Isotopes,6th. ed. (1967)
11. P. Mukherjee and A. K. Sengupta — Nucl.Instr.Meth.68,165 (1969).

FURTHER STUDIES OF K X-RAY EMISSION FROM ^{252}Cf FRAGMENTS

S.S. Kapoor, D.M. Nadkarni, S.R.S. Murthy,
V.S. Ramamurthy and P.N. Rama Rao
Nuclear Physics Division
Bhabha Atomic Research Centre, Bombay-85

INTRODUCTION

For a detailed understanding of K X-ray emission in fission, it is important to investigate the shape of the K X-ray emission distribution function $f(n)$, where $f(n)$ represents the fraction of events in which n K x-rays are emitted from individual fragment nuclei via internal conversion process during the cascade γ deexcitations. In this work K X-ray emission from ^{252}Cf fission fragments has been studied to determine for specified fragment charges (a) the average K X-ray yields per fission emitted in a time region of upto 110 nsec and upto 1000 nsec after fission, (b) the first moment ($\overline{n}$) and the second moment ($\overline{n^2}$) of the function $f(n)$ and (c) whether the average X-ray yield from fragments of specified ch charge $Z_L(Z_H)$ is altered if only those fission events are selected in which the complementary fragment $Z_H(Z_L)$ has emitted a K X-ray.

EXPERIMENTAL METHOD AND ANALYSIS

The fission fragments from the ^{252}Cf source were detected in 2π geometry by a parallel plate mini-ionization chamber filled with pure Argon gas and operated with an electric field of 1 KV/cm. A ^{252}Cf source of strength about 5×10^5 fissions per minute coated on a nickel backing formed the cathode of the ionization

chamber, which had thin perspex windows. The energies of the X-rays were measured by two cooled Si(Li) detectors, A and B, each of size 1 cm^2 x 0.3 cm placed at a distance of about 2.0 cms on either side of the source foil. The energy resolutions of the X-ray spectrometers A and B, interms of the FWHM of 26.25 keV line of ^{241}Am were 0.8 keV and 1.0 keV respectively. The pulses from the ion-chamber and the X-ray detectors were amplified and fed to discriminators to cut off the natural alpha pulses and noise pulses respectively. The outputs of the discriminators were fed to two double coincidence and a triple coincidence units ($2\tau \approx 1\mu sec$). The double coincidence spectrum was also seperately recorded on an analyser for 2τ = 110 nsec. The triple coincidence pulses (E_{XA} E_{XB} F) and the double coincidence pulses ($E_{XA}F$, $E_{XB}F$), after suitably scaling down, gated the 4-parameter system through an OR gate. The outputs from the fission fragment detector and the two X-ray detectors were fed to the three ADC's of the system. The data were punched, event by event, on a paper tape.

The recorded data were analysed to obtain the following spedtra: (i) the independent energy spectra of K x-rays detected in A- and B- systems [$N_A(E)$ & $N_B(E)$] , (ii) the energy spectra $N_A^L(E)$, $N_A^H(E)$ and $N_A^C(E)$ of K X-rays detected in system A for the triple coincidence events for those cases in which the photons detected in the system B belong to the energy regions of the light fragment K X-rays (10-24 keV) heavy fragment K X-rays (24-50 keV) and compton scattered gamma rays

of 50-60 keV, respectively. A typical K X-ray spectrum $\{N_A(E)\}$ is shown in Fig.1. Using a least square fitting code[1] all the spectra were analysed to determine the K X-ray yields per fission from fragments of specified Z. The compton scattered gamma ray backgrounds, detector efficiencies, and X-ray transmissions were appropriately taken into account in the analysis.

Fig.2 shows the observed K X-ray intensities per fission versus Z_H for time ranges of 0-110 nsec and 110-1000 nsec. The presence of a predominantly delayed *component is observed for* $_{52}Te$. *The K X-ray yield per* fragment obtained ~~from Fig.2~~ and using calculated fragment charge yield[2] is shown in Fig.3. It is found that in heavy fragment regions (Z = 51-57) the X-ray yield from odd Z fragments is significantly higher than that from even Z fragment nuclei, and the yield increases in the deformed $N \gtrsim 88$ region. The results are attributed to lower level spacings for odd Z nuclei in the undeformed region and for all nuclei in the deformed region. From the analysis of triple and double coincidence data, the K X-ray yield per fragment for specified Z was also determined for those cases in which the *same fragment* is known to have already emitted one K X-ray. From these results, also shown in Fig.3, it is concluded that for almost all fragment charges the second X-ray emission probability is significantly large implying that X-ray emission is, in general, a cascade process. This cascade X-ray emission is particularly predominant for odd Z heavy fragments (53, 55, 57) and for all fragments in the *deformed region*

For these cases the additional number of K X-rays per fragment is more than one, showing that the cascade may contain more than two K X-rays from each of these fragment nuclei. These results can be expressed in terms of the second moment $\overline{n^2}$ of the X-ray distribution function $f(n)$ which is related to the measured quantities by the expression,

$$\overline{n^2(Z_H)} = \overline{n(Z_H)} \left[\frac{\nu_{xH}}{\eta(Z_H)} \frac{Y_x^{H_x}(Z_H)}{Y_x(Z_H)} + 1 \right]$$

where Y_x and $Y_x^{H_x}$ are the unbiased X-ray yields per fission and the X-ray yields per fission when one X-ray from the same fragment is already detected in detector B respectively. Here ν_{xH} represents the total number of heavy fragment K X-rays per fission detected in detector B and $\eta(Z_H)$ is the efficiency of detection in detector B of X-rays emitted from charge Z_H. $\overline{n(Z_H)}$ is the unbiased K X-ray yield per fragment from Z_H. A similar expression was used for $\overline{n^2(Z_L)}$. The values of $n^2(Z)$ thus obtained are shown in Fig.4, where it can be seen that the large multiciplity of X-ray emission is less probable for the light fragment groups as compared to that from the heavy group. In particular for $Z = 53,55,57$ $\overline{n^2}$ is about 1 and for $Z \gtrsim 59$ $(N > 88)$, $\overline{n^2}$ is nearly 2, showing significantly large probability for multiple X-ray emission in these cases.

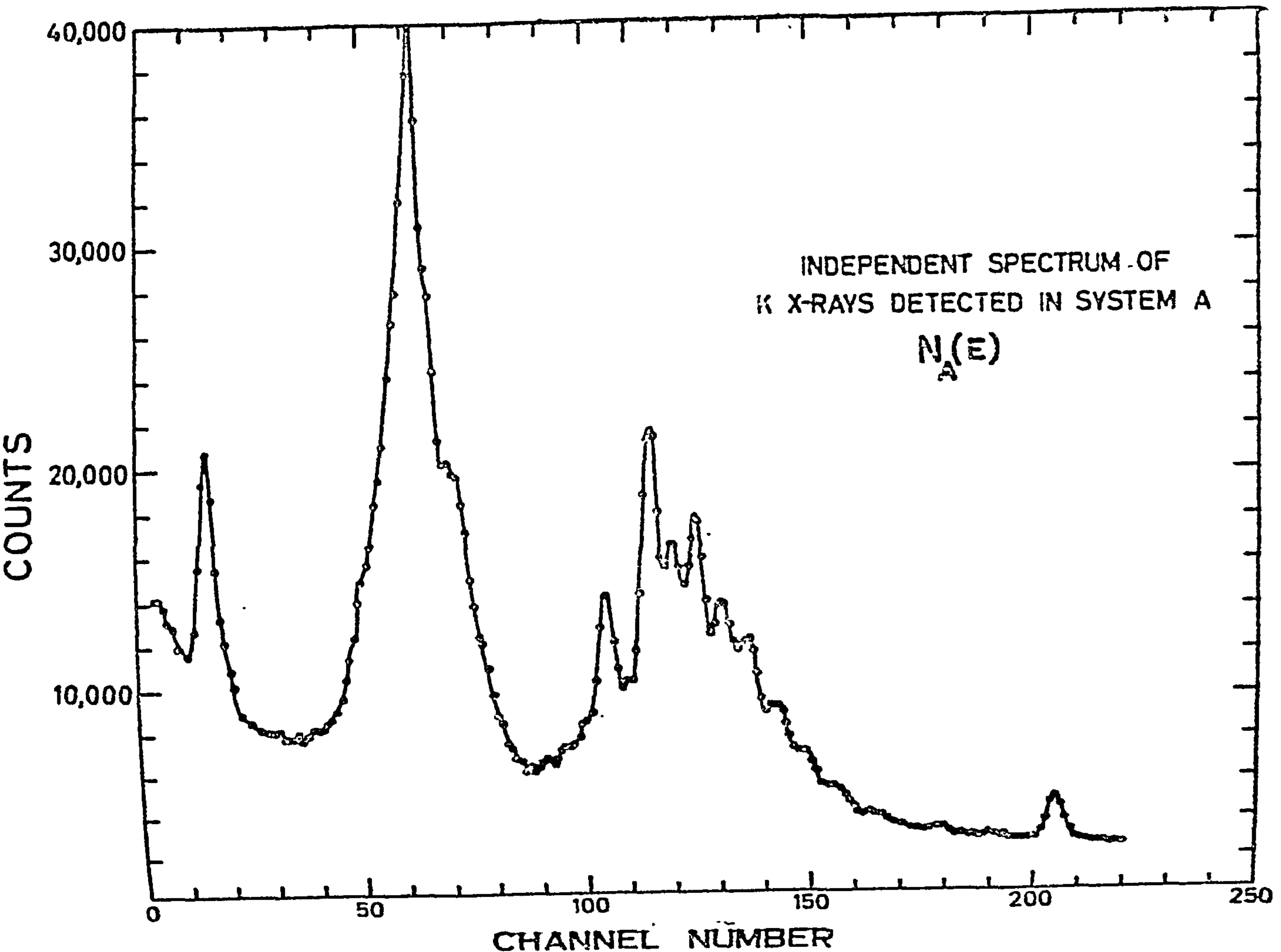
In Fig.5, we have shown $K^H(Z_L)$ $\{K^L(Z_H)\}$ versus (Z_L, Z_H), where $K^H(Z_L)$ represents the probability of enhancement (or decrease) of X-ray emission from charge $Z_L(Z_H)$ when the complementary charge $Z_H(Z_L)$ has

necessarily emitted a K X-ray. The observed value of K different from unity is interpreted as follows: The K X-ray emission probability from fragment charge $Z_L(Z_H)$ varies with the isotopic composition. This leads to a distribution of isotopes for the complementary charge $Z_H(Z_L)$ different from normal in those cases where an X-ray is known to have been emitted from $Z_L(Z_H)$, leading to a value of K different from unity. One possibility in this connection is the presence of odd-even effect on X-ray yields with respect to neutron number for a specified Z. If however, X-ray yields are assumed to vary smoothly with neutron number, the observed value of $K > 1$ in some cases shows that the variation of X-ray yields with respect to neutron number N in these cases has an opposite behaviour for complementary charges in the light and the heavy groups. It may be remarked that the neutron shell $N = 82$ could give rise to this trend. Further, the presence of a genuine correlation in X-ray emission from pair fragments due to the common conditions existing at scission cannot be excluded.

REFERENCES

1. S.K. Kataria, S.S. Kapoor, S.R.S. Murthy and P.N. Rama Rao, Nuclear Physics A154, 458 (1970).

2. R.L. Watson, H.R. Bowman and S.G. Thompson, Phys. Rev. 162, 1169 (1967).


INDEPENDENT SPECTRUM OF
K X-RAYS DETECTED IN SYSTEM A
$N_A(E)$
COUNTS
40,000
30,000
20,000
10,000
CHANNEL NUMBER
0
50
100
150
200
250

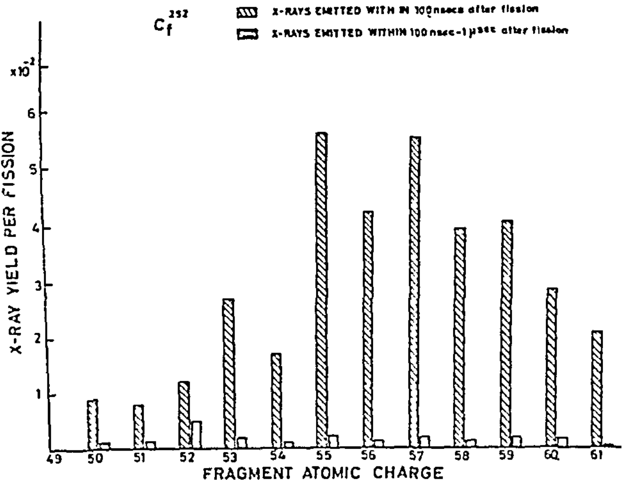

C_f^{252}
X-RAYS EMITTED WITH IN 100nsec after fission
X-RAYS EMITTED WITHIN 100nsec-1μsec after fission
X-RAY YIELD PER FISSION
x10⁻²
1 2 3 4 5 6
49 50 51 52 53 54 55 56 57 58 59 60 61
FRAGMENT ATOMIC CHARGE

FIG. 2

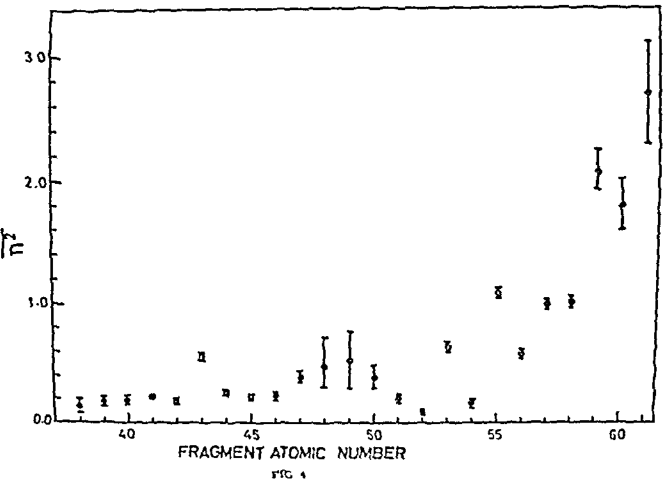


FIG 4

DISCUSSION

P.N. Trehan: Can you explain theoretically the emission of two or three K X-rays from fission fragments.

D.M. Nadkarni: Yes. The same fragment nucleus can emit two or more K X-rays during the γ-deexcitation due to the possibility of internal conversion taking place for each of these transitions. Here we should remember that the vacancy of the K shell is filled in a time of about 10^{-14} sec which is in general, considerably shorter than the half life of the nuclear states undergoing deexcitation.

THE DECAY OF ^{126}I

K. S. N. Murty, B. P. Pathak and M. L. Chatterjee
Saha Institute of Nuclear Physics, Calcutta-9

I. INTRODUCTION

The present work has been undertaken with a view to search for high energy gamma rays in the decay of 13d ^{126}I whose presence indicates levels in ^{126}Te higher than 1425 keV which is the highest level reported by Lagrange et al[1]. The existence of higher levels is possible because the disintegration energy for the β^+ decay of ^{126}I to ^{126}Te is 2150 keV[2]. During the course of the present work, a paper appeared[3] on the decay of ^{126}I. Our results agree with those obtained by these workers.

II. EXPERIMENTAL

The ^{126}I source was produced by fast neutron irradiation of analytically pure ammonium iodide. The cross section for the ^{127}I (n, 2n) reaction being much larger than the cross sections for other [(n, p), (n, α)] reactions, the production of interfering activities is negligible.

Gamma spectra were studied with a 2.5 c.c. Ge(Li) detector in conjunction with a 4096 channel analyzer. The resolution (FWHM) of the system was 3 keV at 1330 keV. The energies and relative intensities of gamma rays are given in Table I. Gamma spectra were also studied with a 3" x 3" NaI(Tl) detector and a 512-channel analyzer.

This confirmed the existence of 2044 keV gamma ray which is too weak to be distinctly seen by means of small volume Ge(Li) detector.

Gamma-gamma coincidence studies were made by using two NaI(Tl) detectors, one of 3" x 3" and the other 2" x 2". Gamma spectra were recorded in coincidence with 388 and 666 keV gamma rays. A weak peak at 1380 keV was observed in the latter spectrum.

III. RESULTS

Our studies confirm the existence of excited levels in ^{126}Te at energies 666.6, 1420.1 and 2044 keV. The existence of the 2044 keV level is suggested by the appearance of a weak line at 1380 keV in the gamma spectrum recorded in coincidence with the 666 keV gamma ray. This result is in agreement with the one obtained by Singh and Taylor[3].

TABLE I

Energies and relative intensities of gamma rays observed in the decay of ^{126}I

Energy (keV)	Relative Intensity	Energy (keV)	Relative Intensity
388.4 ± 0.3	100 ± 5	753.9 ± 0.4	12.3 ± 1
491.3 ± 0.4	8.1 ± 0.7	879.9 ± 0.4	2.2 ± 0.2
511.0	5.6 ± 0.5	1378	(Weak)
666.6 ± 0.4	98 ± 5	1420.1 ± 0.5	0.82 ± 0.2
		2050	(Weak)

REFERENCES

1) J. M. Lagrange et al., Ann. de Phys. 2, 141 (1967).

2) C. M. Lederer, J. M. Hollander and I. Perlman, Table of Isotopes, John Wiley and Sons, (1967).

3) B. Singh and H. W. Taylor, Nucl. Phys. A147, 12 (1970).

DECAY OF ^{68g}Cu (30 sec) and ^{68m}Cu (3.75 min)

V. K., Tikku, H. Singh and B. Sethi,
Saha Institute of Nuclear Physics, Calcutta-9.

INTRODUCTION

The levels in ^{68}Zn have been studied with NaI(Tl)[1] and Ge(Li)[2] detectors by the radioactive decay of ^{68}Cu and ^{68}Ga. Recently ^{68}Cu decay studies were taken up by Ward et al[3] who reported a new activity of 3.8 min. which they assigned to an isomer of ^{68}Cu. There is no published report on the decay scheme of the isomer of ^{68}Cu.

EXPERIMENTAL

The nuclide ^{68}Cu was produced by the fast neutron bombardment of enriched ^{68}Zn as well as specpure ZnO. Apart from ^{68}Cu activities, radioactive nuclides such as ^{63}Zn (38.3 min.), ^{66}Cu (5.1 min.) and ^{65}Ni (2.56 h) were also produced. The decay of the activated enriched ^{68}Zn was followed in an end-window G.M. counter and after subtracting the longer lived components, two activities of 30 sec and (3.75 $\pm$ 0.05) min. were noticed.

The γ-radiations from ZnO bombarded with fast neutrons were recorded on ND 512 channel analyzer using 2.00 cc Ge(Li) detector. The radioactive sources were obtained by bombarding specpure ZnO with fast neutrons. Each time a fresh sample was obtained. The γ-rays of the following energies (intensities) were obtained. 84.6 (95 $\pm$ 5), 110.4 (24.5), 525.7 (100), 577.6 (2.9), 635.9 (15.7), 805.7 (3.0), 1077.7 (82.4), 1260.5 (21.5), 1237.7 (17.9), 1744.9 (1.9), 1883.6 (1.0) keV.

record the decay of the γ-rays, eight consecutive γ-spectra were recorded on 4096 channel analyzer using 2.5 cc Ge(Li) detector. It was noticed that the 84.6, 110.4, 525.7, 635.9 keV γ-rays follow a single half-life of 3.75 min whereas the 1077.7 and 1260.5 keV γ-rays have two half lives, decaying faster in the beginning and ultimately following the 3.75 min half-life.

The beta spectra were recorded with 2 in. dia x 2 in long plastic scintillator using irradiated enriched ^{68}Zn. Four spectra were recorded successively in 128 channels of ND 512 channel analyzer. The Fermi-Kurie plot of the beta spectrum yields four groups of end point energies 4.60, 3.51, 2.70 and 2.26 MeV. The 4.60 MeV group was not seen by the previous workers except Ward et al[3]. The intensity of the group obtained in the present work is 35 %.

In an experiment, the beta activity was fully absorbed upto 3.5 MeV and the decay of the 4.60 MeV group was followed in the end window G.M. counter. The resultant decay curve exhibits two half-lives, 30 sec. for the early part and it follows 3.75 min half-life later on.

To see if the 3.75 min half-life belongs to an isomer of ^{68}Cu, enriched ^{71}Ga was bombarded with fast neutrons and the γ-spectra recorded an Ge(Li) detector. The 84.6, 110.4, 525.7 and 635.9 keV γ-rays were observed. The relative intensities of these γ-rays were observed to be same order as from the fast neutron irradiated ^{68}Zn.

The 577.6, 805.7, 1077.7, 1260.5, 1744.9 and 1883.6 keV γ-rays can be assigned to the unique γ-transitions from the excited levels in ^{68}Zn. The 84.6, 110.4, 525.7 and 635.9 keV γ-rays are assigned to the isomer of ^{68}Cu in agreement with Ward et al[3].

In order to establish the relationship between the γ-rays assigned to the isomer and the well known γ-rays of the decay of 30 sec ^{68}Cu, β-γ and γ-γ coincidence experiments were performed. With gate on integral betas above 100 keV, the γ-rays assigned to the isomer were absent in the coincident γ-spectrum and these γ-rays were seen to be mutually coincident in the γ-γ coincidence experiment. The 84.6 keV γ-ray was not seen to be coincident with any β group in agreement with Ward et al[3]. The coincidence experiments suggest that the isomer state populates the ground state of ^{68}Cu. The fact the well known γ-rays of 30 sec ^{68}Cu follow a composite half-lives supplements the conclusion.

The isomeric cross-section for the yield of ^{68m}Cu and ^{68g}Cu was calculated by studying the decay of the β-ray intensity in an end window G.M. counter and using the equations[4] we obtain $\sigma_m / \sigma_g = 0.7 \pm 0.2$

The ^{68}Zn (n, p) ^{68m}Cu cross-section was determined by comparing the total counts under the 525.9 keV photopeak from ^{68m}Cu and the 1038.69 keV photopeak from ^{66}Cu. The value of (100 ± 17) m b was used for ^{66}Zn (n, p) cross-section[6]. The ^{68}Zn (n, p) ^{68m}Cu cross-section was found to be (4.5 ± 0.8) m b

$\sigma_g = (6.5 \pm 1.3)$ m b and thus $\sigma_{total} = (11 \pm 2)$ m b.

DECAY SCHEME AND DISCUSSION

The decay scheme of ^{68m}Cu and ^{68g}Cu consistent with the experimental observation is given in Fig.

The 4.6 MeV β group observed in the present studies as also by Ward et al[3] can best represent the 30 sec ^{68g}Cu decay to the ^{68}Zn ground state. This implies that the most probable spin of ^{68g}Cu is 1^+.

It is reasonable to describe ^{68}Cu by shell model. The model assigns the 29th proton 2p 3/2 orbit and 2p 1/2 orbit to the 39th neutron. Nordheim strong rule gives 1^+ spin parity value for the ground state of ^{68}Cu in agreement with the experimental observation. Since the isomer is found to exist, it can be explained as arising from the coupling of 2p 3/2 proton to the 1g 9/2 1f 5/2 hole for the neutron and this gives spin parity values of 6^- or 3^- from the Nordheim weak rule or 4^- according Brenen steim rule for particle-hole coupling.

The 84.6, 524.9 and 110.4 keV γ-rays form a cascade between the excited states of ^{68}Cu at 110.4, 655.2 and 720.1 keV. The 110.4 keV is the isomeric ~~state~~ transition. The relative intensities of the 84.6 and 524.9 keV γ-rays are equal within the limits of experimental uncertainties. This supports the cascade nature of these γ-rays.

REFERENCES

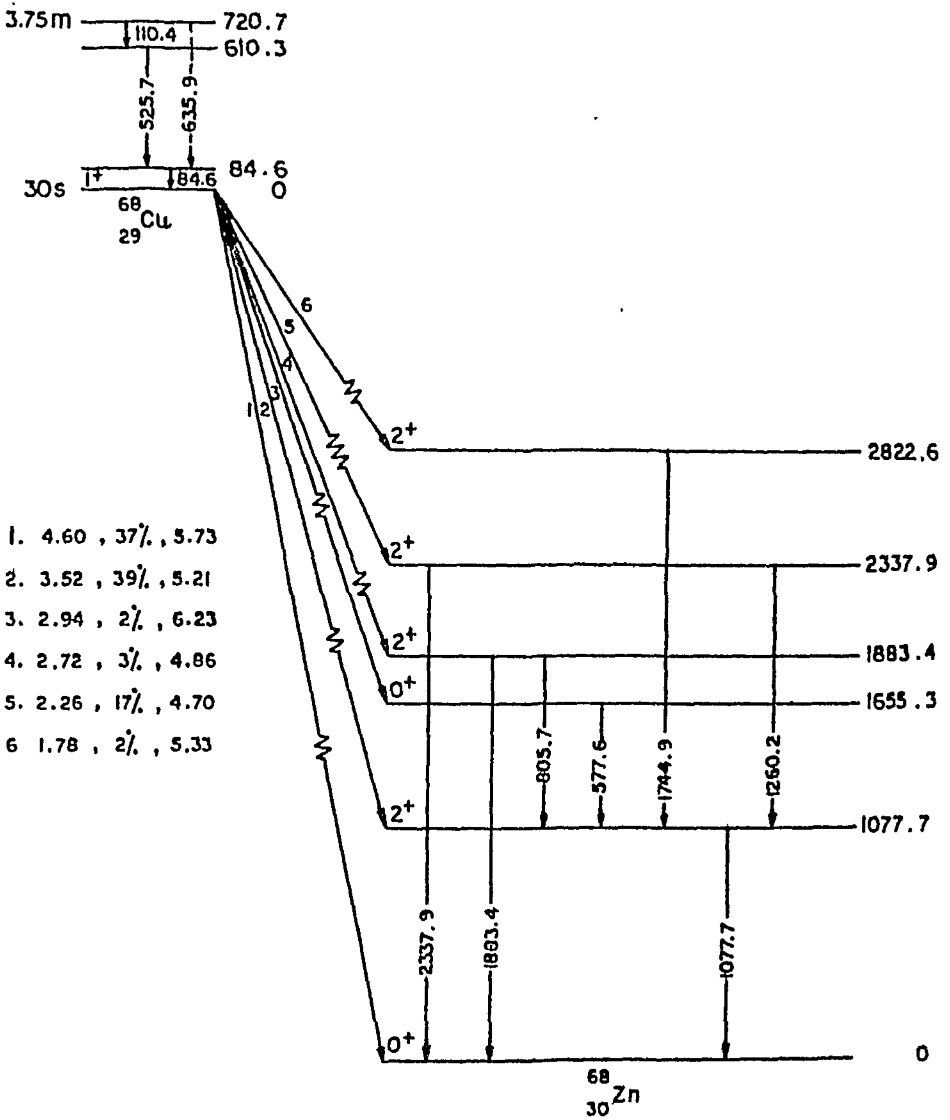
1. H. Bakhru and S. K. Mukherjee, Nucl. Phys., 52 (1964) 125

2. K. Vaughan, A. H. Sher and B. D. Pate, Nucl. Phys., A132 (1969) 561

3. T. E. Ward, H. Ihochi and J. L. Meason, Phys. Rev., - 183 (1969)/802

4. U. Kneissl, H. Schneider, R. Volpel and K. Wolcken, Nucl. Phys., A135 (1969) 395

5. A. S. Gillespie, Jr. and W. W. Hill, Nucleonics, November, 1961.



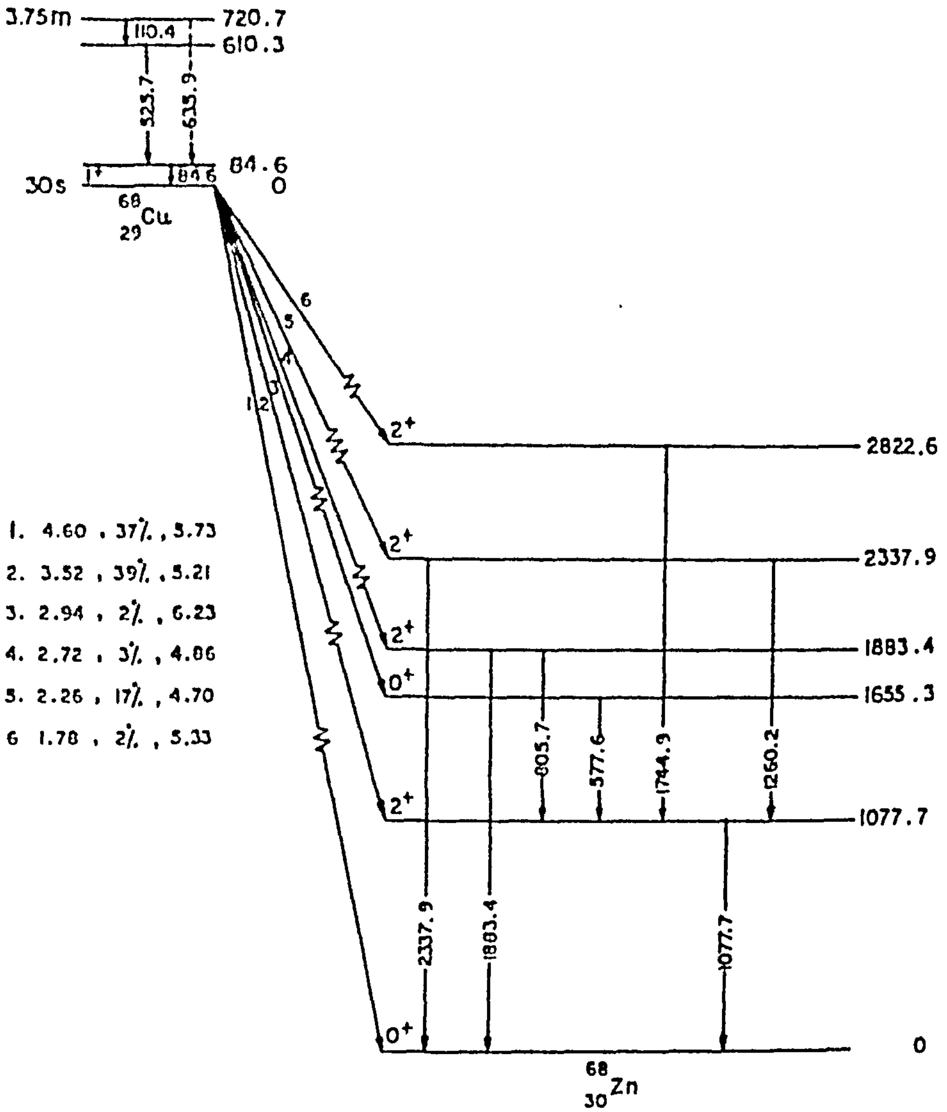
3.75m
720.7
110.4
610.3
525.7
635.9
1+
84.6
84.6
30s
0
68
29 Cu
6
5
4
3
1
2
2+
2822.6
1. 4.60 , 37% , 5.73
2. 3.52 , 39% , 5.21
3. 2.94 , 2% , 6.23
4. 2.72 , 3% , 4.86
5. 2.26 , 17% , 4.70
6 1.78 , 2% , 5.33
2+
2337.9
2+
1883.4
0+
1655.3
805.7
577.6
1744.9
1260.2
2+
1077.7
2337.9
1883.4
1077.7
0+
0
68
30 Zn

HALF-LIFE OF 687.42 keV LEVEL AND ENERGY LEVELS IN ^{147}Pm

H. Singh and B. Sethi,
Saha Institute of Nuclear Physics, Calcutta-9.

The half-life of the 687.42 keV level in ^{147}Pm is measured for the first time using a conventional delayed coincidence set up incorporating an ORTEC time-to-amplitude converter (Model 263) and a 512 channel analyzer (ND-120). The γ-spectra in the decay of ^{147}Nd was also taken on expanded scale (0.37 keV/channel) using Ge(Li) detector in order to look for some uncertain weak transitions.

The half-life was measured by recording time delay between the 233 keV β group feeding the level and the 687.42 keV γ-ray. The β and γ-rays were detected with NE 810 and NE 102A plastic scintillators optically coupled to RCA 7850 photomultipliers and the corresponding channels were set to accept energy intervals of 160-200 keV and 690-770 keV respectively. The prompt time resolution curve for comparison was recorded with a ^{60}Co source. The delayed and the prompt sources were recorded alternately in intervals of 30 min. each and were successively accumulated till a reasonable statistics was obtained. A series of independent measurements were made, changing the energy settings in the start channel, changing the set of coaxial cables introduced in the start and stop channels of TAC. The half-life computed from the moments of the delayed and the prompt curves (Fig.1), as a mean of the independent runs is (0.252 ± 0.100) nsec.

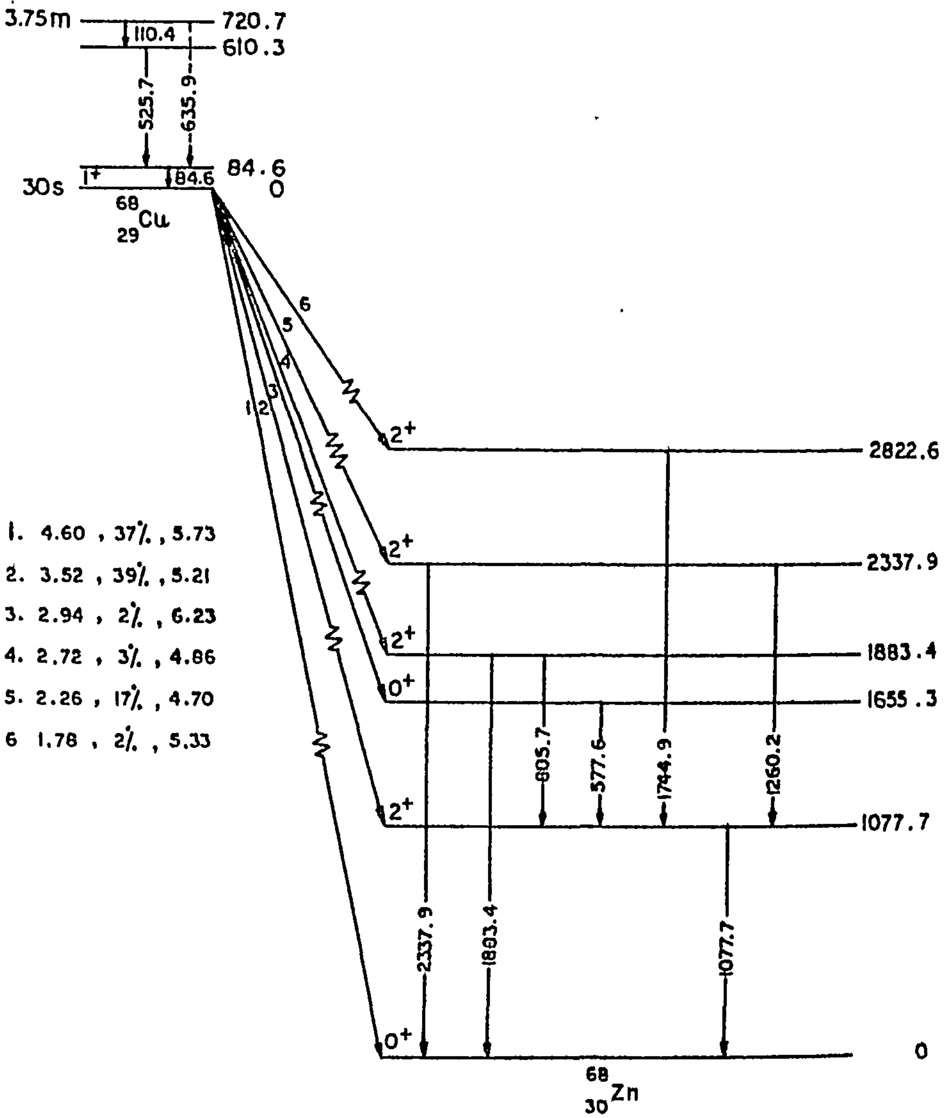

3.75m
720.7
110.4
610.3
523.7
635.9
84.6
0
30s
1+
84.6
68
29 Cu
6
5
4
3
1 2
2+
2822.6
2+
2337.9
2+
1883.4
0+
1655.3
805.7
577.6
1744.9
1260.2
2+
1077.7
2337.9
1883.4
1077.7
0+
0
68
30 Zn
1. 4.60 , 37% , 5.73
2. 3.52 , 39% , 5.21
3. 2.94 , 2% , 6.23
4. 2.72 , 3% , 4.86
5. 2.26 , 17% , 4.70
6 1.78 , 2% , 5.33

HALF-LIFE OF 687.42 keV LEVEL AND ENERGY LEVELS IN ^{147}Pm

H. Singh and B. Sethi,
Saha Institute of Nuclear Physics, Calcutta-9.

The half-life of the 687.42 keV level in ^{147}Pm is measured for the first time using a conventional delayed coincidence set up incorporating an ORTEC time-to-amplitude convertor (Model 263) and a 512 channel analyser (ND-120). The γ-spectra in the decay of ^{147}Nd was also taken on expanded scale (0.37 keV/channel) using Ge(Li) detector in order to look for some uncertain weak transitions.

The half-life was measured by recording time delay between the 233 keV β group feeding the level and the 687.42 keV γ-ray. The β and γ-rays were detected with NE 810 and NE 102A plastic scintillators optically coupled to RCA 7850 photomultipliers and the corresponding channels were set to accept energy intervals of 180-200 keV and 690-770 keV respectively. The prompt time resolution curve for comparison was recorded with a ^{60}Co source. The delayed and the prompt sources were recorded alternately in intervals of 30 min. each and were successively accumulated till a reasonable statistics was obtained. A series of independent measurements were made, changing the energy settings in the start channel, changing the set of coaxial cables introduced in the start and stop channels of TAC. The half-life computed from the moments of the delayed and the prompt curves (Fig.1), as a mean of the independent runs is (0.252 $\pm$ 0.100) nsec.


3.75m
720.7
110.4
610.3
525.7
635.9
84.6
1+
84.6
30s
0
68
29 Cu
6
5
4
3
1 2
2+
2822.6
2+
2337.9
2+
1883.4
0+
1655.3
805.7
577.6
1744.9
1260.2
2+
1077.7
2337.9
1883.4
1077.7
0+
0
68
30 Zn
1. 4.60 , 37% , 5.73
2. 3.52 , 39% , 5.21
3. 2.94 , 2% , 6.23
4. 2.72 , 3% , 4.86
5. 2.26 , 17% , 4.70
6 1.78 , 2% , 5.33

HALF-LIFE OF 687.42 keV LEVEL AND ENERGY LEVELS IN ^{147}Pm

H. Singh and B. Sethi,
Saha Institute of Nuclear Physics, Calcutta-9.

The half-life of the 687.42 keV level in ^{147}Pm is measured for the first time using a conventional delayed coincidence set up incorporating an ORTEC time-to-amplitude converter (Model 263) and a 512 channel analyser (ND-120). The γ-spectra in the decay of ^{147}Nd was also taken on expanded scale (0.37 keV/channel) using Ge(Li) detector in order to look for some uncertain weak transitions.

The half-life was measured by recording [illegible] between the 233 keV β group feeding the level and the 687.42 keV γ-ray. The β and γ-rays were [illegible] NE 810 and NE 102A plastic scintillators [illegible] to RCA 7850 photomultipliers and the [illegible] were set to accept energy intervals of [illegible] and 690-770 keV respectively. The prompt [illegible] curve for comparison was recorded with a [illegible] The delayed and the prompt sources were [illegible]nately in intervals of 30 min. [illegible] accumulated till a reasonable [illegible] A series of independent measurements [illegible] the energy settings in the [illegible] set of coaxial cables introduced [illegible] channels of TAC. The [illegible] of the delayed and the prompt curve [illegible] of the independent [illegible]

In order to know the contribution due to the life time of the 531 keV level, spectral distributions expected of the 531- and 687 keV γ-rays were evaluated by extrapolation of the known spectral distributions in plastic of the 511- and 661 keV γ-rays from ^{22}Na and ^{137}Cs sources. From this information and from the knowledge of the threshold of the energy settings and width of the windows in PHA, it was estimated that the upper limit on the interference of the life time of the 531 keV level could be set at the best at 10%. As such no correction was applied. No interference is expected of the proposed level at 723.48 keV as the only transition of 312.57 keV from this level is biased off in the γ-counter settings. The possible interference from the level at 681.01 keV is negligible due to the weak transitions populating and depopulating it.

The γ-spectrum in the decay of ^{147}Nd was recorded with the help of 2.5 cc Ge(Li) detector and Laben 4096 channel analyzer. The resolution of the γ-spectrometer was 3 keV at 661 keV. New γ-rays of energies 299.65-, 312.57-, 589.98- and 680.78-keV were observed. The decay of these lines was followed for a period of over two months to ascertain their origin and were found to decay with 11 d half-life and thus assigned to ^{147}Pm. The decay scheme to ^{147}Pm was constructed from energy relationship among its transitions (Fig.2). The 589.98 and 680.78 keV γ-rays observed presently were reported earlier by Hill

et al[1] and pnly the former one by Backlin et al[2]. These γ-rays indicate a level at 681.01 keV. The 299.65, 312.57 keV γ-rays were not observed previously by these investigators using Ge(Li) detectors. In the present work a sum peak has been observed at 723.48 keV with the ^{147}Nd source on the top of Ge(Li) detector. It indicates the possibility of a 312.67-411.19 keV γ-γ cascade and a probable existence of a level at 723.48 keV in ^{147}Pm. The log ft values, the energies and the intensities of the β groups to the excited levels in ^{147}Pm were calculated from the corresponding γ-ray values. Except for the slight difference in the intensities of the groups to the levels at 91.03 and 531.94 keV there is a fair agreement with the earlier reports.

TRANSITION RATES

The nature of excitation can be learnt from the knowledge of transition rates. The rates for all the transitions from the 687.42 keV level calculated are compared to those of the Weisskopf estimate.

LEVEL ENERGY 687.42 keV

a) 687.42 keV transition b) 586.13 keV transition

$\delta = 0.82$; $\alpha_t = 0.0059$ $\delta = 0$; $\alpha_t = 0.008$

Retardation factor (F_W) = 2660 F_W = 8.8

Enhancement factor ($1/F_W$) = 2.90

c) 276.0 keV transition

$\delta = \infty$; $\alpha_t = 0.085$

$F_W = 99.7$

d) 197.14 keV transition

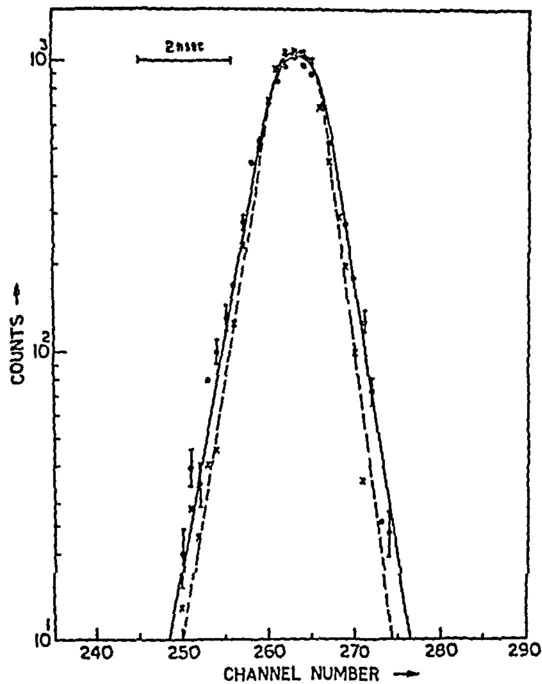
$\delta = 2.33$; $\alpha_t = 0.22$

$F_W = 35$; $1/F_W = 926$

REFERENCES

1) J. C. Hill and M. L. Weidenbeck, Nucl. Phys., A98 (1967) 519

2) A. Backlin and S. G. Malmskog, Arkiv Fysik 34 (1967) 459


2 nsec
COUNTS →
10^3
10^2
10^1
240
250
260
270
280
290
CHANNEL NUMBER →

DISINTEGRATION OF ^{65}Ga

D. Basu
Saha Institute of Nuclear Physics, Calcutta-9

I. INTRODUCTION

The most complete study of the decay of ^{65}Ga with a scintillation spectrometer was made by August and Friichtenicht[1] observing twenty-three gamma rays between 64 to 2330 keV. Li-Scholz and Bakhru[2] observed fifteen gamma rays upto 1414 keV with a Ge(Li) detector, presence of other gallium isotopes in their sample prevented the study of higher energy part of the spectrum. Balanda et al[3] studied the conversion electron spectrum and assigned spin parity to ground and first three excited states of ^{65}Zn. We produced the isotope in very pure state using separated isotope and reported[4] the preliminary results last year. Very recently Holmberg et al[5] reported twenty five gamma rays upto 2365 keV in the Ge(Li) spectra.

Although some twenty two excited states below 3 Mev are known in ^{65}Zn from stripping[6,7] and pick up[8] reactions only a few certain spin parity assignments could be made. Weidinger et al[9] measured the intensities and angular distributions of different neutron groups in ^{65}Cu (p, n) ^{65}Zn reaction using proton energies of 3.6, 4.06, 4.5 Mev and assigned spin parity values to all levels except two, within 1589 keV energy.

II. EXPERIMENTAL TECHNIQUE

Isotopes of zinc were separated in our electromagnetic isotope separator, and were collected in w

cooled copper box. Enriched ^{64}Zn isotope was separated chemically from copper and converted to oxide. Targets were made on aluminium backing and were bombarded with 3.8 Mev protons from our cyclotron. The beam strength was kept at 20-40 μA and the targets were cooled by running water. Each irradiation lasted about 30 mts after which zinc targets were removed from the chamber. Two targets were used alternately for bombardment and several irradiations were performed.

Gamma spectra were recorded using 2.5 cm^3 Ge(Li) detector with an energy resolution of 3 keV at Co^{60}. Spectra were recorded with a 4096 channel LABEN analyser. Spectra were taken in two sections each of 2048 channels, storing the data in the first section for first 15 mts and then in the second for the next 15 mts. This made it possible to follow the decay of each individual gamma giving a possible check against impurities. Standard sources were used for energy and efficiency calibration of the spectrometer.

III. RESULTS

Table I summarises the energies and intensities of gamma rays from the decay of ^{65}Ga. The energy values are accurate within 1 keV and the intensities are within 10 % error limits.

TABLE I. Energies and intensities of gamma rays from the decay of ^{65}Ga.

Energy keV	Relative Intensity	Energy keV	Relative Intensity	Energy keV	Relative Intensity
54		813	0.25	1353	1.31
61		856	0.30	1414	0.36
115	100	867	0.47	1468	0.19
153	15.28	910	1.03	1525	0.02
207	4.12	932	3.00	1750	0.02
654	1.55	1038	0.29	1870	0.01
660	0.60	1047	1.61	1876	0.01
703	0.30	1135	0.50	1962	0.23
715	0.31	1227	1.14	1969	0.27
752	13.4	1261	0.09	2218	0.42
769	1.84	1288	0.09		
796	0.33	1342	0.54		

A comparison with the results of Holmberg et al[5] reveals close agreement between their findings and those of ours. However, we observed new gamma rays at energies 660, 703, 813, 1038, 1288, 1525, 1750, 1870, 1876, 1962, 1969, 2218 and an indication at 1589 keV.

Out of the total thirtyfour gamma rays observed thirty have been fitted in the level scheme shown in Fig.1. Several of the new gammas clearly correspond to transitions from levels at 867, 910 and 1342 to lower states. Two new levels have been proposed at 2077 and 2084 keV to explain the pair of doublets 1870-76 and 1962-69.

Thanks are due to Prof. A. P. Patro for many helpful discussions.

REFERENCES

1) L. S. August and J. F. Friichtenicht, Phys. Rev., 120 (1960) 2072

2) Angela Li-Scholz and H. Bakhru, Phys. Rev., 168 (1968) 1193

3) A. Balanda et al., Acta Phys. Polon., 35 (1969) 301

4) D. Basu, Nuclear and Solid State Symposium, Roorkee (1969)

5) P. Holmberg et al., Acta Phys. Polon, B1 (1970) 59

6) D. Von Ehrenstein and J. P. Schiffer, Phys. Rev., 164 (1967) 1374

7) E. K. Lin and B. L. Cohen, Phys. Rev., 132 (1963) 2633

8) L. C. McIntyre, Phys. Rev., 152 (1966) 1013

9) A. Weidinger et al., Nucl. Phys., A149 No.2, (1970) 241

Fig.1. Decay scheme of 15 min ^{65}Ga.

DECAY OF ^{81m}Se (57 MIN) AND ^{81g}Se (18 MIN)

S. Venkata Ratnam, V. Lakshminarayana and K.L. Narasimham
Laboratories for Nuclear Research
Andhra University, Waltair
AND
M.V. Ramanaiah
Radiochemistry Division, Bhabha Atomic Research Centre,
Bombay.

I. INTRODUCTION

The levels of ^{81}Br were previously studied from the beta decay of ^{81}Se and coulomb excitation[1]. The references to the experimental studies on ^{81}Se decay are summarised in the article of Zoller[2] et al. Three groups have studied this decay with Ge(Li) detectors. Rao[3] et al reported gamma rays upto 829 keV, where as Prawirosoehardjo[4] observed several new transitions, including the newly seen decay of ^{81m}Se to 1146 keV level in ^{81}Br. He also proposed a new level at 815 keV. Zoller et alobtained results which differ from the above two studies. They did not record the 1146 keV transition and on the ohterhand found other gamma rays in ^{81m}Se decay. They also removed the level at 815 keV. The present study is undertaken in as much as there are considerable discrepancies in the above studies.

II. EXPERIMENTAL DETAILS

^{81}Se is produced by ^{80}Se(n,γ) reaction. Enriched samples were obtained from ORNL (as Se metal enriched to 89% in ^{80}Se) and irradiated with thermal neutron flux of 10^{13}n cm^{-2} sec^{-1}, in the research reactor CIRUS, BARC, Bombay. The irradiated samples were allowed to decay for about three hours during which the interfering ^{83}Se(25 Min) act[illegible]

decayed considerably. ^{75}Se is seen to be present, as the main contaminent. The gamma spectra recorded after this time are due to the ^{81}Se isomers in transient equilibrium. The gamma spectra were recorded with a Princeton 4 cm^2 x 5 cm Ge(Li) detector having an over all resolution of 4 keV. These spectra are taken at regular intervals to follow the decay of all the peaks in the gamma spectra. Several samples were bombarded for different intervals of time. This facilitated easy classification of the various transitions following the same half-life. Typical gamma spectra recorded with a 400 analyser are shown in Fig.1 and 2. The energies and relative intensities of the rays thus obtained in the ^{81}Se decay are given in Table 1 along with the results of Zoller et al.

III. RESULTS & DISCUSSION

The decay sbheme to account for the present spectra is shown in Fig.3. The main conclusions are given below:

1) The present study failed to record the 493, 767, 836 and 1146 keV gamma rays previously reported. 2) A weak gamma ray observed at 201 keV is incorporated in the decay scheme between the levels at 767 and 566 keV. 3) A weak gamma ray at 787 keV was reported in Ref.2, but could not be fitted i the decay scheme. This gamma ray is also observed in the present study and fitted between 1352 (newly introduced) ke level and 566 keV level. The new gamma at 1352 keV is the cross-over transition from this state. 4) A gamma ray of 815 keV is introduced to fit this in the level scheme.

5) The 275 keV gamma ray is associated with the decay of

^{81g}Se and is fitted between the 650 and 276 keV levels.
6) A gamma at 801 keV could not be fitted in the level scheme. It cannot however be associated with the decay of ^{83}Se as assigned by Zoller et al.

The beta feeding branches to the 1352 and 815 keV levels are estimated to be (0.056±0.010)% and (0.013±0.01)%. The corresponding log ft values are estimated to be 6.5 and 8.4 respectively. The character of ^{81m}Se is $7/2^+$ while the ground state of ^{81}Br is $3/2^-$. A log ft of 6.5 for the beta branch feeding the 1352 keV state in ^{81}Br is suggestive of an allowed nature. The 1352 keV state decays to the ground as well as 566 keV states, both of which are $3/2^-$. Thus the possible spins for the 1352 keV state are $5/2^+$or $7/2^+$. The spin of 815 keV state may be $5/2^-$ or $7-2^-$ assuming the beta transition feeding the 815 keV state to be of the first forbidden non-unique type. However unique assignments of spin is only possible, if detailed beta decay characteristics are known.

IV. REFERENCES

1. M. Soloman and C. Hojvat, Can.J.Phys.47, 2255 (1969).
2. W.H. Zoller et al, Phys.Rev.185, 1541 (1969).
3. P.V. Rao et al, Phys. Rev.154, 1028 (1967).
4. S. Prawirosoehardjo, Phys.Rev.157, 985 (1967).

TABLE I

Energies & Relative intensities of gamma rays

Notation in Fig.3	Energy (keV)	Present work	Zoller et al[1]
P	103	978.00	1000.00
F	180	0.92	0.80
H	201	0.28	-
N	260	8.20	5.10
O	276	100.00	88.00
L	290	83.00	67.00
J	375	0.50	-
-	491	-	0.01
M	538	6.50	5.70
D	552	11.80	10.20
K	566	32.00	27.00
I	650	3.40	2.90
-	767	-	0.48
B	787	0.38	0.33
G	815	0.10	-
C	829	40.00	33.00
A	1352	0.20	-

CAPTION FOR FIGURES:

FIG. I: Gamma Spectrum in energy range 0.460 keV.

FIG. II: Gamma Spectrum in energy range 500-1350 keV.

FIG. III: Beta = 0.013%(8.4)

Beta = 0.056%(6.5)

ANGULAR CORRELATION STUDIES IN COBALT-59.

K.Venkata Ramana Rao, D.L.Sastry, and V.Lakshminarayana
Laboratories for Nuclear Research, Andhra University,
Waltair. VISAKHAPATNAM-3.(A.P). India.

I. INTRODUCTION.

The low energy level structure of ^{59}Co has been extensively studied using the radioactive decay data(1,2,3) of ^{59}Fe, the (p,p')(4), (He^3,d)(5), and Coulomb excitation studies(6). The early investigations on the radioactive decay of ^{59}Fe established levels at 1100 and 1290 keV in ^{59}Co. The ground, and the 1100 and 1290 keV states were interpreted as single particle $f_{7/2}$, $f_{5/2}$, and $p_{3/2}$ excitations respectively. The later reaction studies, however, suggested 3/2 spin assignments to both 1100 and 1290 keV states. The 1290 keV state predominantly decays to the ground state, the 190-1100 keV cascade decay being weak. Subsequent studies established beta decay of ^{59}Fe to the 1430 keV state in ^{59}Co. The 1430 keV state has a beta feeding of about 1% and decays to ground through two cascades involving the 1290 and 1100 keV states. Thus, in all cases of cascade gammas, the intensities are small. Sum-Coincidence techniques are employed to carry out angular correlations on these cascades in as much as they are superior to the conventional methods.

II. EXPERIMENTAL DETAILS.

The radioactive source ^{59}Fe was obtained as $FeCl_3$ in Hcl solution with a specifi of 4 C/g

of Fe. The source liquid was used in a tubular source holder of perspex, with the scintillation detectors in a 7 cm. geometry. The sum-peak coincidence arrangement used in this study was reported earlier[7]. The decay scheme of ^{59}Fe is shown in Fig: 1, the 7 cm. sum-peak coincidence spectra with zero-, 250 and 400 keV bias are shown in Fig: 2. The peak at 1290 keV is due to the cascade (190-1100) keV. The peak at 1430 keV in the Zero-bias spectrum is due to both cascades (140-1290) keV and (330-1100) keV, while the 1430 keV peak in the 250 keV bias is only due to the (330-1100) keV, the other cascade being removed by the biasing condition. These sum-peak coincidence spectra are recorded for angles 90°, 135°, 180°, 225°, and 270° between the two detectors; the angular position of the detectors is changed every ten minutes and a pooled total of 10,000 true coincidence counts are collected under each peak at each angle. The count rates are fitted to standard polynomials and the resultant angular correlation coefficients are corrected for the finite detector size effects in the usual way.

III. RESULTS AND DISCUSSION:-

The final values of the angular correlation coefficients are : For (190-1100) keV cascade, $A_2 = +(0.028 \pm 0.003)$ and $A_4 = +(0.008 \pm 0.007)$ For the 330-1100 keV cascade, $A_2 = -(0.043 \pm 0.003)$ & $A_4 = -(0.004 \pm 0.003)$; and For the cascade (140-1290) keV $A_2 = -(0.065 \pm 0.004)$ and $A_4 = -(0.006 \pm 0.005)$.

It can be seen that in all cases A_4 values are vanishingly small, and A_2 values are used in the analysis.

The 1100 keV state was strongly excited in (d,d') reaction as well as the Coulomb excitation. On the other hand, the 1290 keV state is not excited in (d,d') and Coulomb excitation. It has a measurable lifetime[8]. It is, therefore, reasonable to assume the 1100 keV transition to be E2, while the 1290 keV transition may be M1 + E2. Thus, the ground, 1100 and 1290 keV states are assumed to be (7/2), (3/2), and (5/2) respectively, and the present correlation coefficient for the 190-1100 keV cascade is employed to obtain the mixing ratio of the 190 keV transition. The analysis yielded a quadrupole content for the 190 keV transition to be (9 ± 1)%.
The 1430 keV state is assumed to be a (1/2) or (3/2) for both spin possibilities. The angular correlation coeffi--cients are used to obtain information on the transitions involved. For an assumed spin of (1/2) for the 1430 keV state, the 140 keV transition turns out to be pure E2, while it has a quadrupole content of (11 ± 4)% for a 3/2 spin assignment, for the 1430 keV state. Assuming the 1290 keV transition to be (92% M1 + 8% E2), the 330 keV transition turns out to be a pure M1 for a spin assignment of (1/2) for the 1430 keV state; the 330 keV transition possess a quadrupole content of (21 ± 1.5)% for a (3/2) spin assignment to the 1430 keV state. Assuming the 1290 keV transition to be a pure E2, the 140 keV transition turns out to possess a quadrupole content of (9 ± 0.8)% for a spin assignment of (3/2) to the 1430 keV state and (5/2) to the 1^

It is desirable to determin the internal conversion coefficients of the low energy transitions in ^{59}Co to uniquely choose from the above possibilities.

REFERENCES:

1. R.L.Heath, C.W.Reich, and D.G.Proctor, Physical Review, 118, 1082, (1960)

2. W.Collin, H.Daniel, O.Mehling, H.Schmidt, G.Spannagel and K.S.Subudhi. Zeischrift Fur Physik, 180, 143, (1964)

3. J.Legrand, J.Morel, and C.Clement. Nuclear Physics, A 142, 63, (1970)

4. M.Mazari, A.Sperderto and W.W.Buechner., Physical Review, 107, 365, (1957)

5. A.G.Blair, and D.D.Armstrong, Physical Review, 140, B-1567. (1965)

6. R.Nordhagen, B.Elbeck and B.Hershkind, Nuclear Physics, A 104, 353, (1967)

7. V.Lakshminarayana, "Invited Talk". Proceedings of the Nuclear Physics & Solid State Physics Symposium" Dec, 1968., D.A.E.,(India), Vol:1., 107, (1968)

8. Y.K.Agarwal, C.V.K.Baba, and S.K.Bhattacherjee, Nuclear Physics, A 99, 457, (1967)

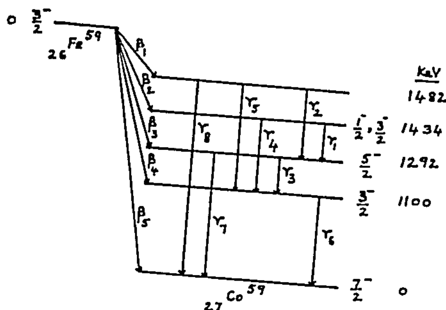


Fig.1. Decay Scheme of ^{59}Fe.

Beta Transitions.

β_1 = 85 keV = 0.1%	β_4 = 467 keV = 52.3%
β_2 = 140 keV = 1.2%	β_5 = 1573 keV = 0.3%
β_3 = 273 keV = 46.1%	

Gamma Transitions.

γ_1 = 142 keV = 1%	γ_5 = 381 keV = 0.02%
γ_2 = 190 keV = --	γ_6 = 1100 keV = 55.2%
γ_3 = 192 keV = 3%	γ_7 = 1292 keV = 43.9%
γ_4 = 335 keV = 0.25%	γ_8 = 1482 keV = 0.1%

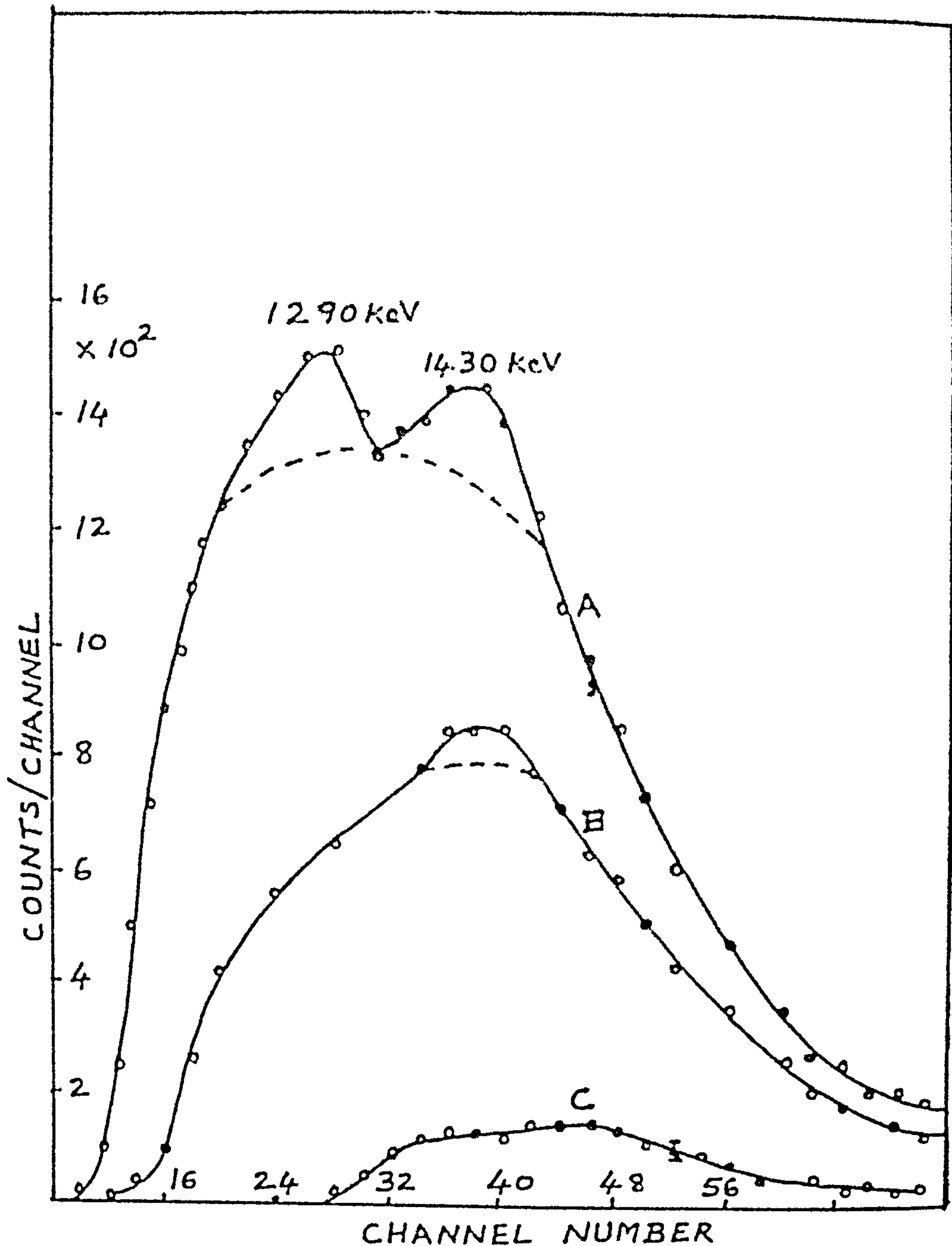


Fig: 2. Sum Peak Coincidence Spectra. - Decay of ^{59}Fe
7 cm. geometry.
A - zero-bias spectrum
B - 250 keV bias spectrum.
C - 400 keV bias spectrum.

INELASTIC SCATTERING OF 40 MEV PROTONS BY ^{58}NI AND ^{60}NI *

N.Lingappa ** and G.W.Greenlees
University of Minnesota, Minneapolis,Minn., U.S.A.

Inelastic scattering studies are normally employed to derive nuclear structure information as an alternative to coulomb excitation studies. The scattering process is highly sensitive to excitation of collective states, and provides a means of studying them. DWBA methods are sufficient to analyse first order excitations. But coupled channel methods can be profitably used to study both first and second order excitations. The following is a study on ^{58}NI and ^{60}NI isotopes.

The 40 Mev proton beam from the Minnesota Linear-Accelerator was used to bombard ^{58}NI and ^{60}NI targets (15-25 mgm/sq.cm.). A 180° magnetic spectrometer with an array of 32 silicon surface barrier detectors in its focal plane was used for detection of scattered protons. The overall resolution was about 200 kev, and was sufficient to study the dominantly excited states.

The experimental angular distributions have been fitted with theoretical calculations from the coupled channel codes[1] JUPITOR-1 and JUPITOR-2. The calculations were done on the CDC-6600 computer of the Univ. of Minnesota. The optical-model parameters used have been shown in Table I . The parameters searched were V, W_x, W_D, and β.

Fig.1 shows the best fits obtained for the collect-

* Work performed under U.S.A.E.C. grant AT-11-1-1265.

** Present Address: Dept. of Physics
Bangalore Univ

TABLE I.

Coupling	^{58}Ni				^{60}Ni			
	V	W_I	W_D	β	V	W_I	W_D	β
0^+_0	42.92	5.47	3.50	---	43.05	2.84	5.14	---
$0^+_0-2^+_1$	43.53	6.48	2.45	0.186	44.00	4.59	3.87	0.206
$0^+_0-3^-_1$	43.33	6.57	2.46	0.177	43.81	4.84	3.84	0.179
$0^+_0-2^+_1-3^-_1$	43.40	6.03	2.48	β_2=0.183 β_3=0.174	44.13	4.43	3.73	β_2=0.203 β_3=0.174

The other optical-model strength and geometry parameters used are available in Ref.2.

TABLE II.

^{58}Ni			^{60}Ni		
β_2	β_{24}	ν	β_2	β_{24}	ν
0.187	0.118	0.63	0.207	0.179	0.86

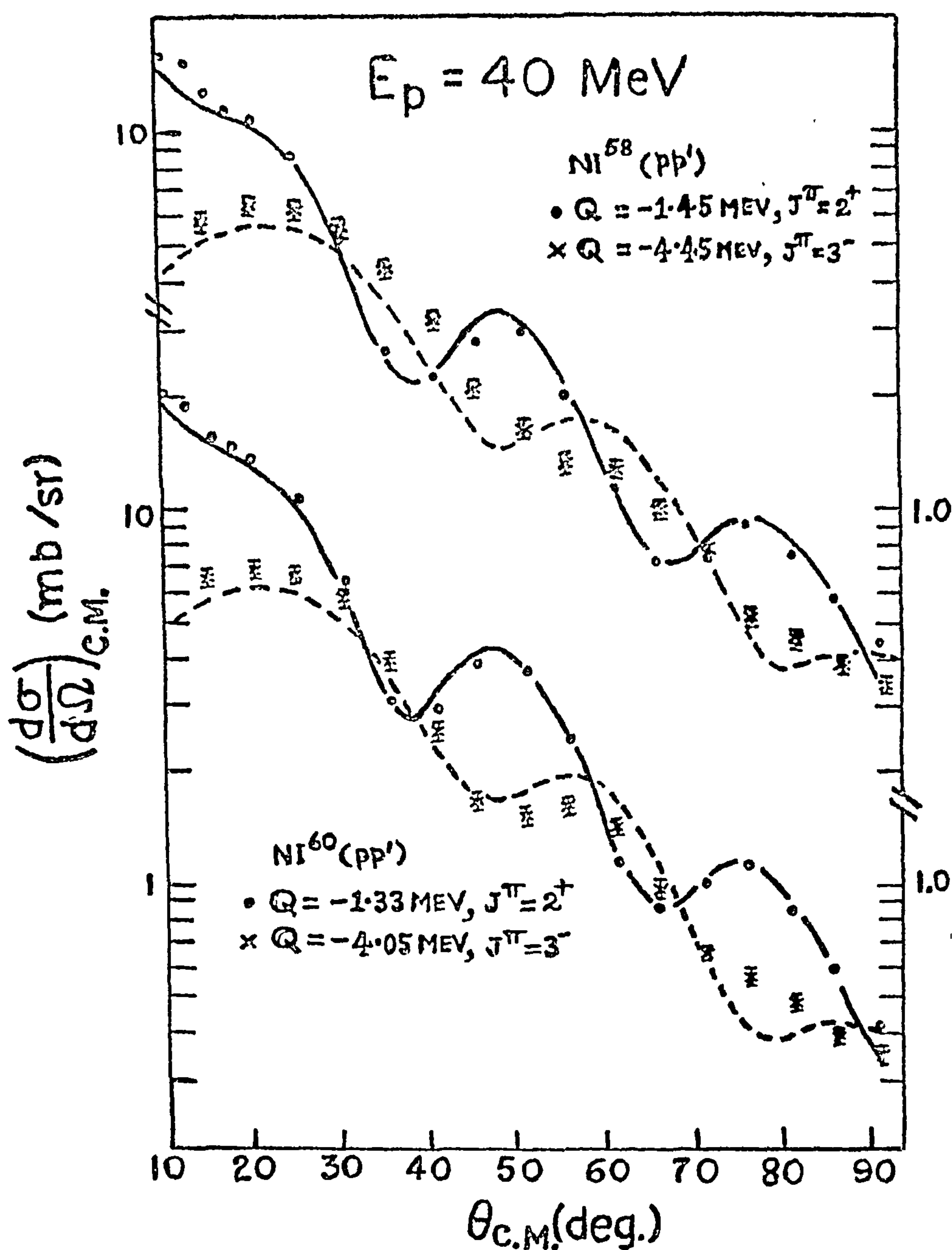


Fig. 1. Inelastic Scattering of 40 MeV Protons by NI^{58} and NI^{60}.

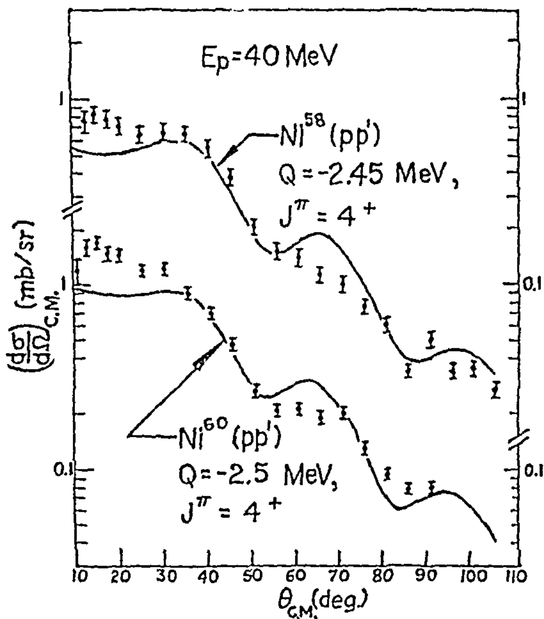


Fig. 2. Inelastic Scattering of 40 MeV Protons by Ni^{58} and Ni^{60}.

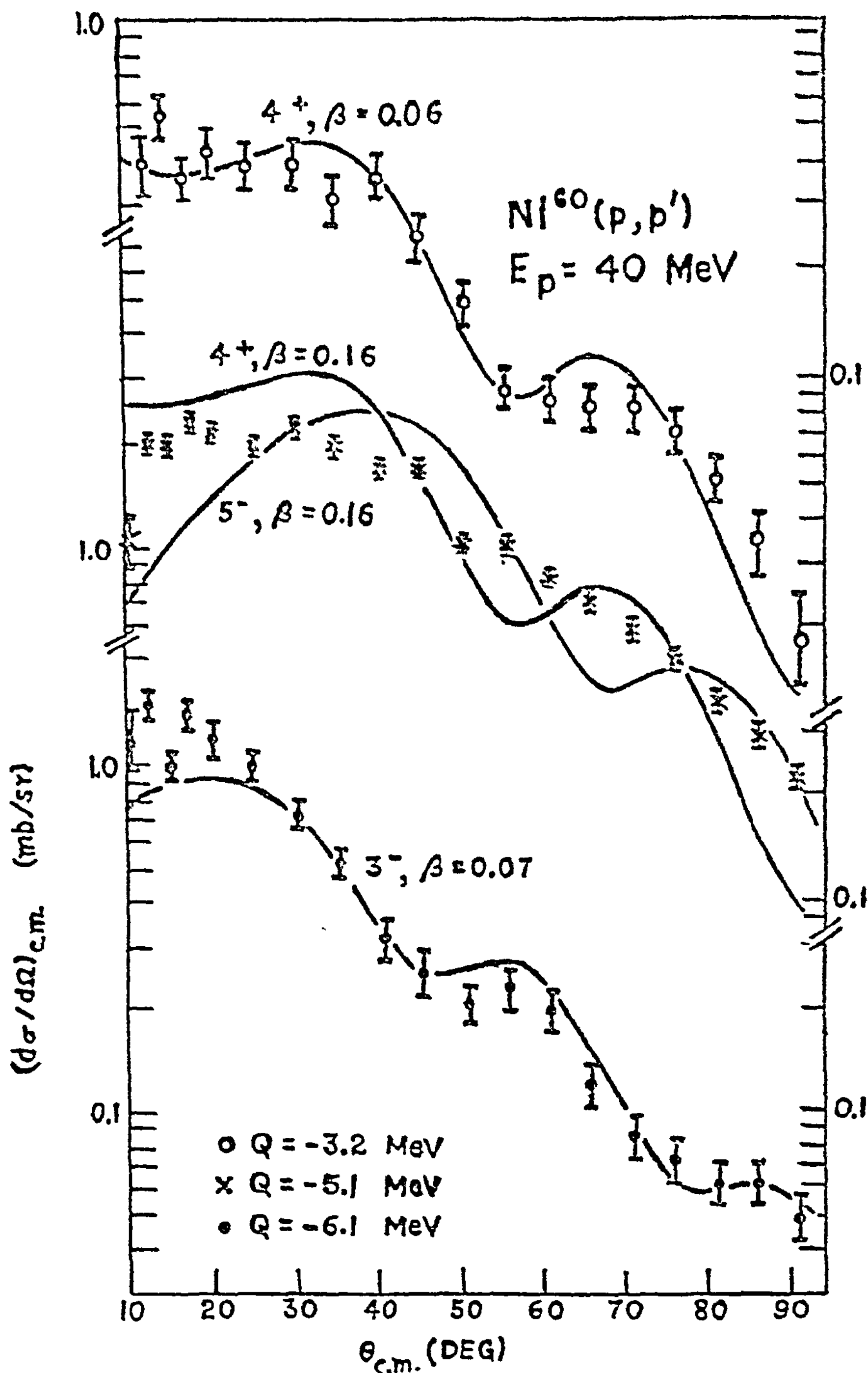


Fig. 3. Inelastic Scattering of 40 MeV Protons by NI^{58} and NI^{60}

DISCUSSION

V. Lakshminarayana: Did you estimate any quadrupole moments for these cases? As you may be aware several cases of vibrational 2 + states are found to have finite quadrupole moment by reorientation effect studies in Coulomb excitation.

N. Lingappa: I do not think there is anything in this method for estimation of possible static quadrupole moments on the quadrupole states. Such a thing is usually done by the re-orientation effect in Coulomb excitation so far as I know.

N.K. Ganguly: B(E2) values would have to correspond to the values. Commensarate values would be obtained if careful evaluation of β is done. 1) For the one-phonon fit there was rather a large difference between the theoretical and experimental value. Would it have been possible to obtain a better fit by varying β . 2) Was there any polarisation measurements done and fits obtained?

N. Lingappa: 1) There was a large difference only for the 4^+ state. But that is th ought to be two phonon in character. An admixture of one phonon into the two phonon state was tried, which as you saw remedied the trouble. All the β parameters were taken as variables in the actual search. The quadrupole and octupole one phonon states fit extremely well. 2) [illegible] tion measurements for the inelastic scatt[illegible]

ON THE DECAY OF ^{142}Pr

K.L. Narasimham and V. Lakshminarayana
Laboratories for Nuclear Research
Andhra University, Waltair

ABSTRACT

The gamma rays in the decay of Pr-142 are studied with a sum coincidence scintillation spectrometer. Two new transitions at 100 and 400 keV are seen in addition to the already observed gamma rays. These are fitted in the decay scheme between the levels at 2080, 1970, 1580 and ground state. The gamma-gamma angular correlations are performed for the 508-1580 cascade to infer about the nature of the 508 keV transition. The present results are consistant with a nearly pure E1 nature for this transition and hence support a 3^- assignment for the 2080 keV level.

GAMMA-GAMMA DIRECTIONAL CORRELATIONS OF THE 552-134 keV CASCADE IN Re^{187}.

M.L. Narasimha Raju, A. Khayyoom and D.L. Sastry,
The Laboratories for Nuclear Research, Andhra University,
Waltair,(A.P.)India.

The level structure of Re^{187} is well established[1]. The 552-134 keV gamma-gamma angular correlation was measured by several authors in the past[2-5]. Arns et al reported a very high positive anisotropy (A_2= 0.316±0.018, A_4= -0.086±0.027) where as Gallagher et al found the correlation to be isotropic with in 1%. Michaelis,and Gupta et al observed small negative anisotropy for this correlation where as Klementovskeya et al observed small positive anisotropy. In view of the above descrepancies it is felt worthwhile to re-measure the 552-134 keV gamma-gamma angular correlation in Re^{187}.

The directional correlation of the above cascade is measured with a conventional slow-fast coincidence scintillation assembly described elsewhere[7]. The system is checked by measuring the 1.17-1.33 MeV gamma-gamma angular correlation in Ni^{60}. The present measurements were done with an effective coincidence resolution of 20 n.s. The angular correlation data were collected at three angles 90°, 135° and 180° and were corrected for the short life of W^{187} and chance coincidences. The pooled up counts at the three angles are normalised and the data are fitted to the standard polynomial

$$W(\theta) = 1 + A_2P_2(\cos \theta) + \quad (co$$

by the method of lest square[8]. T ion

function after correcting for the geometry of both the detectors, is found to be

$$W(\Theta)= 1-(0.028\pm0.015)P_2(\cos\Theta)+(0.012\pm0.017)P_4(\cos$$

This result is fairly in good agreement with that obtained by Michaelis, and Gupta et al and differs cons derably from the values of Gallagher et al, Klementovsk et al and Arns et al. The experimental values of A_2 an A_4 coefficients of the earlier authors together with th values of the present work are tabulated in Table I.

TABLE I

The values of the coefficients of the 552-134 al corr[illegible]on.

	c		A_4
Arns		±0.	0.086±0.027
Gall		Iso	in 1%
Mich		.0	.007±0.0
Kleme		1	isotrop
Gupt		0	0299±C
Prese			012±0.

T c

nt with

REFERENCES

1. K.Way et al. Nuclear Data Sheets, Edited by K.Way etal Academic Press, New York (1965).

2. R.G.Arns, M.L.Wiedenbeck, Nuclear Physics, 19 , 634, (1960).

3. C.J.Gallagher, W.F.Edwards and G.Manning, Nuclear Physics, 19, 18,(1960).

4. W.Michaelis, Nuclear Physics, 45, 573, (1963).

5. S.L.Gupta, M.M.Bajaj and N.K.Saha, Proc.Nat.Inst.Sci. (India), 32, 281, (1966).

6. M.V.Klementovskaya, and P.J.Sharvin, Soviet Physics JETP, 36, 1360, (1956).

7. M.L.Narasimha Raju, D.L.Sastry and E.Kondaiah, Nuovo Cimento, 56, B29, (1968).

8. M.E.Rose, Phy.Rev., 91, 610, (1953).

GAMMA – GAMMA ANGULAR CORRELATIONS IN ^{95}Mo (n,γ) ^{96}Mo REACTION

S.N. Chintalapudi*, D.L. Sastry and Swami Jnanananda**
The Laboratories for Nuclear Research, Andhra University, Waltair

I. INTRODUCTION

The energy levels of ^{96}Mo are known from the decay studies(1) and from (n,γ) studies(2,3). The decay scheme formed from the above studies shows a strong 840 KeV-770 KeV cascade in the low energy group involving the 1.62 MeV-0.776 transition. The internal conversion coefficients were reported(1) to be $(1.2 \pm 0.22) \times 10^{-3}$ and $(1.2 \pm 0.4) \times 10^{-3}$ respectively for the 840 keV and 770 keV gamma rays respectively. The 1.62 MeV state was assigned with a spin of 3^+ or 4^+. The 770 keV transition was established to be of pure E2 nature and the 776 KeV level was assigned a 2^+ character from Coulomb excitation studies(4). The present measurement was undertaken at CIRUS reactor, BARC to analyse the involved spin sequence of the cascade from angular correlation measurements. The results were examined by a parametric plot analysis.

II. EXPERIMENTAL

The experimental arrangement at CIRUS reactor, detection system and experimental condition together with method of collection of data were given in our previous reports(5,6). The target employed was a 99.99% pure natural molybdenum rod, of length 12 mm x 10 mm dia.

* Present Address: Variable Energy Cyclotron Project, BARC Bombay-85.

** Deceased.

The correlation coefficients evaluated were corrected for correlation attenuation as described by White et.al[7].

III. RESULTS AND DISCUSSION

The final correlation function obtained was $W_{\gamma\text{-}\gamma}(\theta) = 1 + (0.09821 \pm 0.008377)\, P_2 \cos\theta + (0.03968 \pm 0.008477)\, P_4 \cos\theta$. On the basis of the Cross Section and the appearance of similar cascades in the decay of ^{96}Nb and ^{96}Tc, the 840 KeV-770 KeV cascades can be ascribed to the ^{95}Mo (n,γ) ^{96}Mo reaction. The ratio of the second excited state to first excited state energy and the ground and first excited state spins of the ^{96}Mo, supported by the absence of direct cross over from the second excited state suggest a quadrupole excitation of the second excited state and hence a 4^+ character to this 1.62 MeV level. The internal conversion studies[1] and (n,γ) studies[2,3] however, do not rule out a 3^+ character to this state and hence two spins sequences $3^+ - 2^+ - 0$ and $4^+ - 2^+ - 0$ for the transition. Since 770 KeV is of pure E2 nature, the 840 KeV in the former case can be either E2 or MI + E2 while in the latter case it must be E2 or M3 + E2. Expressions for $A_k\ (\gamma)$ for the two spins sequences and for the two rays were obtained from

$$A_k\ (\gamma) = A_k\ (L_1 L_1 + 1\ I_i I_i)$$

$$\frac{F_k(L_1 L_1\ I_i I) + 2\delta(\gamma_1)\, F_k\ (L_1 L_1 + 1\ I_i\ I) + \delta^2(\gamma_1) F_k(L_1 + 1 L_1 + 1 I_i I)}{1 + \delta^2\ (\gamma_1)} \qquad - (1)$$

involving the multipole admixture parameter 'δ' (all the terms in the equations have the usual meanings). The F coefficients were taken from Siegbahn[8]. The A_{kk}(Theo) were obtained from

$$A_{kk}(Theo) = A_k(\gamma_1) \times A_k(\gamma_2) \qquad -(2)$$

The parametric plots obtained with A_{22} (Theo) versus A_{44}(Theo) plotted for different values of 'δ' for the 810 keV transition were found inconsistent, for both the spin sequences, with the experimental values and hence the 810 keV was concluded to be of pure multipole nature belonging to either $3^+ - 2^+$ or $4^+ - 2^+$ sequence. In the former case the pure dipole is not permitted by intensity and parity consideration. Assuming E2 nature for 810 KeV for the sequence 3 (2) 2 the A_{22}(Theo) and A_{44}(Theo) are - 0.104 and - 0.08 which are quite contradictory to the experimental values and thus a 3^+ character to the 1.62 MeV level can be completely ruled out. The A_{22}(Theo) and A_{44}(Theo) for the 4(2) 2 sequence are 0.102 and 0.00352 respectively and are considerably in good agreement with the experimental values. It can thus be conculded that the 840 KeV is of pure E2 nature and that the spin sequence for the 1.61 MeV - 0.770 -0.0 MeV transition in Mo^{96} is of a $4^+ - 2^+ - 0^+$ character. These results are also in conformity with the report of Lovas et.al(9).

REFERENCES

1. P. Prieswerk and P. Stahelin
   Helv. Phys. Acta 24 (1951) 300

2. L.G. Kalinkin, A.S. Melioranskii and I.V. Latuhin
   JETP, Vol 33 (8) (1957) 410

3. R.B. Kinsey and G.A. Bartholomew
   Canad. J. Phys. 31 (1953) 1051

4. N.E. Hydenberg and G.H. Temmer
   Phys. Rev. 93 (1955) 617 A

5. Surya N. Chintalapudi, D.L. Sastry and Swami Jnanananda
   Indian J.P & A. Phys Vol.7, No. 8 (1969) 432

6. S.N. Chintalapudi , D.L. Sastry and S. Jnanananda
I.L Nuovo Cimento, Vol. 63 B (1969) 447

7. D.H. White
Nucl. Instr & Methods, 21 2 (1963) 209

8. K. Seigbahn
Alpha, Beta and Gamma Ray Spectroscopy, 1965
North Holland Publishing Co., Amsterdam

9. I. Lovas and Z. Zamori
Nucl. Phys. 39 (1962) 300

Table I

A_n	A_2	A_4
From W (θ) observed	+0.06668 ± 0.007773	+0.04315 ± 0.008301
From W (θ) corrected	+0.09328 ± 0.007958	+0.03771 ± 0.008041
Finite detection size correction factor	1/0.9559	1/0.9559
Corrected A_n	+0.0975 ± 0.008136	0.03932 ± 0.008313
Length and Incident Flux absorption and in the target	(1/0.998833) x (1/0.995333)	(1/0.993560) x (1/0.9935380)
A_n	+0.09821 ± 0.008377	+0.03968 ± 0.008447
Scattering correction factor	1	1
A_n	+0.09821 ± 0.008377	+0.03968 ± 0.008447
	0.110 ± 0.020 (*)	0.040 ± 0.026 (*)

(*) Values reported by Lovas et.al[6]

HALF-LIFE OF 126 keV STATE IN ^{107}Ag

H.C. Jain and S.K. Bhattacherjee
Tata Institute of Fundamental Research, Colaba, Bombay-5

&

C.V.K. Baba
Bhabha Atomic Research Centre, Trombay, Bombay.

I. INTRODUCTION

There has been recently considerable interest in understanding the nature of the low lying energy levels in the odd mass nuclei with $40 \leq Z \leq 50$. The protons in this region are filling $g_{9/2}$ and $p_{1/2}$ shells. One can therefore expect low lying $9/2^+$ and $1/2^-$ levels. These levels are systematically observed in odd mass Rh and Ag isotopes with $1/2^-$ occurring as ground state while $9/2^+$ is found at ~ 100 keV. In addition to these a systematic feature in these nuclei is the presence of $7/2^+$ state very close to $9/2^+$ states - often lower in energy. This $7/2^+$ cannot be a single particle state. K-S coupling scheme (using quadrupole and pairing force) completely fails to account for the small energy spacing between these states. More recently Sherwood and Goswami[1] have explained it by proposing EJPC model. According to this, $7/2^+$ is a three particle state. In that case one expects the M1 transition between $9/2^+$ and $7/2^+$ to be retarded.

II. RESULTS AND DISCUSSION

In last year's conference we presented our results on half-life and magnetic moment of $9/2^+$ state in $^{103}_{45}Rh$. The magnetic moment of $9/2^+$ state agreed well with the theoretical value for $g_{9/2}$ single particle level. While the life-time $T_{1/2} = (1.13 \pm 0.04)$ ns indicated M1 retardation by a factor of ~ 20. The present wor   ais

measurement on life-time of $9/2^+$ state in ^{107}Ag. The source ^{107}Cd was obtained by neutron irradiation of enriched ^{106}Cd. X-rays + 32 keV ($9/2^+ \longrightarrow 7/2^+$) γ-ray were detected in Pb-loaded plastic scintillators, while γ-rays in the energy region from 700 to 1 MeV were detected in 2" thick NaI crystal. The delayed curve, as also the prompt curve taken from a ^{60}Co source are shown in Fig.1. We obtained $T_{1/2}$ = (2.85 ± 0.1) ns.

In addition there are preliminary measurements on life-times of similar $9/2^+$ states in ^{111}Ag and ^{109}Ag at 130 keV and 132 keV respectively. For ^{111}Ag the measurement was done in two ways. In the first, the 70 keV γ-ray was detected in Pb loaded plastic scintillator, while comptons on (415 + 575 + 694) keV γ-rays were detected in 2" thick plastic crystals. In second case 2" thick NaI crystal was used to detect high energy γ-rays above 1600 keV. From both methods, a life-time $T_{1/2}$ = 0.92 ± 0.05 has been obtained. A Pb-loaded plastic for 44 keV γ-ray and 2" thick plastic for comptons of 608 keV were used for ^{109}Ag measurement, which gave $T_{1/2}$=(1.3 ± 0.2) ns for 132 keV ($9/2^+$) state.

The results are tabulated in Table 1. Measurements of L-subshell ratios[2)] for 53 keV transition in ^{103}Rh show that this is predominantly M1 transition. Therefore assuming all these to be pure M1 transition, the M1 retardations have been calculated for Tc, Rh and Ag isotopes. These are also shown in Table 1. One finds a retardation ranging from 21 to 46. If $9/2^+$ is a single particle state as suggested by magnetic moment measurements in ^{103}Rh, then the above mentioned M1 retardations point to the phonon-character of $7/2^+$ states.

References

1. A.T. Sherwood and Goswami, Nucl. Phys. 89, 465 (1966).
2. J.C. Manthuruthil et al., Phys. Rev. 165, 1363 (1968).
3. S.K. Bhattacherjee, H.C. Jain and C.V.K. Baba, Nucl. & Solid State Phys. Symp., Roorkee (1969), and Israel Conf. (1970).
4. Steiner et al., Asilomar Conf. (1967).

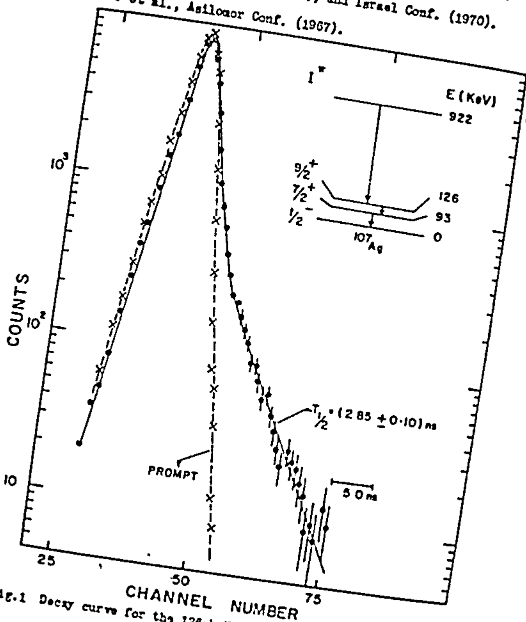


Fig.1 Decay curve for the 126 keV state in ^{107}Ag.

TABLE I

Summary of half-life measurements on $(9/2^{+} \quad 7/2^{+})$ transitions in odd mass Tc, Rh & Ag isotopes.

	ISOTOPES				
	^{99}Tc	^{103}Rh	^{107}Ag	^{109}Ag	^{111}Ag
Energy (keV)	150	53	32.6	44.8	70.4
λ_T(Theory) (for pure M1)	0.1	2.13	11.0	4.4	1.14
$T_{1/2}$ (Expt.) (ns)	(0.192 ± 0.01) [4)]	(1.13 ± 0.04) [3)]	(2.85 ± 0.10) [a)]	(1.3 ± 0.2) [b)]	(0.92 ± 0.05) [b)]
Γ_γ (sec^{-1})	2.7×10^9	1.96×10^8	2.01×10^7	0.99×10^8	3.54×10^8
Γ_γ (S.P.)(sec^{-1})	7.8×10^{10}	4.15×10^9	0.94×10^9	2.5×10^9	9.8×10^9
M1 Retardation	29	21	46	25	28

a) The present measurement.
b) Our preliminary measurement (to be published).

g-FACTOR OF THE 603 keV LEVEL IN ^{124}Te BY BETA-GAMMA PERTURBED ANGULAR CORRELATIONS

A.F. Agnihotry, M. C. Joshi and K.G. Prasad
Tata Institute of Fundamental Research, Bombay-5

I. INTRODUCTION

The possibility of applying the method of perturbed β-γ angular correlation was suggested and applied in the case of $^{154}Eu \rightarrow$ ^{154}Gd by Nielsen(1). In this case the radioactive atoms were implanted in a thin iron foil by an isotope separator. We have applied a similar method to 603 keV (2^+) level of ^{124}Te populated in the decay of ^{124}Sb.

The β-γ angular correlation in $^{124}Sb \rightarrow {}^{124}Te$ ($3^- \xrightarrow{\beta} 2^+ \xrightarrow{\gamma} 0^+$) has been extensively studied by various workers(2,3) (fig.1). It is known to have an anisotropy as large as 40%. The g factor of 603 keV (2^+) level is also determined by various workers(6-8) using the internal fields in iron by the method of perturbed γ-γ angular correlation [PAC]. Since Sb diffuses easily in Fe, it was thought that the uncertainties like lattice damage and interstitial positions, etc. present in the implanted source can be avoided.

II. EXPERIMENTAL

The ^{124}Sb activity was diffused by heating the foil in Argon atmosphere for 200 hrs at 900°C. The tube was very slowly cooled to room temperature. Finally the surface activity was removed by etching the foil with dilute HCl.

The measurement of β-γ angular correlation was done using Anthrecene crystal of 2.5 cm x 1 cm as β detector and 5 cm x 4.5 cm NaI(Tl) as γ detector. The electronics used was conventional slow-fast coincidence circuit with resolving time 50 ns. The source was mounted in the tips of a small electromagnet of C t

vaccum. The β gate was accepted above 1600 keV. The β-γ angular correlation was measured at seven angles.

The field measurement was performed by reversing the current for four different magnetizing ampere turn values i.e. 20, 40, 120 and 320. The effect of stray magnetic field was checked at each magnetising current using "Sb in Cu" source prepared in exactly the same way as "Sb in Fe". In each case more than a million counts were collected.

The γ-γ PAC measurement was also carried out using 1690 - 603 keV ($3^- \longrightarrow 2^+ \longrightarrow 0^+$) cascade to check the β-γ measurement. This cascade is relatively free from interferences. The field measurement in this case was carried out at 320 ampere turns.

III. RESULTS

The β-γ angular correlation was measured and it compares well with the measurement of others[2,3]. For the field measurement the movable γ counter was fixed at $\theta = 135^\circ$ and counting rate was measured by reversing the field direction. The rotation of the angular correlation $\omega\tau$ was deduced from this. It was noticed that at the highest magnetizing current i.e. 320 ampere turns a large stray field effect was observed for "Sb in Cu" source. Fig.2 is the plot of corrected $\omega\tau$ values as a function of magnetizing current. It is seen from the curve drawn through first three points that almost full saturation field is reached beyond 50 ampere turns. The last point is not taken into consideration as the correction in this case is large (70%). The saturation value of $\omega\tau$ is taken as

$$(\omega\tau)_{SbFe} = (0.71 \pm 0.20) \times 10^{-2}$$

The g factor is given by

$$\omega\tau = g\,\mu_N \frac{H_{eff}}{\hbar}\,\tau$$

where μ_N is the nuclear magneton, H_{eff} is the effective magnetic

field at Te nucleus, τ the lifetime of the nuclear state. We h[ave] taken H_{eff} = 620 ± 20 KG (Frenkel)[4] and τ = 8.5 ± 0.5 psec (Stelson)[5]. The g factor is

$$g = 0.28 \pm 0.05$$

The g factor using γ-γ PAC gives

$$g = 0.31 \pm 0.06$$

Table below gives the comparison of present measurement with others. Our value compares well with that of Bhattacherjee(6) and Heestand(9[)]

Cascade (keV)	$\omega\tau$	g	Ref.
1690 γ - 603 γ	$(0.66 \pm 0.24)10^{-2}$	0.22 ± 0.05 (both)	Bhattacherjee[6]
722 γ - 603 γ	$(0.54 \pm 0.13)10^{-2}$		
722 γ - 603 γ	$(0.97 \pm 0.13)10^{-2}$	0.32 ± 0.02	Murray[7]
1690 γ - 603 γ	$(0.75 \pm 0.13)10^{-2}$	0.40 ± 0.23	Bozek[8]
IMPACT (Coulomb Exci.)	$(1.29 \pm 0.9)10^{-2}$	0.21 ± 0.05	Heestand[9]
3500 β 603 γ	$(0.71 \pm 0.20)10^{-2}$	0.28 ± 0.05	Present
1690 γ 603 γ	$(0.80 \pm 0.28)10^{-2}$	0.31 ± 0.05	Present

(6) Phy.Lett. 24B, 651 (1967). (7) Can. J. Phys. 45, 1600 (1967). (8) Asilomar Page 158 (1967). (9) Nucl. Phys. A133, 310 (1969).

IV. DISCUSSION

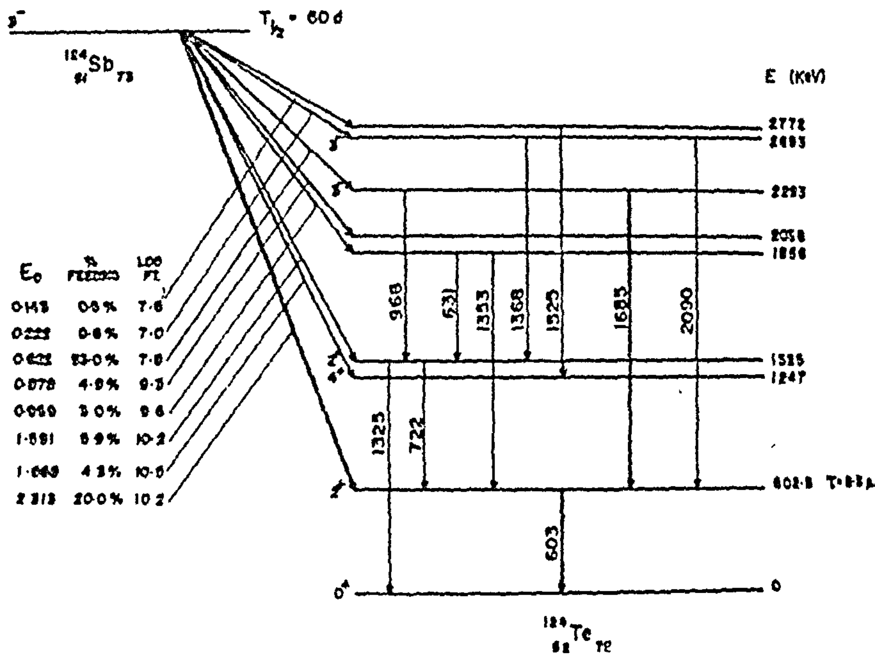
These measurements show that β-γ PAC can be applied in favourable cases. The present case also indicates that foil saturation is reached even at small magnetizing currents. It may also be possible [t]hat in some ferromagnetic media like perm-alloy of high retentivity [e]ven the retained field after removal of the external field may be [en]ough to give saturation value of $\omega\tau$.

[REF]ERENCES

K. Bonde Nielsen; Phy. Lett. 25B, 206 (1967).

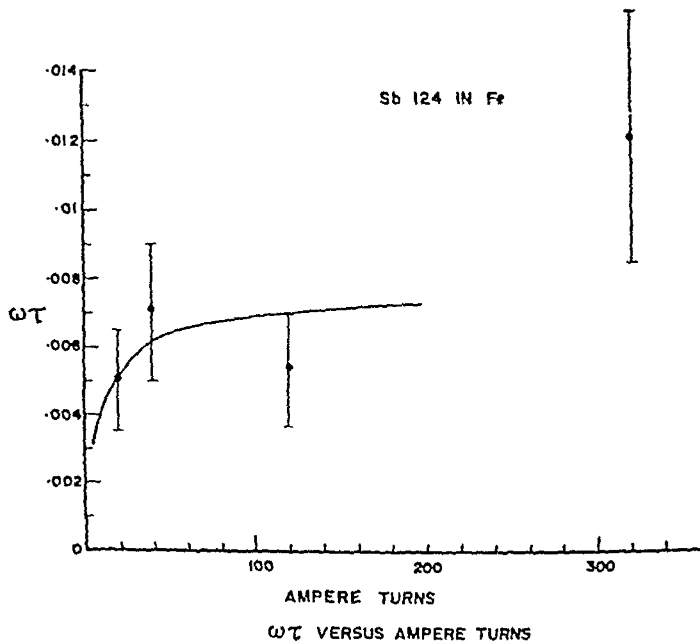
R.M. Steffen; Phys. Rev. Lett. 4, 290 (1960).

S.K. Mitra; Nucl. Phys. 47, 293 (1963).



T½ = 60 d
124Sb
E (KeV)
E0
968
631
1368
2090
1325
722
603
0
124Te

FIG. 1



Sb 124 IN Fe
ωτ
·014
·012
·01
·008
·006
·004
·002
0
100
200
300
AMPERE TURNS
ωτ VERSUS AMPERE TURNS

FIG. 2

4. R.B. Frenkel et al; Phys. Lett. 15, 223 (1967).

5. P.H. Stelson; Nuclear Data 1, 651 (1967).

DISCUSSION

P.G. Hansen: Just a technical question - How big was the correction for the stray field?

A.P. Agnihotry: The correction for the stray field was as large as 70% in the case of highest magnetizing current i.e. 320 ampereturns. But this point is not taken into consideration for calculation of NJ. The correction was small at the other lower magnetizing currents which are used for calculation of NJ.

Ge(Li) - Ge(Li) COINCIDENCE STUDIES IN ^{147}Pm

R. Singh and G.K. Mehta
Indian Institute of Technology, Kanpur-16

I. INTRODUCTION

The decay of ^{147}Nd has been investigated by many workers using various techniques. In 1967, Pashandy et al[1] reported many new levels in ^{147}Pm based on their conversion electron studies. Recently some elaborate NaI(Tl)-NaI(Tl) sum coincidence measurements[2] were made to look at the level structure of this nucleus again. This paper describes the measurements of gamma rays using two Ge(Li) detectors with fast-slow coincidence technique which were made to corroborate earlier work using sum coincidence technique[2] with a view to get conclusive information on the complicated level structure of ^{147}Pm nucleus.

II. EXPERIMENTAL

The source of ^{147}Nd was obtained from B.A.R.C. and purified in an ion-exchange column at T.I.F.R., Bombay. The experimental set-up used for Ge(Li)-Ge(Li) coincidence work is shown in Fig. 1. The two detectors used have volumes of 6 cm^2 x 7 mm and 6 cm^2 x 5 mm which give energy resolutions of 3.0 keV and 3.5 keV respectively for ^{137}Cs gamma rays. The time resolution of the fast coincidence circuit is 40 ns. Detailed measurements are made to get the contributions of Compton distributions of higher energy gamma rays in the photopeaks to the coincidence spectra.

III. RESULTS

The singles spectra of ^{147}Nd were recorded with the 7 mm Ge(Li) detector at various intervals of time to look for the contaminant gamma rays. On the basis of singles spectra the gamma energies 91, 120.5, 154.6, 184, 155.9, 211.5, 223.5

345, 356.3, 388.3, 405.5, 410.5, 440, 450, 457.3, 489.9, 531, 589, 594.8, 654, 660, 685.8 keV are found to belong to the decay of ^{167}Tm.

Because of low intensities of some of the gamma rays and poor efficiency of our detectors only few coincidence spectra could be taken. The results are discussed below.

The 91 keV gate: The peaks, observed in the 91 keV gate fast slow coincidence spectrum, which cannot be accounted for even after adding the chance and Compton contributions correspond to the gamma ray energies 91, 120.5, 154.8, 184, 195.9, 228.5, 275.5, 319.5, 345, 356.3, 440, 589 and 594.8 keV. The 91 keV peak provides a confirmation for the level at 182 keV. The 120.5, 275.5 and 319.5 keV gamma rays give evidence for levels at 685.8, 531 and 410.5 keV. The 184 keV gamma ray arises from the transitions 275-91-0 giving a definite indication of a level at 275 keV. Occurrence of a very weak peak at 228.5 keV coupled with 457.3 keV in singles gives an indication of the 228.5 keV level. The 660 keV level gets confirmation from weak indication of [illegible] keV in this coincidence spectrum and 660 keV in singles spectrum. Rest of the gamma rays arise from well known transitions.

The 120.5 keV gate: The gamma rays found in genuine coincidence with 120.5 keV gamma are of 91, 154.8, 194, 319.5 and 410.5 keV energies. The 91 and 319.5 keV gamma rays appear due to 531-410.5-91-0 transition. The gamma ray of 194 keV appears through 725-531-410.5 transitions whereas 154.8 and 410.5 keV result from 685.8-531-410.5 and 531-410.5-0 respectively. However, presence of 120.5 keV level does not seem to be necessary to infer any transition.

The 319.5 keV gate: In the spectrum strong peaks are observed at 91, 120.5 and 275.5 keV and some weak gamma rays are seen at 154.8, 194, [illegible], and 356.5 keV. All the strong peaks and those at 154.8 and 194 keV arise from well known transitions. However, 2?1.5 and 356.5 result

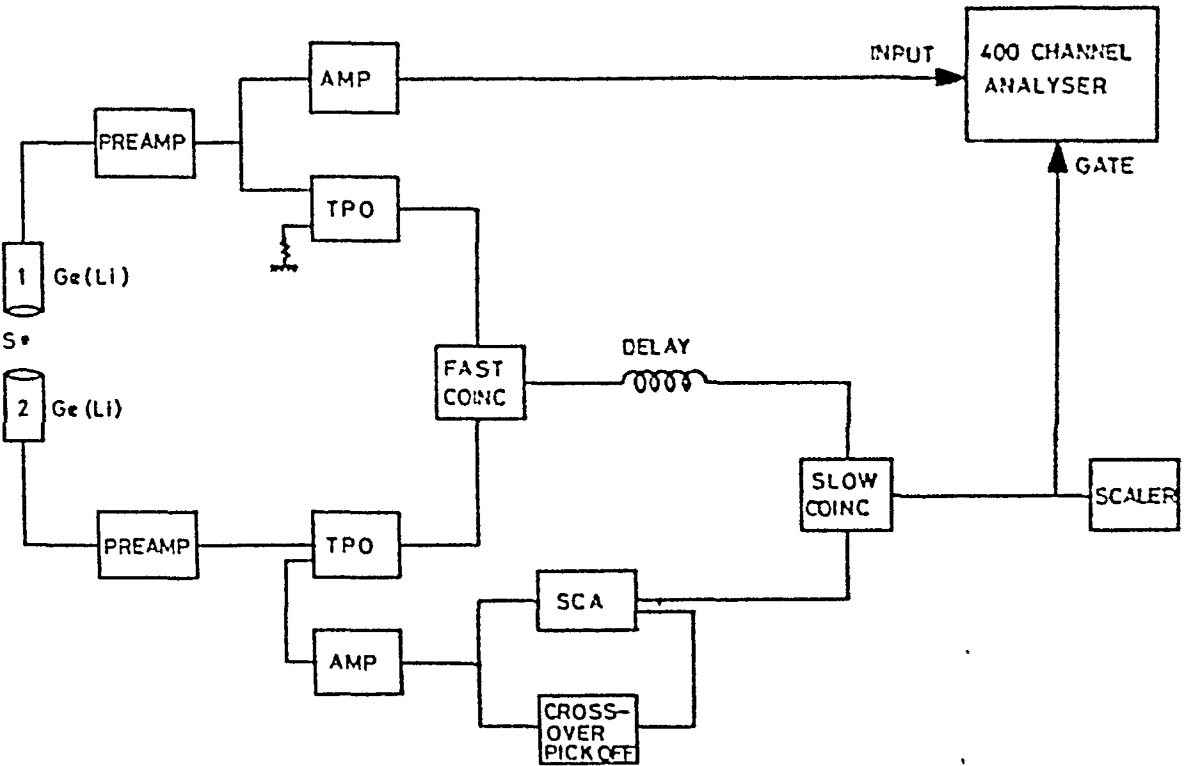
level at 319.5 keV for their explanation.

The spectrum taken with 390.9 keV gate established the transitions 409.9-91-0 and 685.8-489.9-91 without giving any indication of 320.9 keV level. 182 keV gate coincidence spectrum showed 319.5-182, 189.9-182 and 531-182 transitions clearly. Another spectrum was taken with 211.5 keV gate which confirmed the transitions 685.8-531-319.5-0 and 725-531-319.5 with a very small indication of the transition 319.5-182 and did not indicate the existence of any level at 211.5 keV as suggested in reference (1).

The level scheme of ^{147}Pm based on our studies is shown in Fig. 2. The level and the transitions shown with dotted lines are the ones which get evidences either from the singles spectra or from quite weak indications in the coincidence spectra. The present work combined with the earlier sum coincidence measurements shows beyond any doubt that there are no levels at 211.5, 320.9, 471, 552 and 763 keV in ^{147}Pm which were reported by Das'andy et al[1].

REFERENCES

1. D. Bas'andy and A.A. El-Naliem; Z. Naturf. 22A, 154 (1967).
2. C. [illegible], G.K. Mehta, S.K. Chaturvedi and N. Nath (to be published).



Ge(Li) – Ge(Li) fast slow coincidence set up.

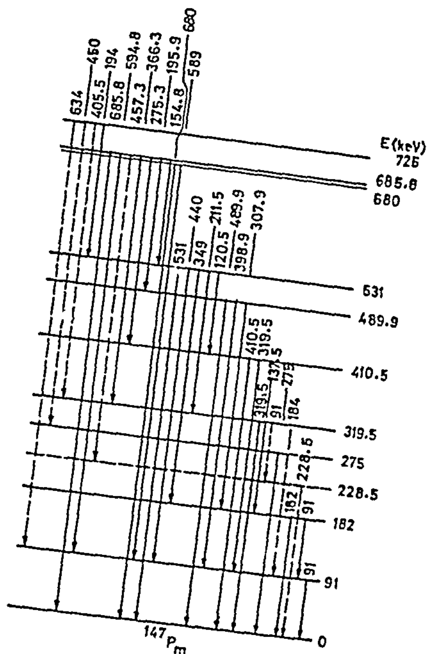


FIG. 2

Fig. 2. Level scheme of ^{147}Pm.

DISCUSSION

B.B. Singh: What was the duration of time in which sum peaks in singles were observed.

R. Singh: It was about half an hour. In fact the source was quite strong.

K.P. Gopinathan: 1) What are the firm evidence for the 182 keV level? 2) What accuracy can you place on the energies of the levels from the cascade cross-over consistency? 3) I have looked for a possible 91 keV transition from a 182 keV level with a Ge(Li) detector of resolution $<$ 0.5 keV but failed to find it. I strongly suspect possibility of impurity in your sample.

R. Singh: 1) The 91 keV gate coincidence spectrum give a beautiful peak at 91 keV and the 182 keV gate spectrum gives 137.5 keV, 307.9 and 349 keV peaks. 2) This is 0.5 keV. 3) No matter what is the resolution of the detector, singles spectrum is not enough to exclude this level because the 182 keV transition is quite weak. We have worried enough to look for the impurities.

DECAY OF ^{115m}Cd AND THE EXCITED LEVELS OF ^{115}In

S.N. Chaturvedi[+], C. Rangacharyulu[++], G.K. Mehta[+] and N. Nath[+]
++ I.I.T., Kanpur; + Banaras Hindu University, Varanasi - 5.

I. INTRODUCTION

Radioactive decay of 143 days ^{115m}Cd has been studied by several investigators[1-7]. Rao et al [4] proposed the decay scheme using electronic summing scintillation spectrometer and assigned new levels at 650 and 1560 keV along with several new gamma transitions. Subsequently Graefee et al [6] studied the decay scheme of ^{115m}Cd and ^{115g}Cd using Ge(Li) - NaI(Tl) coincidence measurements. They have indicated new levels at 828 and 936 keV following the decay of ^{115m}Cd and several gamma components reported by Rao et al have not been observed in their studies. However among all the earlier studies there has always been some inconsistencies in the number of levels and the number of gamma transitions. The present investigation has been carried out to examine the inconsistancies in more details employing Ge(Li) detector and sum coincidence scintillation spectrometer.

II. EXPERIMENTAL DETAILS

Singles spectra were taken with Ge(Li) detector having 3 keV resolution at 662 keV. A conventional fast - slow sum coincidence set-up is used in present studies. The 56 AVP tubes mounted with 1½" x 2" NaI(Tl) crystal were used as scintillation detecto

resolving time of fast coincidence circuit was 30 ns. The sum gate width used was about 50 keV.

III. RESULT AND DISCUSSIONS

The singles spectrum of ^{115m}Cd in two energy ranges were taken to cover the entire range of gamma rays. Several such spectra were recorded at different time intervals in order to follow the half life of observed gamma rays before ascribing each to the decay of ^{115m}Cd. Several impurity peaks are present in the spectrum and ^{134}Cs is found to be one of them. Gamma rays of following energies were observed in the decay of ^{115m}Cd : 106, 157, 227, 336, 485, 492, 592, 828, 934, 1133, 1290, 1420 and 1450 keV.

The sum coincidence spectra were recorded at 1450, 1420, 1290, 1133, 934 and 598 keV gates. In the analysis of spectra the effect of photo-compton summing was also accounted.

The sum coincidence spectra at 1450 keV gate does not provide any cascade transition. The 1450 keV gamma ray observed in the Ge(Li) singles spectrum is due to a cross-over transition.

The sum coincidence spectrum at 1420 keV gate gives the gamma rays of energies 227, 485, 592, 828, 934 and 1133 keV which are clearly observed in the spectrum. These are ascribed to the following decay modes :

1420 ⟶ 1133 ⟶ 0; 1420 ⟶ 934 ⟶ 0 and 1420 ⟶ 828 ⟶ 0.

This provides and evidence for a level at 828 keV. The 1420 keV gamma ray observed in Ge(Li) spectrum shows a cross-over transition from this level.

The spectrum gated at 1290 keV shows the existence of 167 and 1133 keV gamma rays due to 1290→1133→ 0 decay mode. A cross over transition from this level is also observed in Ge(Li) spectrum.

The spectrum gated at 1133 keV does not show any genuine gamma ray peak. The 1133 keV gamma ray observed in singles spectrum leads us to the conclusion that 1133 keV level has only a cross-over transition.

The sum coincidence spectrum at 934 keV gate gives an indication of 106 and 828 keV pair. This can be accounted as 934⟶828⟶0 decay mode. Thus here is an additional evidence for the existence of 828 keV level and a gamma ray of energy 106 keV. A cross-over transition from 934 keV level is also observed in the Ge(Li) singles spectrum.

The sum coincidence spectrum at 598 keV gate gives an indication of 106 and 492 keV gamma rays which can be ascribed to the 934⟶828⟶336 keV decay mode. *This also confirms the level at 828 keV and the gamma* rays of 106 & 492 keV energies.

The 828 keV level is based on the evidences from 1420 and 934 keV gated spectra. The 1420 keV gated sum coincidence spectrum clearly indicates a new transition of 592 keV between the 1420 and 828 keV states. The 934 and 598 keV gated spectrum confirms the existence of 106 and 492 keV gammas and a level at

828 keV which is also in accordance with Graefeé et al [6]. Like most of the earlier studies except Graefee et al we also find the existence of 287 keV gamma ray arising between the 1420 and 1133 keV states. In present investigation we do not find any evidence for levels at 650 and 1560 keV reported earlier by Rao et al [4].

A level scheme of ^{115}In from the decay of ^{115m}Cd has been constructed based on the present studies and is shown in figure 1 .

REFERENCES

1. J.B. Van Den Kool et al; Physica 29 (1963) 140
2. R.P. Sharma & H.G. Devare; Phys. Rev. 131 (1963) 384
3. J.P. Hurley et al; Nucl. Phys. 47 (1963) 93
4. V.V. Rao et al; Nucl. Phys. 51 (1964) 442
5. V.R. Pandharipande et al, Phys. Rev. 136 (1964) 346
6. G. Graefee et al; Phys. Rev. 149 (1967) 884
7. J. McDonal et al; Nucl. Phys. A104 (1967) 177.

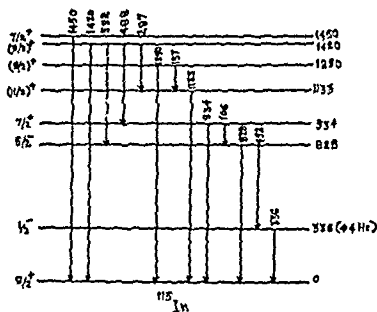


Fig.1. DECAY SCHEME OF ^{115m}Cd

DISCUSSION

K.L. Narasimham: Please explain the method of distinguishing between the results inferred from the sum coinc. spectra at 1450 and 1420 since the full energy peak at this energy extends by 140 keV however accurately the window is set.

S.N. Chaturvedi: There was a gate width of ± 75 keV only in each case and thus there is no question of interference in 1420 and 1450 keV gate spectrum.

K.G. Prasad: There has been extensive studies on the decay of ^{115m}Cd by various methods. What is the purpose of studying this by the sum coincidence method?

S.N. Chaturvedi: Recent studies by Graefee et al has shown some confusion in the population of ^{115}In levels following the decay of ^{115m}Cd particularly the (106 + 492) keV cascade transition. Present studies were made to see such inconsistencies in more details and a level scheme consistent with singles and sum-coincidence studies has been proposed. However, spin and parity assignments of the higher excited states has not reached to a compromise as yet. To do this, relative intensity measurements has also been carried out and theoretical calculations will be made to have a compromise between the experimental and theoretical results.

P.G. Hansen: The sum-coincidence method permits one clean experiment, the selection of the highest sum line in the spectrum. For lower settings one gets false peaks. What have you done to get rid of these?

S.N. Chaturvedi: Sum-coincidence method for cascade studies is definitely troublesome at lower energy gates where true to chance coincidence ratio becomes poorer. But in our case the lowest sum peak gate was of 598 keV where we had true to chance ratio of the order of 20:1. However in the analysis part of the sum-coincidence spectrum several sum-gates were also taken into account for intercascade studies.

SUM COINCIDENCE STUDIES ON ^{131}Ba

C. Rangacharyulu and G.K. Mehta
Department of Physics
Indian Institute of Technology, Kanpur-16

The gamma rays following the electron capture decay of ^{131}Ba have been investigated by many workers[1-5]. The present investigation was undertaken to assign the gamma ray energies precisely and to establish the genetic relations of the gamma rays.

The measurements were done in two stages. In the first, singles spectra were recorded with a Ge(Li) detector of resolution FWHM~3keV at 662keV. The spectra were recorded at regular intervals to follow the decay of gamma rays. This was done to ensure that the gamma rays being considered are really of ^{131}Ba. Some impurity gamma rays were also observed but those could be easily distinguished from the genuine ones. With these studies, the gamma rays of ^{131}Ba are found to be of the following energies: 54.6; 78.9; 82.3; 92.2; 123.5; 133.4; 157.3; 215.7; 239.6; 247.0; 249.5; 294.5; 373.0; 404.3; 420.3; 451.6; 461.5; 480.6; 486.5; 496.5; 572.0; 585.0; 620.0; 675.4; 696.3; 832.7; 915.0; 924.9; 959.9 and 1048.4 keV.

Second stage was the sum coincidence studies using a pair of scintillation detectors. The detectors were of 1½"ϕ x 2" NaI(Tl) crystals mounted on 56 AVP photomultiplier tubes. The spectrometer also has fast-slow coincidence with a fast resolving time 2τ≈30 n sec. The block diagram of the set up is shown in Fig. 1.

Sum coincidence spectra were recorded with gates at 1048, 925, 833, 696, 620, 404, 373 and 216 keV. There are no levels at 925, 833 and 404 keV, but these spectra were recorded to study the double cascades in 1048.4→123.5, 1013.5→215.7 and 620.0→215.7 keV modes of decay.

Horen et al[1] reported a transition of 967 keV as 1048.4→78.6 mode of decay. Murthy et al[3] confirmed this but Mangal et al[5] rule out this possibility. In our present investigation, we observe a 969 keV gamma ray in Ge(Li) spectrum. Our 1048 keV gated sum coincidence spectrum also gives a clear indication of 967 and 79 keV pair. These two observations lead to the conclusion that 1048→79 keV transition exists.

The sum coincidence spectrum with gate at 697 keV showed a pair of gamma rays of energies 528 and 169 keV. To fit this gamma pair in the decay scheme, we have to include a level at 528 keV. As can be seen later, there is further evidence for 528 keV level from 404 keV gated sum coincidence spectrum.

The sum coincidence spectrum at 585 keV gate shows '' two pairs of gamma rays, 506, 79 and 369, 216. The former pair is recently reported by Kucarova et al[4] and the latter by Mangal et al[5]. The pair 506, 79 keV gamma rays leads to the inclusion of a transition 585.0→ Mangal et al[5] explained the gamma pair 369 and 216 keV as 585→373→ mode of decay. But our Ge(Li) spectrum rules out the possibility of the existence of 212 keV gamma ray, whereas 369 keV is not completel ruled out. So our results favour the 585→215.7→0 mode of decay.

The sum coincidence spectrum with gate at 404 keV. shows a gamm pair 312 and 92 keV which could be explained only as 528→215.7→123 mode of decay. Thus here is another evidence for the existence of a level at 528 keV.

Karlsson[2] with his Ge(Li) studies proposed a new gamma ray of energy 324 keV as 697→373 mode of decay. We do not get any indicati for this gamma ray.

Horen et al[1] reported the following cascade modes of decay of

not [illegible] the [illegible] in our [illegible] coincidence spectrum with [illegible] at 216 keV. [illegible] our Ge(Li) singles spectrum shows gamma [illegible] of energies 70.0; [illegible] 92.[illegible] 133.5 and 153.4. There is no [illegible] of 137.4 keV [illegible] in this spectrum. Thus we conclude that the first two modes of [illegible] exist, while the third mode of [illegible] 215.7→70.0→0 is doubtful.

CONCLUSION

[illegible] level at 529 keV, based on our sum coincidence spectrum with [illegible] at 6[illegible]7 keV and 404 keV.

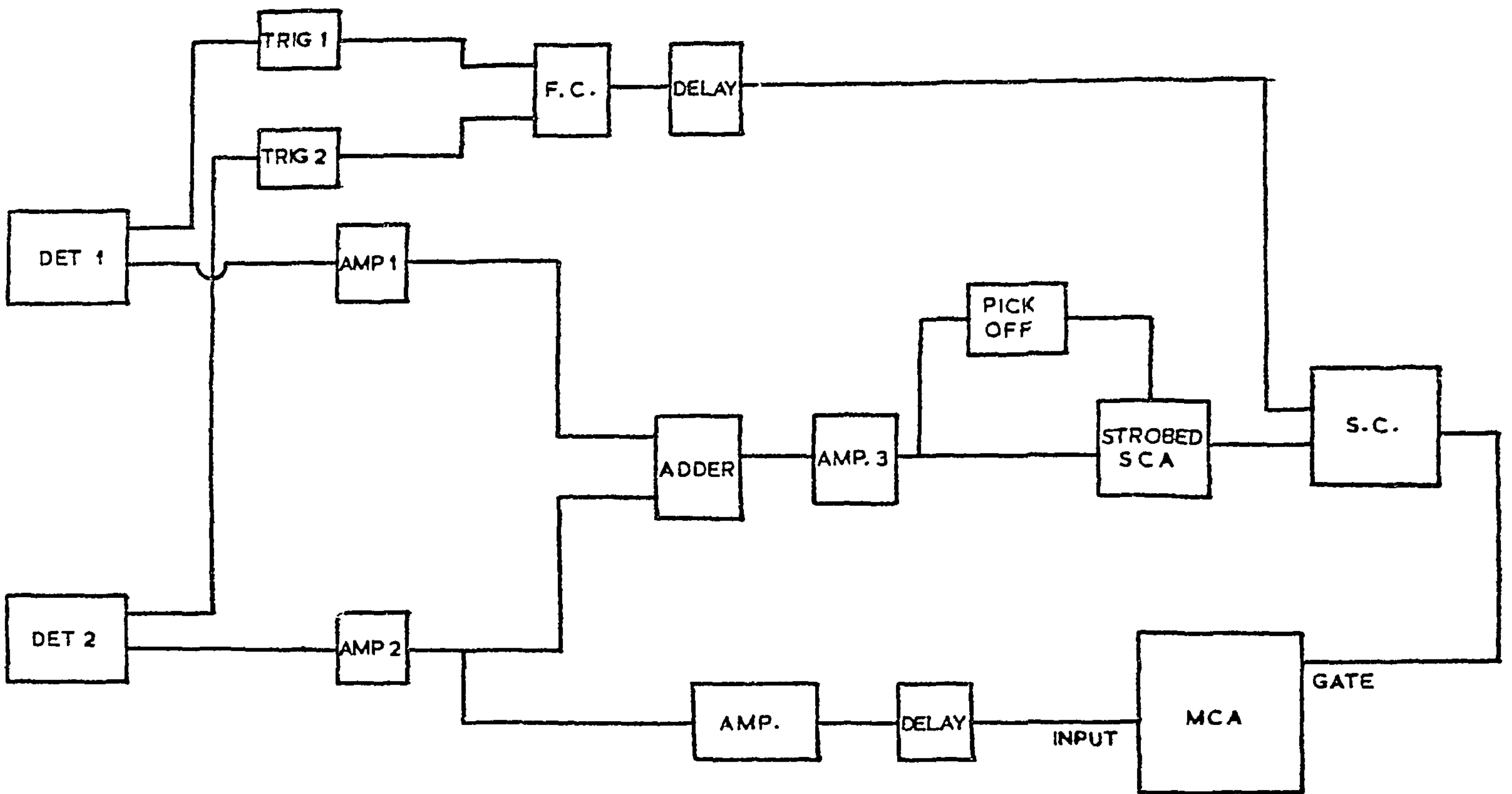
The transition [illegible]→70.[illegible] keV first reported by Kitamura et al[4] is confirmed in the present study. There is no evidence for 5[illegible]3 keV [illegible] reported by them. The evidence for 506 keV gamma ray comes from 5[illegible]5 keV gated sum coincidence spectrum. The same spectrum also provides evidence for coincidence between 216 and 360 keV [illegible]. This was first reported by [illegible] et al[5]. We differ from them in that our result favours the transition 505→215.7→0 mode of decay [illegible] 505→373.0→0 mode of decay proposed by them.

Our study does not give any positive evidence for the [illegible] 215.7→70.0 mode of decay.

A level scheme constructed to be consistent with our results is shown in FIG. 2.

[illegible]

[illegible] et al [illegible] 8135, (1964) 3[illegible]1
[illegible] 33 (1967) 47
[illegible] 21 (1967) [illegible]
[illegible] 7 (1963) 433
[illegible] (1966) 1[illegible]



SUM-COINCIDENCE SET-UP
FIG.1

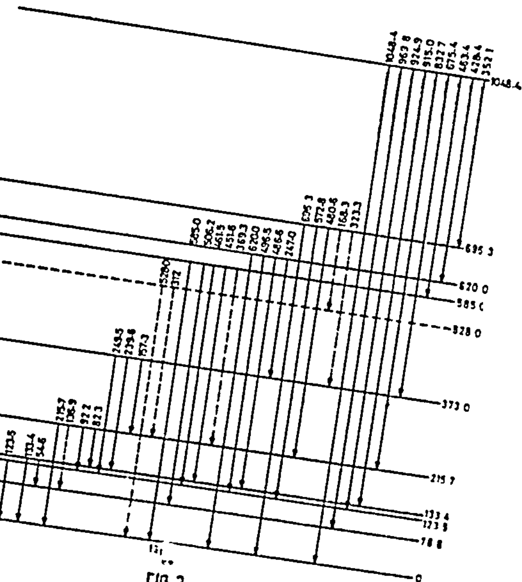

1048.4
963.8
924.9
915.0
832.7
675.4
453.4
428.4
352.1
1048.4
635.3
620.0
528.0
373.0
215.7
133.4
123.5
78.8
0

FIG. 2

DECAY OF Sr^{85m}.

K L NARASIMHAM, M N SITARAMANATH, AND V LAKSHMINARAYANA,
Laboratories for Nuclear Research, Andhra University, Waltair

AND

A P PATRO
Saha Institute of Nuclear Physics, Calcutta.

I. INTRODUCTION

The low lying levels of ^{85}Rb and ^{85}Sr are studied from ^{85m}Sr decay with scintillation and magnetic spectrometers[1]. There are no recent investigations on this decay except the measurement of ^{85}Sr ground state decay energy, of McDonnel et al[2]. The present study is undertaken to make a high resolution spectroscopic investigation of the gamma rays following ^{85m}Sr decay.

II. EXPERIMENTAL DETAILS

Enriched ^{86}Sr (98%) obtained from ORNL is bombarded with 14 MeV neutrons from the Cockcroft Walton accelerator* at SINP, Calcutta. The gamma spectra are recorded with a 2.5 c.c Ge(Li) detector(which gave a full energy peak of FWHM 2.5 keV for ^{137}Cs gamma rays) at the cyclotron division of the above institute.

A typical gamma spectrum recorded with Nuclear Data 512 analyzer is shown in Fig.1. The spectra are taken at regular intervals of 70 minutes and all the peaks in this spectrum are seen to follow this half-life characteristic of ^{85m}Sr. The

* The authors are thankful to Prof. S.K. Mukherjee for allowing us to carry out these irradiations.

energy calibration of the detector is ~~done~~ carried out by recording standard gamma spectra in presence of the experimental source. The relative photopeak efficiency data for this detector was obtained[3] using ^{152}Eu as standard. Using this data, the number of counts under the fullenergy peaks were corrected for detector efficiency to obtain the relative photon intensities. The errors in the relative intensities include the uncertainities in measuring the photopeak areas and those in the detection efficiency.

The energies and relative intensities obtained in the present work are shown in Table I along with the results of Sunyar[4]. ~~In the present study the peak at~~ The 232 keV peak in the scintillation spectrum of Sunyar is resolved now into two peaks at 232 and 237 keV in the present study.

III. <u>DISCUSSION</u>

The electron capture branching intensity to the 151 keV level in ^{85}Rb can be estimated provided the relative intensities of the unconverted gamma rays and conversion coefficients are known. For this purpose the conversion electron data of Sunyar et al is assumed. The ratio of the conversion electron intensities of the 151 and 232 + 237 keV transitions (obtained with a lens spectrometer~~s~~) and the K-conversion intensities of the 232 and 237 keV transitions (obtained with a 180° spectrometer) are assumed. From the present results and the above data, the K-conversion coefficients for 232 and 237 keV

transition are obtained and these are normalized relative to the K-conversion coefficient for the 151 keV transition[5]. These results are shown in Table II along with interpolated theoretical conversion coefficients (calculated taking into account the finite nuclear size, electron binding energies etc) of Haeger and Seltzer[6]. From these results the electron capture branching ratio is obtained as 12.9% The log ft value for this branching is calculated (using the value 1007 keV for the electron capture decay energy of ^{85}Sr ground state from the results of McDonnel et al) as 4.6 indicating an allowed nature for this transition.

The ground state spin and parity of ^{85}Sr and ^{85}Rb are known to be $\frac{9}{2}^{+}$ and $\frac{5}{2}^{-}$. It can be seen from the table that the present value of the conversion coefficient for the 232 keV transition is consistant with M1 + E2 nature. The conversion coefficient of the 237 keV transition however, suggests a E3 nature for this transition. In the earlier studies a spin of $\frac{1}{2}^{-}$ was suggested to the 237 keV state. This assignment needs the 237 keV transition to be M4. The theoretical value of the conversion coefficient for M4 is much larger (1.85) than the present experimental value. It therefore appears that either the character of the 237 keV state is $3/2^{-}$ or the ground and the 232 keV states, have spins 7/2+ and 9/2+ respectively. The allowed nature of the beta feeding to the 151 keV state of ^{85}Rb from the 237 keV state of ^{85}Sr cannot rule out the possibilities $1/2^{-}$ or $3/2^{-}$ for the 237 keV state.

TABLE I

Gamma energies and relative intensities in the decay of ^{85m}Sr.

Energy (keV)		Relative intensity	
Present work.	Sunyar et al.	present work.	Sunyar et al.
151.2	150	12.8 ± 1	16.53
232.1	225	100	100
237.8	233	4.8 ± .3	1.54
EK branching (1%)		12.5	14

TABLE II

K conversion coefficients for 232 and 237 keV transitions.

Transition Energy keV	Theoretical values			Present work	Sunyar
232.1	M1 .0164	E1 .009	E2 .0485	.023±.005	.026
237.8	M4 1.85	E3 .09	E4 .03	.16±.05	-

REFERENCES

1. Sunyar et al, Phy. Rev. 86 (1952) 1023.
2. Hollander, Table of Isotopes, 1968, John Wyly & Co. N.Y.
3. McDonnel et al, Nucl. Phy. 127, 85.
4. A.P. Patro et al, Private communication.(1969).
5. I. Bergstrom et al, Phy. Rev. 79 (1950) 537.
6. Haeger and E.C. Seltzer, Nuclear Data (1968) A4, 1.

COUNTS / CHANNEL (ARBITRARY UNITS)

151·2

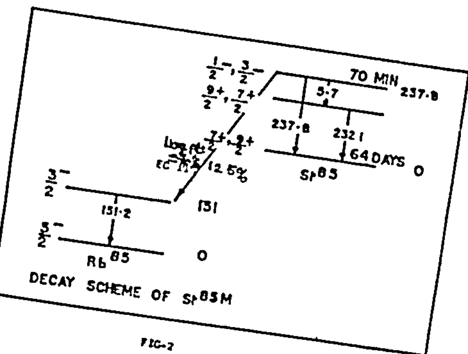
231·1

237·8

CHANNEL NUMBER

100 140 180 220

FIG 1. GAMMA SPECTRUM OF Sr 85M



DECAY SCHEME OF Sr 85M

FIG-2

BETA-GAMMA DIRECTIONAL CORRELATION MEASUREMENTS IN THE DECAY OF Pr-142.

A. KHAYYOOM, M.L. NARASIMHA RAJU and D.L. SASTRY
The laboratories for Nuclear Research, Andhra University, Waltair.

1. INTRODUCTION

The decay scheme of Rr-142 is known from earlier works[1]. The decay of Pr-142 proceeds to the first excited state of Nd-142 with an intensity of 3.7% which subsequently decays to the ground state by the emission of 1576Kev gamma radiation. The ground to ground beta transition taking place between Pr-142 and Nd-142 has intensity of 96.3%. The beta-gamma cascade which is of present interse follows the spin seuence $2^-(\beta)$ $2^+(\gamma)$ 0^+. The inner beta group has an end point energy of 582Kev and has an allowed spectral shape[4] with a log(ft) of 7.1. The (ξ) value for Pr-142 is 13.45 which is relatively larger than the end point energy 2.149mc^2 units . Thus here is a case with charecterstics which fits into the ξ approximation[2,3] The validity of the ξ approximation requires a first forbidden beta transition to exhibit all the allowed charecteristics concerning the log(ft) value (ie) shape and beta-gamma anisotropic. Hence a measurement of the beta-gamma anisotropy forms a critical test for the validity of ξ approximation. If the ξ approximation holds good the anisotropy is expected to be of small magnitude of order $1/\xi$. Previous data on directional correlation measurements

have been available only from the work of Hess et al[4]. They only mentioned that the anisotropy is of the order of zero with in experimental errors. However in this work one finds the absence of the actual energy dependence of the beta-gamma angular correlation function. So it is felt worth while to carry out a systematic measurement of the energy dependence of the beta-gamma directional correlation.

II. EXPERIMENTAL DETAILS

The experimental set-up consists of a conventional slow-fast coincidence spectrometer described else where[5]. The isotope Pr-142 is obtained from B.A.R.C. Bombay in the form of paroscodemium chloride in liquid form. The source is prepared by slowly evoparating to dryness a drpp of Pr-142 on a mylar film of thickness 0.6 mg/cm^2 over an area of 3mm diameter. A drop of insulin is added to the same to aid uniform spreading of the source. The source is centred properly so as to ensure that the variation of the count rate in the movable gamma detector is less than 1%.

In the integral correlation experiment beta particles of energy above 200Kev are accepted in the beta channel, and in gamma channel the photo-peak of 1576Kev gamma is accepted with a window of 150Kev. The differential correlation experiment was conducted at four beta energies in the range 200-500Kev in steps of 100Kev using a ten

channel analyzer.

III. RESULTS

The integral correlation data are fitted to the standard polynomial

$$W(\theta) = 1 + A_2P_2(\cos\theta) + A_4P_4(\cos\theta)$$

by the least squre fit due to Rose[6]. The angular correlation function after correcting for geometry of both the detectors is found to be

$$W(\theta) = 1 + (0.025 \pm 0.01169)\, P_2(\cos\theta) + (0.012 + 0.0148) \times P_4(\cos\theta)$$

The differential correlation data are summerised in table I, after correcting for gamma-gamma background and geometry of both the detectors. It may be noted that no resolution correction has been applied for the finate resolution of the beta spectrometer as the resolution correction is expected to fall with in the limits of exptal errors. From the table it may be noted that the beta-gamma anisotropy is very small and the energy dependance of the angular correlation function is also small. These two factors are consistent with the log(ft) value of the 582Kev beta transition and its allowed shape. Thus it may be concluded from the present work that the main features of the 582Kev beta transition in Pr-142 are in accordence with the validity of the ξ approximation.

TABLE I

Energy mc^2 units	Anisotropy A	Correlation co-eft. ϵ	Reduced correlation co-eft. ϵ'
1.391	0.008±0.019	0.005±0.012	0.008±0.018
1.587	0.018±0.023	0.013±0.015	0.013±0.016
1.783	0.045±0.026	0.032±0.017	0.026±0.013
1.979	0.042±0.022	0.03 ±0.015	0.02 ±0.009

REFERENCES

1) S. Raman Nucl. Phy. A113, 803 (1968)

2) Kotani T, Ross M, Phy. Rev 113,B 1467 (1965)

3) Kotani T, Phy. Rev. 114, 795 (1959)

4) R. Hess, P. Lipnik, F.S.Perdrisat and J.W. Sunier, Nucl. Phys 54, 673 (1964)

5) M.L. Narasimha Raju, D.L.Sastry and E. Kondiah; Nuovo Cemento 56,B29 (1968)

6) Rose M.E.; Phy. Rev. 91,610 (1953)

GAMMA-GAMMA ANGULAR CORRELATIONS IN Nd-147.

B.R. Sastry, K.L. Narasimham and D.L. Sastry.
The Laboratories for Nuclear Research,
Andhra University, Waltair, India.

I. INTRODUCTION

The properties of gamma transitions in ^{147}Pm were studied earlier[1,2] through gamma-gamma angular correlations following the beta decay of ^{147}Nd. Spring[3] studied the angular correlations for some of the cascades in ^{147}Nd and analysed the results assuming the 91 keV transition to be nearly 0-4% E2. The mixing ratios of the second transitions (in cascades involving 91 keV gamma ray) extracted were therefore associated with large errors. When the 440-91 cascade correlation is studied[2] employing conventional fast-slow arrangement, the observed coincidences had to be corrected for the 400-90 and 599-91 cascade contributions and the 533 keV intence transition which largely contributes to chance coincidences. Both these are eliminated when the coincidence spectra are recorded setting the sum coincidence gate at 533 KeV, in addition to the doubled efficiency inherent of the sum-coincidence arrangement. In the present investigation the 440-91 keV transition is studied using the sum-coincidence arrangement and the 6 599-91 keV transition is studied with a conventional fast-slow assembly.

II. EXPERIMENTAL

The source ^{147}Nd employed in this study is obtained from the BARC, Bombay. The sum coincidence arrangement consisted of two well matched 1½" X 2" NaI(Tl) -6292 crystal- photomultiplier combinations arranged in 7 cms geometry. The coincidence spectra were recorded on a 100 channel analyser at 90°, 135° and 180° angles between the detectors. These were employed, after correction for chance and detector geometry to fit in the

polynomial ofo the form $W(\Theta)= 1+ A_2P_2(\text{Cos}\ \Theta) + A_4P_4(\text{Cos}\Theta)$ and the angular correlation coefficients were calculated employing the White's method.

III. RESULTS

The A_2 and A_4 obtained for the two cascades studied presently are given below.

Cascade	A_2	A_4	$Q= \frac{\delta^2}{1+\delta^2}$
91-599 keV	0.01945±0.05	0.3679±0.054	0.18±0.14
91-440 keV	0.06295 ±0.0261	0.023 ±0.027	0.3 ±0.08

Assuming 0.8% E2 for the 91 keV transition[4] the mixings for 440 and 599 keV transitions are extracted using the single transition curves of Arns and Widenbeck[5].

IV. DISCUSSION

Assuming the 91 keV transition to be 0.8% E2, the present investigation yielded the quadrupole content of the 440 keV gamma ray to be (0.3 ± 0.08). This is in agreement with the value reported in ref.2. The quadrupole admixture for the 599 keV gamma ray is extracted to be(0.18 ± 0.14) which is consistant with a 5/2+ for the character of the 690 keV state. The higher value of the quadrupole admixture is ruled out on the basis of the δ^2 Vs energy curves due to Westemberger et al[6].

V. REFERENCES

1. Table of Isotopes 1968.
2. M.S. Rajput et al, Indian Journal of Physics, 42, 7(393) 1968.
3. Spring , Physics Letters, 7, 218, 1963.
4. Ranakumar N., Ph.D. Thesis.
5. Arns and Widenbeck, Physical Review, 111, 1623.
6. Westenberger et al , Phy. Rev., 123, 1812, 1963.

DECAY OF EUROPIUM-148*

V.Lakshminarayana
Laboratories for Nuclear Research,
Andhra University, Waltair

and

J.H.Hamilton, S.Brahmavar and D.Dunn
Vanderbilt University, Nashville, U.S.A.

I INTRODUCTION

Negative parity states with spins between 1 and 5 are expected as a result of interaction between quadrupole and octupole vibrations in spherical even-even nuclei. Some of these states were located in ^{148}Sm in earlier studies. Decay of ^{148}Eu provides a convenient means to look for these states the ground state character of ^{148}Eu being 4$^-$. A number of energy levels in ^{148}Sm were introduced by Cline[1] based on his studies using a Ge(Li)-NaI(Tl) system essentially by energy sums. In particular this study could not resolve the coincidence relationships for gamma energies 550 and 553 keV and 611 and 630 keV. The present study is therefore carried out with two Ge(Li) detectors and the Nuclear Data 2048 multi-parameter counting system.

II Experimental Details

^{148}Eu source is produced by (p,2n) reaction on enriched ^{149}Sm at a 12 MeV proton energy in ORNL cyclotron. A small quantity of the source contained in a perspex source holder is held symmetrically between the two detectors. The Ge(Li) detectors are of 50 c.c.

* Work carried out at Vanderbilt University

each and yielded a resolution of 2.8 KeV for ^{60}Ni 1332 KeV gamma rays. A block diagram of the experimental set-up is shown in Fig. 1. Singles spectrum, background spectrum and singles spectrum with external standards are recorded each for 12 hours. The 4096 X 4096 coincidence data is recorded on magnetic tapes for 4 days. During this time X and Y projections are stored alternatively in the system memory. Later the magnetic tape data is used to successively feed back into the system memory the coincidence spectra for 8 selected gates and the corresponding background. The background subtracted spectra for gates 414, 550, 553, 611, 630, 870, 1034 and 1622 KeV are used in the final interpretation.

III Results and Discussion

The coincidence data ... mmarised in Table 1. The level scheme of ^{148}Sm ... from the coinci-
dence data is shown in Fig. ... dev
fr ... results of Cline a ... udi
... re summarised b
(a) ... transition i.
and ... instad of
... in earl
(b) ... 53)
...
... transi
states to ...

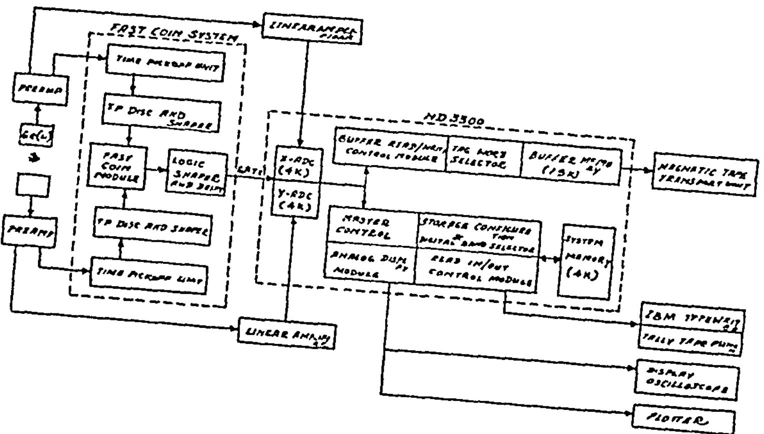


Fig. 1. Block diagram of the experimental arrangement.

TABLE 1

COINCIDENCE DATA

Gate Energy (KeV)	Coincident Gammas (KeV)
1622	550,630
1034	550,630
870	550,611,770,799
630	311,414,502,550,553,620,654, 683,715,726,896,916,930,968, 990,1014,1034,1104,1147,1207, 1236,1310,1344,1461,1543, 1622 and 1650
611	311,414,433,550,572,654,683, 799,870,1063,1329 and 1363
553	414,433,550,611,630,654,683
550	All gammas for 611 and 630 KeV gates. Additional lines at 1183,1355,1409 and 1560
414	coincidences supporting above data

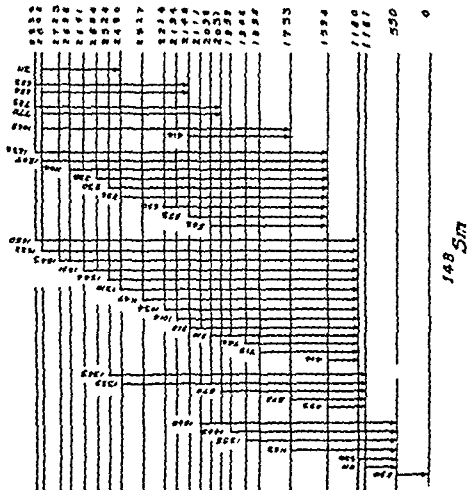


Fig.2. Level scheme of ^{148}Sm to account for the coincidence data

(c) Two new levels at 1959 and 2111 KeV are introduced to account for the 1409 and 1561 KeV lines in the coincidence spectrum with gate 550 KeV.

(d) Two new levels at 2584 and 2698 KeV are introduced to account for the 990 and 1104 KeV lines in the coincidence spectra with gates 414, 550 and 630 KeV.

The level scheme shown in Fig.2 differs considerably from that shown in the table of isotopes[2].

REFERENCES

1. J. Cline Nuclear Physics 96, 97 (1967)

2. Table of Isotopes : C.M.Lederer, J.M.Hollander and I.Perlman, 6th edition, John Wiley (1968)

TRIPLE GAMMA COINCIDENCE AND ANGULAR CORRELATION STUDIES IN Cd^{110} FROM THE DECAY OF Ag^{110m}

U.S. Pande and B.P. Singh
Physics Department, University of Roorkee, Roorkee

I. INTRODUCTION: Decay Scheme of Cd^{110} following the decay of Ag^{110m} has been studied by many investigators.[1] Gamma-gamma angular correlation studies do not reveal unique value of spins of the excited levels involved and multipolarity of the transitions are different by different workers, therefore triple gamma angular correlation studies are taken up.

II. EXPERIMENTAL SET UP: Three NaI(Tl) detectors (spectrometers) have been used for the triple gamma coincidence and angular correlation studies. The mounting of these three detectors have been done in two geometries. (1) Putting all the three detectors in the plane of the table equidistant from the source. The two detectors are fixed perpendicular to each other and the third detector is movable in opposite quadrant, one of the fixed detector always detects the first gamma of the cascade. The other two detectors detect the 2nd and third gamma rays of the cascade, let us call this the 'P' geometry. (2) Two detectors are in the plane of the table and one perpendicular to the plane of the table. All the three are equidistant from the source. One of the detectors, on the plane of the table is fixed and always detects the first gamma ray of the cascade and the other one is movable. The detector perpendicular to the plane of the table is fixed and makes the angle of 90° with both the detectors, let us call this the C geometry. Two coincidence units are used in these studies. A gate of gamma-gamma coincidence of 658 keV (selecting in 4 volts channel width) and 884 keV (in integral spectrum above 500 keV) is formed using one coincidence unit. This gate is one of the input of the

second coincidence unit and other input of the 2nd coincidence unit is from the first detector which scans the spectrum in one volt channel width. The single gamma ray spectrum along with triple gamma ray spectrum is shown in Fig.1(a) which clearly indicates the peak corresponding to 1384 keV-884 keV-658 keV cascade.

RESULTS: The angular correlation studies are done keeping the 1384 keV at photopeak in 4 volts channel width and other gamma rays are selected as mentioned above. The movable detector was kept at various angles of 90°, 112.5°, 135°, 157.5° and 180°. The angular correlation function was calculated by the method of least square fit(The results are obtained without applying solid angle correction ,this correction is considered in the theoretical calculations of angular correlation coefficients). The correlation function thus obtained are:

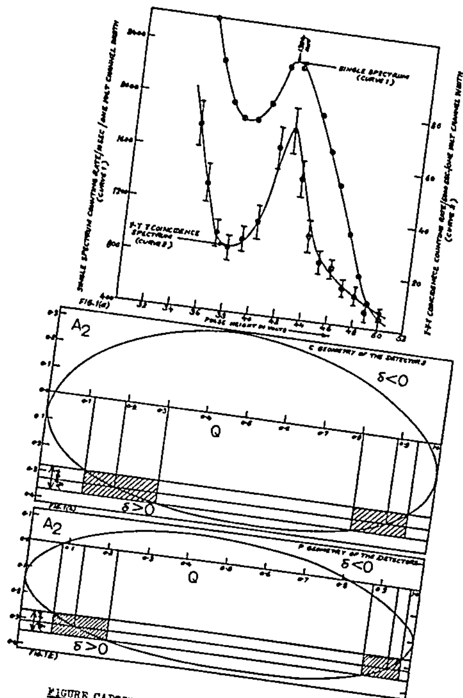
For P geometry $W(\theta) = 1 - (0.317 \pm 0.036) P_2(\cos\theta) + (0.030 \pm 0.042) P_4(\cos\theta)$

For C geometry $W(\theta) = 1 - (0.324 \pm 0.043) P_2(\cos\theta) + (0.080 \pm 0.070) P_4(\cos\theta)$

DISCUSSION: Level scheme for this cascade is given[1] as

$6,5,4+ \xrightarrow[(M_1+E_2)?]{1384\,keV} 4+ \xrightarrow[E_2]{884\,keV} 2+ \xrightarrow[E_2]{658\,keV} 0+$
?

884 keV and 658 keV are taken to be pure E_2 by experimental studies (mainly conversion coefficient ~~data~~ and gamma-gamma angular correlation data). 1384 keV is taken to be mixture of dipole and quadrupole radiations. The theoretical plot for angular correlation coefficient A_2 versus Q ($Q = \delta^2/1+\delta^2$ where δ is amplitude mixing parameter) has been done for both the geometries P and C taking spin 5 to 2926 keV level by the method already reported.[2] It has been shown by Litherland et al.[3] that if both 884 keV and 658 keV gamma rays are E_2 then if detectors detecting 2nd gamma ray and third gamma ray of the cascade are interchanged, the triple gamma angular correlation coefficients are the same. The A_2 exp. in c geometry cuts the



<u>FIGURE CAPTION</u>

Fig.1(a) Triple gamma coincidence spectrum alongwith single specturm.

Fig.1 b) Theoretical plot of A_2 versus Q for the 'C' geometry of the detectors.

Fig.1 c) Theoretical plot of A_2 versus Q geometry of the detectors.

graph (A_2 versus Q) at two points giving $Q_1 = 0.18^{+0.12}_{-0.08}$ and $Q_2 = 0.89^{+0.06}_{-0.09}$. The latter value is rejected on the basis that 1384 keV is mainly M_1 with mixture of E_2. The $A_2^{exp.}$ in Þ geometry cuts the graph (theoretical A_2 versus Q) giving $Q_1 = 0.155^{+0.085}_{-0.06}$ and $Q_2 = 0.94^{+0.04}_{-0.06}$. The latter value is rejected as done in P geometry. The Q_1 in two geometries are almost same within experimental error. The mean value thus is $Q_1 = 0.17^{+0.13}_{-0.07}$ giving $\delta = 0.45^{+0.20}_{-0.12}$. Similar plots of A_2 versus Q were done taking the spin value of 6 and 4 for 2926 keV level in both the geometries The experimental value neither touches the curves nor cuts it Thus these spin values of 6 and 4 are rejected.

Therefore this study gives the spin value of 5 to the 2926 keV level with $Q = 0.17^{+0.13}_{-0.07}$ for 1384keV transition.

REFERENCES:

1. Table of Isotopes, C.M. Lederer et al. (1965) Sixth Edition John Wiley and Sons Inc. New York, LONDON. Nuclear Data Sheets (1959-65) Academic Press, New York, London.
2. U.S. Pande and B.P. Singh, Indian Journal of Pure and Applied Physics, Vol.8, July 1970 p. 401-405.
3. Litherland, A.E. and A.J. Ferguson 1961, Canad. J. Phys. 39, 788.

DISCUSSION

N.G. Puttaswamy: What are the new assignments from these studies?

U.S. Pande: Spin of 5 is confirmed for 2926 KeV level. Spin value of 4 and 6 are rejected by these studies.

GAMMA-GAMMA-GAMMA DIRECTIONAL ANGULAR CORRELATION STUDIES IN Dy^{160} FROM THE DECAY OF Tb^{160}

U.S. Pande and B.P. Singh
Physics Department, University of Roorkee, Roorkee

The sign of $\delta(\langle I \| L'\pi' \| I \rangle / \langle I \| L,\pi \| I \rangle)$, the amplitude mixing ratio of gamma transition has been the subject of investigation by gamma-gamma angular correlation studies. The importance of the sign of the 'δ' has been arroused by K. Kumar,[1] if the determination of sign of δ is independent of phase convention. The opposite sign of 'δ' has been obtained for the middle gamma of three gamma cascadé when the angular correlation of Ist and 2nd and the angular correlation of 2nd and 3rd cascade are done. It means that if the angular correlation studies of three gamma cascade (using three detectors) are done the sign of δ should always be negative due to phase convention (according to Biedenharn and Rose[2] definition) and therefore the absolute sign of 'δ' shall be positive if the experimental value obtained by triple gamma angular correlation is negative, and negative if experimental value is positive. This gives the importance of three gamma cascade angular correlation studies.

Decay of Tb^{160} to Dy^{160} has been studied by many workers.[3,4] There is a very intense three gamma cascade of 298 keV - 879 keV - 87 keV. 879 keV transition is definitly the admixture[3,4] of M_1 and E_2 which is the middle gamma. 298 keV is taken as pure E_1 (but recently[4] small admixture of M_2 has also been considered, but this does not effect the sign of δ in 879 keV transition in which we are interested) and 87 keV is taken[3,4] as pure E_2

Three NaI(Tl)(detectors) spectr ters used.
The mounting of these detectors have
geometries: (i) Putting all the th
plane of the table equidistant fro
detectors are fixed perpendicular

third is movable in the opposite quadrant. The movable detector detects the third gamma of the cascade. The two fixed detectors detect the Ist and 2nd gamma rays of the cascade (say this the 'p' geometry). (ii) In the second geometry two detectors are in the plane of the table and one perpendicular to the plane of the table which is fixed and detects the 2nd gamma of the cascade (say this the 'c' geometry). One detector in the plane of the table is fixed and always detects the first gamma of the cascade and other one in the plane, is movable making angles, of 90^{o} to 180^{o} with the detector in the plane of the table. The liquid source in the form of $TbCl_3$ in HCl was sealed in a perspex container of 3mm x 3mm.

Two coincidence units of the resolution of the order of 10^{-7} sec. are used. The gamma-ray in 2 volts (1 volt=10keV) channel width at 87 keV was chosen in movable detector (spectrometer). Gamma ray in another detector (assigned to detect 2nd gamma of the cascade) are chosen above 500 keV using it as integral. These are the inputs for the Ist coincidence unit. The out put of this coincidence unit forms the gate for the input of the 2nd coincidence unit and other input is from the detector assigned to detect the Ist gamma of the cascade, which scans the spectrum in one volt channel width. Thus the triple coincidence alongwith single spectrum is shown in Fig.1 (chance coincidence counts has been subtracted after putting delay in 2nd coincidence unit). The peak due to 298 keV cascade is clearly indicated alongwith Compton distribution. Considering the decay scheme the Compton contribution of other four'three triple gamma cascades' shall also be in the photopeak of 298 keV. But this shall not be more than 5% and does not effect our results.

The angular correlation studies were made keeping

the gamma ray at photopeak of 298 keV in 4 volts channel width. The angular correlation result by the method of least squ-re fit without applying solid angle correction are as follows

P geometry $W(\theta) = 1 - (0.217 \pm 0.042) P_2(\cos\theta) + (0.076 \pm 0.046) P_4(\cos\theta)$

C geometry $W(\theta) = 1 - (0.127 \pm 0.017) P_2(\cos\theta) - (0.047 \pm 0.020) P_4(\cos\theta)$

The theoretical plot angular correlation coefficients A_2 versus $Q (Q = \delta^2/1+\delta^2)$ has been done for both P and C geometry taking the spin sequence as $2^- \xrightarrow[E_1]{298\,\mathrm{KeV}} 2^+ \xrightarrow[(E_2+M_1)]{379\,\mathrm{KeV}} 2^+ \xrightarrow[E_2]{597\,\mathrm{KeV}} 0^+$ by the method already reported.[5]

Fig.2 and 3 give the theoretical plot of A_2 versus Q for C and P geometry respectively. The experimental value as shown in graph cuts the curve giving the range of Q from 0.73 to 1.0 $\delta > 0$ in C geometry and $Q_1 = 0.02^{+0.20}_{-0.01}$ $\delta < 0$ and $Q_2 = 0.98 \pm 0.01$ $\delta > 0$ in P geometry. 'δ' should have the same sign in both the geometry therefore Q_1 in P_2 geometry is rejected while Q_2 is taken. The mean value of Q lies from 0.73 to 1.00 in C_2 geometry on the other hand the value in P_2 geometry is 0.98 ± 0.01. Considering the small error in this value and this value lies in the range of Q obtained in C geometry it is more appropriate to take $Q = 0.98 \pm 0.01$ giving $\delta = +7.00^{+2.95}_{-1.36}$. The absolute sign of δ should be negative to make experimental sign of 'δ' positive. The δ with absolute sign is $-7.00^{+2.97}_{-1.38}$.

REFERENCES

1. K. Kumar Phys. Letters Vol. 29B No.1(1969).
2. L.C. Biedenharn and M.E. Rose, Rev. Mod. Phys. 25,729 (1953).
3. Nuclear Data Sheets (1959-65) Academic Press, New York.
4. J.M. Jaklevic, et al. Nucl. Phys. A99 (1967) 83-99.
5. U.S. Pande and B.P. Singh, Ind. J. Pure and Applied Phys. Vol.8, July (1970) p.401-405.

third is movable in the opposite quadrant. The movable detector detects the third gamma of the cascade. The two fixed detectors detect the Ist and 2nd gamma rays of the cascade (say this the 'p' geometry). (ii) In the second geometry two detectors are in the plane of the table and one perpendicular to the plane of the table which is fixed and detects the 2nd gamma of the cascade (say this the 'c' geometry). One detector in the plane of the table is fixed and always detects the first gamma of the cascade and other one in the plane, is movable making angles, of 90° to 180° with the detector in the plane of the table. The liquid source in the form of $TbCl_3$ in HCl was sealed in a perspex container of 3mm x 3mm.

Two coincidence units of the resolution of the order of 10^{-7} sec. are used. The gamma-ray in 2 volts (1 volt=10keV) channel width at 87 keV was chosen in movable detector (spectrometer). Gamma ray in another detector (assigned to detect 2nd gamma of the cascade) are chosen above 500 keV using it as integral. These are the inputs for the Ist coincidence unit. The out put of this coincidence unit forms the gate for the input of the 2nd coincidence unit and other input is from the detector assigned to detect the Ist gamma of the cascade, which scans the spectrum in one volt channel width. Thus the triple coincidence alongwith single spectrum is shown in Fig.1 (chance coincidence counts has been subtracted after putting delay in 2nd coincidence unit). The peak due to 298 keV cascade is clearly indicated alongwith Compton distribution. Considering the decay scheme the Compton contribution of other four'three triple gamma cascades' shall also be in the photopeak of 298 keV. But this shall not be more than 5% and does not effect our results.

The angular correlation studies were made keeping

the gamma ray at photopeak of 298 keV in 4 volts channel width. The angular correlation result by the method of least squ're fit without applying solid angle correction are as follows

P geometry $W(\theta) = 1 - (0.217 \pm 0.042) P_2(\cos\theta) + (0.076 \pm 0.046) P_4(\cos\theta)$

C geometry $W(\theta) = 1 - (0.127 \pm 0.017) P_2(\cos\theta) - (0.047 \pm 0.020) P_4(\cos\theta)$

The theoretical plot angular correlation coefficients A_2 versus $Q (Q = \delta^2/1+\delta^2)$ has been done for both P and C geometry taking the spin sequence as $2^- \xrightarrow[E_1]{299\ \mathrm{KeV}} 2^+ \xrightarrow[(E_2+M_1)]{319\ \mathrm{KeV}} 2^+ \xrightarrow[E_2]{97\ \mathrm{KeV}} 0^+$ by the method already reported.[5]

Fig.2 and 3 give the theoretical plot of A_2 versus Q for C and P geometry respectively. The experimental value as shown in graph cuts the curve giving the range of Q from 0.73 to 1.0 $\delta > 0$ in C geometry and $Q_1 = 0.02^{+0.20}_{-0.01}$ $\delta < 0$ and $Q_2 = 0.98 \pm 0.01$ $\delta > 0$ in P geometry. 'δ' should have the same sign in both the geometry therefore Q_1 in P_2 geometry *is rejected while Q_2 is taken. The mean value of Q lies* from 0.73 to 1.00 in C_2 geometry on the other hand the value in P_2 geometry is 0.98 ± 0.01. Considering the small error in this value and this value lies in the range of Q obtained in C geometry it is more appropriate to take $Q = 0.98 \pm 0.01$ giving $\delta = +7.00^{+2.95}_{-1.36}$. The absolute sign *of δ should be negative to make experimental sign of 'δ'* positive. The δ with absolute sign is $-7.00^{+2.97}_{-1.38}$.

REFERENCES

1. K. Kumar Phys. Letters Vol. 29B No.1(1969).
2. L.C. Biedenharn and M.E. Rose, Rev. Mod. Phys. 25,729 (1953).
3. Nuclear Data Sheets (1959-65) Academic Press, New York.
4. J.M. Jaklevic, et al. Nucl. Phys. A99 (1967) 83-99.
5. U.S. Pande and B.P. Singh, Ind. J. Pure and Applied Phys. Vol.8, July (1970) p.401-405.

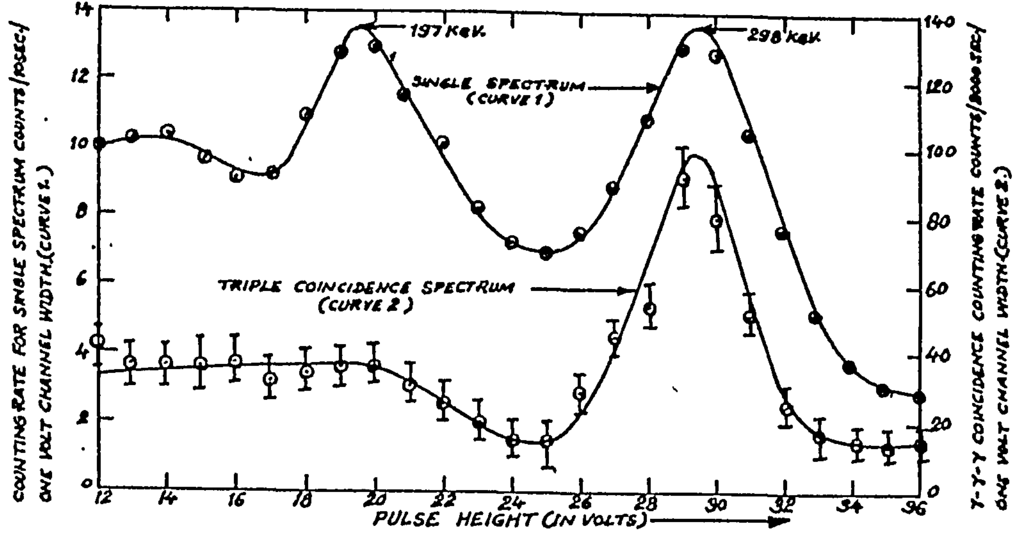


Fig.1. Triple gamma coincidence spectrum alongwith Single Spectrum.

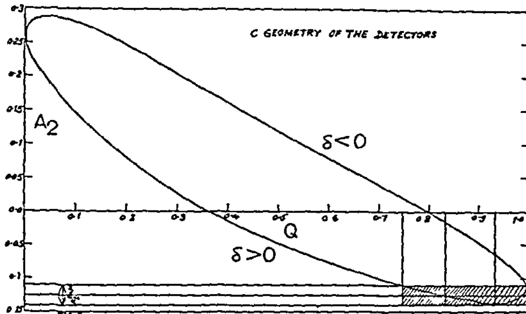


Fig.2. Theoretical plot of A_2 versus Q for the 'O' geometry of the detectors.

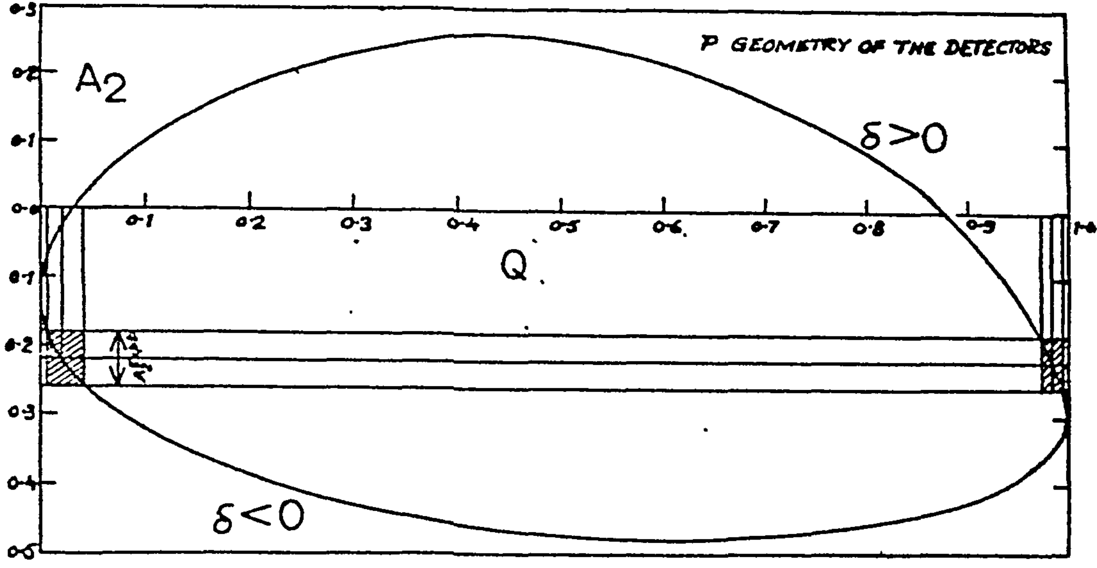


Fig.3. Theoretical plot of A_2 versus Q for the 'P' geometry of the detectors.

INTERNAL BREMSSTRAHLUNG FROM ^{32}P

M.S. Powar and M.Singh
Physics Department, Punjabi University, Patiala.

I. INTRODUCTION

The Internal Bremsstrahlung (IB) accompanying the allowed beta decay in ^{32}P (with E_{β}^{max} - 1.71 MeV) has been investigated by several workers in the last three decades. While some of the measurements show an overall agreement with the K.U.B. theory[1,2] corrected for Coulomb effects[3], the others show a wide disagreement. Most of the earlier measurements were confined to low photon energies (below 250 keV) and agreed reasonably with the theory. The later measurements, covering photon energy region upto or slightly higher than 1 MeV, disagree among themselves. Measurements of Murty and Jnanananda[4] showed good overall agreement between experiment and theory upto photon energy of 1 MeV within about 15 percent. But later measurements of Kreische et. al[6] showed a wide departure from theory ranging from 8 to 100 percent in the same energy region. Berenyi and Varga in their recent detailed studies, point out that the excesses observed by earlier workers can be satisfactorily ascribed to the presence of External Bremsstrahlung (EB) produced by the beta radiation. Their results show agreement with Coulomb corrected KUB theory within 6 % for photon energies upto 1 MeV. The present authors have considered it important to carry out measurements up to photon energies very close to E_{β}^{max}

in order to check the theory more rigorously in these limits. This communication gives a preliminary report of these measurements.

II. EXPERIMENTAL

A major difficulty while working in photon energy region above 1 MeV is the low intensity of IB radiation and resulting poor statistics. In order to overcome this, a sufficiently strong carrier free ^{32}P source (2 mc) supplied as H_3PO_4 in dilute HCl by BARC Bombay, was prepared on a thin polythene film (1.47 mg/cm^2) supported on aluminium ring of inner diameter 5.1 cm. The source material was uniformly distributed on a circular area of 4mm diameter with the help of plane insulin solution.

The IB spectrum was recorded with a single channel gamma ray spectrometer using 7D8 NaI (Tl) crystal of 1.75" diameter and 2" thickness, supplied by Harshaw Co, coupled to 6292 Dumont photomultiplier. The detector was placed at a distance of 10 cm from the source and shielded with 4 cm thick lead lined inside with thin aluminium sheet. The beta particles emitted by the source were absorbed in an ebonite disc 600 mg/cm^2 placed at a distance of 2 cm from the source. The channel width was varied from 5 keV to 30 keV taking care to ensure that the channel width at any energy was smaller at least by a factor of 3, than the line resolution at that energy. Sufficient counts were recorded so as to ensure counting statistics better than 3% even at 1500 keV. Proper checks to ensure the absence of electronic drift were made.

III. CORRECTIONS TO IB DISTRIBUTION .

The pulse height distribution of IB was corrected for background, deadtime of electronic assembly, energy resolution, Compton distribution, Iodine K-X ray escape, photofraction and detector efficiency. The resolution correction was applied by the method given by Novey.[7] Compton correction was calculated by approximating the shape of the Compton distribution for a given energy to a straight line. K-X ray correction was applied by using the data given by Crouthamel.[8] The IB distribution was also corrected for the backscattered radiation. Complete spectra of Hg^{203}, Ce^{141}, Cr^{51}, Mn^{54}, Rb^{86} and Cs^{137} sources were recorded under the above experimental conditions to determine the various correction factors experimentally.

IV. RESULTS and DISCUSSION

The corrected I B photon distribution, obtained as described above, has been normallised to the theoretical K.U.B curve at 100 keV and presents IB photons per meV per beta disintegration as a function of photon energy (Fig, 1). The K.U.B coulomb corrected curve due to Lewis and Fordis also shown. The present results agree with the theory to within 15% upto 700keV while in the energy region 700 keV to 1500 keV the agreement is within 20%. The results are somewhat lower than the Lewis and Ford[3] curve and agree more closely with the uncorrected K.U.B curve above 700 keV thus meaning perhaps that the Lewis and Ford correction is an over estimation. A more detailed study is under progress and will be reported later on.

The authors are indebted to Professor B.S. SOOD for constant encouragement and excellent facilities for work.

REFERENCES

1. J.K.Knipp and G.E.Uhlenbeck; Physica 3, 425,(1936)

2. F. Bloch; Phys. Rev. 50, 272,(1936).

3. R.R.Lewis and G.W.Ford; Phys. Rev. 107, 756,(1957).

4. K.N.Murthy and S.Jnanananda; Nuovo Cimento B 46,217,(1966).

5. W.Kreische, W.Lampart and G.Loos; Nucl.Phys. A107,601, (1968).

6. D.Berenyi and D.Varga; Nucl.Phys.A138, 685,(1969).

7. T.B.Novey; Phys. Rev. 89, 672, (1953).

8. C.E.Crouthamel, Applied Gamma Ray Spectrometry; Pergamon Press (1960).

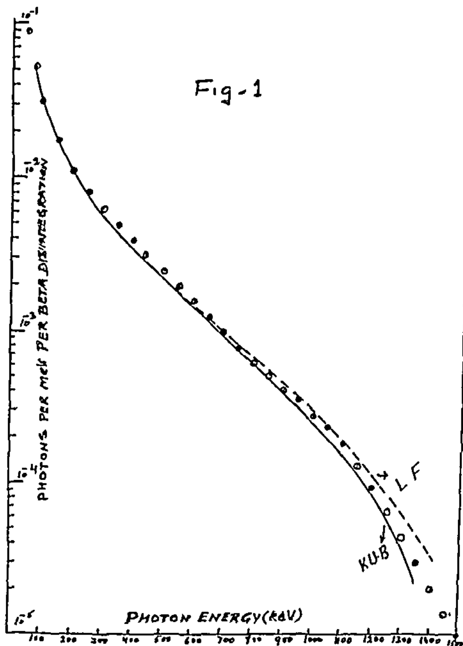


Fig-1
PHOTONS PER MeV PER BETA DISINTEGRATION
PHOTON ENERGY(keV)
LF
KUB

MEASUREMENT OF THE CIRCULAR POLARIZATION OF THE GAMMA RAYS FROM ^{141}Ce AND ^{186}Re AS A FUNCTION OF BETA-RAY ENERGY

J.C. Palathingal
University of Cincinnati, Cincinnati, Ohio(USA)
and Madras Christian College, Madras-59

ABSTRACT

The importance of determining the nuclear matrix elements governing beta transitions in the study of nuclear structure has been realised in recen years. Various research groups have accordingly searched for these by computer analysis of all availa ble experimental data. It is found that the relation between beta-ray energy and the circular polarization of the cascade gamma rays is generally the most sensitive parameter to be used in such computer analysis

We have measured the above parameter in ^{141}Ce and ^{186}Re. We used a back-scattering type Compton polarimeter for measuring circular polarization. It is found that in ^{141}Ce, the circular polarization is a fast-varying function of beta energy. In ^{186}Re, the variation is considerably slower. The results ar compared with the predictions of Manthuruthil and Poirier*. The agreement lends support to the values of nuclear matrix elements obtained by them through computer analysis of available experimental data.

* J.C. Manthuruthil and C.P. Poirier, to be publish

NUCLEAR MATRIX ELEMENTS OF ^{122}Sb - BETA DECAY+

J.C. Palathingal

Physics Department, University of Cincinnati, Cincinnati, Ohio

I. INTRODUCTION

Any $2^- \rightarrow 2^+$ first-forbidden beta transition is characterized by two major matrix elements of tensor rank zero (scalars), which are symbolized as $\int \vec{\sigma}\cdot\vec{r}/\rho$ and $\int i\gamma_5$, three of tensor rank one (vectors), $\int \vec{r}/\rho$, $\int \vec{\sigma}\times\vec{r}/\rho$ and $\int i\vec{\alpha}$, and one of tensor rank two, $\int B_{ij}/\rho$. Employing the generalized theoretical expressions for the various experimental parameters related to such a beta transition taking into account the finite nuclear charge distribution, Manthuruthil and Poirier[1] sought for possible solutions for the six matrix elements through a computer analysis, resulting in two sets of matrix elements as possible solutions. It was shown that a choice between the two sets could be made through a measurement of the correlation between beta-ray energy and gamma-ray circular polarization.

II. EXPERIMENTAL DETAILS

The circular polarization of the gamma rays of ^{122}Sb may be written as ,

$$\mathcal{P}_\gamma = \frac{A_1(\beta)\, A_1(\gamma)\, P_1(Cos\theta) + A_3(\beta)\, A_3(\gamma)\, P_3(Cos\theta)}{1 + A_2(\beta)\, A_2(\gamma)\, P_2(Cos\theta)}$$

The dependence of $\mathcal{P}_\gamma$, the polarization on beta-ray energy

+ Supported by the U.S. National Science F

* Presently at Madras Christian College,

was investigated in the present experiment, for $\overline{\cos\theta}=-0.79$). The sources were of thickness about 10^{-4} g/cm^2, sandwiched between two films of mylar of thickness 6.4×10^{-4} cm. The coincidence-time resolution (2τ) was about 5 nanoseconds for the entire experiment, and the proportion of random-coincidence count rate to total-coincidence count rate varied between 3% and 28%. Through a combination of magnetic shielding and microvariation of the photomultiplier voltage in phase with magnetic field reversal of the polarimeter[2], the gain shift in the phototube output due to the reversal of magnetization was generally kept within 10^{-4}.

III. RESULTS AND DISCUSSION

In Fig. 1, the values of P_γ obtained presently for three beta-energy intervals are shown, along with values computed from the two alternate sets of nuclear matrix elements. The present data clearly shows a P_γ-behaviour of increasing with energy, agreeing with Set I. Further evidence in support of Set I as the correct choice is provided by the small values of P_γ obtained in the present and earlier[3] experiments for integral beta spectrum including low energy-beta rays. For integral spectra given by W (kinetic energy + rest energy, in units of rest energy) $>$ 1.20, 1.49 and 1.68, the present experiment yielded P_γ - values +0.006(020), +0.030(014) and +0.028(028) respectively, and the measurement by Deutsch and Lipnik[3] for W $>$ 1.49 gave +0.023(023). The following values of the matrix elements are thus obtained.

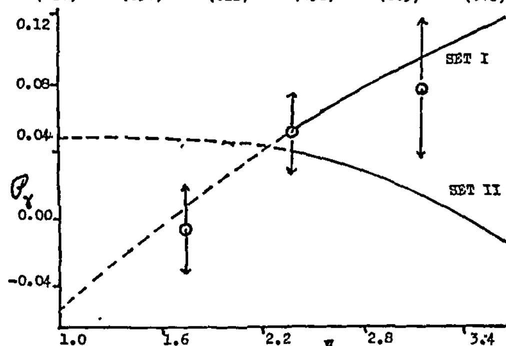


Fig.1

In the shell-model picutre, the 1.40 MeV-beta decay of ^{122}Sb is characterized by the transition of a neutron in a $h_{11/2}$ state to a proton in a $g_{7/2}$ state. Therefore the fact that the $\int \vec{\sigma}\cdot\vec{r}/\rho$-matrix element is dominating suggests that there should be a large degree of shell mixing in ^{122}Sb. Kisslinger and Wu[4], using a special potential, have shown that $\int B_{ij}/\rho$ may be reduced greatly from unity due to cancellation effects. It is interesting to note that the value in the present case is nearly equal to the matrix element of the unique $2^- \rightarrow 0^+$ transition of ^{122}Sb to the ground state of ^{122}Te, estimated to be 0.245. It should also be noted that the corresponding matrix element of the $3^- \rightarrow 2^+$ transition of ^{124}Sb in which also [illegible]

from a $h_{11/2}$ shell is transformed into a proton in a $g_{7/2}$ shell has a value 2-3 x 10^{-2}, much smaller than the value 1.5 to be expected from shell-model considerations, and the value 0.34 predicted by Kisslinger and Wu.

Since the vector-matrix elements, $\int i\vec{\alpha}$ and $\int \vec{\lambda}/\rho$ are relatively small in this beta transition, it is not possible to make this ratio a test case of the CVC theory. On the other hand, the ratio of $\int i\gamma_5$ and $\int \vec{\sigma}.\vec{\lambda}/\rho$ has been determined to be $0.175^{+0.043}_{-0.037}$. This is in agreement with the value 0.208 estimated from the formula of Ahrens and Feenberg[(5)] based on the shell model of the nucleus, and general physical arguments regarding the Coulomb and nuclear contributions to the semiempirical mass formula for nuclei.

REFERENCES

1. J.C. Manthuruthil and C.P. Poirier, Nucl. Phys. A 118, 657 (1968).
2. J.C. Palathingal, Rev. Sci. Instr. 40, 266 (1969).
3. J.P. Deutsch and P. Lipnik, J.Phys. Rad. 21, 806 (1960)
4. L.S. Kisslinger and C.S. Wu, Phys. Rev. 136, B 1254 (1964).
5. T. Ahrens and E. Feenberg, Phys. Rev. 86, 64 (1952).

DISCUSSION

P.G. Hansen: I am aware that the theoretical analysis was not part of your investivation. Nevertheless I wonder whether you would like to comment on the possible role of systematic experimental error might play in these elaborate χ^2 fits etc?

J.C. Palathingal: The experiments sound quite good. A reliable check is obtained from the fact that the value is smallinspite of the fact that various experiments and different experimental groups are involved.

ANGULAR DEPENDENCE OF PAIR ANNIHILATION RADIATION

M.Biswas*, S.C.Roy and A.M.Ghose
NUCLEAR PHYSICS LABORATORY, BOSE INSTITUTE, CALCUTTA-9.

I. INTRODUCTION.

Calculations based on the quantum theory of radiation[1] indicates that annihilated pairs should in general have an angular dependence with the direction of the incident photon. To the best knowledge of the authors no theoretical or experimental data exists in the literature near the threshold of the pair production phenomena. In the experiments[2-5] which have been performed in the past isotropic distribution of annihilation pairs with respect to the incident photon have been assumed for the calculation of the cross-sections. An attempt has been made in our laboratory to check whether the annihilated pairs have an angular variation with respect to the incident photon and thus to check the validity of the previous investigations.

II. METHOD.

In the conventional pair production cross-section measuring system the difficulty arises in separating the Compton continuum from the photopeak due to annihilated radiation. In the present experiment the

---

* Guest worker from New Alipore College cut .

Compton continuum was eliminated very efficiently employing a special method of photopeak sharpening in scintillation spectrometers[6,7]. In this method the detector employed is a single crystal two photomultiplier combination and the spectrum is scanned from one photomultiplier coincidence gated by other. Proper gating eliminates the Compton continuum from the photopeak to a large extent. The scatterers used were cylindrical in shape to adopt the cylindrically symmetrical disposition of the experimental set up.

III. EXPERIMENT.

A 100 mCi C_o^{60} source is placed within a massive lead block, the radiation from the former is extracted using a tapering rectangular slit. The scatterer is placed directly in line with the source at the centre of an iron table. The iron table is graduated to facilitate the placing of the detector at any desired angle. The detector is surrounded with lead bricks to reduce the unwanted background. The detector was first calibrated with a standard Na^{22} source and the proper gate was set so that the photopeak of 0.511 MeV was completely separated. Figure 1 shows the single spectrum of Na^{22} without coincidence and the properly gated coincidence spectrum eliminating the compton continuum to a large extent. The scatterer was then placed in proper position removing the Na^{22} source and the coincidence spectrum for annihilated pairs was

obtained directly from a 128-channel analyser.

IV. RESULTS & CONCLUSION.

The photopeaks obtained experimentally due to annihilated pairs from lead scatterer obtained at three different angles are shown in figure 2. It is clear from the figure that the intensity annihilated radiation has a decreasing trend towards lower angles. The experiment was repeated with scatterers of different thickness and placing the detector diametrically opposite to each of the angle obtaining the same decreasing trend. From this we conclude that pair annihilated radiation has an angular dependence with respect to the incident photon and the re-evaluation of pair production cross-section is essential at this energy region.

Absolute pair production cross-section using the method is in progress.

ACKNOWLEDGEMENT.

Our thanks due to Dr. S.M. Sircar, Director, Bose Institute for his kind interest in this work. One of the authors (SCR) is thankful to the Department of Atomic Energy for awarding him a Senior Research Fellowship to carry out this work. Partial support for this work have been obtained from US National Bureau of Standards.

REFERENCES.

1. Heitler, W. - Quantum Theory of Radiation (Oxford) Third Edition, Chapter V.

2. Hahn, B etal - Helv. Phys. Acta (1952), 25, 505.

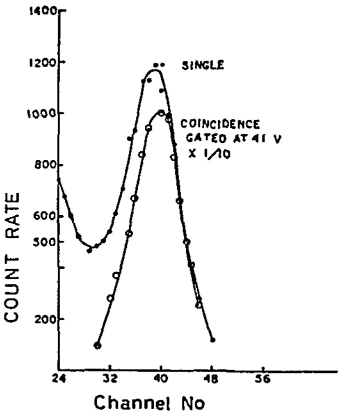
3. Dayton, I.E. - Phys. Rev. (1953), 89, 544.

4. Standil, S. etal. - Canad. J. Phys. (1957), 35, 1156.

5. Rama Rao, J. etal. - Proc. Phys. Soc. (1963), 81, 949.

6. Roy, S.C. etal. - Proc. Nucl. Phys. Symposium, (1968), Vol. II, 193.

7. Roy, S.C. etal. - Nucl. Instr. & Methods. (1969) 67, 318.


SINGLE
COINCIDENCE
GATED AT 41 V
X 1/10
COUNT RATE
1400
1200
1000
800
600
500
200
24
32
40
48
56
Channel No

COUNT RATE
240
210
180
150
120
90
60
30
θ=90°
28
36
44
140
120
100
80
60
40
20
θ=105°
θ=120°
30
38
46
54
Channel No

THE DECAY OF ^{131}I*

K.K.Suri** and P.N.Trehan
Department of Physics, Panjab University, Chandigarh-14

INTRODUCTION

In the negaton decay of ^{131}I to ^{131}Xe, the existence of gamma rays of energy 272, 318, 325, 358, 405 and 643 KeV and a level at 405 keV are controversial. Furthermore the various reported values of a_k(80 keV) are in poor agreement. In view of these controversies, the decay of ^{131}I has been investigated with the help of NaI (Tl) crystals (Pair of 3"x3" and one 1-1/2" x 1/4" sizes) in slow-fast coincidence, (τ = 50 nsec), modified sum coincidence and sum-peak coincidence modes. The results of these investigations are presented in this paper.

RESULTS AND DISCUSSION

A level scheme of ^{131}Xe based on the present work and previous investigations is given in fig. 1.

The sum-coincidence spectrum with the sum-gate set at 640 keV supports the existence of 318-325 keV cascade. Also on the basis of the same spectrum one concludes that either one or both of 272-364 and 358-284 keV cascades may be present.

The sum-coincidence spectrum with the sum gate set at 723 keV shown in fig. 2, supports the existence of 318-405, 643-80 and 358-364 cascades.

---

* Work supported by the Department of Atomic Energy, Government of India and the National Bureau of Standards, Washington, DC.

** Department of Applied Sciences, Panjab Engineering College, Chandigarh.

Figure 3 (curve a) shows the high energy portions of the adder spectrum in almost 4π geometry. The three sum-peak coincidence spectra with the integral biases set at 0,120 and 250 keV are shown in Fig. 3 (curves b, c, and d respectively). From the attenuation of the peak at 723 keV for the various integral biases, one concludes that in addition to the 643-80 keV cascade, the level at 723 keV deexcites itself either by one or both of 318-405 and 358-364 keV cascades. Thus on the basis of both the sum-coincidence and sum-peak coincidence spectrum studies, the existence[3)] of the weak gamma transition of energy 318, 325, 358, 405 and 643 keV and a weakly populated level at 405 keV is confirmed. It has not however, been possible to show the existence of 272 keV gamma ray[3)] .

The K-shell conversion of the 80 keV transition has been measured by setting gate at 284 keV. For this study, 284 keV gamma ray was detected by 3"x3" NaI (Tl) crystal and 80 keV gamma ray was detected by $1\frac{1}{2}$" x $\frac{1}{4}$" NaI (Tl) crystal. After applying usual corrections, we get $a_k = 1.31 \pm 0.18$. This value of 'a_k' when compared with the theoretical values obtained from the tables of Hager et al[3)] confirms M 1 character for this transition.

The 284-80 keV angular correlation was measured by putting the gates to cover 284 and 80 keV photopeaks. The correlation coefficients after applying corrections on account of finite size of detectors are:

$$A_2 = 0.011 \pm 0.012 \qquad A_4 = -0.002 \pm 0.015$$

From the comparison between the experimental[2)] and theoretical values[3)] for K/L, L1/L2 and L1/L3 for 284 keV transition pure E2 character can be assigned to 284 keV gamma ray. Assuming the

spin-parity[3] of the ground state to be $3/2^+$ and that of 364 keV level to be $5/2^+$ and the above mentioned characters of the transitions involved, the experimental values of A_2 and A_4 agree only with $5/2^+$ (E2) $1/2^+$ (M1) $3/2^+$ spin-parity sequence for the 284-80 keV cascade.

REFERENCES:

1. P.C.Mangal, S.P.Sud and P.N.Trehan, Ind. J.Pure Appl. Phys. 12 (1967) 596.

2. G.Graeffe and W.B.Walters, Phys. Rev. Vol. 153 (1967) 1321.

3. R.G.Hager and E.C.Seltzer, Nuclear Data, 4A (1968) 86.

Figure 3 (curve a) shows the high energy portions of the adder spectrum in almost 4π geometry. The three sum-peak coincidence spectra with the integral biases set at 0,120 and 250 keV are shown in Fig. 3 (curves b, c, and d respectively). From the attenuation of the peak at 723 keV for the various integral biases, one concludes that in addition to the 643-80 keV cascade, the level at 723 keV deexcites itself either by one or both of 318-405 and 358-364 keV cascades. Thus on the basis of both the sum-coincidence and sum-peak coincidence spectrum studies, the existence[3)] of the weak gamma transition of energy 318, 325, 358, 405 and 643 keV and a weakly populated level at 405 keV is confirmed. It has not however, been possible to show the existence of 272 keV gamma ray[3)].

The K-shell conversion of the 80 keV transition has been measured by setting gate at 284 keV. For this study, 284 keV gamma ray was detected by 3"x3" NaI (Tl) crystal and 80 keV gamma ray was detected by $1\frac{1}{2}$" x $\frac{1}{4}$" NaI (Tl) crystal. After applying usual corrections, we got $a_k = 1.31 \pm 0.18$. This value of 'a_k' when compared with the theoretical values obtained from the tables of Hager et al[3)] confirms M 1 character for this transition.

The 284-80 keV angular correlation was measured by putting the gates to cover 284 and 80 keV photopeaks. The correlation coefficients after applying corrections on account of finite size of detectors are:

$$A_2 = 0.011 \pm 0.012 \qquad A_4 = -0.002 \pm 0.015$$

From the comparison between the experimental[2)] and theoretical values[3)] for K/L, L1/L2 and L1/L3 for 284 keV transition pure E2 character can be assigned to 284 keV gamma ray. Assuming the

spin-parity[3] of the ground state to be $3/2^+$ and that of 364 keV level to be $5/2^+$ and the above mentioned characters of the transitions involved, the experimental values of A_2 and A_4 agree only with $5/2^+$ (E2) $1/2^+$ (M1) $3/2^+$ spin-parity sequence for the 284-80 keV cascade.

REFERENCES:

1. P.C.Mangal, S.P.Sud and P.N.Trehan, Ind. J.Pure Appl. Phys. 12 (1967) 596.
2. G.Graeffe and W.B.Walters, Phys. Rev. Vol. 153 (1967) 1321.
3. R.G.Hager and E.C.Seltzer, Nuclear Data, 4A (1968) 86.

Fig: 1 Decay scheme of ^{131}I

Fig: 2 Sum-coincidence spectrum of ^{131}I with gate set at 723 keV .

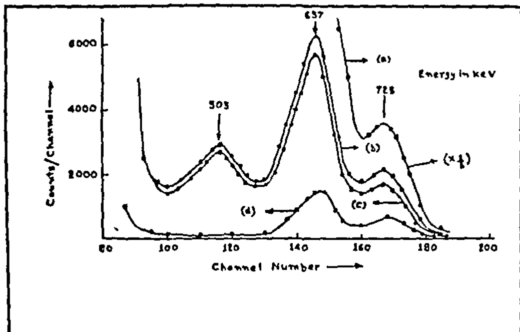


Fig: 3 Curve (a) high energy portion of the adder spectrum, curves (b), (c) and (d) are sum-peak coincidence spectra with crystals in 4π geometry, with biases set at 0, 120 and 250 keV respectively of ^{131}I.

THE DECAY OF ^{160}Tb TO LEVELS IN ^{160}Dy *

K.K.Suri** and P. N. Trehan
Department of Physics, Panjab University, Chandigarh-14.

INTRODUCTION

In the beta decay of ^{160}Tb to ^{160}Dy a level at 1535 KeV has been recently proposed by Ludington et al [1]. The existence of a level at 1287 is controversial. Further the assignment of spins to the levels at 1049 and 1359 KeV is also somewhat doubtful.

In view of the above the level scheme of ^{160}Dy has been investigated with the help of a pair of 2"x2" NaI (Tl) crystals in slow-fast coincidence (τ = 50 nsec) and in modified sum coincidence modes [2]. The results of these investigations are being presented in this paper.

RESULTS AND DISCUSSION

A level scheme of ^{160}Dy based on present work and previous investigations is given in fig. 1.

Gamma - gamma coincidence spectrum, with gate set at 197 KeV, after substraction of the interference of 216 and 299 KeV gamma transitions in the gating channel shows up peaks due to 1003 and 1250 KeV gamma rays in addition to the other well-known coincident gamma rays. The existence of 1003-197 and 1250 -197 KeV cascades support the existence of levels at 1287 and 1535 KeV respectively.

---

* Work supported by the Department of Atomic Energy, Government of India and National Bureau of Standards, Washington D.C.

**Department of Applied Sciences, Panjab Engineering College, Chandigarh.

Table-1

Summary of the mixing ratio analysis of the directional correlation data in ^{160}Dy

Cascade (KeV)	A_2	A_4	Possible Spin-parity sequence	Transition (KeV)	Multipole admixture (%) and Mixing ratio assignment
[illegible]	[illegible] ±0.023	0.010±0.011	$2^-(D,Q)2^+(Q)0^+$	299	E2+M1 (≤0.2% M1); $\delta = 0.01^{+.004}_{-.01}$
[illegible]	[illegible]	-0.107±0.010	$2^-(D,Q)2^+(D,Q)2^+$	879	M1+E2 (93.8 - 98% E2); $\delta = -5.7^{+1.8}_{-1.3}$
[illegible]	[illegible]	[illegible]	$3^+(D,Q)2^+(Q)0^+$	962	M1+E2 (95.0- 99% E2); $\delta = -7.0^{+2.9}_{-2.8}$.
[illegible]	[illegible]	[illegible]	[illegible]	1272	E1+M2 (0.2-5.5% M2) $\delta = +0.071^{+0.024}_{-0.140}$
[illegible]	[illegible]	[illegible]	[illegible]	1170	E1+M2 (≤ 1.5% M2) $\delta = -0.07^{+0.052}_{-0.071}$
[illegible]	[illegible]	[illegible]	[illegible]	[illegible]	E1+M2 (1.0 -6.66 M2) $\delta = 0.19^{+.07}_{-.09}$

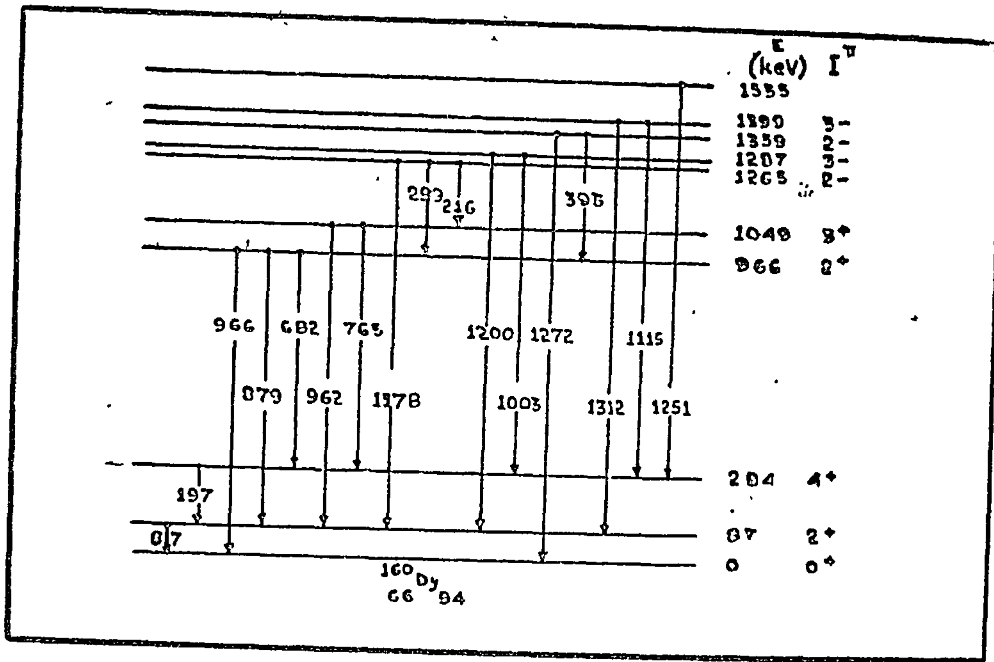


Fig: 1 Level scheme of ^{160}Dy

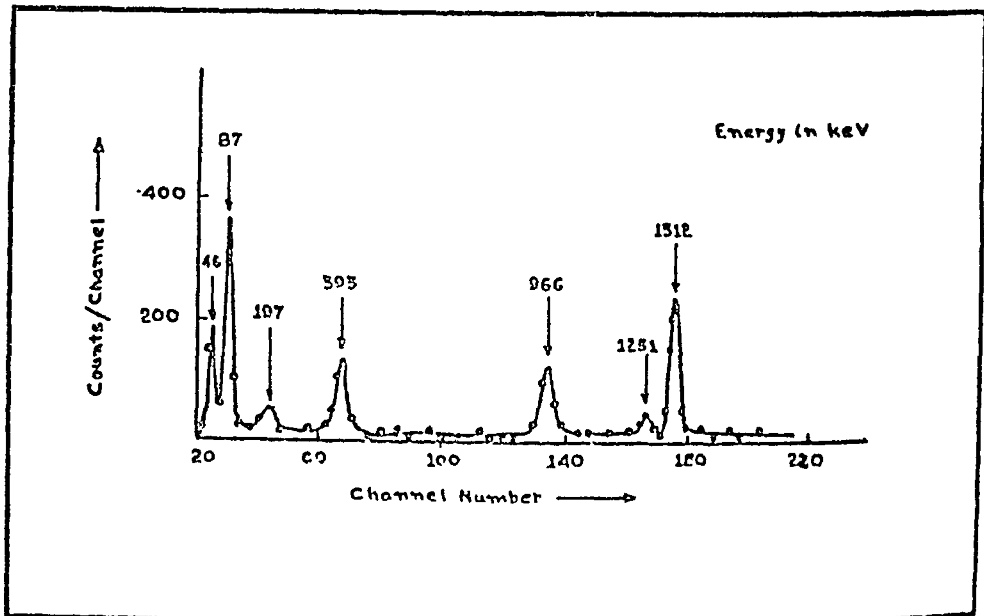


Fig: 2 Sum-coincidence spectrum of ^{160}Tb with gate set at 1400 keV.

DECAY OF ^{107}In

M. B. CHATTERJEE and B. B. BALIGA
Saha Institute of Nuclear Physics, Calcutta-9.

I. INTRODUCTION

The study of the level scheme of ^{107}Cd was done by Basu and Patro[1] in 1963 in our laboratory. Since then no new information has appeared in the literature. The level scheme proposed by them was on the basis of gamma-ray singles measurement with NaI and sum coincidence with NaI x NaI scintillation spectrometers. So it was proposed to study the nucleus again with the Ge(Li) detector. The ^{107}Cd lines were identified from the characteristic decay of ^{107}In. Many more lines have been observed than reported earlier.

II. EXPERIMENTAL

Enriched sample of ^{106}Cd (77.94%) was bombarded for one lifetime of ^{107}In (32 min.) with the internal proton beam of energy 3.8 Mev. Sample was pressed into a gold-backed target and bombarded with a proton beam of current $\sim$ 50 μA 32 min. ^{107}In activity was produced through (p,γ) reaction. The gamma-rays were detected with the Ge(Li) detector of about 3 KeV resolution. The detector is an assembly from ORTEC having 5 cm^2 surface and 5 mm depletion thickness followed by a TENNELEC FET preamplifier and an ORTEC amplifier. The spectrum was taken in two sections with 4096 LABEN anal, section spectrum was recorded upto 3 Mev channels.

III. RESULTS

The lines which showed the lifetime of ^{107}In were taken as the lines belonging to ^{107}Cd. The ^{107}Cd nuclei produced further decayed to ^{107}Ag with a lifetime of 6.5 hrs. We observed no more ^{107}Ag lines besides 93.1 KeV line as expected. 99.65% of ^{107}Cd decays to 93.1 KeV level of ^{107}Ag. Other lines belonging to ^{107}Ag are weak enough and we have not observed them. ^{111}In (2.81 d) is also produced through (p,γ) and (p, n) reactions from the ^{110}Cd and ^{111}Cd impurities present in the sample. We have used the two well known ^{111}In lines advantageously to calibrate the spectrum.

In the low energy region we have observed a few lines which come from impurities. The lines were identified as from iron and zinc. Zinc is suspected to be an impurity in the gold backing of the target.

The strongest line observed in ^{107}Cd spectrum (Fig.1) is of energy 204.4 KeV. The next strong line is of energy 321.1 KeV. The highest energy line observed in the spectrum is of energy 2871 KeV. We have observed several new gamma rays which are not reported earlier. The error in energy measurement in our case is within one KeV in the energy region upto 500 KeV. In the high energy region the error in energy measurement is larger because of non-linearity.

Relative intensities of the gamma-rays have been measured with respect to the strongest line 204.4 KeV. The table-I gives the energies and intensities of the

lines assigned to ^{107}Cd.

These results are preliminary and the work is still in progress.

Thanks are due to Prof. A. P. Patro and Prof. B. Basu for many helpful discussions.

REFERENCES

1. B. Basu and A. P. Patro, Nucl. Phys. 46, 59 (1963).

Table 1

Energies and relative intensities of gamma lines in ^{107}Cd

Energy (KeV)	Relative Intensity	Energy (KeV)	Relative Intensity
204.4	100	(1044)	1.81
321.1	19.36	1061	1.26
(365.2)	6.90	1270	13.15
553.9	1.74	(1346)	3.36
599.4	1.07	1378	3.43
604.5	3.60	(1411)	3.75
(612.0)	1.46	1643	3.28
728.7	6.29	1778	2.93
762.5	2.13	1922	3.45
809.8	7.11	(1982)	(5.38)
(902.6)	1.73	(2004)	(5.29)
916.3	2.70	(2063)	(3.41)
(922.8)	3.31	2302	2.73
(1000)	2.87	2871	1.55
1038	0.98		

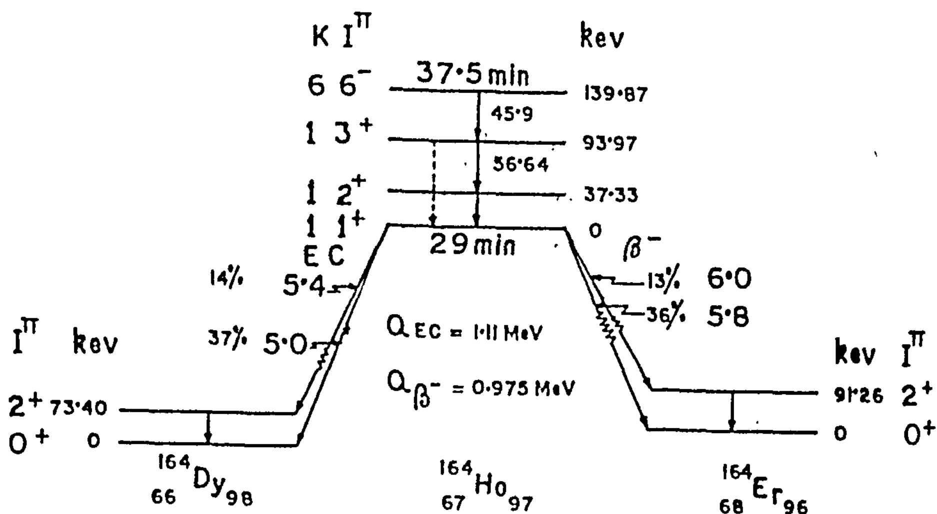
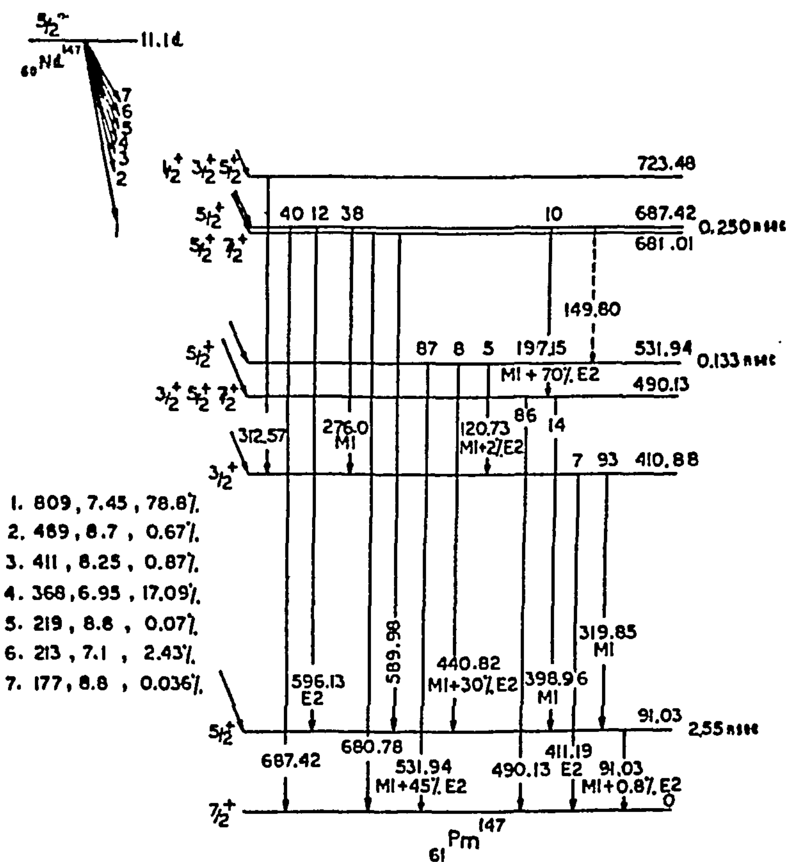


FIG:1. DECAY SCHEME OF ^{164}Ho



CHANNELLING OF PROTONS IN A SINGLE CRYSTAL OF SILICON

K.G. Prasad, R. P. Sharma and J.K. Srivastava
Tata Institute of Fundamental Research, Bombay-5

When energetic charged particles are incident on a single crystal within a critical angle, ψ_c, with respect to a crystal axis or a plane, they get channelled. In such a case these particles are not able to approach the crystal atoms nearer than the Thomas Fermi screening distance "a". Thus the yield of those phenomenon requiring closer encounter with the atoms such as the wide angle Rutherford scattering, production of inner shell x-rays and nuclear reactions, etc is minimum. Hence the observation of such processes is a sensitive method of studying channelling phenomenon.

Lindhard[1] has shown on the basis of continuum approximation that for the particles of charge Z_1e and energy E, the critical angle is given by $\psi_c \simeq \sqrt{\frac{2 Z_1 Z_2 e^2}{E d}}$ provided $\psi_c \lesssim \frac{a}{d}$ where Z_2e is the charge of the target nucleus and d the lattice spacing in the direction of the row. The minimum yield is shown to be $\chi_{min} \simeq \pi \langle a^2 + \rho^2 \rangle N d$, ρ^2 and N being the mean square amplitude of lattice vibrations and the atomic density in the crystal, respectively.

The experimental arrangement for observing the channelling phenomenon consists of a double axis Goniometer capable of tilting as well as rotating with respect to the incident beam. It is essential to vary the crystal orientation in extremely fine steps. For this purpose reduction gear arrangements were provided for the movements about the two axes. In this arrangement it was possible to change the angles in steps of 0.19°. In the present experiment a well polished Si single crystal with $\langle 111 \rangle$ axis perpendicular to the plane of the crystal was bombarded with well collimated 2-3 MeV

protons from the Van de Graaff accelerator at Trombay. The back scattered protons were detected in a Si surface barrier detector. Only those particles of energy corresponding to the scattering from just below the surface of the target were counted. Figure 1 shows some of the major dips obtained with 2 MeV protons.

Our results (Table 1) seem to agree well with those of others reported earlier[2].

Table 1

Results for E = 3.0 MeV

Plane	χ_{min}		Ψ_c	
	Present work	Others[2]	Present work	Others[2]
{100}	0.48 ± 0.05	0.42±0.03	0.074°	0.070°
{110}	0.35 ± 0.05	0.31±0.03	0.066°	0.087°
{111}	0.42 ± 0.05	0.36±0.03	0.032°	0.092°

The channelling effect has been used as powerful tool, both in solid state and nuclear physics as indicated below:

(a) Solid State Physics

1. Precise orientation of single crystals.
2. Locating foreign atoms in the crystals introduced by thermal diffusion or implantation.
3. Study of surface contamination and dislocation.
4. Crystal defects and radiation damage.

(b) Nuclear Physics

1. Lifetimes of the fission events[4].
2. Nuclear reaction times[5].

   These times are in the range 10^{-14}-10^{-18} seconds.
3. Production of highly polarized deutrons beams[6].

(c) Other applications

1. Channelling effects in the light emission from He ion beams

excited by a gold single crystal (beam foil spectroscopy)[7].

2. Study of channelling of electron and positron by observing bremsstrahlung radiation[8].

3. Rosette motion in negative particle channelling[9].

REFERENCES

1. J. Lindhard; Dan. Vid. Selsk. Mat. Fys. Medd 35, No.14 (1965).
2. J.A. Davies, J. Denhartog and J.L. Whitton; Phy. Rev., 165, 345 (1967).
3. Various papers in Proc. of Chalk River Conference, Can. J. Phys. 46, No.6 (1968).
4. W.M. Gibson and K.O. Nielsen; Phys. Rev. Lett. 24, 114 (1970).
5. M. Maruyama et al.,Nucl. Phys., A145, 581 (1970).
6. M. Kaminsky; Phys. Rev. Lett., 23, 819 (1970).
7. T. Andersen et al., Phys. Lett., 33A, 121 (1970).
8. R.L. Walker et al., Phys. Rev. Lett. 25, 5 (1970).
9. H.J. Kreiner et al., Phys. Lett., 33A, 135 (1970).

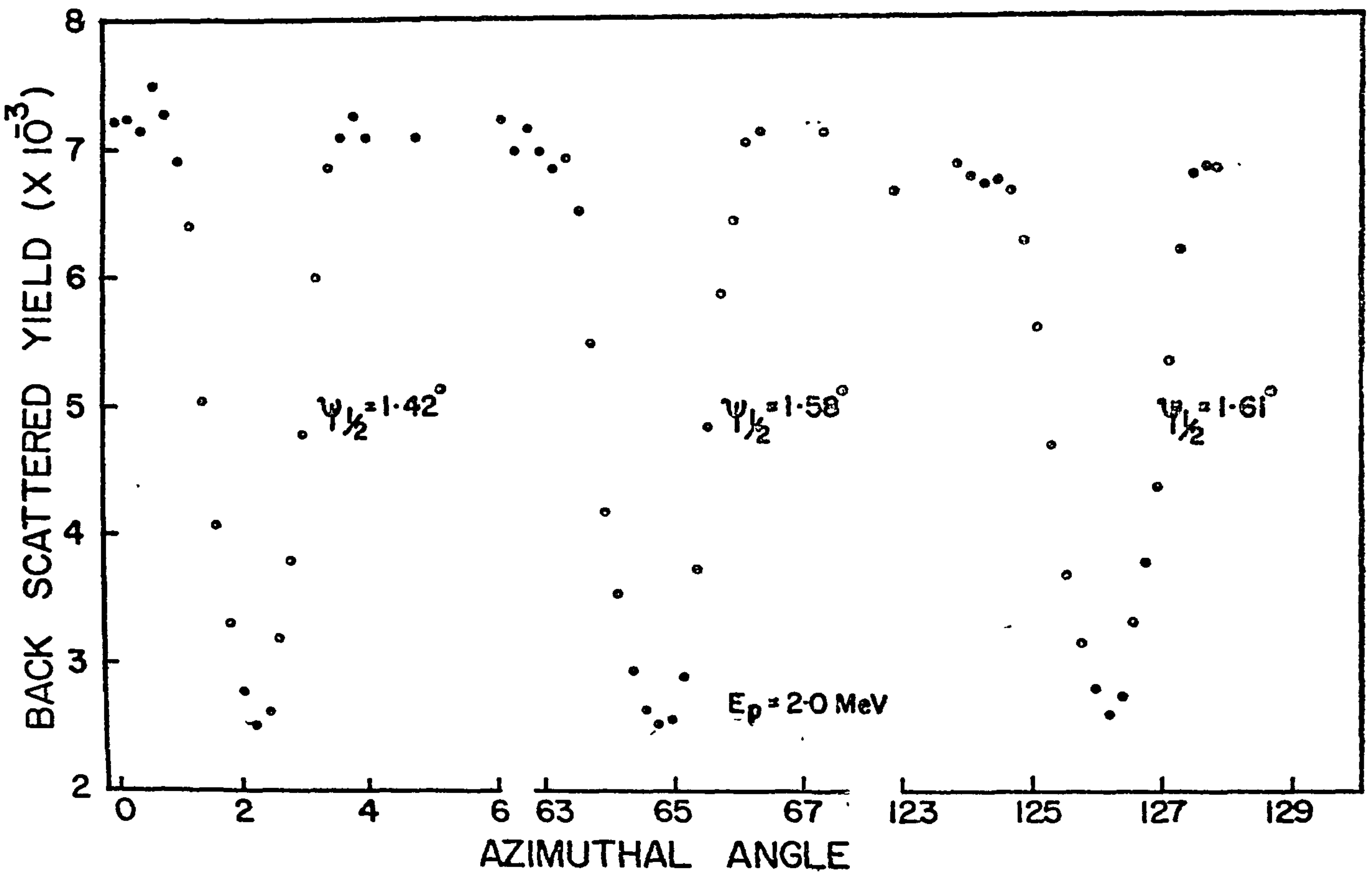

BACK SCATTERED YIELD (X 10^{-3})
8
7
6
5
4
3
2
0
2
4
6
63
65
67
123
125
127
129
AZIMUTHAL ANGLE
$\psi_{1/2} = 1.42°$
$\psi_{1/2} = 1.58°$
$\psi_{1/2} = 1.61°$
$E_p = 2.0$ MeV

FIG. 1

EXPERIMENTAL METHODS AND TECHNIQUES

A PRE-INJECTION e/m ANALYSER SYSTEM FOR USE WITH VAN DE GRAAFF ION SOURCES

S.N. Misra and M.R. Dwarkanath
Bhabha Atomic Research Centre, Bombay - 85.

I. INTRODUCTION

Acceleration of multiply charged ions (particularly He^{++}) enhances the energy range of Van de Graff Accelerators. Since R.F. ion source put out only 1% of total ion yield as He^{++}, post acceleraction separation by analysing magnet requires large helium beams to be accelerated. This causes severe loading of the accelerating tube. Instead, we first separate the He^{++} from the He^{+} by employing crossed electric and magnetic fields and selectively inject only the He^{++} into the accelerating tube.

II. DESCRIPTION

The basic design of the system closely follows the design of Taylor and Weil[1]. The He^{++} extraction test bench is built around a ORTEC model 320 ion source. Prefocussing of the divergent beam is best achieved by an Einzel lens which produces focussing without accelerating the ions and this immensely increases the resolving power of the analyser. A schematic of the set up is shown in Fig.1. The crossed field analyser consists of electric and magnetic fields perpendicular to each other and to the direction of the ions. A fixed magnetic field of 900 gauss is produced across a pole gap of 3.5 cm by a bank of 24 ceramic permanent magnet wafers and the continuously variable electric field is produced by applying 0-1600 volts across a pair of parallel plate electrodes kept 2.5 cm apart. A 3 mm acceptance aperture kept below the analyser, allows un
cted beam to enter the accelerating tube.

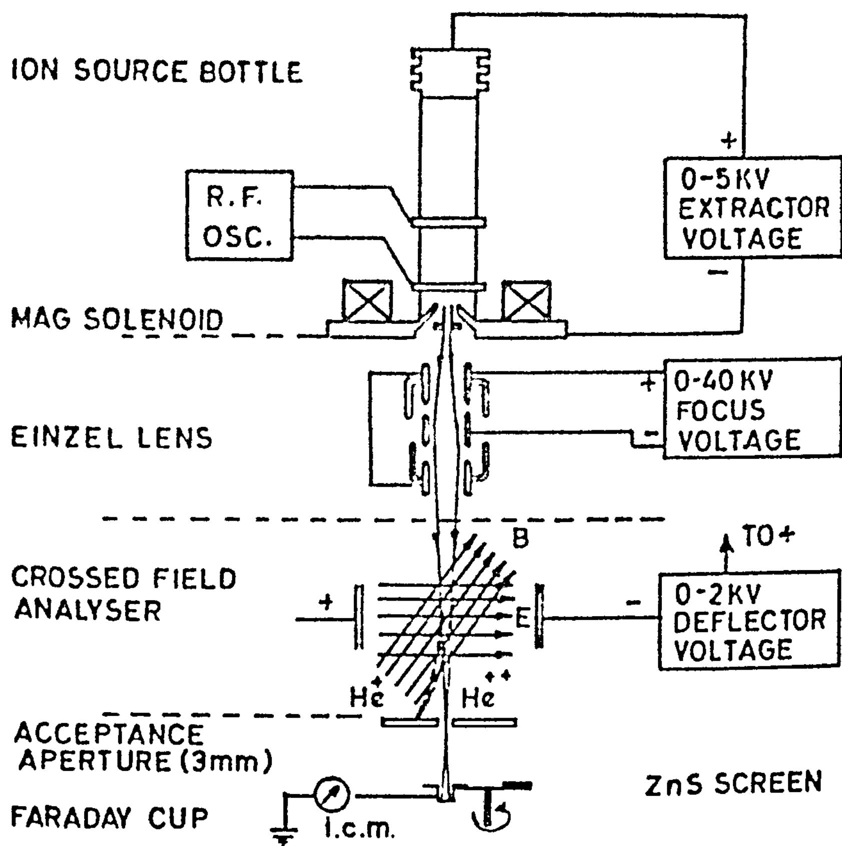


FIG.1. SCHEMATIC OF He^{++} ION SOURCE

III. EXPERIMENT

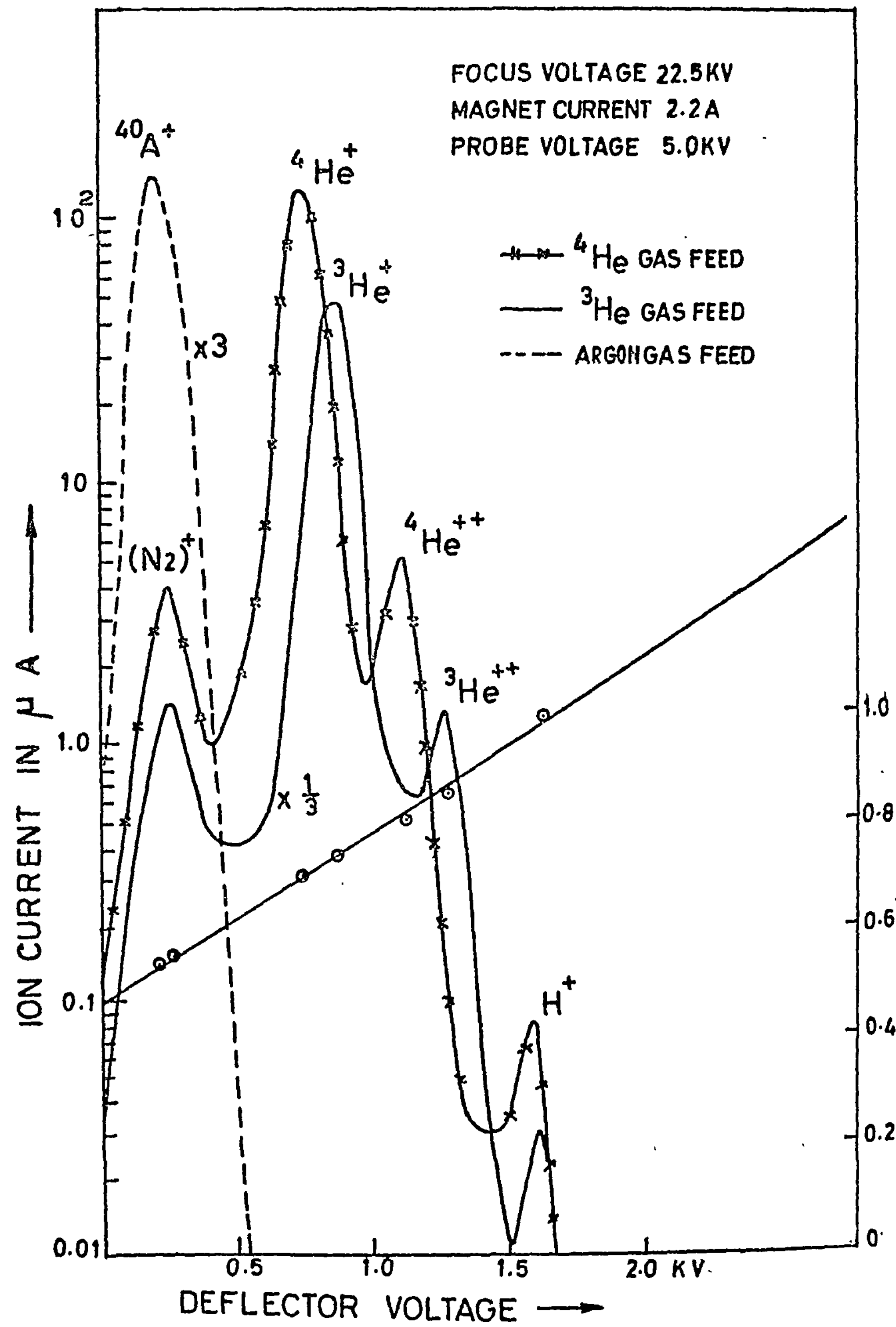
After each reconditioning, the ion source is replaced on the test bench and pumped for at least 24 hours. This is followed by a period of baking the ion source with helium gas to remove hydrogen occluded in the walls of the source bottle. Having thus prepared the ion source for putting out a good yield of the He^{++} ions, the source magnet, the gas leak, the extractor, focus and deflector voltages are adjusted to maximise the He^{+} ion yield. The deflector voltage is then turned down to zero and is gradually increased in small suitably chosen steps (~50 volts). The ion current is recorded for each deflector voltage setting and a graph is plotted of the ion current against the deflector voltage. Fig. 2 shows such a graph for three different gasses, ^{4}He, ^{3}He and ^{40}A, feeding the ion source. The graphs show several peaks, the most prominent being due to singly ionised ions.

IV. RESULTS AND ANALYSIS

Tentatively, the different peaks in Fig. 2 are identified with different ions and the deflector voltages (Vd) at which the peaks appear are determined. A graph of $\sqrt{Z/M}$ vs Vd should be a straight line as the condition for transmission for the beam is

$$\sqrt{\frac{Z}{M}} = \left(\sqrt{\frac{Mp}{2eV}}\ \frac{C}{BD}\right) Vd$$

Where Ze is the charge of the ion, M is the mass of the ion in units of the proton mass Mp, D is the spacing between electrodes, B the magnetic field and V is the extraction voltage. The quantities in parenthesis are constant for a given extraction voltage. Fig. 2 also shows a graph of $\sqrt{Z/M}$ Vs Vd. The experimental po



FOCUS VOLTAGE 22.5KV
MAGNET CURRENT 2.2A
PROBE VOLTAGE 5.0KV
^{4}He GAS FEED
^{3}He GAS FEED
ARGONGAS FEED
$^{40}A^{+}$
$^{4}He^{+}$
$^{3}He^{+}$
x3
$(N_2)^{+}$
$^{4}He^{++}$
$^{3}He^{++}$
x $\frac{1}{3}$
H^{+}
10^{2}
10
1.0
0.1
0.01
0.5
1.0
1.5
2.0 KV
1.0
0·8
0·6
0·4
0.2
0
ION CURRENT IN μ A
DEFLECTOR VOLTAGE

FIG.2

nicely on a straight line confirming the earlier assignment for the various peaks.

However, Z/M does not uniquely define the nature of the ion. The peak corresponding to $Z/M = \frac{1}{2}$ may be due to both $^4He^{++}$ and $(H\ H)^+$. But the $(H\ H)^+$ contribution must be very small since the yield of H^+ is itself very small. In the case of $^3He^{++}$, $Z/M = 2/3$. It is inconceivable that any other ion may be producing this peak. Hence, it seems reasonable to conclude that the He^{++} yield from the test bench assembly is about 1-2 μa.

REFERENCE

1. I.J. Taylor and J.L. Weil, Nuclear Instruments and Methods 34(1965), 197-201.

DISCUSSION

P.K. Ghosh: What is the ion source pressure at which you observe 99% He^+ and 1% He^{+2}?

S.N. Misra: Gas pressure feed 1×10^{-4} m of H_g. inside the ion source bottle 1×10^{-5} m of Hg and system's vacuum in Einzel lens was in the region 1.5 x 10^{-6} mm of Hg

S.B. Karmohapatro: Since there will be no focussing of the analysed beam what will be the width of the beam and what will be the transmission?

S.N. Misra: There is no focussing in the test bench system after analysis. But once it is fitted in the accelerators, the accelerators single gap focussing lens works for it. At present focussed spot of 3 mm. has been obtained at acceptance aperture el itself.

EFFECT OF ABSORBER THICKNESS ON NARROW-BEAM-COLLIMATED GEOMETRY CONDITION

S. Gopal, H. Sanjeevaiah and B. Sanjeevaiah
Department of Physics, University of Mysore, Manasagangotri.
Mysore-6

I. INTRODUCTION

A number of measurements on photon attenuation coefficients have been made from time to time using narrow-beam-collimated geometry. In all these experiments it is tacitly assumed that the multiple scattered photons from the absorber do not reach the detector and hence the good geometry condition is preserved. But it may be expected that the number of multiple scattered photons reaching the detector would increase as the absorber thickness increases. This aspect has been overlooked in the measurements of attenuation coefficients[1-9]. Therefore it is felt necessary to investigate the effect of absorber thickness on the narrow-beam-collimated geometry condition.

II. EXPERIMENTAL

The narrow-beam-collimated geometry set-up similar to that of Davisson and Evans[1] is used in this experiment; but the diameters of the slits are halved and the distance between the source and the detector is doubled. These alterations were made to reduce the solid angle subtended by the detector at the absorber. The advantages in reducing the solid angle are:

(i) the compton scattered photons reaching the detector can be neglected[10];

(ii) the coherently scattered photons reaching t det r

nonuniformity in the thickness of the absorbers were calculated using the relation given by Carter et al [9]. This correction was found to be less than 0.05%.

III. RESULTS

The photopeaks observed for different absorber thicknesses are displayed in figure 1. The percentage resolutions calculated from the photopeaks and the corresponding linear attenuation coefficients are tabulated in Table I.

Table I

Thickness t gm/cm^2	% Resolution	μ cm^2/gm	μt
0 A	10.5	-	-
3.6979 B	10.5	0.1073±0.0007	0.3967
8.3336 C	11.4	0.1079±0.0008	0.8992
11.9989 D	11.6	0.1089±0.0008	1.3067
15.5476 E	11.8	0.1097±0.0012	1.7055

The results clearly show that for $t \lesssim 3.7$ gm/cm^2, the attenuation coefficient and percentage resolution of the detecting system remain fairly constant. Therefore it may be seen that the narrow-beam-collimated geometry condition is preserved and the number of multiple scattered photons reaching the detector is negligible for values of $\mu t < 0.5$, where μ is the attenuation coefficient in the material for the incident photons.

ACKNOWLEDGEMENT

The aut rateful to Prof. S.Chandrasekhar, He of the de for p the facilities to t thes atio

vis Ev . Rev. 81, 40

lga . 952).

ede Re 9 (1962

e . Rev.

shmi
66).

Phys.

ok
s 7

er

24,

(1952)
7

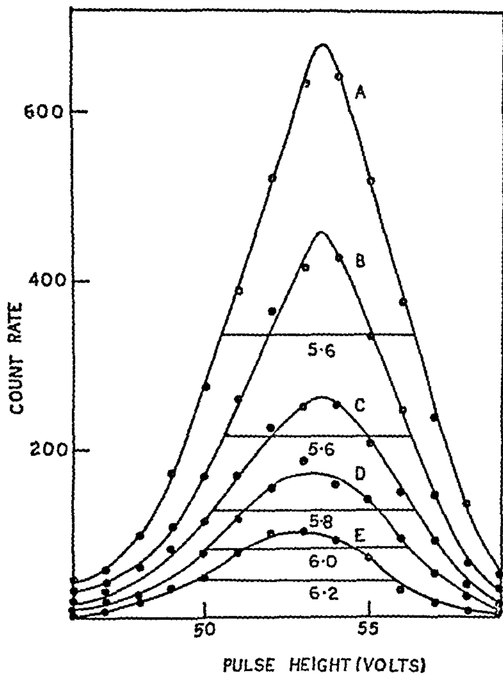


Fig. 1 The spectra of 662 keV gamma rays for different absorver thicknesses.

A LIQUID ARGON IONIZATION CHAMBER AS A COUNTER FOR α-PARTICLES.

B.Y. Deshpande, S.K. Pardhasaradhi and R. Ramanna
Technical Physics Division, Bhabha Atomic Research Centre, Bombay-85.

I. INTRODUCTION

Liquid argon as a counting medium in an α-particle ionization chamber has been described by several authors. The method of nuclear pulse technique has also been used to get information about the physical properties of the liquid. It has been reported by Malkin and Shultz[1] that for pure liquid argon electron drift velocity increases as a square-root of electric field, whereas Williams[2], Swan,[3] and Pruett and Broida[4] report saturation of drift velocity at high fields.

In the present investigation we report the dependence of pulse height, energy resolution, and charge collection efficiency on parameters like electric field, Argon gas pressure, volume of the counter, and molecular impurities in the liquid. Results are discussed in terms of the recombination mechanism.

II. EXPERIMENTAL

In our experiments we have used a three parallel-plate structure dipped in liquid argon. Am^{241} α-sources of 0.5 μC strength each are electro-deposited on the outer plates. The central plate acts as the collecting electrode. In this configuration one of the counters is kept as a reference when parameters for the other are changed. Liquid argon is produced in a copper cup attached to a cold finger dipped in liquid nitrogen. Prior to liquefaction argon gas is purified by repeatedly passing it over copper and magnesium traps

heated to 600°C.

The counter is connected to a low-noise charge-sensitive pre-amplifier, main amplifier, and a 512-pulse height analyser. Measurements are taken for electronic charge collection.

III. RESULTS AND DISCUSSION

α-particle spectra, pulse heights, and energy resolutions as functions of electric field, inter-electrode spacing for the experimental counter, and the superincumbent argon gas pressure are shown in Figs. 1-3. Pulse height measurements are reproducible within ± 1 channel; total counts under the peak also tally with the strength of the source. Introduction of oxygen, nitrogen, or forming gas (10% hydrogen in nitrogen) suppressed the pulses completely; purification of this impure gas restored the spectra fully.

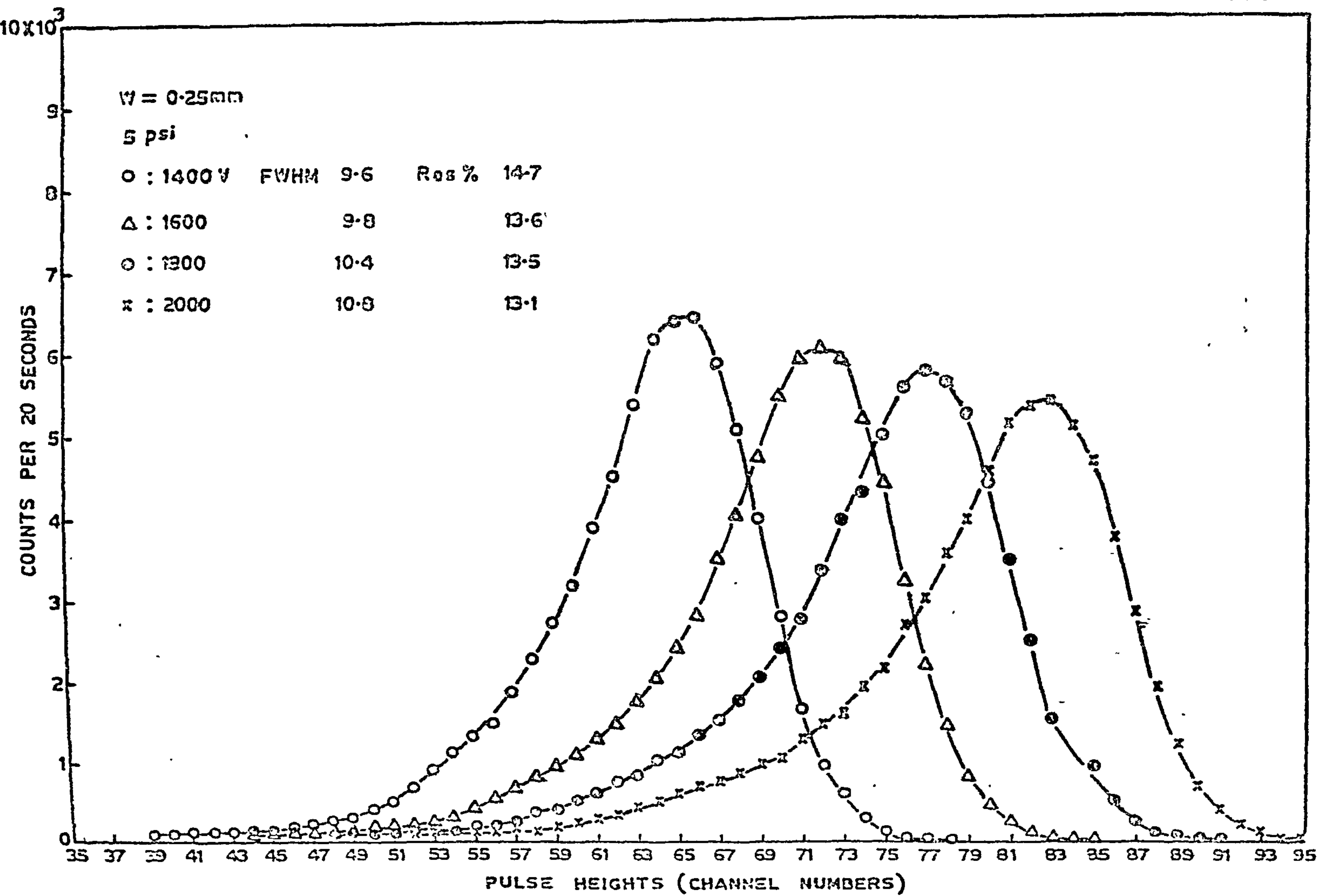
From the experimental data it is seen that for a given separation and gas pressure, pulse height increases with electric field without showing saturation even at high fields of the order 100 kV/cm. This may mean that more and more charge is coming from the columnar region. But it is also found that for the same electric field E pulse heights are different for different separations and pressures. At higher pressures pulse heights are always found to be higher indicating that columnar recombination alone does not govern the response of the counter. Dependence of pulse height on separation W clearly indicates the presence of trapping and recombination of the charge. However, under pure recombination law pulse heights must increase as W is reduced. To the contrary, it is observed that there is an optimum separation for which maximum pulse height is obtained. This volume effect seems to be an additional factor which determines

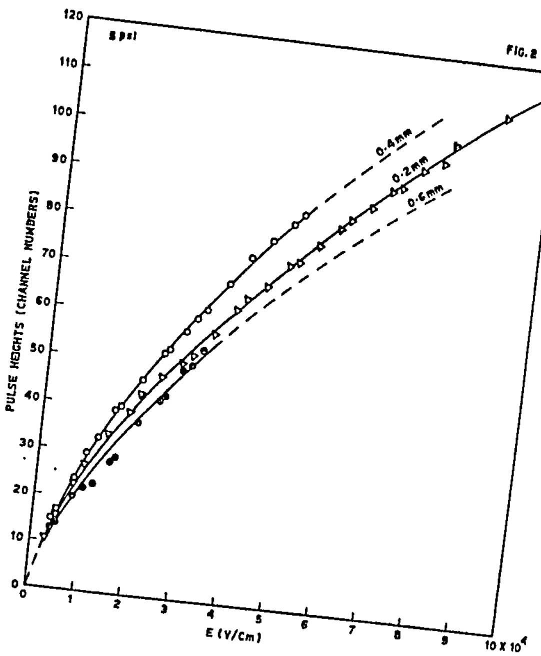
the response of the counter. Williams[2] in his measurements also noticed such an effect which, however, he attributed to systematic errors.

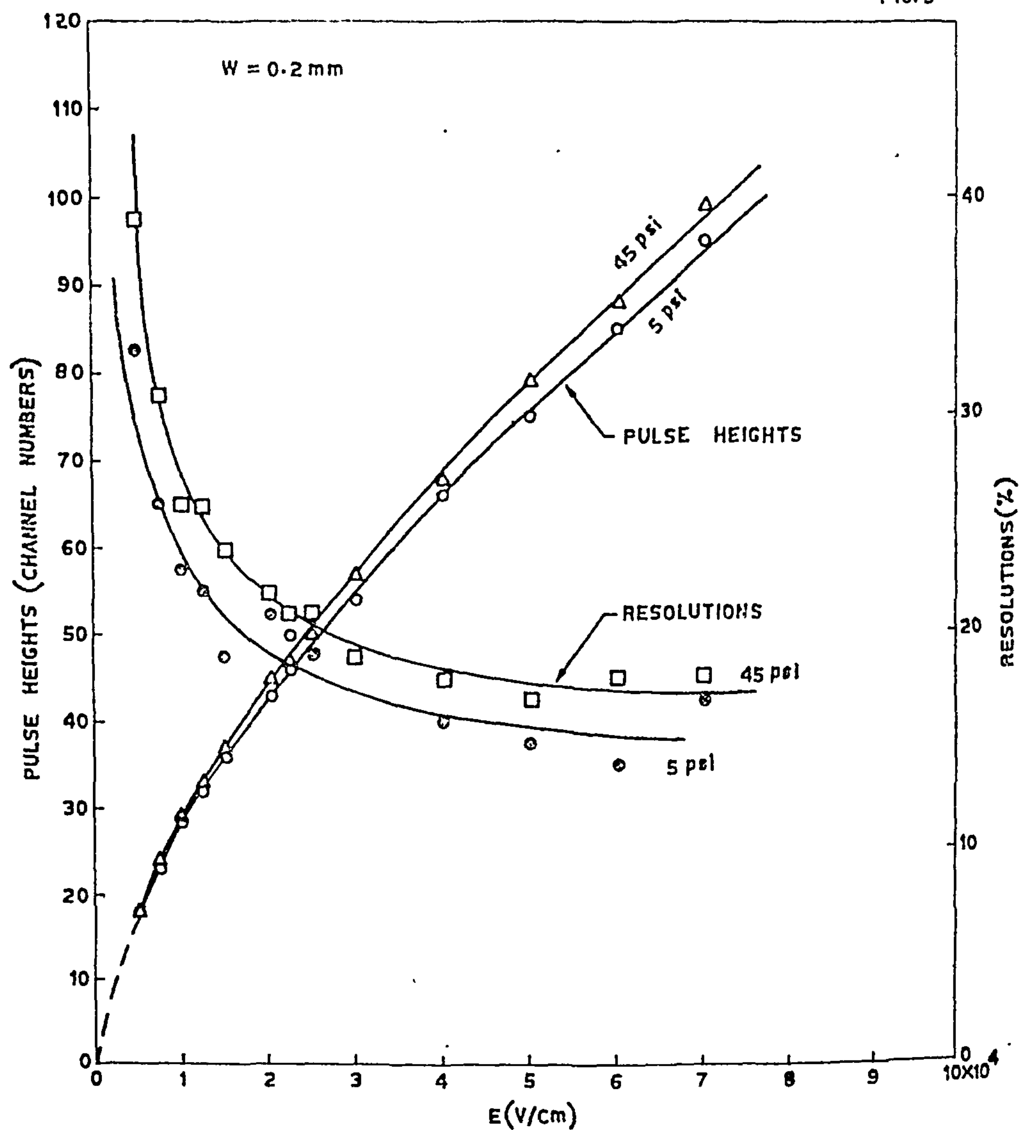
We propose to attribute the volume effect to some sort of short range internal electric field which essentially screens the external field. This causes reduction in the pulse height. The concept of internal field is further supported by the fact that with increasing pressure the pulse heights are found to increase. This means under high pressure the effect of internal field is reduced. In essence, we may say that pulse heights are governed by three factors; columnar recombination, trapping and recombination of charge during transit, and by the internal field.

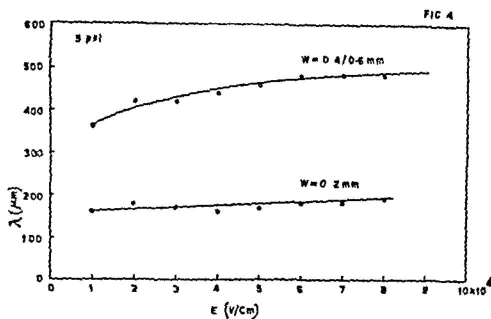
Internal field as postulated here could arise due to potential wells in the liquid, polarization effects of the liquid medium, positive ion space charge, space charge due to trapped carriers, or due to the presence of ionized impurities in the liquid. An estimate of the magnitude of the internal field from the recombination law gives some clue to its exact origin..

When pulse heights are governed only by the free carrier recombination statistics, charge collection efficiency η is given by the familiar Hecht-relationship: $\eta = (\lambda/W) [1 - \exp(-W/\lambda)]$. Here λ, the drift length, is the distance the charge traverses in electric field E during its lifetime τ. If v_d is the drift velocity, and μ is the mobility, then $\lambda = v_d\tau = \mu E\tau$. From the pulse height ratio for W=0.4 mm and 0.6 mm at a given field, we find λ. This is repeated for different fields. Then using these values of λ, the effective λ at the corresponding fields for the W = 0.2 mm data are evaluated.


FIG. 1
W = 0·25mm
5 psi
o : 1400 V FWHM 9·6 Res % 14·7
Δ : 1600 9·8 13·6
⊙ : 1800 10·4 13·5
x : 2000 10·8 13·1
10X10^3
COUNTS PER 20 SECONDS
PULSE HEIGHTS (CHANNEL NUMBERS)


8 psi
FIG. 2
PULSE HEIGHTS (CHANNEL NUMBERS)
E (V/Cm)
0.4mm
0.2mm
0.6mm
0
10
20
30
40
50
60
70
80
90
100
110
120
1
2
3
4
5
6
7
8
9
10 X 10^4


FIG. 3
W = 0·2 mm
45 psi
5 psi
PULSE HEIGHTS
RESOLUTIONS
45 psi
5 psi
PULSE HEIGHTS (CHANNEL NUMBERS)
RESOLUTIONS (%)
E (V/cm)
10X10^4
0
10
20
30
40
50
60
70
80
90
100
110
120
1
2
3
4
5
6
7
8
9


FIC 4
5 psi
W = 0.4/0.6 mm
W = 0.2 mm
λ (μm)
E (V/Cm)
10x10^4
600
500
400
300
200
100
0
0
1
2
3
4
5
6
7
8
9

Results of these calculations are shown in Fig. 4.

From these results it is seen that the drift length saturates at high electric fields for small as well as large separations. Saturation can arise due to saturation of drift velocity or due to trapping. If we now assume that the drift velocity saturates, as it cannot increase indefinitely and as is also reported by other investigators, we may conclude that the charge transport is governed by the internal electric field of the kind peculiar to liquid state. Its magnitude is such that it reduces the drift velocity to about one third of its value.

IV. REFERENCES

1. M.S. Malkin and H.L. Shultz, Phys. Rev. 83, 1051 (1951).
2. R.L. Williams, Canad. J. Phys. 35, 134 (1957).
3. D.W. Swan, Proc. Phys. Soc. 83, 659 (1964).
4. H.D. Pruett and H.P. Broida, Phys. Rev. 164, 1138 (1967).

DISCUSSION

M.R. Bhiday: Have you looked at the pulse shape?

R.Y. Deshpande: Yes, but not very much in details. The rise-time is about a μ sec. and seems to be independent of electric field for high fields.

M.G. Betigeri: 1) Does the resolution also show an optimum behaviour as a function of W. 2) How do you estimate τ .

R.Y. Deshpande: There is no optimum in resolution with respect to the separation W. 2) We have not estimated τ .

USE OF LIQUID CRYSTALS AS MEDIA FOR CONTINUOUSLY SENSITIVE CHAMBERS FOR THE REGISTRATION OF ELEMENTARY PARTICLES

A.K. Jalaluddin and Hashmat Husain
Aligarh Muslim University, Aligarh, U.P.

Liquid crystals are groups of substances which do not transform into the isotropic liquid phase directly on melting. They can exist in a phase intermediate between the solid and liquid phases (mesophase). In the mesophase, these substances possess fluidity but at the same time also preserve certain degree of alignment of its molecules which explain their anisotropy. According to the degree and nature of the molecular alignment liquid crystal are classified as nematic, smetic, and cholesteric.[(1-3)] Due to their extraordinary behaviour liquid crystals have found a large number of applications in the measurement of surface temperature and its variations, in the detection, control and modulation of electric, magnetic and optical signals, and also in magnetic resonance spectroscopy as solvents. In the present paper we suggest a use of liquid crystals as chamber media for the registration of elementary particles.

Thick layers of nematic liquids (e.g. p-azoxyanisole, 4,4'-bis(methoxy) azoxybenzene) appear turbid due to the nonhomogeneity of the orientation of their molecular aggregates along some preferred direction. It has been found that complete orientation of the liquid in thick layers can be achieved with relatively low magnetic field strengths (1-2 KiloGauss).[(4)] This is due

to the diamagnetic anisotropy of the volume elements and the free mobility of the molecules. Static and low frequency electric fields also have similar orienting effects on nematic liquid crystals.[5,6] When a nematic sample, sandwitched between two transparent, conducting tin oxide-coated glass plates, is subjected to an electric field the molecules (except those at the surface) reorient themselves in a preferred direction. If such a sample is viewed along the direction of alignment between crossed polaroids, the field looks dark due to the extinction of the transmitted light.[7] In the case of p-azoxyanisole, domains have been observed under the influence of external electric fields.[8] The relaxation time for the fundamental particles in the nematic mesophase, as measured by varying the frequency of the applied alternating field, has been found to be of the order of $\sim 10^{-5}$ sec.[2] A schematic diagram of the experimental setup used by us to study the transparency of crystalline liquid samples is shown in figure 1. In our experiments, we have found that the transparency of p-azoxyanisole falls drastically with the application of electric fields, both D.C. and A.C., of strengths $\sim 10^{4}$ V/cm, whereas in the case of a mixture of cholesteryl chloride, cholesteryl nonanoate, and oleyl cholesteryl carbonate (30%, 56% and 14% by wt. respectively), which is normally milky in look, becomes clear on the application of D.C. fields of $\sim 10^{5}$ V/cm. Our experiment with the cholesteric mixture

corroborates the observation recently reported by several authors,[9] according to whom the increase in the transparency of the mixture is due to the transition of the sample from the cholesteric to the nematic state.

The deformation energy involved in the above transitions is very small (in the case of a nematic layer of 4, 4'-bis(methoxy) azoxybenzene this energy $\sim 10^{-5}$ erg. cm^{-3}).[3] The transition from the forced homogeneous molecular alignment to the natural alignment of a crystalline liquid sample with the turning off of the external field is spontaneous. The initiation of deorientation is favoured at those points where the kinetic energy of the molecules is appreciably greater than the average value. It is therefore expected that if the withdrawal of the external field is controlled by the incidence of an elementary particle on the sample, the thermal 'spikes' produced by the high energy secondary electrons along the path of the particle may very well act as initial centres of deorientation of molecules, analogous to the formation of bubbles in a Bubble Chamber.[10] The further spreading of the deorientation should be spontaneous and its rate determined by the thermal conductivity of the medium. The deorientation may spread over a sphere of radius $\sim 10^{-2}$ cm(suitable for photographing the region in polarized light) within few microseconds. Such a 'track' may be made to look bright in a dark background by suitably orienting the polars.

Since the above device will be controlled by the incident particles themselves it will remain almost continuously sensitive to incident particles.

Elaborate experimental investigations of some of the aspects of the above problem are in progress.

REFERENCES

1. G.H. Brown and W.G. Shaw, Chem.Reviews 57, 1049(1957)

2. G.W. Gray, Molecular Structure and Properties of Liquid Crystals, Academic Press, New York (1962).

3. A. Saupe, Angewandte Chem., Int.Ed.,7, 97(1968).

4. W. Møll and L.S. Ornstein, Proc. Acad.Sci.Amsterdam 21, 259(1918)

5. L.S. Ornstein and W.Kast, Trans.Faraday Soc.29,931 (1933).

6. K.Herrmann, A.H.Krummacher and K. May, Z.Physik,73, 419(1932).

7. J.A.Castellano and M.T.McCaffrey, Liquid Crystals and Ordered Fluids, Plenum Press, New York(1970).

8. R. Williams, J.Chem.Phys. 39, 384(1963).

9. J.J.Wysocki, J.E.Adams and D.J. Olechna, Liquid Crystals and Ordered Fluids, Plenum Press,New York (1970).

10. N.B. Dolone(Ed), Puzyrkovie Kamery, Gosatomizdat, Moscow(1963).

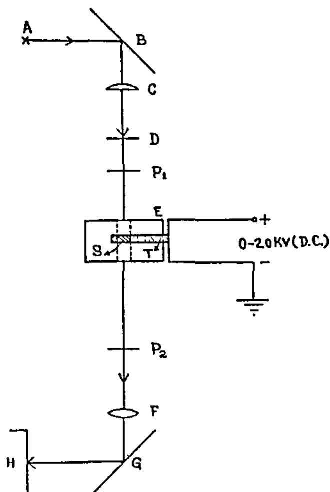


Fig.1. Schematic diagram of the Experimental Setup to Study Transparency of Liquid Crystals.
A-Source; B and G - mirrors; C and F - lenses; D-Diaphragin; P1 and P2-polarizer and analyzer respectively; E-heating stage; S-sample sandwiched between tin oxide-coated transparrent glass slide and cover plate; T-teflon spacer; H-photomultiplier.

DISCUSSION

S.V. Subramanyam: It is the cholesteric liquid crystal that is sensitive to scattering properties (and a sample of this was displayed by the author too!). But why nematic type was chosen for detection is not clear.

A.K. Jalaluddin: In order to make a cholesteric mixture clear one has to apply a field of the order of $\sim 10^5$ V/cm. This strength is very large compared to that required in the case of a nematic sample (e.g. substituted benziledene aniline).

MEASUREMENT OF LOW REACTION CROSS-SECTIONS WITH DIELECTRIC TRACK DETECTORS

D.S. Srivastava
Aligarh Muslim University, Aligarh, India

and

G. Somogyi, B. Schlenk and I. Hunyadi
Institute of Nuclear Research of the Hungarian Academy of Sciences, Debrecen, Hungary

I. INTRODUCTION

Because of very low reaction cross-sections the data on angular distribution of α-groups emitted in many nuclear reactions are completely missing for low bombarding energies in the literature. The obvious difficulties in such measurements are large backgrounds and the error caused due to changes in the beam current for different angular settings of a conventional detector during long exposures. The discovery of dielectric track detectors in which the track diameter is a very sensitive function of type and energy of particle opens new possibilities for such measurements[1,2]. These detectors have the added advantages of giving permanent record of particle tracks without fading and of being insensitive to β-particles, γ-rays, X-rays light rays etc. In a previous paper[3] we have established the accuracy of plastic detectors in angular distribution measurements by comparing their results with those measured by a semiconductor detector in the case of $^{19}F(d,\alpha)^{17}O$ nuclear reaction. In this paper we present experimental data for the angular distribution and yields of α_0 and α_1 groups emitted in the $^{27}Al(d,\alpha)^{25}Mg$ nuclear reaction at E_d=650,585 and 540 keV measured by using plastic track detectors. For this reaction no data is available below E_d=1.2 MeV. Some typical problems encountered during the present measurements will also be briefly described along with their solutions.

II. EXPERIMENTAL

A collimated beam of deuterons accelerated in the cascade generator of the Institute of Nuclear Research, Debrecen, was allowed to fall at 45° upon a very thin Al- target mounted in the centre of the vacuum irradiation chamber simil   to .

one described in Ref.1. The target was made by evaporating spectroscopically pure Al on thin copper backings of about 0.3 mg/cm^2. The target thickness was determined by measuring the γ-peak shift of the 340 keV $^{19}F(p,\alpha\gamma)$ resonance line as described elsewhere.[4] Two bent cellulose acetate plastic sheets (Cellit-T, manufactured by I.C.I., London) used as detectors were mounted along the curved circular wall of the irradiation chamber, one for receiving the α-particles at the forward angles (20^o-90^o) and the other at the backward angles (90^o-165^o). In such a geometrical arrangement[1] the emitted α-particles entered the detector surface at right angles at every lab-angle.

Some preliminary irradiations and etchings showed that on the irradiated surface of the detectors, tracks due to ^{3}He particles were also formed. These particles were produced due to d + d reaction taking place on the deuterium self-target developed on the Al target. These tracks had very large density and due to their low energy they appeared on the etched surface of the detectors after a relatively shorter etching time. Because of their large track density these tracks produced circular opal spots marking the area of the detector exposed at every lab-angle. This was used with advantage to count the desired α-tracks lying in this area.

As the energy of a given group of α-particles varies with lab-angle, the tracks belonging to α-particles of same group did not appear on the etched surface of the detectors simultaneously and did not have equal diameters at a given etching time. This difficulty was overcome by suitably retarding the α-particles at various lab-angles using Al foils of appropriate thickness so that they had nearly same (minimum) energy (within $\pm$ 0.1 MeV) at all lab-angles as at 165^o.

Due to long exposure time in the vacuum chamber of the accelerator a layer of AlN got developed on the surface of the Al target and resulted into disturbing α-particles from the ^{14}N (d, α) reaction. The α_0 and α_1 groups from the

^{27}Al (d, α) ^{25}Mg reaction to be studied lay energetically between the α_1 and α_2 groups from the ^{14}N (d, α) reaction. To avoid the disturbing effect of nitrogen α_1 groups the thickness of detector sheets were chosen in such a way that their etchable part passed through the sheets and their tracks could not be etched. Thus before mounting it as detector the thickness of the available 100 μ thick Cellit-T plastic had to be reduced to about 39 μ. This was done in two steps: first by etching it into a solution containing 30 gm $K_2Cr_2O_7$ + 95 cc H_2SO_4 + 120 cc H_2O, at 60°C for about 2.5 hours its thickness was reduced to 45 μ and then the remaining 6 μ were removed in the track etching solution (20 gm NaOH + 16 gm KOH + 4.5 gm $KMnO_4$ + 90gm H_2O) at 60°C. This two step process was found necessary to avoid any change in track growing features of the plastic caused by the possible diffusion of the dichromate solution. Further, the bulk etch rate in the dichromate solution was very large and it did not etch any background tracks present in the plastic which might cause error. On etching the plastic detectors from the back side the tracks belonging to α_0 and α_1 groups from the ^{27}Al (d, α) ^{25}Mg nuclear reaction appeared in succession and could be counted.

To illustrate the planning of such measurement by plastic track detectors the real situation at the bombarding energy E_d = 650 keV will now be described. Using suitable Al foils we could so adjust that the energy of α-particles at every lab-angle from the α_0 group of ^{27}Al (d, α) ^{25}Mg reaction would be E_{α_0} = 5.9 MeV, from α_1 group it would be E_{α_1} = 5.4 MeV and from α_2 group it would be E_{α_2} = 5.0 MeV within ± 0.1 MeV. The ranges of these particles from our calculated range energy curves[5] were found to be R_{α_0} = 36.5 μ, R_{α_1} = 31 μ and R_{α_2} = 27.5 μ within ± 1 μ. With the absorbing foil used in this case the energy of the disturbing α_1 group from ^{14}N (d, α) reaction lay in the energy region 6.45-7.55 MeV at various lab-angles corresponding to a range in Cellit of ∠.5
After knowing this, (38 ± 1) μ thick Cellit -

were used for actual measurements. With this thickness the end-point of the α_0 tracks could be reached after removing 1.5 μ thick layer of plastic from the back side of the detector by etching but for track counting under optical microscope the most suitable diameter (of $\sim$5 μ) could be reached after 4 μ removed layer from the end-point of the track. As the plastic was etched from both the sides upto this stage, the remaining thickness of the plastic at the stage of counting of α_0 group was $[38-2\ (1.5+4)] = 27\ \mu$. On reaching good countable size for α_1 and α_2 groups from the $^{27}Al(d,\alpha)^{25}Mg$ nuclear reaction, the remaining thickness after etching would be 16 and 9 μ respectively. Handling of such thin plastics is practically very difficult. To avoid this difficulty the plastic was first etched from both the sides and when the ^3He tracks marked the boundary of the irradiated area to be counted in and the α_0 group had appeared on the back surface, the counting of the α_0 was performed and then the etching of the plastic was continued only from the back side of the detector to reach the α_1 group thus avoiding too much thinning up of the plastic detector as well as the growth of the otherwise disturbing ^3He tracks. The measurement of α_2 group could not be made as very thin plastic sheets (12 μ) were left after the counting of α_1 group.

III. RESULTS

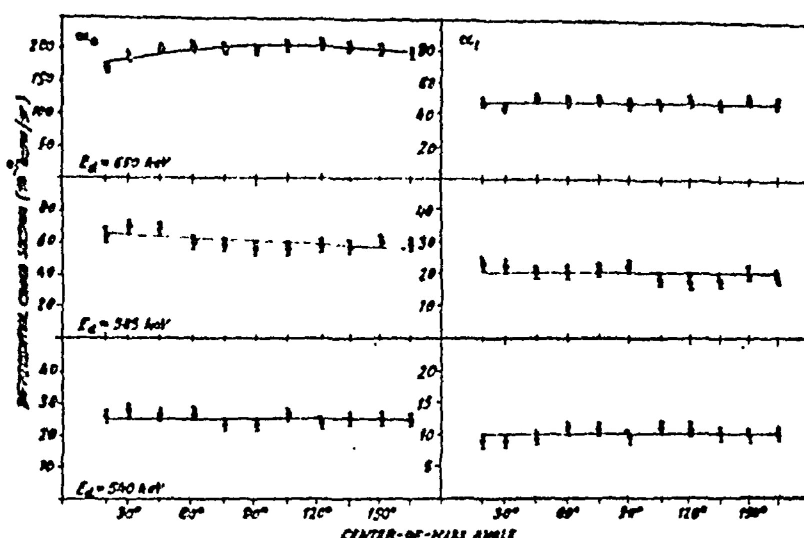
The absolute differential cross-sections of the α_0 and α_1 groups emitted in the $^{27}Al(d,\alpha)^{25}Mg$ nuclear reaction in the centre-of-mass system at E_d = 650, 585 and 540 keV bombarding deuteron energies are shown in the figure. The bars in the figure represent the error of the relative angular distribution. According to the uncertainities in the target thickness determinations, the errors in the absolute cross-sections are estimated to be 35% in general. The angular distributions which are nearly isotropic have been analyzed in terms of the Legendre Polynomials as published elsewhere.[4] The curves in the figure are the least square fits of the experimental points to the series of Legendre Polynomials. Assuming statistical compound reaction mechanism the relative intensity ratio of the two

measured α- groups could be reproduced[4] by a simple calculation giving the statistical weight factors for the alpha transitions concerned.

It is believed that the method described can be used for the study of (p,α), (d,α), and (t,α) nuclear reactions. At low neutron energies the study of (n,α)nuclear reactions is also feasible. At high neutron energies, however, the α-tracks from the $^{12}C(n,n')3\alpha$ reaction due to the carbon content of the plastics cause disturbing background.

REFERENCES:

1. G. Somogyi, B. Schlenk, M. Várnagy, L.Meskó and A.Valek: Nucl. Intr. Meth. 63, 189 (1968).
2. G. Somogyi and B. Schlenk: Proc. Intern.Topical Conf. Nucl. Track Regist. in Insulating Solids and Appl. Clermont-Ferrand, France, May 6-9, 1969.
3. L. Meskó, B. Schlenk, G. Somogyi and A. Valek: Nucl. Phys. A130, 449 (1969).
4. I. Hunyadi, B. Schlenk, G. Somogyi and D.S. Srivastava: "Investigation of $^{27}Al(d,\alpha)^{25}Mg$ nuclear reaction in the Energy Range E_d = 650-540 Using Plastic Track Detector" Acta Physica Academiae Scientiarum Hungaricae (to be published).
5. G. Somogyi, M. Várnagy and G. Petö: Nucl. Instr. Meth. 59, 299 (1968).



Angular distribution of α_0 and α_1 groups emitted in the $^{27}Al\ (d,\alpha)\ ^{25}Mg$ nuclear reaction at bombarding deuteron energies E_d = 650, 585 and 540 keV as measured by using plastic track detectors.

DISCUSSION

M.R. Bhiday: 1) Have you made an estimate of energy resolution? 2) What is the exact method of this estimation?

D.S. Srivastava: 1) Yes, it is 150 keV at 3 MeV. It is also different for different plastics and varies with etching conditions viz., cellulose nitrate gives least resolution, cellulose acetate more and polycarbonates most. For a given plastic the resolution increases with etching time. 2) It is based on our experimental experience. It can also be seen from our measurement of $D(t)$ curves to be published in "Interm Journal of Radiation and Isotope".

"MEASUREMENT OF MAGNETIC FIELD INDEX 'n' OF THE 5 Mev BETATRON BY AN A.C. POTENTIOMETER"

M.R. Bhiday and V. N. Bhoraskar
Department of Physics, University of Poona, Poona-7(India)

I. INTRODUCTION

The field index 'n' of the betatron can be determined accurately by measuring the fields at different radial points in the median plane. However, the magnet current should be stable for accurate measurement of the magnetic fields at various points. In addition, if a small search coil is used for this purpose an accurate knowledge of its constants is also required.

Because of the eddy currents, the flux in the magnet is not in phase with the current in the magnetising coils and with a small search coil used to measure the magnetic field by balancing its induced voltage with some external standard voltage, the inequality(2) of the phases of these voltages becomes a problem and the use of a phase shifter is essential.

The method described in this note for measurement of the field index 'n' of the 5 Mev betatron, we have in this laboratory, is independent of the current in the magnet as well as the constants of the coils used, and the difficulty of phase difference is also removed.

II. THEORY

If a small coil of N turns is placed in the uniform gap of the betatron, the e.m.f. induced at the time t due to the magnetic field $B = B_o \sin \omega t$ is given by

$$E_o = - N \frac{d\phi}{dt} = - NAB_o \omega \cos \omega t \qquad \ldots\ldots \qquad (1)$$

If another measuring search coil of turns N_1 is kept at a radial distance r in the median plane of the betatron, the induced e.m.f. at the time t in this coil is

$$E_r = - N_1 \frac{d\phi_1}{dt} = - N_1 A_1 B_r \omega \operatorname{Cos} \omega t \quad \ldots\ldots (2)$$

If the two ends of the coil kept in the central part of the betatron are connected to a standard potentiometer wire of length L, and if the e.m.f. from the measuring coil is balanced across the potentiometer wire for length ℓ, then

$$\frac{B_r}{B_o} = R\ell \quad \ldots\ldots (3)$$

where R is a constant.

Similarly for the radial position $(r + \Delta r)$ of the measuring coil, if the length of the potentiometer wire required for the balance is ℓ_1, then we have

$$\frac{B_{r+\Delta r}}{B_o} = \frac{B'_{r+\Delta r}}{B'_o} = R\ell_1 \quad \ldots\ldots (4)$$

The terms $B'_{r+\Delta r}$ and B'_o arise due to the fluctuations in the current if any, but the ratio remains the same.

From eq. (3 and 4)

$$\frac{\Delta B_r}{B_r} = \frac{\Delta \ell}{\ell} \quad \ldots\ldots (5)$$

if $(r + \Delta r) > r$ then $\ell_1 < \ell$.

As $n = - \dfrac{dB_r/B_r}{dr/r} = - \dfrac{\Delta B_r/B_r}{\Delta r/r}$ from (5)

$$n = - \frac{\Delta \ell/\ell}{\Delta r/r} \quad \ldots\ldots (6)$$

III. RESULTS AND CONCLUSION

A standardising search coil and a measuring coil were mounted in the central uniform gap and in the outer non-uniform gap of the betatron magnet respectively. The position of the latter could be known accurately in the

median plane. The voltages induced in the two coils were always found to be in phase and were put over a standard A.C. potentiometer. The balance point determined by a vibrational galvanometer was accurate to $\pm$ 1 m.m.

The value of n at any radial distance r in the median plane can be determined by multiplying the value of $\frac{1}{B}\frac{dB}{dr}$ read from fig. (1), by the r of the corresponding point. The variation of the 'n' with 'r' is shown in fig. (2).

It is clear from fig. (2) that the condition[3] for double focussing is obeyed only in a region 7 cm. $< r <$ 10 cms. of the median plane and the stable orbit[1] could be fixed at the radial distance r equal to 8.25 cms.

IV. ACKNOWLEDGEMENT

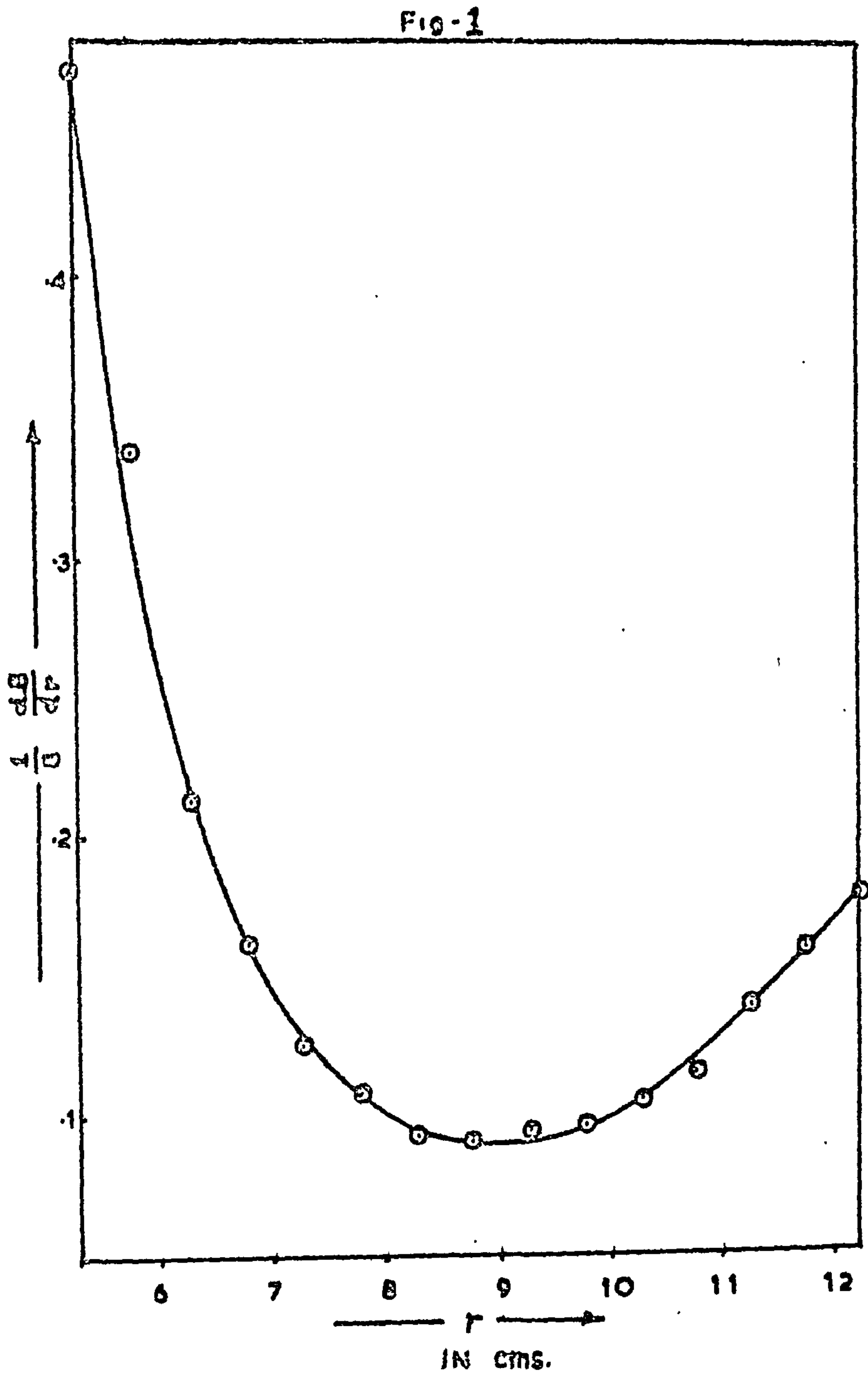
We are grateful to Prof. Wernholm, Royal Institute of Technology, Sweden for his gift of 5 Mev betatron for our research work.

V. REFERENCES

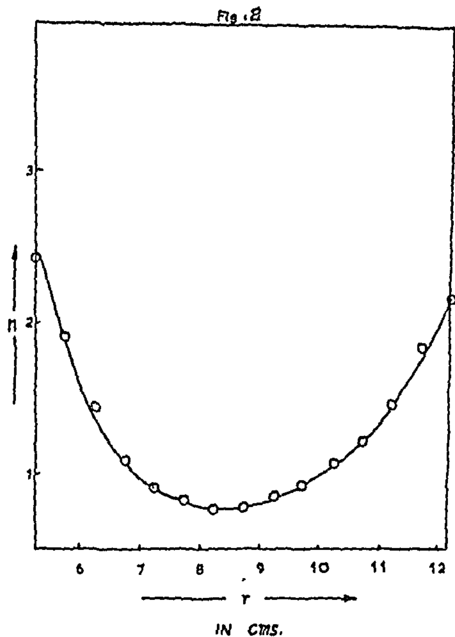
(1) Goward, Dain, Nature, 159, 636, 1947.

(2) Kerst, Phys., Rev., 60, 47, 1941.

(3) Kerst, Serber, Phys., Rev., 60, 53, 1941.



Figure(1) : Variation of $\frac{1}{B}\frac{dB}{dr}$ with the radial distance r.



Figure(2) : Variation of " n " with the radial distance r.

DISCUSSION

A. Jain: What is the accuracy in the measurement of the field index?

V.N. Bhoraskar: 2% in n value.

S.B. Karmohapatro: Is it required to see whether there is any loss of intensity due to inaccuracy in measurement in n.

V.N. Bhoraskar: Yes, I agree. But basically we are only shifting the orbit by momentarily pulsing the magnetic field, and expect the beam to emerge as it is in the stable orbit.

MASS SPECTROSCOPIC DIAGNOSTICS OF THE VACUUM ARC

V.S.Venkatasubramanian and P.T.Rajagopalan
Department of Physics, Indian Institute of Science, Bangalore-12.

I. INTRODUCTION

Mass spectrometry is a valuable tool for the diagnostics of electrical discharge phenomena, as a knowledge of the isotopic composition provides useful information on the role of the electrodes and ambient gas in the initiation and maintanence of the discharge, While, the distribution of ions in different ionisation states enables the plasma temperature and electron pressure to be calculated. In this paper, we present the results of mass spectrometric studies on the vacuum arc which have a bearing on two aspects of the vacuum arc discharge, (a) the transition from 'anode' to 'cathode' type of arcing, and (b) the temperature distribution in the vacuum arc column.

II. EXPERIMENTAL DETAILS

The measurements were made with a Nier-Johnson type double-focusing mass spectrometer constructed in this laboratory[1,2]. The vacuum arc source was of the simple door-bell type in which the arcing contacts were actuated by an externally mounted, a.c. fed electromagnet. The arcing voltage 6-24V was supplied by external batteries with inductance and/or resistance in series. Waveforms of arcing voltage and current were monitored with a CRO, and for the current range employed (gap current pulses 4-30A, and average arc currents 0.2-2A) the waveforms revealed 'showering', i.e., interrupted arcs due to discharging and recharging of the local capacitance. The circuit parameters could be adjusted for showering times to have values in the range 5-200 sec. A monitor electrode at the exist of the electrostatic analyser was used to measure a constant fraction of the total ion current, and the ra s

of resolved isotopic to monitor currents taken as a true measure of the ion current.

III. ANODE AND CATHODE ARCS

A study of electrode effects in some arc ion sources has been given by Honig[3]. The observation of two types of contact arcs was first made by Holm[4] on the basis of electrode erosion measurements; a more exhaustive study by Germer[5] established the feature of these distinct arc types, viz., the anode arc vaporising material from the anode leaving a crater, and interpreted as due to vaporisation of the anode by electrons initiating the arc, and the cathode arc evaporating cathode material in an array of tiny pits and interpreted as due to vaporisation at field emission spots and sputtering.

A mass spectroscopic study of this effect has been carried out by measuring the intensities of singly and doubly charged ionic species with sissimilar electrodes, for both small and large showering times. This is achieved by arcing the contacts (a) with no inductance is series, when the showering times are short $\sim 5 \mu$sec., and (b) with a 100 μH series inductance, when the showering times are $\sim 100 \mu$sec. The series resistance is adjusted so that the peak gap currents are nearly the same for the cases compared. The Table 1 gives the distribution of both cathode and anode material ions.

The measurements show that with no series L, and hence small showering times, the ions consist mainly of the anode material, while with longer showering intervals, there is a predominance of cathode ions. In the latter case, the relative abundances of multiply charged ions is higher. Thus the results confirm the existence of two arc types recognised in opening contacts.

TABLE 1

RELATIVE ION ABUNDANCES WITH DISSIMILAR ELECTRODES

Cathode	Series L .	Al^{+} .	Al^{++} .	Cu^{+} .	Cu^{++}.
Cu	Nil	7.0	2.5	4.5	1.2
Al	Nil	2.5	0.7	5.0	2.5
Cu	100 μH	20	12	95	68
Al	100 μH	55	50	13	6

(b) Fe-Cu couple.

Cathode	Series L .	Fe^{+}	Fe^{++}	Cu^{+}	Cu^{++}
Fe	Nil	4.0	2.4	5	2.0
Cu	Nil	5.0	1.8	2.0	1.1
Fe	100 μH	65	55	30	28
Cu	100 μH	25	20	45	35

IV TEMPERATURE DISTRIBUTION IN THE VACUUM ARC.

The mass spectrum from a vacuum arc between similar electrodes is mainly composed of atomic ions M^{+} M^{++} and M^{2+} and the molecular ion M_2^{+}. There is good evidence that high pressure arcs of duration 100 sec., and higher are in local thermodynamic equilibrium[6]. Thus if the vacuum arc is assumed to have a uniform plasma temperature and electron pressure, these parameters can be determined from a knowledge of singly and multiply charged ions, using the well-known Saha formula,[7]

$$\frac{n_{n+1}\, n_e}{n_n} = 2\, \frac{u_{n+1}(T)}{u_n(T)} \cdot \frac{(2\pi m k)^{3/2}}{h^3}\, T^{3/2}\, e^{-\{E_n - \Delta E_n\}/kT}$$

where n_{n+1} and n_n are the number densities of the $(n+1)$-fold, and n-fold ionised species, n_e the number density of electrons, u_{n+1}, u_n are the partition functions for the $(n+1)$-fold, and n-fold ionised atoms, E_n is the ionisation energy for the process $n^{+} \rightarrow (n+1)^{+}$; and ΔE_n is the lowering of ionisation energy due to [illegible] fields in the plasma.

Further, the relative abundances of atomic and molecular ions can be computed from the dissociation formula[8] and Saha equation,

$$\ln \frac{n_A n_B}{n_{AB}} = \ln K = \frac{D}{kT} + \frac{3}{2} \frac{\pi m k T}{h^2} - \ln \frac{8\pi^2 I}{h^2} + \ln\left[1 - e^{-h\nu/kT}\right] + \ln \frac{2 g_A g_B}{g_{AB}}$$

where D is the dissociation potential, I the moment of inertia, and ν the vibration frequency of the molecule, and g the statistical weights. If these equations are used with the observed abundances of atomic and molecular ions, it is not possible to arrive at a consistent and physically plausible set of values of T and n_e, for two reasons - (a) the observed abundances of molecular ions correspond to much lower temperatures than for multiply charged ions, (b) rather too high electron pressures ($\sim 10^4$ atmos.) have to be assumed to explain the observed multiple charge abundances, as pointed out by Franzen and Schuy[9].

The assumption of a uniform temperature for the arc column appears unrealistic. Actually, the temperature distribution in a cylindrical arc has been considered by Maecker[8] on the basis of energy balance equations, and for high pressure arcs with molecular gases, consists of a core, surrounded by a plateau with small temperature gradient corresponding to a region where thermal conduction is enhanced by transport of dissociation energy by diffusing molecules. A similar zoning of the arc structure is expected for the vacuum arc, with plateaus corresponding to (a) molecular recombination and dissociation, (b) single ionisation (c) double ionisation etc. The electron density, after the initial rapid rise due to onset of ionisation, does not however, increase much with temperature, the decrease in gas density being offset by enhancement due to multiple ionisation.

In the table below, we give the values of the relative abundances $\frac{M^{2+}}{M^+}$, $\frac{M^{3+}}{M^+}$ and $\frac{M_2^+}{M^+}$ for the vacuum arc,

calculated with the assumption of a uniform

$$n_e = 10^{19}/\mathrm{cm}^3,$$

and an arc column temperature distribution consisting of (a) a core of temperature T_1, where M^{2+} and M^{3+} predominate, (b) an intermediate zone of temperature T_2 (c) a periphery of temperature T_3 where molecular ions prevail, and compare these with observed values in our measurements. The method of calculation of M^{2+}, and M^{3+} is outlined in Reference[7], while the classic paper of Russel[8] on stellar abundances of molecules is followed for the calculation of M_2^+, the recent mass spectroscopic values of dissociation and ionisation energies of C_2 being used.

TABLE II

Material	T_1	T_2	T_3	$\frac{M^{2+}}{M^+}$	$\frac{M^{3+}}{M^+}$	$\frac{M_2^+}{M^+}$	$\frac{M^{2+}}{M^+}$	$\frac{M^{3+}}{M^+}$	$\frac{M_2^+}{M^+}$
	(10^4 °K)			(Calc.)			(Obs.)		
C	4.0	2.0	0.8	0.1	-	0.20	0.12	-	0.18
Al	3.7	2.6	0.4	0.86	0.2	0.1	0.8	0.2	0.1
Fe	3.4	2.5	-	1.2	0.17	-	1.2	0.15	-
Cu	4.1	2.8	-	0.65	0.1	-	0.6	0.1	-

It is thus possible to choose a set of values of T_1, T_2 and T_3 that are consistent with experimental data on abundances. Further, these temperatures are broadly in accordance with optical spectroscopic data in Gerdien and other high pressure high temperature arcs.

REFERENCES

1. V.S.Venkatasubramanian; Ind. J. Pure App. Phys., 6, 706, (1968).
2. V.S.Venkatasubramanian and H.E.Duckworth; Canad. J. Phys., 41, 234, (1963).
3. R.E.Honig; Advances in Mass Spectrometry, Vol.3, (Institute of Petroleum, London, 1966) p.101.
4. E.Holm and R.Holm; Z.Angew. Phys., 6, 352, (1954)
5. L.H.Germer; J. Appl. Phys., 19, 1067, (1958)
6. H.Maecker; Discharge and Plasma Physics Univ. New. Eng. Press, Armidale, Chap.19. N.S.W., 1964.
7. Data for Plasmas in Local Thermodynamic Equilibrium. Ed.H.W.Drawin; (Gauthier-Villars, Paris, 1965.)
8. H.N.Russel; Astrophys. J. 79, 317, (1934).
9. J.Franzen and K.D.Schuy; Phenomena in Ionised Gases; (Int. Conf. Belgrade, 1965) Vol.3. p.242.

DISCUSSION

Jayakumar: What was the power at which the arc was operated?

P.T. Rajagopalan: The power at which the arc was operated was varied from about 6 watts to 25 watts corresponding to the voltage across the electrodes being varied between 6 and 25 volts at an average arc current of about one ampere.

S.B. Karmohapatro: What is the R.P. of your instrument? Why do you require double focussing?

P.T. Rajagopalan: The resolving power of the instrument is about 1 in 50. Double focussing is required while using ion sources like the vibrator arc source which produce ions of large energy spread.

A VERSATILE MOSSBAUER SPECTROMETER

V.S. Indurkar and P.K. Patwardhan
Electronics Division
Bhabha Atomic Research Centre
Trombay - Bombay.

I. INTRODUCTION

Mossbauer spectroscopy is widely used in Nuclear Physics, Solid state physics, and more recently for chemical structure [illegible]. This is usually done by moving the source or absorber relative to each other, which imparts the doppler modulation to the recoil-free gamma radiation so as to produce resonant absorption.

The production of precisely controlled velocity is [illegible] either by mechanical(1), or by electromechanical(2-4) means. Constant velocity, linearly increasing velocity and sinusoidal velocity are some of the more common modes of motion employed.

Mechanical means of producing [illegible] low velocities have [illegible] limited success(2). However, electromechanical methods are being used with good success in Mossbauer spectrometry for [illegible] velocities or linearly increasing velocities. An important advantage of the electromechanical method is that it lends itself [illegible] to the instantaneous velocity corrections, employing [illegible] feed-back.

In these electromechanical vibrator is used [illegible] with velocity transducer for velocity feedback [illegible] instantaneous velocities accurately and is applicable to all [illegible] the modes of motion.

It has been pointed by [illegible] and [illegible] et al.(2,[illegible]

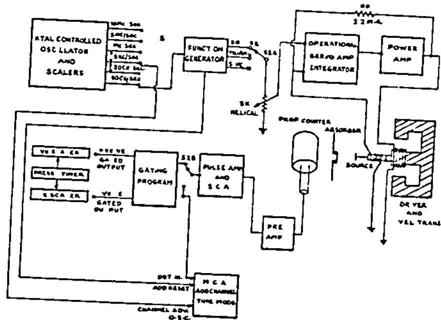
that there is a distinct advantage constant velocity mode enjoys over the constant acceleration type of instrument, in investigations of selected regions of Mossbauer spectrum. The spectrometer described here can be used either in constant velocity or linearly increasing velocity mode. For constant velocity mode of analysis, a pair of scaler-timer is the additional requirement. This unit can be used when selected regions of an absorption spectrum are to be observed in constant velocity mode. Higher drive velocities are obtainable from this spectrometer in linearly increasing velocity, mode, which is usecul in the Rare-earth region.

When coupled to Multichannel analyser the spectrometer furnishes for to and fro cycle of movement (Cohen type)(3), or the converse is also possible (Kankelleit type)(4). In the first case the analyser is reset at appropriate times when the drive movement cycle is complete.

II. FUNCTIONAL DESCRIPTION

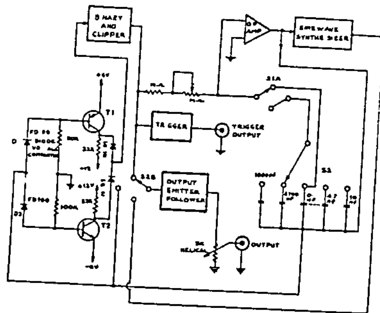
Fig. /1/ shows the functional block diagram of this spectrometer. A Function generator has a binary triggered by the diode comparator. The input to this diode comparator can either be the positive or negative going voltage levels of the triangular waveform, or an externally fed squarewave such as a squarewave generated by scaling down of crystal controlled oscillator output, or the 200, $\overline{200}$ Binary output of a 400-channel analysor(4). The binary output is shaped through operational integrator and diode sine wave synthesiser. Fig. /2/ shows the schematic of this function generator.

Function generator output (square, triangular or sinusoidal voltage sweep), is fed to the differential input of the operational amplifier module through a wire wound helical potentiometer, which controls the maximum velocity swing. The other input to operational



FUNCTIONAL BLOCK SCHEMATIC

Fig 1



FUNCTION GENERATOR

Fig 2

amplifier is the output of velocity sensing coil of the linear velocity-transducer. The error signal thus produced is amplified and integrated in second operational amplifier module and is then fed to the DC-coupled power amplifier.

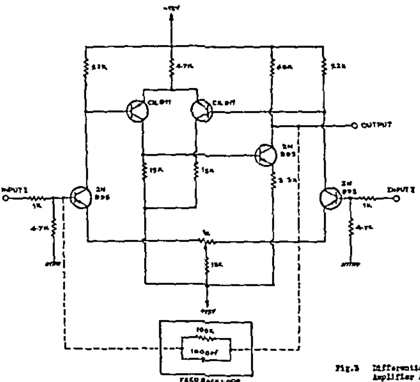
The operational amplifier used is a discrete component packaged module based on Grigsons[6] design, used as a common element in function generator, servo-feedback amplifier and integrator loop. It has a high open loop gain, good stability.

Power amplifier used is a wide band transformerless audio amplifier with high power output. DC-couplings are maintained throughout this power stage and sufficient negative feedback has been provided to eliminate any oscillatory mode as well as stabilising it against any voltage drifts. Fig. /3/ shows the operational amplifier and power amplifier used.

III. FEEDBACK AND REDUCTION OF POSITION DRIFTS.

The velocity feedback loop is around the amplifier-integrator, power amplifier and electromechanical feedback coupling through velocity transducer, where dc electrical couplings, rigid mechanical couplings and sufficiently stiff suspensions are maintained to reduce chances of any longitudinal mode resonances[3] and velocity distortions. Large amount of local negative feedback is also applied to ensure stability of the system.

Position drifts are caused due to random voltage fluctuations at the power amplifier output unaccompanied by the input voltage variations. The power amplifier output is dc coupled to the input of servo amplifier through a high resistance Rf (fig.1) in the negative feedback manner. Thus any random position drifts are reduced to extremely small value.



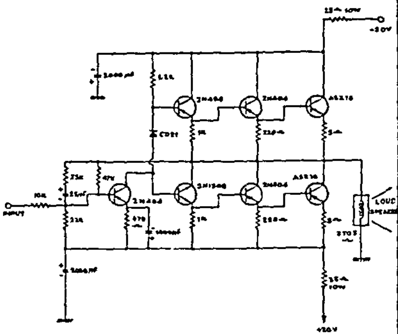


Fig.3 Differential Input Operational Amplifier And Power Amplifier.

However, it should be noted that since stabilisation by use of this feedback is only at the cost of total power gain, the actual amount of feedback is dependent on the total allowable gain-reduction and a proper balance has to be struck between the two.

IV. ELECTROMECHANICAL DRIVE

The doppler motion is generated by means of electromechanical drive assembly. A high compliance bass range loudspeaker (Deconed) is used as a driver. This is coupled to the moving member of a linear velocity transducer type 6LV2, used to sense the instantaneous velocities and for velocity feedback. The moving member is supported by 15 mil thick beryllium copper suspension. A set of six screws on transducer mounting are used to align the position of the transducer coil housing.

V. PERFORMANCE, CALIBRATION AND RESULTS.

Mossbauer absorption spectra were taken with this Spectrometer in both constant velocity and linearly increasing velocity mode. A 5 millicurie Co^{57} source in palladium matrix (25 μ)-thickness was used at room temperature. Fig. /4/ shows the hyperfine splittings in case of metallic iron of natural composition. It was pointed by Preston et.al[7] that the seperation between 1st and 2nd, 2nd and 3rd, 4th and 5th and 5th and 6th dips of natural iron splittings should be equal to the excited state splitting g_1=2.244 mm/sec. Using this value Fig./4/ yields the average velocity per channel = 0.07271 mm/sec, Table 1 shows the calculated velocity positions of six lines as compared to the standard velocity positions as given by Preston et.al.[7]. This shows the maximum velocity deviations better than ± 0.003 mm/sec, for full scale of 10.657 mm/sec.

The spectrometer is also being used in velocity regions higher than 10 mm/sec. In these regions rare earth systems such as Europium with 21.7 Kev line is being used. This aspect of the spectrometer and



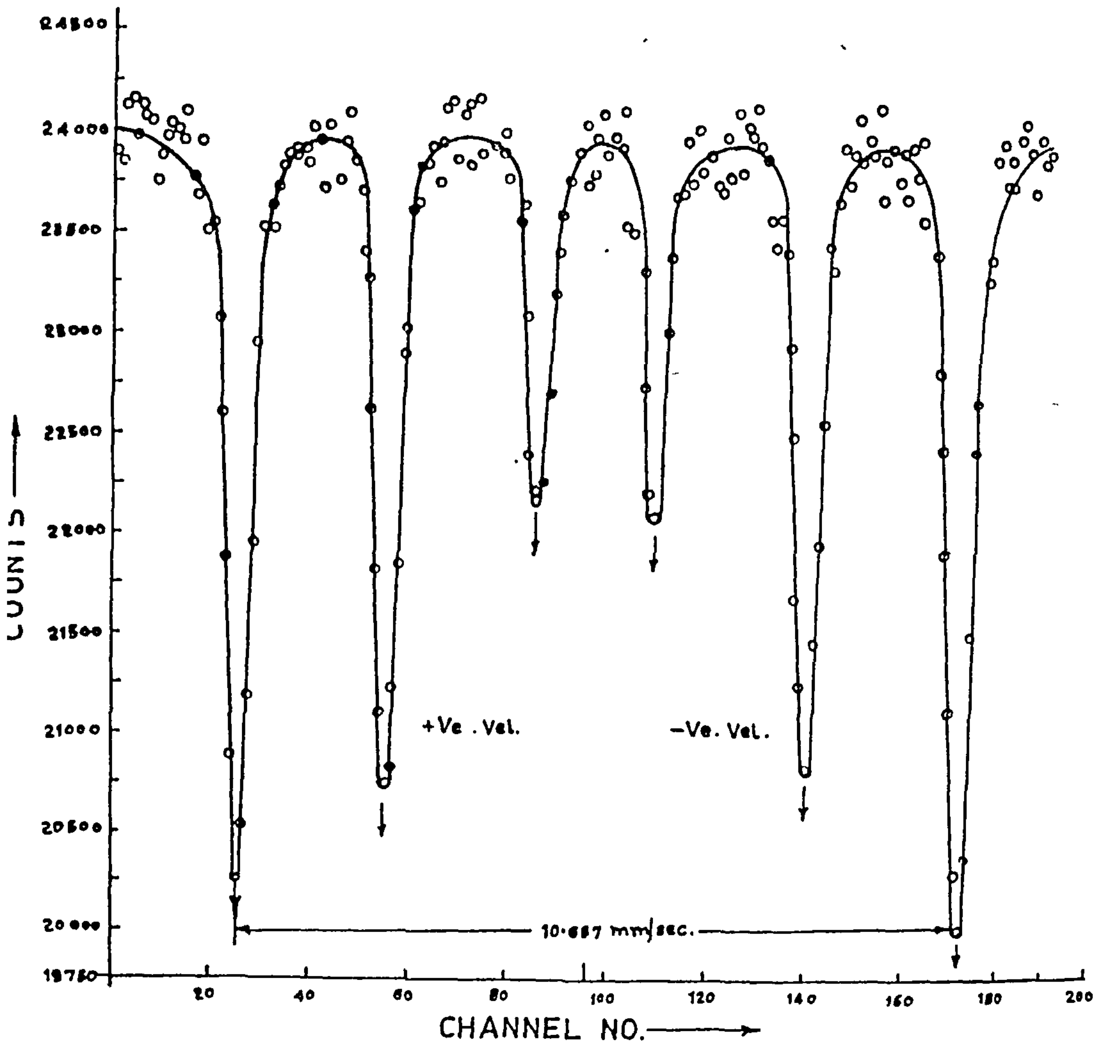


Fig.4 Mossbauer Absorption Spectrum (Const.Acc. Mode). Co^{57}(Pd) Vs.Natural Iron Foil(25u).

and the results are being communicated elsewhere.

VI. <u>ACKNOWLEDGEMENTS</u>

Authors wish to thank Shri A.L.Khandwe and Shri N.S.Samu their cooperation in the experimental work. They are also thankful t A.S.Rao, Director,Electronics Group and Shri G.H.Vaze, Head Electronic Division for their interest in this work.

<u>REFERENCES</u>

1. R.Booth, et.al.Nucl, Instr. & Meth. Vol.25(1963) pp.1
2. G.K.Weirthiem, 'Mossbauer effect principles & applications' pp.21.
3. R.L.Cohen, et.al.Rev.Sci.Instr.Vol.34(1963) pp.671.
4. R.Kankeleit, Rev Sci.Inst.Vol.33 (1964) pp.194.
5. H.Brafmn, et.al.Nucl.Instr. & Meth. Vol.42(1966) pp.245.
6. C.W.Grigson,Elect.Engg.Vol.36 (July 1964) pp.456.
7. Preston et.al.Phy.Rev.Vol.128 (1962) pp. 2207
8. 'Mossbauer effect data Index' (1958-65) by Muir, Ando & Coogan.

<u>TABLE 1</u>: Comparison of calculated and standard velocity positions for the Magnetic Hyperfine splitting of natural iron in Fig. 4. Source: Co^{57} 5 millicurie(Pd), at room temperature. Standard positions are as given by Preston et.al.(7).

Sr. No.	Position	Calculated Velocity mm/sec.	Standard Velocity(as by Preston et.al(7))mm/sec.
1.	25 Channel	+ 5.311055	+ 5.328
2.	55 Channel	+ 3.129755	+ 3.084
3.	86 Channel	+ 0.875745	+ 0.840
4.	109 Channel	- 0.796565	- 0.840
.	139.75 Channel	- 3.039055	- 3.084
	171.50 Channel	- 5.34096	- 5.328

A METHOD OF MEASUREMENT OF ABSOLUTE DISINTEGRATION RATE OF A RADIO-ACTIVE SOURCE

O.P. Joneja, J.S. Coachman and M.P. Navalkar
Nuclear Physics Division
Bhabha Atomic Research Centre, Trombay, Bombay-85.

There are essentially two direct methods for finding absolute disintegration rate of radio-active sources.

a) The use of detectors with a well defined solid angle

b) Coincidence method

The latter is especially attractive since the disintegration rate can be determined without the actual knowledge of detector efficiencies. The present report describes a method for finding disintegration rate of radio-active sources for which the maximum β-energy is much larger than γ-energy.

The major problems encountered in coincidence technique are

a) Conversion electrons

b) γ efficiency of β crystal

The latter appears in the expression for disintegration rate in two forms.

a) γ ray alone getting into β crystal resulting in a detectable pulse.

b) γ ray and β particle getting into crystal resulting in a detectable pulse.

A method which overcomes the disadvanteges of the coincidence
chnique has been suggested by Frosch et al and can be applied to
io-active sources having maximum β energy greater t ray
gy. Au^{198} which satisfies the above requirement
employed for measurement of thermal fluxes can

this method. Besides Au^{198}, other sources such as Al^{28}, Zr^{97}, Xe^{97}, Xe^{133m}, Xe^{135m}, Yb^{177} etc. can also be used with this method.

It can be shown that if N_{β} , N_{γ} and $N_{\beta\gamma}$ are the counting rates in β, γ and $\beta\gamma$ coincidence channel, then under certain assumptions

$$\frac{N_{\beta} N_{\gamma}}{N_{\beta\gamma}} = N_{0}\left[1 + \left(\frac{F_{1(\beta+\gamma)}}{F_{1\beta}} - 1\right) E'_{1\gamma}\right]$$

where N_0 = absolute Disintegration rate

$F_{1\beta}$ = Fraction of β spectra accepted electronically by the β detector

$F_{1(\beta+\gamma)}$ = Fraction of β and γ spectra accepted electronically by the β detector

and $E'_{1\gamma}$ = Probability that a γ ray entering the β crystal gives rise to a pulse

The experimental procedure consists in plotting $N_{\beta} N_{\gamma}/N_{\beta\gamma}$ (corrected for effects such as background, dead time, chance coincidence etc.) as a function of the solid angle subtended by β detector at the source (i.e. proportional to inverse square of the distance between β detector and source) and extraploating the curve at zero geometry to find the intercept which gives the disintegration rate independent of γ efficiency of β crystal.

EXPERIMENTAL DETAILS AND RESULTS

A block diagram of the experimental arrangement which consists of a standard coincidence set up is shown in Fig.(1).

Spec-pure gold foils were irradiated in reactor APSARA and counted in the present experimental set up at different distances of β crystal. A plastic scintillator of ½" thick was used as

a β detector. β bias was adjusted above the maximum energy of converted electrons. Standard procedure for background, dead time corrections etc. was followed.

The experimental results were analysed on CDC-3600 using the standard method of least square fitting and are shown in Fig. (2). It is seen from Fig.(2) that a straight line as predicted by theory is obtained. The uncertainty calculated by the method of propagation of errors was about 1% in N_0.

CONCLUSIONS

Using irradiated gold foils, it has been shown that the present method which is independent of the γ efficiency of β crystal and also the knowledge of internal conversion coefficient, could be used for determining absolute disintegration rate.

BLOCK DIAGRAM OF THE EXPERIMENTAL SET-UP

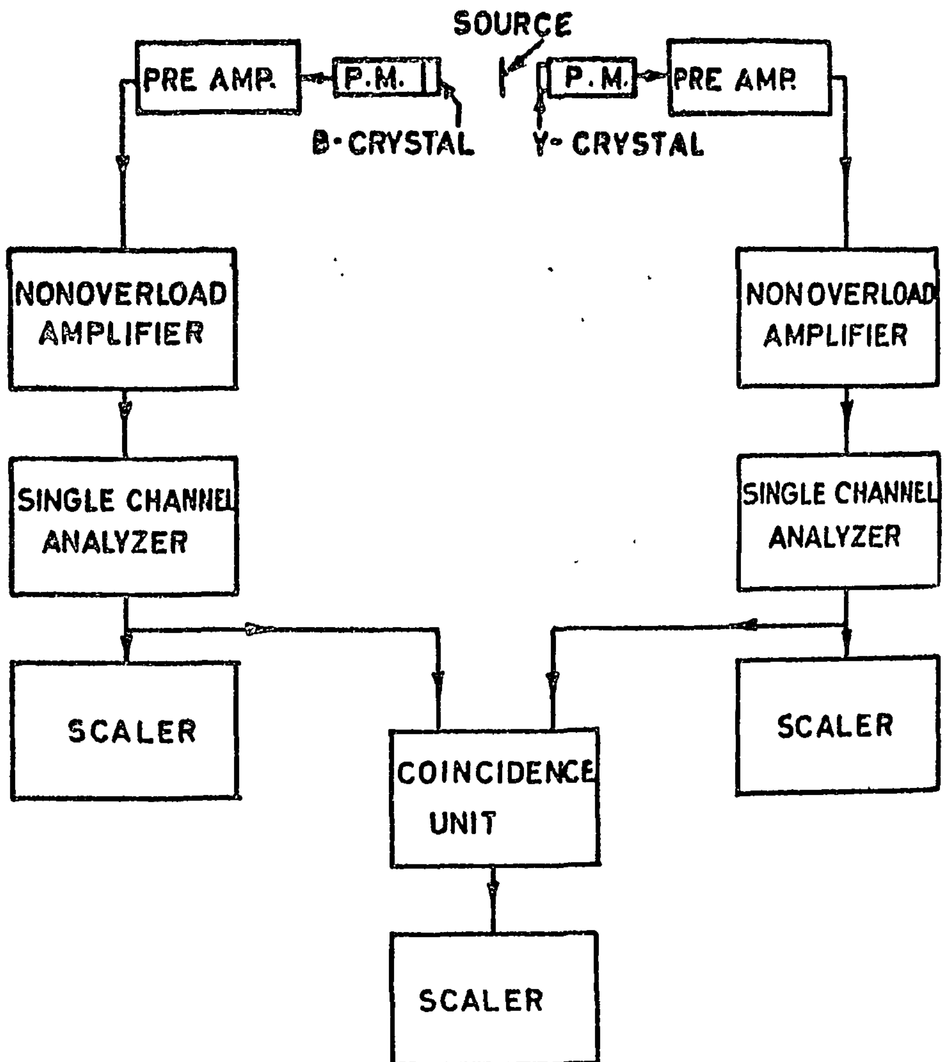
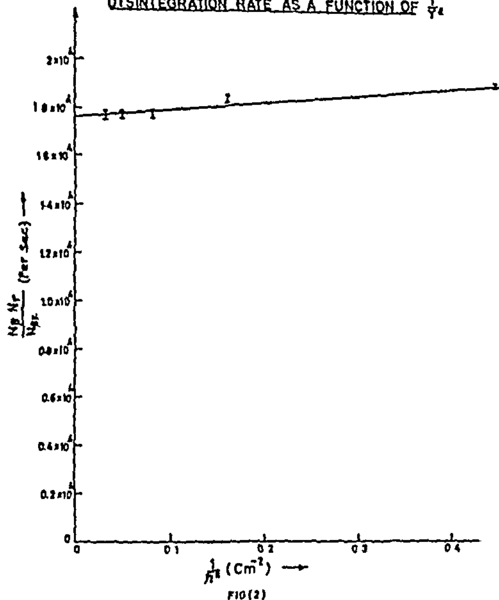


FIG - 1


DISINTEGRATION RATE AS A FUNCTION OF $\frac{1}{r^2}$
2×10⁴
1.8×10⁴
1.6×10⁴
1.4×10⁴
1.2×10⁴
1.0×10⁴
0.8×10⁴
0.6×10⁴
0.4×10⁴
0.2×10⁴
0
$\frac{N_\beta N_\gamma}{N_{\beta\gamma}}$ (Per Sec)
0
0.1
0.2
0.3
0.4
$\frac{1}{R^2}$ (Cm⁻²)

FIG(2)

A HIGH CURRENT ELECTRON IMPACT ION SOURCE

A. K. Hui and P. K. Ghosh
Indian Institute of Technology, Kanpur-16

I. INTRODUCTION

A high current electron impact magnetron ion source capable of delivering ion currents of the order of milliamperes is described. The ion source is a modified version of the type described by Singer et al.[1] The major changes are, use of the ion source magnetic field as a variable parameter, use of the ion source housing as the outer anode, and ruggedized construction. Since this ion source delivers ion currents at very low extraction potentials, i.e., in the ev range, the ions in the beam should have relatively high energy homogeneity when accelerated to kev or mev region. Consequently, this offers certain definite advantages over rf discharge ion sources. In the latter type, energy homogeneity of the extracted ion beam is considerably inferior as little control can be exercised on the energy of the electrons existing in discharge plasmas.

II. EXPERIMENTAL

The present ion source contains ten 7 cm long 1 mm diameter tungsten wires connected in series for the filament and these are cylindrically arranged on a 4.5 cm diameter circle around a 6.5 mm diameter central anode. The latter is concentric with a 9 cm diameter outer anode which also acts as the ion source housing. Axially, the ion source is about 9.5 cm long. The ions are

through a 2 cm diameter aperture located at the center of the outer anode. The metallic parts of the ion source are made of 304 stainless steel and the insulating parts are of mica. The ion source is water cooled. Internal assembly of the flange mounted source is shown in Fig. 1.

The electromagnet around the ion source with 9 cm diameter pole pieces associates with it a coil made of about 2500 turns of 20 SWG wire capable of carrying 2 amp of continuous current and significantly higher currents for short periods. Mappings show that the magnetic field between the poles is highly inhomogeneous as might be expected. Typically, for 4 amp of magnet current, on the polar axis which coincides with the central anode, it shows a field of about 400 gauss at the center of the ion source and about 700 gauss on the pole face.

For the present experiments, the anode potential was clamped to ground and the filament which is heated with 50 Hz ac floated negative dc with respect to the anodes. This potential difference, or the Ionizing Voltage (I.V.), is an approximate measure of the electron energy in the ion source. In a typical ion source operation, a filament current of 60 amp requires about 50 volts ac and this results an anode current of about 5 amp. The ion energy is controlled by the ion extraction potential.

III. RESULTS

Most measurements of ion currents with the present ion source were made with nitrogen as the experimental gas. The results obtained with oxygen are quite similar.

Some typical results for nitrogen at 10^{-4} torr gauge pressure are shown in Fig. 2. The solid lines show the variation of the ion current as a function of the magnetic field intensity and Ionizing Voltage, as measured about 10 cm outside the ion exit aperture. The results shown refer to an extraction potential of 60 volts with respect to the aperture. The magnetic field intensity refers to that at the center of the ion source. It is apparent from the data that the dependence on the magnetic field is not strong. The behaviour of the ion current as a function of the filament current at constant Ionizing Voltage and magnetic field intensity is shown by the broken line. In the operational region, the ion current is a sensitive function of the filament current.

The ion source is presently being used for ion optical spectroscopic work. With suitable dimensional changes this should be useful in accelerators and in other experimental work where high current low energy ion beams are required.

The authors wish to gratefully acknowledge support from the Petroleum Research Fund of the American Chemical Society.

REFERENCE

1. Stanley Singer, N. G. Kim, L. V. [illegible], and K. [illegible], J. Phys. Chem. 69, 799 (1965)

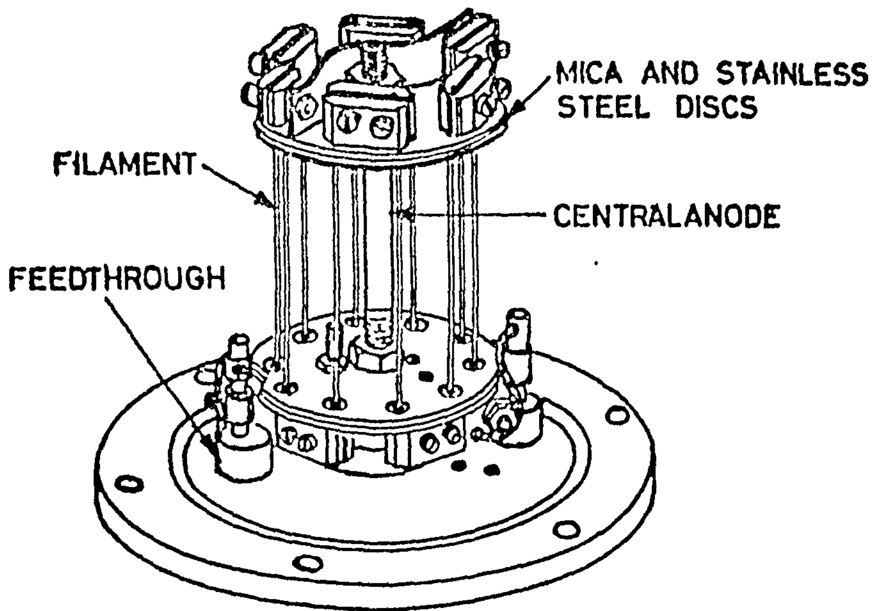


FIG. 1 - Ion Source Assembly

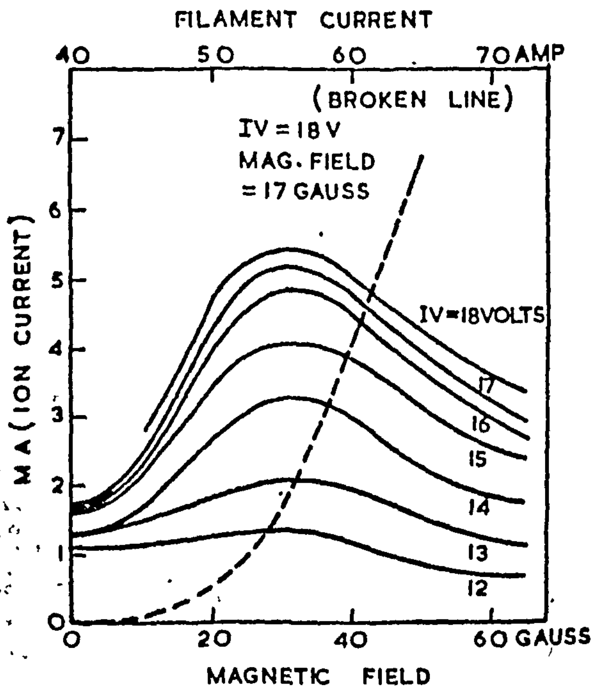


Fig. 2 Variation of Ion Current with
(a) Magnetic Field (Solid Lines), and
(b) Filament Current (Broken Line)

DISCUSSION

S.N. Misra: 1) What is the material of aperture used? 2) Are you using any insulating sleeve at aperture?

P.K. Ghosh: 1) Stainless steel 304. 2) No.

V.N. Bhoraskar: If the cathode is directly heated by 50c/s current, will the voltage between the anode and the cathode remains the same?

P.K. Ghosh: No, the variation is dependent on the magnitude of the 50 cps voltage used to heat the filament.

V.N. Bhoraskar: Is there any advantage of grounding the anode?

P.K. Ghosh: Yes, the outer anode also serves the purpose of the ion source housing and no additional housing is required.

S.B. Karmohapatro: With such low extraction voltage how such high current is extracted.

P.K. Ghosh: The ion exit aperture is rather large. This apparently permits enough field penetration to result in the observed ion currents.

S.B. Karmohapatro: 1) Whether you extract ions radially or axially. 2) By axial extraction do you expect higher ion current.

P.K. Ghosh: 1) Ions are extracted radially. 2) It is difficult to predict. The geometry of the internal assembly of the ions source is presently not convenient

for axial extraction.

S. Chatterjee: How do you measure the extracted ion-current?

P.K. Ghosh: With the help of a faraday cup and a milliammeter.

Characteristics of a Duoplasmatron Ion Source.

D. K. Mukherjee and R. S. Bhattacharya.
Saha Institute of Nuclear Physics, Calcutta-9.

INTRODUCTION

The Duoplasmatron Ion Source which is a high intensity type of source has got some advantages e.g. high currents, high ionization efficiency etc.

We have reported here some preliminary operational characteristics of a Duoplasmatron (1) ion source using neon gas. The results which are in the low energy and low efficiency region are not reported earlier. Low energy operation is important for Isotope separators for preparing isotopictargets and the low efficiency operation of the source is useful for direct enhancement of the multiply charged ions for accelerators.

EXPERIMENT

The Duoplasmatron used here is the standard Von - Ardenne type [1,2] of source with a ferromagnetic anode and an intermediate electrode. A schematic diagram of the experimental set-up is shown in fig. I. The ion beam from the plasma chamber is extracted by supplying a positive accelerating voltage to the source. The extractor electrode is usually given a low negative voltage. The extractor is followed by einzel lens with proper focussing voltage, which focusses the ion beam into a faraday cage. Pressure inside the discharge chamber was measured by an air calibrated thermocouple gauge, and the pressure out :· by

an Ionisation gauge, GIC011 (CVC).

The first part of our present work deals with the dependence of the extracted ion current on the pressure in the discharge chamber[3]. When the pressure outside the chamber was steady at about 9×10^{-6}mm. of mercury, the pressure inside was about 1×10^{-3}mm. or less. After degassing the filament for about 15 mins. with a constant heating current of 40 Amp., neon gas was fed inside and the arc voltage was supplied. The pressure outside the source was about 2×10^{-5}Torr, when the arc discharge was generated with an arc voltage of 150-200 volts. Then we started with as high a pressure inside the source, as was possible to get an ion current $\sim 10^{-7}$A with a low accelerating voltage. We went on lowering the pressure by means of a needle valve noting at the same time the variation of the ion current with pressure in the chamber with accelerating voltage as a parameter. The magnetic field was fixed at 2 KG.

After getting an optimum value of pressure in the chamber (Pi), we tried to verify the $V^{3/2}$ dependency[4,5] of ion current in the low accelerating voltage range (1-6KV) with arc discharge current (I_A) and the pressure Pi as parameters. The magnetic field was fixed at 2.2KG.

After keeping the pressure Pi at 4.5×10^{-2}mm. the arc voltage Varc and the magnetic field (600 G) fixed, the arc current was varied by changing the heating current of the filament and the dependency of the ion current I_c on I_A for a particular accelerating voltage (6KV) was

noted.

RESULTS

In fig. 2, we have shown the variation of I_e with Pi. This shows that for a particular value of the filament current [illegible] there is an optimum value of pressure ($2x10^{-2}T$) at which the extracted ion current is maximum[3] and is smaller on either side of it. Fig. 3 shows the dependency of ion current [illegible] on the accelerating voltage. In the first curve we have the values of I_e for different values of V for some particular value of I_A at a particular pressure [illegible]. In the second figure [illegible] pressure Pi is changed and the corresponding I_e is noted as a parameter. The solid lines in both the curves are with a slope of 3/2. Our experimental points in both the curves show some departure from this line and the slopes of the best fitting straight lines of our results are found to be 1.3. In fig. 4, the ion current I_e shows a similar tendency[5], [illegible] for a particular value of Pi the current I_e increases with I_A increasing, reaches a maximum and then falls with further increase in I_A. This shows that for a particular pressure there is an optimum value of arc current I_A for which the extraction is maximum.

From figs. 2 and 4, it is thus evident that the extracted ion current [illegible] the pressure inside[illegible] [illegible] with [illegible] arc current.

DISCUSSION

From our present work [illegible] plasmatron ion source, the extracted [illegible] altered only by changing the pressure [illegible]

discharge which in turn depend on filament heating current, Pressure inside the Discharge chamber and the magnetic field. The extraction of the beam also has been shown[4,5] to have $V^{3/2}$ extraction voltage dependence indicating its space charge limitation. In our present results, it departs from this dependence. In this work though we have not reported any dependency of ion current on the magnetic field there are results of other workers. There is an optimum value of the arc current depending on the pressure inside for an optimum extraction.

In these measurements we have dealt with low accelerating voltages since low energy ion beam, if can be extracted from a Duoplasmatron with high intensity, can be used directly for target preparation with-out prior deceleration near the target as is required for nuclear spectroscopy work. With low arc current i.e., with lower efficiency there remains a possibility of the presence of some neutral atoms inside, which may produce more multiply-charged ions by ionatom collisions.

REFERENCES

1. M. Von Ardenne "Tabellen der Electronenphysik, Ionenphysik and Ubermikroskopie Deut. Verlag. Wiss. Berlin, 1954.
2. C. D. Moak, et al. Rev. Sci. Instr. 30. 694 (59)
3. VEB VaKutronik, Dresden-Manual of Duop. Ion Source
4. O. Almen & K. O. Nielson-Nucl. Instr. 1 (1957) 302.
5. N. Wells and P. R. Hanley Accl. Conf. Washington, 1969
6. A. Septier et al. Nucl. Instr. 38 (1965) 41.

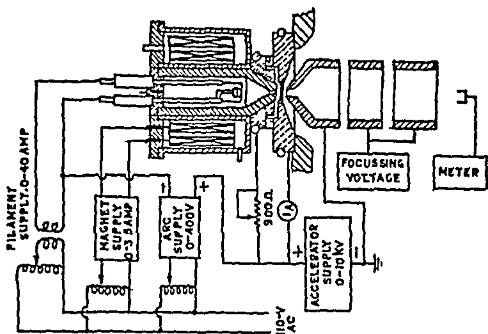

FILAMENT SUPPLY 0-40 AMP
MAGNET SUPPLY 0-3.5 AMP
ARC SUPPLY 0-400V
900Ω
I_A
ACCELERATOR SUPPLY 0-10KV
FOCUSSING VOLTAGE
METER
110-V AC

FIG. 1.

FIG. 2.

Pl = 2x10^{-2} T
o Iarc = 500 mA.
● Iarc = 480 mA.
X Iarc = 460 mA.

SLOPE = 3/2

Pl 1·3x10^{-1} T
o Iarc = 325 mA
Pl = 1·1x10^{-1} T
● Iarc = 360 mA
Pi = 6·5x10^{-2} T
X Iarc = 420 mA

SLOPE = 3/2

ION CURRENT I_c (μA)

ACCELERATING VOLTAGE V (Kv)

FIG. 3.

V_{ACC} = 6 Kv
Pi = 4·5x10^{-2} T
Imag = 1 Amp.

ION CURRENT I_c (μ Amp)

ARC DISCHARGE CURRENT I_A (m Amp)

FIG. 4.

DESIGN OF A CONTROLLED ν_z SECTOR FOCUSSED ISOCHRONOUS CYCLOTRON FOR MESON FACTORIES

A.Jain and A.S.Divatia
Bhabha Atomic Research Centre, Trombay, Bombay-85

I. INTRODUCTION

The extension of the sector focussed isochronous cyclotron upto the 1 GeV region has been attempted by various workers with varying degrees of success.[1,2,3] Two basic requirements must be met with in designing the sectors of an AVF cyclotron-(i) isochronism, and (ii) correct axial focussing.

For isochronism the time averaged magnetic field $\langle B \rangle$ must increase with the radius according to relativistic requirements[1,4] the strong field hill sector must be continuously flared to subtend an angle at the centre[5] which we put in the form

$$\eta(r) = 2\cot^{-1}\left\{\frac{B_H}{B_V}\left(\cot\left[\frac{\pi}{N}\cdot\frac{\langle B\rangle - B_V}{B_H - B_V}\cdot\frac{B_H}{\langle B\rangle}\right] - \cot\frac{\pi}{N}\right) + \cot\frac{\pi}{N}\right\} \cdot (1)$$

For correct axial focussing the vertical betatron frequency must lie in an operation band away from serious resonances. This can be done by suitably choosing the flutter function F^2 and the spiral angle ϵ in the equation derived by various authors[5,6]

$$\nu_z^2 = -n + F^2\left(1 + 2\tan^2\epsilon\right) \qquad (2)$$

In the attempts mentioned earlier, correct axial *focussing* has been obtained either by searching for a suitable magnetic potential with a digital computer[2] or by adjusting F^2 with the radius[1]. The latter implies a pole gap varying with the radius which may prove inconvenient for large proton machines. We outline here a method to obtain simultaneous isochronism and correct focussing by a simple analytical technique.

II. DESIGN THEORY

Using the hard edge approximation[5] we

vertical frequency equation when sector entry and exit spiral angles are unequal to be

$$\nu_z^2 = \frac{F^2}{2}\left\{\frac{1}{K}\left[\tan(\epsilon_1+K) - \tan(\epsilon_2-K)\right] + \tan(\epsilon_2-K)\left[\tan(\epsilon_1+K)+\tan(\epsilon_2-K)\right]\right\} \quad \cdots (3)$$

which reduces to the well tested Eq.2 when $\epsilon_1 = \epsilon_2 = \epsilon$. The first square bracket contains the Thomas and Laslett and the second the Kerst alternating-gradient effects.

Referring to Fig.1, suppose the hill sectors have been designed till the radius r=a. Let the angle subtended at the centre by the arc AB at r=a be η_0 and arc A'B' at r=a + Δa be $\eta_0 + \Delta\eta_0$ where

$\Delta\eta_0$ = required increment in the hill angle for isochronism obtained by differentiating Eq.1.

Let us introduce a spiral angle ϵ_1 (angle between the radius vector and tangent to the sector) at A and ϵ_2 at B. Let the corresponding contributions at the centre be $\Delta\theta_1$ and $\Delta\theta_2$, and for isochronism the net increase in hill angle $\Delta\theta = \Delta\theta_2 - \Delta\theta_1$ must be such that

$$\Delta\eta_0 = \Delta\theta \qquad (4)$$

Since $\Delta a \ll a$, the portions of the curves AA' and BB' can be assumed linear and from triangles ACA' and BCB'

$$\Delta\theta_1 = \epsilon_1 - \sin^{-1}\left[\frac{a}{a+\Delta a}\sin\epsilon_1\right]$$
$$\Delta\theta_2 = \epsilon_2 - \sin^{-1}\left[\frac{a}{a+\Delta a}\sin\epsilon_2\right] \quad \cdots (5)$$

and substituting in eq (4)

$$\Delta\eta_0 = \left[\epsilon_1 - \sin^{-1}\left(\frac{a}{a+\Delta a}\sin\epsilon_1\right)\right] - \left[\epsilon_2 - \sin^{-1}\left(\frac{a}{a+\Delta a}\sin\epsilon_2\right)\right] \cdot\cdot(6)$$

Thus we notice that the spiral angles introduced at any radius affect both axial focussing (Eq.3) and increase in average field due to sector flaring (Eq.6). For reasonable conditions, the transcendental equations (3) and (6) can be solved simultaneously to yield a set ϵ_1 and ϵ_2 satisfying both isochronism and a correct ν_z at each radius. The process is repeated for several radii and the polar co-ordinates of the sectors generated from Eq.(5).

Since Eq.(3) is approximate, a reiterative corrective procedure

is required. Using the preliminary design a scale model and orbit integration studies are required to indicate the deviation $\Delta\nu_z$ and $\Delta(\Delta\eta_0)$ and the corrections $\Delta\epsilon_1$ and $\Delta\epsilon_2$ can be obtained by solving the set

$$-\Delta\nu_z = \frac{\partial f_1}{\partial\epsilon_1}\Delta\epsilon_1 + \frac{\partial f_1}{\partial\epsilon_2}\Delta\epsilon_2$$
$$-\Delta(\Delta\eta_0) = \frac{\partial f_2}{\partial\epsilon_1}\Delta\epsilon_1 + \frac{\partial f_2}{\partial\epsilon_2}\Delta\epsilon_2 \quad (7)$$

obtained by differentiating Eq (3) and (6). The process is rapidly converging since Eq.(3) is a good first approximation.

III. RESULTS

Using the above method, we present the sector shapes for a 938 MeV proton machine having the indicated parameters.

N = 8 Bcentral = 6.772 Kg. B_H = 14.900 Kg B_V = 6.157 Radius = 400 cms

Rad cms	Energy Mev	⟨B⟩ kG	θ_1°	θ_2°	ϵ_1°	ϵ_2°	F^2	K	ν_z	η_0°
100	22.8	6.94	-	-	22.2	25.2	.129	.040	0.28	4.0
150	53.8	7.16	7.6	11.9	31.8	37.2	.152	.049	0.28	5.2
200	102.6	7.51	16.1	22.1	39.2	47.8	.178	.060	0.28	7.0
250	177.6	8.05	25.0	33.6	46.0	58.8	0.2	.072	0.28	9.7
300	295.7	8.91	34.1	46.9	53.8	71.8	0.2	.083	0.28	14.1
350	499.6	10.38	44.2	64.2	57.7	86.6	.177	.083	0.28	21.6
400	938.3	13.55	54.2	89.9	-	-	-	-	-	38.0

The deviations expected in the experimental values of ⟨B⟩ are within 15% as seen by comparison with an approximate method(7), those in ν_z are within 25%, since Eq.(3) when applied to the sectors of the VEC under construction promises to hold within 25%(8). The final test of the table lies in a scale model and orbit integration studies(4) using the measured magnetic field.

IV. CONCLUSION

Because of two spiral angles, this appears to be more flexible and systematic for

isochronous cyclotrons near the GeV region (e.g. meson factories and synchrotron pre-injectors) where a large (several hundred per-cent) sector flaring is encountered and simultaneously a precisely controlled ν_z value is required along the radius to escape the various resonances[1,2,3] which arise due to the wide energy range. Variable energy operation could best be achieved[9] by negative ion accelera-tion and subsequent stripping at the desired radius.

REFERENCES

1) Blosser et al., Rev. Sc. Inst. 29 (1958) 819
2) Kerst et al., Rev. Sc. Inst. 31 (1960) 1076
3) Proceedings of the Conf. on S.F. cyclotrons, 1962, Nucl. Inst. & Meth. 18, 19 (1962) 387-478
4) M.M.Gorden and T.A. Welton, ORNL-2765
5) Progress in Nuclear Techniques & Instrumentation Vol.1(1965)1-101, North Holland Pub. Co.
6) Principles of Cyclic Particle Acc., J.J.Livingood, D.Van Nostrand & Co.(1961) Chap 13.
7) B.L.Cohen et al, Nuc. Inst & Meth 6 (1960) 105
8) A.Jain, VEC technical note.
9) Proc. Int. Conf. on SFC and Meson factories, 1963 CERN 63-19, 318.

FIG. -1

DISCUSSION

P.N. Trehan: Are there any designs available of this kind of meson factroy?

A.S. Divatia: Yes. The Swiss Nuclear Institute (S.I.N) is constructing a 500 MeV Isochronous cyclotron, with a 70 MeV isochronous cyclotron as injector, for use as a meson factory. But this is of the "seperated sector" type i.e. no valleys. Also, our design technique is analytically different.

S. Chatterjee: Have you estimated ν_r for each value of ν_z ? One has to think about the resonances to avoid any blow-up.

A.S. Divatia: Yes, We have estimated ν_r for each value of ν_z along the radius, and designed the sectors such as to avoid all possible "avoidable" resonances. However, the unavoidable radial resonance $\nu_r = 3/2$ at half the proton rest mass has to be overcome and the unavoidable $\nu_r = 2$ resonance occurs and rests the upper energy limit at 938 MeV.

ION OPTICS IN THE BEAM TRANSPORT SYSTEM OF THE VARIABLE ENERGY CYCLOTRON AT CALCUTTA

A. Jain and A.S. Divatia
Bhabha Atomic Research Centre, Trombay, Bombay - 85

I. EXTERNAL ION OPTICS OF THE 224 cm. VARIABLE ENERGY CYCLOTRON

The principle magnetic elements of the ion optical system of the Variable Energy Cyclotron at Calcutta are shown schematically in Fig.1. The quadrupole lenses Q1 and Q2 focus the beam at the slit S1 of the 159.5° double focussing (n = 1/2) analysing magnet system M1 having a resolution of 14.5 Kev/mm. An intermediate image formation and hence two quadrupole lenses are necessary if the beam dispersion produced by the cyclotron fringing field is to add to that produced by the analysing magnet. The slit S2 of the analysing magnet selects 1/40 of the analysed beam current and reduces the initial energy spread from about 600 Kev to 15 Kev. The quadrupole Q3 focuses the analysed beam near the entry pont of the switching magnet SW2 which can be made to bend the beam into any of the six high resolution caves C4, C5, C6, C7 C8 & C9. The maximum bend of 55° is specifically shewn. The quadrupole lens Q4 next focuses the beam into the experimental target T. The position of the first switching magnet SW1 is also shown which can switch the unanalysed beam into either of the three high intensity caves C1, C2 and C3.

II. PROGRAM ENVELOPE

The program ENVELOPE has been developed here in Fortran IV for the CDC 3600 computer. The program contains subroutines for the motion in a drift space, quadrupole magnet lens system, switching magnet, slit, analysing magnet system, etc. If the se parameters of the beam transport elements in the syst

in the data, the subroutines are called in the same sequence. The beam envelope is traced in a desired number of steps using the appropriate transfer matrix of the magnetic element and treating the length along the optic axis in this matrix as a variable. The final beam parameters due to one subroutine are automatically fed as the initial beam parameters in the succeeding subroutine. This makes any general arrangement of elements possible in the system. Several systems can be studied in a single run. A write-up of the program with the beam dynamics used can be found elsewhere.(1)

The main difficulty experienced was in assigning the quadrupole lens doublet currents I_1 and I_2 which will produce the required beam characterestics at the next slit. We have obtained the currents I_1 and I_2 by solving a set of simultaneous transcendental equations by the Newton Raphson approximation technique. For a double image at I (Fig.1) we solve the set

$$\left.\begin{array}{l} q_{12} \simeq 0 \\ q_{32} \simeq 0 \end{array}\right\} \qquad (\text{Table 1})$$

and for a double waist at I, the set

$$\left.\begin{array}{l} x \simeq 0 \\ y \simeq 0 \end{array}\right\}$$

where x and y are given by,

$$\begin{aligned} x &= q_{11} x_0 + q_{12} x_0' \\ x' &= q_{21} x_0 + q_{22} x_0' \\ y &= q_{31} y_0 + q_{32} y_0' \\ y' &= q_{41} y_0 + q_{42} y_0' \end{aligned} \qquad (1)$$

and the co-efficients are functions of the parameters as defined in Table 1 and Fig.1.

III. STUDIES OF THE VEC ION OPTICAL SYSTEM

The program has been used to generate the beam envelope through the VEC Beam Transport System described in Fig.1. Details of the envelopes generated can be found elsewhere.(1) We find that the

TABLE 1.

$$q_{11} = \alpha_{3h}(\alpha_1 - L_2 K_1 \beta_1) - K_1 \beta_1 \beta_{3h}/K_3 + L_4[K_3 \beta_{3h}(\alpha_1 - L_2 K_1 \beta_1) - \alpha_{3h} K_1 \beta_1]$$

$$q_{12} = q_{11} L_0 + \alpha_{3h}(\beta_1/K_1 + L_2 \alpha_1) + \alpha_1 \beta_{3h}/K_3 + L_4[K_3 \beta_{3h}(\beta_1/K_1 + L_2 \alpha_1) + \alpha_1 \alpha_{3h}]$$

$$q_{21} = K_3 \beta_{3h}(\alpha_1 - L_2 K_1 \beta_1) - \alpha_{3h} K_1 \beta_1$$

$$q_{22} = q_{21} L_0 + K_3 \beta_{3h}(\beta_1/K_1 + L_2 \alpha_1) + \alpha_1 \alpha_{3h}$$

$$q_{31} = \alpha_3(\alpha_{1h} + L_2 K_1 \beta_{1h}) + \beta_3 K_1 \beta_{1h}/K_3 + L_4[\alpha_3 K_1 \beta_{1h} - K_3 \beta_3(\alpha_{1h} + L_2 K_1 \beta_{1h})]$$

$$q_{32} = q_{31} L_0 + \alpha_3(\beta_{1h}/K_1 + L_2 \alpha_{1h}) + \beta_3 \alpha_{1h}/K_3 + L_4[\alpha_3 \alpha_{1h} - \beta_3 K_3(\beta_{1h}/K_1 + L_2 \alpha_{1h})]$$

$$q_{41} = -K_3 \beta_3(\alpha_{1h} + L_2 K_1 \beta_{1h}) + \alpha_3 K_1 \beta_{1h}$$

$$= q_{41} L_0 - K_3 \beta_3(\beta_{1h}/K_1 + L_2 \alpha_{1h}) + \alpha_3 \alpha_{1h}$$

$\alpha_1 = \cos(K_1 L_1)$ $\alpha_{1h} = \cosh(K_1 L_1)$ $\beta_1 = \sin(K_1 L_1)$ $\beta_{1h} = \sinh(K_1 L_1)$

$\alpha_3 = \cos(K_3 L_3)$ $\alpha_{3h} = \cosh(K_3 L_3)$ $\beta_3 = \sin(K_3 L_3)$ $\beta_{3h} = \sinh(K_3 L_3)$.

sequence and positioning of elements described in Fig.1 is highly efficient and with minor adjustments can be made to yield merely 100 transport efficiency (i.e. no loss of particles). For a high transmission through the analysing magnet, we were required to solve the set,

$$x \simeq 0$$
$$y' \simeq 0 \qquad \text{for Q2.}$$

IV. DESIGN STUDIES

The program can also be used to design new beam transport systems. If the system requirements are known, several sequences and positioning of elements can be visualised and the corresponding beam envelopes generated. The correct sequence and positioning can be reached rapidly in a few runs and parameters like quadrupole current requirements, etc., obtained.

A sub-routine for the program to solve upto twenty simultaneous transcendental equations by the Newton Raphson method is under preparation for optimisation studies.in Beam Transport elements.

REFERENCES

(1) BARC Report, under preparation.

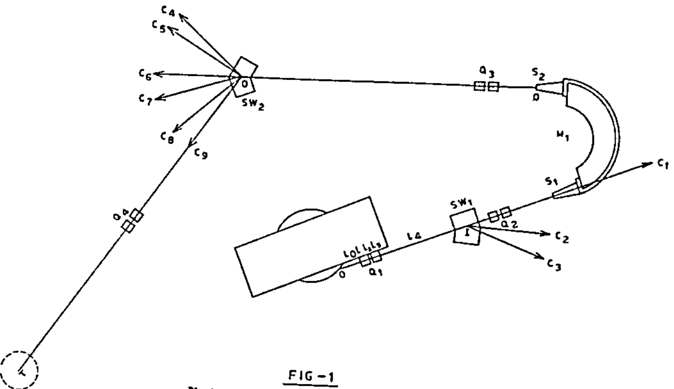


FIG - 1

Fig 1 The principle elements of the ion optical system of the 224 cm Variable Energy Cyclotron at Calcutta

A temperature compensated Hall probe (Model T-6010 of F.W.Bell, Inc.) alongwith a gaussmeter (Model 640 of F.W.Bell, Inc.) was used as the field measuring equipment. Absolute field measuring accuracy of this system is ± 0.5% upto 10 kilogauss. Positioning jig for the probe and its mounting arrangement are shown in fig.1. Radial and angular positions of the probe can be controlled within 0.05 cm. and 0.25 deg. respectively. Median plane can be located within 0.05 cm.

All the points at which measurements are taken lie on a polar grid. Radial scanning was done from 2.1 cms. to 16.1 cms. in 1 cm. intervals. Azimuthally, for the first eight radii, 0-360 deg. and for other seven radii, 0-120 deg. region was scanned in 4 deg. intervals, in both reverse and forward directions. Shortening of the scan for last seven radii was due to the obstruction of the motion of the probe by the magnet yoke. At each radius data was taken for 4 currents viz. 1,2,3 and 3.5 amp.

III. RESULTS

Fig. 2 shows the plot $B(r,\theta)$ vs. θ at a radius 7.1 cms for the current 3.5 amp.

Fig. 3 shows the plots $\langle B(r)\rangle$ vs. radius for all the currents. Some deviations are observed, due to a drift in the current caused by heating.

In fig. 4 amplitudes of 3rd, 6th and 9th harmonics vs. radius have been plotted for all the currents.

Table I gives the first harmonic coefficients, in gauss, for different currents.

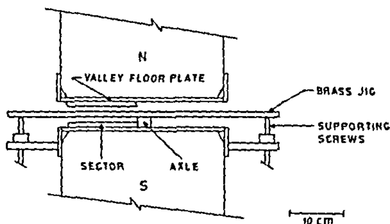


Fig. 1 a : General layout of the experimental set-up.

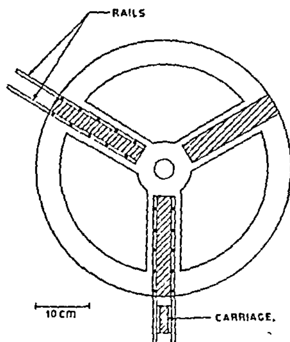


Fig. 1 b Positioning brass jig with the carriage.

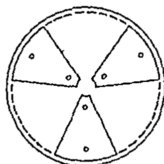


Fig. 1 c

Valley floor plate with radial sectors screwed on it.

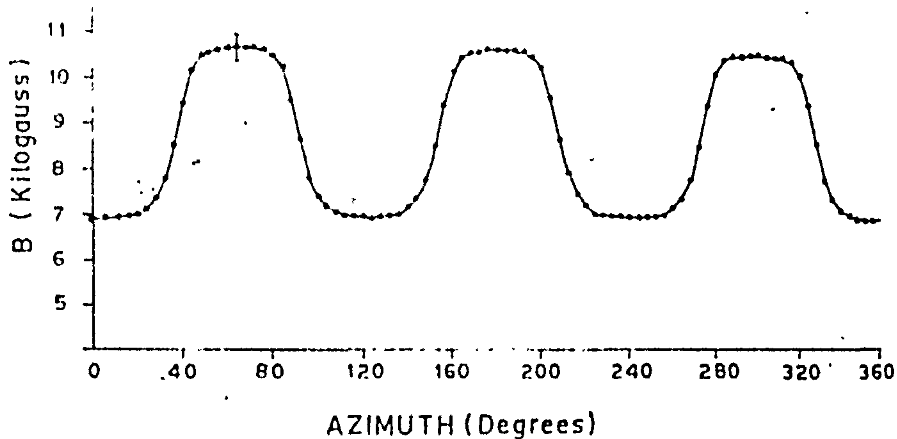


Fig. 2 : Measured magnetic field vs. azimuth for a given radius.

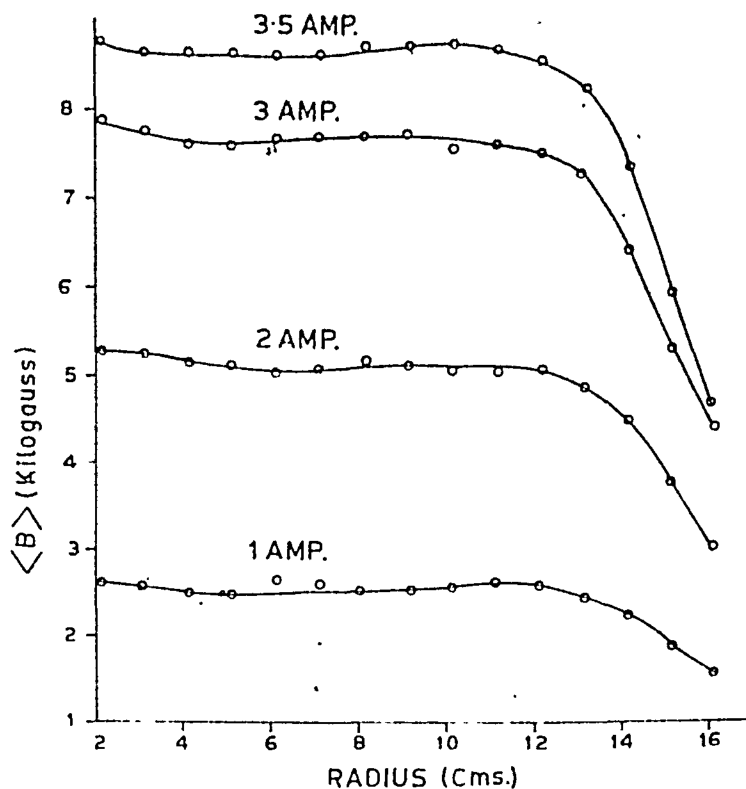


Fig. 3. : Azimuthally averaged magnetic field vs. radius for various currents.

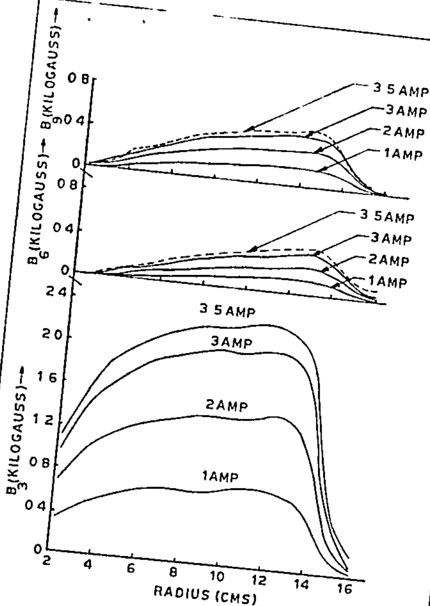


Fig. 4 : Amplitudes of the third, sixth and ninth harmonics vs. radius for various currents.

Table I

Radius (cms)	1 amp. a_1	1 amp. b_1	2 amp. a_1	2 amp. b_1	3 amp. a_1	3 amp. b_1	3.5 amp. a_1	3.5 amp. b_1
2.1	14.3	6.4	20.2	38.7	8.1	12.4	18.2	18.5
3.1	2.4	18.5	6.8	2.0	9.6	35.5	2.6	64.7
4.1	0.3	- 1.9	5.4	-2.2	- 1.2	14.7	-19.5	0.6
5.1	- 0.7	- 0.4	- 5.7	26.6	- 6.3	19.4	- 5.7	31.4
6.1	- 1.3	9.7	-12.7	-1.1	- 0.3	9.8	-21.4	12.4
7.1	- 2.1	- 3.2	-19.5	14.3	21.3	11.3	-20.8	17.6
8.1	0.7	- 9.9	-15.5	7.3	-15.2	- 3.2	-25.8	14.1
9.1	- 6.3	1.3	-16.0	9.1	- 7.4	2.5	-27.2	15.6

Absolute accuracy at any point is better than 3%; this takes account of positioning errors and current drift. For the reason given above, only the harmonics which are multiples of 3 were found out beyond the eigth radius.

REFERENCES

1. N.F. Verster and H.L. Hagedoorn; Nucl. Instr. & Meth. 18 - 19, 327 (1962)

2. R.E. Berg, H.G. Blosser and W.P. Johnson; Mich. State Univ. Cyclotron Project Report, MSUCP - 22 (1966).

DISCUSSION

V.N. Bhoraskar: Have you consider the stability of the magnetising current?

R.K. Bhandari: Current instability contributes an error of about 0.5% of the reading. Reported accuracy 3% takes account of this error.

[illegible]

[illegible]

[illegible]

[illegible]

I. [illegible]

[illegible]

$$[illegible](s) = [illegible] + \sum [illegible]$$

[illegible] only [illegible] [illegible] all.[1,2] [illegible] of [illegible] or total beam [illegible]. [illegible] a first [illegible] of [illegible] high efficiency [illegible]. A series of [illegible] relating various [illegible] their first [illegible] contributions, are [illegible].

II. [illegible] FIRST [illegible]

To make the calculations [illegible] following assumptions

(1) If a magnet [illegible] contains [illegible] gap is inversely [illegible]

i.e. [illegible] = Constant/g

[illegible] based [illegible] assumption on the [illegible] the total magnetic [illegible] as the relationship [illegible]. Using a [illegible] that [illegible] assumption holds [illegible]

of these calculations.

ii) First harmonic caused by the loss of N fold symmetry due to an inaccurate sector can be calculated by Fourier analysing a step wave whose half periods or amplitudes are slightly unequal corresponding to the machining or positioning error.

Using these assumptions, we list the general expressions derived[3] in the following table.

Table 1.

Type of error	Relationship between constructional errors and first harmonic ΔB
1. Non-parallity of pole pieces	$\Delta B_a = B_{Av}\, r.\delta / 2.R_0.(g_1 + \delta/2)$
2. Machining of sectors	$\Delta B_b = 2\sqrt{2N}\,(B_H - B_{Av})\,\delta\theta/\pi$
3. Positioning of sectors on pole-tip.	$\Delta B_c = 2\sqrt{2N}\left(1 + \cos\frac{\pi}{N}\right)^{1/2}(B_H - B_{Av})\,\delta\beta/\pi$
4. Tapering of Sector edges	$\Delta B_d = 2\sqrt{2N}\,(B_H - B_{Av})\,t.\delta\phi/\pi.r.\sin\phi$
5. Thickness of sectors	$\Delta B_e = 2\sqrt{N}\,\sin\left(\frac{\pi}{2N}\right) B_H.\delta z/\pi.g_h$
6. Flatness of sectors	$\Delta B_f = 2\sqrt{N}\,\sin(\pi/2N)\, B_H.\delta g/2\pi g_h$
7. Parallity of sectors	$\Delta B_g = 2\sqrt{N}\,\sin(\pi/2N)\, B_H.\Delta/2\pi g_h$
8. Concentricity of Pole-pieces	$\Delta B_h = 2\sqrt{2N}\,(B_H - B_{Av})\,\Delta y\,(1 + \tan\omega/2)/2\pi.r.$

III. TOTAL FIRST HARMONIC

The total first harmonic is the sum of the individual first harmonics added with their proper phase. Since the exact phase of the error cannot be predicted, by applying the statistics of independent errors, it has been shown[3] that the most probable sum in this case also reduces to the root square sum given by

$$\Delta B = \sqrt{\Delta B_a^2 + \Delta B_b^2 \cdots \Delta B_n^2} \qquad (3)$$

IV. RESULTS

Using the expressions listed in Table 1, the total first harmonic for the parameters and tolerances of the Texas A & M University cyclotron is calculated to be 3.6 gauss at r = 10 cms

for an average field of 8.25 Kgauss; the actual measured value is 2.0 gauss[4]. The corresponding value for the Calcutta cyclotron is expected to be 3.9 gauss. In fig.1 are compared the theoretical and experimental values of the first harmonic as a function of the cyclotron radius.

V. CONCLUSION

Considering the large number of derivations involved and the statistics due to uncertainty in phase, there is a reasonable agreement between the theoretical and experimental measurements. Thus, using these general expressions, tolerances for the sectors of an AVF cyclotron magnet having N sectors and of any dimension can be simply prescribed which will keep the total first harmonic content below the critical permissible level. Such tolerances largely influence the technical feasibility of a cyclic accelerator of large dimensions.

REFERENCES

1. Theory of Cyclic Acc., Kolomensky & Lebedev, North Holland Pub Co. (1966) 31
2. Progress in Nuc. Techneques & Instrumentation, North-Holland Publishing Co., (1965), 29.
3. A.Jain and A.S.Divatia, To be published
4. Private communication from Mr. W.A.McFarlin, Cyclotron Institute, Texas A & M University.

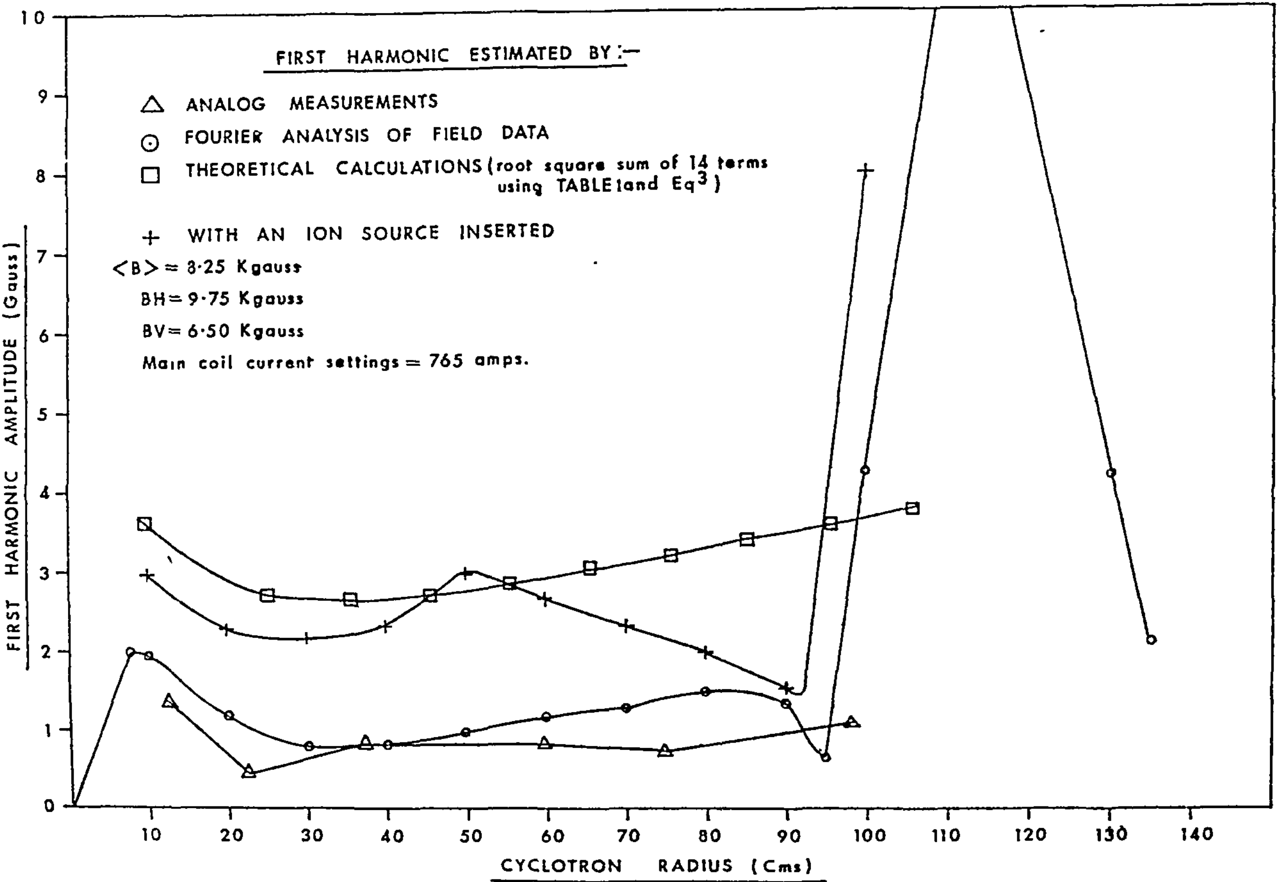


Fig.1. Comparison of the calculated and measured first harmonic amplitude of the Texas A & M University Cyclotron.

TEMPERATURE EFFECTS ON ELECTROSTATIC PROBE MEASUREMENT IN HIGH PRESSURE PLASMA

V.K. Rohatgi
Bhabha Atomic Research Centre
Trombay, Bombay-85.

I. INTRODUCTION

Practically no information has been located regarding a charge emitting probe and its application as a plasma diagnostic tool. The present study was undertaken to investigate the effect of temperature on the charge collection property of a probe. The object of this paper is to summarize the results of this study.

II. THE EXPERIMENT

The plasma was generated in a 1cm diameter channel confined by insulated molybdenum disks with tungsten inserts. A probe similar to the stack disk was located halfway in the column. The stack including the probe attained high temperatures due to the heat from the plasma. The stack was enclosed in an inert gas chamber to prevent it from oxidation during the experiment. Other details of the apparatus have been published earlier[1]. At fixed arc current and steady state collector temperature the probe characteristics were plotted directly on an x-y recorder. The probe temperature was measured by a lead sulfide photodetector whose output voltage was related to the target temperature.

III. RESULTS

The current voltage characteristics of molybdenum and

tungsten probes in 1 atm argon plasma of 125A arc are presented i
Fig.1. The low temperature probe data ($T \leq 500°K$) has been anal
on the basis of ion collection probe theory, assuming no charge e
ssion from the collector surface[2].

At higher temperatures when thermionic emission begins
appear both ions and electrons contribute to the probe current.
the mobility control flow expressions for ions and electrons it i
possible to show that for electron density upto 10% of the ion de
the reduction in the space charge field is less than 4%. Hence i
that case one can neglect the electron emission and use the probe
to study the charge distribution as in the case of a low temperat
probe. As expected, the results thus obtained (Fig.2) indicate t
in the case of an electron emitting probe the charge density and
gradient are slightly reduced when compared with a water cooled p

Estimates of electron temperature made from the water
cooled probes compared favourably with the spectroscopic determin
tions[3]. However, Fig.1 shows that the quantity $(di/dV)_{V=0}$ in
eases with probe temperature. This implies that the T_- estimated
from the high temperature probe data would be lower than T_- obtai
from the water cooled probe data. Thus it is concluded that high
temperature probe measurements provide an under-estimate of plasma
electron temperature.

The dependence of current on the surface temperature
the collector is shown in Fig.3. From simple calculations based o
the Richardson equation and the kinetic theory of gases it is poss
to show that in the present example the current at lower temperatu

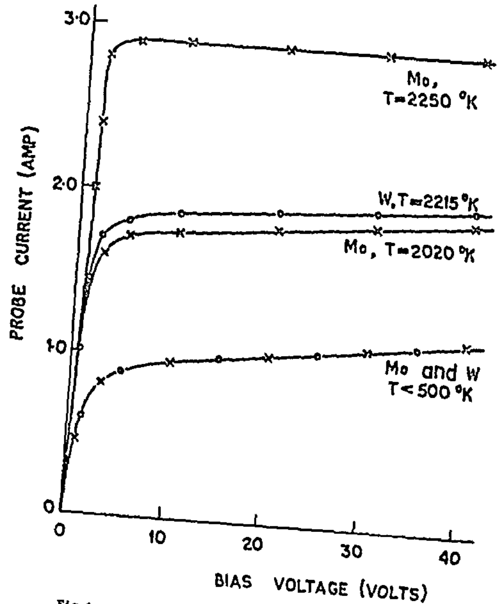


Fig.1. Current-voltage characteristics of molybdenum and tungsten probes in argon plasma of 125A arc.

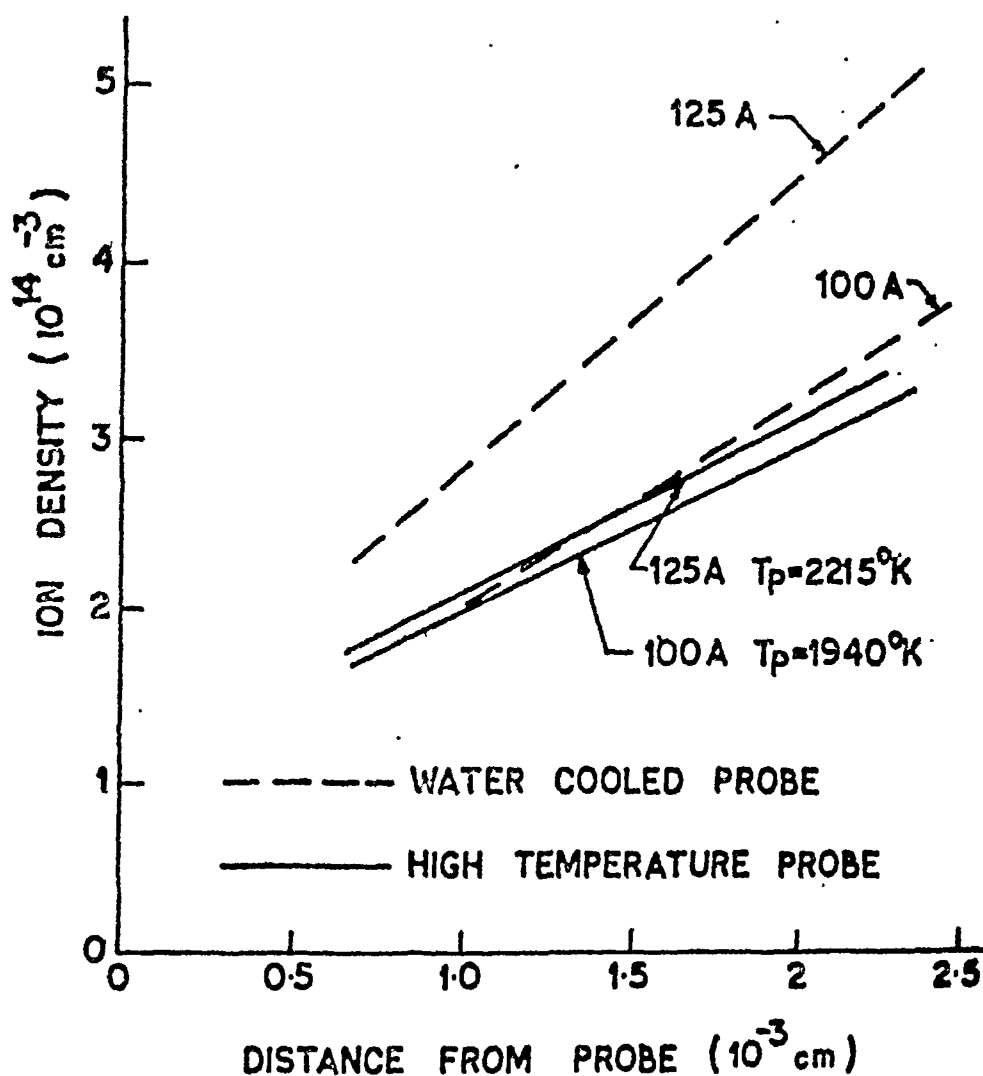


Fig.2. Charge distribution in the boundary layer of a negatively biased probe in argon plasma at 1 atm. Full line, high temperature probe; broken line, water cooled probe.

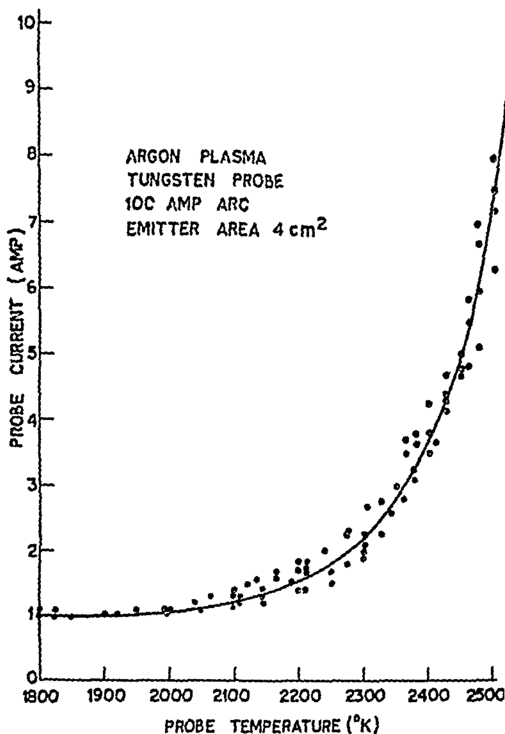


Fig.3. Dependence of current on temperature of a tungsten probe in argon plasma of 100A arc.

($T \leq 2000°K$) is mainly due to the ion collection and that it remains constant throughout the range of the experiment. The data also permits an evaluation of the effective work function of tungsten which in this case is found to be 3.54ev. This value of work function is appreciably lower than the reported work function of 4.5ev for tungsten[4] in vacuum. It has been shown that the reduction in the work function of the emitter is due to the presence of ion space charge field in a manner described by the Schottky effect[5].

REFERENCES

1. V.K. Rohatgi, A IAA. J., 4, 1852 (1966)
2. V.K. Rohatgi, Int. J.Electron., 24, 257(1968)
3. V.K. Rohatgi, Brit.J.App.Phy.,(J.Phys.D.),1, 485 (1967).
4. D.E. Gray, Am.Inst.Phys.Handbook(McGraw Hill Book Co., New York 1963) 2nd Edition, Table 9 j - 1.
5. V.K. Rohatgi, J.App.Phys.(To be published).

DISCUSSION

M.R. Bhiday: In a fixed probe (w.r.t.) electrodes, the probe is looking at a very negligible fraction of the plasma. How much faith can be placed on the calculations of E?

V.K. Rohatgi: Within the accuracy of the measurements and the resolution of probe studies the field has been found to be uniform over a section larger than the probe size.

VELOCITY MEASUREMENT IN RF PLASMA JET

Jayakumar and A.S. Paithankar
Technical Physics Division, Bhabha Atomic Research Centre,
Trombay, Bombay-85(AS).

I. INTRODUCTION

Preliminary measurements of the velocities of the Argon plasma jets generated in the quartz tube placed in the induction coil of an rf oscillator have been reported in this paper. The knowledge of this important parameter is essential for understanding various phenomena taking place in the plasma and also for improving the efficiency and performance of different technical applications of the jet. Numerous methods are available for the plasma jet velocity measurements. The measurement of plasma jet in MHD channel[1] is carried out by discharging a capacitor in flowing plasma. The flight of ion cloud created is recorded by means of 2 photomultiplier system. The velocity of the plasma jet can also be computed by measuring the MHD voltage generated. Both these methods are based on the assumption that the relative velocity of plasma jet and ion is zero. There are various other methods such as water-cooled probe[2] to measure the impact pressure and spectroscopic technique[3] which determines the temperature distribution and hence the velocity distribution. But all these measurements have been shown to have their own drawbacks[4]

In the present experiment, the plasma jet velocity was measured by using luminous particle tracer technique.[4, 5]

III. EXPERIMENTAL

The schematic diagram of the experimental apparatus is

shown in Figure 1. The high frequency generator used was a 6KW, 12 MH_z oscillator. The plasma torch consisted of a 35 mm i-d quartz tube open at one end surrounded by a water cooled copper coil with five turns and 4 cm overall length. The plasma gas was introduced in the tube tangentially. This tangential flow of the gas stabilizes the plasma and insulates it from the wall of the tube.

The plasma jet was started by increasing the generator power to about 80% and introducing a graphite rod in the quartz tube. The arc is struck by heating the graphite by induction and adjusting the gas flow. Once the arc was stabilized the graphite rod was removed. Each time the plasma gas flow-rate, and the power in the tube was kept constant. The constancy of the power input to the plasma was monitored by keeping note of grid and plate current of the oscillator. The power input in the plasma was estimated to be 1.5 KW. After stabilizing the plasma jet a fine mesh ($\sim$40 μ) of graphite power was introduced from top and the path of the particles were traced taking piroutres with Lica camera with a shutter speed of about 2 msec. The calibration of the camera shutter speed was done with tektronics 585A oscilloscope. Photographic enlarger was used to measure the length of the streaks produced by the particles. The scale factor of the image was determined by comparing the diameter of the plasma tube as it appeared on the negative with its actual diameter, and velocities were determined by dividing the streak length of the particle by exposure time.

In order to locate the radial position of the particles, three dimential mapping technique was used. The side view of the p

plasma jet was reflected with the help of mirror in such a way that front view and side view could be seen side by side. Knowing the position of the track with respect to centre of the tube, the radial position of the track was determined.

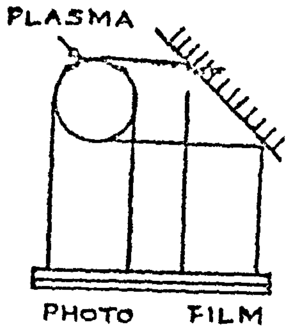
III. RESULTS

About 200 tracks in about 50 photographs were studied and velocity of the jet was determined. Fig.2 shows the radial distribution of jet velocity for given distance from the edge of the plasma tube. The average velocity was found to be 8 m/sec.

Thanks are due to Shri C. Ambasankaran for his encouragement and keen interest in the work.

IV. REFERENCES

1. S. Suckewer and Z. Celinsh; Intd. symp. on MHD electrical generation 1, 303, 1964.
2. J. Grey et al. A I A A J, 4, 98, 1966.
3. F. Gotmohlish et al. A I A A J, 4, 1085, [illegible]
4. S.V. Desai et al. Rev. of Sc. Int. [illegible], [illegible], [illegible]
5. R.M. Fristrom and A. Westenberg; (Flame [illegible]; (McGraw Hill Book Co., N.Y., 1965) [illegible]



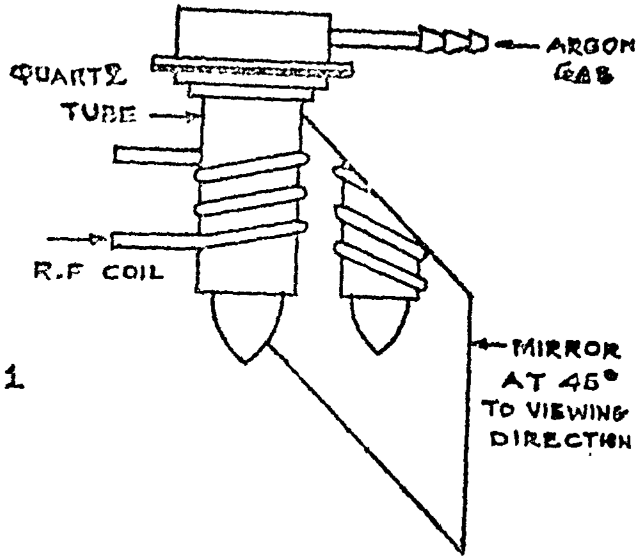


fig 1

VELOCITY M/SEC.

12·0
10·0
8·0
6·0
4·0
2·0

Z=0
Z

Z=0 MM
Z=4 MM
Z=10 MM

RADIAL DISTANCE M.M.

4·0 8·0 12·0 16·0 20·0

FIG. 2

ELECTROTHERMAL EFFICIENCY OF D.C. PLASMA JETS

A.S. Paithankar, Jayakumar, P.S.S.Murthy, and P.R. Vanjpe
Technical Physics Division, Bhabha Atomic Research Centre,
Trombay, Bombay-85(AS).

I. INTRODUCTION

The knowledge of the heat balance in the flames generated in the D.C. plasma jets is a necessary prerequisite for employing these devices for technological applications. This information is necessary for determining the various reaction rates and the electrode life. This paper provides an estimate of the efficiency of the plasma jets developed in BARC. The studies were made on a 30 KW non-transferred arc torch, and a 120 KW transferred arc torch. The losses in the plasma torch and useful power were obtained from calorimetric and metal cutting speed measurements.

II. EXPERIMENTAL

The torches tested were gas vortex stabilized torches comprising a 10mm dia thoriated tungsten cathode and a copper nozzle anode separated from the cathode by araldite. The torches were built for ceramic spraying and metal cutting. These were used with suitable transductor controlled power supplies. The tests were made for 6mm dia orifice with a 2.5cm long non-transferred flame and the transferred arc torch was tested for 3 mm nozzle orifice.

III. RESULTS AND DISCUSSION

The total power input to the torch is divided into

1) Electrode loss, 2) Radiation loss and 3) power carried away by the flame. In most torches the radiation loss is negligible and electrothermal efficiency of the torch is given by:

$$\eta = \frac{Pin - Pel}{Pin} \times 100$$

$$= \frac{\text{Total power in the jet}}{\text{Power input}} \times 100$$

where Pin is the power input and Pel is the power loss in electrodes.

However in the case of transferred arc torch the anode loss appears as useful heat and hence much higher efficiency is obtained. The analysis of various losses is as follows.

The anode: The anode is usually the stabilizing nozzle and the losses can be equated to $j_a(\phi_a + V_a + \frac{3KT}{2e})$ KW/cm^2 where j_a is the current density at the anode, ϕ_a the work function, V_a the anode potential fall and T is the gas temperature. To this loss is added the convective and radiative losses. In practical devices these losses are kept below 100KW/cm^2 for copper, to avoid excessive erosion. The cathode: The total cathode losses are due to cathode fall + heat gain due to convection and radiation + resistive losses.

The major loss in gas stabilized torches is due to cathode fall and is equal to:

$$j_k(V_k - \phi_k - V_e)$$

where V_k is the cathode fall, j_k the cathode current density, ϕ_k the work function and V_e is the voltage equivalent of thermal energy of electrons.

The efficiency of non-transferred arc torch with Argon at 32 volts and 450 Amps was calculated to be 78% and with Nitrogen at 75 volts and 400 amp was about 83%. The large efficiency is apparently due to vortex flow.

The above discussion is valid also for transferred arc devices, though here the main anode loss appears as useful heat. However there is a loss due to the auxiliary nozzle. This loss can be calculated by treating the nozzle as a metal interface at plasma potential and can also be measured calorimetrically. In a typical experimental case this loss for Argon - Nitrogen mixture as plasma gas was estimated to be about 6 KW and confirmed by experimental measurement.

The heat transferred to the work piece in the case of a transferred arc device can be calculated from sample experiment. In cutting process a large portion of heat is conducted away along ll of the work piece and is spent unprofitably in heating the job. e heat balance in the case of metal cutting has been calculated by enthal(1) and Rykalin(2) assuming a superposition of the fields of nt heat sources. The efficiency of kerf melting (fusion cutting) of the total heat transfer to the job is given by

$$\eta_K = \frac{5\ vt/4a}{2\left(1 + 5\ \frac{vd}{4a}\right)} \quad \text{where } a = \frac{X}{C\rho}$$

v is the cutting speed, t is the thickness of material, X the conductivity, C the sp. heat and ρ is the sp. gravity of the

Thus the total heat transferred in cutting process is given by

$\frac{1}{\eta}$ v d t ρTm C. where d is the kerf width and Tm is the melting point of the material.

The overall electrothermal efficiency of the transferred arc was found to be 90%, the efficiency of heat transfer to the work-piece for 1" thick stainless steel at 100 cm/sec. cutting efficiency was 45% and the actual(cutting efficiency,corresponding to heat used for cutting) was about 25%. The measurements were for A, N_2 mixture with 250 volts arc voltage and 400 amps current.

The anode erosion was found to be much larger in Nitrogen than Argon. This is attributed to the fact that despite the higher efficiency in Nitrogen the anode flame ends in a finer spot for N_2 increasing the power density.

Assuming the electrode losses to appear fully in anode the nozzle will erode considerably if the spot is smaller than 1mm. However with Argon the flame assumes the full channel diameter and the loss is below 50 KW/cm^2 for the mentioned operation. The cathode erosion was too small to be measurable.

Thanks are due to Shri C. Ambasankaran for his encouragement and interest in our work.

IV. REFERENCES

1. D. Rosenthal; Theory of moving sources of heat and its application to metal treatment, Pergamon Press, 1946.

2. N.N. Rykalin; Computing thermal phenomenon of welding practice, Berlin, Verlag Technik, 1957.

COMMUNICATIONS RECEIVED BUT NOT PRESENTED

the formula for computing the cross section comes out to be :

$$\sigma = \frac{A(1+\alpha)\lambda}{\theta \epsilon \phi N (1-e^{-\lambda t})(e^{-\lambda t_a} - e^{-\lambda t_b})}$$

where A is the photopeak area of the selected gamma ray in time $(t_b - t_a)$, α is the internal conversion coefficient, λ is the decay constant of the product nucleus, θ is the branching ratio for the gamma ray in question, ϵ is the effective efficiency of the detector including the solid angle and self absorption corrections, ϕ is the incident neutron flux, N is the number of irradiated target nucleus. ~~is the decay constant of the product nucleus~~ and t is the duration of irradiation. By comparision method, the capture cross section for the reaction in question comes out to be,

$$\sigma = \sigma_1 \cdot \frac{A(1+\alpha)N_1\epsilon_1\theta_1 (1-e^{-\lambda t_1})(e^{-\lambda_1 t_{a_1}} - e^{-\lambda_1 t_{b_1}})}{A_1(1+\alpha_1)N\epsilon\,\theta (1-e^{-\lambda t})(e^{-\lambda t_a} - e^{-\lambda t_b})}$$

where the symbols with subscript 1 refers to the standard reaction. Out of all the quantities entering in this equation $\sigma_1, \alpha, \alpha_1$, θ and θ_1 are taken from the literature[2,3], the decay constant λ is determined by measuring the half life of product nucleus, N & N_1 are calculated by knowing the mass of targets irradiated, photopeak areas A and A_1 are determined experimentally, photopeak efficiency ϵ and ϵ_1 is taken from earlier work.[4]

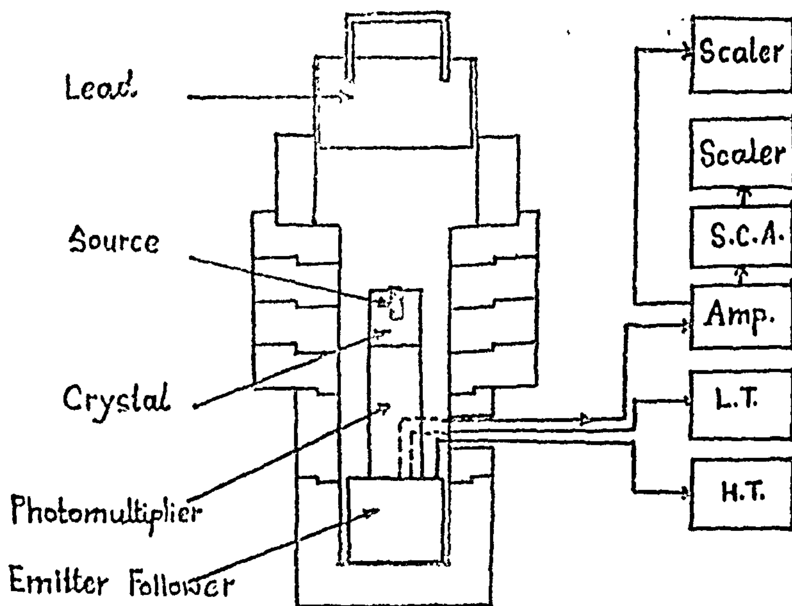
Following the method of Booth et al[5] we have also calculated the capture cross section at 24 keV with the help of equation,

$$\sigma = \sum_{J} \frac{2J+1}{2(2I+1)} \frac{1}{2}\pi\left(\frac{2.6\times10^{6}}{E_n}\right)\frac{\Gamma_\gamma}{D}\left[1-(b\pi)^{1/2}\left(1-\frac{2}{\sqrt{\pi}}\int_0^{\sqrt{b}}\exp(-t^2)dt\right)\right]$$

where J is the total angular momentum of compound nucleus, I is the spin of target nucleus, E_n is the incident neutron energy in eV, Γ_γ is the radiation width, D is the average level spacing and $b = \Gamma_\gamma/2V_0\Gamma_n^0$; V_0 is penetration factor and Γ_n^0 is the reduced neutron width. Here V_0 is taken to be unity for zero angular momentum. The parameters I, J, Γ_γ, D, E_n are taken from earlier works [6,7]. The value of these parameters were taken as the average over all the S-wave resonances. The contribution due to the p-wave neutron has been assumed to be almost zero and the low energy resonance parameters can be used at E_n = 24 keV. For zero spin target nuclei the average level spacing has been taken to be equal to the observed level spacing whereas for non zero-spin target nuclei, the average level spacing is taken to be twice of the observed level spacing [8].

A comparision is made between the measured neutron capture cross section and the theoretically calculated ones and is shown below.

Target Nucleus	σ (mb) exp.	σ (mb) theo	Target Nucleus	σ (mb) exp	σ (mb) theo
^{55}Mn	41	43.4	^{114}Cd	287	253.9
^{63}Cu	28	22.6	^{127}I	638	672
^{75}As	160	94.3	^{139}La	13	12.08
^{98}Mo	121.5	140.7	^{141}Pr	82	60



COUNTING SET-UP

REFERENCES

1) T. B. Ryves et al; Journal of Nuclear Energy Parts A/B, 1966, Vol.20, 249.

2) L.A.Sliv and I.M.Band, Tables of I.C.C., Alpha-, Beta-and Gamma-Ray spectroscopy Vol.2 (1965)1639.

3) Jack M. Hollander, Berkeley; Table of Isotopes (1967) 6th Edn

4) P.N. Tiwari & E. Kondaiah (Unpublished work)

5) R. Booth et al; Phys. Rev. 112 (1958) 226

6) A.K. Chaubey & M.L. Sehgal; Phys. Rev. 152 (1966) 1055.

7) B.N.L. 325 (1958) Second Edn.

8) Carter, Harvey, Hughes and Pilchev; Phys. Rev. 96 (1954) 113.

DEEXCITATION PHENOMENA IN PROMPT FISSION FRAGMENTS

Ratna Sarkar and Aparesh Chatterjee

Saha Institute of Nuclear Physics, Calcutta-9

An attempt to treat the fission energy kinetics at the scission point from our RGM-PES approach[1] reproduced the observed energy release E_R, the fragment excitation energy U_F and the kinetic energy T_F with fair success in 5 nuclei[2]. Further improvements[3] of the RGM allow us to study (a) the prompt γ-decay processes and (b) the dependence of U_F on the excitation of the fissioning nucleus.

We recall that the quadrupole-monopole interaction energy E_q of the recoiling fragments were assumed[1,2] to give rise to E2 type prompt γ-rays. We assume here that (i) $E_q = E_\gamma^{max}$ where E_γ^{max} is the energy available in prompt γ-decay, and that (ii) E_γ^{max} is divided into the number n_γ of cascade E2 transitions of mean energy E_γ. Assuming the deexcitation sequence of the prompt fragment A_{F*} to be

$$A_{F*} \xrightarrow[\nu_F]{n} A_{F'*} \xrightarrow[n_\gamma]{\gamma} A_{F'} \quad , \qquad (1)$$

where ν_F is the number of prompt neutrons ahead of $A_{F'*}$ from which n_γ γ-rays are emitted leaving $A_{F'}$ in the ground state.

We assume, as is customary,

$$(E_\gamma^{max})_{av} \approx \tfrac{1}{2}E_\gamma^{max} \approx \tfrac{1}{2}B_n = n_\gamma \cdot E_\gamma \quad , \qquad (2)$$

where B_n is the mean neutron binding energy of the fragments.

The predictions of $(E_\gamma^{max})_{av}$ and n_γ for the ^{236}U, ^{252}Cf fissioning nuclei[3] agree fairly well with the experimental observations of Johanson[4] and Maier-Leibnitz et al.[5]

The dependence of U_F on the available energy U_I of e

fissioning nucleus I has the remarkable features that (i) the strong shell structure effects found in threshold fission in the fragments seem to be selectively wiped out gradually with increasing excitation[6] and that (ii) the kinetic energy T_F remain roughly constant (decrease is observed in a few cases); the excess energy thus goes to increase the intrinsic energy of the system in such a way that higher excess energies smooth out the variations of fragment intrinsic energies.

If ΔU_I is the excess internal energy of I to be shared with the excess energies ΔU_L and ΔU_H of the light and heavy fragments L and H, then

$$\Delta U_I = \Delta U_L + \Delta U_H . \quad (3)$$

We recall that the RGM interaction energy $\delta\epsilon$, really being a measure of the chaos introduced in a nuclear system due to the presence of extracore nucleons, predicts that the midshell nuclei enjoy a "saturation configuration" in their ground states. If $\delta\epsilon_{max}$ is the midshell RGM correction, and $\delta\epsilon$ that for a local species, then $(\delta\epsilon_{max} - \delta\epsilon)_F$ is a measure of the lack of saturation of F. We define the energy partition condition in the fragments to be

$$\Delta U_L / \Delta U_H = (\delta\epsilon_{max} - \delta\epsilon)_L / (\delta\epsilon_{max} - \delta\epsilon)_H . \quad (4)$$

Limiting ourselves to the range $3 \lesssim U_I \lesssim 50$ MeV, a simple statistical treatment with Le Couteur and Lang's approximation for the mean temperature T of evaporated neutrons[7] gives

$$1/T = [d \ln \rho(U_F)] / dU_F \approx (a_F / U_F)^{\frac{1}{2}} . \quad (5)$$

We have used our calculated a-parameters[8] throughout.

The fragment excitations for the threshold fission and fission at 11.1 MeV excitation of the ^{227}Ac nucleus have been

calculated and compared with the data of Schmitt and Konecny[9] of the ^{226}Ra+p reaction at 13.0 proton energy. Similar comparison has been made for the ^{234}U fission reaction at 0, 15, and 18 MeV excitations through the ^{233}U+n reaction data with thermal neutrons[10], and ^{230}Th+α reaction[11] at 25.7 and 29.5 MeV, respectively. The predictions that (i)ν_p increases in absolute magnitude, (ii) the neutron yield peak shifts to heavier mass, and (iii) the peak-tovalley ratio of the sawtooth yield curve gradually decreases, are all verified experimentally.

REFERENCES

1. R. Sarkar and A. Chatterjee, Phys. Lett. 30B(1969)313; Phys. Rev. C1(1970)619; R. Sarkar, unpublished
2. R. Sarkar and A. Chatterjee, Proc.L.E.N.P.&S.S.Symp.(1969)
3. R. Sarkar and A. Chatterjee, Phys. Lett. 33B(1970)263
4. S. Johanson, Nucl.Phys.60(1964)378; 64(1965)147
5. H. Maier-Leibnitz et al., I.A.E.A. Fission Conf. (1965)
6. V. S. Ramamurthy et al., Phys. Rev. Lett. 25(1970)386
7. K.J. Le Couteur and D.R.Lang, Nucl.Phys. 13(1969)32
8. S. K. Ghosh et al.,Proc. L.E.N.P.&S.S. Symp. (1969)
9. H.W.Schmitt and E. Konecny, Phys.Rev.Lett. 16(1966)1008
10. V. F. Apalin et al., Nucl. Phys. 71(1965)553
11. H. C. Britt and S. L. Whetstone, Phys.Rev. 133(1964)B603

optical-model potential is intrinsically energy dependent and nonlocal. So that the OMP - $\mathcal{V}_{op}$ at the incident nucleon energy E, may be written as

$$\mathcal{V}_{op}(E;\vec{r},\vec{r}') = V_N(E)g_v(\vec{r},\vec{r}') + iW_N(E)g_w(\vec{r},\vec{r}'), \qquad (1)$$

where $\vec{r}$ is the incident nucleon coordinate.

In writing eq.(1) it has of course been assumed that the form factors of the potential are independent of E. This seems justified because in phenomenological analyses geometrical parameters of the potential are found to vary little over a wide energy range.

If following Perey and Buck[5], we also assume that the non-local nature of the potential may be described by taking the form factors:

$$g_v(\vec{r},\vec{r}') = f_v(p)\frac{e^{-s^2/\delta_v^2}}{(2\pi\delta_v^2)^{3/2}},\quad g_w(\vec{r},\vec{r}') = f_w(p)\frac{e^{-s^2/\delta_w^2}}{(2\pi\delta_w^2)^{3/2}}, \qquad (2)$$

where $\vec{p} = (\vec{r}+\vec{r}')/2$; $s=|\vec{r}-\vec{r}'|$ and δ_v and δ_w are respectively the non-locality parameters of the real and imaginary parts, we obtain for the equivalent local optical-model potential - (V+iW) the expression

$$V + iW = V_N(E)f(r)e^{-\alpha_v(E+V+iW)} + iW_N(E)f_w(r)e^{-\alpha_w(E+V+iW)} \qquad (3)$$

with $\alpha_v = m\delta_v^2/2\hbar^2$ and $\alpha_w = m\delta_w^2/2\hbar^2$; m is the nucleon mass. Since the quantities α_v and α_w are quite small+ and in the low energy region under consideration W is also small, we obtain from eq.(3)

$$W(E,r) = \frac{W_N(E)f_w(r)e^{-\alpha_w(E+V(E,r))}}{1+\alpha_v V_n(E,r)e^{-\alpha_v(E+V(E,r))}}, \qquad (4)$$

where $V_n(E,r) = V_N(E)f_v(r)$

III. DISCUSSION

It follows from ref.[4] that because of the dispersion relation $V_n(E)e^{-\alpha_v E}$ and $V(E)$ are essentially constant near zero energy. So that the energy dependence of $W(E,r)$ as given by eq. (4) is essentially determined by the factor $W_N(E)e^{-\alpha_w E}$ in the numerator.

Basic theories predict that $W_N(E)$ is proportional to the state density of the target nucleus[1], so that $W_N(E)$ is expected to increase rapidly with E. On the other hand $e^{-\alpha_w E}$ is a decreasing function of

+ Perey and Buck[5] used $\delta_v = \delta_w = .85$ fm. This gives $\alpha_v = \alpha_w = .008$ MeV^{-1}. For $\delta_w = 1.2$ fm, $\alpha_w = .017$ MeV^{-1}

E. Thus the energy dependence of $W(\vec{r})$ is weak compared to that of $W_N(E)$. This clearly shows that the physical argument that the magnitude of the imaginary potential increases with the number of absorbing channels, and, therefore, with energy [illegible] more appropriately to the *nonlocal imaginary potential* [illegible] than to the local imaginary potential depth, the energy [illegible] of which is in fact somewhat reduced due to the [illegible].

Now in the low energy region $W(E)$ [illegible] to have some positive slope, we, therefore, have from [illegible] the condition

$$dW_N(E)/dE \geqslant \alpha_N W_N(E) \qquad (5)$$

Next we discuss the radial distribution of $W(\vec{r})$ as given by eq. (4). We, do this for *E = 0* [illegible] for simplicity, E from the arguments of various quantities. For simplicity we also [illegible] the second term (which is small [illegible]) in the denominator in eq. (4) the effect of which will [illegible] later. We thus write eq. (4) as

$$W(r) \approx W_0 f_N(r) e^{-\alpha_N V(r)}$$

It follows from the argument [illegible] expected to be appreciable [illegible] face region where the real [illegible] therefore, (for simplicity, [illegible] value upto $r = r_0$ where [illegible] falls to 10% of its value [illegible]

$$W(r_0)/W(0) = e^{\alpha_N V(0)}$$

Thus an enhancement of W [illegible] clearly indicated. However, [illegible] nds sensitively on the [illegible] $V(0)$ = 50 Mev, [illegible]

As regards the [illegible] easy to see that [illegible] in the surface [illegible] (ref.[5]) so that [illegible] Since $V_N(r)$ is [illegible] that $W(r)$ [illegible] to be help[illegible]

It [illegible] on of the [illegible] al [illegible]

surface peaking in the (local) imaginary potential.

REFERENCES

1. G.E. Brown, Unified Theory of Nuclear Models (North-Holland Pub. Co. Amsterdom, 1964) Chapter, 9
2. P.E. Hodgson, Ann. Rev. Nucl. Sci. 17 (1968)1
3. C.A. Engelbrecht and H. Fiedeldey, Ann. Phys. 42 (1967)262
4. I. Ahmad and M.Z. Rahman Khan, Nucl. Phys. A141 (1970)7
5. F.G. Perey and B.Buck, Nucl. Phys. 32 (1962)353

STUDY OF (p, p') AND (p, n) REACTIONS IN Be^9

J. Mahalanabis
Saha Institute of Nuclear Physics, Calcutta-9

ABSTRACT

We have calculated the cross-sections for (p, p') and (p, n) reactions in ^9Be at medium energies, leading to excitation of the 2.43 MeV state ($5/2^-$) in Be^9 and ground state of ^9B (isobaric analouge state), respectively. The results are compared with the available experimental data. It is seen that better fit is obtained with Wilkinson' wavefunction rather than the oscillator wavefunction.

ELASTIC AND INELASTIC SCATTERING CROSS-SECTIONS OF CHROMIUM, IRON AND NICKEL

S.B. GARG and B.P. RASTOGI
Reactor Engineering Division
Bhabha Atomic Research Centre, Bombay-85.

I. INTRODUCTION

Chromium, iron and nickel are the main constituents of stainless steel which is commonly used as a structural and canning material in fast power reactors. In a typical fast reactor the content of stainless steel varies from 25% to 30% of the core volume. Though chromium, iron and nickel are poor moderators, yet they are good enough to degrade the spectrum by elastic and inelastic collisions in fast systems. It is, therefore, imperative to have the correct estimate of their elastic and inelastic scattering cross-sections.

The measured information on these cross-sections is rarely available throughout the entire energy range 1.0 - 10.0 MeV. Thus the only way of generating suitable numbers is to interpolate or extrapolate between the measured points. Optical and statistical models are two such tools that provide a means of extrapolation and interpolation.

In optical model analysis phase shifts are correctly calculated by fitting the experimentally measured elastic scattering cross-sections and their angular distributions. This is achieved by finding a suitable potential which approximately represents the

interaction between the projectile and the target. Such a potential consists of two parts - the real and the imaginary. The real part of the potential accounts for the refraction of the incident particles through the target nucleus and gives the potential scattering or shape elastic cross-section. The imaginary part of the potential accounts for the absorption of the incident particles in the target nucleus and gives the cross-section for the compound nucleus formation. The subsequent decay of the compound nucleus leads to the split of the reaction or compound nucleus formation cross-section into compound elastic and inelastic scattering cross-sections. The total cross-section is obtained by adding the shape elastic and the reaction cross-sections.

In the present study the real and the imaginary parts of the potential have been determined by fitting the measured elastic scattering cross-sections and their angular distributions wherever such information was available in the energy range 1.0 - 10.0 MeV. Saxon form has been used for the real part and the Gaussian form for the imaginary part.

II. THE X^2 CRITERION

The quantity X^2 is defined as

$$\chi^2 = \sum_n \left\{ \sum_i \omega_i \left(\sigma_i^{calc} - \sigma_i^{exp} \right)^2 + \frac{1}{N} \sum_j \omega_j \left(d\sigma_j^{calc} - d\sigma_j^{exp} \right)^2 \right\}$$

Where the left inner sum is taken over the quantities which are not angular distributions and the right inner sum is taken over those quantities which are angular distributions; and the ω_i , ω_j are the weights.

There are six parameters of the optical model potential, namely, U,W,r,a,b and V_{sO}. In the calculations a search of these parameters is made by varying them in such a way that a minimum value of x^2 is obtained. A computer program AUTO was adapted for use on CDC-3600 to do the automatic search and sean of these parameters. This program allows the simultaneous variation of five parameters. In this study the search is limited to U, W and γ only. V_{sO} is fixed at zero value since no attempt is made to fit the polarization measurements - the data being not available. The values of a and b are fixed at 0.65 and 0.45 respectively.

The computer programme AUTO is coupled to another programme ABACUS which is based on the optical and Hauser - Feshbach models.

III. CALCULATIONS

The optical model parameters for chromium have been obtained by fitting the measured elastic angular distributions at 0.98 and 2.35 MeV. Above 2.35 MeV only the elastic scattering cross-sections have been fitted. The excitation cross-sections have been

TABLE I

	Cr			Fe			Ni		
E (MeV)	$\sigma_e^{(c)}$ (Barns)	$\sigma_e^{(m)}$ (Barns)	$\sigma_{in}^{(c)}$ (Barns)	$\sigma_e^{(c)}$ (Barns)	$\sigma_e^{(m)}$ (Barns)	$\sigma_{in}^{(c)}$ (Barns)	$\sigma_e^{(c)}$ (Barns)	$\sigma_e^{(m)}$ (Barns)	$\sigma_{in}^{(c)}$ (Barns)
4.0	2.72	2.84	0	1.44	1.19	0.2	2.92	2.85	0
3.0	2.76	2.59	0.21	2.45	2.42	0.71	2.31	2.15	0.65
4.0	2.64	2.47	0.56	2.05	2.19	0.51	2.02	2.00	0.45
5.0	2.26	2.27	0.63	2.41	2.10	0.85	-	-	-
6.0	2.59	2.34	0.54	2.49	2.38	0.64	2.49	2.16	0.57
7.0	2.57	2.35	0.48	2.28	2.17	0.53	2.32	2.14	0.58
8.0	2.20	2.07	0.46	2.14	2.0	0.46	2.11	2.03	0.54
9.0	2.11	1.97	0.39	1.96	1.91	0.42	1.90	1.81	0.59
10.0	1.76	1.63	0.58	1.79	1.71	0.41	1.80	1.83	0.76

STATUS OF ^{239}PU CAPTURE TO FISSION CROSS-SECTION RATIO MEASUREMENTS

B. P. Rastogi and S. K. Kapil
Bhabha Atomic Research Centre, Bombay 85

Introduction

The capture to fission ratio (α) in the keV energy range is an important nuclear physics parameter for the design, breeding potential and economics of large fast reactors. Large [illegible] fast reactors have a neutron spectrum which is degraded enough to give significant absorptions in the fissile element in the keV range. This is particularly true of systems having appreciable amounts of light materials as core constituents e.g. steam cooled fast reactors.

In this paper the status of the measurements of fission to capture cross-section ratio of Pu-239 (α-239) in the keV range is reviewed.

Until 1967 capture to fission ratio values of Pu-239 (α-239) used were mostly based on measurements made in [illegible] or earlier. In Fast Reactor Physics Symposium in 1967 at [illegible] measurements of alpha in Kev range report by Schomberg et al [1] were on the average about 1.8 times higher than the available values.

For a 2000 litre Sodium cooled core the predicted loss of breeding gain due to this change in alpha would be about [illegible] for oxide fuel, and about 40% for carbide fuel, affecting the [illegible] very adversely. For the steam cooled reactor the breeding gain would [illegible]. It has been estimated that for an [illegible] the uncertainity in α should be less than [illegible].

As the change in α-239 suggested [illegible] would greatly affect the breeding [illegible] a lot of effort has been put [illegible] differential and integral [illegible] laboratories.

Differential [illegible]

Values of α-239 [illegible] fission cross-section [illegible] sections using a [illegible] the energy range from [illegible] keV. [illegible] particularly above [illegible] values, and the [illegible]

Ryabov et al (2) have measured α-239 in the energy range between 5ev and 20 KeV on the Pulsed Reactor IBR using TOF and cadmium loaded scintillation detector. Capture and fission gamma rays were differentiated by the delayed coincidence due to fission neutron capture in cadmium giving a gamma cascade with 9.2 MeV energy. Values reported are higher than Schoemberg's measurements in the .1 to 1 KeV range and lower than prevalent values between 2 and 20 KeV. Due to limited energy resolution in the KeV range this experiment is useful only for the sub-KeV energies.

Czirr (3) used Pu metal foils with a one litre scintillation detector for fission and capture events. Pulse shape discrimination was used for distinguishing between the two. TOF method was used for energy determination and energy range of 1 to 10 KeV was covered.

Gwin et al (4) measured α-239 over the neutron energy range 0.02 eV to 30 KeV. Neutrons from a pulsed source impinged on Pu-239 sample in the centre of a large scintillator which detected prompt gammas from fission and capture. For fission event detection a Pu-239 ionization chamber was used for the lower energy part, at higher energies metal foils of Pu-239 were used and the difference in pulse height distributions of fission and capture gammas was used. Values from these measurements lie between ENDF/B and Shoemberg measurements.

Table I shows a comparison of the results of various measurements.

Integral Measurements

Integral measurements can provide a check on the accuracy of the differential data by comparing the spectrum averaged values from integral experiments with calculations based on the differential data.

Sehgal et al (5) used an under-moderated PuAl-D_2O lattice with varying amounts of Boron poison. A comparison of calculated and measured reactivities for different poisoning showed qualitatively that α-239 should be about 1.5 times higher than the ENDF/B values.

Bretcher et al (6) measured alpha in Assembly 24 of ZPR-9 (median fission energy 13 KeV) by reactivity-reaction rate technique. Experimental values of α-239 with Li-6 and U-238 (with α-238 obtained radiochemically) as reference absorbers were .497 and .525 respectively. Based on ENDF/B data and a recently evaluated set (9) the calculated values are 0.352, and 0.597 respectively.

Iskenderian (7) made measurements of α-239 on EBWR in the epicadmium energy range. In EBWR about 20% of the epicadmium fissions and captures

take place in the range of .1 to 100 KeV. He found good agreement with ENDF/B calculations and found that increasing α in the .1 to 100KeV energy range by 50%, increase in epicadmium alpha is 8%. In view of poor sensitivity, this experiment is of limited value in resolving the α-239 value in KeV range.

Integral measurement of α-239 was made by Anderson et al (10) in FRO critical facility in cores 5 and 8 with median U-235 fission energy of 50 and 180 keV respectively. Core 5 was made to simulate a steam cooled fast reactor. Reactivity-Reaction Rate method was used with B-10 as the reference absorber. Theoretical calculations based on cross-section set with α-239 higher than the prevalent values in the energy range by about 30% are compared with the experimentally deduced α-239 in the table given below. For comparison data the results for U-235, for which the capture to fission ratio data is much better known are also given.

Nuclide	Assembly	Experimental	Calculated
Pu-239	5	0.42 ± .05	0.36
	8	0.17 ± .07	0.20
U-235	5	0.43 ± .04	0.32
	8	0.24 ± .05	0.25

It is seen that for the soft spectrum core 5, even for U-235 (test of experimental accuracy) the agreement is poor.

Adamson et al (11) used the same method and same samples as those used by Andersson et al, for measurements in Zebra core 6, a core of 247 litres simulating PuC fuel. Experimental and calculated (using FD2 cross-section set) α-239 values were 0.36 ± .09 and 0.23 respectively.

Till et al (8) used the null reactivity zoned assembly (NCTR) technique on ZPR-III assembly 55 (Pu fuelled with 28.5% flux below 25 KeV) and ZPR-VI assembly 24-A (U235 fuelled with 8.4 cm radius Pu zone). With K_∞ of unity for the null reactivity zone, total fission source is equated to total absorption in zone to get alpha. The measured and calculated alpha values based on different differential measurements are shown below. Also shown for assembly 55 (ZPR-III) is calculation of α-239 based on the evaluated set (9).

Assembly	Experiment	ENDF/B	Gwin	Schoemberg	Kapil evaluated (9)
24A	.420 ± .05	.3193	.4206	.5429	
55	.426 ± .03	.2920	.3947	.4940	.4565

Conclusion

There is a fair amount of divergence among the differential measurements of the capture to fission ratio of Pu-239 in the range 100 eV to 20 KeV. But it can be said that the value of this ratio is higher than

the values used earlier as well as ENDF/B data and the ratio is lower than the data of Schoemberg et al over most of the energy range considered. Of the differential measurements so far, the values obtained by Gwin et al seem to be the best set.

Many integral experiments have sensitivities which only point to the above two qualitative conclusions and very few of them are useful in choosing values of α-239 on a quantitative basis. The present situation may be summarised by the results of a recent comparison of calculations for a 2500 litre sodium cooled PuO_2 fuelled reactor using the best estimates of data available at various laboratories of the world. The calculated α-239 values ranged from 0.251 to 0.334.

Table I

Energy KeV	Gwin	Ryabov	Czirr	Schoemberg
.1 - .2	0.94	1.10		0.96
.2 - .3	0.95	1.26		0.92
.3 - .4	1.20	↑		1.45
.4 - .5	0.47	|		0.75
.5 - .6	0.72	|		0.64
.6 - .7	1.83	1.977		2.09
.7 - .8	0.95	|		1.38
.8 - .9	0.96	|		1.25
.9 - 1	0.67	↓		0.97
1 - 2	0.92	0.79	0.74	1.06
2 — 3	1.18	↓	0.80	1.30
3 - 4	0.88	↑	0.66	1.19
4 - 5	0.84	|	0.68	1.13
5 - 6	0.83	0.36	0.68	1.19
6 - 7	0.79	|	0.70	1.33
7 - 8	0.60	|	0.51	0.96
8 - 9	0.43	|	0.46	0.73
9 - 10	0.52	↓	0.50	1.05
10 - 15	0.44	↑		1.00
15 - 20	0.32	0.35		0.82
20 - 30	0.27			0.65

References

1. Schoemberg et al: Fast Reactor Physics Symposium, Karlsruhe, 1967
2. Ryabov et al: Atomnaya Energia, 24, 351, 1968
3. Czirr: Trans. Am. Nucl. Soc. 12, 261, 1969
4. Gwin et al: Nucl. Sc. & Eng. 40, 306, 1970
5. Sehgal et al: Trans. Am. Nucl. Soc. 11, 202, 1968
6. Bretcher et al: Nucl. Sc. & Eng. 39, 368, 1970; ANL-7410, pp. 172
7. Iskenderian: ANL-7610, pp. 184, 1970
8. Till et al: ANL-7610, pp. 176, 1970
9. Kapil: BARC-I/96, 1970
10. Andersson et al: Fast Reactor Physics Symposium, Karlsruhe, 1967
11. Adamson et al: ANL-7320

NEUTRON DISTRIBUTION IN NUCLEI FROM ISOBARIC ANALOGUE STATES

M. Murthy
Department of Physics
Indian Institute of Technology, Kanpur-16

1. INTRODUCTION

The parameters describing the charge distributions of the protons in the nucleus, have been obtained with ever increasing accuracy from experiments on electron scattering and muonic X-rays[1]. The information on neutron distribution is, however, very much less detailed. Bethe and Siemens[2] have employed the Fermi model for the nucleus and have found that the half density radius for the neutron distribution is only about 0.1 fm less than that of the protons. In this paper, we have used the method of Nolen et al[3] who suggested that the displacement energies between isobaric analogue states could be used along with the accurately determined charge radii to entract information about the radial distributions of neutrons in nuclei.

2. Details of Calculations

It can be easily shown that the energy shift between isobaric analogue states is caused only by the charge dependent part of the nuclear Hamiltonian. We have considered the energy shift due to the following charge dependent perturbations:- (a) the neutron-proton mass difference, (b) the Coulomb interaction, (c) the electromagnetic spin-orbit interaction and (d) the charge dependence of the specifically nuclear forces. We then have the experimentally known[4] displacement energies (after taking the n-p mass difference into account) given by

$$\Delta E_d(\text{expt}) = \Delta E_{\text{Coulomb}} + \Delta E_{\text{s.o.}} + \Delta E_{\text{c.d.}}$$

In the above equation, the terms on the right hand side denote the energy shifts due tothe charge dependent perturbations mentioned above.

(i) Coulomb interaction: In isobaric analogue states, one of the excess neutrons in the parent state is converted into a proton in the analogue state. The interaction of this proton with the Coulomb field of the charge distribution due to the protons in the core gives the Coulomb displacement energy. Assuming that the radial distribution of the neutron excess in the parent state is the same as that of the proton in the analogue state, the direct term of the Coulomb interaction is given by

$$\Delta E_c(\text{direct}) = e\int_0^{\infty} V_c(r)\, \rho_{exc}(r)\, d^3r$$

where $\rho_{exc}(r)$ denotes the radial distribution of the neutron excess and $V_c(r)$ is the Coulomb potential due to the charge distribution of the protons in the core.

If $\rho_n(r)$ and $\rho_p(r)$ denote the radial distributions of the neutrons and protons, respectively, then

$$\rho_{exc}(r) = \rho_n(r) - \rho_p(r)$$

also

$$V_c(r) = \int_{\infty}^{r} \frac{Ze}{r'^2}\left[\int_0^{r'} \rho_p(r'')\, d^3 r''\right] dr'$$

The exchange term is given by

$$E_c(\text{exchange}) = \sum_{\substack{\text{all protons}\\ \text{neutron exc.}}} \iint \psi_p^*(\vec{r}_1)\, \psi_{exc}^*(\vec{r}_2)\, \frac{e^2}{r_{12}}\, \psi_p(\vec{r}_2)\, \psi_{exc}(\vec{r}_1)\; d\vec{r}_1\, d\vec{r}_2$$

$$\Delta E_{\text{Coulomb}} = \Delta E_c(\text{direct}) + \Delta E_c(\text{exchange}).$$

ii) <u>The electromagnetic spin-orbit interaction:</u> This arises due to the difference between the intrinsic magnetic

moments of the neutron and proton. This results in the neutron and proton experiencing different forces while moving through the electromagnetic field generated by the other nucleons. The expression[5] for spin-orbit perturbation

$$H_{s.o.} = \frac{e\hbar^2}{2m^2c^2} (\mu_p - \mu_n) \sum_{i=1}^{A} \frac{1}{r_i} \frac{dV_c(r_i)}{dr_i} \vec{l}(i).\vec{s}(i)\vec{\tau}_z(i)$$

from which the energy shift $\Delta E_{s.o.}$ can be calculated.

(iii) Charge dependence of the specifically nuclear forces. We have used the general form for the charge dependent nucleon-nucleon interaction given by

$$H_{c.d} = V(r_{ij}) \Big[(p + r\vec{\sigma}(i).\vec{\sigma}(j))(\tau_z(i) + \tau_z(j)) + (q + s\,\vec{\sigma}(i).\vec{\sigma}(j)(\tau_z(i)\tau_z(j) - \tfrac{1}{3}\vec{\tau}(i).\vec{\tau}(j)) \Big]$$

The charge dependent parameters p, q, r and s have been determined earlier[6] from a least squares analysis. Thus the energy shift $\Delta E_{c.d.}$ can be evaluated.

3. RESULTS

The experimental displacement energies used are $^{13}C-^{13}N^{*}=2.268$ MeV and $^{18}O-^{18}F^{*} = 3.522$ MeV Calculations have been made both with harmonic oscillator and Woods-Saxon wave functions and the results are given in the Table I. Thus in order to compensate for the corrections and reach an agreement with the experimental values of the displacement energies, the direct term has to be increased which is done by adjusting the radius of the neutron excess distribution. Our calculations show that the radius of the neutron distribution is not likely to fall much outside that for the protons. The present model indicates that displacement energies between iso

TABLE I

Determination of parameters of neutron distribution

(a) From harmonic oscillator charge distribution and wave functions

NUCLEUS	Estimates of different contributions to displacement energy (in MeV)				Root mean square radius (fm)		
	Coulomb interaction						
	Direct term	Exchange term	Spin orbit interaction	Charge dependence	Proton distribution	Neutron excess distribution	Neutron distribution
^{13}C	3.935	-0.251	-0.058	-0.103	2.32	2.39	2.35
^{18}O	4.471	-0.386	-0.089	-0.201	2.77	3.15	2.85

(b) From Fermi charge distribution and Woods-Saxon Wave functions

^{13}C	3.659	-0.228	-0.064	-0.099	2.32	2.55	2.41
^{18}O	4.278	-0.329	-0.068	-0.164	2.77	3.35	2.93

states are useful in probing detailed differences in nuclear structure.

REFERENCES

1. Landolt-Bornstein, 1967, Nuclear Radii (Berlin; Springer-Verlag).
2. Bethe, H, and Seimens, S., Phys. Lett 27B (1968) 549.
3. Nolen, J.A., and Schiffer, J.P., Phys. Lett 29B (1969) 396.
4. Harchol, M., et al, Nucl. Phys. A90 (1967) 459.
5. Murthy, M., Y.R. Waghmare, Nucl. Phys. A139 (1969) 579.
6. Murthy, M., J. Phys. A (Gen. Phys.), Vol. 2 (1969) 672.

COMPARISON OF THE CENTRIFUGAL STRETCHING MODEL AND THE VARIABLE MOMENT OF INERTIA MODEL

P.C. Sood
Physics Department, Banaras Hindu University, Varanasi-5.

We had proposed[1] a simple version of the centrifugal stretching model (CS model) for the phenomenological description of the rotational sequence of low lying levels in various nuclei. Recently another model, called the variable moment of inertia (VMI) model, has been suggested[2] for this purpose. In the following we compare these two models both with regard to their physical assumptions as well as their mathematical formulations and comment on the features revealed through such a comparison.

In the CS model the hydrodynamical concept of assuming the moment of inertia $\mathcal{J}$ being proportional to β^2 (where β represents the nuclear deformation) is adopted and the equilibrium deformation β_o is obtained by minimizing the energy with respect to the variable β. In the VMI model, on the other hand, $\mathcal{J}$ is assumed proportional to β and then $\mathcal{J}$ itself is regarded as the variable with respect to which the energy is minimized to determine the equilibrium ('ground state') value $\mathcal{J}_o$. In both models we are led to a relation giving the angular momentum I dependence of the moment of inertia $\mathcal{J}_I$ and also a set of parametric equations for the level energies E_I. Let us compare these relations.

The I-dependence of the moment of inertia in the VMI model is given (vide their eq.(7)) as

$$\mathcal{J}_o / \mathcal{J}_I = 1 - \frac{I(I+1)}{2C\mathcal{J}_I^3} \quad \ldots\ldots \quad (1)$$

which can be rewritten as

$$\frac{I(I+1)}{4C\mathcal{J}_o^3} = \tfrac{1}{2}\left(\mathcal{J}_I/\mathcal{J}_o\right)^2 \left\{\left(\mathcal{J}_I/\mathcal{J}_o\right) - 1\right\} \quad \ldots\ldots \quad (2)$$

The corresponding relation of CS model (vide their eq.(6) is

$$\mathcal{J}_I/\mathcal{J}_o = \frac{1}{(1-V)^2} \quad \ldots\ldots \quad (3)$$

Using eq.(3) we get

$$\tfrac{1}{2}\left(\mathcal{J}_I/\mathcal{J}_o\right)^2 \left\{\left(\mathcal{J}_I/\mathcal{J}_o\right) - 1\right\} = \frac{(1-V)^{-2} - 1}{2(1-V)^4}$$

$$= \frac{1 + 2V + O(V^2) - 1}{2(1-V)^4}$$

$$\approx \frac{V}{(1-V)^4} \text{ to the first order } \ldots\ldots \quad (4)$$

which, according to eq. (9) of CS model, is

$$= \frac{I(I+1)}{D} \quad \ldots\ldots \quad (5)$$

Thus from eqs.(2), (4) and (5) above we see that the I-dependence of the moment of inertia is same in the first order in both the models under the correspondence of the respective parameters given by the relation

$$D = 4C\mathcal{J}_o^3 = \frac{2}{\sigma} \quad \ldots\ldots \quad (6)$$

Similarly one may compare the expression for the energy from the CS model (vide their eq.(7))

$$E_I = \frac{\hbar^2}{2\mathcal{J}_o} I(I+1)(1-V)^2(1+V) \quad \ldots\ldots \quad (7)$$

with the corresponding expression of the VMI model

(vide their eq.(16))

$$E_I = \frac{\hbar^2}{2\mathcal{J}_0} I\,(I+1)\ \frac{(3r_I - 1)}{2\,r_I^2}\ ;\ r_I = \mathcal{J}_I/\mathcal{J}_0 \ldots \quad (8)$$

Now we may write

$$\frac{(3\,r_I - 1)}{2\,r_I^2} = \frac{1}{2}\left(\mathcal{J}_0/\mathcal{J}_I\right)^2 \left\{3\left(\mathcal{J}_I/\mathcal{J}_0\right) - 1\right\}$$

$$= \frac{1}{2}\left(\mathcal{J}_0/\mathcal{J}_I\right)\left\{3 - \left(\mathcal{J}_0/\mathcal{J}_I\right)\right\}$$

which, with substitution from eq. (3) above, becomes

$$= \frac{1}{2}(1-V)^2\left[3 - (1-V)^2\right]$$

$$= \frac{1}{2}(1-V)^2\left[3 - 1 + 2V + O(V^2)\right]$$

$$\approx (1-V)^2(1+V) \quad \text{to first order} \ldots\ldots \quad (9)$$

thus establishing the equivalence of eqs.(7) and (8) in the first order.

In view of this first order equivalence of the basic equations of the two models, their predictions will not differ significantly for well deformed and moderately deformed nuclei thus resulting in the similar agreement with the experiment for these cases. Further the smooth transition from the deformed region to nearly spherical structure so well brought out [3] by the CS model is also in evidence[2] in the VMI model. However the CS model is somewhat better off than the VMI model on two important points. The first point is that while the validity of VMI model holds only for energy ratio $E_4/E_2 \gtrsim 2.23$, the CS mod val right upto the vibrational limit value of rgy

ratio. The second point is that while in the VMI model a physical meaning for their parameter σ has been sought rather unsuccessfully by looking for its un-defined correlation with B(E2) ratios, the corresponding parameter D of the CS model has been shown[4] to have a well-defined relationship with the β-vibrational energies.

REFERENCES

1. P.C. Sood, Can. J.Phys. 46, 1419 (1968)
2. M.A.J. Mariscotti, G. Scharff - Goldhaber and B. Buck, Phys. Rev. 178, 1874 (1969)
3. P.C. Sood, J.Phys. Soc. Japan, 26, 1059 (1969)
4. P.C. Sood, Prog. Theo. Phys. (Japan) 41, 545 (1969)

AN EFFECTIVE Λ-N INTERACTION

Fawzia Hasan, M.Z. Rahman Khan and Q.N. Usmani
Department of Physics, Aligarh Muslim University, Aligarh.

In the present work we aim to determine an effective Λ-N potential for the relative s- and p-states assuming a shell model description of the system with the Λ-particle and the nucleons moving in the same harmonic oscillator well for a given hypernucleus. We assume the nucleon core as remaining unchanged by the presence of the Λ-particle. This allows us to take the same oscillator frequency for the core and the hypernucleus. We take into account the variation of the oscillator frequency with mass number. This is accomplished by fixing the harmonic oscillator frequency from the root mean square radii of the core nuclei as determined from electron scattering. We also take into account the centre of mass energy by subtracting the kinetic energy operator for the centre of mass motion from the core and hypernuclear Hamiltonians.

The Λ-N interaction is taken as a central, two-body charge independent potential. No specific shape has been assumed for the interaction. Following a procedure due to Moshinsky[1], we expand it in terms of a series of velocity dependent potentials in increasing powers of the momentum, but all of zero range. The coefficients of the terms in this series are the successive moments of the potential. Since the Λ-N force is short range we retain only the first two terms of the series

and higher moments to be negligible.

We assume the hypernuclear spin to be $|J_N - 1/2|$, with J_N being the ground state spin of the core nucleus. In the shell model picture, this corresponds to the case when the singlet interaction is more attractive than the triplet[2].

Assuming a j-j coupling scheme for the nucleons and the Λ-particle the Λ-binding energy B_Λ is expressible in terms of the four Λ-N relative matrix elements $\langle nl | v_s^{\,l} | nl \rangle$, where n is the harmonic oscillator radial quantum number, l is the relative orbital angular momentum and s can be 0 and 1 corresponding to the singlet and triplet interaction respectively. The separation into relative and centre of mass wave functions is done with the Smirnov transformation[3] for particles of unequal mass.

The four relative matrix elements can be expressed in terms of six parameters, the first two moments of the potential and the singlet and triplet potential depths in the relative s- and p- states. These parameters are determined by a least squares fit to the experimental Λ-binding energy data. Initially we assume charge-independence, so the Λ-binding energies of mirror nuclei were averaged. Also the oscillator frequencies were taken to be the same for nuclei of the same mass number[4]. For various reasons the hypernuclei ${}_\Lambda H^3$, ${}_\Lambda He^6$, ${}_\Lambda Li^9$, and ${}_\Lambda Be^9$ were not included in the present analysis, but we hope to include them in future.

In the Table we display the Λ-binding energies as obtained from our analysis along with their experimental values[5]. The least square value is 0.6.

Hypernucleus	B (exp) (Mev)	B (cal) (Mev)
H^4	2.295	2.238
He^4	2.295	2.238
He^5	3.08	3.113
He^7	4.79	5.099
Li^7	5.57	5.268
Be^7	4.79	5.099
Li^8	6.815	6.696
Be^8	6.815	6.696
B^{10}	8.62	9.134
B^{11}	10.18	10.266
B^{12}	11.10	10.781
C^{13}	10.51	10.536

The effect of charge- symmetry breaking was also taken into account and was found to be small.

In the above analysis of the s- and p- shell hypernuclei the second moment was found to be a little large than the first. Since the least square value obtained is very small it may be hoped that the introduction of the third moment would not make much difference to the fit. It can, therefore, be concluded that the third and higher moments are negligibly small. The largeness of the second moment, with the third and fourth moments taken to be zero can be reproduced by an effective interaction which changes sign near the origin. This is also

characteristic feature of the Volkov[6] effective interaction in the harmonic oscillator basis.

The potential depths obtained were larger than those obtained in earlier analysis. However, the values of the volume integrals are roughly the same. The p-state depths were found to be large and repulsive in contradiction to earlier qualitative analysis[7].

In future we intend to carry out a more detailed analysis in the same spirit as the one mentioned above.

REFERENCES

1. M. Moshinsky, Nucl. Phys. 8 (1958) 19.

2. R.H. Dalitz, Nuclear Interactions of the Hyperons, p. 24. Oxford University Press, 1965.

3. M.M. Bakri, Nucl. Phys. 96A (1967) 115.

4. M. Bauten et al. Nuc. Phys. 100A (1967) 90.

5. G. Bohm et al., Nucl. Phys. B4 (1968) 511;
G. Bohm et al., Nucl. Phys. B12 (1969) 1.

6. W.H. Bassichis and A. Gal, Phys. Rev. 1C (1970) 28.

7. R.C. Herndon, Y.C. Tang and E.W. Schmid, Phys. Rev. 159 (1967) 853.

AN EFFECTIVE Λ-NUCLEON INTERACTION

Fawzia Hasan and M. Z. Rahman Khan
Department of Physics, Aligarh Muslim University, Aligarh

ABSTRACT

A phenomenological study of the effective two-body Λ-N interaction is made from the binding-energy data of the s- and p- shell hypernuclei within the framework of the shell-model. The Λ-N interaction is taken as central and spin-dependent. The radial part of the interaction has been expanded in terms of a series, the coefficients of which are the successive moments of the potential. The binding-energy is expressed in terms of six independent parameters: the first two moments and the singlet and triplet potential depths, in the relative s- and p- states. These parameters are determined by a least square fit to the experimental data. A good fit is obtained. The effect of charge-symmetry breaking has also been taken into account and is found to be small.

EFFECT OF RESCATTERING ON THE ABSORPTION OF FREE PIONS IN COMPLEX NUCLEI

R. S. Kaushal
Physics Deoartmeñt, Indian Institute of Technology, Kanpur

ABSTRACT

The rescattering process is known to make important contributions to the nuclear absorption of bound pions with two-nucleon emission and to the radiative capture of pions. Here we calculate the rescattering corrections to the nuclear absorption of free pions with single-nucleon emission in perturbation theory. As the contribution of incoherent rescattering is expected to be small the calculations are made only for coherent rescattering under some simplifying assumptions. The results are applied for pion absorption in ^{12}C nucleus.

STATES OF ^{8}Be FROM THE ANALYSIS OF $^{7}Li(p,\alpha)^{4}He$ REACTION DATA

N.Kumar
Physics Department, Indian Institute of Technology, Kanpur

and F.C.Barker
Research School of Physical Sciences,
The Australian National University, Canberra

I. INTRODUCTION

The $^{7}Li(p,\alpha)^{4}He$ reaction goes through the formation of the ^{8}Be compound nucleus and its analysis gives information about the α-emitting (even spin and positive parity) states of ^{8}Be lying in the region of 20 MeV excitation energies. The differential cross-sections of this reaction, using both polarized(1,2) and unpolarized(3,4) beams of protons, have been measured upto energies, E_p, of about 12 MeV for incident protons. Most of the experimental data obtained in these studies are consistent except(5) for the measurements of absolute cross-section of this reaction. The total cross-section curve of this reaction seems to be dominated by two peaks lying at E_p = 3.0 and 5.6 MeV. To determine the properties of levels contributing to these two peaks, many theoretical analyses have been attempted(6-9), but none of them appears to be adequate enough to explain all the experimental data over a long energy range, and the results from these analyses are not consistent with each other. Furthermore, some of the analyses suffer from the use of a formula having sign errors(10). Thus in view of all these, we have attempted to analyse the data of this reaction upto E_p = 7 MeV, and have attempted to obtain consistency with $\alpha+\alpha$ elastic scattering data, and to some extent the $^{6}Li(d,\alpha)^{4}He$ reaction data.

II. METHOD OF ANALYSIS

The general expression for the differential cross-section of a reaction initiated by a polarized be of particles has been taken from the revie cl Welton(11); and has been reduced to t

EFFECT OF RESCATTERING ON THE ABSORPTION OF FREE PIONS IN COMPLEX NUCLEI

R. S. Kaushal
Physics Department, Indian Institute of Technology, Kanpur

ABSTRACT

The rescattering process is known to make important contributions to the nuclear absorption of bound pions with two-nucleon emission and to the radiative capture of pions. Here we calculate the rescattering corrections to the nuclear absorption of free pions with single-nucleon emission in perturbation theory. As the contribution of incoherent rescattering is expected to be small the calculations are made only for coherent rescattering under some simplifying assumptions. The results are applied for pion absorption in ^{12}C nucleus.

STATES OF ^{8}Be FROM THE ANALYSIS OF $^{7}Li(p,\alpha)^{4}He$ REACTION DATA

N.Kumar
Physics Department, Indian Institute of Technology, Kanpur

and P.C.Barker
Research School of Physical Sciences,
The Australian National University, Canberra

I. INTRODUCTION

The $^{7}Li(p,\alpha)^{4}He$ reaction goes through the formation of the ^{8}Be compound nucleus and its analysis gives information about the α-emitting (even spin and positive parity) states of ^{8}Be lying in the region of 20 MeV excitation energies. The differential cross-sections of this reaction, using both polarized[1,2] and unpolarized[3,4] beams of protons, have been measured upto energies, E_p, of about 12 MeV for incident protons. Most of the experimental data obtained in these studies are consistent except[5] for the measurements of absolute cross-section of this reaction. The total cross-section curve of this reaction seems to be dominated by two peaks lying at E_p = 3.0 and 5.6 MeV. To determine the properties of levels contributing to these two peaks, many theoretical analyses have been attempted[6-9], but none of them appears to be adequate enough to explain all the experimental data over a long energy range, and the results from these analyses are not consistent with each other. Furthermore, some of the analyses suffer from the use of a formula having sign errors[10]. Thus in view of all these, we have attempted to analyse the data of this reaction upto E_p = 7 MeV, and have attempted to obtain consistency with $\alpha+\alpha$ elastic scattering data, and to some extent the $^{6}Li(d,\alpha)^{4}He$ reaction data.

II. METHOD OF ANALYSIS

The general expression for the differential cross-section of a reaction initiated by a polarized beam of particles has been taken from the review article of Welton[11]; and has been reduced to the expression for

the total cross-section, σ_{tot}, and the coefficients A_L and B_L of the Legendre polynomials in the expansions of the polarization efficiency and the angular distribution of a reaction[1]. The reaction matrix elements appearing in these expressions have been then expressed in terms of the energy independent level parameters a_c, B_c, E_λ and $\gamma_{\lambda c}$ by using the multi-level R-matrix theory as reviewed by Lane and Thomas[12]. For a particular channel c, a_c and B_c denote the channel radius and the boundry condition parameter; while for a particular level λ, E_λ and $\gamma_{\lambda c}$ stand for the eigenenerg and the reduced width amplitude respectively. The chan index c designates the channel quantum numbers $\alpha \ell S$, whe α denotes the channel in question (in subsequent discussion we use the index p for the ingoing ^7Li+p channel, and α for the outgoing $\alpha+\alpha$ channel), ℓ the relative orbital angular momentum in the channel, and S the channel spin formed by the vector addition of the intrinsic spins of the channel particles. (For the outgoing $\alpha+\alpha$ channel, we need not specify ℓ and S values, as S is always equal to zero, and ℓ is automatic ally determined once the spin J of the compound state is specified.)

To include very approximately the contribution from the levels not included explicitly, we use $\alpha+\alpha$ elastic scattering data[13], assuming that imaginary parts of the phase shifts and sharp changes in the real parts may be attributed to levels being included explici ly; while the general trends of the real parts arise due to the other nearby levels. Further, to include approx. the contribution from the competing channels (i.e. all other possible channels except the ingoing ^7Li+p and the outgoing $\alpha+\alpha$ channels), we assume that the whole contribution from the competing channels comes from the $^7Li^*+p$, ^7Be+n and $^7Be^*+n$ channels, and from p-wave nucleons alone. Since the reduced width amplitudes for the ^7Be+n and $^7Be^*+n$ channels are taken to be the same,

the ^7Be+n and $^7Be^*$+n channels.

For a fixed set of values of a_c and B_c, and for a fixed number of levels of definite spin J, fit to the data are obtained by varying E_λ and $\gamma_{\lambda c}$ till a minimum in χ^2 is achieved.

III. FITTING PROCEDURE AND RESULTS

In the energy region under consideration, results obtained from the analysis of the $^7Li(p,\alpha)^4He$ reaction data are expected to be consistent with those from related reactions, such as the $\alpha+\alpha$ elastic scattering and the $^6Li(d,\alpha)^4He$ reactions. Darriulat[13] has extracted complex phase shifts from the observed $\alpha+\alpha$ scattering cross-sections. About 20 MeV excitation energies, E_x, in ^8Be, the energy dependences of these phase shifts suggest the presence of 0^+ levels near 20 and 23 MeV; 2^+ levels at 16.6, 16.9, 19.9 and 22.2 MeV; and a 4^+ level near 19.8 MeV. In the last few years, the $^6Li(d,\alpha)^4He$ reaction data obtained by using unpolarized beams of deutrons have also been analysed by two different groups of workers[7,14]. The studies of these authors seem to indicate the presence of 2^+ levels at E_x = 22.5 and 25 MeV; and a 0^+ or a 4^+ level somewhere in between these two 2^+ levels. Recent shell model calculations by one of us[15] including only the states of the lowest configuration, and in which the matrix elements of the effective interaction have been determined by fitting the excitation energies and other properties of levels in the nuclei of mass number 6 to 9, predict the even spin, +ve parity and T=0 states of ^8Be at roughly the same excitation energies at which they are suggested by the $\alpha+\alpha$ scattering phase shifts and the $^6Li(d,\alpha)$ data. Then if the 2^+ states are assumed to be the main contributing factor to the data of this reaction as indicated by the previous analyses[6-9] of this reaction, then $\alpha+\alpha$ scattering phase shifts, the analyses of the $^6Li(d,\alpha)$ data and the shell model calculations indicate that the main contribution to the data of this reaction upto E_p = 7 MeV may come from 2^+ levels lying at E_x = 16.6, 16.9, 19.9 and 22.2 MeV in ^8Be. Out of

TABLE I

Level parameters for states of ^{8}Be obtained from best fits to the $^{7}Li(p,\alpha)^{4}He$ reaction data upto E_p = 7 MeV. Eigenenergies are in MeV, while the reduced width amplitudes are in $MeV^{\frac{1}{2}}$. Reduced widths denoted by $\gamma_{\lambda p \ell S}$.

J of Levels / Parameters	0	0	2	2	2	2
E_{λ}	19.7	21.7	15.8	20.1	22.2	25.0
$\gamma_{\lambda p11}$	-0.93	-0.81	0.48	-0.24	0.02	0.57
$\gamma_{\lambda p12}$	0.0	0.0	0.76	0.27	-0.34	0.75
$\gamma_{\lambda p31}$	0.0	0.0	0.08	-0.10	0.03	0.31
$\gamma_{\lambda p32}$	0.0	0.0	-0.49	0.12	-0.06	-0.06
γ_{α}	-0.03	0.002	0.13	0.21	-0.15	0.02
$\gamma_{\lambda c^*}$(+)	0.67	0.43	-0.46	0.47	-0.24	0.22

(+) Here c^* refers to the $^{7}Li^{*}+p$ channel only.

a_p	a_{α}	B_p(p-wave)	B_p(f-wave)	B_{α}
4.22 fm.	6.0 fm.	-1	-3	0

these four 2^+ levels, the 16.6 and 16.9 MeV levels appear[16] to contain about equal intensities of T=0 and T=1 components. As these levels lie close together and below the energy region of interest, we may approximate by taking their eigenenergies as equal, and may assume that their contributions are the same as those of the unmixed T=0 and T=1 states. Then including only the contribution from the T=0 state, the main contribution to the data of this reaction may come from 2^+ states lying at 16.8, 19.9 and 22.2 MeV. Then using for these three 2^+ levels the values of the p-wave nucleon reduced width amplitudes as calculated from the shell model calculations, and the eigenenergies and α-particle reduced widths as chosen to fit approximately the $\alpha+\alpha$ scattering d-wave phase shifts[13], we have predicted fits to σ_{tot}, A_L and B_L data. These fits seem to have the general features

of the experimental curves[1-4]. Then using these values of parameters as good starting values, we have obtained fits to the data in which we have also included two 0^+ levels at about E_x = 19 and 22 MeV, and a 2^+ level at about 25 MeV, as suggested by the $\alpha+\alpha$ scattering and the $^6Li(d,\alpha)^4He$ data respectively. The obtained fits to the data are very satisfactory, and are definitely much superior than those of the previous authors[6-9], with a χ^2/N value of 2.27. The final values of the level parameters are displayed in table I.

It is interesting to note from our attempt that the experimental data of the $^7Li(p,\alpha)^4He$ reaction upto E_p = 7 MeV can be reasonably well explained by using indications about the numbers and positions of the 0^+ and 2^+ states of the ^8Be as suggested by $\alpha+\alpha$ scattering phase shifts, the analyses of the $^6Li(d,\alpha)^4He$ reaction data, and the shell model calculations of Kumar[15]. Since the results obtained from the previous analyses[6-9] of this reaction had no consistency with $\alpha+\alpha$ and the $^6Li(d,\alpha)$ data, the present consistency seems to indicate that our results are definitely better. Further, our attempt seems to confirm that while other levels are needed to correct the behaviour of the calculated curves, the main contribution to the data of this reaction upto E_p = 7 MeV comes from three 2^+ levels.

From the present analysis, two new 0^+ levels have been found to be present in ^8Be around E_x = 20 MeV. The presence of these levels was only indicated previously by the behaviour of the $\alpha+\alpha$ phase shifts, but not confirmed by ány any analysis of the experimental data. Thus it would be interesting to carry out a detailed R-matrix analysis of the $\alpha+\alpha$ phase shifts in the region of 20 MeV excitation energies in ^8Be to fix the properties of these levels. Polarization data of the $^6Li(d,\alpha)^4He$ reaction are now available. Analysis of these data would also prove very useful.

REFERENCES

1. C.Petitjean and L.Brown; Nucl.Phys. A111, 177(1968).

2. G.R.Plattner, T.B.Clegg and L.G.Keller; Nucl.Phys. A111, 481(1968).

3. F.Hirst and R.Uebergang; Aust.J.Sci.Res. 4A, 284 (1951).

4. G.S.Mani, R.Freeman, F.Picard, A.Sadeghi and D.Redon; Nucl.Phys. 60, 588(1964).

5. G.M.Lerner and J.B.Marion; Nucl.Instr. and Meth. 69, 115(1969).

6. R.A.Lux, Ph.D. thesis, University of Wisconsin (1963).

7. R.M.Freeman and G.S.Mani; Proc.Phys.Soc. 85, 267 (1965).

8. M.Borsaru, M.Cenja, C.Hategan, and E.Iliescu; Rev. Roum.Phys. 12, 661(1967).

9. M.Dayhuff and R.G.Seyler; Bull.Am.Phys.Soc. 14, 1213 (1969).

10. N.Kumar and F.C.Barker, to be published.

11. T.A.Welton, in Fast Neutron Physics Part II, ed. J.B. Marion and J.L.Fowler, Interscience publishers (1963).

12. A.M.Lane and R.G.Thomas; Rev.Mod.Phys. 30, 257(1958).

13. P.Darriulat, Ph.D. thesis, University of Paris (1965).

14. T.U.Chan, J.P.Longequeue and H.Beaumevieille; Nucl. Phys. A124, 449(1969).

15. N.Kumar, to be published.

16. F.C.Barker; Nucl.Phys. 83, 418(1966).

ELECTRON SCATTERING FORM FACTORS FOR C^{13}

Raj K. Gupta
Physics Department, Panjab University, Chandigarh

ABSTRACT

An analysis of the elastic and inelastic form factors, obtained at the Saskatchawan Accelerator Laboratory, Saskatoon, Canada, will be reported. The rms charge radius for C^{13} is obtained and the calculations of the inelastic form factors using various model wave-functions, are compared with the experimental data.

ION-OPTICS OF A SPLIT-POLE MAGNETIC SPECTROGRAPH BY METHOD OF RAY-TRACING

S. Das and N. Sarma
Nuclear Physics Division
Bhabha Atomic Research Centre, Trombay, Bombay-85

I. INTRODUCTION

Calculations on the ion-optical properties of a split-pole magnetic spectrograph described by Enge (1) have been done both analytically (2) and by ray tracing methods (3). In the present calculations the equation of motion for the charged particles has been formulated more accurately. This equation is used as the input for a ray-tracing computation of the trajectories of the particles. Results thus obtained have been compared with those of Enge and Visweswariah.

II. THEORY

It can be shown that the most general equation of motion in the median plane of a spectrograph for a particle of mass m, charge q is

$$\frac{d^2y}{dx^2} = -\frac{h(s)}{R}\left[1+\left(\frac{dy}{dx}\right)^2\right]^{3/2}$$

where $h(s) = \frac{B_{z,0}}{B_0}$; $B_{z,0}$ is the induction in the median plane and B_0 is the uniform field at the median plane within the pole gap (Fig.II)

The above equation was solved numerically using the Runge-Kutta method of integration for particles of a specified divergence α . Calculations were made for a range of radius values upto a maximum of 90 cms. The characteristics of the spectrograph were then determined by the behaviour of the

trajectories at the focal plane. In this calculation two types of fringing field at the pole boundary have been considered;

(1) SCFF (sharp cut-off) and

(2) EFF (Extended fringing field)

III. RESULTS

We have computed the exit angle (ϵ_1''), angle of deviation (ϕ') and the virtual image distance (l_1'') due to circular sector; radian-plane magnification, aberration, dispersion, resolution and final focal-plane location of the entire spectrograph. A correction for kinematic line broadening has also been taken into account.

Our computations are generally in better agreement with ref.(2) than the calculations of Spencer & Enge (3). However experimental data are not available at present for comparison.

REFERENCE

1. H.A. Enge, Nucl. Instr. and Methods, 28 (1964) 119
2. M.N. Visweswariah and S. Sarma, Nucl. Instr. Methods, 54(1967)181
3. J. Spencer and H.A. Enge, Nucl. Instr. and Meth. 49 (1967) 181

Position of the focal surface and aberration

Radius	X in cms.	Y in cms.	Aberration
40	[illegible]	-23.173	0.00101
50	174.314	-33.22	0.0032
60	198.16	-42.915	0.0051
70	221.59	-52.4	0.00687
80	244.788	-61.83	0.00768
90	267.825	-71.2	0.0083

Characteristics of Pole-Piece I

R	ϵ_1''		ϕ'		ℓ_1''	
	*Theoretical	Ray Tracing	*Theoretical	Ray Tracing	*Theoretical	Ray Tracing
50	14° 30'	14° 30'	40° 54'	40° 54'	-90.76	-90.0
60	9° 54'	10° 0'	34° 12'	34° 6'	-88.0	-88.4

Radius in cms.	Median-plane magnification(KH)			Dispersion(D)			Momentum Resolution(R)		
	Ref.2	Ref.3	Present work	Ref.2	Ref.3	Present work	Ref.2	Ref.3	Present work
40	0.35	0.337	0.31523	2.16 2.13	1.99	2.06057	2744.4	2650	2905.2
50	0.348	0.3365	0.310055	1.99 1.98	1.905	1.9962	3164.4	3145	3576.8
60	0.35	0.34	0.31	1.89	1.84	1.96586	3591.1	3650	4227.55
70	0.3535	0.344	0.31238	1.83	1.7875	1.92354	4002.2	4120	4789.35
80	0.358	0.348	0.315963	1.79	1.7525	1.8982	4395.5	4555	5340.1
90	0.364	0.354	0.32002	1.75	1.725	1.86586	4766.6	4970	5830.0

* Ref. 2

FIG I SHOWS THE POLE FACE LAYOUT OF SPHS

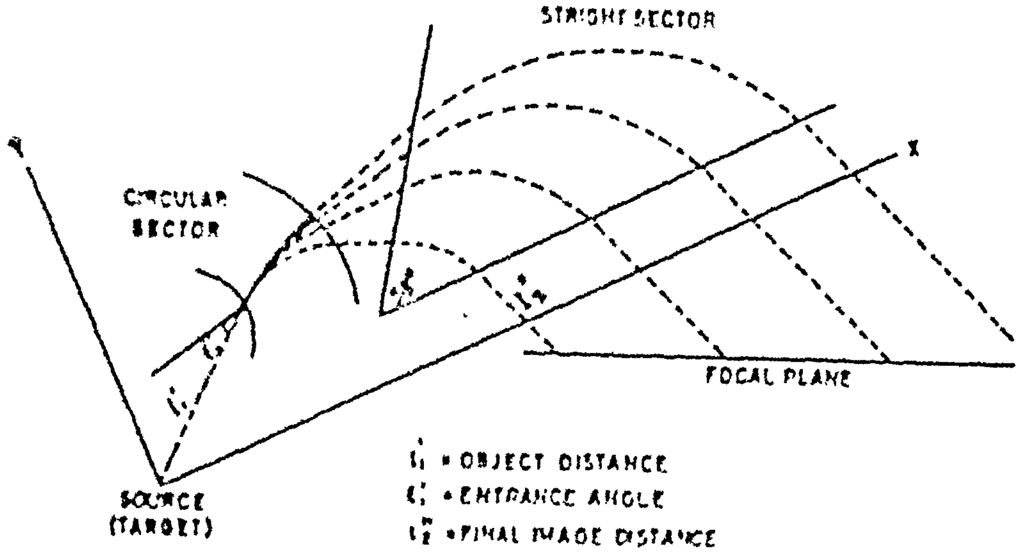
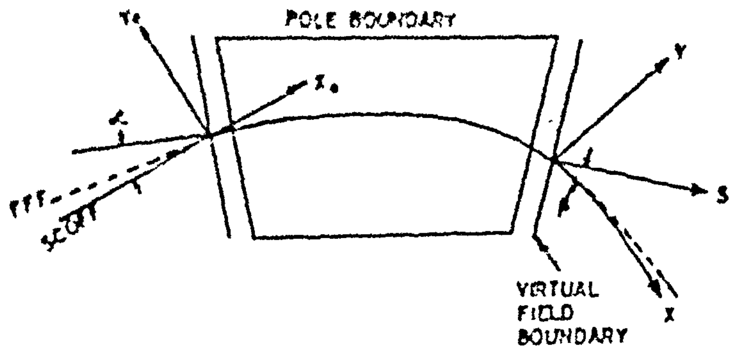


FIG II



β IS THE EXIT ANGLE, D IS THE AIR GAP AND S IS A NON-DIMENSIONAL CO-ORDINATE WHICH MEASURES THE DISTANCE ALONG THE NORMAL IN UNITS OF D.

RF MEASUREMENT OF THE COMPLEX CONDUCTIVITY OF A PLASMA BY AN EXTERNAL PROBE

J. N. Maiti and J. Basu
Saha Institute of Nuclear Physics, Calcutta-9

ABSTRACT

The complex conductivity of a plasma in a discharge tube has been measured with an rf external probe by using an impedance method. The probe consists of a coil placed around the discharge tube and the method lies in determining the conductivity from the measurement of the coil impedance with plasma inside the tube, normalised with respect to that without plasma. The complex conductivity of a plasma generated in a hot cathode argon discharge has been measured at different discharge currents and gas pressures. The values of the electron density and electron collision frequency in the plasma, obtained from the conductivity measurement, are found to be in reasonable agreement with the values calculated from the measured Langmuir probe data.

HYPERFINE FIELD ON Tc IN Ni

R.C. Chopra, S. H. Devare and H.G. Devare
Tata Institute of Fundamental Research, Bombay-5

The method of PAC is one of the various experimental tec ques[1] available for the study of hyperfine interactions. It is to determine the hf-fields if the nuclear g-factor is known, and v versa.

The hf-field acting on technetium in nickel has been measu using time-differential-perturbed angular correlation (TDPAC) techni que. The knowledge of the nuclear g-factor was not essential since measurements were made with Mo^{99}-Ni alloy sources as well as Mo-metal sources. The hf-field was determined by the ratio of the two Larmour frequencies.

I. EXPERIMENTAL

Natural Molybdenum was irradiated for three days in CIRUS in a neutron flux of 10^{13} n/cm^2/sec. The alloy was prepared by melting the activity in a furnace with proper quantity of nickel. The alloy was then pressed to a thin foil, cut into small pieces and annealed for 6 hrs. at 800°C. The Mo^{99}-Ni alloy contained 3.8 at % of Mo.

In the decay of Mo^{99} to Tc^{99}, the 740-181 keV γ'-γ cascade was used for the measurements. Partial decay scheme of $Mo^{99} \rightarrow Tc^{99}$ is given in Fig.1. 2" x 2" NaI(Tl) crystals mounted on RCA 6810A photomultipliers were used as γ-detectors. The typical FWHM of the 511-181 keV prompt was 2.7 ns.

An external field of 20.5 KG was used with Mo-metal sources while in the case of Mo-Ni alloy sources the polarising field was 7.1 KG. A water cooled electromagnet[2] was used for producing the desired fields.

II. RESULTS

In a magnetic field, applied in a plane perpendicular to the plane of detectors, the angular correlation of two gamma rays can be expressed as

$$W(\theta, H, t) = \sum_{k=0}^{k_{max}} A_k P_k(\cos(\theta - \omega_L t)) \quad \text{---(1)}$$

The Larmour frequency ω_L is given by

$$\omega_L = g \mu_N H_{eff.}/\hbar$$

where g is the nuclear g-factor of the intermediate state, μ_N the nuclear magneton and $H_{eff} = H_{int} + H_{ext}$.

The coincidence counting rate is given by

$$C(t) = e^{-t/\tau} W(\theta, H, t).\text{Const} \quad \ldots\ldots\ldots\ldots(2)$$

τ being the mean life of the intermediate level. Counts were collected for both field directions (positive and negative) at an angle of 135°. A quantity R(t) is defined as

$$R(t) = \frac{2(C^+(t) - C^-(t))}{C^+(t) + C^-(t)} \quad \ldots\ldots\ldots\ldots\ldots(3)$$

$C^+(t)$ and $C^-(t)$ being the coincidence counts for positive and negative direction of the field respectively. For $A_2 \gg A_4$, (3) reduces to

$$R(t) = \frac{6 A_2 \sin 2\omega_L t}{4 + A_2}$$

A plot of R(t) against t is shown in Fig.2 for the case of ^{99}Mo-Ni alloy.

The internal field acting on Tc in Ni was determined to be:

H_{int} = -31.6 KG ± 4% .

III. DISCUSSION

Gerdau's group[3] has determined the field on Tc in Ni to be -41 KG ± 10% which is in agreement with our value. The internal fields for 12 solutes in Fe, Co, Ni have recently been estimated[4] and it is found that conduction electron polarisation alone can fit for the experimental values of H_{hf}. The predicted value for the field on Tc in Ni is -55 KG which fairly agrees with our result.

REFERENCES

1. A.J. Freeman and R.E. Watson; in Magnetism (Rado-Suhl), IIA, Ch.4, Academic Press, New York, 1965.

2. P.N. Tandon; Thesis, University of Bombay, 1967 (unpublished).

3. E. Gerdau et al (Private communication).

4. D.A. Shirley, S.S. Rosenblum and E. Matthias; Phys. Rev. 170, 363 (1968).

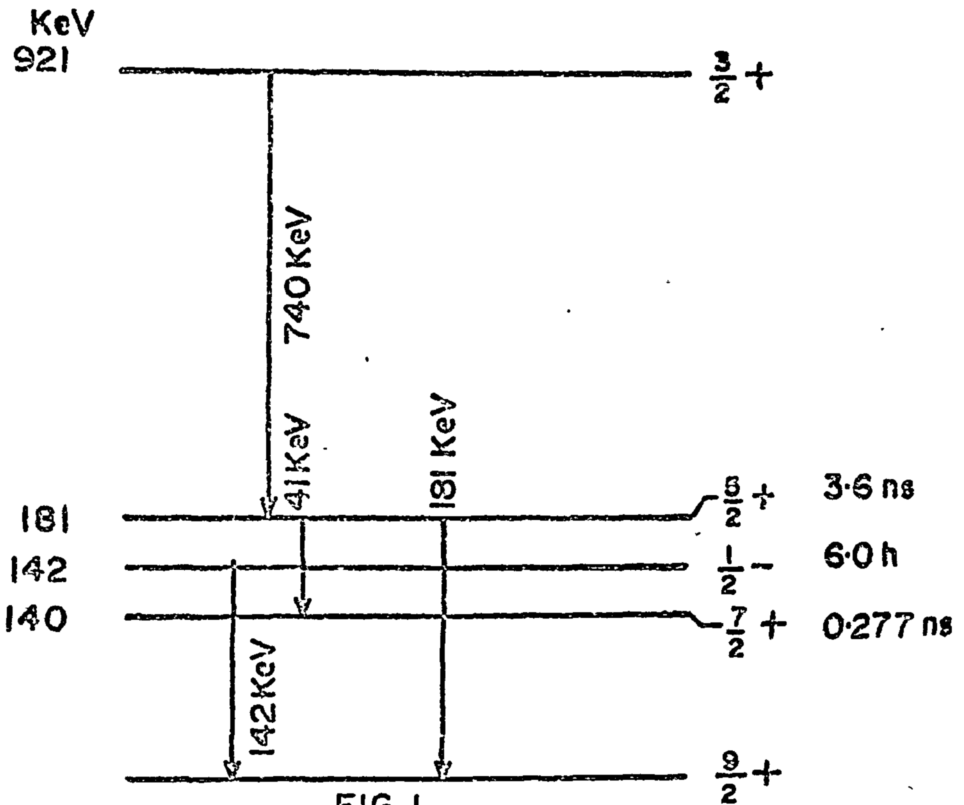


FIG. I

PARTIAL DECAY SCHEME OF Tc^{99}

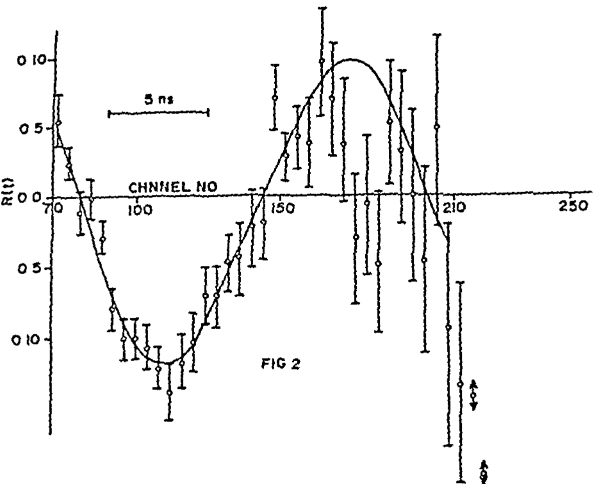


FIG 2

INTERNAL BREMSSTRAHLUNG SPECTRUM FROM ^{32}P.

N. Nath, S. Mitra, A.K. De, A.K. Das, and P.C. Bhattacharya,
Department of Physics, Calcutta University.

I. INTRODUCTION

The problems in connection with internal bremsstrahlung (IB) in beta decay are not yet solved in spite of numerous experimental and theoretical studies during the recent years. A survey of Persson[1] reveals explicitly that the disagreement lies not only between theory and experiment but also among the individual experiments.

It was therefore decided to carry out a critical analysis of the problem. There is a considerable number of measurements [2-13] for ^{32}P source. These are in more or less agreement (except [10]) for smal photon energies. Considerable discrepancies occur, however, at higher photon energies[8-13]. At the highest photon energies (~1200 investigated, some experimental results [10,12] differ by as much as 100%. In the cases of other isotopes the observed deviations are much greater.

We give a preliminary report of the IB spectrum measurement for ^{32}P using a modified geometrical arrangement similar to that used by Baronyi and Varga[13].

II. EXPERIMENTAL

The geometrical arrangement used in the present investigation is shown in Fig.1. Previous workers placed beta absorber half way between the source and the detector using a lead collimator. The present experimental arrangement is designed to ensure that a

minimum EB contributes to the measurements and corrections can be applied for it. As concluded from Fig. 2, the optimum place of the absorber is not midway between the detector and the source. For the present geometry of source-crystal distance (20 cm) and crystal diameter (3.8 cm), the absorber is placed at 15 cm from the crystal.

The geometrical arrangement and associated circuitries (e.g., super-stable high voltage, linear amplifier, single channel analyser, electronic timer etc.) is housed in an airconditioned room at a fixed temperature of $74^{0} \pm 1^{0}$ F and the supply voltage is stabilised by an A.C. voltage stabiliser. The amplifier characteristic and analyser stability was checked frequently by a precision pulser and a pulse oscilloscope.

The energy calibration was performed with a suitable set of standard γ-ray lines covering the entire range of interest. During each of the three runs with $\sim 300 \mu c$ ^{32}P source, analyser window was adjusted by the precision pulser and varied according to Kelley's considerations, i.e., $< 1/3$ FW-energy-HM at that energy. Sufficient care is taken to avoid spurious effects. Corrections are made for several factors such as background, energy resolution, backscattering, compton & iodine K-escape electrons, geometrical & gamma detection efficiency of the crystal and absorption of the radiation between the source and the detector. The experimentally recorded pulse height distribution after various mentioned corrections are converted to the probability for IB production per 1 Mev energy per beta disintegration in the range (60-1250)KeV on an absolute basis.

III. COMPARISON WITH THEORY

Fig. 3 shows the experimental and theoretical spectra. The solid lines shows the KUB theory and the dotted line the coulomb corrected theory of Lewis & Ford[15]. According to Nilsson[14], coulomb correction factor (1 + πaZW/p) should be replaced by Fermi function. For low values of Z (as the case here) the two factors are essentially the same.

Ford & Martin[16] considered the so-called detour transitions to IB accompanying nuclear beta decay. This is not so important for allowed decay (eg., ^{32}P). Double Internal Bremsstrahlung (DIB) proposed by Jastram & Vanderleeden [16, 17] should occur with the probability $\sim a^2$ and should have negligible influence on the measurements of single IB which in the same approximation has the probability $\alpha=1/137$.

IV. DISCUSSION AND CONCLUSION

Our results show consistency with the KUB theory in the region (100-500) KeV. In the region (500-1250)KeV there is a definite disagreement between experiment and theory even considering the coulomb effect, the experimental distribution being in excess over the theory on the average of 30%. Moreover the deviation increases with energy from 15% at 600KeV to 50% at 1250KeV. This conclusion is at par with that of Liden & Starfelt[8]. Narasimhamurty & Jnanananda[11] found that in the energy region from (100-500)KeV there is a small but definite experimental excess of 15% over the KUB theory while above 600KeV the experimental distribution coincides with the theoretical distribution. Their experimental arrangement though similar to ours can not be called ~~called~~ good 'geometry' because they placed the beta

absorber half way between the source and the detector.

In spite of the experimental inconsistencies that might be present ~~present~~ in our measurements an experimental excess over the KUB theory is obtained in the present experiment in the high regions.

... ...

The authors wish to thank Mr. A.Das for assisting the construction of the experimental arrangement.

References:

1. B.I.Persson, Proc. Conf. on electron capture etc., Debrecen, Hungary, pp. 142, (1968).

2. L. Madansky & F. Rasetti, Phys. Rev. 83, 187 (1951).

3. T.B. Novoy, Phys. Rev. 89, 672 (1953).

4. P. Bolgiano et al., Phys. Rev. 89, 679 (1953).

5. A. Michalowicz, J.PHYS. et Radium, 15, 156, (1954).

6. M. Goodrich & W.B. Payne, Phys. Rev. 94, 405 (1954).

7. M.A.Hakeem & M. Goodrich, Nuclear Phys., 31, 322 (1962).

8. K.Liden & N. Starfelt, Phys. Rev. 97, 419 (1955).

9. K.A. Korotkov and A.M. Chernikov, Bull. Acad. Science USSR, 24, 899, (1961).

10. H. Langevin-Joliot, Ann. de Phys. 2, 16 (1957).

11. K. Narasimhamurty & S. Jnanananda, Nuovo Cim. 46B, 217 (1966).

12. W.Kreische et al., Nuclear Phys. A107, 601 (1968).

13. D. Bernyi & D. Varga, Nuclear Phys. A138, 685 (1969).

14. S.B. Nilsson, Ark. Fys. 10, 467 (1956).

15. R.R.Lewis & G.W.Ford, Phys. Rev. 107, 756 (1959).

16. P.S. Jastram and J.C. Vanderleeden, Phys. Letters, 19,29(1965).

17. P.S. Jastram and J.C.Vanderleeden, Phys. Rev. C, 1 (1970).

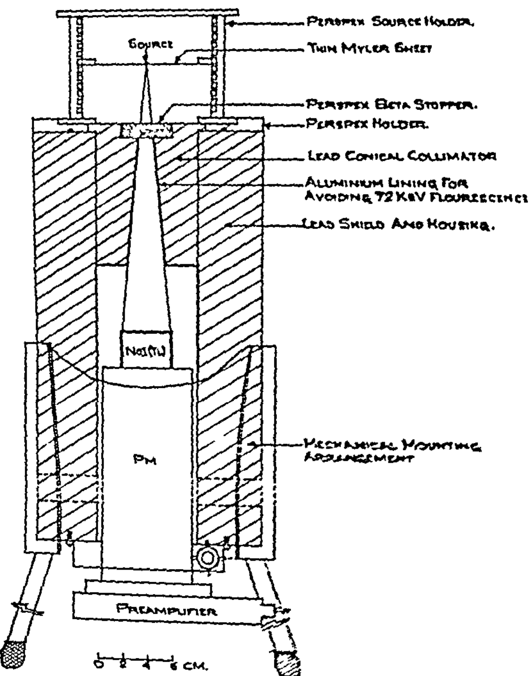


Fig. 1

Crossectional view of the geometrical arrangement for for the measurement of IB in the present study.

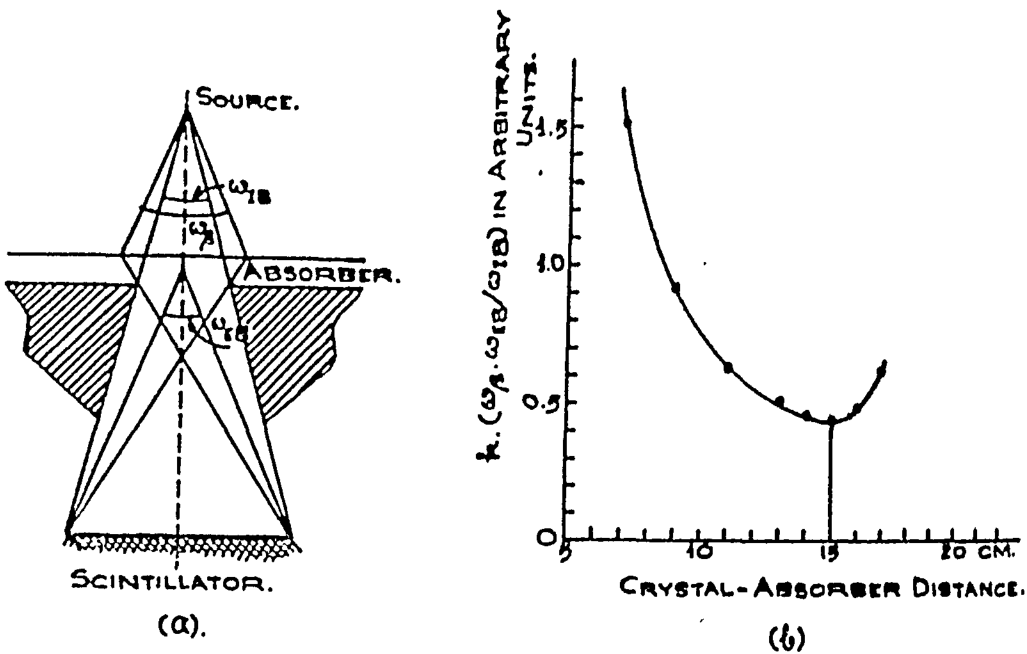


FIG. 2.

Fig. 2. (a) The approximate plane equivalents of the solid angles in the geometrical arrangement of IB measurement.

(b) The variation of the combination of the solid angles as a function of the crystal-absorber distance (Source-crystal distance 20 cm, Crystal size ∅ 3.8 cm and absorber thickness 1 cm.

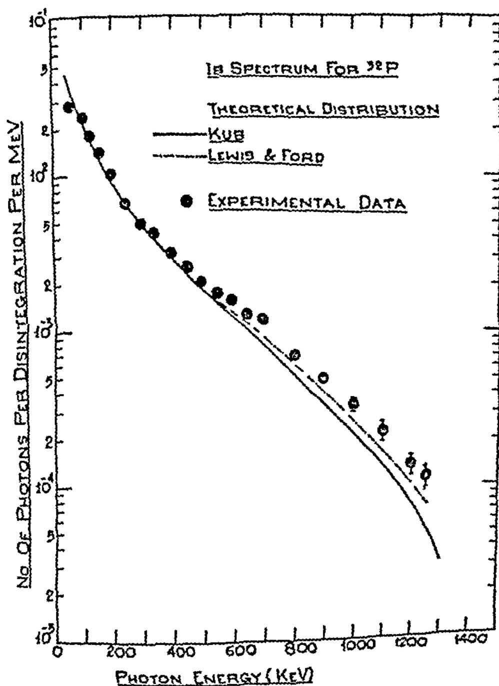


FIG 3

The inner bremsstrahlung spectrum for ^{32}P

MEASUREMENT OF THE (82L-212γ) ANGULAR CORRELATION IN ^{121}Te

H. S. Sahota
Physics Department, Punjabi University, Patiala-4

ABSTRACT

Measurement of the angular correlation of 11/2 - 3/2 - 1/2 cascade in ^{121}Te has been performed with L-conversion electrons and γ rays. The measured value of the correlation A_{22} = 0.020 ± 0.03 agrees with the findings of Marelius et al[1] but differs very much from the result A_{22} = -0.007 ± 0.007 of Goldberg and Frankel[2] using a thin lens beta spectrometer as a fixed detector for electrons and a scientillation counter for the movable detector. The L-subshell particle parameter for the 82 keV M_4 transition has been evaluated and compared with the theory of Hager and Seltzer.

(1) A. Marelius, H. Pettersson, S Tornkvist, S. E. Hagglund and R. Dumitrescu, Arkiv fur Fysik, 37, 435, (1968)

(2) N. Goldberg and S. Frankel; Phys. Rev 100, 1350 (1955)

AUTHOR INDEX

NUCLEAR PHYSICS